Geochemical study on reservoir and source rock asphaltenes and their significance for hydrocarbon generation

vorgelegt von
Diplom-Geologe
Eric Lehne

von der Fakultät VI – Planen Bauen Umwelt
der Technischen Universität Berlin
zur Erlangung des akademischen Grades

Doktor der Naturwissenschaften
- Dr. rer. nat. –

genehmigte Dissertation

Promtionsausschuss:

Vorsitzender:	Prof. Dr. Ugur Yaramanci
Berichter:	Prof. Dr. Brian Horsfield
Berichter:	Prof. Dr. Wilhelm Dominik

Tag der wissenschaftlichen Aussprache: 09. Oktober 2007

Berlin 2008

D 83

Abstract

Non-isothermal open system pyrolysis - gas chromatography and bulk petroleum generation experiments were performed on type II-S petroleum asphaltenes, source rock asphaltenes and related source rock kerogens to evaluate petroleum composition and generation timing. The results show that despite the traditionally assumed similarities between petroleum asphaltenes and their related kerogens, significant differences in petroleum generation timing and composition occur, at least for the studied type II-S petroleum system. Petroleum asphaltenes and source rock asphaltenes are less stable and show tighter petroleum formation windows than kerogens when extrapolated to geological heating rates. However, no obvious structural links were found that could directly explain the observed reactivity differences from bulk kinetic measurements. But, the amount of organic sulphur is not proportional to the reactivity of petroleum generation from asphaltenes at lower thermal stress. More likely is, that kerogens and asphaltenes posses different positions and types of sulphur bonds resulting in cracking of covalent bonds at different levels of thermal stress.

Source rock asphaltenes, related kerogen, and oil asphaltene pyrolysates show major structural differences and differ in aromaticity and organic sulphur content. Highest aromaticity was found in pyrolysates of source rocks asphaltenes, medium from kerogens, and lowest aromaticity in pyrolysates formed from petroleum asphaltenes. In addition, the highest organic sulphur content was identified in kerogen pyrolysates, whereas pyrolysates of both types of asphaltenes do not show a major difference in the content of organic sulphur. Based on the *n*-alkyl chain length distribution the kerogen pyrolysates predict the field of the paraffinic-naphtenic-aromatic low-wax oil generating facies. Pyrolysates of both asphaltene types plot at a triple point predicting P-N-A low and high wax, as well as paraffinic oil generating facies. These predictions however do not correlate with the asphaltic natural oils found in this petroleum system. The pyrolysates from both types of asphaltenes, as well from

kerogens show differences such as alkane / alkene ratios, xylene distributions, and toluene/ xylenes ratios, which can be attributed to different concentrations of precursors within the asphaltene and kerogen macromolecules.

Micro-scale sealed vessel pyrolysis (MSSV) experiments were applied on reservoir asphaltenes from a sulphur-rich sequence from Southern Italy in order to compare their petroleum and gas generation characteristics, in terms of primary and secondary gas generation, as well as the compositional kinetic prediction of determining the actual products that will be released from the asphaltene under specific geologic conditions.. The outcoming results were compared to MSSV products formed from an immature source rock kerogen of the same petroleum system in terms of chemical structural differences, as well as differences in gas formation, isotopic composition of products and compositional kinetics. The detailed compositional information from non-isothermal MSSV pyrolysis indicate that hydrocarbons formed from the oil asphaltenes show lower aromaticity and lower content of organic sulphur than products from source rock kerogen. Primary gas and secondary gas kinetics evaluated on petroleum asphaltene products result in similar geological prediction as gas formation from the source rock kerogen. Nevertheless, the GOR of product formed from the asphaltenes is much lower than that formed from the kerogen. Carbon isotopes measured on gas formed from these different types of asphaltenes and the kerogen reveal that differences are most probably related to different maturities and gas generating precursor structures. The C_{6+} oil like kinetics and geological predictions are nearly identical for hydrocarbons formed from the oil asphaltene and the kerogen. The simulation experiments using MSSV-pyrolysis illustrated that compositional features of hydrocarbons formed from asphaltenes are very similar to compositional feature found for natural petroleum. This was especially the case of *n*-C_{6-14}, *n*-C_{15+}, aromatic compounds and NSO like compounds. For that reason a compositional kinetic

model for C_{6+} formation was build up for the asphaltenes from the Italian petroleum system, which reflects the major characteristics of oils formed in this area.

Asphaltenes from reservoir oils, source rock bitumen and the kerogen of related source rocks of the Duvernay Formation (WCSB) have been studied in order to compare their petroleum generation characteristics. Open system bulk petroleum pyrolysis for bulk kinetic evaluation and geological extrapolation and pyrolysis GC experiments for petroleum compositional characterisation were applied in order to evaluate the reliability of petroleum asphaltenes in source rock evaluation studies in which a potential source rock sample is not available. Kinetic parameters and resulting geological extrapolations of petroleum formation calculated on immature source rock kerogens and asphaltenes fit exactly to corresponding parameters measured on asphaltenes precipitated on low mature oils. In contrast molecular characteristics such as aromaticity and the amount of alkylated thiophenes reveal highest values in source rock asphaltenes, while oil asphaltenes demonstrate lowest aromaticity. Source rock kerogens seem to represent an intermediate between both types of asphaltenes at low levels of maturity. Interestingly the molecular ratios observed in products formed from oil asphaltenes fit exactly to those observed in natural oils and support the application of petroleum asphaltenes to predict petroleum formation and especially petroleum compositional characteristics.

Further on, reservoir asphaltenes isolated from crude oils from Nigeria onshore were investigated in terms of bulk kinetic parameters, structural moieties, such as aromaticity and *n*-alkyl chain length distribution obtained from open-system pyrolysis, as well as hydrocarbon generation characteristics based on MSSV pyrolysis. Bulk kinetic measurements on oil asphaltenes predict peak hydrocarbon generation for geological temperatures of 145°C. This predicted temperature correlates with hydrocarbon generation for example in the western part of the Anambra Basin in Nigeria onshore. The *n*-alkyl-chain distribution of investigated Nigerian oil asphaltene pyrolysates predicts the facies generating high-wax P-N-A-oils or

paraffinic oils. The changes for facies recognition based on the *n*-alkyl chain length distribution of asphaltene pyrolysates correlates with facies changes due to variations of terrestrial input obtained from biomarker parameters of related crude oils. Hydrocarbons formed from the Nigerian reservoir asphaltene show a strong heating rate dependency for the *n*-alky-chain length distribution and for the generation of aromatic hydrocarbons, like alkylbenzenes and alkylphenols. Compositional kinetic parameters of oil and gas formation obtained from oil asphaltene pyrolysates show high values together with the early potential for the generation of gas, which may support that the original source rock of these oils correspond to a type II/III organic matter. The simulation experiments using MSSV-pyrolysis illustrated that compositional features of hydrocarbons formed from Nigerian asphaltenes are very similar to compositional feature found for natural petroleum. For that reason a compositional kinetic model for C_{6+} formation was build up for the asphaltenes from Nigeria onshore. This model reflects the major characteristics of NSO lean oils formed in this delta system.

Acknowledgment

This study is part of the Industry Partnership Programme “Asphaltenes as geochemical markers” at the GFZ-Potsdam. I am grateful to the companies Shell, ENI-Agip, Norsk Hydro, Statoil and ConocoPhillips for financial support. Very special thanks to Dr. Volker Dieckmann for supervising this thesis and for managing the IPP-project. As well I gratefully acknowledge Professor Dr. Brian Horsfield for suggestions and support during my time at the GFZ-Potsdam.

Thanks for analytical support to the technical stuff Cornelia Karger, Kristin Günther, Michael Gabriel, and Anke Sobotta at the GFZ-Potsdam, section 4.3, especially to Ferdinand Perssen for assistance during the pyrolysis experiments. I thank also Dr. Rolando di Primio for his suggestions concerning asphaltenes, and Dr. Heinz Wilkes for constructive comments regarding biomarkers.

Also I would like to thank my friends and colleagues at section 4.3 for the time we had.

Content

1. Introduction

1.1 Nature and characteristics of asphaltenes

1.1.1 Occurrence and definition of asphaltenes

A petroleum reservoir fluid is a complex polydisperse mixture consisting of light and heavy paraffins, aromatics, resins and asphaltenes. Both, asphaltenes and resins are non-crystalline, aromatic heterocompounds with aliphatic substitutions and they form the polar fractions of crude oil and source rock bitumen (Pfeiffer and Saal, 1940; Tissot and Welte, 1984). The asphaltenes show highest molecular weight and polarity of all fractions in those oils and bitumens. Resins have a strong tendency to associate with asphaltenes. Such association determines, to a large extent, their solubility in crude oil (Koots and Speight, 1975).

The term asphaltene was coined by Boussingault (1837), who described the constituents of some bitumens (asphalts) found in Eastern France and in Peru. He named the alcohol insoluble, essence of turpentine soluble solid obtained from the distillation residue "asphaltene", since it resembled the original asphalt.

The asphaltene fraction of a petroleum crude is defined according to Nellensteyn (1924) as the fraction insoluble in low boiling point paraffin hydrocarbons, but soluble in carbon tetrachloride and benzene. According to Pfeiffer (1950) asphaltenes are defined as the fraction insoluble in *n*-heptane but soluble in toluene. Other authors classified asphaltenes as insoluble fraction in light gasolines and petroleum ether (Marcusson *et al.*, 1931; Hubbard and Stanfield, 1948). In contrast to resins, the asphaltenes are precipitated in the presence of ether.

Nowadays, asphaltenes are always defined based on solubility as insoluble in paraffin hydrocarbons but soluble in polar/aromatic chemicals such as toluene, xylene (Hirschberg *et al.*, 1984; Speight *et al.*, 1984; Leontaritis and Mansoori, 1988; Kawanaka *et al.*, 1989;

Speight, 1999). Resins instead are defined as the fraction of the desasphalted oil that is strongly adsorbed in surface-active materials such as alumina, or silica, and can only be desorbed by a solvent such as pyridine or a mixture of toluene and methanol (Speight, 1999; Andersen and Speight, 2001).

1.1.2 Structure and physical-chemistry of asphaltenes

The "solubility class" definition of asphaltenes generates a broad distribution of molecular structures that can vary greatly from one crude oil to another. In general, asphaltenes are characterized by fused aromatic rings, aliphatic side chains, and polar heteroatom-containing functional groups. From a physical point of view, they can be described as aggregates with a fused aromatic core with polar heteroatom functionality, capable of accepting or donating protons (Spiecker *et al.*, 2003). The mechanism of aggregation is linked to π-π overlap between aromatic sheets and to hydrogen bonding between functional groups.

A number of investigators have constructed model structures for asphaltenes, resins, and other heavy fractions based on physical and chemical methods. Physical methods include IR, NMR, ESR, mass spectrometry, X-ray, ultra-centrifugation, electron microscopy, small angle neutron scattering, small angle X-ray scattering, quasi-elastic light scattering spectroscopy, VPO, GPC (Priyanto *et al.*, 2001). Chemical methods involve oxidation, hydrogenation (Priyanto *et al.*, 2001). A common tool in geochemistry is the pyrolysis of asphaltenes, because asphaltenes decompose, forming hydrocarbons and volatile products, when heating them above 300°C (Rubinstein *et al.*, 1979).

Fig 1 - Fig 3 show selected proposed structures of asphaltene molecules, which include the atoms carbon, hydrogen, oxygen, nitrogen, sulphur contained in both polar and non-polar groups. Two of the representative structures for the asphaltene molecule in Fig 1 belong to the Atabasca tar-sand bitumen and petroleum bitumens (Suzuki *et al.*, 1982).

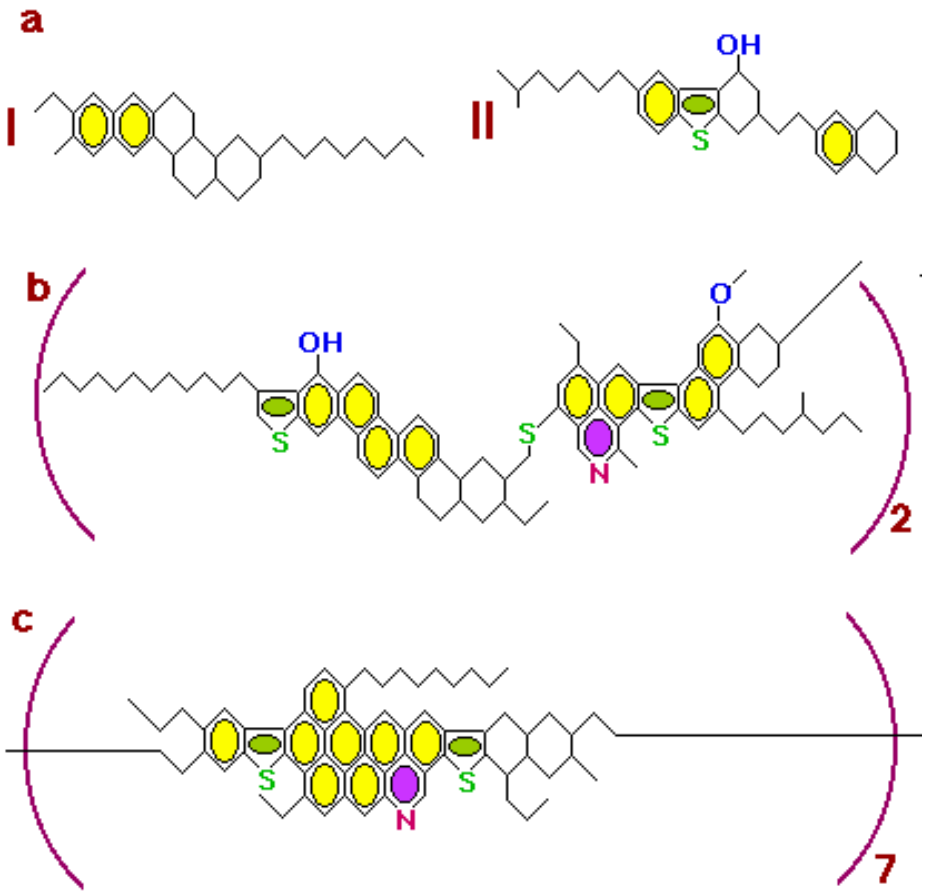

Fig 1 Average molecular structural models of the fractions of Athabasca tar-sand bitumen and petroleum bitumens; (a) resin fraction with two subgroups (I, II), (b) asphaltene fraction of tar-sand bitumen; (c) asphaltene fraction of petroleum bitumen proposed by Suzuki *et al.* (1982)

Oxygen may be present in heterocyclics, but occurs mainly in functional groups, either terminal (-OH) or in cross-linking position (-O-). Nitrogen occurs entirely in heterocyclics, whereas sulphur is confined to heterocyclics, but can appear in sulphides distinguished in labile thiols and stable thioethers in cross-linked positions (Moschopedis *et al.*, 1979; Pelet *et al.*, 1986).

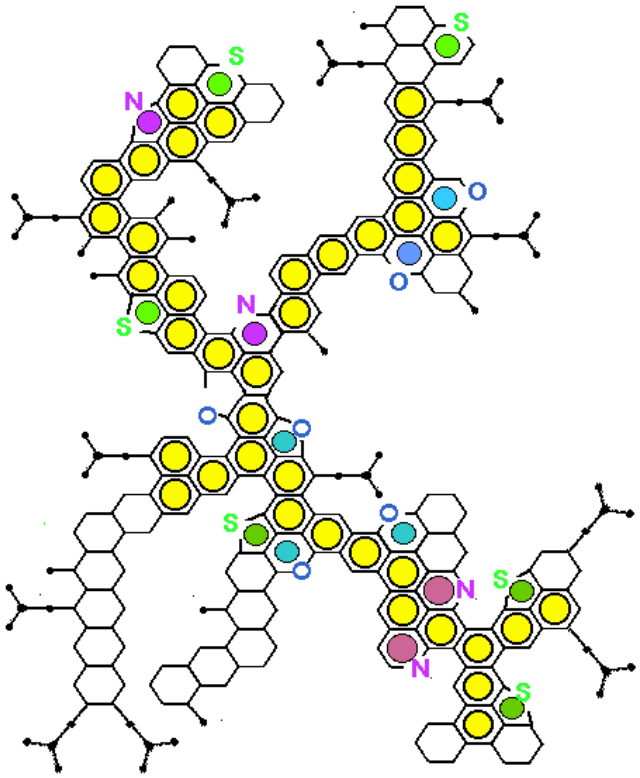

Fig 2 Molecular structure of asphaltene proposed for Maya crude (Mexico) (after Mansoori (1995) and ref. therein).

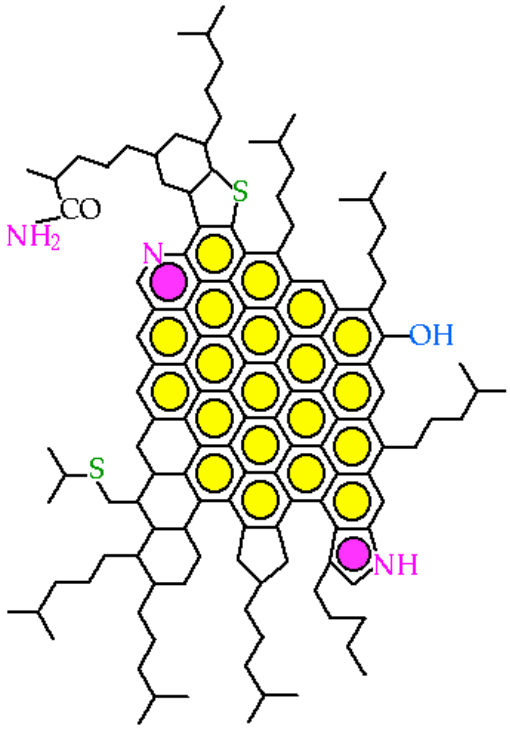

Fig 3 Molecular Structure of Asphaltene proposed for 510C Residue of Venezuelan Crude by Carbognani (1992)

The asphaltene fraction contains the largest percentage of heteroatoms (O, S, N) and organometallic constituents (Ni, V, Fe) in the crude oil. Therefore, several authors mentioned metalporphyrins, derived from chlorophylls and bacteriochlorophylls (Baker and Louda, 1986), as central chemical structure of asphaltene macromolecules (Premovic and Jovanovic, 1997; Marquez *et al.*, 1999; Groenzin and Mullins, 2001; Premovic *et al.*, 2002).

1.1.3 Size of asphaltene particles

The determination of asphaltene molecular mass is complicated by the tendency of asphaltene molecules to associate with each other and with other petroleum constituents, and reported molecular masses vary from 900 to 300 000 Da (Speight *et al.*, 1985), or 1000 to 200 000 Da (Mansoori, 1995). But it is generally concluded that asphaltene fractions from typical crude oils have a number average molecular weight of 1200-2700 Da and a molecular mass range of 1,000-10,000 Da or higher (Speight *et al.*, 1985; Acevedo *et al.*, 2005). Intermolecular association phenomena are primarily responsible for observed molecular weights up to and in excess of 100,000 Da (Speight *et al.*, 1985).

Asphaltene particles can assume various forms when mixed with other molecules depending on the relative sizes and polarities of the particles present (Yen and Chilingarian, 1994). In addition, they behave as lyophobic and steric, and they posses electrostatic and associative forces. Asphaltene molecules have a high degree of polynuclear aromaticity. It has been recognized that petroleum asphaltene may form micellar particles in aromatic and, or polar solvents such as toluene and methylnaphthalene (Yen and Chilingarian, 1994; Galtsev *et al.*, 1995; Sheu and Mullins, 1995). Asphaltene flocs (random aggregates) can form steric-colloids in the presence of excess amounts of resins and paraffinic hydrocarbons (Park and Mansoori, 1988; Priyanto *et al.*, 2001) as shown in Fig 4. Asphaltene molecules may have an

average molecular diameter around 5 N m. The size distribution of asphaltene micelles may have an average size around 25 N m, whereas micellar coacervates may have sizes >25 N m. Several experimental investigations have indicated that asphaltene micelles could be of spherical-like, cylindrical-like or disk-like form (Espinat and Ravey, 1993; Yen and Chilingarian, 1994). All these investigations are indicative of the fact that asphaltene particles may self-associate, but not flocculate, and form micelles in the presence of aromatic hydrocarbons (or other polar solvents) as shown in Fig 5.

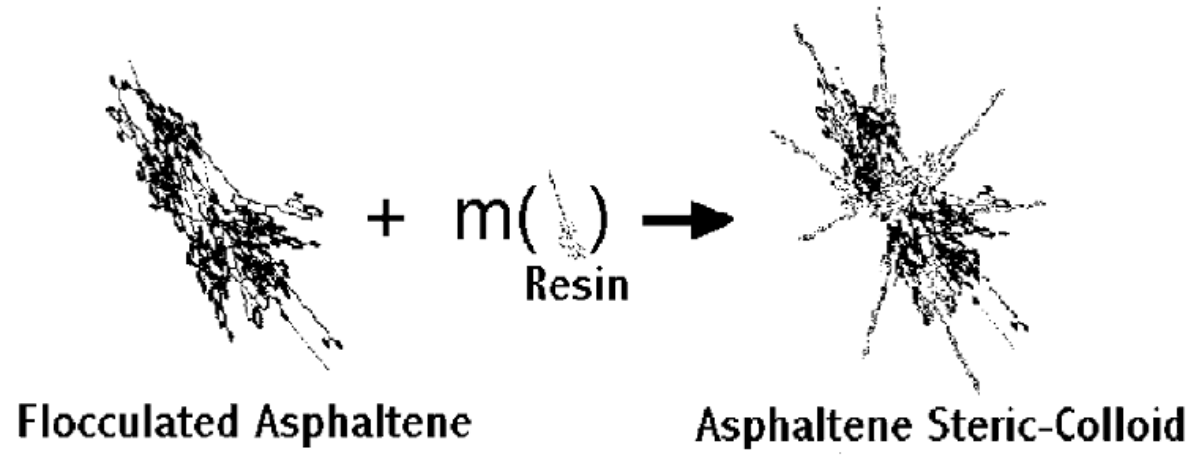

Fig 4 Steric-colloid formation of asphaltene flocs (random aggregates) in the presence of excess amounts of resins and paraffinic hydrocarbons (Priyanto *et al.*, 2001).

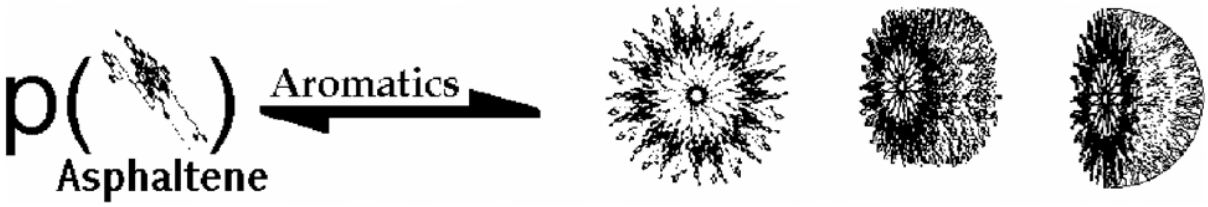

Fig 5 Micellization (self-association) of asphaltene due to increase in aromaticity (polarity) of its medium (Priyanto *et al.*, 2001).

1.2 Asphaltenes in industry

1.2.1 Asphaltene deposition and its problems

Heavy organics (asphaltene, resin, wax, and organometallic compounds) deposition is a common problem in all sections of the oil industry, including oil production, transportation, and processing (Sheu *et al.*, 1991; Mansoori, 1996; Escobedo and Mansoori, 1997; Mansoori, 1999). Deposition of these materials may cause a number of difficulties including wettability reversal, permeability reduction, increased pressure drop, well and pipeline plugging and finally production rate reduction (Park and Mansoori, 1988; Schantz and Elliot, 1994; Storm *et al.*, 1994; Mansoori, 1996; Escobedo *et al.*, 1997; Kocabas and Islam, 1998; Almehaideb, 2004). Asphaltenes have also been found to facilitate the formation of extremely stable water-in-crude oil emulsions, which increases production problems (Berridge *et al.*, 1968; Sheu and Shields, 1995; McLean and Kilpatrick, 1997).

Depositions of the heavy organics present in oil could happen due to various causes depending on their molecular nature. Paraffinic wax may be deposited due to lowering of the crude oil temperature and formation of crystalline solids (Afanasev *et al.*, 1993; Trindade *et al.*, 1996; Mansoori, 1999; Yang and Kilpatrick, 2005). More common is asphaltene deposition, which causes major difficulties in petroleum mixtures, such as petroleum reservoir fluids. Resins are not known to deposit on their own (Mansoori, 1996), but they deposit with asphaltenes as shown in Fig 4. The reasons for the asphaltene deposition can be cited to many factors including variations of temperature, pressure, composition due to mixing with gasolines, flow regime, and wall and electrokinetic effect (Mansoori, 1996, 1999).

1.2.2 Asphaltene deposition and its control

Asphaltenes may be destabilized in any area of the oil production facility from the near well bore area to the refinery feed stock. For that reason several studies have been carried out for the use of fouling of catalysts, coking, and promotion of emulsions during the crude oil processing (Andersen and Speight, 1999; Peramanu *et al.*, 1999; Wu *et al.*, 2000; Leon *et al.*, 2001; Monteagudo *et al.*, 2001; Alboudwarej *et al.*, 2002; Ostlund *et al.*, 2002; Pan *et al.*, 2002; Alboudwarej *et al.*, 2003; Parra-Barraza *et al.*, 2003; Spiecker *et al.*, 2003; Almehaideb, 2004; Hong and Watkinson, 2004; Hu *et al.*, 2004; Mousavi-Dehghani *et al.*, 2004; Oh *et al.*, 2004; Trejo *et al.*, 2004; Ibrahim and Idem, 2005; Juyal *et al.*, 2005; Stark and Asomaning, 2005). Flocculation and deposition of asphaltenes can be controlled using various production and chemical treatment techniques. Production techniques include for example reduction of shear, elimination of incompatible materials from asphaltic crude oil streams, minimization of pressure-drops in the production facility and minimization of mixing of lean feed stock liquids into asphaltic crude streams (Escobedo *et al.*, 1997; Mansoori, 1999). Chemical treatment techniques include the addition of dispersants, antifoulants, and aromatic solvents which may be used to control asphaltene deposition. Dispersants work by surrounding the asphaltene molecules similar to the natural resin materials. Aromatic solvents for asphaltene deposits need to have a high aromaticity to be effective, and antifoulants have proven effective in condensate stabilization units in gas plants (de Boer *et al.*, 1995; Peramanu *et al.*, 1999; Leon *et al.*, 2001; Ostlund *et al.*, 2002; Juyal *et al.*, 2005; Stark and Asomaning, 2005).

1.3 Asphaltenes in reservoir geochemistry

1.3.1 Asphaltenes in natural systems

Asphaltene precipitation in natural systems can induce the formation of tar mats along migration pathways or in petroleum reservoirs (Dahl and Speers, 1986; Wilhelms and Larter, 1994a, b; Dou *et al.*, 1998). As a consequence of the formation of tar mats in the "near well bore" region, feeding channels or along migration paths, these tar mats act as barrier in reservoir systems, resulting in reduced flow as the deposit thickness increases. Wilhelms and Larter (1994b) explained tar mat formation by asphaltene precipitation due to gas injection into a migrating or stationary petroleum charge. Additionally, precipitation controlling factors, such as pressure reduction during migration and influx of asphaltic-rich petroleum from the carrier, might have an impact as well (Wilhelms and Larter, 1994b; Larter and Aplin, 1995). A comparison study to identify petroleum formation characteristics from tar mats and oil asphaltenes from the Northern Viking Graben area in the Norwegian North Sea was recently published by Keym and Dieckmann (2006). The authors confirmed that generated pyrolysis products from tar mats are similar to those from oil asphaltenes in terms of bulk and resolved composition, illustrating their common origin. Processes related to the origin and occurrence of asphaltenes in the subsurface have been proposed by Wilhelms and Larter (1994a; 1994b). They suggest the existences of asphaltene precursors, so called asphaltene-precursor-entities (APE). According to these authors, asphaltene-molecules are kept in solution by steric stabilization and due to changes in solvent properties of the oil these APE´s start to aggregate and probably form lyophilic micelles.

The theory of hydrocarbon generation of kerogen thermal degradation was gradually developed in the 1960´s (Louis, 1964; Philppi, 1965; Albrecht and Ourission, 1969).

Concerning the origin of asphaltenes in petroleum and bitumen, it has been proposed that the major part of asphaltenes or asphaltene-precursor-entities are formed during the early stages of thermal maturation by the rupture of labile bonds in the kerogen structure and they are thought to act as intermediates in crude oil generation (Béhar *et al.*, 1984; Tannenbaum and Aizenshtat, 1985; Solli and Leplat, 1986). Pelet *et al*. (1986) proposed that asphaltenes are structural equivalents of kerogens, and that only their solubility allows them to migrate in petroleum. Thus, oil asphaltenes are considered to be reservoired fragments of the source rock kerogen (Pelet *et al.*, 1986). During thermal evolution asphaltenes undergo compositional changes, just as kerogens do (Durand and Monin, 1980; Béhar *et al.*, 1984; Castex, 1985; Pelet *et al.*, 1986).

1.3.2 The use of asphaltenes in exploration

Pyrolysis of asphaltenes isolated from crude oil yields an oil-like product that contains hydrocarbons. The distributions of these hydrocarbons have been reported to provide information on the source and maturity of the asphaltenes and therefore on the oils (or bitumens) that contain them (Rubinstein *et al.*, 1979; Béhar *et al.*, 1984; Jones and Douglas, 1987; Jones *et al.*, 1988). In the case of biodegraded oils, hydrocarbon distributions obtained from related oil asphaltene pyrolysates offer essential informations for oil/oil correlation (Rubinstein *et al.*, 1979; Béhar *et al.*, 1984; Magnier and Huc, 1995).

In the last few years asphaltenes have become of immense interest for exploration techniques, since it was reported that they possess structural features of the related source rock kerogens (Béhar *et al.*, 1984; Tannenbaum and Aizenshtat, 1985; Pelet *et al.*, 1986; Solli and Leplat, 1986; Sinninghe Damsté *et al.*, 1989; Tissot, 1989; Muscio *et al.*, 1991; di Primio *et al.*, 2000). This is because the use of asphaltenes from crude oils may help to overcome the lack

of source rock samples in basin analysis when reliable predictions for the generation of hydrocarbons are required. Potential source rocks are described in terms of quantity, quality and level of thermal maturity of organic matter (Peters, 1986; Bordenave *et al.*, 1993), but pertinent source rock information is frequently absent because exploratory drilling do not reach deeply buried source facies. Even if the source is reached samples are often inappropriate for reliable oil-source rock correlation due to low maturity or organic facies variation. Especially passive margins are amongst the most prospective areas for future hydrocarbon exploration and the assessment of their potential requires understanding the processes involved in continental break-up and margin development. This is for example the case where deep basinal pre-salt sediments with sustained source potential are occurring below salt structures and post-salt organic-rich sediments. The tracing of migration pathways and predicting oil-gas fractionations in pre-rift sediments is particularly difficult as calibration source facies are not available. The approach of using asphaltenes for source rock evaluation can be called "geochemical inversion" (Bissada *et al.*, 1993). The use of asphaltenes in inferring the source rock properties has already demonstrated in various publications in terms of chemical and physical properties (Kruge *et al.*, 1996; Werner *et al.*, 1996; Xiao *et al.*, 1998; Nali *et al.*, 2000; Odden *et al.*, 2002; Sun *et al.*, 2003). For example, Werner *et al.* (1996) published an approach of viscosity prediction of petroleum fluids during expulsion based on an investigation of phase behaviour and precipitation of asphaltenes in different mixtures. Xiao *et al.* (1998) studied asphaltenes from humic coal extracts and crude oils from China in terms of microscopic fluorescence and reflectance. They documented that asphaltene reflectance is hinged on source rock type, and varies systematically with the maturity of related oils and coal extracts. Nali *et al.* (2000) proposed the Tmax of asphaltenes measured by Rock-Eval pyrolysis as a parameter for oil maturity assessment. Their experimental results on many samples from different areas and containing different organic matter types,

demonstrated that that kerogen Tmax values are close to those of related source rock asphaltenes. The use of isotopic composition of oil asphaltenes for oil/source correlation was shown by Odden *et al.* (2002). They investigated the isotopic compositions of oil asphaltenes from different oil fields in the Northern Sea, and showed that the isotope composition varies with terrestrially influenced facies.

Pyrolysis-gas chromatography (Py-GC) of asphaltenes isolated from crude oils or rock extracts have been the subject of several previous investigations, which provided informations for source rock correlation (Béhar *et al.*, 1984; Béhar and Pelet, 1985; Cassani and Eglinton, 1986; Solli and Leplat, 1986; Jones *et al.*, 1988; Horsfield, 1989; Horsfield *et al.*, 1991; Muscio *et al.*, 1991; Horsfield *et al.*, 1993; Horsfield *et al.*, 1994). Examples for the use of py-GC include analysis of biomarker skeletons in asphaltenes for correlating crude oils and likely sources (Béhar and Pelet, 1985; Cassani and Eglinton, 1986; Jones *et al.*, 1988; Horsfield *et al.*, 1991), asphaltene physical and chemical properties for defining permeability barriers in reservoirs (Wilhelms and Larter, 1994a), as well as for the prediction of petroleum gas-oil ratios (Horsfield *et al.*, 1991; Muscio *et al.*, 1991; Horsfield *et al.*, 1993). For example Muscio *et al.* (1991) and Horsfield *et al.* (1993) have shown that the chain length distribution and bulk GOR (gas to oil ratio) of source rock asphaltene pyrolysates respectively is similar to the kerogen of the same source rock within the oil window maturity range.

In addition hydrocarbon prediction using bulk kinetic parameters derived from asphaltenes have been established (di Primio *et al.*, 2000; Dieckmann *et al.*, 2002). Dieckmann *et al.* (2002) applied bulk kinetic concepts on oils formed from marine carbonate source rocks and illustrated that due to the lean organic content of the source rock, asphaltenes were degraded in part, indicating geological expulsion temperature. Such stabilisation was supported by previous results from Khavari-Khorasani *et al.* (1998) who studied kinetics on asphaltenes which precipitated along a migration route and which was originally generated in carbonate

source rocks as well. More recently Skeie *et al.* (2004) have applied asphaltene kinetics precipitated from type II marine oil on an exploration area, in order to represent the oil generating facies of the heterogeneous Draupne Formation. Here the kinetics of petroleum asphaltenes were similar to the kerogen of the organic rich and marine Draupne Facies, while the mixed type II/III facies, which still has an oil prone character, was proposed to be unimportant for oil accumulation. Keym *et al.* (2006) have also shown for the Draupne Formation that kinetic studies on asphaltenes can help to overcome uncertainties associated with petroleum formation from heterogeneous source rocks. The majority of the studies however focused on type II marine settings and were limited to petroleum formed from the Draupne Formation, the Kimmeridge Clay in the North Sea or the Duvernay Formation in Canada. Less has been reported about the application of type II-S asphaltenes in a similar context. Di Primio *et al.* (2000) have published that the thermal degradation of asphaltenes related to type II-S kerogen occurs at earlier stage than the degradation of related sulphur rich kerogens. They mentioned that oil asphaltenes represent the labile fragments of the related source rocks of the same maturity sequence.

2 Goals and Approach

The aim of the present thesis is to provide new insights on structural moieties of asphaltenes and related bulk kinetic parameters of asphaltene decomposition for determining the timing of oil generation for geological predictions. The goal of the current study was to compare asphaltenes from reservoir oils with those of related source rock bitumens and related kerogens. For the present study we focussed on samples from a type II-S system in Southern Italy, a type II system in Canada, and a type II/III system in Nigeria, in order to compare hydrocarbon generation characteristics of asphaltenes from different depositional environments.

The objectives for the present study can be summarized as followed:

- To study facies and maturity control on asphaltenes
- To investigate the effect of long-time-storing on asphaltene composition
- To compare asphaltenes from reservoir oils with those of related source rock bitumens and kerogens in terms of bulk kinetic parameters and product compositional features, or gas generation characteristics for the different petroleum systems
- To compare petroleum and gas generation characteristics of reservoir asphaltenes, in terms of primary and secondary gas generation, as well as the compositional kinetic prediction of determining the actual products that will be released from the asphaltene under specific geologic conditions

Because it is known that asphaltene from type II-S sequence differs from asphaltenes from type II organic matter (di Primio *et al.*, 2000; Dieckmann *et al.*, 2002), oil asphaltenes, source rock asphaltenes and related kerogens from a Triassic source rock in Italy and from the Duvernay Formation were compared in detail. Additionally, oils and related asphaltenes from Nigeria onshore, sourced from type II/III organic matter, were also investigated in terms of

structural moieties. As well compositional kinetic analysis calculated from MSSV experiments was performed to compare MSSV products from reservoir asphaltenes with those of source rock kerogens in terms of structural moieties, like aromaticity and organic sulphur content, generation of primary and secondary gas as well as calculated compositional kinetic predictions, and finally differences in the isotopic composition of asphaltene and kerogen products.

In the **first part** (chapter 5) of this work, source rock samples and crude oils from South-Italy, the Duvernay Formation and Nigeria onshore are presented and discussed for their basic chemical and physical composition. The source rock samples were investigated using Rock-Eval to determine their source rock potential. The crude oils were studied for chemical composition, light-hydrocarbons, and biomarker distributions in terms of oil-source correlation using MPLC, GC-MS and Tvap-GC.

The **second part** (chapter 6) provides a comparison investigation of oil asphaltenes precipitated with different *n*-alkane solvents in terms of structural differences, bulk kinetics and consequences for geological predictions. For this study the topics are:

- To investigate reservoir asphaltenes isolated with different solvents in terms of structural moieties for oil-source correlation as well as geological predictions for hydrocarbon generation based on asphaltene kinetics
- To investigate temperature influence during precipitation on structural moieties, like aromaticity, of reservoir asphaltenes from Nigeria

In the **third part** (chapter 7) of this thesis, a detailed investigation of asphaltenes from reservoir oils, source rock asphaltenes, and related source rock kerogens from a sulphur-rich sequence situated in Southern Italy was performed. Non-isothermal open system pyrolysis

experiments were performed on immature source rocks as well as source rock asphaltene and asphaltenes precipitated from crude oils. Kinetic parameters calculated on immature source rock kerogens, source rock asphaltenes, as well as petroleum asphaltenes are discussed in terms of structural moieties and bulk kinetics. Micro-scale sealed vessel pyrolysis (MSSV) experiments were applied on reservoir asphaltenes in order to compare their petroleum and gas generation characteristics, in terms of primary and secondary gas generation, as well as the compositional kinetic prediction of determining the actual products that will be released from the asphaltene under specific geologic conditions. The main goals can be summarized as followed:

- To compare source rocks kerogens and relevant source rock asphaltenes, as well oil asphaltenes in terms of bulk kinetics and geological predictions
- To compare asphaltenes isolated from crude oils with those of source rock bitumen and related source rock kerogens in terms of product compositional features, such as aromaticity, paraffinicity, organic sulphur content, or gas generation characteristics
- To discuss kinetic parameters calculated on kerogens, source rock asphaltenes, and petroleum asphaltenes in terms of structural moieties
- To study the petroleum and gas generation characteristics from oil asphaltenes in terms of primary and secondary gas generation, as well as the compositional kinetic prediction of the molecular composition of the C_{6+} hydrocarbon fraction
- To compare MSSV products from reservoir asphaltenes in terms of compositional differences with those of immature source rock kerogen previous investigated
- To study differences in the isotopic composition of asphaltene and kerogen products

The **fourth part** of the present thesis (chapter 8) provides a comparison study for asphaltene kinetics and asphaltene product compositional characterization from a type II sequence from

the Duvernay Formation (WCSB). Here, the main topics for the Duvernay Formation (WCSB) in chapter 8 are as followed:

- To investigate reservoir asphaltenes in terms of bulk kinetics for oil-source correlation as well as geological predictions for hydrocarbon generation based on asphaltene kinetics
- To study kerogens, source rocks asphaltenes and relevant oil asphaltenes over a very wide maturity range in terms of structural moieties for compositional characteristics such as aromaticity, paraffinicity and the amount of organic sulphur
- To compare MSSV products from reservoir asphaltenes in terms of compositional differences with those of immature source rock kerogen previous investigated

Finally, the **fifth part** (chapter 9) provides a comparison study for asphaltene kinetics and asphaltene product compositional characterization from a type II/III deltaic sequence Nigeria onshore. Here, the topics are:

- To investigate reservoir asphaltenes in terms of structural moieties for oil-source correlation as well as geological predictions for hydrocarbon generation based on asphaltene kinetics
- To investigate primary and secondary gas generation, as well as the compositional kinetic prediction of the molecular composition of the C_{6+} hydrocarbon fraction resulted from asphaltene decomposition using MSSV.

3 Geological Background and Sampling Details

In order to study structural and compositional differences between asphaltenes and kerogens, samples from Southern Italy, Western Canada, and Nigeria onshore were investigated. We studied samples from three different types of petroleum systems, as source rock – asphaltene correlation may vary for different types of source rock settings. The samples from Southern Italy are sourced from a carbonate sequence that is rich in organic sulphur (type II-S). Source rocks and crude oils from the Duvernay Petroleum System (Canada) are originated from a pure marine environment (type II). The samples from Nigeria onshore are related to a deltaic sequence with characteristic terrestrial organic input (type II/III). For reasons of confidentiality detailed information to location or geological setting of samples from Southern Italy or Nigeria cannot be given in this study.

3.1 Southern Italy

3.1.1 Petroleum Geology

Hydrocarbon accumulations in Italy are of economic interest since first geological studies in the 50's suggested the areas of the Po Basin, Southern Alps, Northern Apennines and the Southern Italian region, mainly Sicily on- and offshore as favorable for hydrocarbon exploration and exploitation (Facca *et al.*, 1951; Beneo, 1952; Hoover, 1953; Reeves, 1953; Beneo, 1955, 1956; Colombo and Sironi, 1959; Kafka and Kirkbride, 1959).

For the present study we investigated samples from an oil field of Southern Italy located in the central western Mediterranean, which is a segment of the Alpine collisional belt developing along the Africa-Europe plate boundary (Catalano *et al.*, 1996; Catalano *et al.*, 2002). It links the African Maghrebides with Calabria and the Apennines, and extends from the Corsica Sardinia block across Sicily to the Pelagian Platform. Fig 6 shows the sketched

map with main tectonic features and basins of the area. The known stratigraphy and facies domains of this area are mainly based on seismic profiles calibrated by well logs and dredge haults.

The western and central Sicily region is characterized as a thin skinned imbricate wedge of Triassic to Lower Pleistocene carbonate and siliclastic rocks (Giunta, 1993; Catalano *et al.*, 1994; Catalano *et al.*, 1996; Butler *et al.*, 1997). The deposition of carbonate sediments alternating pelagic, platform and transitional facies lasted until the Middle Miocene. During the Messinian the area of study was part of a major, regionally widespread evaporite basin (Novelli and Mattavelli, 1988; Mattavelli and Novelli, 1990a; Ruvo *et al.*, 2003). Organic-rich carbonate-evaporitic and carbonate-siliceous rocks are worldwide the sources of large quantities of heavy oil deposits (Powell, 1984; Zumberge, 1984; Tannenbaum and Aizenshtat, 1985; Mattavelli *et al.*, 1993; Khavari-Khorasani *et al.*, 1998; Riboulleau *et al.*, 2000; Hetenyi *et al.*, 2002; Hetenyi *et al.*, 2004).

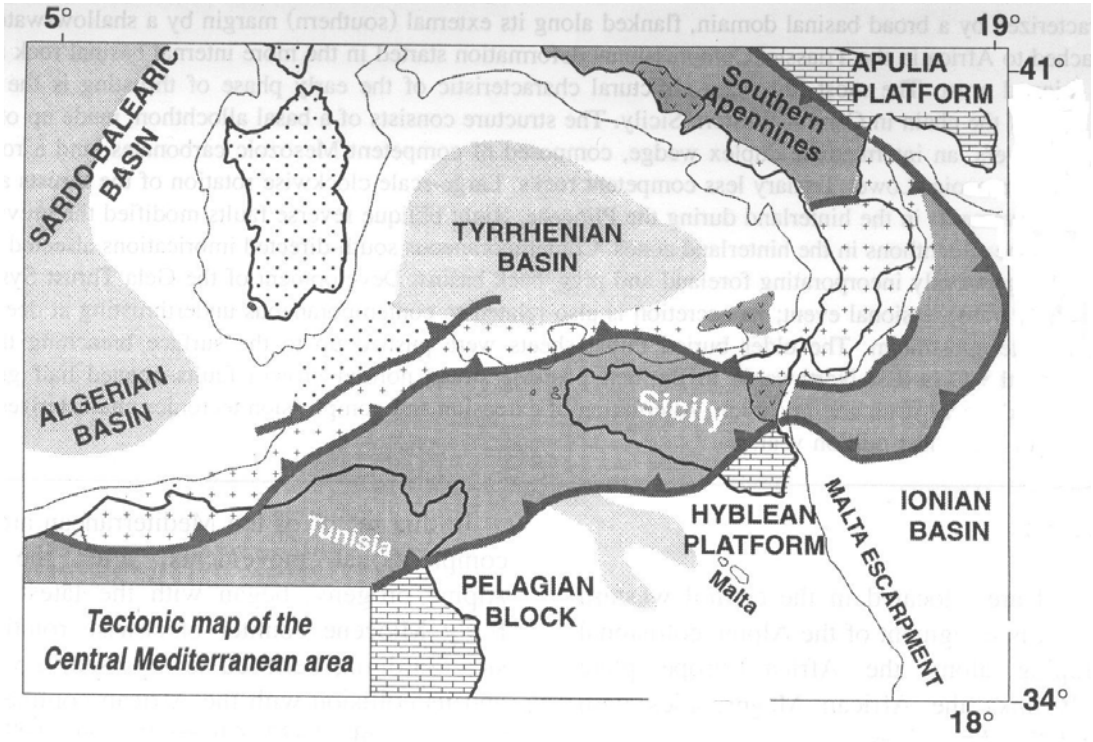

Fig 6 Scheme of the studied area with main tectonic structures (after Catalano *et al.* 1996*)*.

The most crude oil accumulations in Southern Italy are sourced from Upper Triassic formations (Stefani and Burchell, 1993). The Norian and Rhaetian of Southern Italy was characterized by the occurrence of carbonate platforms, which in turns might have been bridged with depositional platforms in Northern Italy by the Abruzzo Platform, and later on separated by hemi pelagic troughs (di Stefano, 1990). In these troughs deep-sea pelagic facies were deposited, with the uppermost Triassic often represented by radiolarites. The Triassic carbonate platform successions of Southern Italy are normally organic lean and dominated by shallowing up peritidal cycles (Stefani and Burchell, 1993). During the Late Triassic times important source facies were deposited in form of organic-rich "lenses" in different portions of the platform, and show often varying facies types where clays and carbonates alternate at different scales (Brosse *et al.*, 1989; Brosse *et al.*, 1990; Stefani and Burchell, 1993). These depositional variations result in different oil types, for example mainly shaly or carbonate sourced (Ruvo *et al.*, 2003), and oils sourced from facies of variable hypersaline conditions (Stefani and Burchell, 1993; Peterson, 1994). The oils generated from these facies intervals contain significant amounts of sulphur and are generally thought to be thermally immature (Novelli *et al.*, 1988; Moretti *et al.*, 1990; di Primio and Horsfield, 1996; Holton, 1999). It is generally assumed that high viscosity, heavy oils form at low levels of thermal maturity (Tissot *et al.*, 1987; Baskin and Peters, 1992). However, the maturity of these organic-rich rocks varies a great deal from area to area and is related to the geodynamic evolutions during Tertiary tectonics (Novelli *et al.*, 1988; Lentini *et al.*, 1996). Source rocks often reached maturity only when buried under thick fore deep sediments and when involved in compactional tectonics. The tectonic evolution of this region has controlled the development of two main groups of structural traps suitable for hydrocarbon accumulation (Monaco *et al.*, 2000; Tortorici *et al.*, 2001). The first group is associated with Pleistocene fold-and-thrust systems, represented by large anticlines and duplexes. The second group has developed

during the last stage of continental collision in the Pleistocene and is represented by strike-slip related structures.

Brosse *et al.* (1990) suggested two different migration episodes, with a more "shaly oil" migration during Jurassic times, and a Pleistocene migration of "carbonate oil", resulting in different oil types in different structural traps. The following works explained local different oil types associated with different traps due to remobilization combined with localized faulting processes (Ruvo *et al.*, 2003).

3.1.2 Sample description

Source rocks from South Italy studied for this project consist of 16 samples from cores and 5 samples from cuttings. The oils from South Italy can be described as heavy black oils with API gravities ranging from 2° to 33° API. Based on previous information provided by ENI, the sample set comprises two biodegraded oils with 2.62° and 9.9° API. Furthermore, in order to study the storage effect on reservoir asphaltenes, two oils have been supplied from a fresh sampling and from long-time stored samples to provide a sample set in order to investigate the effect of storage on structural moieties in asphaltenes. Table 1 shows the source rock and crude oil samples with information to TOC and API gravity.

Source rocks			Crude oils			
sample	TOC (%)	note	sample	well	° API grav.	note
G000642	4,39	core sample	G000393	A	9,9	Biodegraded
G000645	3,46	core sample	G000394	A	2,62	Biodegraded
G000646	0,41	core sample	G000395	A	10,4	Low Maturity
G000647	2,93	core sample	G000396	A	11,5	Low Maturity
G000648	1,37	core sample	G000397	A	9	Low Maturity
G000649	6,76	core sample	G000398	B	19,35	Intermediate Maturity
G000650	1,29	core sample	G000399	B	19,35	Intermediate Maturity
G000651	2,34	core sample	G000400	B	19,35	Intermediate Maturity
G000652	11,80	core sample	G000401	C	33,5	High maturity
G000653	2,89	core sample	G000402	A	8,5	Low Maturity
G000654	8,76	core sample	G000403	A	8,5	long-time stored
G000655	4,03	core sample	G000404	A	10,4	long-time stored
G000656	7,05	core sample				
G000657	0,75	core sample				
G000660	0,67	core sample				
G000661	6,65	core sample				

Table 1 Samples with information to TOC or API gravity.

3.2 The Duvernay Petroleum System (WCSB)

3.2.1 Petroleum Geology

The Duvernay Formation in central Alberta/Canada represents one of the most important sources for petroleum in the Western Canada Sedimentary Basin. These reservoirs are mainly situated along the Rimbey-Meadowbrook reef belonging to the Late Devonian Frasnian Woodbend Group. The deposition of the Duvernay Formation occurred as the result of subsidence during the Laramide orogeny (Deroo *et al.*, 1977; Creaney and Allan, 1990).

The Formation comprises two principal lithofacies, (1) a lime mudstone with varying degrees of bioturbation indicating relatively oxygenated conditions and (2) an organic-rich laminated mudstones deposited in deep water euxinic conditions (Creaney and Allan, 1990; Requejo *et al.*, 1992; Requejo *et al.*, 1994; Chow *et al.*, 1995; Li *et al.*, 1997; Dieckmann, 1998; Li *et al.*, 1998). Organic matter has thought to be preserved by bottom-water anoxia and is associated with clay minerals (Dieckmann, 1998). For palaeoenvironment characterization the probable presence of green sulphur bacteria and a water column rich in hydrogen sulphide is indicated by the specific geomarker 1,2,3,4-tetramethylbenzene (TMB), which can be found in natural products as well as in pyrolysates (Hartgers *et al.*, 1994b; Clegg *et al.*, 1997). These green sulphur bacteria (*Chlorobiacea*) are known to reproduce only in sulphate and hydrogen sulphide-rich water bodies (Abella *et al.*, 1980). Their occurrence is restricted to Palaeozoic source rocks and is known to be maturity as well as facies dependent. Two major facies have been recognized for the Duvernay Formation, as a result of varying depth of water during its deposition (Chow *et al.*, 1995). In the East Shale Basin (Fig 7) the Duvernay Formation overlies platform carbonates of the Cooking Lake Formation with minor discontinuity and surrounded by lower Leduc Formation reefs. In the West Shale Basin, the Duvernay Formation conformably overlies rocks of similar lithology, called the Majeau Lake Member, which predates reef growth (Creaney and Allan, 1990).

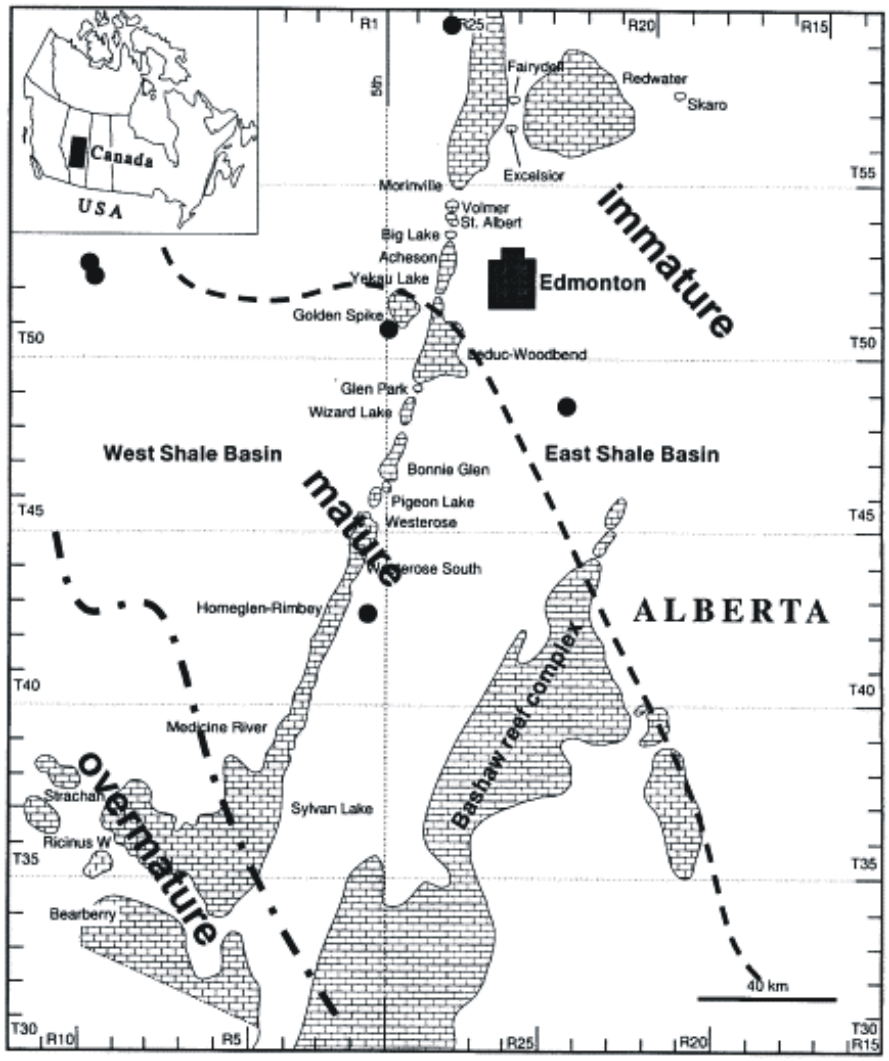

Fig 7 Study area and sampled wells in the Alberta Basin (modified after Dieckmann *et al. (*2004*)*; Li *et al.* (1998). The regional maturity trend is based on source rock screening by Rock-Eval and TOC (after Stoakes and Creaney (1984)).

The Duvernay Formation occurs widely throughout Alberta with increasing maturity going from the north-east to the south-west. Large areas of the Duvernay Formation are oil-prone, but, light oils and gas were also generated at high maturity. Crude oil along the Rimbey-Meadowbrook reef is found in up-dip reservoirs (e.g. Acheson, Big Lake and St. Albert); whereas gas is generally present in down-dip reservoirs like, for example, Homeglen-Rimbey and Bonnie Glen (Fig 8). This pattern and also the fact, that most down-dip reservoirs are filled to their spill points led to the Gussow model of differential entrapment (Gussow, 1968).

Later on Stoakes and Creaney (1984; 1985) and Li *et al.* (1998) established secondary petroleum migration models along the Rimbey-Meadowbrook reef.

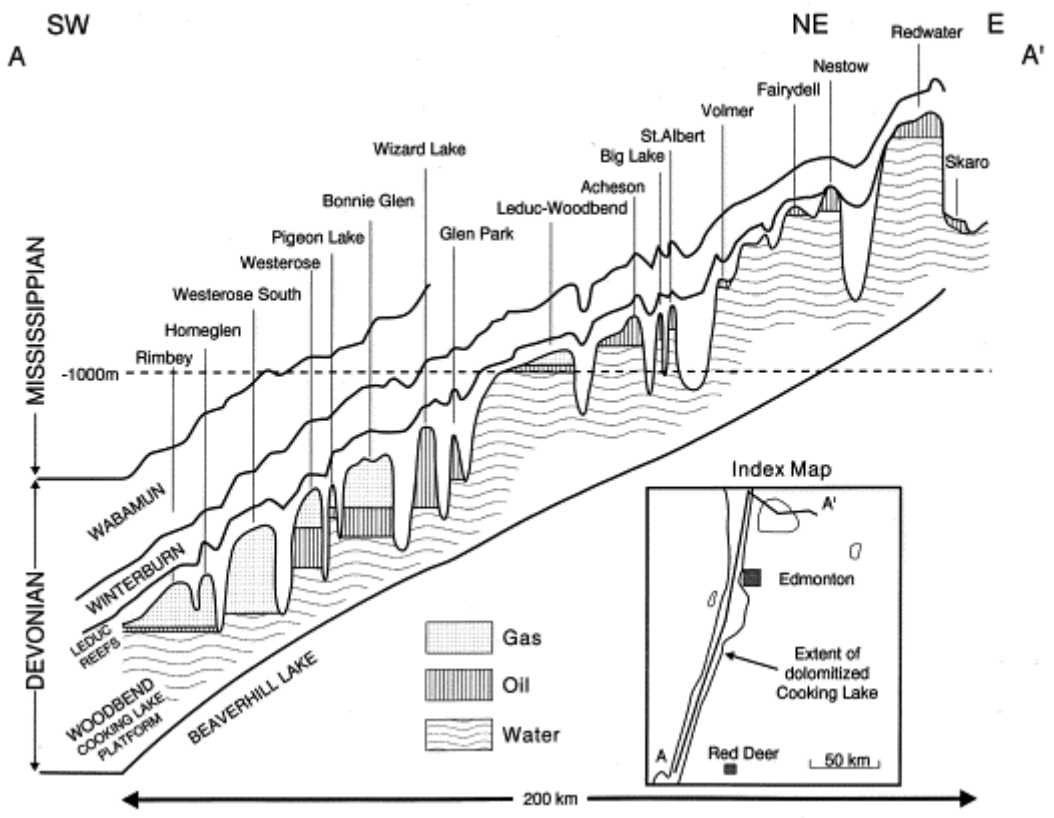

Fig 8 Geological profile through the Rimbey-Meadowbrook reef-system showing the distribution of oil and gas reservoirs (after Stoakes and Creaney (1985)).

3.2.2 Sample description

The sample set of the Duvernay Formation in central Alberta/Canada comprises 33 core samples from 13 different wells containing variations in facies types, and 8 crude oils with API gravities from 36° to 52°. Core samples are from depth between 1144 m and 2976 m and cover a full maturity range from immature to overmature. Table 2 shows the source rock and crude oil samples with information to location, depth and API gravity.

	Source rocks		
sample	**well**	**depht (m)**	**TOC (%)**
G000541	Redwater	1144,3	3,05
G000542	Redwater	1147,3	5,36
G000545	Redwater	1153,9	9,33
G000546	Redwater	1157,2	4,69
G000548	Tomahawk	2335,3	5,72
G000549	Tomahawk	2335,8	6,53
G000550	Tomahawk	2336,2	9,62
G000553	Tomahawk	2338,8	9,57
G000559	Leduc	1783,5	0,61
G000560	Norbuck	2640,6	0,74
G000562	Norbuck	2648,3	4,36
G000564	Forgotsen Burk	1934,2	9,71
G000570	Forgotsen Burk	1944,8	10,30
G000575	Imperial Armena 3	1575,4	1,94
G000579	Can Gulf Dom Red.	1146,7	14,80
G000581	Can Gulf Dom Red.	1153,2	3,25
G000583	Can Gulf Dom Red.	1155,8	7,60
G000586	Imperial Kingman	1404,2	2,37
G000587	Imperial Kingman	1404,5	3,21
G000592	Imperial Kingman	1406,7	3,37
G000593	Imperial Kingman	1416,9	1,78
G000596	Ferrybank	2243,3	5,03
G000598	Ferrybank	2245,3	0,73
G000600	Ferrybank	2248,6	4,04
G000601	Imperial Cynthia	2971,5	1,48
G000602	Imperial Cynthia	2971,9	1,28
G000603	Imperial Cynthia	2973,7	4,19
G000607	Imperial Cynthia	2976,1	1,90
G000610	Sarcee et al Pibroc	1395,7	9,37
G000615	Sarcee et al Pibroc	1402,9	8,47
G000631	Banff Imperial	1677,6	5,54

	Crude oils			
sample	**well**	**depht (m)**	**° API grav.**	**note**
G000405	Redwater	943 - 999	36	black oil
G000406	Leduc Woodbend	1623 - 1631	38	black oil
G000407	Homeglen Rimbey	2410 - 2411	44	black oil
G000408	Leduc Woodbend	1522 - 1548	37	black oil
G000409	Judy Creek	2575 - 2577	39,5	black oil
G000410	West Pembina	3069	39,37	light oil
G000411	West Pembina	3753 - 3761	52,36	light oil
G000412	West Pembina	3364 - 3380	47,1	light oil

Table 2 Duvernay samples with information to location, depth and TOC or API gravity.

3.3 Nigeria onshore

3.3.1 Petroleum Geology

The Niger Delta, which builds out into the Gulf of Guinea on the Atlantic coast of West Africa, is one of the largest modern delta-systems on earth. The delta is situated at the seaward end of the Benue Trough, which consists of Cretaceous sediments of Albian to Maastrichian age (Haack *et al.*, 2000). Following the opening of the Equatorial Atlantic Ocean in the late Early Cretaceous (Benkhelil, 1989; Mulaski *et al.*, 1995), a delta had built out over the continental margin (Damuth, 1994). Today, the Niger Delta Basin is one of the most prolific deltaic hydrocarbon provinces in the world. Fig 9 shows the schematic map with main depositional belts of the Niger Delta.

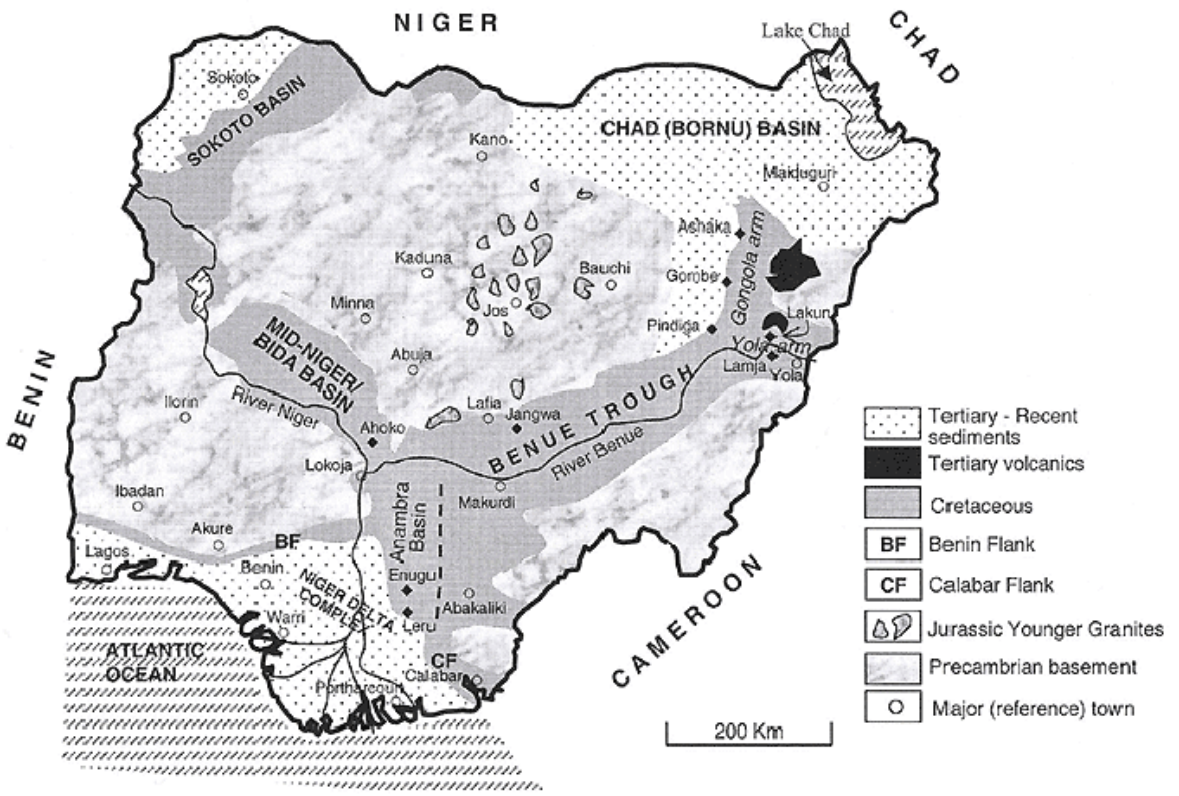

Fig 9 Schematic map of the Niger Delta showing the distribution of depositional and structural belts (after Wehner (2005)).

Oil exploration in Nigeria was started in 1951 and resulted in commercial production since 1956 (Haack *et al.*, 2000). The principal source for oil and gas in the Niger Delta are type II, II-III and type III kerogens (Haack *et al.*, 2000). Deposits formed in marine deltaic environments are predominantly derived from allochthonous material (Coleman, 1988; Galloway and Hobday, 1996). Continental-derived materials such as spores/pollen, terrestrial organic matter (peat, coal, plant debris) and minerals are transported to the ocean via rivers and/or the atmosphere. Thus, continental-derived material is generally abundant in deltaic deposits. About 55% of terrigenous carbon is particulate, and is thought to be refractory compared to autochthonous carbon produced by phytoplankton. Therefore, particulate carbon has the potential to accumulate in marine and estuarine sediments, and deltaic and shelf systems. However, commercial oil deposits derived from type III organic matter have been identified in a number of basins worldwide (Durand and Paratte, 1983; Bertrand *et al.*, 1986; Mukhopadhyay *et al.*, 1989; Littke *et al.*, 1990; Boreham and Powell, 1991; Clayton *et al.*, 1991; Powell *et al.*, 1991; Powell and Boreham, 1994; Thompson *et al.*, 1994; Clayton, 1998; Boreham *et al.*, 1999; Kotarba *et al.*, 2002).

The stratigraphic sequence of the Niger delta consists of mainly three thick rock units, which are from shallowest to the deepest 1) the Benin Formation composed of sandstone in a fluvial and coastal environment, 2) the Agbada Formation, which is interbedded sandstones and shales deposited in a transitional to marine paralic environment, and finally 3) the Akata Formation with massive marine shales Fig 10. The organic matter of both, the Akata and the Agbada Formations is geochemically very similar (Ekweozor and Daukoru, 1994).

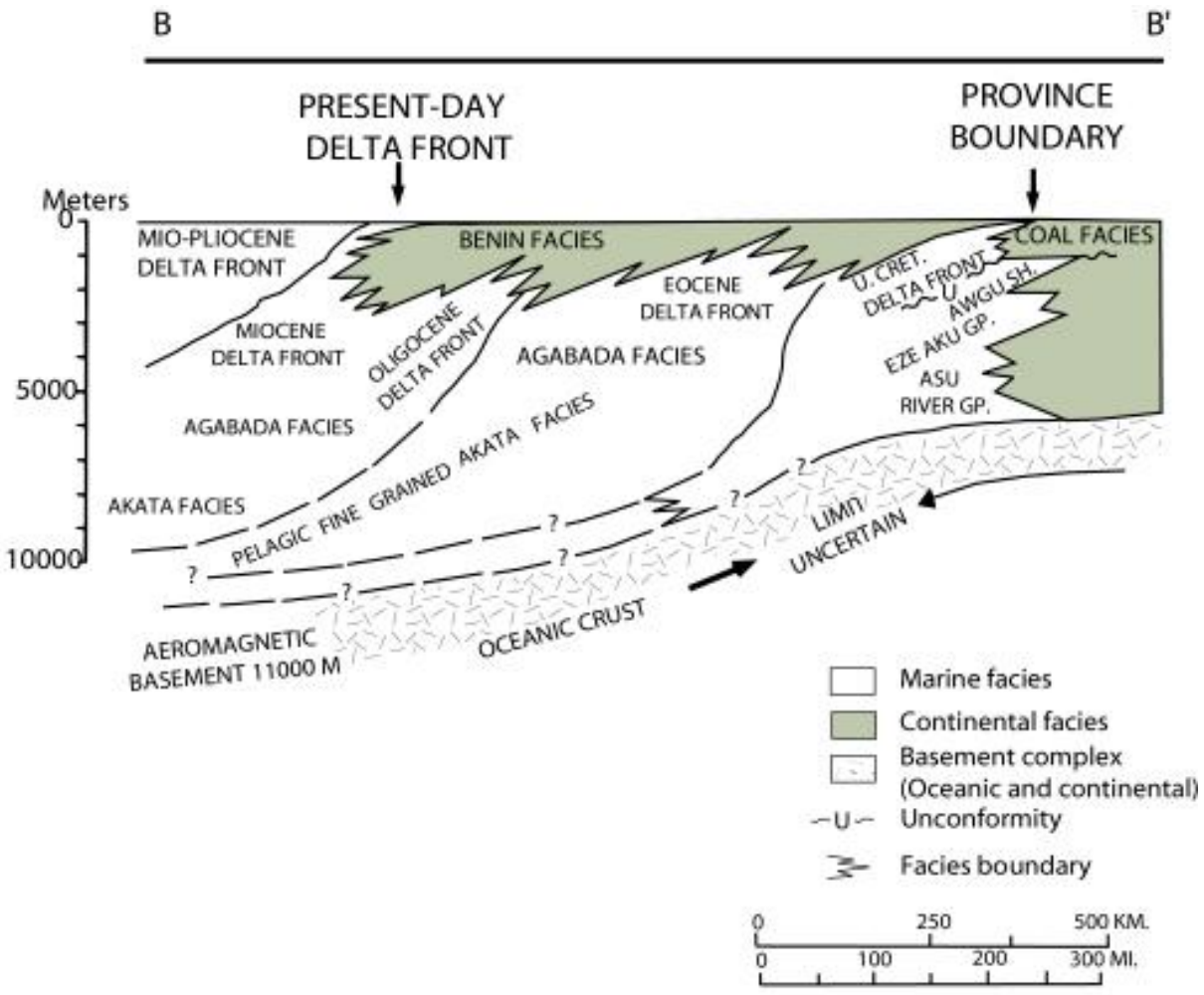

Fig 10 Averaged cross section through the Niger delta from offshore region (B) to province boundary in the onshore region (B´) (Tuttle *et al.*, 1999).

It is generally assumed that oil and gas in the Niger Delta is mainly sourced from terrestrial and nearshore marine palaeoenvironments. The geochemistry of the sedimentary organic matter, as well the crude oils, has been studied in detail by previous works (Evamy *et al.*, 1978; Ekweozor *et al.*, 1979, 1981; Udo and Ekweozor, 1990; Ekweozor and Daukoru, 1994; Ukpabio *et al.*, 1994; Nwachukwu *et al.*, 1995; Thomas, 1995; Mosto Onuoha and Ekine, 1999; Tuttle *et al.*, 1999; Haack *et al.*, 2000; Eneogwe and Ekundayo, 2003; Eneogwe, 2004; Obaje *et al.*, 2004).

3.3.2 Sample description

Crude oils from Nigeria were provided by Shell. The Nigerian samples set consist of 10 crude oils with API gravities from 21° - 41°, which represent a biodegradation sequence. Table 3 shows crude oil samples with information to API gravity and biodegradation.

Crude oils			
sample	**well**	**° API grav.**	**note**
G000502	A	24,5	biodegraded
G000503	A	22,5	biodegraded
G000504	A	39,9	
G000505	A	37,6	
G000506	A	21,1	biodegraded
G000507	A	30,6	biodegraded
G000508	A	35,5	
G000509	A	34,2	
G000510	A	37,1	
G000511	A	41	

Table 3 Nigerian samples with information to API gravity.

4 Methodology

4.1 Sample preparation

4.1.1 Soxhlet extraction

Powdered source rocks were extracted for 24h by a Soxhlet extractor to yield the source rock bitumen. Soxhlet extraction, invented for the extraction of lipids from a solid material (von Soxhlet, 1879) is usually required when the desired extractable compounds have only a limited solubility in a solvent. A schematic representation of a Soxhlet extractor is shown in Fig 11.

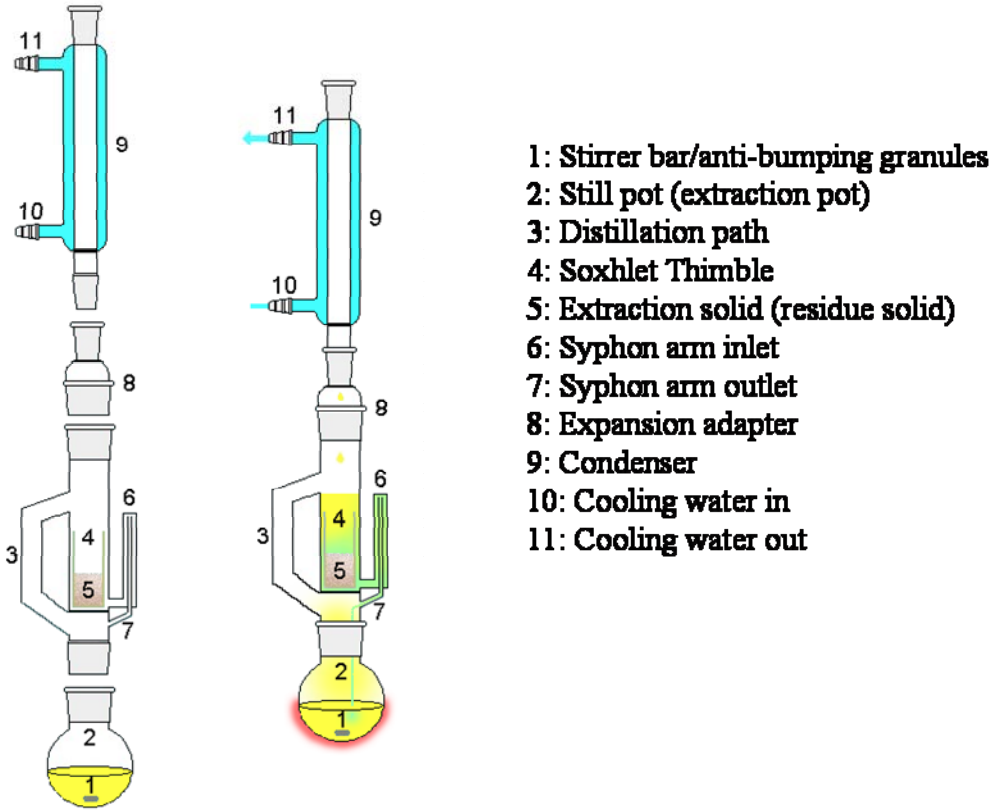

Fig 11 A schematic representation of a Soxhlet extractor (Wikimedia Foundation, 2006)

For the present study 25 g of powdered source rock were filled inside a solvent pre-cleaned extraction thimble made from filter paper, which was placed into the main chamber of the Soxhlet extractor. The extraction pot was filled with 150 ml of solvent, a mixture of

dichloromethane and ethanol in ratio 99:1, and the solvent was heated to reflux. The solvent vapour travelled up a distillation arm, and flooded into the chamber housing the thimble of source rock powder. The condenser ensured that any solvent vapour cooled and dropped back down into the chamber housing, where the source rock bitumen dissolved in the solvent mixture. When the Soxhlet chamber was filled up with solvent, the chamber was automatically emptied by a siphon side arm, with the solvent and dissolved bitumen running back down to the distillation flask. This cycle was allowed to repeat over 24 hours.

After extraction the solvent was removed by turbo vaporization, and source rock bitumen was dried under nitrogen gas.

4.1.2 Asphaltene precipitation

4.1.2.1 Italian and Duvernay samples

Several methods have been proposed for asphaltene separation prior to characterization studies, and each of these methods may suffer from some deficiency which renders it unsuitable for universal application. Asphaltene properties vary with the separation method and with individual techniques, like ageing time, solvent/crude oil ratio, solvent type, oil type and temperature and pressure influence (Ignasiak *et al.*, 1977; Rubinstein *et al.*, 1979; Jones *et al.*, 1988; Myhr *et al.*, 1990; Gürgey, 1998; Agrawala and Yarranton, 2001; Hu and Guo, 2001; Alboudwarej *et al.*, 2002; Parra-Barraza *et al.*, 2003). Most common is the isolation of asphaltenes by following the IP143, NFT60115 or ASTM D3279 methods, which uses *n*-heptane for solvent precipitation. Additionally, the method ASTM D2007-80 is used for *n*-pentane insoluble asphaltenes. A comparison study on the bulk chemical composition of asphaltenes isolated with different *n*-alkane solvents is presented in chapter 6.

Asphaltenes isolated with different *n*-alkanes solvents show minor differences in terms of aromaticity, distribution of organic sulphur compounds, GOR´s, and chemical kinetics and progressive transformation of organic matter. Based on the results from this precipitation experiment, we decided to separate asphaltenes from crude oils and bitumen by precipitation with *n*-hexane (except for Nigerian crude oils), because asphaltenes isolated with *n*-hexane are intermediate in terms of structural moieties and show best results for kinetic parameters.

For asphaltene precipitation a 60-fold excess of *n*-hexane was added to 5 ml of crude oil dissolved in 0.5 ml dichloromethane. The mixture was stirred for 5 min. in an ultrasonic bath and allowed to settle for 48 hours. Then the asphaltenes were filtered by vacuum filtration and washed with fresh *n*-hexane. After drying under a gentle stream of nitrogen gas, the asphaltenes were weighed and further on purified in a second and third step by re-precipitation with *n*-hexane from the solution in dichloromethane followed by cleanups.

100 mg of dried source rock bitumen was dissolved in 1 ml of dichloromethane again and asphaltenes were precipitated with a 60-fold excess of *n*-hexane as described above followed by second and third step of re-precipitation and replicate cleanups with fresh solvents.

4.1.2.2 Nigerian samples

For the Nigerian crude oils, we isolated asphaltenes by precipitation with hot *n*-heptane solvent to separate asphaltenes and high-wax compounds. Aside from resins it is well-known that waxy material is easily co-precipitated during asphaltene separation methods (Heath *et al.*, 1997; Thanh *et al.*, 1999; del Carmen Garcia *et al.*, 2000). Special separation techniques (Heath *et al.*, 1997; Musser and Kilpatrick, 1998; Thanh *et al.*, 1999) are not practical for this study, because these techniques are proposed for only a few ml of crude oils, and due to the low asphaltene content (5 – 200 mg/ l crude oil) of the Nigerian oils we needed a few hundred ml of crude oil to isolate sufficient amounts of asphaltenes for our study. Because high-wax

compounds start to precipitate at low temperatures (Afanasev *et al.*, 1993; Hsieh, 1999), we decided to isolate asphaltenes using the 60-fold excess of hot *n*-heptane solvent (65°C). After 48 hour's settlement, the mixture was again stirred for a few minutes by ultrasonic, then heated up (65°C) and finally filtrated. In the same way the asphaltenes were purified by multiple precipitation steps. Since no research has studied the effect of solvent temperature on the bulk chemical composition of isolated asphaltenes, we precipitated asphaltenes from the most biodegraded Nigerian crude oils by the common precipitation method using *n*-hexane as well, and compared them to asphaltenes isolated with hot *n*-heptane in terms of aromaticity (chapter 6).

4.2 Analytical methods

Rock-Eval

Rock Eval pyrolysis was used to identify the type, richness, quality and thermal maturity of source rock samples. Rock-Eval pyrolysis was performed with a Rock-Eval 6 instrument. Technical descriptions of Rock-Eval 6 are given by Béhar *et al.* (2001) and Lafargue *et al.* (1997; 1998). The Rock Eval pyrolysis method consists of a programmed temperature heating (in a pyrolysis oven) in an inert helium atmosphere to quantitatively and selectively determine (1) the free hydrocarbons contained in the sample and (2) the hydrocarbon- and oxygen-containing compounds (CO_2) that are volatilized during the cracking of kerogen. Products released from the source rocks were detected by flame ionisation (FID) and thermal conductivity detectors (TCD).

For analysis the pyrolysis oven is kept isothermally at 300°C for 3 min. and the free hydrocarbons are volatilized and measured as the S1 peak. The temperature is then increased from 300° to 600°C (at 25°C/min). This is the phase of volatilization of the very heavy

hydrocarbons compounds (>C_{40}) as well as the cracking of non-volatile organic matter. The hydrocarbons released from this thermal cracking are measured as the S2 peak (by FID). The temperature at which S2 reaches its maximum depends on the nature and maturity of the kerogen and is called Tmax. The CO_2 issued from kerogen cracking is trapped in the 300°-390°C range. The trap is heated, and CO_2 is released and detected on a TCD during the cooling of the pyrolysis oven (S3 peak).

In summary, the basic parameters obtained by Rock-Eval pyrolysis are:

S1 = the amount of free hydrocarbons (gas and oil) in the sample (in milligrams of hydrocarbon per gram of rock). S1 normally increases with depth. Contamination of samples by drilling fluids and mud can give an abnormally high value for S1.

S2 = the amount of hydrocarbons generated through thermal cracking of non-volatile organic matter. S2 is an indication of the quantity of hydrocarbons that the rock has the potential of producing should burial and maturation continue.

S3 = the amount of CO_2 (in milligrams CO_2 per gram of rock) produced during pyrolysis of kerogen. S3 is an indication of the amount of oxygen in the kerogen and is used to calculate the oxygen index.

Tmax = the temperature at which the maximum release of hydrocarbons from cracking of kerogen occurs during pyrolysis (top of S_2 peak). Tmax is an indication of the stage of maturation of the organic matter.

TOC = total organic carbon content of samples, determined by adding the residual organic carbon detected in pyrolysis residues to the pyrolyzed organic carbon, which in turn is measured from the hydrocarbon compounds issuing from pyrolysis.

The following parameters can be calculated from Rock Eval pyrolysis data:

HI = hydrogen index (HI = [100 x S2]/TOC). HI is a parameter used to characterize the origin of organic matter. Marine organisms and algae, in general, are composed of lipid- and

protein-rich organic matter, where the ratio of H to C is higher than in the carbohydrate-rich constituents of land plants.

OI = oxygen index (OI = [100 x S3]/TOC). OI is a parameter that correlates with the ratio of O to C, which is high for polysacharride-rich remains of land plants and inert organic material (Tissot and Welte, 1984).

PI = production index (PI = S1/[S1 + S2]). PI is used to characterize the evolution level of the organic matter.

Elemental analysis

Elemental analysis of carbon, hydrogen, nitrogen and sulphur were measured on a Leco CHNS-932 analyser. For the measurement of C, H, N and S the sample is burned at 1000 °C in an oxygen flow. The combustion gases CO_2, H_2O, NO_x and SO_2 are transported into a reduction device by a helium flow where the nitric oxyd NO_x is reduced to N_2 and free oxygen is bound. The detection of combustion gases CO_2, H_2O and SO_2 is done through selective IR-detectors. After detection of those gases the amount of remaining nitrogen is detected via thermal conductivity.

Medium Pressure Liquid Chromatography (MPLC)

The MPLC system was equipped with a thermo deactivated silica 100 precolumn and a LIChroPrep Si60 main column with *n*-hexane as mobile phase (Radke *et al.*, 1980). This analytical technique was used to separate crude oils into aliphatic, aromatic and resin and asphaltene fractions. The aliphatic fraction was detected by infrared (IR) and the aromatic fraction was determined by ultraviolet (UV) - detector. 5α-androstane and 1-ethylpyrene were used as internal standards.

Gas Chromatography - Mass Spectrometry (GC-MS)

The aliphatic and the aromatic hydrocarbon fractions were analyzed for biomarker using a gas chromatographic system coupled with a mass spectrometer. Compound separation was performed on an Agilent 6890 Series GC-instrument equipped with a PTV injection system and a fused silica capillary column (SGE BPX5; 50 m length, inner diameter = 0.22 mm, film thickness = 0.25 μm). Helium was used as carrier gas, and the temperature of the GC oven was programmed from 50°C (1 min) to 310°C at a rate of 3°C/min, followed by an isothermal phase of 10 min. The injector temperature was programmed from 52°C to 300°C at a rate of 12°C/sec. For compound identification, the gas chromatographic system was linked to a Finnigan MAT 95 XL mass spectrometer operating in the electron impact mode (70 eV). Full scan mass spectra were recorded from *m/z* 50 to 650 at a scan rate of 1 s per decade and an interscan delay of 0.2 s, resulting in a scan cycle time of 1.3 s.

Thermovaporisation Gas Chromatography (Tvap –GC)

For whole oil analysis the crude oils were injected onto quartz wool in glass capillary tubes of ca. 30 mm length, which were then sealed (Muscio *et al.*, 1994). The quartz wool and the capillary tubes were pre-cleaned by heating to 300°C for several hours. For the analysis the glass tubes were cracked at 300°C within the piston device of the Quantum MSSV Thermal system, after thermal outer-surface pre-cleaning and flushing the sealed glass capillaries. The mobilized products were collected in a cryogenic trap at -196°C. By heating the trap to 300°C, the products were released onto a dimethylpolysiloxane-coated column (0.52 μm film thickness) fitted into an Agilent GC 6890A gas chromatograph equipped with FID, and employing helium as carrier gas. Quantification of the products was performed using *n*-butane

as external standard. Peaks were identified and quantified based on reference chromatograms using Agilent ChemStation software.

Open-system-pyrolysis-GC and GC-MS

Open-system pyrolysis was performed using the same instrument configuration as described for thermovap-GC. For whole rock analysis 5-10 mg of each powdered sample was weighed into a glass capillary tube and held in place using thermally pre-cleaned quartz wool. Asphaltenes were mixed with thermally pre-cleaned quartz sand in the weight ratio 1:5, and 5 mg of this mixture was weighed into the glass capillary. Products released over the temperature range up to 300°C were vented to remove volatile or occluded compounds. Detection of pyrolysis products was carried out using a FID, carrier gas flow was regulated at 30 ml/min with a split ratio of 1:15. Pyrolysis products were released over the temperature range of 300 – 600°C (40°C/min) and collected in a liquid nitrogen-cooled trap. By heating the trap to 300°C the products were released and measured online by gas-chromatography. N-butane was used as a standard to quantify generated products. Identification of peaks based on reference chromatograms was done using Agilent ChemStation software.

GC-MS was performed on selected samples of source rock and asphaltene pyrolysates. The pyrolysis products were measured by a Thermo Finnigan Trace GC with Trace DSQ-MS (electron energy 70 eV) equipped with a dimethylpolysiloxane coated column of 0.25 μm film thickness. Peaks were integrated from the total ion current trace using the software Xcalibur (Version 1.3) by Thermo Finnigan.

Open-system-stepwise-pyrolysis-GC

The analysis was performed using the same Agilent GC 6890A gas chromatograph equipped with a Flame Ionisation Detector (FID), as described above. As well the sample preparation was carried out the same way described for open-system-pyrolysis before. The samples have been heated up with a heating-rate of 5.0K/min to a specific end-temperature of either 350, 380, 400, 420, 450 or 500 °C. The pyrolysis products released up to the decided end-temperature were collected in a liquid nitrogen-cooled trap, and finally released by heating the trap to 300°C and measured online by gas-chromatography. The identification and quantification of peaks based on reference chromatograms was done manually with the software Agilent ChemStation.

Gas chromatography combustion isotope-ratio mass spectrometry (GC-C-IRMS)

The stable carbon isotopic composition of pyrolysis products from petroleum asphaltenes and kerogens was measured by GC-C-IRMS. The system consisted of a GC unit (6890 Series, Agilent Technology, USA) connected to a Finnigan MAT GC III combustion device coupled via open split to a Finnigan MAT 253 mass spectrometer (ThermoElectron, Germany). Organic compounds in the GC effluent were oxidised to CO_2 in the combustion furnace at 940^{o}C on a CuO/Ni/Pt catalyst. CO_2 was transferred on line to the mass spectrometer to determine carbon isotope ratios. Asphaltenes were mixed with thermally pre-cleaned quartz sand in the ratio of 1:5 and 8-17 mg of this mixture were analysed with a GC split ratio of 1:30. The injector was set at 50°C for 1 minute and then heated at 700°C min^{-1} to 300°C. The samples were separated on a fused silica capillary column (HP Ultra 1, 50 m x 0.32 mm ID, 0.52 µm FT, Agilent Technology, USA). The temperature program started at 40°C, was held

for 3 min isothermally, and then increased at 2°C min^{-1} to 100°C. The temperature was then increased by 4°C min^{-1} to 310°C, and held at that temperature for 30 minutes. Helium, set to a flow rate of 1.0 ml min^{-1}, was used as carrier gas.

Bulk pyrolysis for kinetic model input

Programmed open-system pyrolysis with online FID was performed on a modified Humble SR-Analyzer. About 30 - 80 mg of each powdered whole rock sample and mixture of thermally pre-cleaned quartz with asphaltenes (ratio 5:1) were heated at different heating rates of 0.1, 0.7 and 5.0 K/min. A constant flow of carrier gas (45 ml/min) was maintained in order to transport all pyrolysis products to the FID for continuous measurement of bulk formation rates. The bulk petroleum formation curves measured at the three laboratory heating rates served as input for the kinetic model. The activation energy distribution (Ea) and frequency factor (A) were evaluated using KINETICS 2000® and KMOD® software. The mathematical model is described by Burnham *et al.* (1987). It is based on kinetic analysis of formation rate (dM/dT) versus temperature (T) curves, assuming in each case that n=25 first-order reactions with activation energies spaced between 46 and 70 kcal/mol and a single pre-exponential factor A.

Three different heating rates, including slow heating rates of 0.1 and 0.7 K/min, were used in order to ensure slow temperature measurement for the artificial maturation experiments. The use of such slow heating rates is important, since fast laboratory heating rates in kinetic studies may lead to an invalid temperature measurement during the simulation experiments (Burnham *et al.*, 1988; Schenk and Dieckmann, 2004), which results in unrealistic geological extrapolations.

Micro-scale sealed vessel pyrolysis (MSSV) - non-isothermal-closed-system-pyrolysis

Micro-scale sealed vessel (MSSV) pyrolysis experiments have been conducted at temperatures between 300 and 600°C with three different heating rates of 0.2, 0.7 and 5.0 K/min for asphaltenes as well as for kerogens. Details of this procedure have been reported in Horsfield *et al*. (1989). Briefly, an accurately weighed aliquot (ca. 1mg) asphaltene was diluted with fine-grained quartz powder by a ratio of 1:5. The sample was purged for 5 min. at 300°C to eliminate volatile compounds and small glass beads were introduced in 40µl glass tube and sealed. The tubes were isothermally heated using a GC oven and finally cracked within the piston device of the Quantum MSSV Thermal system to enable on-line analysis of the maturation products with gas chromatography (GC). Products were quantified using an external butane standard. For identification of pyrolysis peaks GC-MS was performed on selected samples of different temperatures. Here the pyrolysis products were measured by a Thermo Finnigan Trace GC with Trace DSQ-MS (electron energy 70eV) equipped with a dimethylpolysiloxane coated column of 0.25 µm film thickness. A number of pyrolysis products were identified for selected samples. Peaks were integrated using the software Xcalibur (Version 1.3) by Thermo Finnigan from the total ion current trace.

Fig. 12 shows the work-flow of the analytical methods used for each sample set to achieve the presented goals of this study.

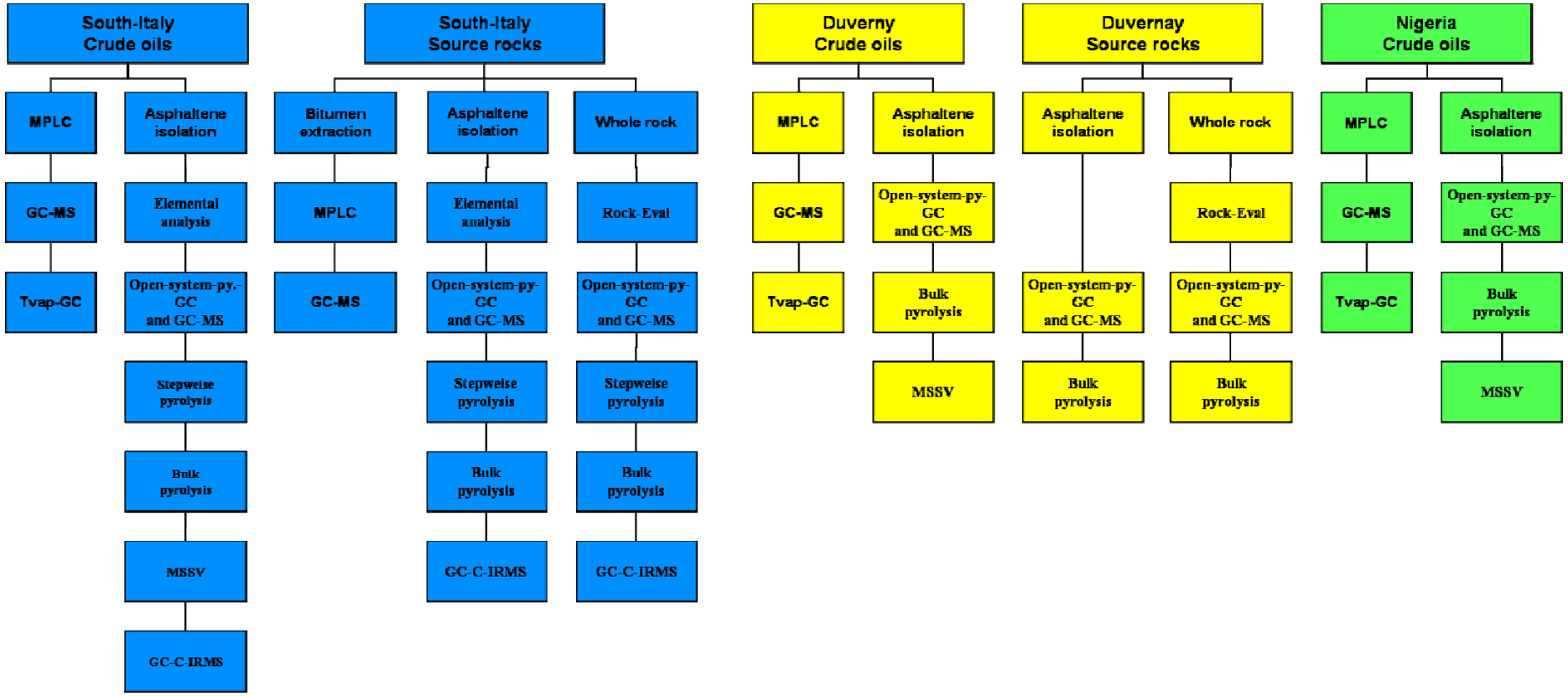

Fig 12 Analytical flowchart for the samples of this study.

5 Basic Chemical and Physical Characterization

5.1 Southern Italy

5.1.1 Source rock screening

The source rocks from Southern Italy studied for this project consist of 16 samples from cores of different wells. Samples from the same area have already studied by di Primio and Horsfield (1996).

The cored source rock samples were subdivided for the present study into shales and laminated mudstones, both of which are of a dark brownish or greyish colour. The mudstones show fine laminae of organic matter, which are oriented either parallel or slightly oblique to bedding. The shales are darker in colour, and show higher organic matter content, which is orientated parallel to their bedding. Fig 13 and Fig 14 show selected photos from samples G000645, G000646, and G000654. The changes from shale to laminated mudstones indicate either climatic or tectonic events for alternations from subtidal to intertidal environment. High organic matter content in this type of shale samples can be interpreted as originated from microbial mats in a hypersaline carbonate lagoon environment (Kenig and Huc, 1989; Gelin *et al.*, 1995; Schaefer *et al.*, 1995; di Primio and Horsfield, 1996).

The quality of the organic matter of the source rocks was investigated by Rock-Eval and TOC analysis. The data show strong variations due to different lithofacies. Table 4 provides Rock-Eval data and macroscopic characteristics of Italian source rocks. The shale samples have high TOC values ranging from 2.89% to 11.8% TOC and the Hydrogen Indices (HI) range from 613 to 909 mg HC/g TOC. These latter values indicate kerogens falling in fields for type I and II (Tissot and Welte, 1984) (Fig 15).

Sample G000654
Tmax 421 °C
TOC 8,76 %

Fig 13 Photo of core sample G000654.

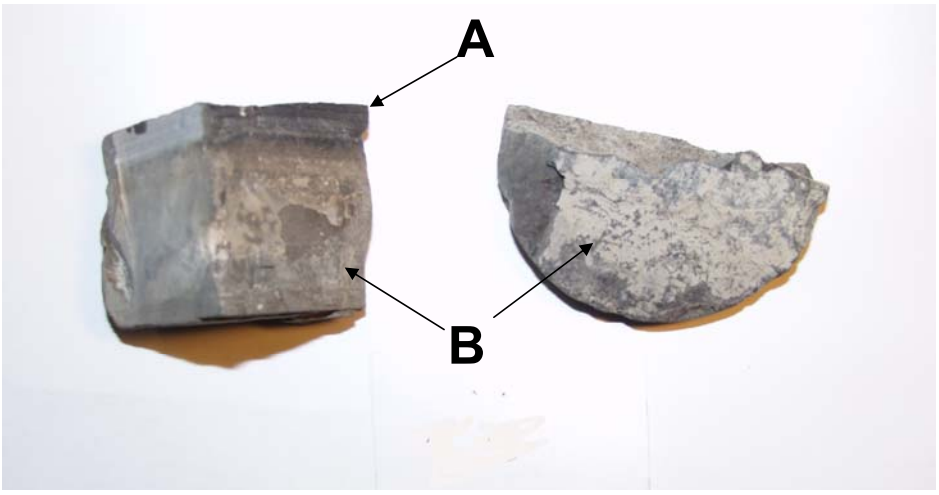

A:
Sample G000645
Tmax 434 °C
TOC 3,46 %

B:
Sample G000646
Tmax 429 °C
TOC 0,41 %

Fig 14 Photo of core samples G000645, and sample G000646.

Sample	HI	OI	PI	TOC (%)	Tmax (°C)	macroscopic charcteristics
G000642	779	15	0,01	4,39	422	shale
G000645	742	13	0,04	3,46	434	shale
G000646	471	39	0,41	0,41	429	mudstone
G000647	613	17	0,01	2,93	418	shale
G000648	691	45	0,03	1,37	416	mudstone
G000649	763	9	0,03	6,76	414	shale
G000650	567	44	0,04	1,29	414	mudstone
G000651	650	28	0,02	2,34	416	mudstone
G000652	816	7	0,01	11,80	421	shale
G000653	670	23	0,03	2,89	417	shale
G000654	909	10	0,02	8,76	421	shale
G000655	759	20	0,02	4,03	413	shale
G000656	817	8	0,03	7,05	415	shale
G000657	583	73	0,04	0,75	419	mudstone
G000660	572	57	0,02	0,67	409	mudstone
G000661	686	10	0,02	6,65	439	shale

Table 4 Rock-Eval data for Italian source rocks.

The maturity of the studied shales is low with Tmax around 413°C. The same is true for the mudstones, which show Tmax values around 409°C (Fig 15). Espitalié *et al*. (1985) mentioned that type II-S kerogens enter the oil window at lower temperatures than type II kerogens. The HI for the mudstone samples range from 471 to 691 mg HC/g TOC, indicating a kerogen type II. Fig 16 shows the TOC range for studied source rock samples. The sample G000661 represents an exception and is very different to the rest of the studied sample set. The Tmax of this sample is with 439°C significantly higher but the HI of 691 mg HC/g TOC is similar to those of the shale and mudstone samples.

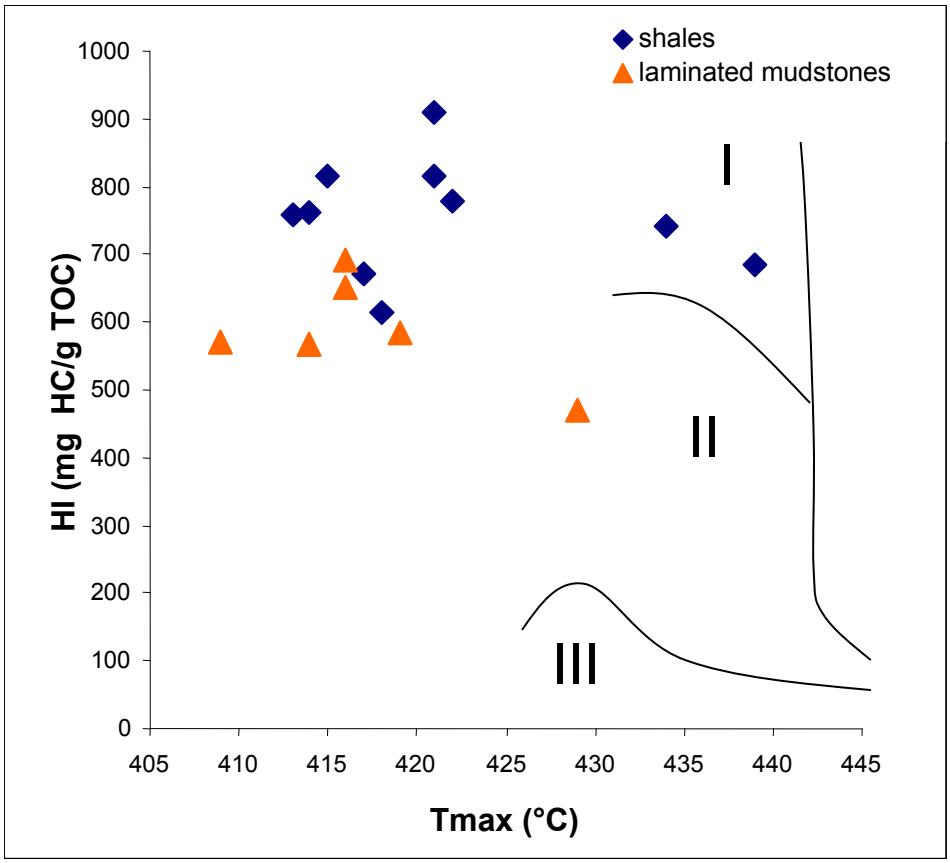

Fig 15 Pseudo-van-Krevelen diagram with Tmax versus HI for the Italian source rock samples (after Espitalié *et al.* (1985)).

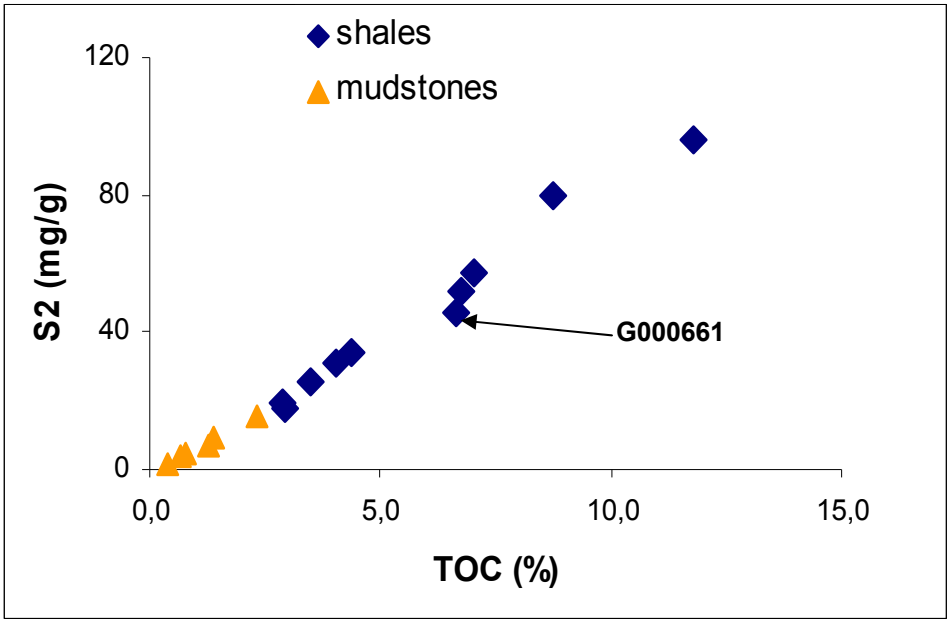

Fig 16 Rock-Eval S2 and TOC for source rocks from Southern Italy.

5.1.1.1 Source rock bitumen

For oil-source correlation using biomarkers, selected powdered source rocks were extracted for 24h by Soxhlet (with a mixture of dichloromethane and ethanol in ratio 99:1) to yield the source rock bitumen. After drying the bitumen under nitrogen gas, 100mg bitumen was dissolved in 0.5 ml of dichloromethane and asphaltenes were precipitated using *n*-hexane solvent. After filtration of the asphaltenes, the bitumen was separated into saturates, aromatics and NSO fractions by medium pressure liquid chromatography (MPLC) (Fig 17). The Italian source rock bitumens show in general high contents of NSO compounds between 73 – 81 %, and saturates do generally not exceed 10 %. There are two samples which differ from the others in the distribution of compound classes. The sample G000650 display higher amounts of aliphatic hydrocarbons, whereas the sample G000661 differs from the others by lowest amounts of NSO compounds (50%) and highest contents of aromatic hydrocarbons.

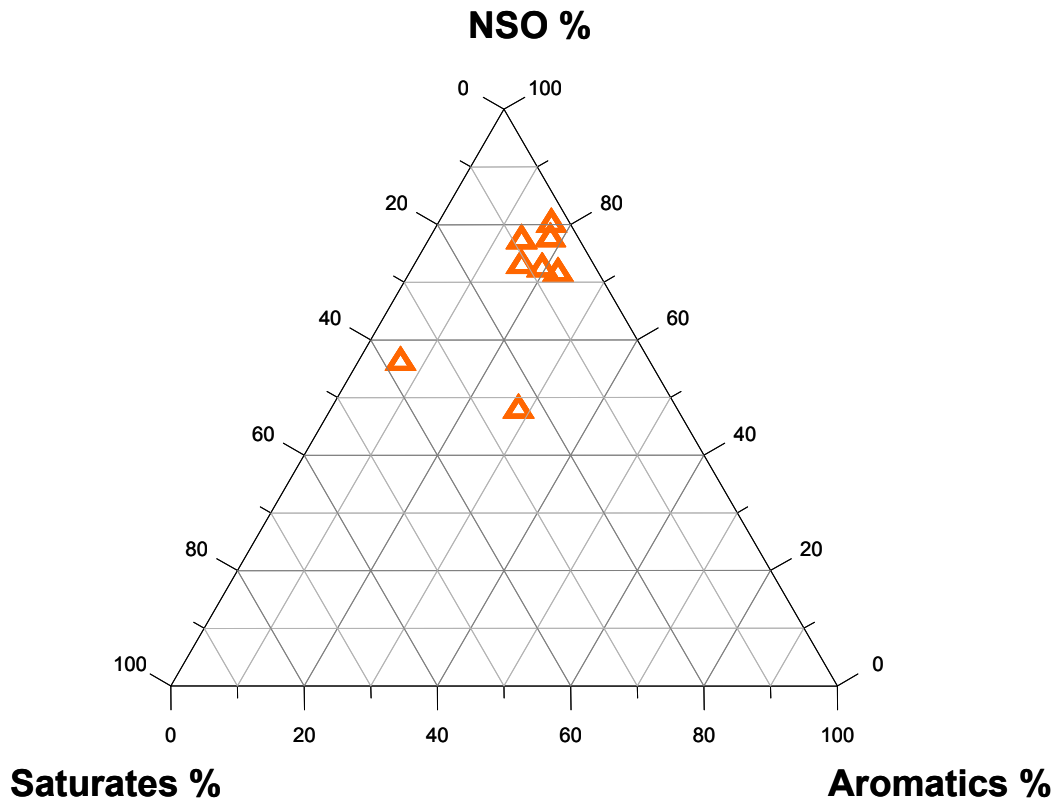

Fig 17 Ternary diagram showing the compound class distribution of the Italian source rock bitumen.

5.1.2 Crude oil screening

5.1.2.1 Bulk composition

Fig 18 shows the bulk composition of the studied Italian oils in terms of NSO, saturates and aromatics. Based on MPLC-analysis the oils from Southern Italy are generally dominated by polar compounds and asphaltenes. The lowest content of NSO compounds (ca. 10%) were monitored in the crude oil with 33° API, whereas the API gravity of the other oils decreases with increasing proportion of the NSO fraction. This figure also separates fresh oils from biodegraded oils. The biodegraded oil sample (G00394) with an API gravity of 2.64° show total content of NSO and asphaltene fractions of about 85%. The second biodegraded oil sample (G000393) shows NSO content of only 65%, indicating that the original, non-biodegraded oil was relatively NSO lean. The generally low API gravities of these heavy crude oils were explained by Novelli *et al.* (1988) as a result of high expulsion efficiency controlled by high heating rate, fast subsidence and over pressuring during Tertiary tectonics.

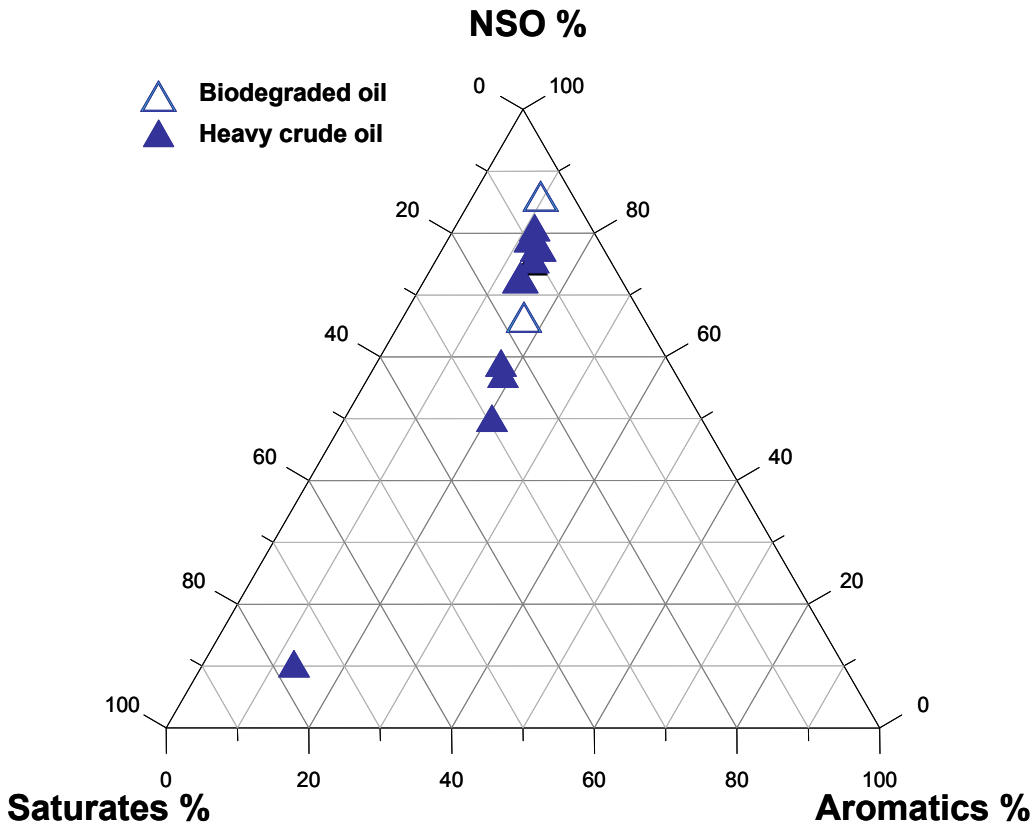

Fig 18 Ternary diagram showing the compound class distribution of the Italian crude oils.

Selected chromatograms from thermovaporisation - whole oil analysis for the investigated Italian oils are presented in Fig 20. Apart from the two very strong biodegraded oils, the less degraded crude oils show a bimodal distribution pattern for the homologous series of *n*-alkanes up to *n*-C_{30}. The most prominent aromatic compounds in all investigated oils (Fig 20) are in increasing order of GC retention time toluene, ethylbenzene, m,p-xylene, and o-xylene. All oils show a very high hump of GC unresolved compounds. Fig 19 shows a plot of the GC hump (%) versus the API gravity for respective crude oils. For the two biodegraded oils at least 90 – 94% of all compounds are situated in the GC-hump. Lowest percentage of unresolved compounds (62%) was monitored for the crude oil G000401 with an API of 33.5°. Interestingly, the long-time-stored samples, produced in 1960 and 1963, show lower amounts of unresolved compounds than their fresher counterparts.

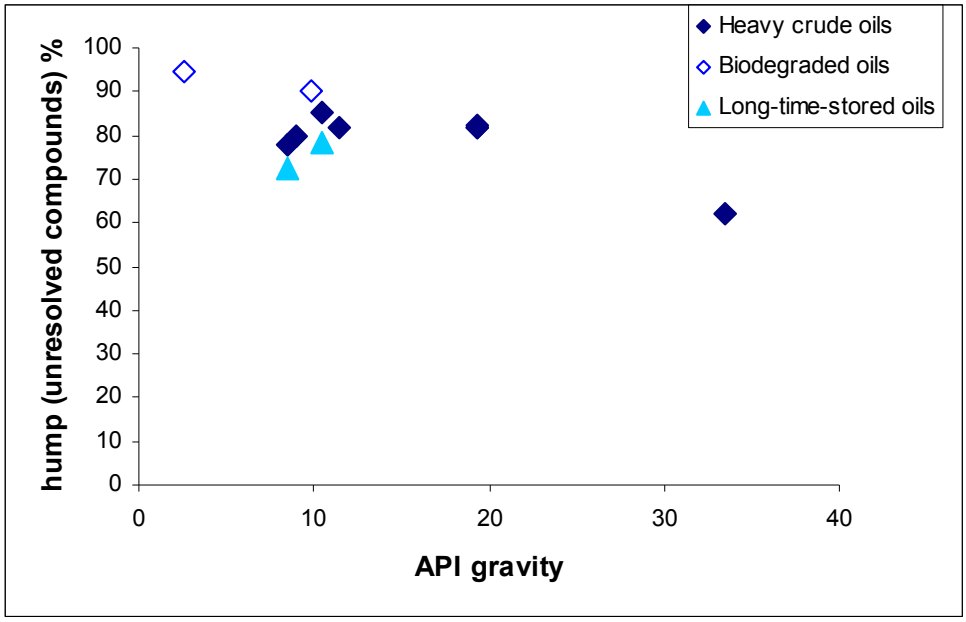

Fig 19 Diagram with the GC hump (%) versus the API gravity for crude oils from Southern Italy.

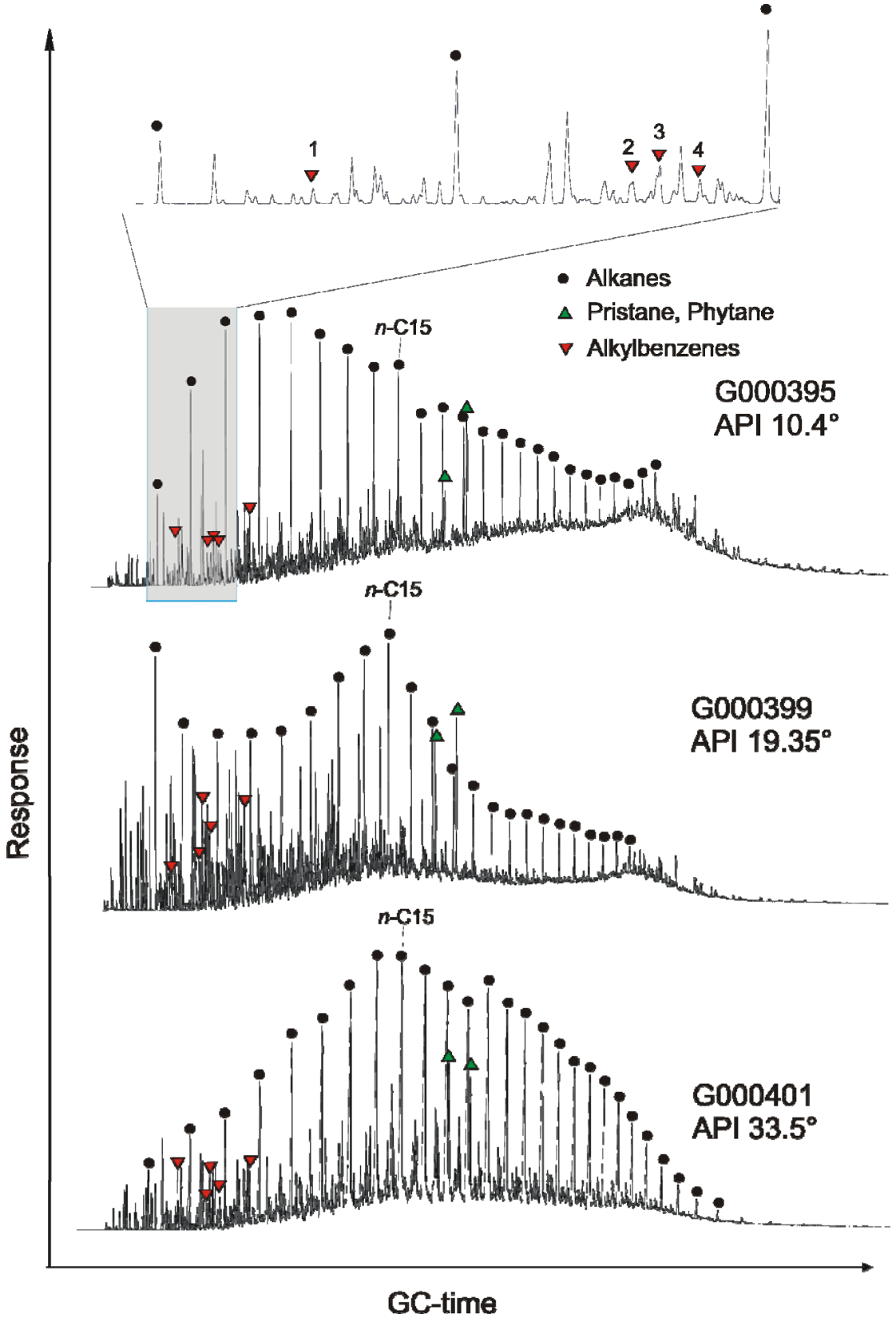

Fig 20 Thermovaporisation GC traces of 3 Italian oil samples are shown with increasing API gravity. Alkanes from *n*-C_7, pristane and phytane, as well most prominent alkylbenzenes are marked. The alkylbenzenes are corresponding to retention time from left to the right: toluene (1), ethylbenzene (2), m,p-xylene (3), o-xylene (4), and trimethylbenzene.

5.1.2.2 Biomarkers

The recognition of biogenic inputs in the sedimentary organic matter record is usually obscured by post-depositional diagenic transformations, which modify the original composition. The study of the genesis of fossil molecules in these environments has been one of the main research focuses in geochemistry in last years. According to the biomarker concept, certain organic compounds occurring in crude oils and sediments can be traced back to a precursor compound in the biosphere, if the basic skeleton of the geochemical product preserves an unambiguous link with its biogenetic precursor (Higby Schweitzer, 2004).

Biomarkers are complex molecular fossils derived from once living organisms (Peters *et al.*, 2005). Because these biological markers can be measured in oils as well as in source rock bitumen, they provide a tool to correlate oil families and to relate oils with source rocks. Thus biomarkers provide informations on the organic matter in the source, environmental conditions during deposition and burial, thermal maturity experienced by a source rock or crude oil, degree of biodegradation, and sometimes the age of organic matter (Peters *et al.*, 2005).

Since different depositional environments are characterised by different assemblages of organisms, the distribution of their preserved biomarkers is generally used to correlate oils and bitumen. As well biomarker parameters are an effective tool to rank the relative maturity of petroleums throughout the entire oil-generative window.

Especially organic-rich source rocks formed in carbonate-evaporitic palaeoenvironments, like the source rock samples from Southern Italy, are associated with high biological productivity. The dissolved carbonate is a reserve of inorganic carbon for photosynthesis that affords a larger biomass than in the corresponding neutral eutrophic environments (Talling *et al.*, 1973; Grimalt *et al.*, 1991). The organisms living in these environments must be halophilic, or at least be tolerant to certain amounts of dissolved salts by evaporation. This of course limits the biodiversity of prokaryotic and eukaryotic species. Therefore these environments are often

attributed to the high presence of cyanobacteria, purple bacteria, sulphur-reducing bacteria and the so-called "microbial mats" (Kenig and Huc, 1989; Gelin *et al.*, 1995; Schaefer *et al.*, 1995; di Primio and Horsfield, 1996). Several studies up to now have focussed on the biogenic inputs in evaporitic environments for a number of different basins worldwide (Connan and Dessort, 1987; Barbe *et al.*, 1990; Grimalt *et al.*, 1991; Grimalt *et al.*, 1992; Carpentier *et al.*, 1993; Keely *et al.*, 1993; Teixidor *et al.*, 1993; Gelin *et al.*, 1995; Kenig *et al.*, 1995; Schaeffer *et al.*, 1995; Sinninghe Damsté *et al.*, 1995; Campos *et al.*, 1996; di Primio and Horsfield, 1996; Russel *et al.*, 1997; Grice *et al.*, 1998b; Putschew *et al.*, 1998; Schaeffer-Reiss *et al.*, 1998; Vaz dos Santos Neto *et al.*, 1998; Abdullah, 1999; Rodrigues *et al.*, 2000; Bao and Li, 2001; Cabrera *et al.*, 2002; Perez *et al.*, 2002).

Alkane distribution

Common for all less biodegraded oils from Southern Italy is an unusual high amount of *n*-C_{14} and *n*-C_{15}, as shown in Fig 20. Most prominent is the high content of *n*-C_{15}, some crude oils show additionally high contents of *n*-C_{14}. In recent sediments these components are generally indicative of bacterial contribution or certain microalgae, and they have been found in pure cultures of *Desulfovibrio desulfuricans* (Boon *et al.*, 1977), cultures of sulphate-reducing bacteria (Grimalt *et al.*, 1992; Russel *et al.*, 1997), cyanobacterial mats (Boon *et al.*, 1983), cultures of *Bacillu*s species (Kaneda, 1967), sedimentary microbial populations (Volkman *et al.*, 1980; Grimalt and Albaigés, 1987; de las Heras *et al.*, 1997), and in cell walls of saline tolerant microalgae (Grice *et al.*, 2003). Their occurrence in the present study is consistent with high sulphate-reducing activity associated with carbonates and reduced sulphur. Microbial mats are formed by a sequence of different bacterial colonies (cyanobacteria, filamentous bacteria, sulphur purple bacteria), and periodically detrital sedimentation and recolonization on the detritus (Kenig *et al.*, 1990). The presence of these *n*-alkanes in the

Italian crude oils cannot be connected to outline bacterial input. The slightly enhanced concentrations for *n*-C_{14} and *n*-C_{15} in these crude oils point more to an unusual source.

The most mature oil with an API gravity of 33.5° show also unusual high amounts of *n*-C_{19}, which in young sediments has been referred to an input of marine algae (Youngblood *et al.*, 1971). Because of the relative high content of pristane (Pr/Ph = 1) in the same sample, it is possible that this oil is sourced from a different environment or sourced under different redox conditions. As well, the higher pristane content in this sample might be related to faster decomposition of phytane than of pristane at higher level of thermal maturity, as reported by Tang and Stauffer (1995) to occur for Monterey kerogen pyrolysates.

A minor preference of odd over even carbon number *n*-alkanes in the range *n*-C_{23} to *n*-C_{29} was found in the low mature crude oils, which generally peaks in *n*-C_{25} and *n*-C_{27}. These odd over even predominance is often attributed to land plant cuticular waxes (Tissot and Welte, 1984). Di Primio (1995) has shown in his microscopy study that macerals of land plants are missing in the source rocks from Southern Italy, and suggested microbial mats as source for higher contents of odd carbon numbered alkane in the range *n*-C_{29} to *n*-C_{31}. The author also mentioned that the algae *Botryococcus*, which reflects odd over even dominance in this range as well (Metzger *et al.*, 1986), could be excluded as alternative source due to the hypersaline environment inferred for the source rocks. Microbial mats as probable source for odd over even alkane dominance was also mentioned in other studies (Boon *et al.*, 1983; Kenig *et al.*, 1990). However, more recently it was proven that for example *Botryococcus braunii* is saline-tolerant and often found in consequently saline lacustrine environments (Grice *et al.*, 1998a; Audino *et al.*, 2002; Grice *et al.*, 2003; Volova *et al.*, 2003).

Pristane and phytane

The low Pr/Ph ratios (Pr/Ph < 1) for all Italian oils indicate consistently anoxic conditions (Didyk *et al.*, 1978; Peters, 1986; Bordenave, 1993). Besides the redox potential of the

environment, the nature of the contributing organisms, and production additives could also modify the Pr/Ph ratios. However, according to the relatively low value observed in the entire section, other derived input probably did not essentially affect the Pr/Ph values. Ten Haven *et al.* (1987) proposed that the Pr/Ph ratio cannot be used as an indicator for oxygen levels. But, in hypersaline environments of deposition an application of the Pr/Ph ratio can be expected to be successful. The occurrence of laminations in the Italian source rocks and, according to previous work (di Primio and Horsfield, 1996), the organic sulphur incorporation also suggests that sediments were deposited in oxygen-depleted basin (Orr, 1986; Haas, 2002; Peters *et al.*, 2005). Johns *et al.* (1980) explained the dominance of phytane in anoxic sediments in that chlorophylls have reached the sediment without being degraded. When hydrolysis then liberates phytol from the chlorophyll molecules in the anoxic zone only reduction to phytane is likely. Low Pr/Ph ratios from saline environments were also explained by Nissenbaum *et al.* (1972) and ten Haven *et al.* (1987) as resulted from the breakdown of isoprenoid glycerol ether lipids in halophilic bacteria, which increases the phytane concentrations. However, several works proposed other precursors than outlined chlorophyll for Pr and Ph. These alternative precursors for Pr are bound tocopherols (Goossens *et al.*, 1984; Koopmans *et al.*, 1999), ether lipids from archaea (Navale, 1994), and zoo-plankton (Blumer *et al.*, 1969), whereas ether lipids from archaea have also been suggested as precursors for Ph (Risatti *et al.*, 1984; Rowland, 1990; Navale, 1994).

Fig 21 shows a cross-plot of pristane/*n*-C_{17} versus phytane/*n*-C_{18} after Peters *et al.* (1999) from whole-oil chromatograms of Italian oils. Here, it is illustrated that the heavy black oils fall in the field of type II organic matter, which is according to Peters *et al.* (1999) as well indicative for more reducing depositional environments. The sample G000401 (API 33.5°) differs in this plot as well (Pr/Ph = 1), and exhibits a less anoxic depositional environment. As a consequence of degradation effects, the ratios of both biodegraded samples do not fall in the field of type II organic matter. Beside, the observed trend for the heavy crude oils is not

proportional to the API of related oils. The three intermediate mature crude oils with 19.35° API present highest ratios for pristane/*n*-C_{17} and phytane/*n*-C_{18} for the illustrated heavy crude oils in Fig 21.

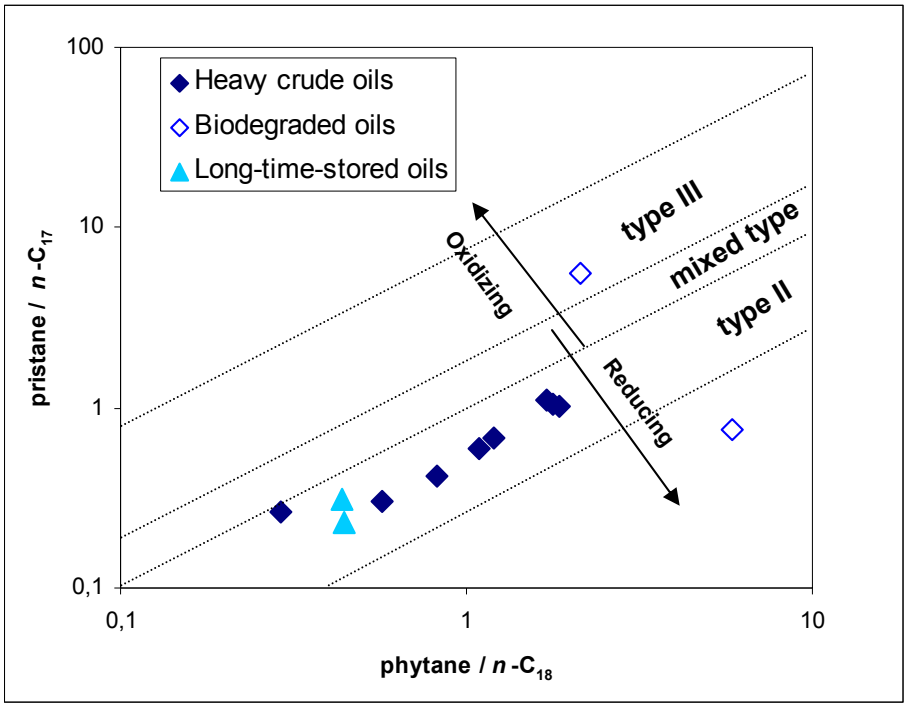

Fig 21 Plot of pristane/*n*-C_{17} vs. phytane/*n*-C_{18} from whole-oil chromatograms of Italian oils (after Peters *et al.* (1999)).

Hopanes and steranes as maturity parameter

Hopanes and steranes are trace compounds (ppm) in oils and bitumen, and they are analysed using gas chromatography / mass spectrometry. Hopanes are pentacyclic hydrocarbons of the triterpane group believed to derive from bacteriohopanoids in bacterial membranes, whereas steranes are tetracyclic hydrocarbons derived from sterols, which are membrane and hormone components in eukaryotic organisms (Peters *et al.*, 2005). Hopane and sterane distributions are convincing maturity parameters and also used for oil-source correlations.

Relevant biomarker parameters for the oils and source rock bitumen from Southern Italy are presented in Table 5.

Sample		Gammacerane Index	Homohop. Index	C_{31} Homohop. Izom.-Index	C_{32} Homohop. Izom.-Index	Ts/(Ts+Tm)	Hop-Mor-Ratio H/(H+M)	C_{29}Ts Index	Sterane-Isom. 20S/(20S+20R) αααC_{29}	Sterane-Isom. ββ/(ββ+αα) C_{27}	Pr/Ph
G000393	crude oil	0.35	0.04	0.53	0.57	0.44	0.80	0.23	0.57	0,00	0.62
G000394	crude oil	0.05	0.06	0.57	0.59	0.05	0.92	0.04	0.58	0,00	0.50
G000395	crude oil	0.36	0.05	0.50	0.50	0.29	0.86	0.16	0.57	0.12	0.40
G000396	crude oil	0.30	0.03	0,57	0.57	0.29	0.88	0.11	0.60	0.32	0.56
G000397	crude oil	0.33	0.02	0.51	0.54	0.32	0.86	0.12	0.53	0.11	0.40
G000398	crude oil	0.35	0.07	0.59	0.60	0.41	0.87	0.18	0.67	0.25	0.55
G000399	crude oil	0.36	0.07	0.59	0.60	0.43	0.88	0.15	0.62	0.26	0.66
G000400	crude oil	0.36	0.07	0.57	0.61	0.44	0.88	0.24	0.59	0.28	0.65
G000401	crude oil	0.12	n.d.	0.58	0.69	0.69	0.94	0.40	n.d.	0.52	1,00
G000402	crude oil	0.32	0.05	0.53	0.54	0.27	0.87	0.11	0.56	0.31	0.45
G000403	crude oil	0.30	0.03	0.55	0.57	0.28	0.88	0.11	0.64	0.36	0.37
G000404	crude oil	0.31	0.04	0.50	0.54	0.33	0.85	0.15	0.53	0.31	0.41
G000642	bitumen	0.33	0.11	0.19	0.18	0.11	0.80	0.11	0.17	-	n.d.
G000648	bitumen	0.45	0.02	0.21	0.29	0.12	0.84	0.19	0.20	-	n.d.
G000649	bitumen	0.33	0.07	0.23	0.20	0.06	0.83	0.07	0.18	-	n.d.
G000650	bitumen	0.37	0.08	0.18	0.07	0.16	0.90	0.14	0.19	0.24	n.d.
G000651	bitumen	0.19	0.11	0.23	0.18	0.08	0.85	0.22	0.25	-	n.d.
G000652	bitumen	0.14	0.03	0.19	0.17	0.04	0.80	0.09	0.17	-	n.d.
G000654	bitumen	0.27	0.08	0.21	0.11	0.05	0.79	0.09	0.08	-	n.d.
G000656	bitumen	0.22	0.06	0.25	0.24	0.06	0.80	0.15	0.32	-	n.d.
G000661	bitumen	0.46	0.13	0.56	0.53	0.36	0.89	0.19	0.44	0.38	n.d.

Gammacerane Index = gammacerane / (gammacerane + C_{29} 17α(H), 21β(H)-homohopane)

Homohopane Index = C_{35}-homohopane / (C_{31}- + C_{32}- + C_{33}- + C_{34}- + C_{35}-homohopane)

C_{31} Homohopane Izom.-Index = 22S C_{31}-homohopane / (22S + 22R C_{31}-homohopane)

C_{32} Homohopane Izom.-Index = 22S C_{32}-homohopane / (22S + 22R C_{32}-homohopane)

Ts/(Ts+Tm) = C_{27} 18α(H)-trisnorhopane II / (C_{27} 18α(H)-trisnorhopane II + C_{27} 17α(H)-trisnorhopane)

Hopane-Moretane-Ratio = C_{29} 17α(H), 21β(H)-homohopane / (C_{29} 17α(H), 21β(H)-homohopane + βα-moretane)

C_{29}Ts Index = C_{29} 18α-(H)-30-norneohopane / (C_{29} 18α-(H)-30-norneohopane + C_{29} 17α(H)-hopane)

Sterane-Isom. 20S/(20S+20R) αααC_{29} = C_{29} 5α(H), 14α(H), 17α(H) 20S / (ααα20S + ααα20R)

Sterane-Isom. ββ/(ββ+αα) C_{27} = C_{27} 14β(H), 17β(H) / (ββ + αα)

Pr/Ph = pristane /phytane

Table 5 Biomarker parameter for Italian crude oils and selected source rock bitumen.

The steranes in Italian oils and bitumens are dominated by (20*S*)- and (20*R*)-cholestane and (20*S*)- and (20*R*)-ethyl-cholestane. The ratio of 20*S*/(20*S*+20*R*) of C_{29}-sterane is higher for crude oils compared to the ratios of source rock bitumen, indicating different levels of maturity for crude oils and bitumens (Fig 22).

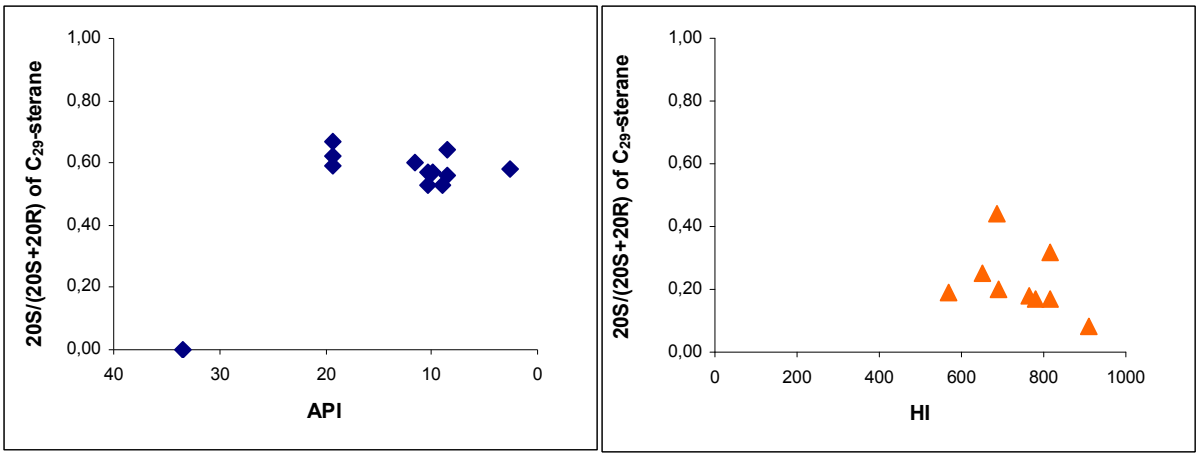

Fig 22 Ratio of 20*S*/(20*S*+20*R*) of C_{29}-sterane versus the API for crude oils (left), and versus the HI for source rock bitumen (right).

The hopane-moretane ratio for all crude oils is nearly equal with ranges from 0.85 to 0.94 and is only slightly higher than the moretane ratio of source rock bitumens, which range between 0.80 and 0.90. But, this moretane ratio might not be a useful maturity parameter for oils and source rocks from Southern Italy, because the moretane ratio is predicated on certain source rock environmental conditions, as well, the occurrence of moretane is more attributed to terrestrial organic matter (Isaksen and Bohacs, 1995; Peters *et al.*, 2005; Younes, 2005; Justwan *et al.*, 2006) than to organic matter found in hypersaline environments.

The ratio of 22*S*/(22*S*+22*R*) of C_{31}- and C_{32}-homohopanes (*m/z* 191) are nearly the same for all Italian crude oils. But compared to the ratio calculated for source rock bitumen, crude oils show higher amounts of 22*S*, the geological epimer, compared to the biological precursor 22*R*. The 22*S*/(22*S*+22*R*)-ratio for bitumen varies from 0.18 to 0.25, whereas the same ratio from crude oils ranges from 0.49 to 0.58. This reflects the immature character of investigated

source rocks. However, various authors have shown that homohopane isomerization as maturity parameter is not very reliable, especially for immature source rocks deposited under hypersaline conditions (ten Haven *et al.*, 1986; Peters *et al.*, 1990).

The maturity parameter Ts/(Ts+Tm) measured in samples from Italy ranges from 0.05 to 0.44 for the immature oils, and shows a value of 0.69 for the crude oil with API of 33.5° (G000401)(Fig 23 top left). As it can be seen from Fig 23 (top right), source rock bitumen show ratios which vary from 0.04 to 0.12, pointing to the immaturity of that source rocks.

However, as well this maturity parameter might not be reliable for the studied samples from Southern Italy, since Ts/(Ts+Tm) is commonly used as a maturity parameter for oils of very homogenous sources (Seifert and Moldowan, 1978; Riva *et al.*, 1988) as well as oil samples representing the same facies (Jones and Philp, 1990). Bakr and Wilkes (2002) studied the occurrence and distribution of carbazoles and benzocarbazoles in crude oils from the Gulf of Suez in Egypt in terms of facies and depositional environment. The authors have shown that the biomarker parameter Ts/(Ts+Tm) is controlled by variations of facies and depositional environment, but not by maturity.

The observed trend for Ts/(Ts+Tm) versus the API in Fig 23 for the Italian crude oils is more similar to a biodegradation trend, since the strongest biodegraded oil show lowest ratio of Ts/(Ts+Tm) and do not reveal any indication of the originally maturity. As well, crude oils and source rock bitumen from Italy show strong variations of biomarkers for oil -oil and oil – source correlation, probably due to variations of biogenic input during changes from subtidal to intertidal environments. Hence, the use of Ts/(Ts+Tm) as maturity parameter for the samples from Italy must be questioned. Besides, it has proposed that source rock lithology may influence the variability of Ts/(Ts+Tm) as well (Rullkötter *et al.*, 1984; Rullkötter *et al.*, 1985; Riva *et al.*, 1989; Waples and Machihara, 1991; Bakr and Wilkes, 2002). Riva *et al.* (1989) have demonstrated that the Ts/(Ts+Tm) ratio decreases as the proportion of shale in calcareous facies decreases. This leads to very low Ts/(Ts+Tm) ratios in carbonate source

rocks, like published by several authors (McKirdy *et al.*, 1983; Rullkötter *et al.*, 1984; Rullkötter *et al.*, 1985; Riva *et al.*, 1989; Mattavelli and Novelli, 1990b). And at least, this explains that the low Ts/(Ts+Tm) ratios for studied source rock bitumen from Southern Italy are controlled by lithology and not only by maturity. The same oil and bitumen characteristics might be valid for the C_{29}Ts index, which commonly increase parallel to Ts/(Ts+Tm) with increasing maturity (Fowler and Brooks, 1990; Riediger *et al.*, 1990; Peters *et al.*, 2005). Studied samples from Italy show the same trend for C_{29}Ts index versus API like previously observed for the Ts/(Ts+Tm) parameter, indicating that this parameter might also be affected by biodegradation of oils (Fig 23 bottom).

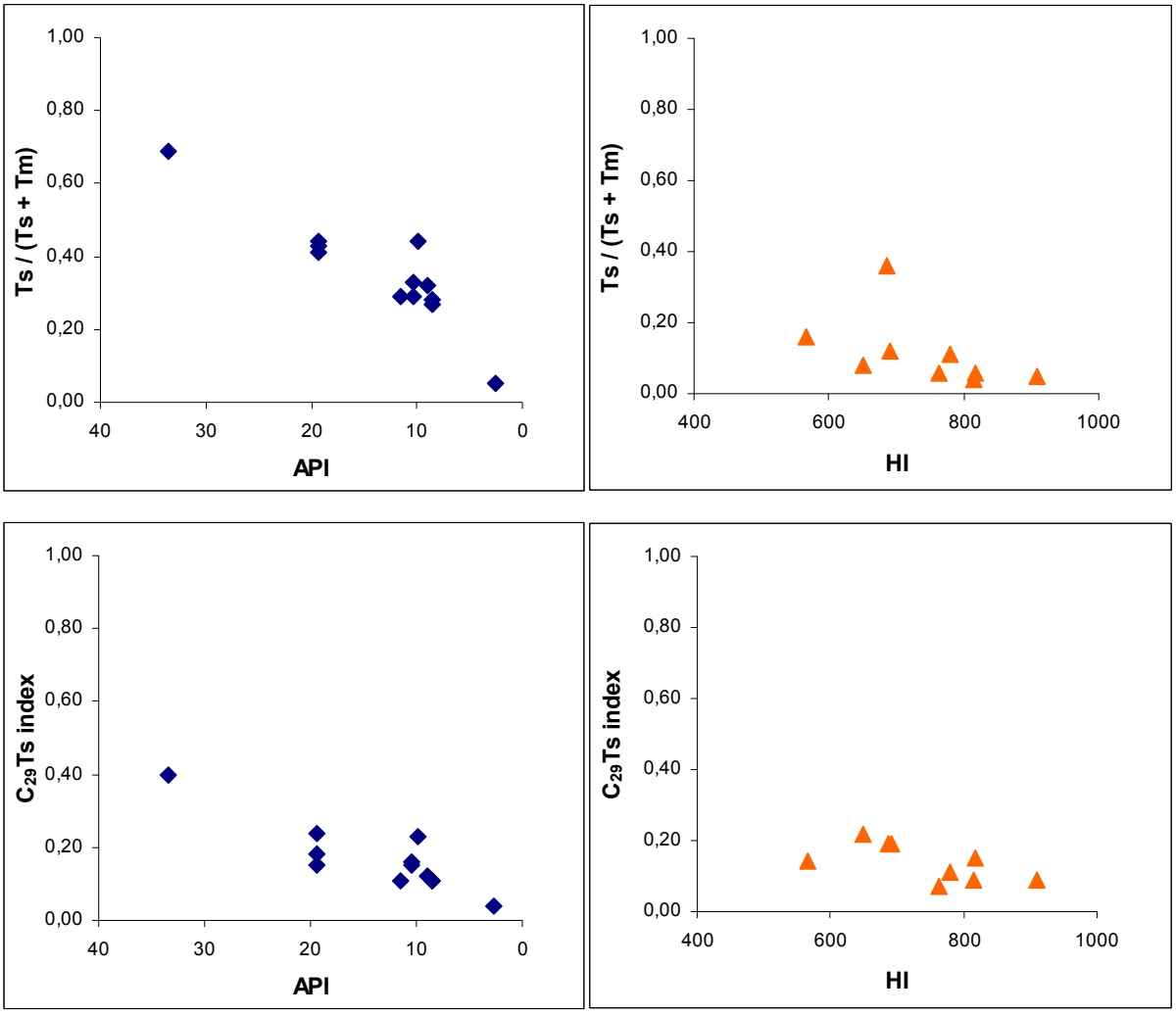

Fig 23 Maturity parameter Ts/(Ts+Tm) versus the API for Italian crude oils (top left), and versus the HI for source rock bitumen (top right), and the C_{29}Ts index versus API for the same oils (bottom left), and versus HI for same bitumens (bottom right).

The sterane-isomerization index $\beta\beta/(\beta\beta+\alpha\alpha)$ of C_{27} steranes in Italian crude oils increases with increasing maturity. The $\beta\beta$ C_{28} and C_{29} steranes could not be quantified in all oils, for the reason that they are either virtually absent, or co-eluted or else they occur in too low quantities in some cases. In most source rock bitumens, however, none of these $\beta\beta$ steranes could clearly be identified due to their low amounts in those bitumens. This is in contrast to previous works of ten Haven *et al*. (1986) and McKirdy *et al*. (1983), who proposed that $\beta\beta$ steranes are abundant in oils and sediments from hypersaline environments even during early diagenesis. Peters *et al*. (2005) mentioned the sterane isomerization index to be independent of source organic matter input, but can be affected by source rock mineral matrix (McKirdy *et al.*, 1983; Huang *et al.*, 1990). For studied oils from Italy the ratio $\beta\beta/(\beta\beta+\alpha\alpha)$ of C_{27} steranes fits best, because their values appears slower to reach the equilibrium than other sterane maturity parameters (Seifert and Moldowan, 1986). Fig 24 shows a plot of C_{27} $\beta\beta/(\beta\beta+\alpha\alpha)$ steranes versus C_{29} 20*S*/(20*S*+20*R*), which was originally proposed as a plot of $\beta\beta/(\beta\beta+\alpha\alpha)$ versus 20*S*/(20*S*+20*R*) of C_{29} steranes established by Seifert and Moldowan (1986).

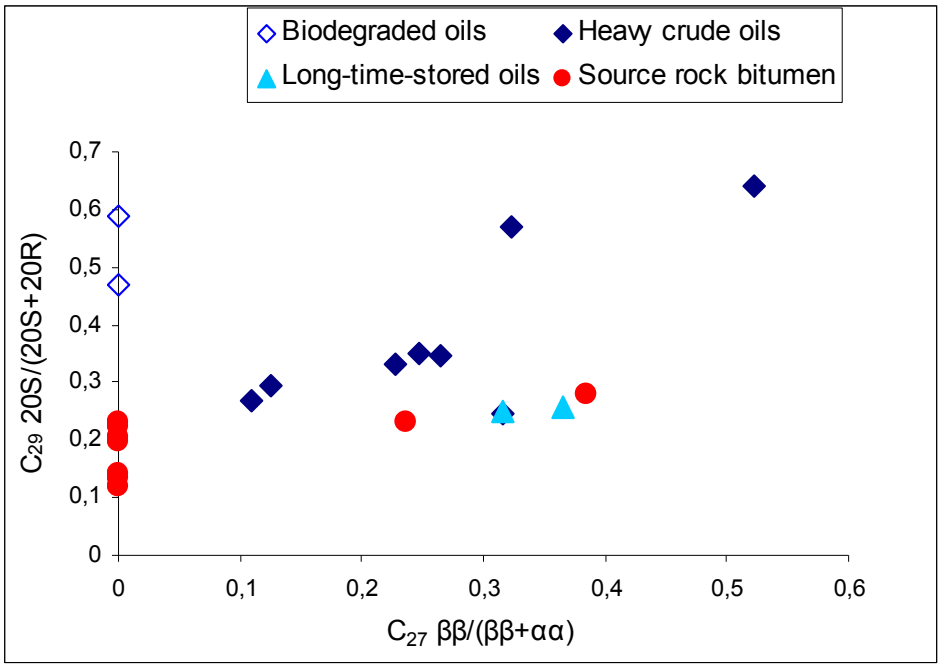

Fig 24 Plot of C_{27} $\beta\beta/(\beta\beta+\alpha\alpha)$ versus C_{29} 20*S*/(20*S*+20*R*) steranes of Italian crude oils and bitumen (modified after Seifert and Moldowan (1986)).

From Fig 24 it is evident that both of these maturity parameters are affected by biodegradation and long-time storing, because degraded and stored oils plot far away from the other heavy crude oils. The C_{27} $\beta\beta/(\beta\beta+\alpha\alpha)$ sterane isomerization ratio is not useful for studied source rock bitumen from Southern Italy, because $\beta\beta$ steranes could not be quantified in most bitumens.

To conclude, crude oils and source rock bitumen from Southern Italy demonstrate different levels of maturity based on biomarker maturity parameters. Less degraded and non stored oils demonstrate an early stage of thermal maturity using the parameters C_{27} $\beta\beta/(\beta\beta+\alpha\alpha)$ and C_{29} 20*S*/(20*S*+20*R*), whose values correspond to an vitrinite reflectance value of 0.7 – 0.8 Ro%, as shown in Fig 25a. Bitumen show an immature stage of maturity, corresponding to a vitrinite reflectance of 0.4 – 0.5 Ro% (Fig 25b).

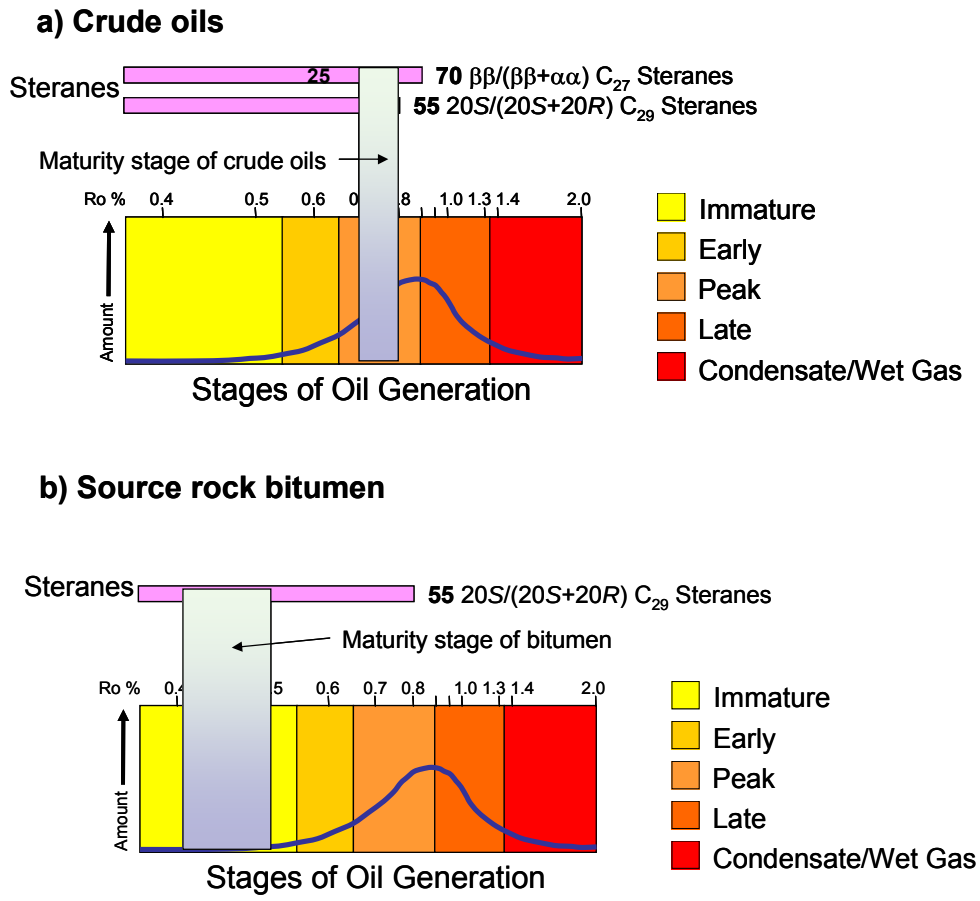

Fig 25 Biomarker maturation parameters are shown versus vitrinite reflectance and a generalized oil generating curve for a) Italian crude oils, and b) source rock bitumen from Italy (based on Mackenzie (1984), Peters et al. (2005))

Hopanes and steranes for oil - source rock correlation

Ternary plots of sterane carbon number are often used to facilitate oil–oil and oil–source rock correlation and to provide a general comparison of depositional environments (Peters *et al.*, 2005). Fig 26 shows the distribution of αααC_{27}, C_{28} and C_{29} steranes in crude oils and source rock bitumen. The ααα C_{28} sterane was not detected in all source rock bitumen, which might be indicative of a very low input of diatoms and haptophyceae algae (Volkman, 1986), or more likely, it might be related to the C_{28} sterane being absent in specific evaporitic environments (Albaigés *et al.*, 1986; Quesada *et al.*, 1997). However, crude oils differ from most bitumen in that they show higher amounts of αααC_{29} sterane, which is normally attributed to land plant organic matter (Peters *et al.*, 2005). Matsumo *et al.* (1982) and Fowler and Douglas (1987) mentioned that C_{29} steranes could also derived from cyanobacteria, which types more to the common nature of the studied oils. But, it is notable that crude oils with higher API (19° – 33°) show also higher contents of C_{27} sterane (~ 40%), indicating a more algal source for these oils (Volkman, 1986).

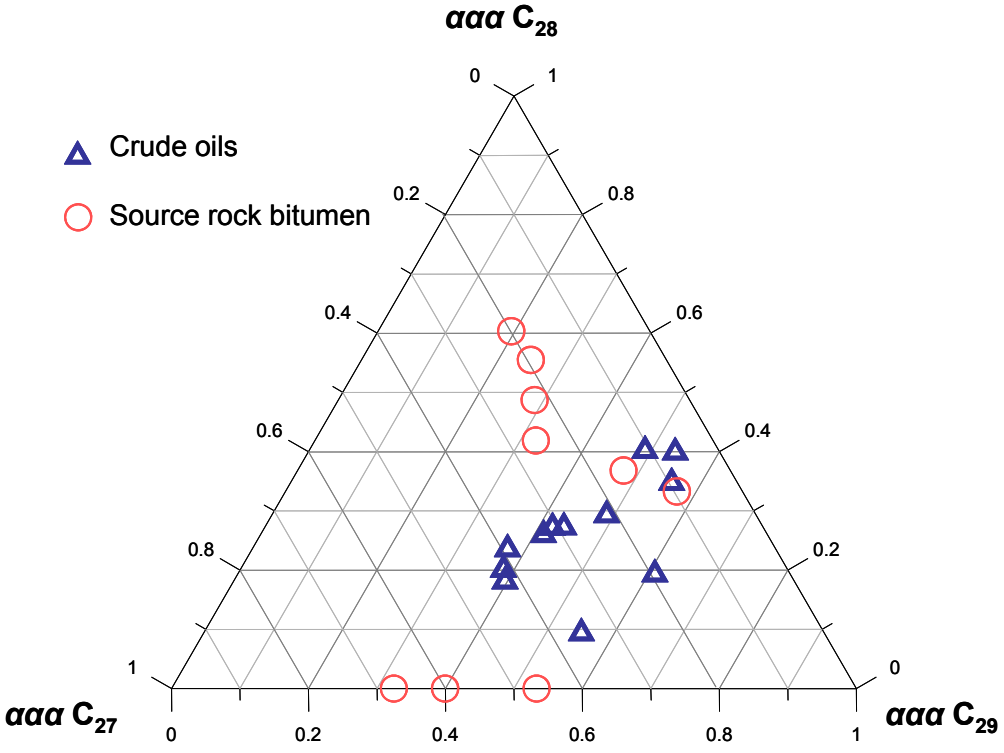

Fig 26 Ternary plot showing sterane composition of crude oils and source rock bitumen for Italian samples.

As it can be seen from Fig 26 the distribution of αααC_{27}, C_{28} and C_{29} steranes do not provide any facial relationship neither within the crude oils and source rock bitumen nor between the oils and bitumen.

The high contents of methylsterane and dinosterane in Italian crude oils and bitumens are also remarkable, indicating a strong organic input of dinoflagellates and bacteria (Robinson *et al.*, 1984; Chen and Summons, 2001; Zhang *et al.*, 2003; Peters *et al.*, 2005). Methylsteranes and dinosteranes are commonly cited to be indicative of lacustrine depositional environments (Summons *et al.*, 1987; Summons *et al.*, 1992; Meyers and Ishiwatari, 1993; Hanson *et al.*, 2000; Chen and Summons, 2001; Holba *et al.*, 2003; Zhang *et al.*, 2003). Other depositional palaeoenvironments for the occurrence of these sterane-types were given by Hofmann *et al.* (1993) and Schaeffer *et al.* (1995), who referred the presence of dinoflagellates in this type of palaeoenvironment to marine waters with a moderate salinity. The functionalized precursors dinosterol and dinostanol for dinosteranes (Withers, 1983) are present in marine as well as in non-marine dinoflagellate species (Curiale, 1987; Summons *et al.*, 1987; Peters *et al.*, 2005). Jiamo *et al.* (1990) have shown that bitumens from source rocks deposited under hypersaline conditions contain less C_{28} vs. C_{29} methylsteranes compared to brackish lacustrine environments, which is attributed to species differences in different environments. The dominance of C_{29} methylsteranes was also found in the studied samples from S-Italy, which would type to dinoflagellates of a more marine-like species. Crude oils as well as source rock bitumens contain high amounts of gammacerane (*m/z* 191), which represents a marker for highly saline depositional environments (ten Haven *et al.*, 1989), and a reducing palaeoenvironment in a stratified water body where the source rock was deposited (Moldowan *et al.*, 1985; Mello *et al.*, 1988; Connan and Nissenbaum, 2004). The functionalized precursor tetrahymanol of gammacerane is found in several species of the protozoan *Tetrahymena* (ten Haven *et al.*, 1989; Venkatesan, 1989), as well as in anaerobic purple bacteria, like for

example *Rhodopseudomonas palustris* (Kleemann *et al.*, 1990). The widespread presence of gammacerane in the studied samples may therefore be related to one or both of these organisms.

Fig 27 shows a plot of the ratio $\alpha\alpha\alpha C_{29}$ / $\alpha\alpha\alpha(C_{27}+C_{28}+C_{29})$ versus the gammacerane index for Italian oils and source rock bitumen. Here, it is obvious that the less degraded crude oils show a relationship of $\alpha\alpha\alpha C_{29}$ / $\alpha\alpha\alpha(C_{27}+C_{28}+C_{29})$ and the gammacerane index, indicated by decreasing of % $\alpha\alpha\alpha C_{29}$ with increasing values for the gammacerane index.

Only two crude oil samples presented in Fig 27 differ from the other oil samples. The samples G000401 (API 33.5°) and G000394 (API 2.62°) show lower indices for gammacerane, and both samples can be considered to be sourced from an different environment, even if a biodegradation effect on the gammacerane index of sample G000394 cannot be excluded. Source rock bitumen, however, do not show a clear relationship of the facies parameter presented in Fig 27, which might be a result of strong facies variations. Only the sample G000661 is definitely an exception. Most biomarker distributions for this sample do not correspond to the other samples, which suggest that sample G000661 is not related to the same source rock facies preserved in the other studied samples. This sample shows highest indices for gammacerane and homohopanes than other source rock samples. Aromatic biomarkers like methylphenanthrenes are also enriched in this sample.

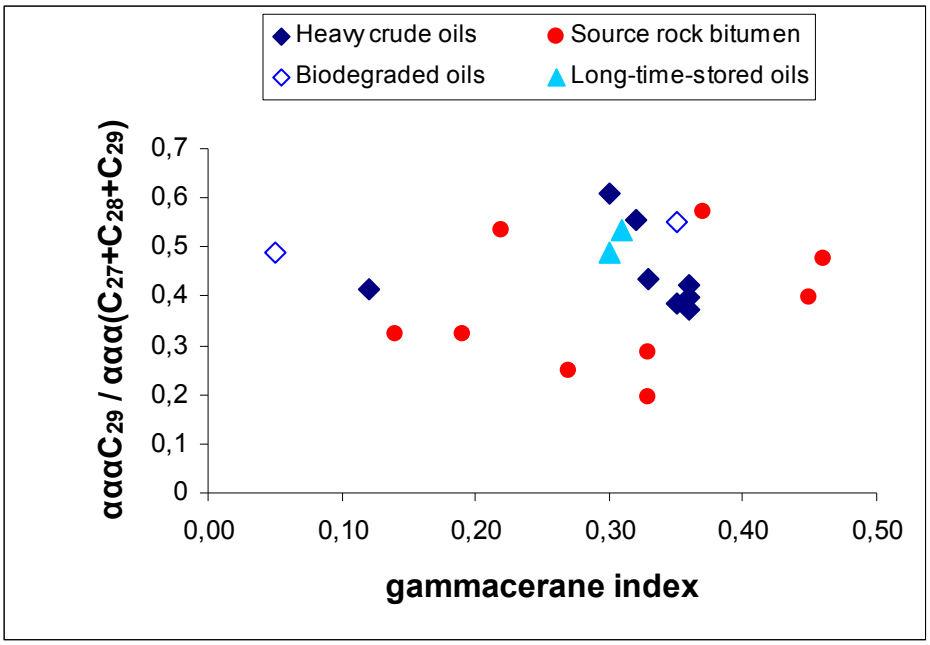

Fig 27 Plot of ααα C_{29} / ααα (C_{27}+C_{28} +C_{29}) versus the gammacerane index for Italian oils and source rock bitumen

5.1.2.3 Light hydrocarbons

Light hydrocarbon parameters are useful for determining oil groups, oil/source rock correlations and influence of source lithofacies (Thompson, 1983, 1988; Mango, 1990; Thompson and Kennicutt, 1990; Mango, 1994; Halpern, 1995; ten Haven, 1996; Jarvie *et al.*, 1997; Odden *et al.*, 1998; Magnier and Trindade, 1999; Wever, 2000; Dieckmann *et al.*, 2002; Cañipa-Morales *et al.*, 2003).

Light hydrocarbons as well as oil asphaltenes were reported to be utilized for providing information concerning source rock facies (Horsfield *et al.*, 1991; ten Haven, 1996; di Primio *et al.*, 1998; di Primio *et al.*, 2000; Nali *et al.*, 2000; Dieckmann *et al.*, 2002). Dieckmann *et al.* (2002) used bulk kinetic analysis of oil asphaltenes and light hydrocarbon analysis to evaluate expulsion temperatures. The authors reported that calculated expulsion temperatures from light hydrocarbons and asphaltene kinetics show an inverse trend, which they referred to different expulsion behaviour of light hydrocarbons and the heavy fractions of oils. Thus, in cumulative petroleum systems, in which low and high maturity charging controls petroleum composition, asphaltene and light hydrocarbon characteristics best reconstruct the full expulsion history.

Fig 28 illustrates two different light hydrocarbon plots for studied Italian oils in order to characterize oils in term of maturity and possible biodegradation. Fig 28 a shows the plot of heptane / iso-heptane values established by Thompson (1983). These values are the principle indices of paraffinicity (Thompson, 1983), with a heptane value = (2-methylhexane + 3-methylhexane) / (1,cis-3-dimethylcyclopentane + 1,trans-3-dimethylcyclopentane + 1,trans-2-dimethylcyclopentane). The isoheptane value is calculated as followed:

Isoheptane value = 100.0 x *n*-heptane / (cyclohexane + 2-methylhexane + 1,1-dimethylcyclopentane + 3-methylhexane + 1,cis-3-dimethylcyclopentane + 1,trans-3-dimethylcyclopentane + 1,trans-2-dimethylcyclopentane + *n*-heptane + methylcyclohexane).

The studied heavy oils in Fig 28a spread from mature to supermature zones in this diagram and display an unusual distribution of light hydrocarbon parameters, which would be more related to high mature or supermature crude oils, whereas the common maturity parameters based on biomarkers suggest a lower maturity for these oils. The paraffinicity values calculated from light hydrocarbons do not reflect the low mature characteristics of the studied oils. As well, the oils do not fallow the trend of increasing paraffinicity values with increasing maturity proposed by Thompson (1983). The lowest paraffinicity indices I and H, according to Thompson, were monitored in the long-time-stored oil (G000404), and the mature crude oil G000401 (33.5° API). The most mature oil sample G000401 has a heptane value of 12.5, and an isoheptane value of 1.8, and plot therefore in the field of mature crude oils. Even, if this reflects the characteristics of the studied oil, it is incongruently to a trend of paraffinicity and maturity for the sample set. Interestingly, the two biodegraded oil samples show extraordinary high heptane and isoheptane values, and do not reflect to have experienced biodegradation. Both biodegraded oils contain relative high amounts of *n*-heptane, and of 2- and 3-methylhexane compared to their other light hydrocarbon, which strongly influence the values of paraffinicity H and even more paraffinicity I (Thompson, 1983).

Galimberti *et al.* (2003) have shown that light hydrocarbons in oils formed from carbonate source rocks do not give reliable maturity indications, because of the unusual formation of C_7 light hydrocarbons from carbonate source rocks. Galimberti *et al.* (2003) explained this anomalous behaviour of light hydrocarbons based on MSSV experiments, in that carbonatic source rocks are able to produce high concentrations of *n*-C_7 in the first phase of oil generation, and that a decrease of *n*-C_7 concentrations, and therefore a decrease in the paraffinicity occurs during increasing maturity. This may lead to an overestimation of oil maturity of the oils like observed for this sample set.

Fig 28 b illustrates the light hydrocarbons characteristics of the Italian oils based on the ratios of toluene / *n*-heptane (aromaticity) and *n*-heptane / methylcyclohexane (paraffinicity) after

Thompson (1988) and Cañipa-Morales *et al.* (2003). These ratios are used to determine alteration processes such as evaporative fractionation, water washing, incipient biodegradation, and maturity. As well in Fig 28b light hydrocarbon parameters do not reflect the common trend of maturity. The mature crude oil G000401, as well as the long-time-stored oil G000404, show lowest ratios and plot in the field of biodegradation. The biodegraded samples instead fall in the field of water washing (G000393), or show an unusual ratio for aromaticity (G000394). It has to be mentioned that sample G000394 with 2.62° API show strong biodegradation of even light hydrocarbons. Light hydrocarbons in this strongest degraded sample are virtually absent or occur in too low concentrations for reasonable quantification. Thus this sample plots far away from other samples and reflect an unusual aromaticity value.

The low maturity oil samples G000402 (8.5° API), G00397 (9° API), and G000396 (11.5° API) fall in the field of water washing due to relative high contents of *n*-C_7 compared to methylcyclohexane. More mature oils with API´s of 19.35° plot in the field of the original oils. This reflects the same inversed maturity trend like observed for the heptane / isoheptane values, which was explained by Galimberti *et al.* (2003) by high concentrations of *n*-C_7 in the first phase of oil generation. Low mature oils show highest paraffinicity based on the ratio of *n*-heptane / methylcyclohexane, and the sample with highest maturity show lowest ratio and fall even in the field of biodegradation of Fig 28 b.

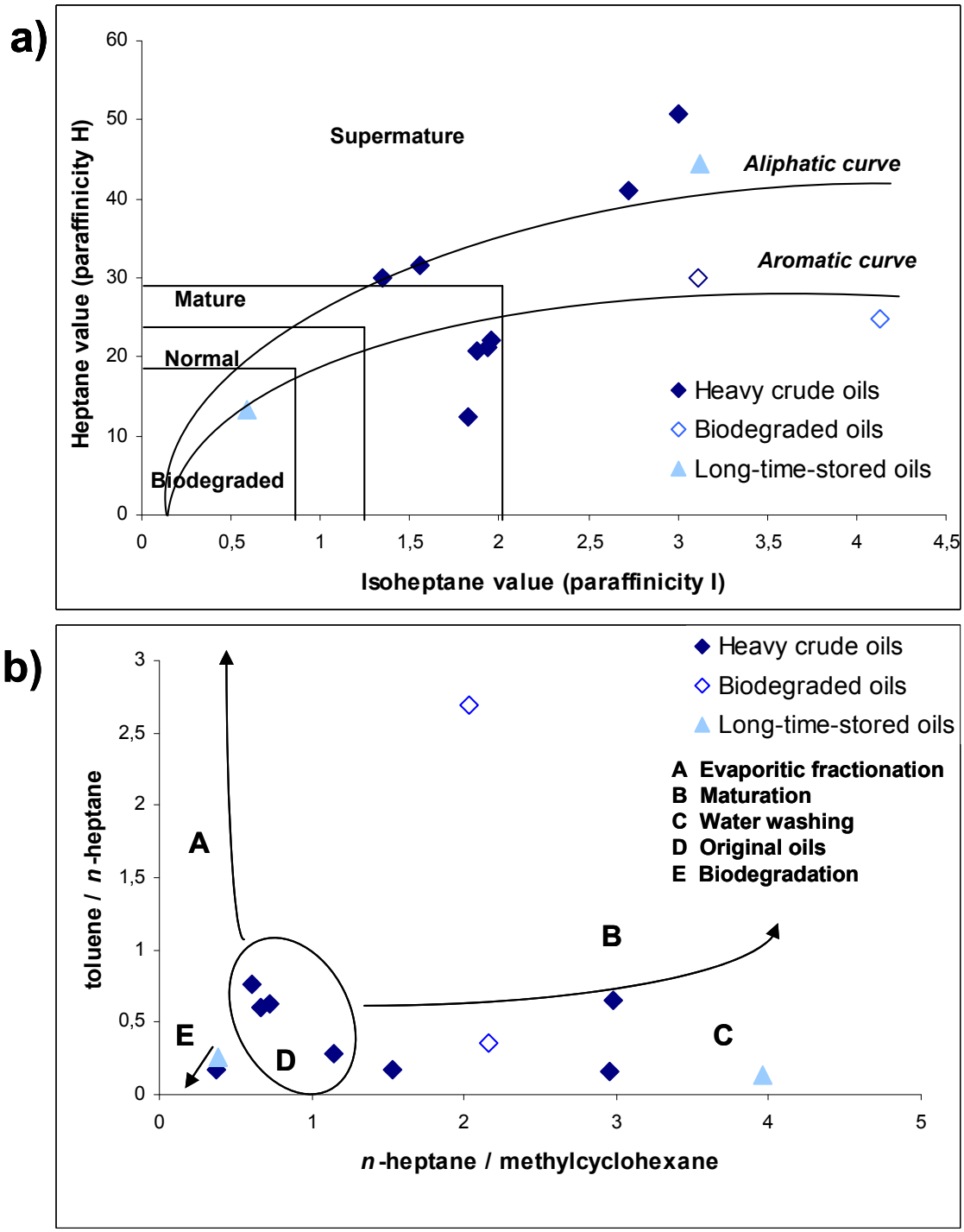

Fig 28 a) The cross plot of paraffinicity H versus paraffinicity I ratio for all investigated crude oils from South Italy (after Thompson (1983)). b) Investigated Italian oils in terms of aromaticity versus paraffinicity (after Talukdar and Dow (1990); modified by Cañipa-Morales *et al.* (2003)).

Fig 29 shows the ratio of paraffinicity F (*n*-heptane / methylcyclohexane) after Thompson (1988) versus the API gravity of Italian crude oils. Here, it is evident that heavy crude oils show decreasing *n*-heptane / methylcyclohexane ratio with increasing API gravity, which is inverse to the paraffinicity index established by Thompson (1983; 1988). Biodegraded and long-time-stored oils do not correspond to the observed trend, probably due to alteration effects.

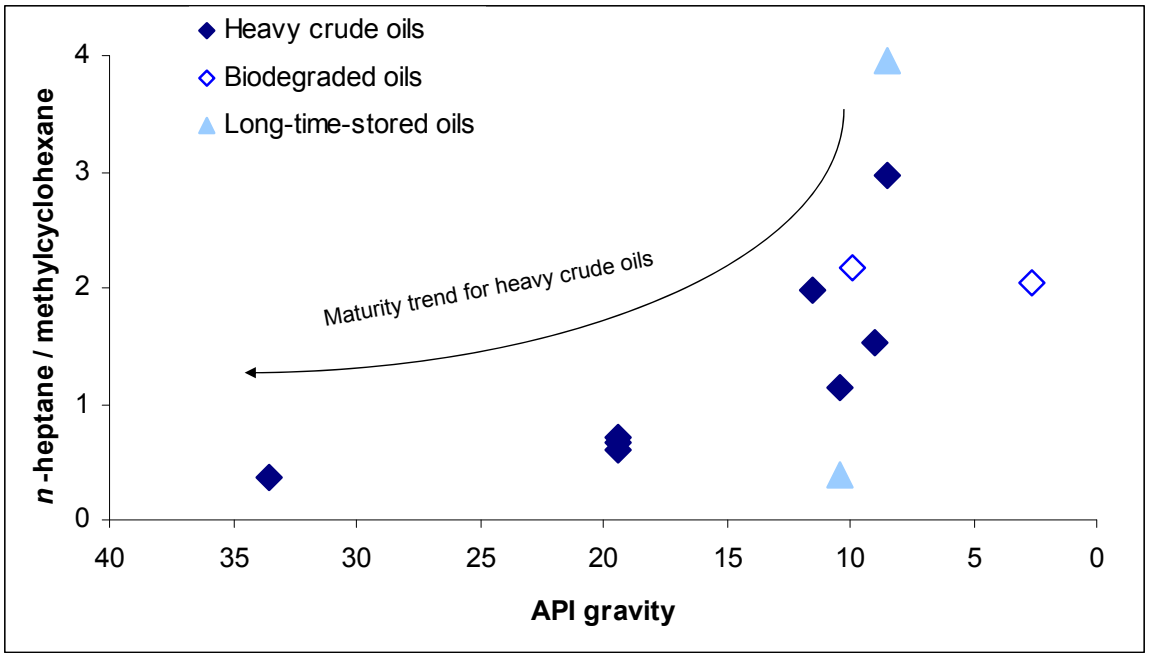

Fig 29 The ratio of paraffinicity F (*n*-heptane / methylcyclohexane) after Thompson (1988) versus the API gravity of Italian crude oils.

5.1.2.4 Long-time storing

Storage effects have a strong impact on the chemical oil composition, especially for light hydrocarbons (Devai *et al.*, 2001; Bastow *et al.*, 2003; Cañipa-Morales *et al.*, 2003). In our study the storage effect strongly influences the characteristics of light hydrocarbons with stored oils (G000403 and G000404) being enriched in 2- and 3-methyl-hexane relative to their fresher equivalents (G000402 and G000395). Fig 30 shows the light hydrocarbon ratios of 2-methylhexane plus 2,3-dimethylpentane versus 3-methylhexane plus 2,4-dimethylpentane established by Mango (1990). All the studied oils fit to a straight line confirming the similar origin of the oils.

In this plot it can be seen that the storage effect strongly influences the characteristics of light hydrocarbons with stored oils being enriched in methylhexanes relative to their fresher equivalents. This phenomenon has also been reported by Cañipa-Morales *et al.* (2003), who studied the effect of evaporisation on the C_{7+} fraction systematically. The authors suggest that methylhexanes are not grossly affected by incipient evaporation or storage effects.

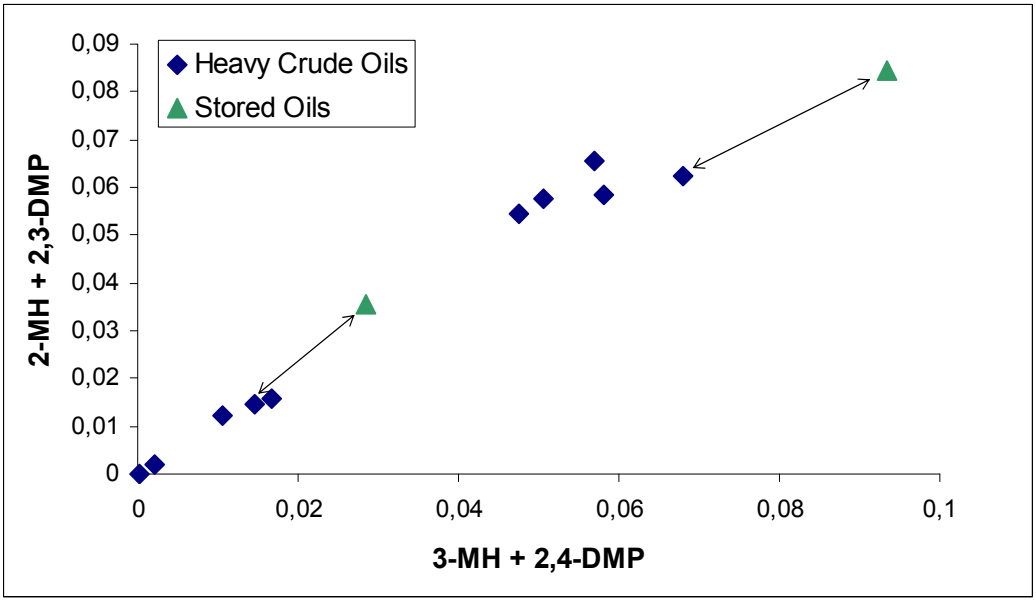

Fig 30 Light hydrocarbon ratios of 2-methylhexane plus 2,3-dimethylpentane versus 3-methylhexane plus 2,4-dimethylpentane established by Mango (1990) for stored oils and fresher crude oils from Italy. Arrows mark the stored oils with their fresher counterparts.

The long-time-stored crude oils G000403 and G000404 were sampled in 1960 and 1963. Nevertheless, it also has to be considered that stored oils are enriched in all light hydrocarbons, but depleted in asphaltene content and as well they show lower % of hump by whole-oil analysis relative to their fresher equivalents (Fig 19). The reason for that might be a possible gravitational fractionation in the storing container resulted in an enrichment of light hydrocarbons in the upper part of the container.

Also, alterations in the *n*-alkane hydrocarbon composition of long-time stored oils have been observed. These consist in the depletion of the alkanes in the range of *n*-C_8 - *n*-C_{14}, and an increase of *n*-alkane higher than *n*-C_{16} compared to the fresher oil. Alterations in the hydrocarbon composition during storage were found by Grimalt *et al.* (1988) of recent sediments. The authors attributed aerobic microbial reworking to be responsible for these changes. The storage effect on studied oils has also influenced some biomarker distributions, like previously presented.

However, beside these differences between long-time-stored oils and their fresher counterparts, their asphaltenes are very similar in terms of structural moieties investigated by open-system-pyrolysis. Minor differences were observed for the distributions of some aromatic hydrocarbons and some alkylthiophenes, which are mostly within the standard deviation of the technical method. An investigation using open-system-pyrolysis GC-MS showed more minor differences in that stored oils show lower concentrations of some cycloalkenes. This was best observed for methylcyclopentadien, which normally is known from industrial pyrolysis of coal tar, and which arise from decomposition of polyaromatic structures (Schmid *et al.*, 1948; Bäuml and Mayr, 1985; Roy, 1999), or from thermal degradation of phenols (Spielmann and Cramers, 1972). But, since most of these minor differences are within the standard deviation of the technical method the asphaltene pyrolysates from long-time-stored oils can thus be used for oil-source correlations, like for example prediction of depositional environment.

5.1.2.5 Biodegradation

Biodegradation is an alteration phenomenon caused by bacteria, the metabolic activity of which is well developed in the presence of nutrient-enriched waters and temperatures not exceeding 80-85°C (Peters *et al.*, 2005). Biodegradation of oil (C_{6+} components) leads to a decrease in saturated hydrocarbon content and API gravity, to a smaller decrease in aromatic hydrocarbons, and an increase of sulphur and metal content, oil density, acidity and viscosity (Volkman *et al.*, 1984; Rowland *et al.*, 1986; Palmer, 1993; Meredith *et al.*, 2000; Taylor *et al.*, 2001; Head *et al.*, 2003; Larter *et al.*, 2003).

The two oils (G000393 and G000394), which have experienced biodegradation have extremely low API gravities with 9.9° and even 2.64°, respectively. Both biodegraded oils differ significant in the alkane distribution and in the hump compared to less biodegraded samples. Fig 31 shows the GC-chromatogram of the biodegraded sample with an API of 9.9° (sample G000393). The oil has still some amounts of light hydrocarbons, and a distinctly high content of unresolved compounds. The *n*-alkanes higher than *n*-C_{22} are biodegraded in this oil. In contrast to that the oil with 2.62° API (sample G000394) shows even depletion in light hydrocarbons most probable due to intensive biodegradation or evaporation fractionation. Biodegradation of light hydrocarbons is well known and stated in various articles (James and Burns, 1984; Horstad and Larter, 1997; Boreham *et al.*, 2001). It is difficult to mention the extent of biodegradation for these oils, due to the present of *n*-alkanes in the range of *n*-C_6-*n*-C_{22}. Following the common scale of Peters *et al*. (2005) these oils would be termed to be moderate biodegraded due to their alkane distribution. Whereas the fact of degraded hopanes in those oils point to a heavy or very heavy rank of biodegradation (Peters *et al.*, 2005). As well the fact of such high contents of unresolved complex components situated in the GC-hump is also contradictory to a moderate biodegradation. The presence of *n*-alkanes in these oils is probably to lead back to a recharge of fresher oil in the reservoir, which is not yet or still not totally degraded. Also, a diesel contamination during production may lead to higher

n-alkane amounts in the whole-oil analysis. This of course leads to a misconclusion of degradation extent when using common biodegradation scales.

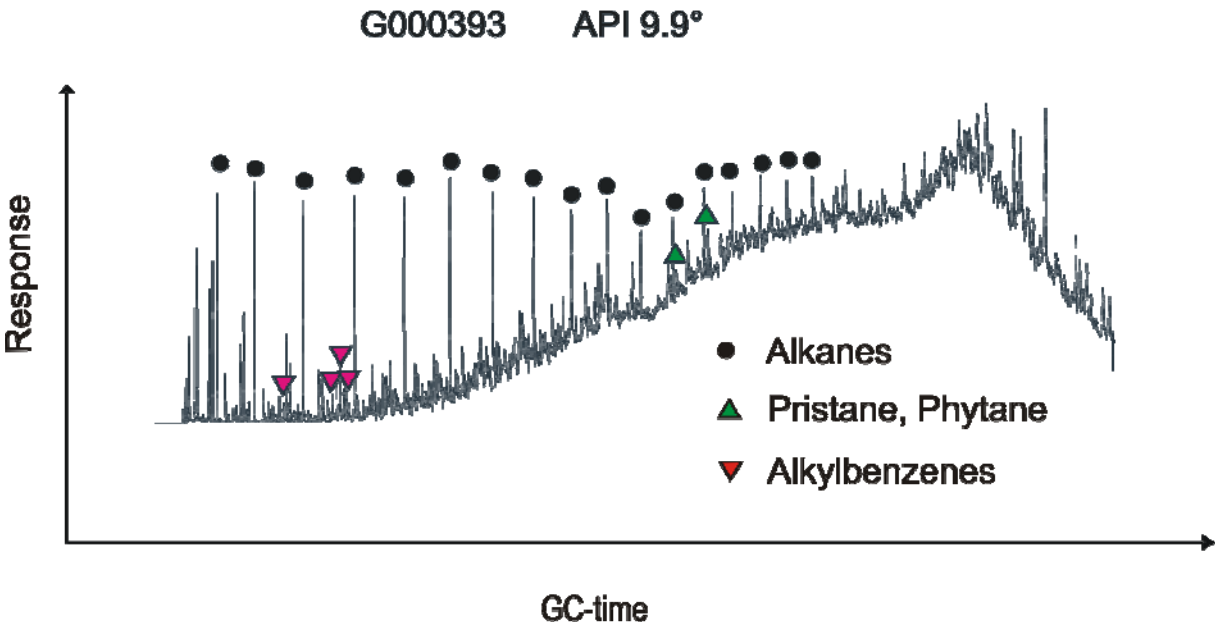

Fig 31 Thermovaporisation GC traces of one biodegraded Italian oil sample. Alkanes from *n*-C_6, pristane and phytane, as well most abundant alkylbenzenes are marked. Benzenes are corresponding to retention time from left to the right: toluene, ethylbenzene, m,p-xylene, and o-xylene.

Moreover, in the biomarker chapter 5.1.2.3 it was shown that the biomarker parameters Ts/(Ts+Tm) and C_{29}Ts index show a trend of biodegradation when plotted versus the API gravity of the oils (Fig 23). In order to investigate a probable degradation of C_{27} 18α(H)-trisnorhopane II (Ts) and C_{29} 18α-(H)-30-norneohopane (C_{29}Ts) the related biomarker parameters from Fig 23 were plotted versus the % of GC unresolved compounds (hump), shown in Fig 32. Here it is additionally evident that both biomarker parameters a grossly affected by biodegradation, because the cross-plots of these biomarkers versus the hump results in a decreasing trend of biomarker ratio proportionally with increasing % of GC-hump, which can only be explained in that both, ratio of biomarker parameter and hump, are associated with biodegradation. The sample G00394 with an API of 2,62° shows highest

percentage of GC-hump and lowest values for Ts/(Ts+Tm) and C_{29}Ts index due to degradation effects, whereas the ratio of 20*S*/(20*S*+20*R*) of C_{29}-sterane for the same sample is higher than for the most of the Italian crude oils. As well, in Fig 32 long-time-stored oils are somewhat different, because of lower % of GC-hump compared to fresher counterparts.

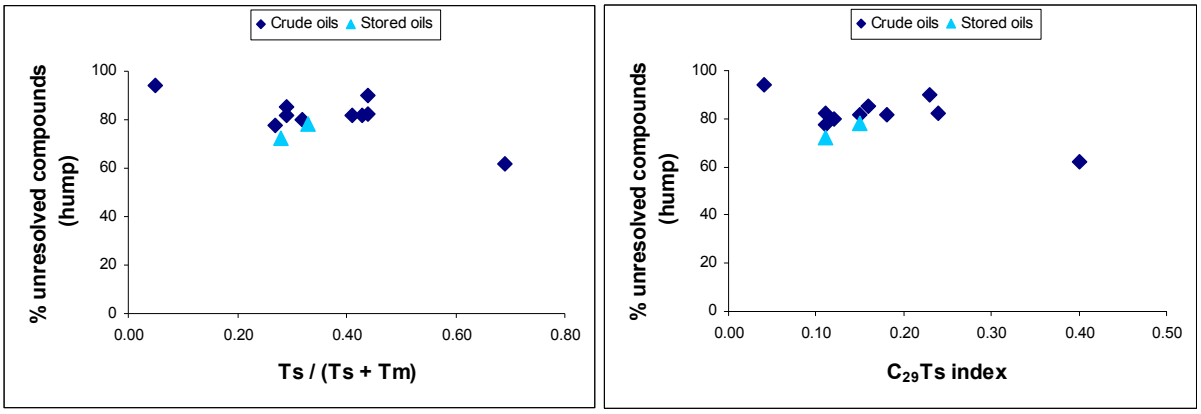

Fig 32 Biomarker parameters Ts/(Ts+Tm) (left) and C_{29}Ts index (right) versus % of GC unresolved compounds (hump) for Italian crude oils

5.1.2.6 Discussion on evidence of anaerobic biodegradation

The biodegradation of oils in the subsurface at oil/water contacts is generally contributed to aerobic bacteria (Peters *et al.*, 2005). However, several works demonstrated anaerobic biodegradation of oils in nature (Stetter *et al.*, 1993; Bodrossy *et al.*, 1995; Beeder *et al.*, 1996; Nilsen *et al.*, 1996; Nilsen and Torsvik, 1996; Connan *et al.*, 1997; Zengler *et al.*, 1999; Wilkes *et al.*, 2000). Jobson *et al.* (1979) had already before shown that sulphate-reducing bacteria are able to grow on oils even when pre-incubated with aerobic bacteria. Sulphate reduction in oil reservoirs may occur for example when sulphate-rich sea waters are injected in the reservoir during secondary oil production. Depletion of *n*-alkanes in crude oils under sulphate-reducing conditions have been reported for natural systems as well as in incubation

experiments (Aeckersberg *et al.*, 1991; Rueter *et al.*, 1994; Coates *et al.*, 1997; Caldwell *et al.*, 1998). Other works reported the degradation of monoaromatic hydrocarbons under sulphate-reducing conditions (Coates *et al.*, 1997; Reinhard *et al.*, 1997; Zhang and Young, 1997), especially for the degradation of benzenes coupled with sulphate reduction (Lovley *et al.*, 1995; Rabus and Widdel, 1995; Rabus and Heider, 1998; Harms *et al.*, 1999; Wilkes *et al.*, 2000). Wilkes *et al.* (2000) have demonstrated the depletion of alkylbenzenes by sulphate-reducing δ-protobacteria of crude oils from the North Sea. The authors isolated two pure cultures, strain oXyS1 and strain mXyS1, and showed that strain oXyS1 preferentially depletes o-xylene and o-ethyltoluene, while protobacteria mXyS1 depletes m-xylenes and m-ethyltoluene. This was also mentioned as specific indicator of initial biodegradation (Wilkes *et al.*, 2000). Fig 33 shows the ratio of o-xylene/(m,p-xylene + o-xylene) versus the API gravity for the crude oils from Southern Italy. The ratio of o-xylene/ Σ xylenes decreases with decreasing API gravity. This would in terms of biodegradation indicate ongoing depletion of o-xylene, probably by similar δ-protobacteria like strain oXyS1, with increasing biodegradation. The xylenes in the strong biodegraded sample G000394 (2.62° API) are virtually absent. The xylene distribution of the oils is thus an evidence for anaerobic biodegradation, since the observed trend refer to oils over a broader API range from 2.6-33.5°. Therefore, this ratio might be also a possible tool to characterize the extent of biodegradation for crude oils from this petroleum system.

Wilkes *et al.* (2000) noticed also that these δ-protobacteria had utilized toluene as well. The sample set of crude oils from Italy do not show any trend of toluene with the API gravity, but the relative low content of toluene in these crude oils in comparison to petroleum from other reservoirs might be a result of initial biodegradation as well.

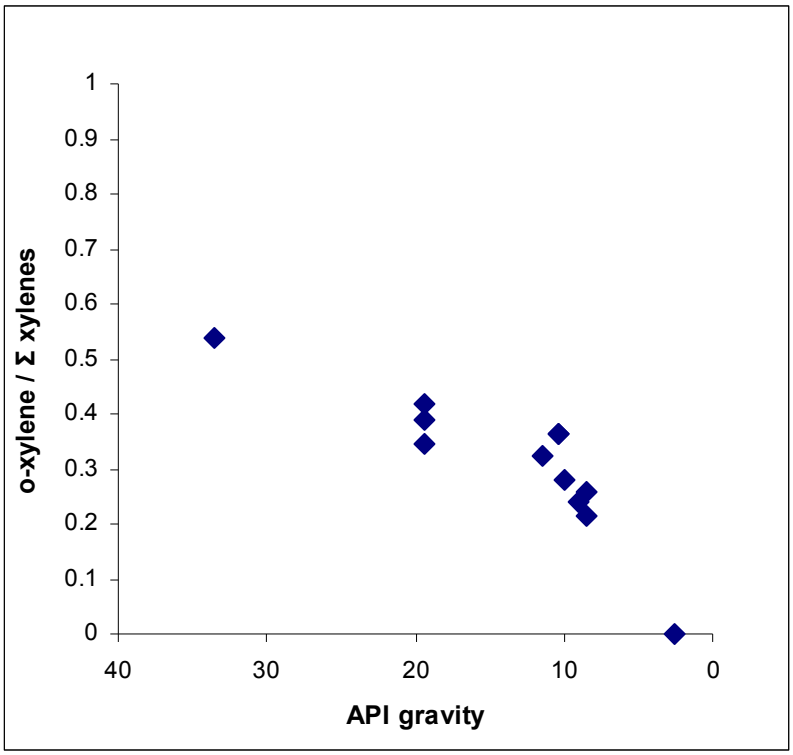

Fig 33 Diagram with the ratio of o-xylene/(m,p-xylene + o-xylene) versus the API gravity for the crude oils from Southern Italy, indication for a depletion of o-xylene due to microbial degradation.

Beside, closed-system maturation experiments on asphaltenes from those crude oils showed as well an increasing ratio of o-xylene/(m,p-xylene + o-xylene) with increasing thermal stress. Thus, the trend observed in Fig 33 might be in part also be related to maturity, at least for the samples with an API between 19° and 33.5°.

For understanding the extent of the observed anaerobic biodegradation it might thus be useful to compare the xylene distribution of oils with them of asphaltenes isolated from those oils. Asphaltenes provide informations about the original composition of degraded oils (Rubinstein *et al.*, 1979; Magnier and Huc, 1995), and it is generally established that asphaltenes are most resistant to microbial metabolism (Magnier and Huc, 1995; Mana Capelli *et al.*, 2001; Chaillan *et al.*, 2004).

Thus, for further studies asphaltenes isolated from crude oils have been studied systematically using open-system pyrolysis-GC. Fig 34 shows the ratio of o-xylene/(m,p-xylene + o-xylene)

versus the API gravity for Italian crude oils in comparison with the ratio of related asphaltene pyrolysates.

From this plot it is evident that reservoir asphaltenes do not show the same trend like observed for the crude oils. First, this shows that oils have experienced strong compositional changes due to anaerobic biodegradation, at least for their xylenes.

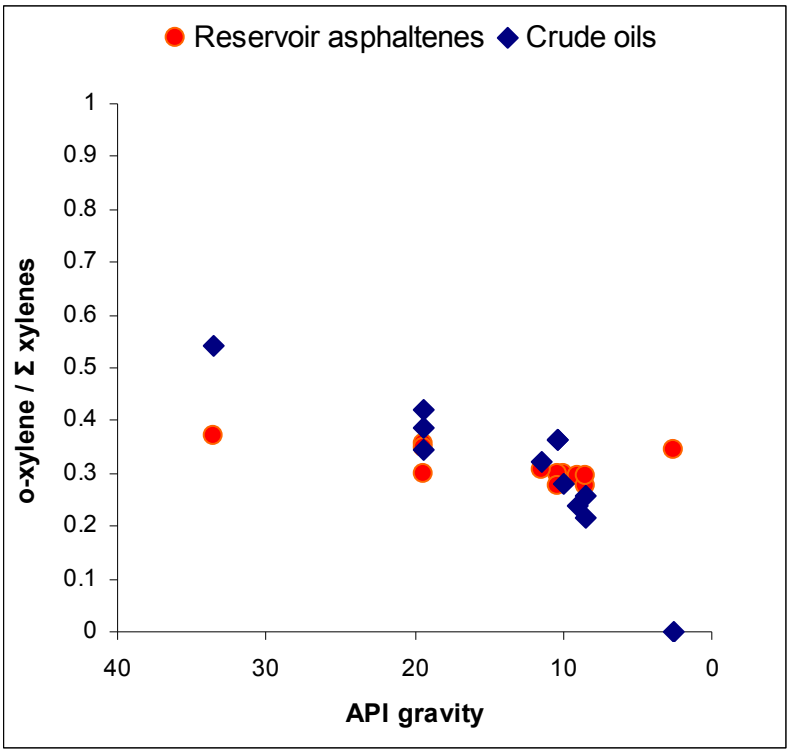

Fig 34 Ratio of o-xylene/(m,p-xylene + o-xylene) versus the API gravity for Italian crude oils and related asphaltenes.

The stored oils and their asphaltenes are not significant different in their xylene distribution compared to their fresher counterparts. This explains that stored and fresher oils do not have a different extent in the anaerobic biodegradation, and thus storage is not one of the factors which influence the observed anaerobic biodegradation.

Unexpectedly, in the range between 33.5 and 9° API the asphaltene pyrolysates show a very slightly decreasing o-xylene ratio with decreasing API gravity. This is somewhat surprising, and queries at first sight the recalcitrance of asphaltenes to biodegradation. But, the respective oil of the asphaltene plotted at 33.5° API was based on biomarkers supposed to be of a

different oil subfamily. It might therefore be more probable that this asphaltene shows a higher xylene distribution, because of compositional differences between those oil subfamilies. This is supported by the asphaltene isolated from oil with 2.62° API from that same oil subfamily. This asphaltene shows the same xylene ratio as the asphaltene from the mature oil with 33.5° API. As well, both samples show highest maturity based on the ratio of 20*S*/(20*S*+20*R*) of C_{29}-sterane, which support as well higher ratios of o-xylene/(m,p-xylene + o-xylene) with increasing thermal stress. The slighter variations in the xylene distribution within the asphaltenes are hence related to compositional variations within the oil subfamilies or thermal maturity and not to biodegradation.

Beside, asphaltene biodegradation is up to day only known, when induced by men, like for example the bioremediation of asphaltenes in oil contaminated soils or waters, using either a pure biological (microbes and fungi) or a combined chemical, biological (oxidizer and microbes) treatment (Rontani *et al.*, 1985; Venkateswaran *et al.*, 1995; Thouand *et al.*, 1999; Kanaly and Harayama, 2000; Balba *et al.*, 2003; Gallego *et al.*, 2006). Rontani *et al*. (1985) were among the first, who studied biodegradation of asphaltenes. They have demonstrated that asphaltenes from Asthart crude oils from the Gulf of Gabes, Tunisia, can be degraded by the metabolic activity of microorganisms isolated from sediments polluted with hydrocarbons from an outlet of a refinery.

As well, it was published that asphaltene biodegradation can occur within the well bore. Pineda-Flores *et al*. (2004) isolated a microbial consortium capable of degrading asphaltenes from one Mexican Maya crude oil. This Maya crude oil sample was obtained from the Blasillo-61 oil well, which is unique for his conditions in terms of salinity and pH.

Premuzic and Lin (1999) and Margesin and Schinner (2000) presented studies of biodegradation under simulated oil well conditions. The authors mentioned that the well bore offers best conditions for biodegradation due to the presence of high-saline waters, higher temperatures and high pressures, and acidic or alkaline pH. Organisms exposed to asphaltenes

during long periods may than have the ability to degrade them (Margesin and Schinner, 2000). Kampfer *et al*. (1993) published that well bores are commonly less dominated by different bacterial populations, depending on environmental conditions, but more by fungi, yeasts, moulds and actinomycetes. Nevertheless, an asphaltene biodegradation occurring naturally and in reservoir is yet not known.

For the studied oils from Southern Italy, it is unlikely that the observed anaerobic biodegradation is associated with the microorganisms living in the well bore, because studied oils are obtained from three different oil wells. In addition, for production the well bore is aerated directly by air injection. This technique promotes rather aerobic than an anaerobic biodegradation (Zekri and Chaalal, 2005).

5.1.2.7 Conclusions

The crude oils from Southern Italy are unusual in terms of their biomarker parameters, light hydrocarbons, as well of their biodegradation.

- Crude oils and source rock bitumens show different levels of thermal maturity based on biomarker maturity parameters. Less degraded and non stored oils demonstrate an early stage of thermal maturity using the parameters C_{27} $\beta\beta/(\beta\beta+\alpha\alpha)$ and C_{29} 20*S*/(20*S*+20*R*), whose values correspond to an vitrinite reflectance value of 0.7 – 0.8 Ro %. Bitumen show an immature stage of maturity, corresponding to a vitrinite reflectance of 0.4 – 0.5 Ro %.
- Biomarker parameters for oil-source correlation do not show a clear relationship between crude oils and source rocks. But, the unusual high concentrations of gammacerane and dinosteranes in oils and bitumens point to a similar origin. Additionally, based on these parameters the crude oils G000394 (API 2.62°) and G000401 (API 33.5°) are probably not part of the same oil subfamily than the other

crude oils. As well, the source rock sample G000661 differs in most biomarker parameters from the other samples.

- Light hydrocarbon parameters for the crude oils from Southern Italy do not reflect low mature characteristics of studied oils. The low mature, heavy oils show an overestimation of oil maturity based on Thompson´s light hydrocarbon parameters, due to high concentrations of *n*-C_7 in the first phase of oil generation (Galimberti *et al.*, 2003). Light hydrocarbon compositional characteristics such as aromaticity and paraffinicity can therefore later not be compared directly to compositional characteristics of asphaltene pyrolysates.
- Long-time storing affected strongly the characteristics of light hydrocarbons with stored oils being enriched in 2- and 3-methylhexane relative to their fresher equivalents. The storage effect on studied oils has also influenced biomarker maturity parameters and the *n*-alkane distribution resulting in the depletion of the alkanes in the range of *n*-C_8 - *n*-C_{14}, and an increase of *n*-alkane higher than *n*-C_{16} compared to the fresher oil.
- Asphaltenes isolated from stored oils and isolated from related fresher oils show minor differences for total yields of some cycloalkenes investigated by open-system-pyrolysis, but are generally within the standard deviation of the technical method. Thus the pyrolysates of asphaltenes isolated from long-time-stored oils can be used for oil-source correlations.
- Low API crude oils from Southern Italy are affected by biodegradation, indicated by an unusual high % of GC-unresolved compounds (hump), depletion of certain alkanes and even of light hydrocarbons. For the studied Italian oils the biomarker parameters Ts/(Ts+Tm) and C_{29}Ts index are grossly affected by microbial metabolism. As well, an anaerobic biodegradation is indicated by the ongoing depletion of o-xylene with decreasing API gravity for these oils.

5.2 Duvernay Petroleum System (WCSB)

5.2.1 Source rock screening

The Duvernay Formation provides a well-known petroleum system on the basis of research reported in literature (Requejo *et al.*, 1992; Creaney *et al.*, 1994). The Duvernay Formation is known as a homogeneous depositional environment of marine organic matter. The potential for petroleum generation for the Duvernay Formation is provided by Rock-Eval analysis. Table 6 provide relevant Rock-Eval data for Duvernay source rocks, previous investigated by Dieckmann (1998). The TOC of studied rocks varies from 0.61 to 14.8%. Hydrogen indices (HI) for the studied source rocks range from 631 to 14 mg HC/g TOC. These are associated with an increase in thermal maturity indicated by Tmax values, which range from 414 to 465 (Fig 35). The HI systematically decreases with increasing maturity within in the pseudo-van-Krevelen diagram. Immature samples with TOC values higher than 2%, S2/S3 ratio > 5 and HI values above 300 mg HC/g TOC can be described as having a good petroleum generation potential (Peters, 1986; Bordenave *et al.*, 1993).

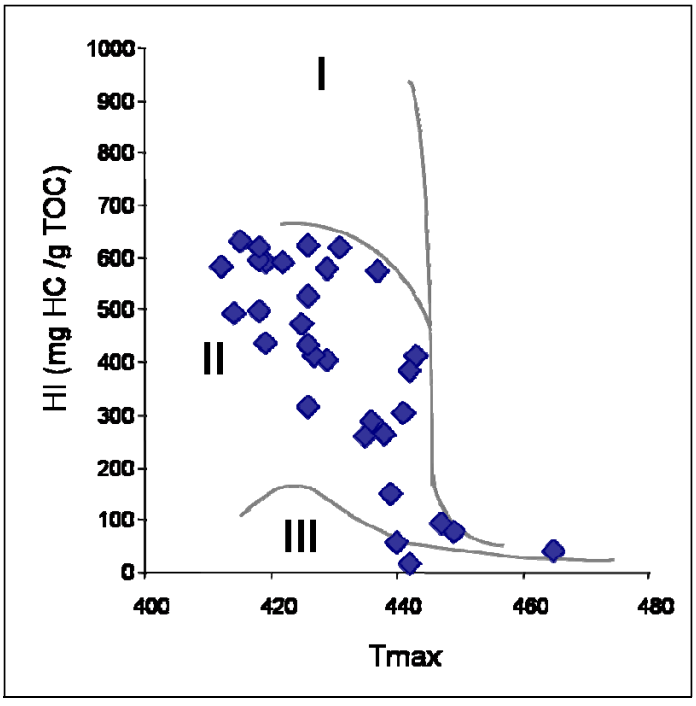

Fig 35 Pseudo-van-Krevelen diagram for the source rocks from the Duvernay Formation (after Espitalié *et al.* (1985)).

Sample	well	HI	OI	PI	TOC (%)	Tmax (°C)
G000541	Redwater	437,38	50,16	0,03	3,05	419
G000542	Redwater	591,42	28,17	0,02	5,36	419
G000545	Redwater	593,57	25,29	0,03	9,33	418
G000546	Redwater	494,03	36,03	0,04	4,69	414
G000548	Tomahawk	526,05	11,01	0,11	5,72	426
G000549	Tomahawk	577,18	6,13	0,11	6,53	429
G000550	Tomahawk	576	11	0,08	9,62	437
G000553	Tomahawk	621,94	4,81	0,09	9,57	426
G000559	Leduc	257,38	0	0,12	0,61	435
G000560	Norbuck	14,86	0	0,76	0,74	442
G000562	Norbuck	40,14	6,42	0,52	4,36	465
G000564	Forgotsen Burk	385,07	2,27	0,13	9,71	442
G000570	Forgotsen Burk	412,82	4,56	0,12	10,30	443
G000575	Imperial Armena 3	405,67	23,71	0,08	1,94	429
G000579	Can Gulf Dom Red.	583,58	26,42	0,07	14,80	412
G000581	Can Gulf Dom Red.	499,38	46,77	0,04	3,25	418
G000583	Can Gulf Dom Red.	631,05	31,97	0,05	7,60	415
G000586	Imperial Kingman	412,24	32,91	0,07	2,37	427
G000587	Imperial Kingman	432,4	31,15	0,07	3,21	426
G000592	Imperial Kingman	473,59	28,49	0,05	3,37	425
G000593	Imperial Kingman	316,85	40,45	0,06	1,78	426
G000596	Ferrybank	286,08	6,96	0,24	5,03	436
G000598	Ferrybank	150,68	21,92	0,29	0,73	439
G000600	Ferrybank	264,85	12,38	0,27	4,04	438
G000601	Imperial Cynthia	55,41	29,73	0,46	1,48	440
G000602	Imperial Cynthia	75,78	18,75	0,43	1,28	449
G000603	Imperial Cynthia	303,1	5,49	0,22	4,19	441
G000607	Imperial Cynthia	92,11	11,58	0,5	1,90	447
G000610	Sarcee et al Pibroc	618,68	14,41	0,05	9,37	418
G000615	Sarcee et al Pibroc	591,5	16,65	0,04	8,47	422
G000631	Banff Imperial	620,94	5,6	0,09	5,54	431

Table 6 Rock-Eval data for source rocks from Duvernay (after Dieckmann (1998)).

Fig 36 shows the TOC range for studied Duvernay source rock samples. The samples from the well Forgotson Burk (G000564, G000570) differ to the other studied source rock samples. Facies variations in the Duvernay Formation were observed before by Li *et al.* (1997) and were shown to affect also the petroleum formation characteristics of the Duvernay Formation (Dieckmann, 1998).

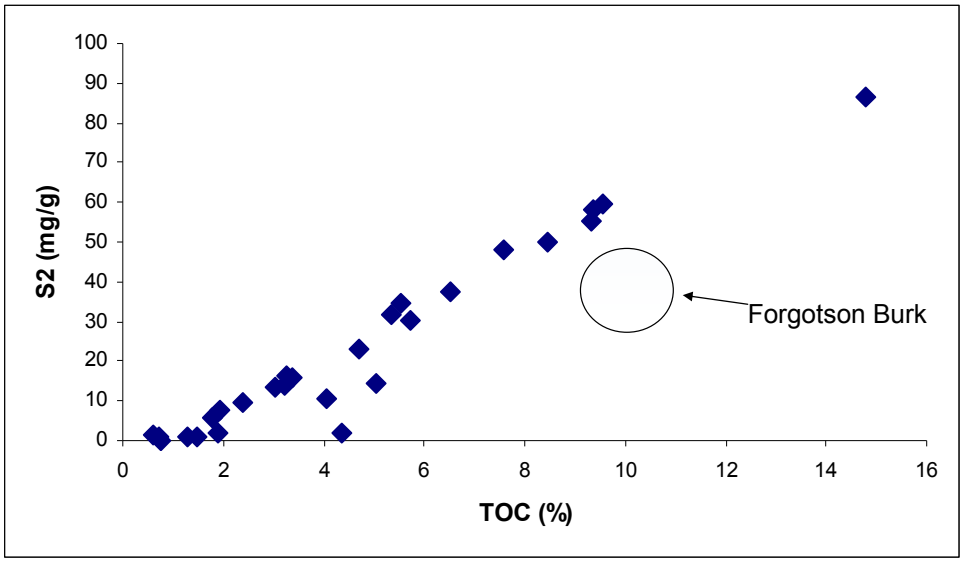

Fig 36 Rock-Eval S2 and TOC for source rocks from the Duvernay Formation.

5.2.2 Crude oil screening

5.2.2.1 Bulk composition

Investigated Duvernay oils consist of black and light oils with API´s ranging from 39° to 52°. Generally, the content of the polar fraction of the light crude oils does not exceed 4%, whereas black oils contain 8-23% (Fig 37). The black oils show decreasing content of the NSO fraction with increasing API gravity. The same is monitored for the light oils G000410 (39.37° API) and G000412 (47.1° API). Only the light oil sample G000411 (52.36° API) differs from that and shows a high content of aromatic hydrocarbons.

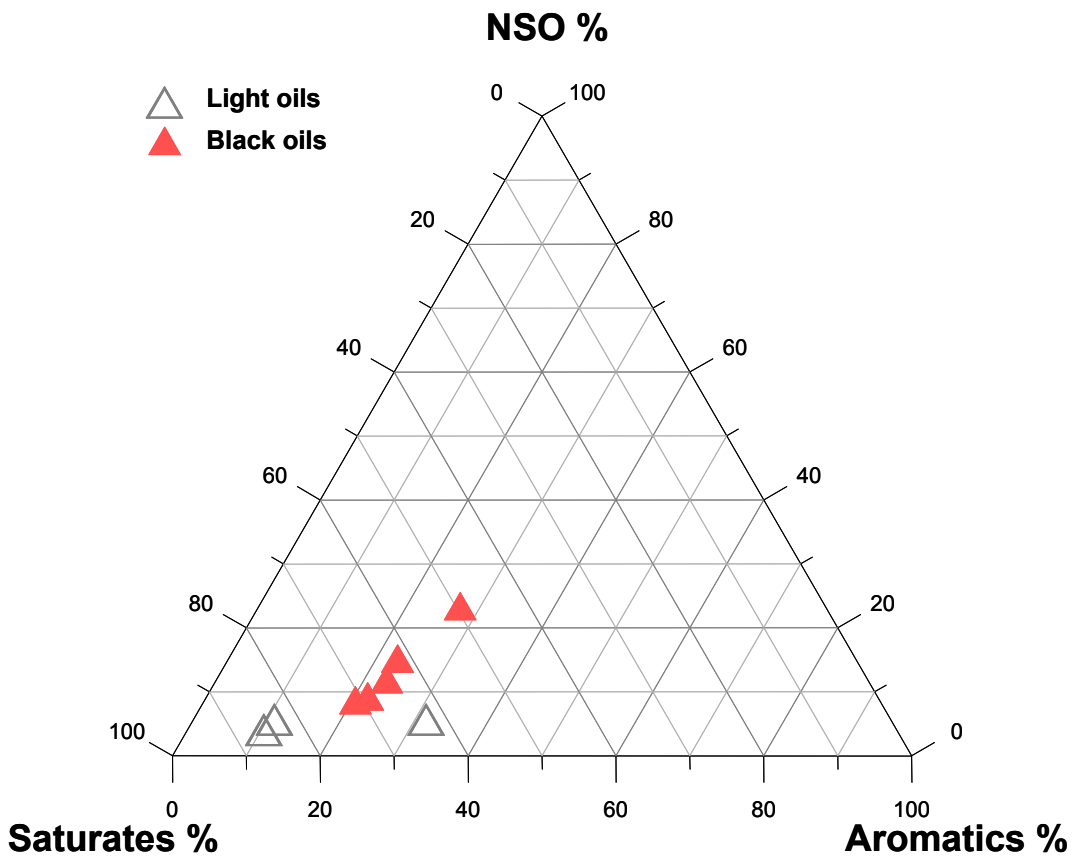

Fig 37 Ternary diagram showing the compound class distribution of the Duvernay crude oils.

Selected chromatograms from thermovaporisation - whole oil analysis for the Duvernay oils are presented in Fig 38. The crude oils show a bimodal distribution of *n*-alkane homologues. Especially the samples with lower API gravities contain a remarkable amount of long-chain alkanes (up to C37). With increasing API gravity the distribution of *n*-alkanes shifts to low molecular weights. Remarkable is the occurrence of 1,2,3,4-tetramethylbenzene in Duvernay crude oils, which is attributed to a specific green-sulphur bacteria (*Chlorobiacea*) (Requejo *et al.*, 1992; Hartgers *et al.*, 1994a).

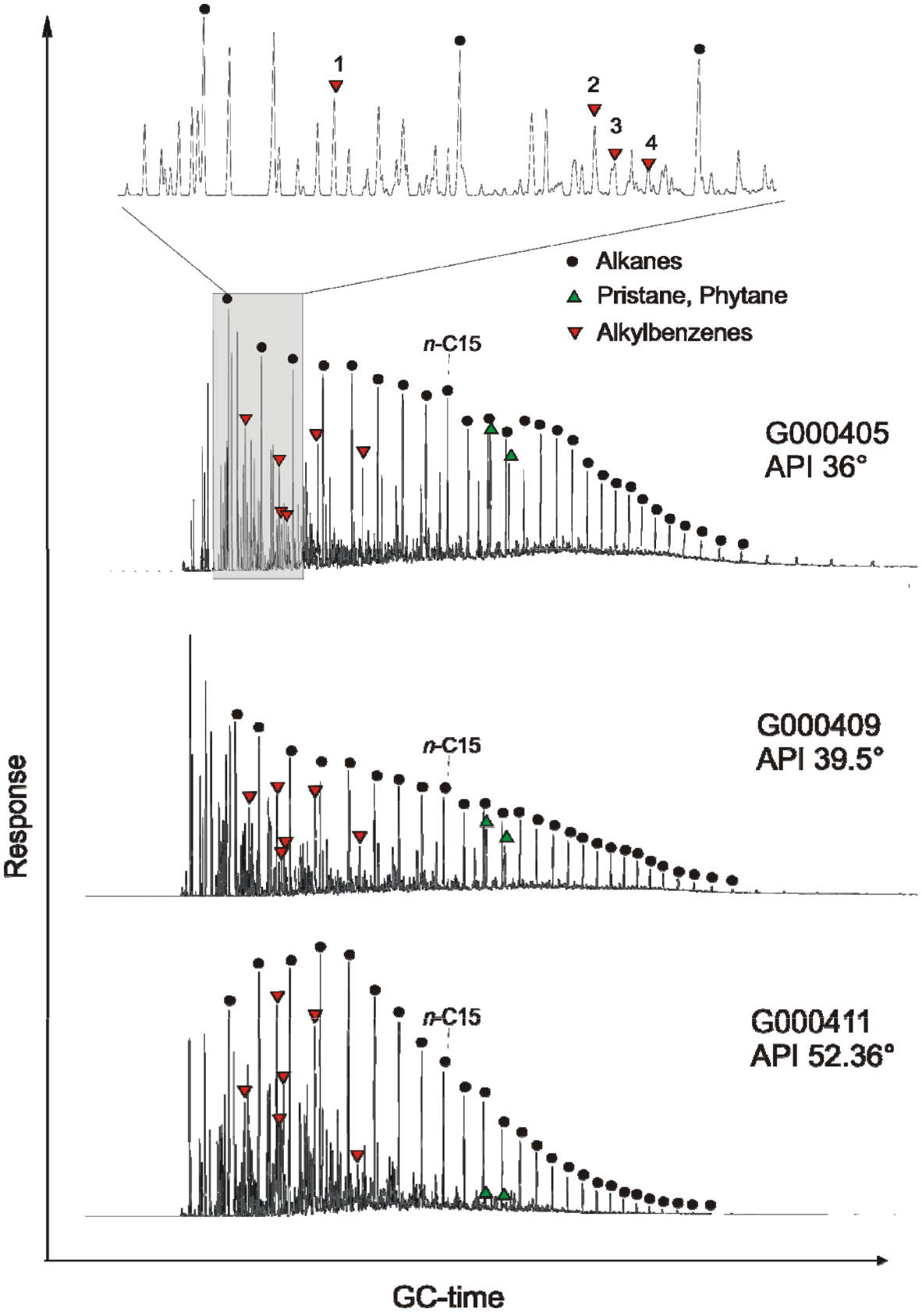

Fig 38 Thermovaporisation GC traces of 3 Duvernay oil samples are shown with increasing API gravity. Alkanes from *n*-C_7, pristane and phytane, as well most abundant alkylbenzenes are marked. Benzenes are corresponding to retention time from left to the right: toluene (1), ethylbenzene (2), m,p-xylene (3), o-xylene (4), trimethylbenzene and tetramethylbenzene.

5.2.2.2 Biomarkers

Pristane and phytane

Pr/Ph ratios higher than 1 for the Canadian crude oils indicate a suboxic redox potential of the depositional environment. The Pr/Ph ratios for Duvernay oils range from 1.32 to 1.94, which is typical for a marine depositional environment (Peters *et al.*, 2005). Fig 39 shows a cross-plot of pristane/*n*-C_{17} versus phytane/*n*-C_{18} after Peters *et al.* (1999) from whole-oil chromatograms of Duvernay oils. The crude oils show a decreasing trend of pristane/*n*-C_{17} versus phytane/*n*-C_{18} with increasing API of those oils. These ratios for the crude oils plot along a straight line referring to homogenous organic matter type in the source rock depositional environment, but they do not plot exactly in the field of type II organic matter in the presented diagram. According to Peters *et al.* (1999) the field of mixed type of organic matter is characterized by the suboxic depositional environment, and therefore the presented diagram is not adequate for the prediction of organic matter type in the case of the Duvernay oils, but can be used to infer the oxicity in the source rock depositional environment.

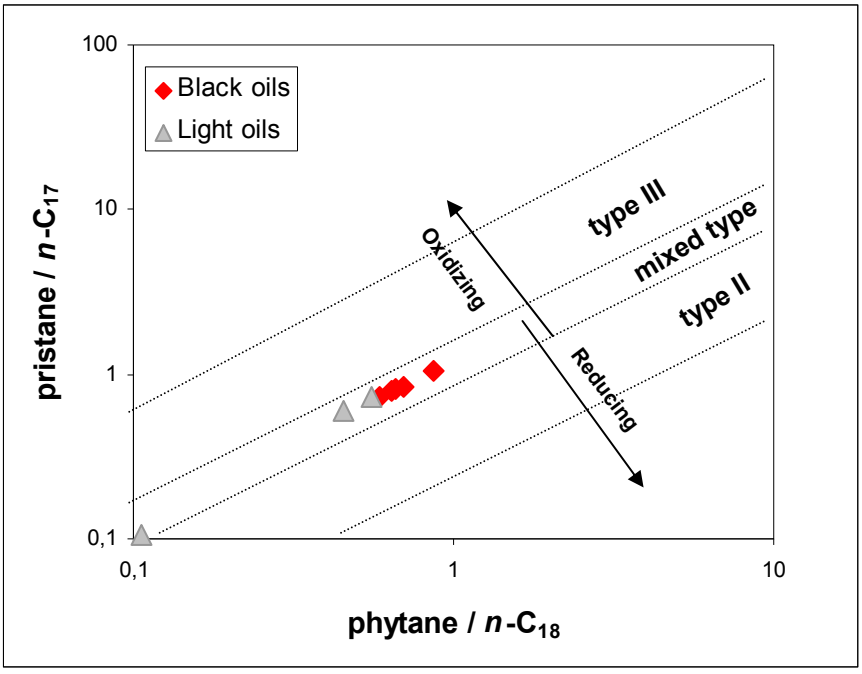

Fig 39 Plot of pristane/*n*-C_{17} vs. phytane/*n*-C_{18} from whole-oil chromatograms of Duvernay oils (after Peters *et al.* (1999)).

Hopanes and steranes as maturity parameter

Table 7 provides relevant biomarker parameters after Dieckmann (1998) of crude oils and source rock bitumen from the Duvernay Formation.

The maturity parameter Ts/(Ts+Tm) shows increasing ratio with increasing maturity as demonstrated in Fig 40. Only the light oil sample G000411 (API 52°) differs from that trend and shows lowest ratio for Ts/(Ts+Tm). For bitumens this ratio increases until Tmax of 435°C where the ratio shows equilibrium with further ongoing maturity (Dieckmann, 1998).

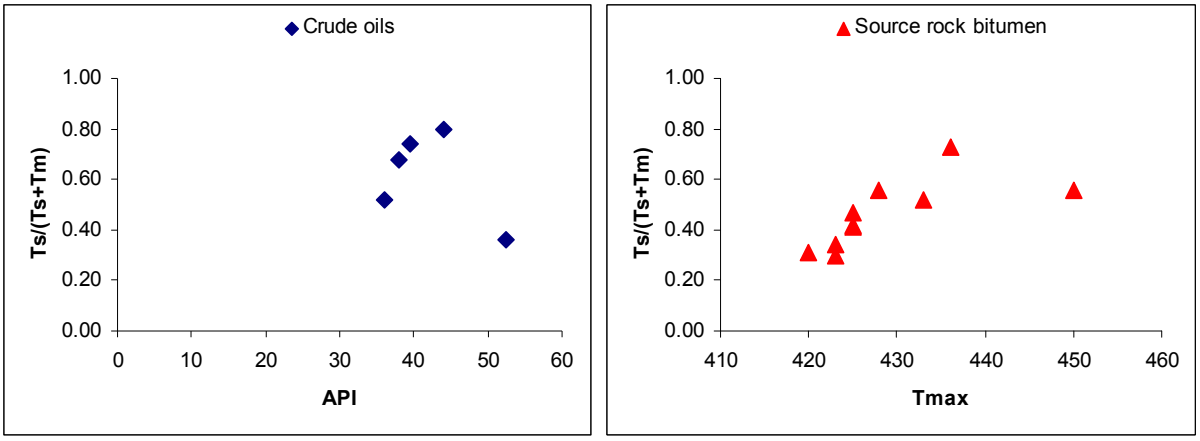

Fig 40 Ts/(Ts+Tm) versus the API for crude oils (left) and versus Tmax for source rock bitumen (right) investigated by Dieckmann (1998)

More maturity parameters are obtained from the sterane isomerization C_{29} $\beta\beta/(\beta\beta+\alpha\alpha)$ and C_{29} 20*S*/(20*S*+20*R*). Values for C_{29} $\beta\beta/(\beta\beta+\alpha\alpha)$ range between 0.66 and 0.73 for the black oils, and at 0.4 for the light oil sample G000410. Interestingly, these ratios decrease with increasing API of related Duvernay oils. This is not observed for the bitumens, whose values range between 0.36 and 0.65. This is illustrated in Fig 41 showing a plot of the ratio C_{29} $\beta\beta/(\beta\beta+\alpha\alpha)$ versus the API for crude oils and versus Tmax for source rock bitumen.

Sample		% αααC_{27}	% αααC_{28}	% αααC_{29}	Sterane-Isom. C_{29} ββ/(ββ+αα)	Sterane-Isom. 20S/(20S+20R)	Ts/(Ts+Tm)	Homohop. Index	Pr/Ph
G000405	crude oil	36.00	17.00	46.00	0.73	0.62	0.52	0.08	1.32
G000406	crude oil	38.00	16.00	46.00	0.72	0.64	0.68	0.14	1.42
G000407	crude oil	41.00	0.00	59.00	0.66	0.66	0.8	0.00	1.61
G000409	crude oil	41.00	19.00	40.00	0.71	0.61	0.74	0.00	1.86
G000410	crude oil				0.4	-	-	-	1.94
G000411	crude oil	-	-	-	-	0.74	0.36	0.11	1.92
G000412	crude oil	-	-	-	-	-	-	-	1.94
42714*	bitumen	26.00	18.00	55.00	0.43	-	-		
42725*	bitumen	33.00	19.00	47.00	0.5	0.58	0.56	0.07	
42728*	bitumen	34.00	18.00	48.00	0.58	0.61	0.52	0.07	
42746*	bitumen	35.00	19.00	46.00	0.4	0.6	0.47	0.06	
42765*	bitumen	30.00	17.00	53.00	0.36	0.58	0.3	0.06	
G000596	bitumen	35.00	19.00	45.00	0.65	0.64	0.73	0.12	
42779*	bitumen	-	-	-	-	0.52	0.56	0.12	
42790*	bitumen	28.00	18.00	54.00	0.41	0.46	0.31	0.05	
42795*	bitumen	25.00	22.00	53.00	0.39	0.5	0.34	0.11	
42802*	bitumen	33.00	20.00	47.00	0.49	0.61	0.41	0.06	
42811*	bitumen	36.00	19.00	45.00	0.45	0.61	0.42	0.07	

Sterane-Isom. ββ/(ββ+αα) C_{29} = C_{29} 14β(H), 17β(H) / (ββ + αα)

Sterane-Isom. 20S/(20S+20R) αααC$_{29}$ = C_{29} 5α(H), 14α(H), 17α(H) 20S / (ααα20S + ααα20R)

Ts/(Ts+Tm) = C_{27} 18α(H)-trisnorhopane II / (C_{27} 18α(H)-trisnorhopane II + C_{27} 17α(H)-trisnorhopane)

Homohopane Index = C_{35}-homohopane / (C_{31}- + C_{32}- + C_{33}- + C_{34}- + C_{35}-homohopane)

Pr/Ph = pristane /phytane

Table 7 Biomarker parameter for Duvernay crude oils and source rock bitumen after Dieckmann (1998). The marked (*) source rock bitumen are not part of the sample set for the present study.

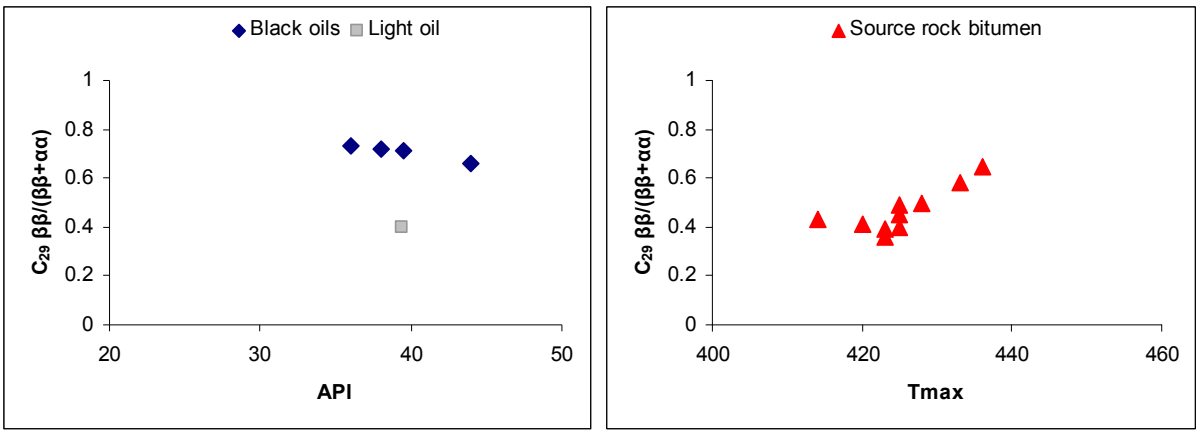

Fig 41 Plot of the ratio C_{29} *ββ*/(*ββ*+*αα*) versus the API for crude oils (left) and versus Tmax for source rock bitumen (right) for the Duvernay Formation.

This observed inverse trend of C_{29} *ββ*/(*ββ*+*αα*) versus API in Fig 41 for the Duvernay oils might indicate that oils have experienced different heating rates in the subsurface (Mackenzie and McKenzie, 1983) or different levels of clay catalysis (Huang *et al.*, 1990; Peters *et al.*, 2005). Alternatively, it is thinkable that this biomarker parameter decrease because of higher maturity, which is described by several authors to occur for the sterane 20*S*/(20*S*+20*R*) parameter (Peters *et al.*, 1990; Marzi and Rullkötter, 1992; Peters *et al.*, 2005).

The C_{29} 20*S*/(20*S*+20*R*) sterane ratio versus API and Tmax for oils and bitumen from the Duvernay Formation is shown in Fig 42. Crude oils and bitumens show ratios, which range from 0.62 to 0.74 for the oils and from 0.46 to 0.64 for bitumens proportionally with increasing maturity. But, this sterane isomerization index might not be a good maturity parameter for the Duvernay oils, because their values exceed the equilibrium which is about a value of 0.52-0.55 (Seifert and Moldowan, 1986; Peters *et al.*, 2005).

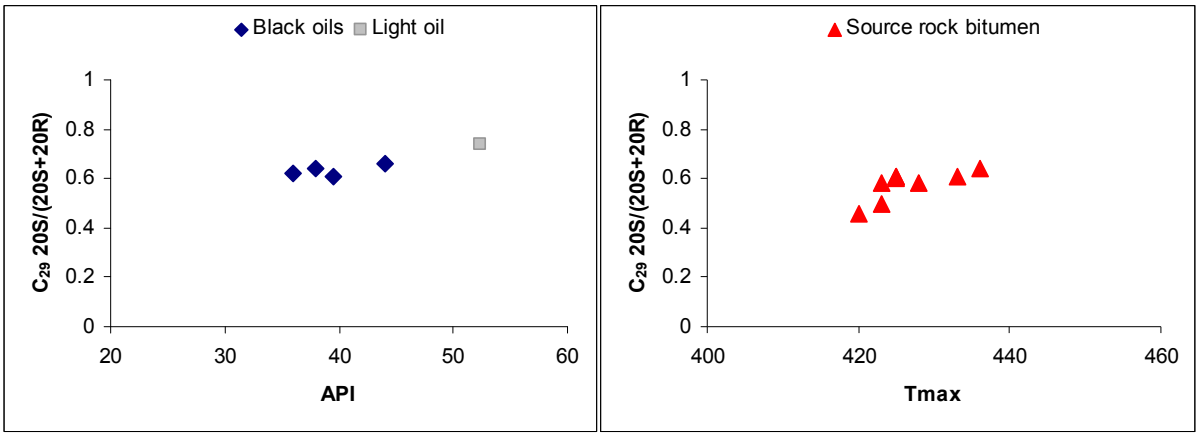

Fig 42 Plot of the ratio C_{29} 20*S*/(20*S*+20*R*) versus the API for crude oils (left) and versus Tmax for source rock bitumen (right) for the Duvernay Formation.

Best maturity parameter for crude oils, except the light oils from the Duvernay Formation is Ts/(Ts+Tm) and for bitumens additionally C_{29} 20*S*/(20*S*+20*R*), based on the interpretations of presented biomarkers. Low mature oils from Duvernay show Ts/(Ts+Tm) values corresponding to a vitrinite reflectance of 0.65 %Ro (Fig 43a). Those values from more mature black oils correspond to a vitrinite reflectance up to 1.1 Ro%. The facies dependency of Ts/(Ts+Tm) (Bakr and Wilkes, 2002), which was discussed for the Italian samples, may not play a role here, because the Duvernay Petroleum System is characterized as being of istry</SECONDARY_TITLE><VOLUME>8</VOLUME><PAGES>1105-

Source rock bitumen yield a correlated vitrinite reflectance of 0.45 Ro% for most immature samples, and a Ro% up to 0.8 based on Ts/(Ts+Tm) (Fig 43b). Values obtained from C_{29} 20*S*/(20*S*+20*R*) measured on source rock bitumen yield higher vitrinite reflectance for more immature source rocks. Here, the biomarker values conform to a vitrinite reflectance of 0.6 %Ro for immature source rocks. Since the values of C_{29} 20*S*/(20*S*+20*R*) for those source rocks are closer to the equilibrium, the vitrinite reflectance obtained from this sterane parameter is more reliable, at least for immature source rocks (Fig 43b).

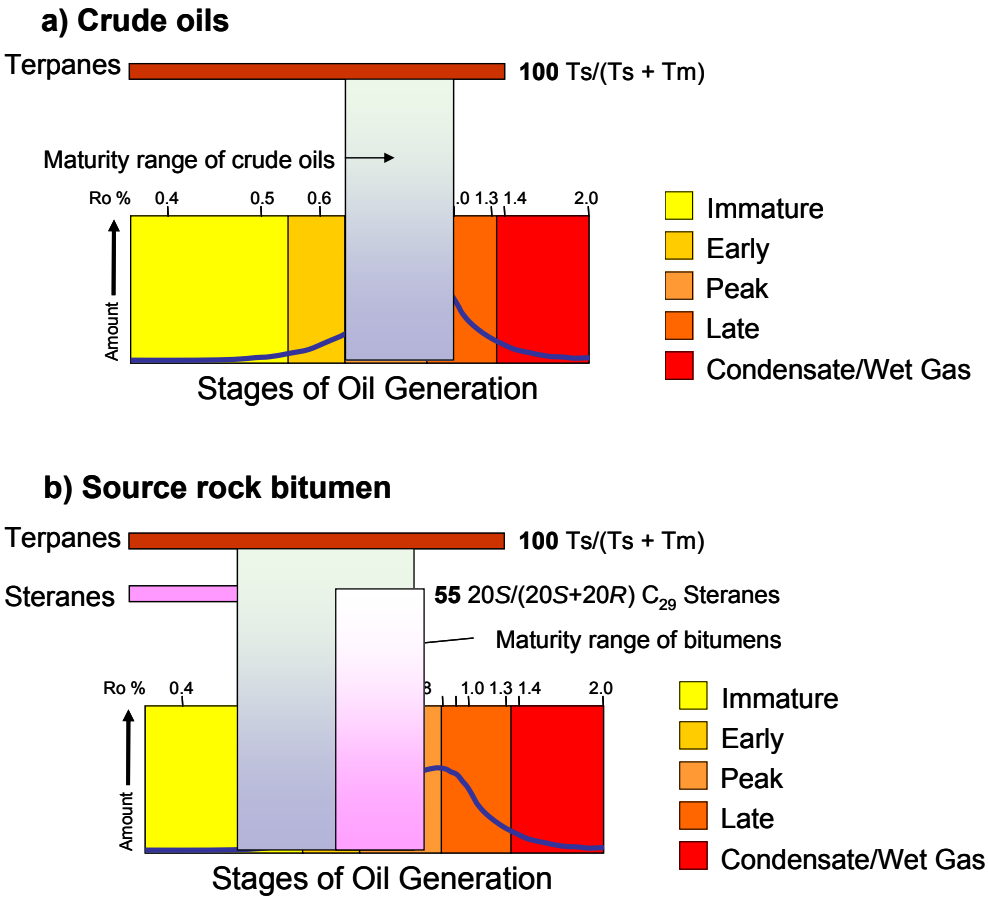

Fig 43 Biomarker maturation parameters are shown versus vitrinite reflectance and a generalized oil generating curve for a) Duvernay crude oils (except light oils), and b) source rock bitumen from the Duvernay Formation (based on Mackenzie (1984), Peters *et al.* (2005))

Hopanes and steranes for oil - source rock correlation

The crude oils from oil fields of central Alberta are generally divided into different oil families and subfamilies, which show characteristic differences in terms of their homohopane distributions (Riediger *et al.*, 1999). Based on the work of Dieckmann (1998), the homohopane distributions of studied samples support the origin being the Duvernay Formation. Li *et al*. (1998) proposed two oil subfamilies for the Duvernay Formation, on basis of the correlation of Ts/(Ts+Tm) ratios with C_{23}-tricyclic terpane/C_{30}- αβ–hopane ratios.

According to these authors, the crude oils studied for this project belong all to the same oil subfamily.

Fig 44 shows the distribution of ααα C_{27}, C_{28} and C_{29} steranes in crude oils and source rock bitumen from the Duvernay Formation. The sterane distributions between those crude oils and bitumens are not so different like observed for the Italian samples. Both, oils and bitumen show similar amount of ααα C_{28} sterane with 20 %, and they differ only in that bitumens contain slightly higher amounts of ααα C_{29} sterane. At least, this sterane distribution points to same facies for oils and source rocks. Samples from the Forgotson Burk well, which are different in facies (Fig 36), will not be taken into account for the further study on bulk kinetic parameters.

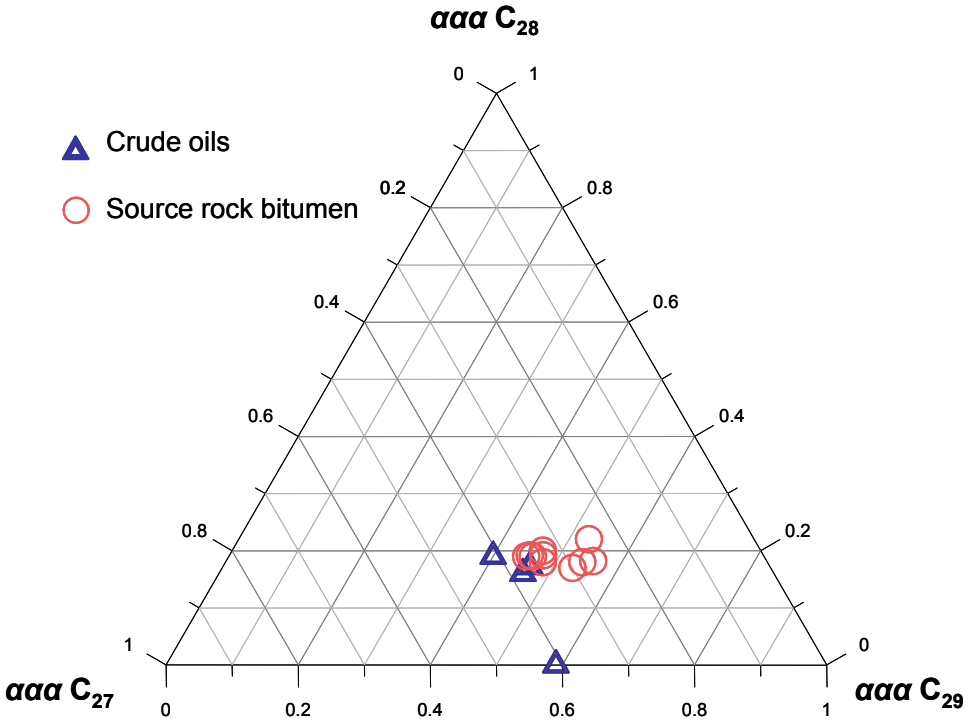

Fig 44 Ternary plot showing sterane composition of crude oils and source rock bitumen for the Duvernay samples.

5.2.2.3 Light hydrocarbons

Fig 45 illustrates the light hydrocarbons characteristics of the studied oils from Duvernay. The diagram with the heptane / isoheptane values established by Thompson (1983) is shown in Fig 45a. The heptane / isoheptane values were calculated as followed:

Heptane value = (2-methylhexane + 3-methylhexane) / (1,cis-3-dimethylcyclopentane + 1,trans-3-dimethylcyclopentane + 1,trans-2-dimethylcyclopentane).

Isoheptane value = 100.0 x *n*-heptane / (cyclohexane + 2-methylhexane + 1,1-dimethylcyclopentane + 3-methylhexane + 1,cis-3-dimethylcyclopentane + 1,trans-3-dimethylcyclopentane + 1,trans-2-dimethylcyclopentane + *n*-heptane + methylcyclohexane).

Light oils and black oils plot mainly in the fields of normal to mature oils. Nevertheless, the black oils within this sample set show some diversity in the heptane value, which is a result of variations in the total yields of 2- and 3-methyhexane compared to the other hydrocarbons of the black oils. These varying yields of methylhexanes do not show any trend with the API gravity of related oils. A reason for that might also be that samples have experienced different ambient conditions during sampling, handling, and transport, because methylhexanes are less effected by evaporisation than other light hydrocarbons (Cañipa-Morales *et al.*, 2003).

Fig 45b illustrates the light hydrocarbons characteristics of the Duvernay oils based on the ratios of toluene / *n*-heptane and *n*-heptane / methylcyclohexane after Thompson (1988) and Cañipa-Morales *et al.* (2003). Cañipa-Morales *et al.* (2003) mentioned that these ratios may still be utilized when partial evaporation during sampling and handling has occurred. Based on this plot the studied oils from Duvernay do not show any indications of a secondary overprint such as biodegradation or water washing.

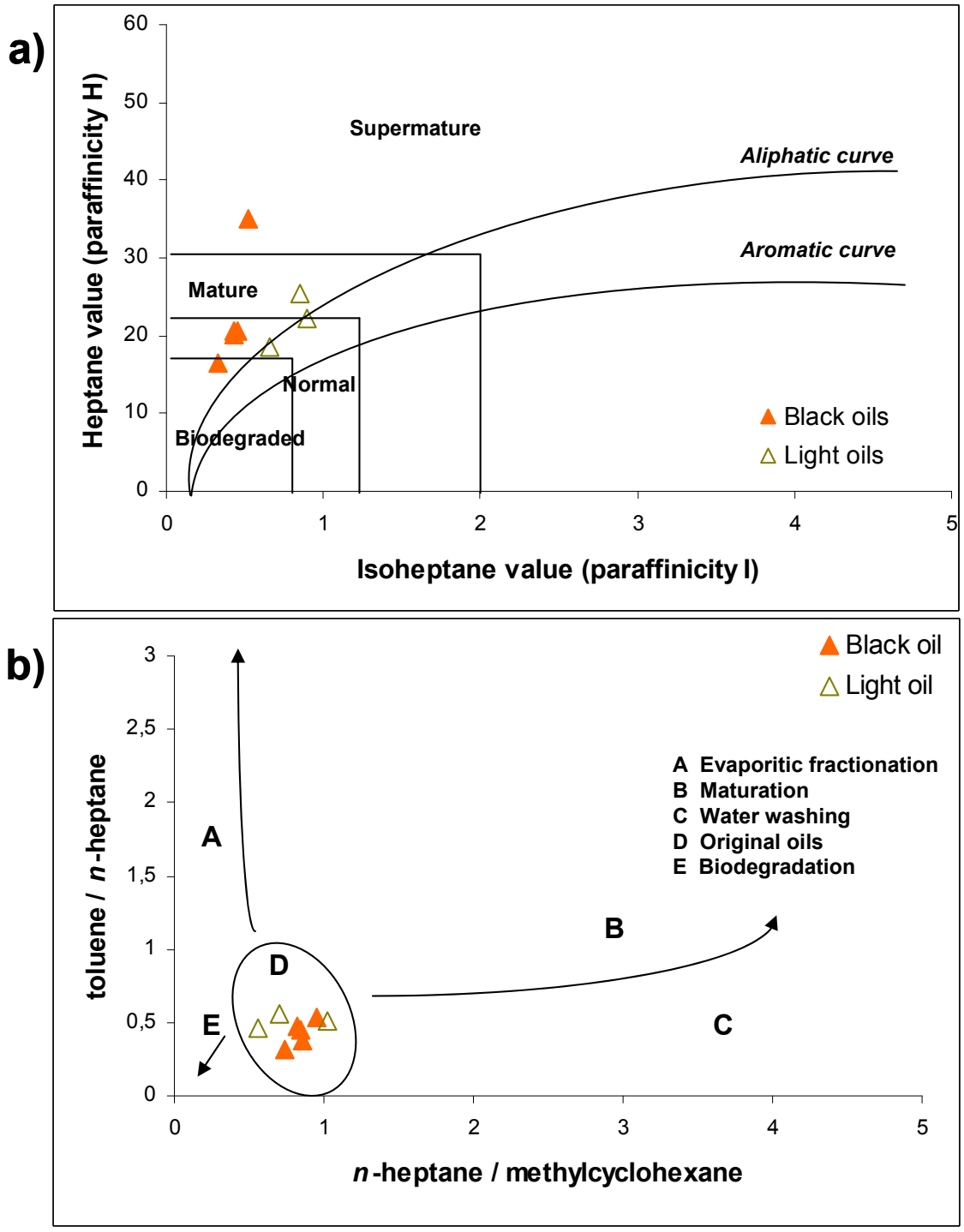

Fig 45 a) The cross plot of paraffinicity H versus paraffinicity I ratio for crude oils from the Duvernay Petroleum System (after Thompson (1983)). b) Investigated Duvernay oils in terms of aromaticity versus paraffinicity (after Talukdar and Dow (1990); modified by Cañipa-Morales *et al.* (2003)).

Fig 46 shows the ratio of paraffinicity F (*n*-heptane / methylcyclohexane) after Thompson (1988) versus the API gravity for Duvernay crude oils. The Duvernay light oils demonstrate lower ratios of paraffinicity F compared to the black oils. Both, black oils as well as light oils from Duvernay show an increasing trend of paraffinicity F with increasing maturity, what is also proposed as general characteristic of this light hydrocarbon parameter (Thompson, 1983, 1988; Cañipa-Morales *et al.*, 2003). As demonstrated already in Fig 29 the heavy crude oils from Southern Italy jar with this general characteristic in that they show decreasing paraffinicity F with increasing maturity.

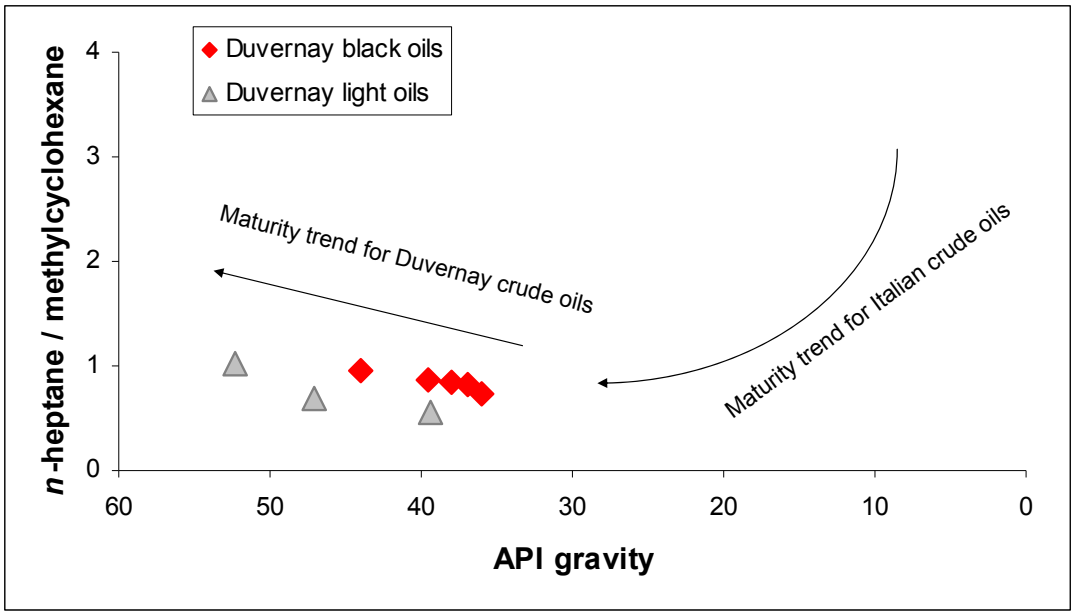

Fig 46 Ratio of paraffinicity F (*n*-heptane / methylcyclohexane) after Thompson (1988) versus the API gravity for Duvernay crude oils.

5.2.2.4 Conclusions

- Low mature oils from Duvernay show Ts/(Ts+Tm) values, which correspond to a vitrinite reflectance of 0.65 %Ro. Those values from more mature black oils correspond to a vitrinite reflectance up to 1.1 Ro%.
- Values obtained from C_{29} 20*S*/(20*S*+20*R*) measured on bitumen yield a vitrinite reflectance of 0.6 %Ro for immature source rocks. Bitumen of mature source rocks yield a correlated vitrinite reflectance of 0.8 Ro% based on the Ts/(Ts+Tm) parameter.
- The distribution of αααC_{27}, C_{28} and C_{29} steranes in crude oils and source rock bitumen from the Duvernay Formation points to same facies for oils and source rocks. Samples from the Forgotson Burk well, which are different in facies, will not be taken into account for the further study on bulk kinetic parameters.
- Based on light hydrocarbon parameters the studied oils do not show any indications of a secondary overprint such as biodegradation or water washing. Therefore, their compositional characteristics such as aromaticity and paraffinicity can later be compared directly to the products formed from the kerogens and asphaltenes.
- Light oils from Duvernay show some differences to the black oils in terms of biomarker and light hydrocarbon parameters. As well, the light oil samples did not contain sufficient amounts of asphaltenes to get precipitated and further on investigated.

5.3 Nigeria onshore

5.3.1 Crude oil screening

5.3.1.1 Bulk composition

The crude oils from Nigeria show API gravities from 21° - 41°. Based on MPLC-analysis the crude oils are dominated by saturated hydrocarbons and have NSO contents from 7 to 21% proportional to the API gravity (Fig 47). Unaltered crude oils with high API gravity up to 41° prove contents of saturated hydrocarbons of 78%. The sample G00502 differs from this trend due to unusual high amounts of NSO-compound up to 37%. This crude oil (24.5° API) is strongly biodegraded but do not reveal the lowest API gravity.

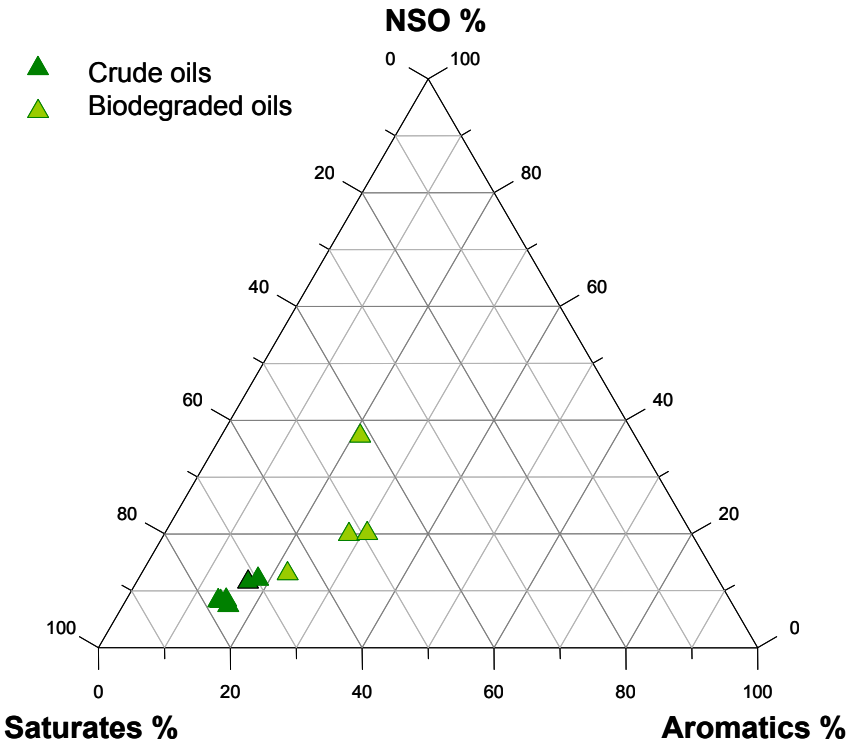

Fig 47 Ternary diagram showing the compound class distribution of the Nigerian crude oils.

Chromatograms of selected, less biodegraded oil samples are presented in Fig 48. The strongly biodegraded samples are presented later on in Fig 57. Unaltered or slightly biodegraded oils with higher API gravity show a bi- to trimodal distribution pattern for the homologous series of *n*-alkanes.

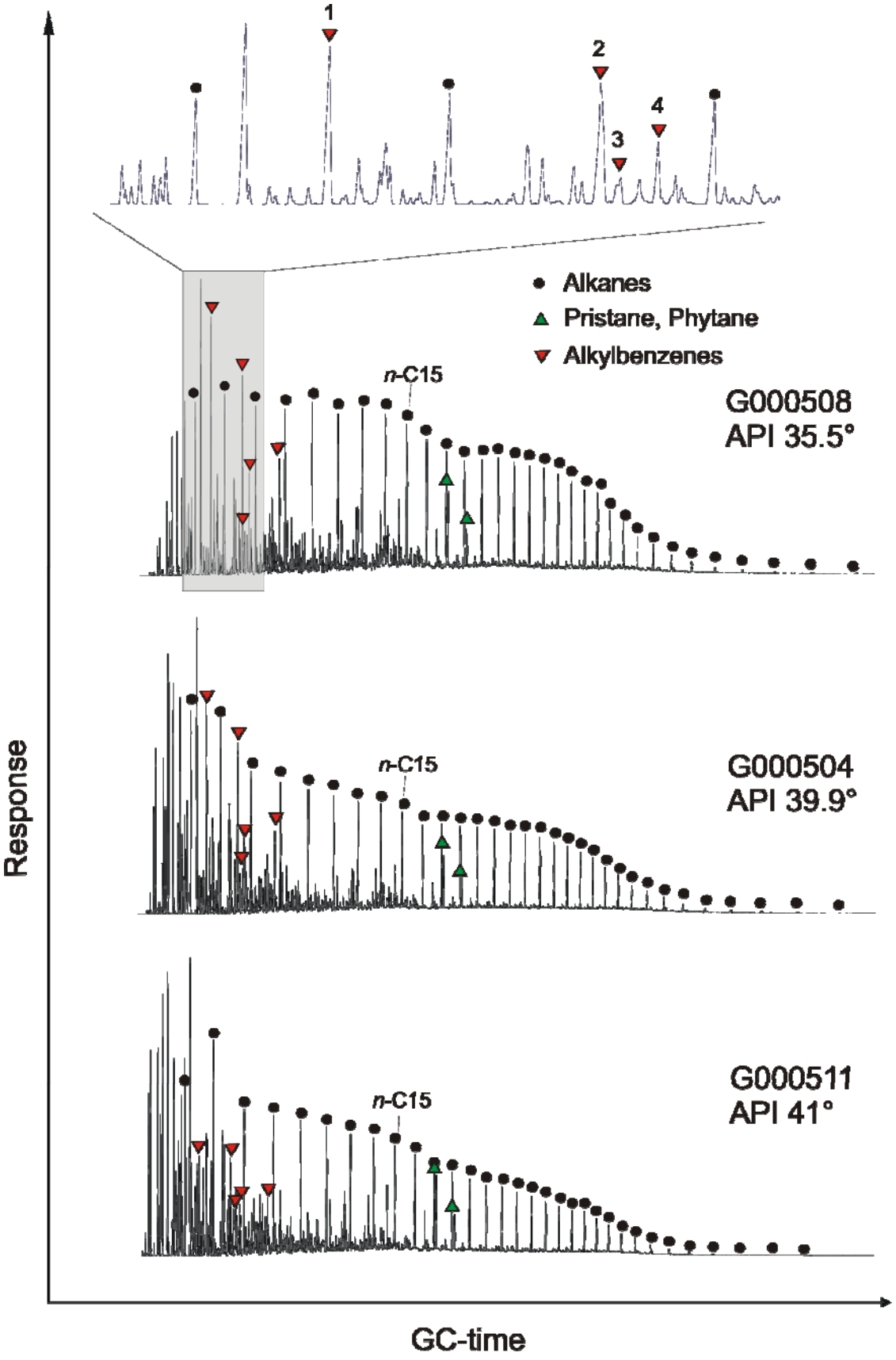

Fig 48 Thermovaporisation GC traces of 3 Nigerian oil samples are shown with increasing API gravity. Alkanes from *n*-C_7, pristane and phytane, as well most abundant alkylbenzenes are marked. Benzenes are corresponding to retention time from left to the right: toluene (1), ethylbenzene (2), m,p-xylene (3), o-xylene (4), and trimethylbenzene.

5.3.1.2 Biomarkers

Alkane distribution

Nigerian oils show in the range between *n*-C_{10} and *n*-C_{17} peaks either in *n*-C_{11} or *n*-C_{14}. Alkanes higher than *n*-C_{18} show again increasing total amount with a peak in *n*-C_{20} or *n*-C_{22} and some oils also in *n*-C_{27}. The even carbon numbered dominance of *n*-C_{20} or *n*-C_{22} is probably the result of reduction of even fatty acids or alcohols (Tissot and Welte, 1984). Only sample G000511 (API 41°) differs and shows a peaks in the odd carbon number alkanes *n*-C_{21} and *n*-C_{27}. The alkanes of all oils in the range between *n*-C_{23} and *n*-C_{31} show a slight predominance of odd over even carbon number, which might be resulted from continental runoff (Kvenvolden, 1962; Tissot and Welte, 1984).

Pristane and phytane

The Nigerian oils have high Pr/Ph ratios from 2.1 up to 3.7, indicative for dysoxic depositional conditions (Peters *et al.*, 2005). The strongly biodegraded oils (G00503 and G000506) show lower ratios of 1.8, probably due to degradation effects.

Fig 49 shows a cross-plot of pristane/*n*-C_{17} versus phytane/*n*-C_{18} after Peters *et al.* (1999) from whole-oil chromatograms of Nigerian oils. The biodegraded oils show a decreasing trend of pristane/*n*-C_{17} versus phytane/*n*-C_{18} with increasing API of those oils, explained by ongoing depletion of *n*-alkanes due to microbial alteration. The unaltered crude oils do not show any trend of those ratios with the API gravity.

All oils plot in the field of type III or at the boundary of type III and mixed type of organic matter shown in the diagram established by Peters *et al.* (1999). This illustrates according to these authors relative high oxicity in the source rock depositional environment and the influence of terrestrial organic matter. Within the less degraded oils the ratio of pristane/*n*-C_{17} shows somewhat higher diversity referring to variations in the oxicity of depositional environment.

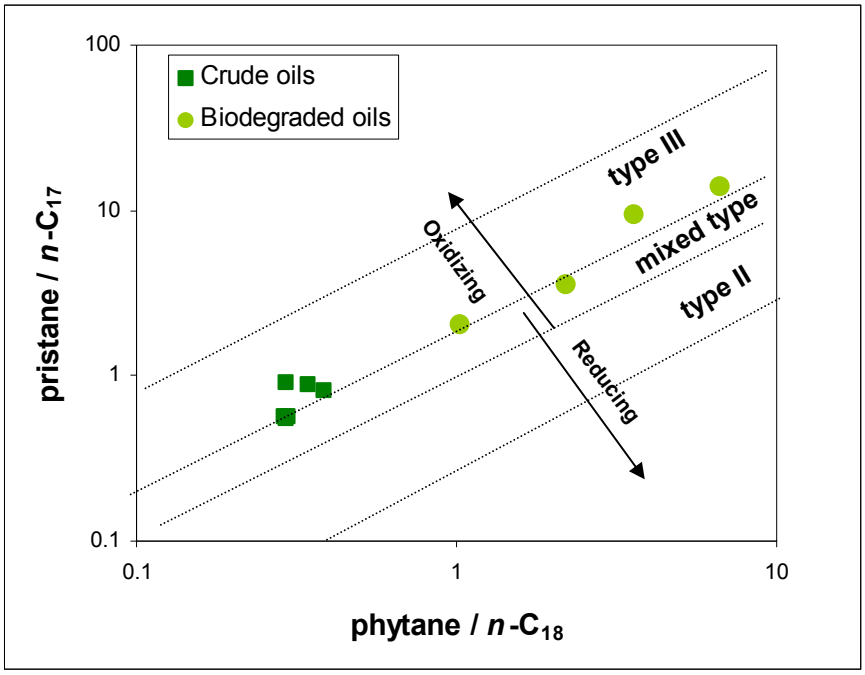

Fig 49 Plot of pristane/*n*-C_{17} vs. phytane/*n*-C_{18} from whole-oil chromatograms of Nigerian oils (after Peters *et al.* (1999)).

Hopanes and steranes as maturity parameter

Relevant biomarker parameters for the Nigerian oils are presented in Table 8. The Table presents parameters of hopanes (top), as well as steranes and the Pr/Ph ratio (bottom).

Sample	Ts/(Ts+Tm)	C_{29}Ts Index	Moretane Ratio M/(H+M)	Oleanane Index O/H	Oleanane-Hop. O/(O+H) Ratio	Homohop. Index	C_{31} Homohop. Izom.-Index	C_{32} Homohop. Izom.-Index	C_{35} Homohop. Izom.-Index
G000502	0.52	0.20	0.10	1.01	0.50	0.03	0.58	0.56	0.58
G000503	0.51	0.23	0.10	1.01	0.50	0.03	0.59	0.56	0.59
G000504	0.59	0.20	0.08	0.98	0.49	0.03	0.58	0.58	0.54
G000505	0.53	0.16	0.09	0.99	0.50	0.03	0.58	0.57	0.56
G000506	0.51	0.20	0.10	1.02	0.50	0.03	0.59	0.57	0.58
G000507	0.54	0.18	0.09	0.98	0.49	0.03	0.58	0.56	0.58
G000508	0.61	0.19	0.07	0.98	0.49	0.03	0.58	0.58	0.55
G000509	0.58	0.19	0.12	1.05	0.51	0.02	0.57	0.58	0.55
G000510	0.44	0.14	0.12	1.03	0.51	0.02	0.56	0.56	0.55
G000511	0.53	0.15	0.10	0.99	0.50	0.02	0.57	0.57	0.54

Sample	Sterane-Isom. 20S/(20S+20R) αααC_{27}	Sterane-Isom. 20S/(20S+20R) αααC_{28}	Sterane-Isom. 20S/(20S+20R) αααC_{29}	Sterane-Isom. 20S/(20S+20R) αααC_{30}	Sterane-Isom. ββ/(ββ+αα) C_{29}	% αααC_{27}	% αααC_{28}	% αααC_{29}	Pr/Ph
G000502	0.43	0.20	0.36	0.43	0.48	31.54	26.58	41.88	2.51
G000503	0.44	0.21	0.35	0.40	0.49	31.48	26.37	42.15	1.94
G000504	0.47	0.22	0.40	0.46	0.51	31.65	26.24	42.11	2.00
G000505	0.44	0.20	0.37	0.41	0.48	31.88	26.92	41.20	2.20
G000506	0.45	0.20	0.36	0.43	0.51	31.27	26.66	42.06	1.82
G000507	0.44	0.21	0.36	0.41	0.48	31.12	26.77	42.11	2.96
G000508	0.48	0.27	0.41	0.49	0.55	29.29	26.73	43.98	2.18
G000509	0.47	0.25	0.38	0.48	0.50	23.01	22.35	54.64	3.70
G000510	0.43	0.19	0.33	0.44	0.46	29.97	27.04	42.99	3.39
G000511	0.44	0.21	0.36	0.44	0.50	28.12	24.82	47.06	2.47

Ts/(Ts+Tm) = C_{27} 18α(H)-trisnorhopane II / (C_{27} 18α(H)-trisnorhopane II + C_{27} 17α(H)-trisnorhopane)

C_{29}Ts Index = C_{29} 18α-(H)-30-norneohopane / (C_{29} 18α-(H)-30-norneohopane + C_{29} 17α(H)-hopane)

Moretane-Ratio = C_{30} βα-moretane/ (C_{30} βα-moretane +C_{30} 17α(H), 21β(H)-homohopane)

Oleanane Index = 18α(H)-oleanane / C_{30} 17α(H), 21β(H)-homohopane

Homohopane Index = C_{35}-homohopane / (C_{31}- + C_{32}- + C_{33}- + C_{34}- + C_{35}-homohopane)

C_{31} Homohopane Izom.-Index = 22S C_{31}-homohopane / (22S + 22R C_{31}-homohopane)

Sterane-Isom. 20S/(20S+20R) αααC_{27} = C_{27} 5α(H), 14α(H), 17α(H) 20S / (ααα20S + ααα20R)

Sterane-Isom. ββ/(ββ+αα) C_{29} = C_{29} 14β(H), 17β(H) / (ββ + αα)

% αααC_{27} = αααC_{27} sterane / ααα(C_{27} + C_{28} + C_{29})

Pr/Ph = pristane /phytane

Table 8 Biomarker parameter for Nigerian crude oils.

Fig 50 shows the plots of Ts/(Ts+Tm) (left) and the C_{29}Ts index versus the API for Nigerian crude oils. Both maturity parameters do not show a trend with the API. The values for Ts/(Ts+Tm) range between 0.44 and 0.61 and those for the C_{29}Ts index between 0.14 and 0.23. These somewhat variations for both parameters within the sample set might rather be related to facies variations than to thermal maturity (Bakr and Wilkes, 2002).

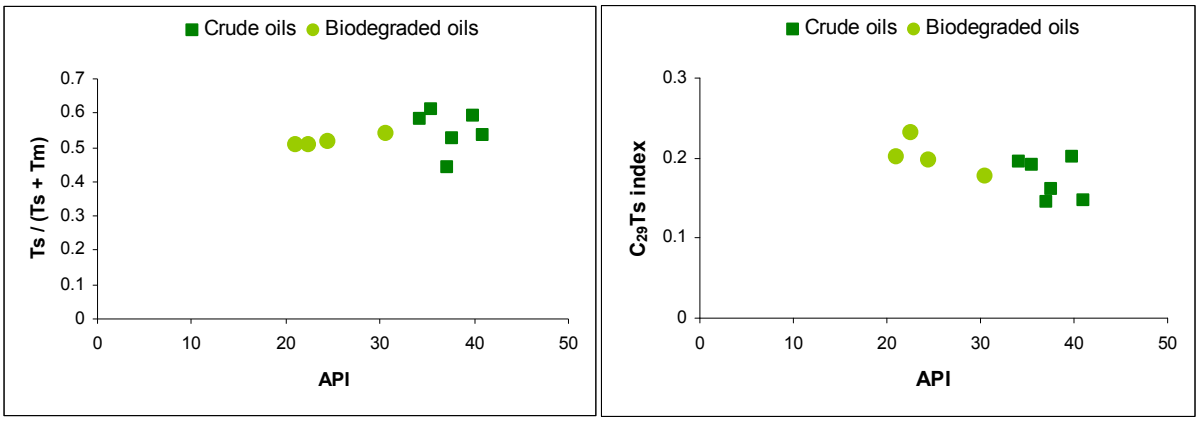

Fig 50 Maturity parameter Ts/(Ts+Tm) versus the API for Nigerian crude oils (left), and the C_{29}Ts index versus API (right).

The homohopane index is very similar for all studied oils and ranges between 0.02 and 0.03. The same is valid for the homohopane isomerization index showing values of 0.56 to 0.58 for example for the C_{32} homohopane. This indicates that all oils are of the same maturity stage. Thus, the API of studied oils is only determined by the degree of biodegradation. This is also obvious when looking at the sterane distributions. Fig 51 shows the ratios of 20*S*/(20*S*+20*R*) of C_{29}-sterane (left) and C_{29} $\beta\beta/(\beta\beta+\alpha\alpha)$ (right) versus the API for Nigerian crude oils. These ratios do not change with the API, which supports once more same maturity stage of those oils.

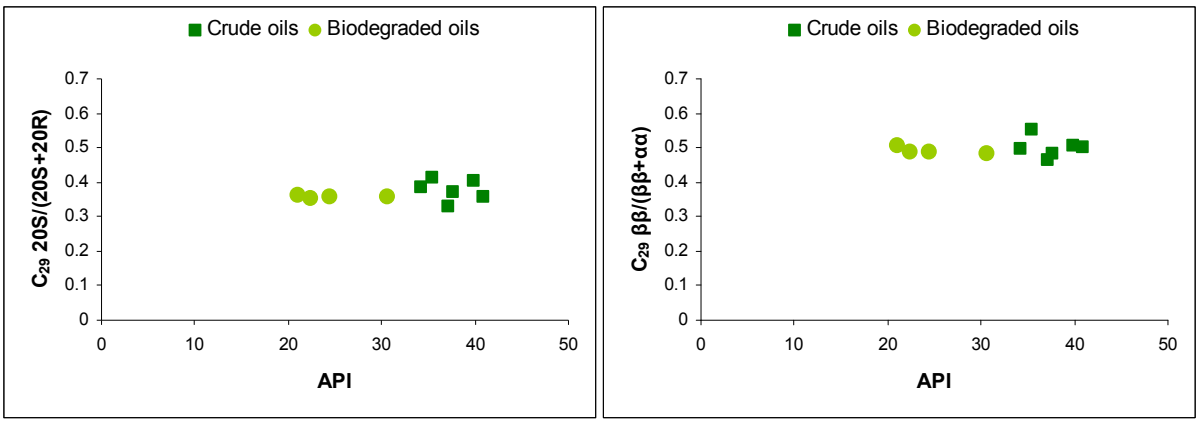

Fig 51 Ratio of 20*S*/(20*S*+20*R*) of C_{29}-sterane versus the API for Nigerian crude oils (left), and the ratio C_{29} *ββ*/(*ββ*+*αα*) versus API for same oils (right).

Fig 52 shows a plot of C_{29} 20*S*/(20*S*+20*R*) versus C_{29} *ββ*/(*ββ*+*αα*) steranes for the Nigerian crude oils (after Seifert and Moldowan (1986)). This cross-check indicates that both maturity parameters seem to be reliable, since the ratios plot along a straight line. Thus, both parameters can be used to determine the rank of maturity for those oils, shown in Fig 53. Based on both parameters the Nigerian oils show an early to near peak hydrocarbon generation corresponding to vitrinite reflectance values of about 0.75 percent (C_{29} 20*S*/(20*S*+20*R*)) and 0.8 percent (C_{29} *ββ*/(*ββ*+*αα*)) (Fig 53).

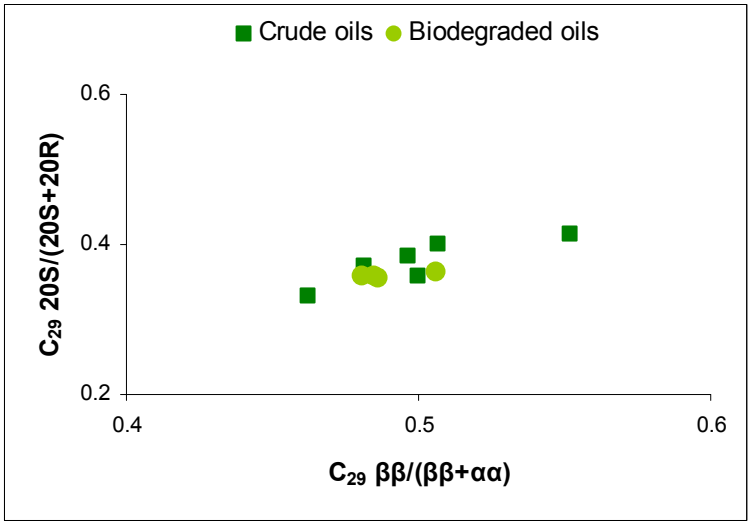

Fig 52 Plot of C_{29} 20*S*/(20*S*+20*R*) versus C_{29} *ββ*/(*ββ*+*αα*) steranes for Nigerian crude oils (after Seifert and Moldowan (1986)).

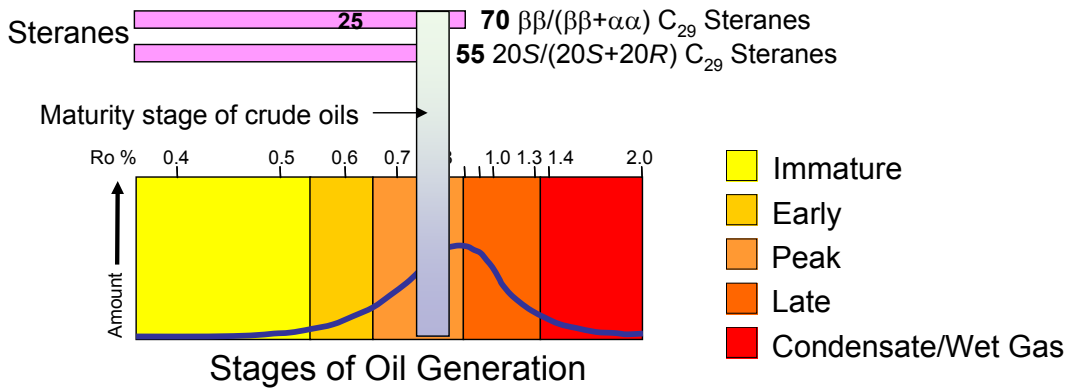

Fig 53 Biomarker maturation parameters are shown versus vitrinite reflectance and a generalized oil generating curve for Nigerian crude oils (based on Mackenzie (1984), Peters *et al.* (2005))

Hopanes and steranes for facies correlation

Fig 54 shows the sterane distribution for crude oils from Nigeria onshore. The Nigerian oils demonstrate similar amounts for $\alpha\alpha\alpha C_{28}$ sterane and slight variations of $\alpha\alpha\alpha C_{29}$ sterane, which can be cited to facies variations.

An outstanding biomarker in the Nigerian oils is the occurrence of 18α(H) oleanane, which is referred to an input of angiosperms (Ekweozor *et al.*, 1979; Ekweozor and Udo, 1988; Riva *et al.*, 1988; Ekweozor and Telnaes, 1990; Nwachukwu *et al.*, 1995; Haack *et al.*, 2000; Eneogwe and Ekundayo, 2003; Eneogwe, 2004). The oleanane index after Ekweozor and Telnaes (1990) (oleanane / C_{30} hopane) is about 1 for all oils. Eneogwe and Ekundayo (2003) classified crude oils from Nigeria in three different families based on light hydrocarbon distributions and biomarker parameters, e.g. oleanane /hopane ratio. According to these authors the oils would be classified as sourced from organic matter with a terrestrial input, but with greater marine affinity. But, the average of C_{29} steranes between 42 – 47 % in the studied

oils is much higher than mentioned from the authors. This observation suggests that the oils are generated from predominantly terrestrial organic matter. As well the presence of high waxy compounds in these oils cite to a terrestrial source. Less biodegraded oil samples show the presence of long-chain *n*-alkanes higher than *n*-C_{40} of waxy origin.

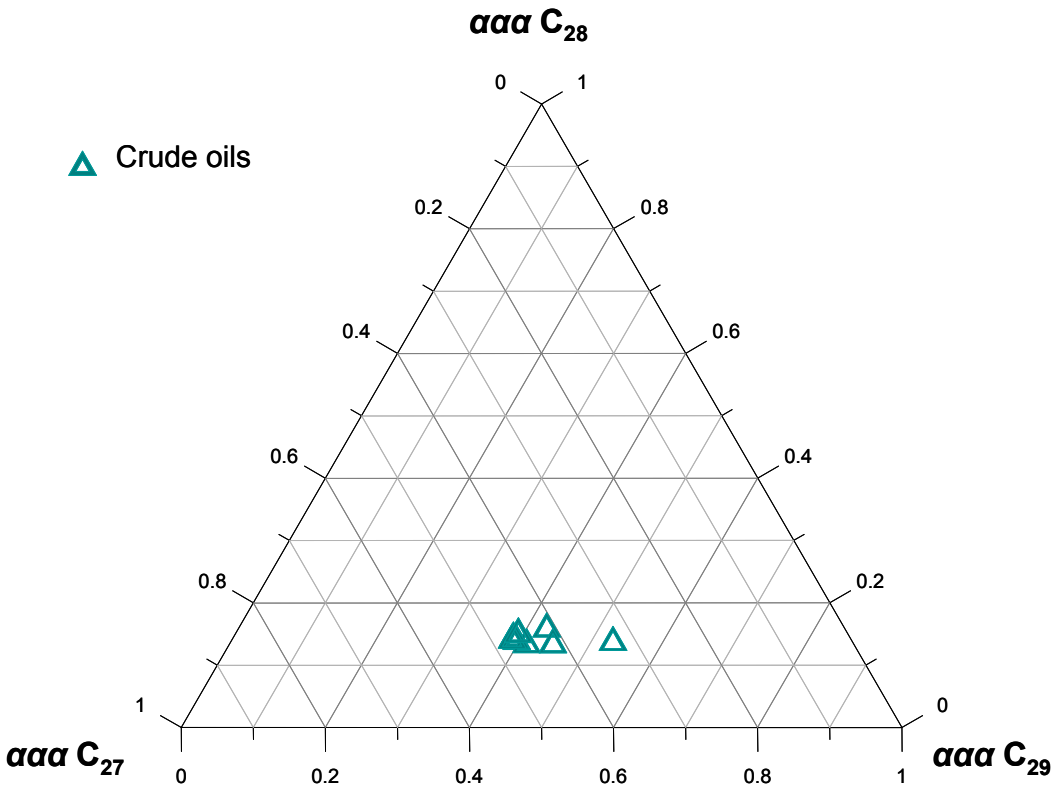

Fig 54 Ternary plot showing sterane composition of Nigerian crude oils.

Facies variations due to different terrestrial organic matter input is also observed in the cross-plot of the moretane ratio versus % of αααC_{29} sterane, as shown in Fig 55. Here, the moretane values slightly increases proportionally with increasing αααC_{29} sterane. Since moretane is attributed to be derived from terrestrial source (Isaksen and Bohacs, 1995; Peters *et al.*, 2005; Younes, 2005; Justwan *et al.*, 2006), the facies variations observed for the Nigerian oils are related to different input of terrestrial organic matter.

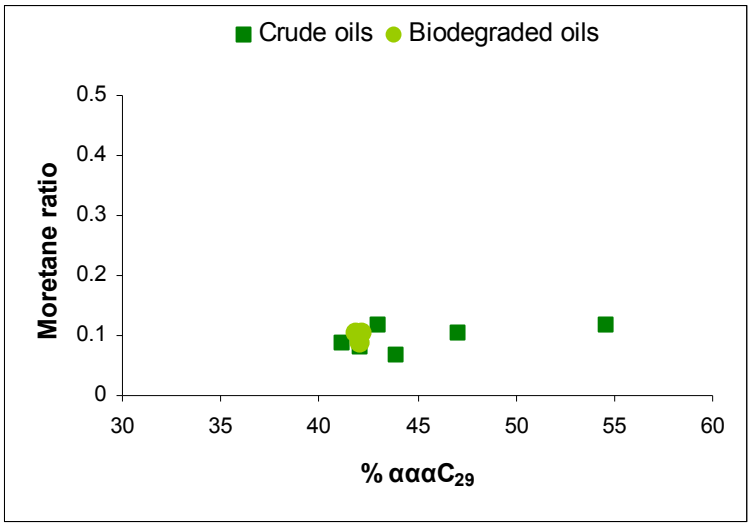

Fig 55 Cross-plot of the moretane ratio versus % αααC_{29} sterane for the Nigerian oils.

Although moretane is usually a maturity parameter (Waples and Machihara, 1990), it can here be used for facies correlations, since all oils are of same maturity, like shown before. This underlines also that moretane is highly facies related, even when used as maturity parameter. Moreover, from Fig 55 it is obvious that the biodegraded oil samples are all of very similar facie pointing to the same oil with different ranks of biodegradation.

5.3.1.3 Light hydrocarbons

Fig 56 illustrates the light hydrocarbons characteristics of the studied oils from Nigeria. The diagram with the heptane / isoheptane values established by Thompson (1983) is shown in Fig 56a. The heptane / isoheptane values were calculated as followed:

Heptane value = (2-methylhexane + 3-methylhexane) / (1,cis-3-dimethylcyclopentane + 1,trans-3-dimethylcyclopentane + 1,trans-2-dimethylcyclopentane).

Isoheptane value = 100.0 x *n*-heptane / (cyclohexane + 2-methylhexane + 1,1-dimethylcyclopentane + 3-methylhexane + 1,cis-3-dimethylcyclopentane + 1,trans-3-dimethylcyclopentane + 1,trans-2-dimethylcyclopentane + *n*-heptane + methylcyclohexane).

The light hydrocarbon parameters from Nigerian oils are very useful to distinguish less degraded from biodegraded oils, like shown in Fig 56a. The unaltered oils plot in the fields of normal to mature oils within the diagram established by Thompson (1983), whereas the biodegraded oil samples plot all in the field of biodegraded oils.

The difference between non-degraded and degraded oils is also obvious in terms of their paraffinicity F (*n*-heptane /methylcyclohexane) in that this parameter shows lower values for degraded oils pointing to be affected by biodegradation (Cañipa-Morales *et al.*, 2003), shown in Fig 56b. The same values of paraffinicity F for all non-degraded oils are as well an additional indication of same maturity stage for the studied Nigerian petroleums. However, from the same figure it is obvious that most oils have experienced secondary overprint due to evaporitic fractionation, probably during reservoir leakage. This is indicated by strong variations of the aromaticity parameter toluene / *n*-heptane.

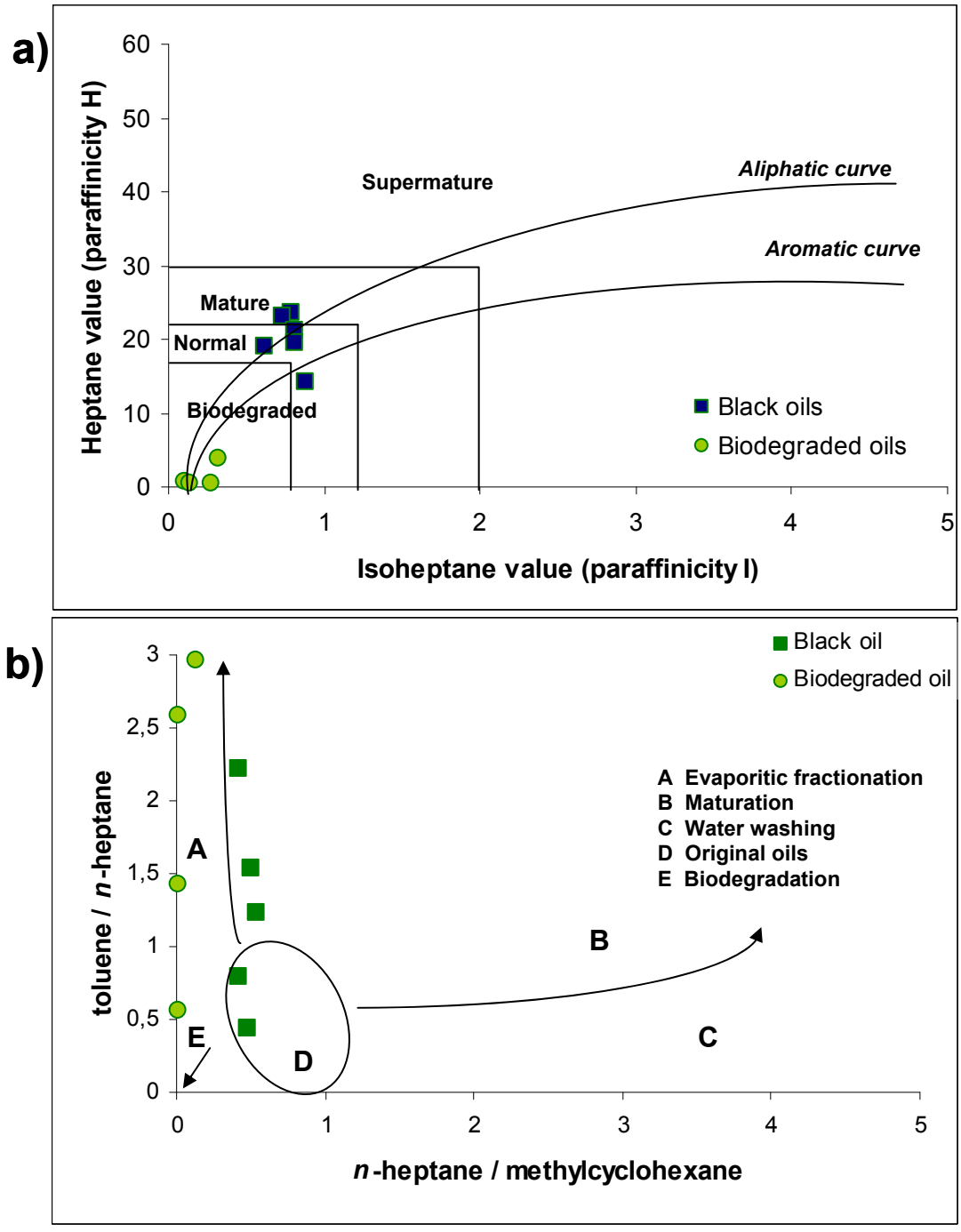

Fig 56 a) The cross plot of paraffinicity H versus paraffinicity I ratio for all investigated crude oils from Nigeria (after Thompson (1983)). b) Investigated Nigerian oils in terms of aromaticity versus paraffinicity (after Talukdar and Dow (1990); modified by Cañipa-Morales *et al.* (2003)).

5.3.1.4 Biodegradation

The three biodegraded Nigerian oil samples in Fig 57 are ranked in order of decreasing hydrocarbon biodegradation and increasing API gravity. The aliphatic hydrocarbons in the oils have been significantly affected by microbial attack relative to aromatic compounds. But these oils show a dominance of pristane and phytane as well as an unresolved hump. The sample G000506 shows depletion of light hydrocarbons as well as normal *n*-alkanes are virtually absent. Interestingly, some alkanes in the range of *n*-C_{12} to *n*-C_{15} are still present, where less biodegraded samples show dominance of these alkanes. Also, *n*-alkanes in the range *n*-C_{21} to *n*-C_{29} are still present in this sample. The sample G000503 differs in that even *n*-alkanes in these ranges are depleted, but this sample still contain higher amounts of light hydrocarbons than the crude oil described before. The sample G000507 with the 30.6° API indicates obviously slighter biodegradation. The *n*-alkanes are still present even when affected by degradation relative to aromatic compounds.

The extent of biodegradation following the scale of Peters *et al*. (2005) for this oil set ranges from 1 for the oil with an API gravity of 34°, and to 4/5 for most biodegraded samples (G000502, G000503 and G000506).

The study by open-system-pyrolysis on pyrolysates of asphaltenes isolated from Nigerian crude oils did not give evidence for any indication of asphaltene biodegradation.

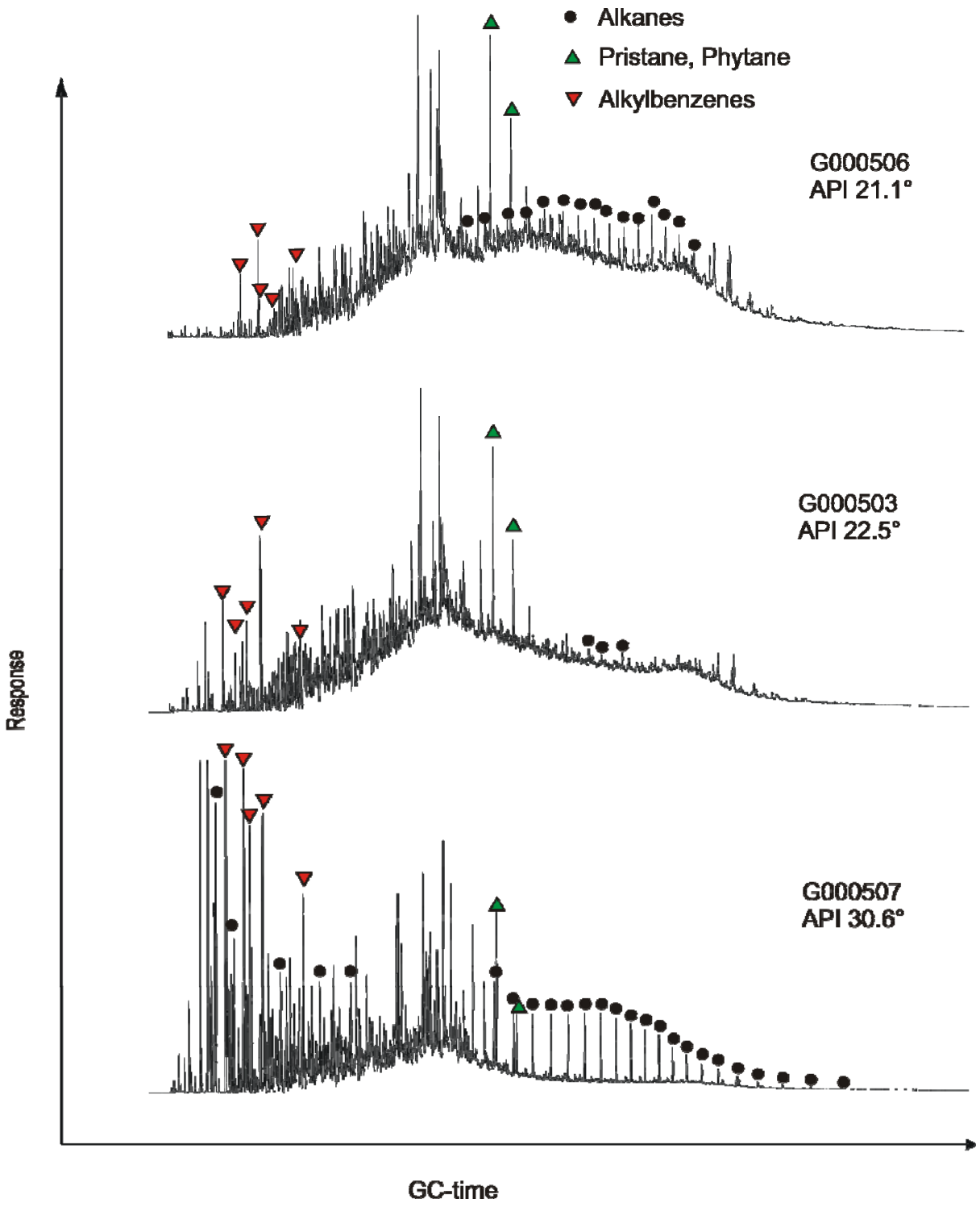

Fig 57 Thermovaporisation GC traces of 3 biodegraded oil samples from Nigeria are shown with increasing API gravity. Alkanes from *n*-C_7 when present, pristane and phytane, as well most abundant alkylbenzenes are marked. Benzenes are corresponding to retention time from left to the right: toluene, ethylbenzene, m,p-xylene, o-xylene, and trimethylbenzene.

5.3.1.5 Conclusions

- All Nigerian oils are of same stage of maturity, corresponding to a vitrinite reflectance of about 0.8 %Ro.
- These oils show minor facies variations probably due to different terrestrial organic matter input indicated by their biomarker distributions.
- Biodegraded oil samples are all of very similar facies pointing to the same oil with different ranks of biodegradation.The extent of biodegradation following the scale of Peters *et al*. (2005) for the most degraded oils is about 4/5, and there is no indication of asphaltene biodegradation.
- The light hydrocarbon parameters from Nigerian oils distinguish unaltered from biodegraded oils. However, most oils have experienced secondary overprint due to evaporitic fractionation. Thus, only their compositional characteristics in terms of paraffinicity should later be compared directly to the products formed from oil asphaltenes.

6 Asphaltene Precipitation Experiments

6.1 Introduction

Asphaltenes are defined based on solubility and not by chemical criteria. Thus, asphaltenes are those compounds in crude oils which precipitate upon addition of excess paraffinic hydrocarbon (Mitchell and Speight, 1973; Hirschberg *et al.*, 1984; Speight *et al.*, 1984; Leontaritis and Mansoori, 1988; Kawanaka *et al.*, 1989; Speight, 1999). The amount of solvent used to precipitate asphaltenes determines their surface properties and the amount of resins to remain attached to the asphaltene molecules (Ancheyta *et al.*, 2002; Parra-Barraza *et al.*, 2003; Pina *et al.*, 2006), since resins are more soluble in light-carbon-number alkanes than the asphaltenes. The volume ratio of solvent / oil therefore determines whether or not resin molecules remain at the asphaltene surface after precipitation. Several works demonstrated that incompletely extracted resins influence properties of asphaltene fraction such as molar mass (Agrawala and Yarranton, 2001; Alboudwarej *et al.*, 2002; Carauta *et al.*, 2005; Creek, 2005). Ancheyta *et al.* (2002) demonstrated that the quantity of asphaltenes precipitated varies with the volume of solvent added, becoming constant after reaching a solvent / oil ratio of 60 ml/g. The quantity of asphaltenes precipitated varies also with the chain length of the *n*-alkane used. Several authors (Mitchell and Speight, 1973; Corbett and Petrossi, 1978; Hotier and Robin, 1983) have demonstrated that the quantity of asphaltenes precipitated varies very little for *n*-alkanes with carbon numbers higher than *n*-heptane and increases significantly for shorter *n*-alkanes. The solvent type influences furthermore other asphaltene precipitation factors, such as the flocculation point, which is the point of incipient asphaltene precipitation. Wiehe *et al.* (2005) have shown that the flocculation point increases as the *n*-paraffin carbon number increases, reaching a maximum at a carbon number of 9 or 10, and then decreases.

Since it is known that the amount of isolated asphaltenes differs with solvent type, it is of interest if the solvent type has an effect on facies correlation using asphaltenes, as well if solvent type has effect on the geological predictions based on asphaltene kinetics. Therefore,

the objective of the present chapter is to investigate the effects of different solvent types on facies correlation utilizing asphaltenes, as well to evaluate the consequences for bulk kinetics on oil asphaltenes and resulting geological prediction.

Within the scope of this study three different crude oils from South Italy (G000394, G000395 and G000398) have been precipitated each with *n*-pentane, *n*-hexane, and *n*-heptane. The API gravity of these oils range from 2.62° to 19.35° and they possess high sulphur contents from 2.64 to 7.17 %. Table 9 shows selected oil samples and bulk characteristics.

sample	API gravity	sulphur content	solvent	wt.-% asphaltenes after 1.precipitation	wt.-% asphaltenes after 2.precipitation	wt.-% asphaltenes after 3.precipitation
G000394	2.62°	7,17%	*n*-C_5	*23,4%*	*20,8%*	*18,7%*
			n-C_6	*32,3%*	*17,5%*	*15,2%*
			n-C_7	*45,6%*	*24,6%*	*13,2%*
G000395	10.4°	6,83%	*n*-C_5	*18,8%*	*17,3%*	*17,1%*
			n-C_6	*17,2%*	*15,1%*	*13,5%*
			n-C_7	*15,6%*	*13,1%*	*12,5%*
G000398	19.35°	2,64%	*n*-C_5	*13,9%*	*12,5%*	*11,3%*
			n-C_6	*20,8%*	*11,9%*	*10,2%*
			n-C_7	*44,5%*	*11,8%*	*8,6%*

Table 9 Selected oil samples with bulk characteristics and percentage of isolated asphaltenes

In order to investigate the influence of asphaltene precipitation solvent on asphaltene kinetics and geological predictions, oil asphaltenes precipitated with different *n*-alkane solvents were submitted to artificial maturation experiments. Further on, asphaltenes isolated with *n*-pentane and *n*-hexane were diluted again, and re-precipitated with *n*-heptane. The maltene fractions (here called *R1* and *R2*) of this experiment were analysed to consider insolubility differences for asphaltenes from those different solvent types.

Fig 58 shows the work-flow diagram for this experiment.

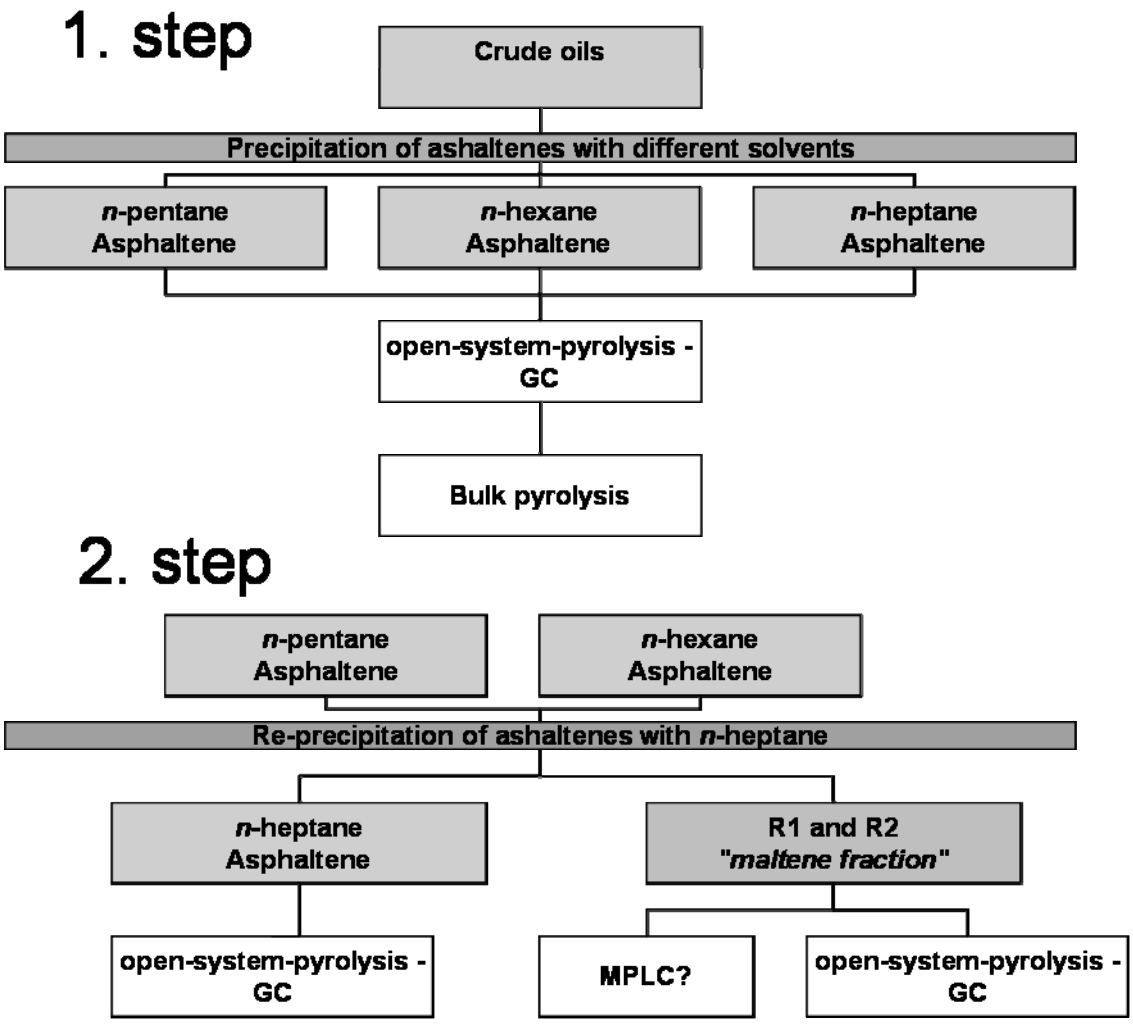

Fig 58 Analytical flowchart for the investigation on asphaltenes isolated with different solvents.

6.2 Amounts of asphaltenes

Yields of precipitated asphaltenes depend on the different solvent types, and also from the number of precipitations. After three precipitation steps asphaltenes precipitated with *n*-pentane provide the highest yields, while *n*-heptane resulted in the lowest quantities of precipitated material. The amount of precipitated asphaltenes decreases as the molecular weight of *n*-alkane solvent increases, like it is mentioned before.

Multiple precipitations is a common tool to purify asphaltenes, for the reason that isolated solids with only one precipitation step may consists still of high amounts of maltenes.

Fig 59 shows varying yields of wt-% of precipitated solids for each precipitation step. Considering isolated solids after three precipitations steps as pure asphaltenes, this example shows that high amounts of maltenes are co-precipitated using only one or two precipitation steps. The amount of precipitated solids decreases with consecutive precipitation. Here, in one example the amount of pure asphaltene after third precipitation is only about 20 wt-% compared to the amount of isolated solids after the first precipitation.

After the first precipitation two crude oils (G000394 and G000398) show extraordinary high yields of precipitated materials for *n*-hexane and even stronger for *n*-heptane solvents. These two crude oils are nearly solid and therefore highly viscous, in contrast to the more liquid crude oil G000395. The reason for the unusual high yields after the first precipitation step from nearly solid oils might be explained by a strong intermolecular association of maltenes and asphaltenes in high viscous crude oils or solid tars. The volume ratio of solvent / oil necessary to isolate pure asphaltenes from crude oils is therefore also determined by the viscosity of certain oil, and also by solvent type, like indicated for two the high viscous oils.

Purifying asphaltenes by multiple precipitation was investigated by Gürgey (1998), who studied the maltene fraction from each precipitation step in terms of biomarker distribution. The author noticed that the isoprenoid, hopane and sterane distribution varies in the maltene fractions from each precipitation step.

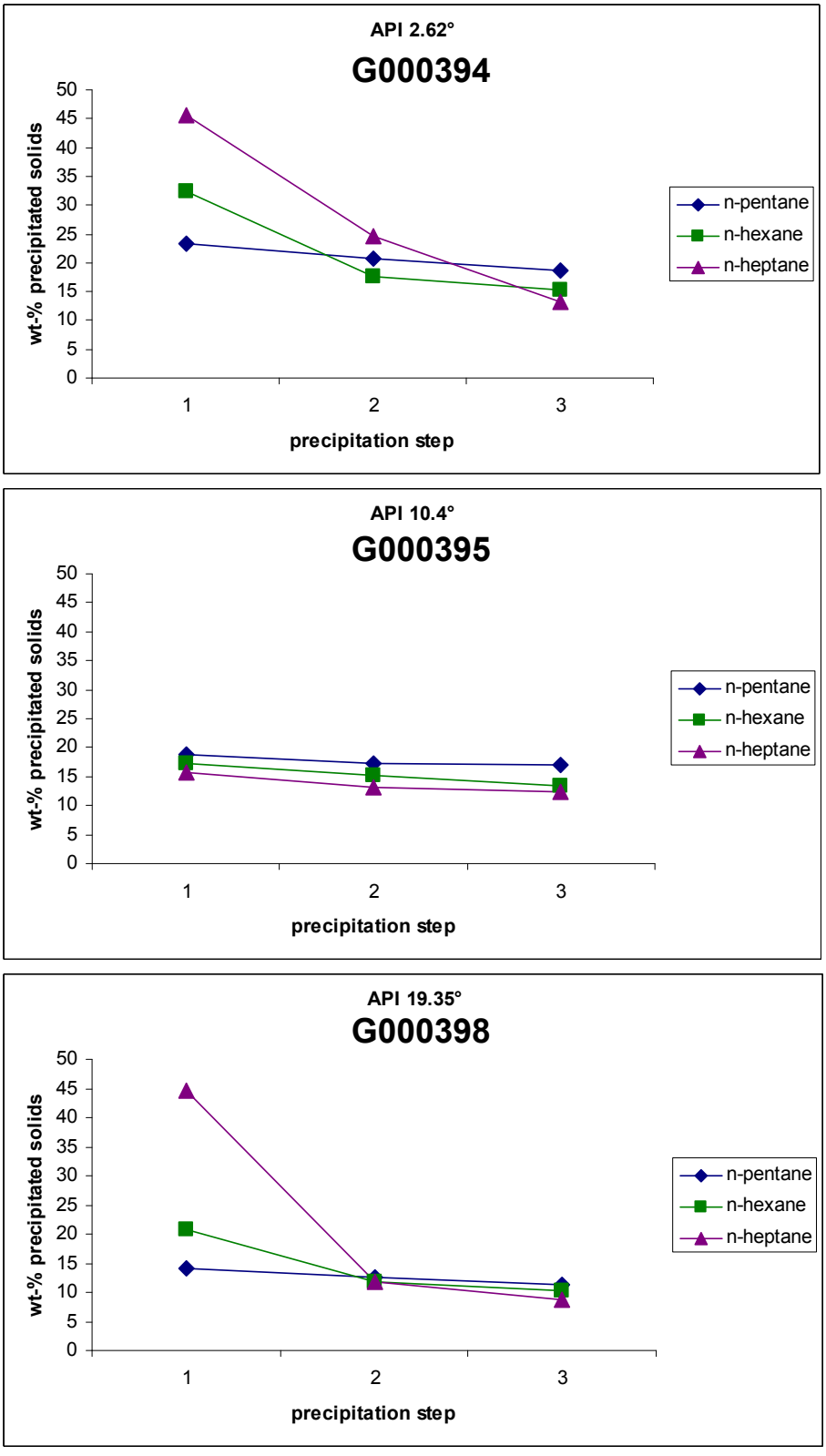

Fig 59 Weight percentage of precipitated organic matter with consecutive precipitation step.

6.3 Asphaltene pyrolysates

6.3.1 Aromaticity

Since our focus concerns the structural characterization of asphaltenes we studied the asphaltenes using open-system pyrolysis, which allows a comparison of asphaltenes in terms of compositional features. The studied samples correspond to the asphaltenes precipitated after the third precipitation step on the respective oils. Speight *et al.* (1984) reported increasing aromaticity based on the atomic H/C ratio for asphaltenes isolated with solvents of increasing carbon number. Since our investigation is limited only to common solvents from *n*-C_5 to *n*-C_7, we are not able to confirm this for the whole spectrum of solvents. Our results indicate a slightly increasing of aromaticity for those asphaltenes, which is within the standard deviation of the technical method (Fig 60). The ratio of aromatic compounds versus *n*-C_{6+}, named aromaticity, is very slightly increasing for corresponding asphaltenes with increasing chain length of solvent.

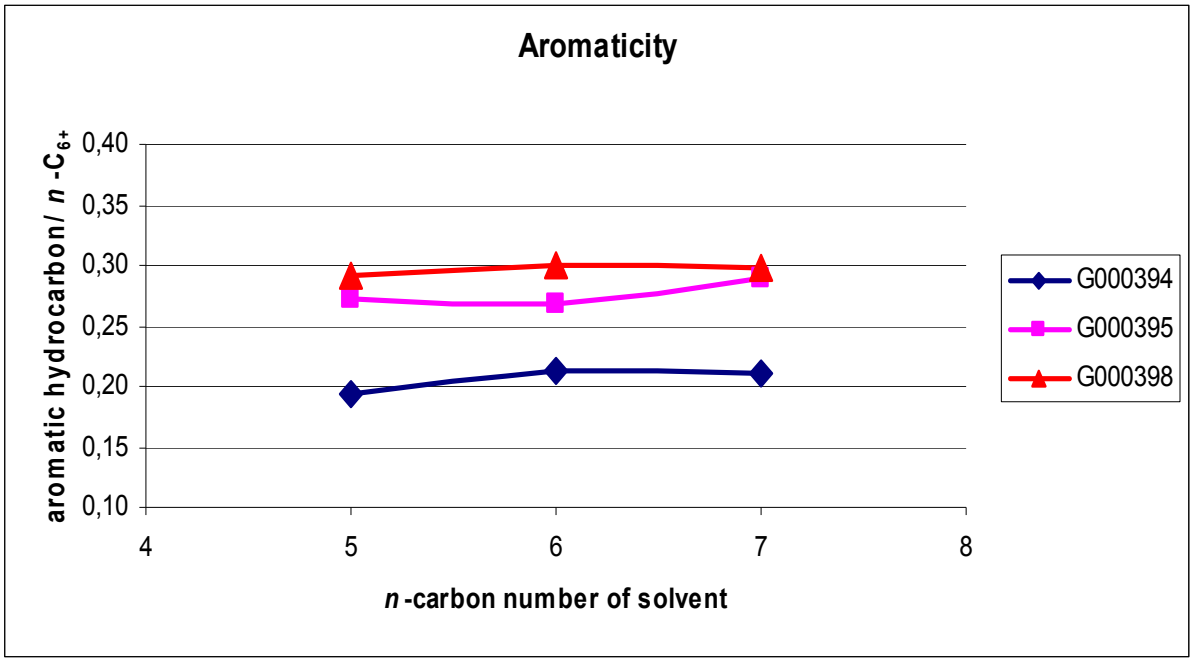

Fig 60 Aromaticity for three asphaltenes each isolated with three different alkane solvents.

6.3.2 Organic sulphur content

When focussed on specific compounds like for example thiophenes, there are more differences determined (Fig 61). Alkylated thiophenes represent the relative enrichment of organic sulphur in organic matter, which in turns can give information about the depositional environment (Sinninghe Damsté *et al.*, 1989; de Leeuw and Sinninghe Damsté, 1990; Eglinton *et al.*, 1990b; di Primio and Horsfield, 1996). In Fig 61 it is demonstrated that the ratio of total thiophenes (2- and 3-methylthiophene, 2,3- / 2,4- and 2,5-dimethylthiophene, and ethylmethylthiophene) versus *n*-C_{6+} slightly increases as the carbon number of solvent increases. But moreover differences are observed when investigating different single organic sulphur compounds, like for example 2,3-dimethylthiophene and 2,5-dimethylthiophene (Fig 61), which are commonly used to predict depositional environment (Eglinton *et al.*, 1990b; di Primio and Horsfield, 1996). In the second plot of this figure it is obvious that general ratios are not spreading, but it is observed that asphaltenes from *n*-pentane yield slightly higher ratios of 2,3-dimethylthiophene than others. However, the ratio of 2,5-dimethylthiophene and toluene, *n*-$C_{9:1}$ plus *n*-$C_{25:1}$ after di Primio and Horsfield (1996) differs from this observation too (Fig 61 right). Here, asphaltenes isolated with *n*-hexane show lowest ratios, whereas *n*-heptane insoluble asphaltenes represent the highest. This inversed behaviour compared to the general increasing trend of thiophenes might also be in part related to increasing amounts of aromatic compounds. Indeed, *n*-hexane isolated asphaltene show highest yields (µg/g asphaltene) of toluene of all studied asphaltene pyrolysates.

The ratios shown in Fig 61 are all obtained from GC-resolved pyrolysates.

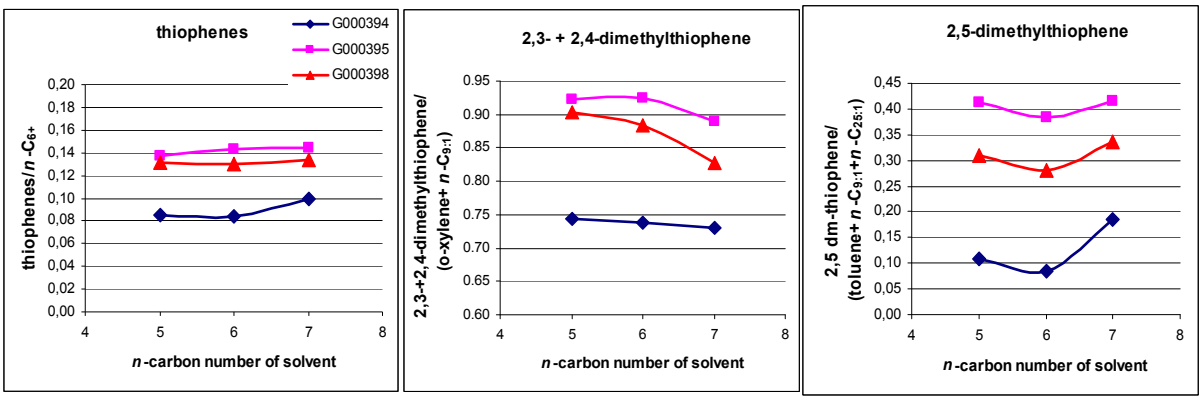

Fig 61 The ratios of total amount of thiophenes vs. *n*-C_{6+} (left), of 2,3-dm-thiophene vs. o-xylene plus nonene (middle), and of 2,5-dm-thiophene vs. toluene plus *n*-$C_{9:1}$ and *n*-$C_{25:1}$ (right) for three asphaltenes each isolated with three different alkane solvents.

The ratio of 2,3-dimethylthiophene and o-xylene versus *n*-$C_{9:1}$ has been chosen as a marker in order to assess the abundance of organic sulfur relative to hydrocarbons in pyrolysates (Eglinton *et al.*, 1990b). Sinninghe Damsté *et al.* (1989) proposed different precursor molecules for different alkylated thiophenes. With reference to them 2,3-dimethylthiophene is related to steroidal isomers, whereas the presence of 2,5-dimethylthiophene is connected with linear precursor isomers.

For this study it is of interest if the observed differences have an impact on predicting the depositional environment using the established diagrams. Fig 62 shows the ternary diagram with the use of 2,3-dimethylthiophene and o-xylene and *n*-$C_{9:1}$ as proposed by Eglinton *et al.* (1990b). Since asphaltenes show unusual low contents of 2,3-dimethylthiophene, the diagram was modified with the sum of 2,3- and 2,4-dimethylthiophene. All investigated asphaltenes predict the field of type II source rock, and none of these asphaltenes isolated with different solvents shows higher differences, which would lead to different predictions. From this figure it gets clear that these observed differences on a molecular level are very small scaled, not evident in ternary diagrams, and therefore they do not influence for example characterization of depositional environment, or have an impact on predicting the depositional environment utilizing petroleum asphaltenes.

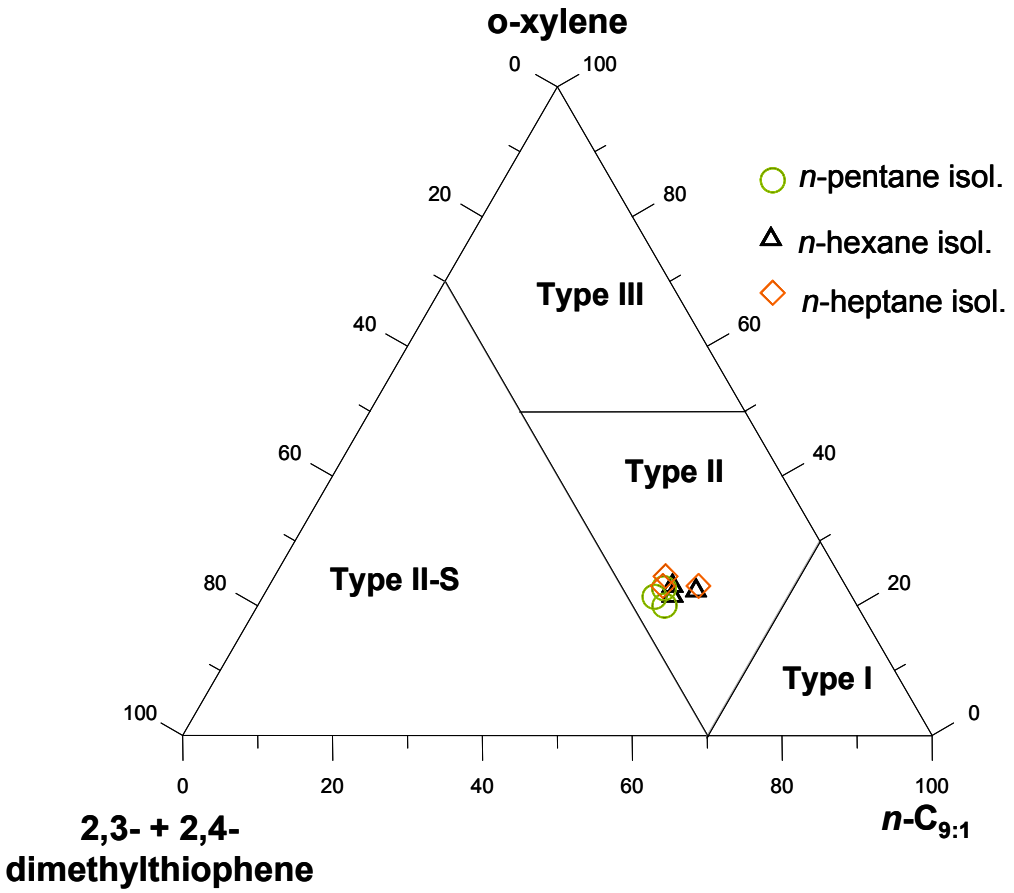

Fig 62 Ternary diagram of 2,3- + 2,4-dimethylthiophene, o-xylene, and *n*-$C_{9:1}$ for investigated reservoir asphaltenes (modified after Eglinton *et al.* (1990b))

6.3.3 GOR´s (Gas to Oil Ratio)

More obvious differences of isolated asphaltenes are found related to gas to oil ratio (GOR). Fig 63 presents the ratios of C_1-C_5/C_{6+} (GOR) of investigated asphaltenes. Changes in the gas to oil ratio are noted in that the GOR slightly increases with increasing carbon number of precipitation solvent. Asphaltenes isolated from *n*-hexane solvents are in all cases intermediate. This also shows that asphaltenes isolated with *n*-pentane display higher amounts of oil precursors than, and asphaltenes isolated with *n*-heptane exhibit highest amounts of gas generating precursors. This is in agreement with the observation of increasing aromaticity for

asphaltenes with increasing carbon number of solvent, where asphaltenes with higher aromaticity contain higher amounts of gas precursors.

More differences, for example the gas wetness (C_2-C_5/C_1-C_5) were not observed, indicating that products from *n*-heptane insoluble asphaltenes are slightly gas richer, but do not differ in terms of dry or wet gas. It is as well remarkable that the gas to oil ratio for asphaltene pyrolysates is inversely proportional to the API gravity of related crude oil. The asphaltenes isolated from the crude oil (G000394) with lowest API gravity show in all cases the highest GOR.

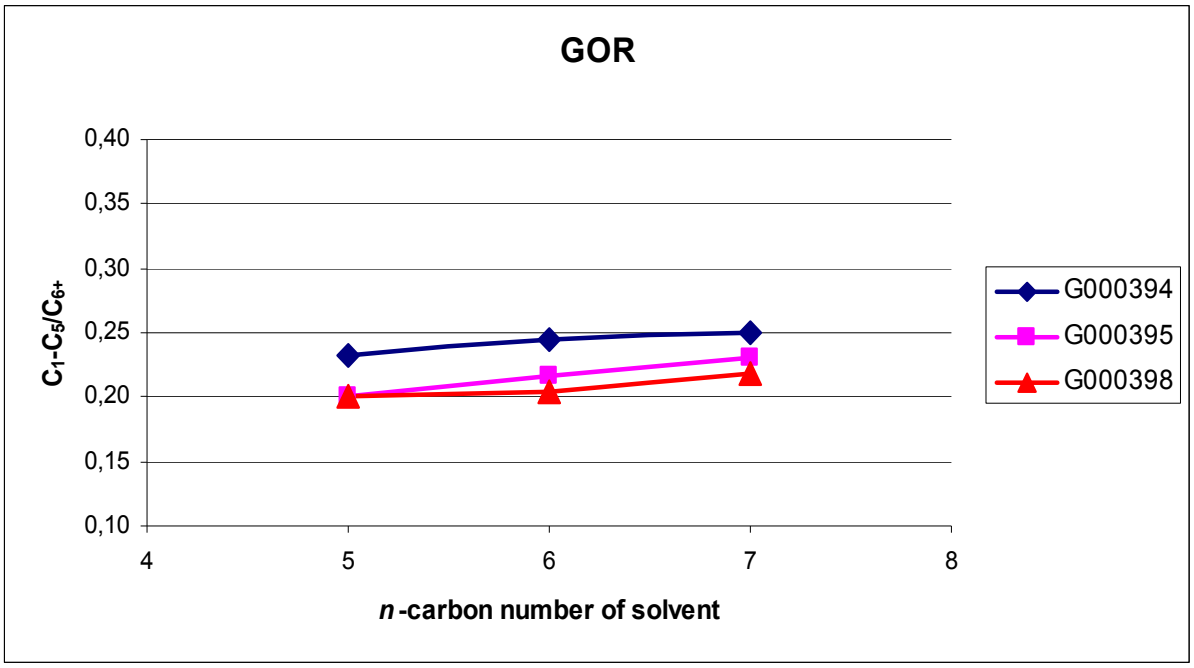

Fig 63 The gas to oil ratios (GOR) for investigated asphaltenes.

6.4 Asphaltene kinetics

In order to investigate the influence of asphaltene precipitation methodology on bulk kinetics and geological predictions, asphaltenes from different solvents were submitted to artificial maturation experiments.

Fig 64 shows the activation energy distribution and the frequency factor calculated on the measured asphaltenes from sample G000395. It can be seen that the asphaltenes precipitated with *n*-pentane show higher activation energies as compared to the other ones, whereas the asphaltenes from *n*-hexane and *n*-heptane do not show significant differences. The mean activation energy for asphaltenes precipitated with *n*-pentane is 54 kcal/mole, whereas the counterparts show Emean activation energy at 51 kcal/mole. Also the frequency factor of pentane-precipitated asphaltenes is with 1,2E+14 s^{-1} higher as compared to the counterparts, which have frequency factors between 1,6E+13 and 2,6E+13 s^{-1}. It is notable, that the activation energy distribution for the asphaltene isolated with *n*-pentane show artifacts in the range of low activation energies, so that realistic frequency factor A and mean activation energy even are higher for this sample.

These unequally transformation behaviour of asphaltenes results in unlike extrapolation to geological conditions. The calculated prediction of hydrocarbon generation for a geological heating rate of 3 K/my is illustrated in Fig 65. Geological temperature values, calculated to the respective bulk petroleum formation rates, are found between 130° and 140°C. Asphaltene from *n*-pentane solvent differs from the other ones in that the predicted geological heating rate is about 10°C higher than for the two other asphaltenes.

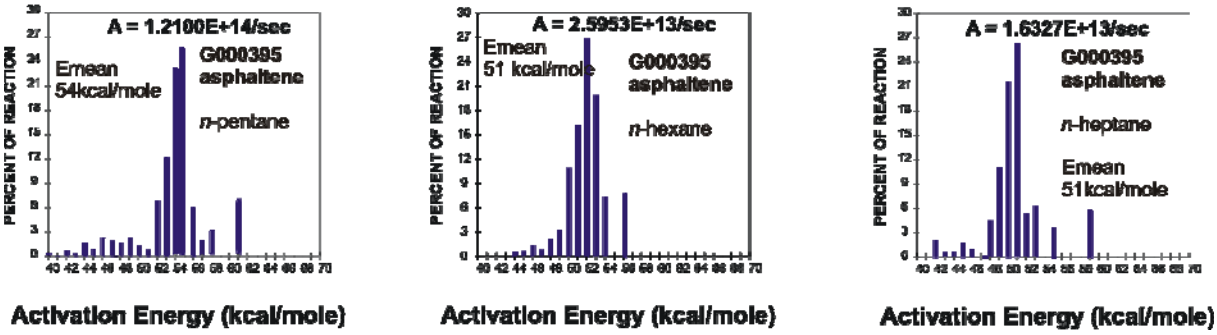

Fig 64 Activation energy distribution and frequency factor for oil asphaltenes precipitated with different alkane solvents from one crude oil (sample G000395).

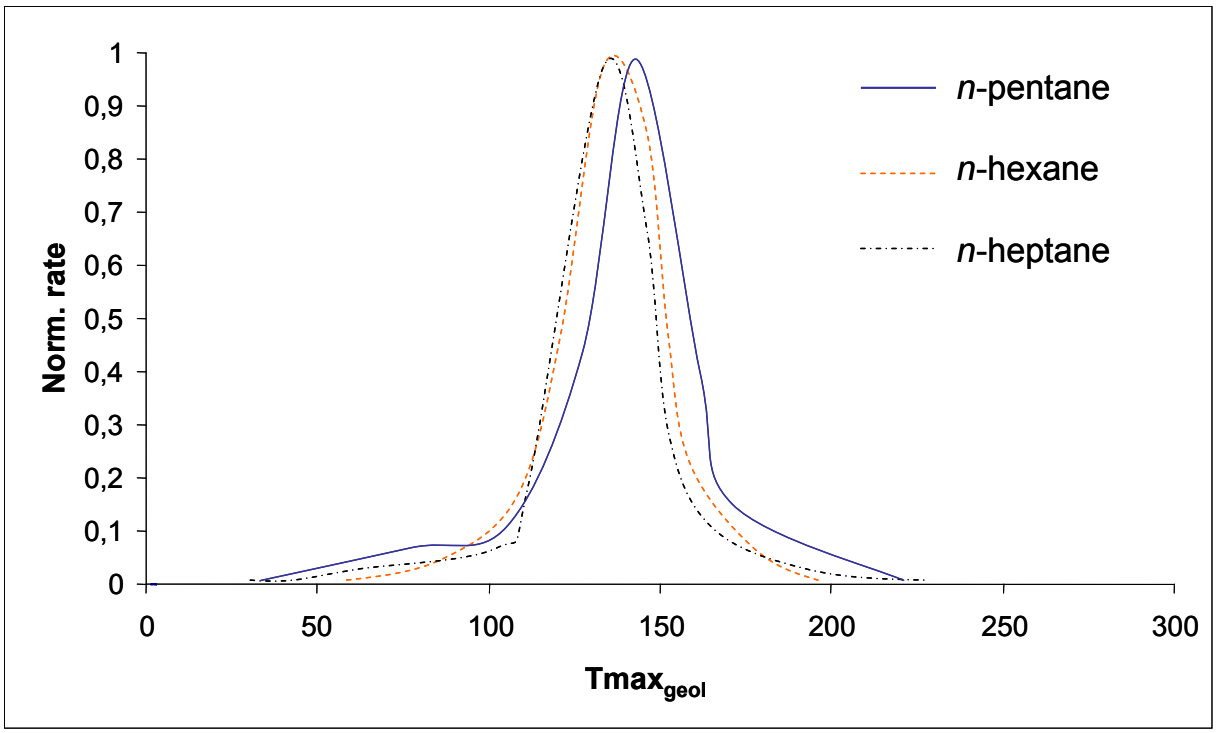

Fig 65 Prediction of bulk petroleum formation from the oil asphaltenes determined for a geological heating rate of 3 K/my using presented samples from Fig 64.

This clearly shows that *n*-pentane insoluble asphaltenes are more stable with respect to the chemical structure and covalent bonds. On the other hand, the same asphaltenes show in their pyrolysates lower GOR´s than their counterparts. Lewan (1998) proposed sulphur radicals as the rate-controlling factor in petroleum formation. These sulphur radicals are likely derived from cleaved C–S and S–S bonds, and the number of these bonds should be proportional to

the rate of thermal cracking. As shown in Fig 61, asphaltenes isolated with *n*-pentane present lower amounts of thiophenes, respectively lower amounts of organic sulphur. The resulting lower concentrations of sulphur radicals in these samples poorer in organic sulphur lead to petroleum formation at higher thermal stress. This explains higher activation energies and geological predictions obtained from *n*-C_5 isolated asphaltenes. The differences of asphaltenes precipitated with different solvents might be thus related to dissimilar processes of aggregation and/or chemical bonding of precursor molecules in the asphaltene macromolecule, like it is provided also for different sulphur containing precursor molecules. An explanation for differences in the chemical structure of asphaltenes based on different aggregation of asphaltene-precursor-entities (APE) due to the chain length of solvent might also be referred to the entropy of mixing of molecules of different sizes (Flory, 1953; Cimino *et al.*, 1995).

Beside, it is thinkable that differences in chemical linking of asphaltene-precursor-molecules like for example metalloporphyrins are also influenced by solvent types. Many authors mentioned these metalporphyrins, derived from chlorophylls and bacteriochlorophylls (Baker and Louda, 1986), as central chemical structure of asphaltene macromolecules (Premovic and Jovanovic, 1997; Marquez *et al.*, 1999; Groenzin and Mullins, 2001; Premovic *et al.*, 2002), and they are proposed to have catalytic effects on hydrocarbon generation (Premovic *et al.*, 1996). Therein might be as well an explanation for variations of stability of investigated asphaltenes, provided that vanadyl- and nickel containing porphyrins would influence bulk kinetics of asphaltenes too.

6.5 Structures related to insolubility differences

Finally, we decided to take a look inside what kind of chemical moieties are precipitated with *n*-pentane and *n*-hexane solvent, but are soluble in *n*-heptane. For that we diluted asphaltenes isolated with *n*-pentane and *n*-hexane in a dichloromethane (0.25 ml CH_2Cl_2/ 50 mg asphaltene), and precipitated each with *n*-heptane again, following the methodology previous described. The new precipitated asphaltenes do not differ from asphaltenes, which were directly precipitated with *n*-heptane.

Therefore we investigated the so-called maltene fraction of this experiment, because there should be the chemical compounds, which were occluded or included in the asphaltene structure using *n*-C_5 or *n*-C_6 solvent, but which were soluble in *n*-C_7 solvent. Fig 66 shows the flowchart for this investigation.

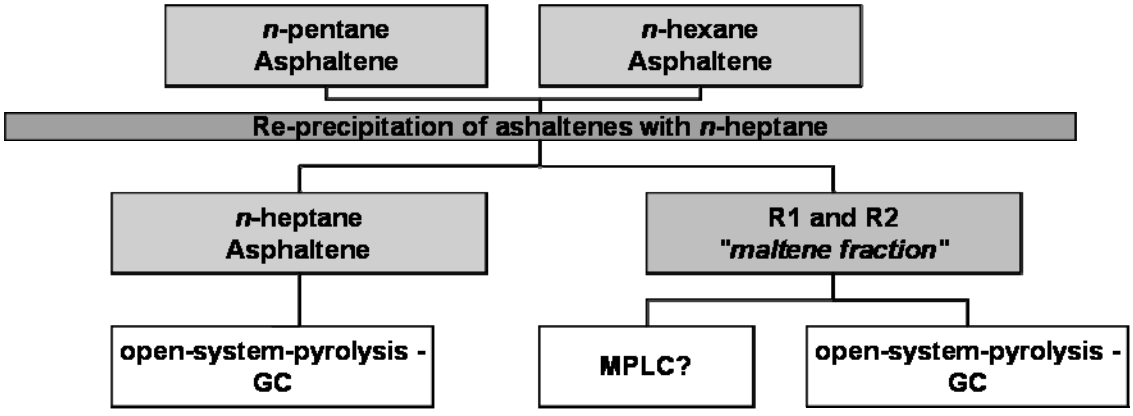

Fig 66 Analytical flowchart for this experiment.

For simplification the so called “maltene” fractions were termed *R1* (*n*-heptane soluble– *n*-hexane insoluble) and *R2* (*n*-heptane soluble– *n*-pentane insoluble). These fractions were concentrated by turbo vaporisation and finally dried under a gentle stream of nitrogen gas for further studies. Table 10 provides a list of weights of precipitants and recovered fractions.

base fraction			recovered fractions		
wt.(mg) asphaltene *n*-hexane	wt.(mg) asphaltene *n*-pentane	solvent	wt.(mg) asphaltene fraction	wt.(mg) maltene fraction *R1*	wt.(mg) maltene fraction *R2*
115,6 mg		*n*-C_7	112,28 mg	3,18 mg	
	153,1 mg	*n*-C_7	145,68 mg		7,22 mg

Table 10 Weights of asphaltene raw material (base fraction) and recovered fractions.

Further on, we tried to take an aliquot of these fractions for quantification and fractionation by liquid chromatography into saturates aromatics and NSO. But, it was noticed that while the pure organic matter from *R1* and *R2* is soluble in *n*-heptane, that same organic matter is still insoluble in *n*-hexane, for that MPLC analysis was hampered. First, this shows that the organic matter from *R1* and *R2* still can be termed by the general definition an "asphaltene", since it is insoluble in *n*-hexane, even if the same organic matter is soluble in *n*-heptane. And second, this shows that the organic matter from *R1* and *R2* are not maltenes *sensu stricto*, because they would have been soluble in *n*-hexane now. For that we investigated *R1* and *R2* further on by open-system-pyrolysis-GC too. Fig 67 shows the selected chromatogram of open system pyrolysis GC experiments on one asphaltene separated with *n*-heptane, and the chromatograms of *R1,* and *R2* respectively. The products from the *n*-heptane insoluble fractions (*R1* and *R2*) are less aromatic than the asphaltene isolated with this solvent. Products from *R1* and *R2* show lower contents of alkylbenzenes and alkylated thiophenes compared to the isolated asphaltene. It is difficult to state precursor molecules for alkylbenzenes in pyrolysates, which originate from cracking reactions via *β*-cleavage relative to the aromatic ring (Hartgers *et al.*, 1994a). It is generally accepted that alkylbenzenes in pyrolysates are derived from aromatization (La Londe *et al.*, 1987; da Rocha Filho *et al.*, 1993; Hartgers *et al.*, 1994a; Saiz-Jimenez, 1995). Derenne *et al.* (1996) have shown that alkylbenzenes in pyrolysates can also be related to a marine microalgae, called *Chlorella marina*.

Some major differences between asphaltenes and *R1, R2* fractions are found in some specific single compounds. The pyrolysates from *R1* and *R2* show distinguish higher amounts of *n*-$C_{18:0}$, resp. *n*-$C_{18:1}$, and an unknown single compound between *n*-C_8 and *n*-C_9, which is marked in Fig 67. The relative amount of these compounds is even higher in *R2* (*n*-heptane soluble– *n*-pentane insoluble).

N-C_{18} alkane is the most abundant hydrocarbon in many yeast and bacterial species (Grimalt *et al.*, 1991). For example non-photosynthetic bacteria may have hydrocarbon distributions dominated by *n*-C_{18} (Han *et al.*, 1968; Han and Calvin, 1969; Bird and Lynch, 1974; Jeng and Huh, 2004), as well halophilic bacteria display a dominance of this *n*-alkane (Grimalt *et al.*, 1992; Teixidor *et al.*, 1993). As already mentioned, the oil samples are sourced from an evaporitic sequence (di Primio and Horsfield, 1996), and for that an input of halobacteria is plausible. Beside, this alkane might also be indicative of autochthonous input (Han and Calvin, 1969; Grimalt *et al.*, 1991).

A dominance of *n*-C_{18} was also reported by Versteegh *et al*. (2004) to occur in "dinocasts" from the Eocene Jatta Gypsum Formation (Pakistan) originated from motile dinoflagellates. The biogenic input of dinoflagellate species in the Italian oils is provided by the abundance of dinosteranes found in those oils, which indicate that the occurrence of *n*-C_{18} in the Italian oils and related asphaltenes might also be attributed to these species. However, beside the origin of the biogenic precursor, the precipitation experiments show that the degree of cross-linking carbon chains, notably with 18 carbon atoms, within the asphaltene macromolecule decreases with increasing carbon number of solvent. This shows changes of chain functionality of isolated asphaltene macromolecules with different paraffinic solvents.

Further difference is observed in that the dominance of even-over-odd carbon number of alkanes in the range *n*-C_{18} – *n*-C_{26} slightly increases from *R1*<*R2*. This observation refers to

differences in aggregation of biogenic compounds between *R1* and *R2*, since even carbon *n*-alkanes are probably the result of reduction of even fatty acids or alcohols (Tissot and Welte, 1984).

The results of the present investigation clearly show that the chain length of solvent has an effect on the chemical structure of precipitated asphaltenes, and that the resulting chemical differences might have an impact on geological predictions for hydrocarbon generation based on asphaltene kinetics.

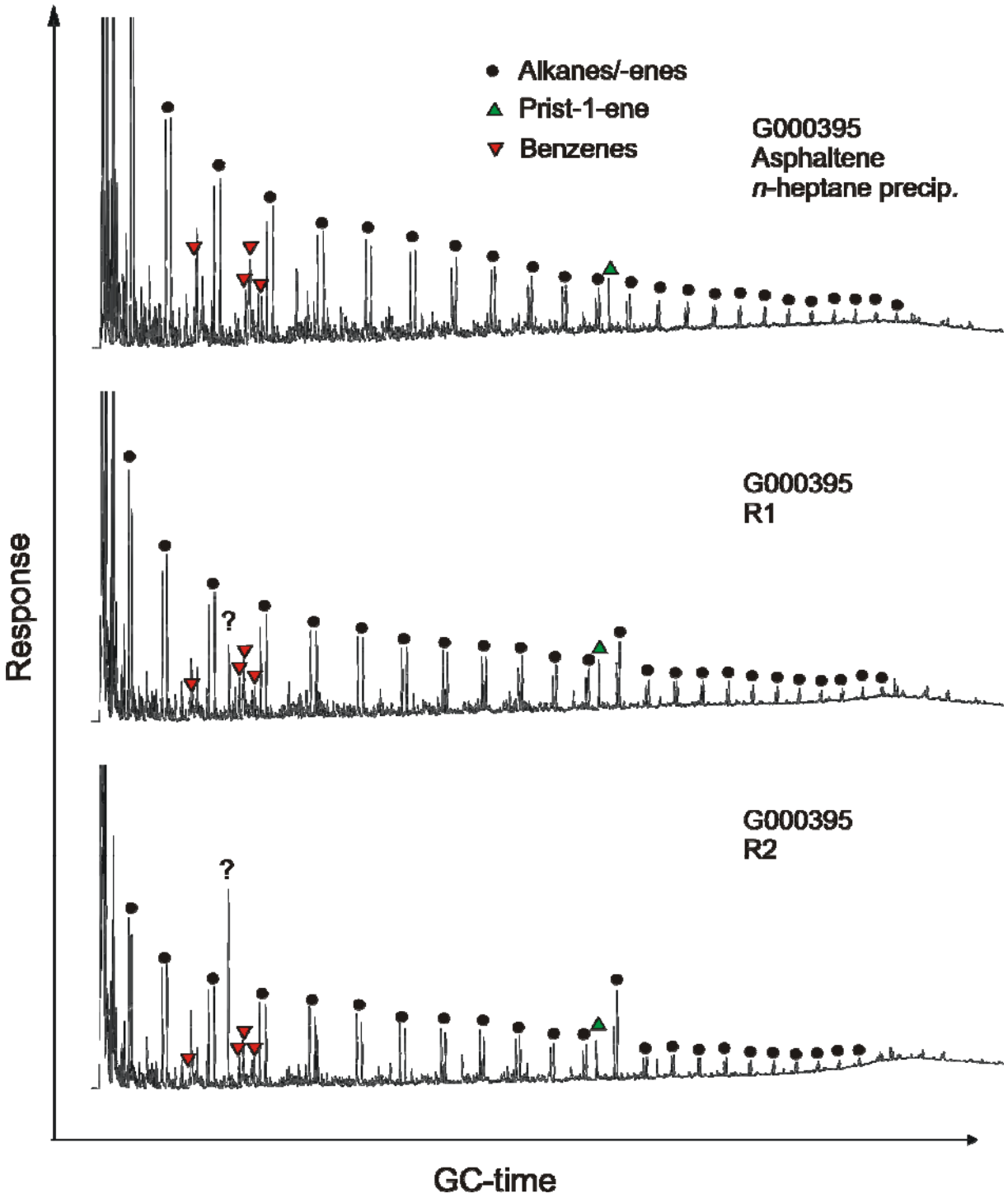

Fig 67 Selected chromatogram of open system pyrolysis GC experiments on one asphaltene separated with *n*-heptane (sample G000395), and the chromatograms of *R1* and *R2* respectively from the same sample. Alkylbenzenes are corresponding to retention time from left to the right: toluene, ethylbenzene, m,p-xylene, and o-xylene.

6.6 Separating asphaltenes from high-wax compounds

Crude oils sourced from terrestrial organic matter containing large amounts of hydrocarbons above C_{40}, have the potential to give rise to serious wax deposition problems during production, and in some cases within the reservoir itself (Afanasev *et al.*, 1993; Trindade *et al.*, 1996; Mansoori, 1999; Yang and Kilpatrick, 2005). The same is valid for asphaltene separation from high waxy crude oils, for those special separation techniques have been proposed (Heath *et al.*, 1997; Musser and Kilpatrick, 1998; Thanh *et al.*, 1999; del Carmen Garcia *et al.*, 2000; Yang and Kilpatrick, 2005). The classical view is that high wax, low sulphur oils were commonly associated with non-marine strata (Tissot and Welte, 1984). Tissot and Welte (1984) further summarised the geological settings for the occurrence of high wax oil as: (i) rift valleys of lower Cretaceous in the area of South Atlantic Ocean; (ii) paralic environments where high wax oils are associated with coal beds; (iii) continental lowlands with non-marine sedimentation. Petroleum wax hydrocarbons are not just simply composed of *n*-alkanes. Musser and Kilpatrick (1998) and Hsieh *et al*. (2000) discerned two distinct groups of petroleum waxes, which they termed microcrystalline and paraffinic. The microcrystalline waxes were composed of aliphatic hydrocarbon compounds containing a substantial amount of alkyl branching and naphtenic rings, whereas paraffinic waxes consist of hydrocarbon chains with few or no branches. While high wax oil occurrences are often associated with restricted types of basins and stratigraphic sequences, many of which are non-marine in origin, recent research (Thanh *et al.*, 1999; Hsieh *et al.*, 2000; Hsieh and Philip, 2001) has shown that waxy compounds are in fact ubiquitous components of crude oil (including marine oils). This implies that macerals other than higher plant exinite and vitrinite, e.g. marine or lacustrine alginite, may be the source of wax hydrocarbons in oils. The parent source rock must contain significant concentrations of long-chain and high molecular weight aliphatic structural moieties, either present as free (extractable) compounds or as molecular components covalently-bound within macromolecular organic phases (resins, asphaltenes and

kerogen), in order to generate a high content of waxes in the oils. Both, the initial biological input to sediments and the effect of depositional and diagenetic factors in preserving molecular features of lipids will control the occurrences and concentrations of long-chain aliphatic groups in source rocks, thus critically influencing their capability to generate high wax oil (Yang and Kilpatrick, 2005).

In order to avoid contamination risk of waxy compounds, we decided to isolate asphaltenes using hot *n*-heptane solvent (65°C), based on the assumption that high-wax compounds start to precipitate at low temperatures (Afanasev *et al.*, 1993; Hsieh, 1999). The effect of temperature on asphaltene separation in a degassed Chinese crude oil from Caoqiao (Shengli Oil Field) was previously investigated by Hu and Guo (2001). The authors showed that the amount of isolated asphaltenes decreases with increasing solvent temperature. But, no research has studied the effect of solvent temperature on the bulk chemical composition of isolated asphaltenes. Therefore, we precipitated asphaltenes from the most biodegraded crude oils by the common precipitation method using *n*-hexane as well, and compared them to asphaltenes isolated with hot *n*-heptane in terms of their aromaticity by pyrolysis (Fig 68).

In all cases the asphaltenes isolated with *n*-hexane at room temperature display higher aromaticity than their counterparts separated with hot *n*-heptane. This is of course related to temperature effect, because in general the aromaticity increases with increasing carbon number of solvent type (Speight *et al.*, 1984), which is contrary to the present observation. This is also remarkable when bearing in mind that asphaltenes isolated with hot *n*-heptane are purer in long-chain *n*-alkanes than asphaltenes precipitated with *n*-hexane at room temperature.

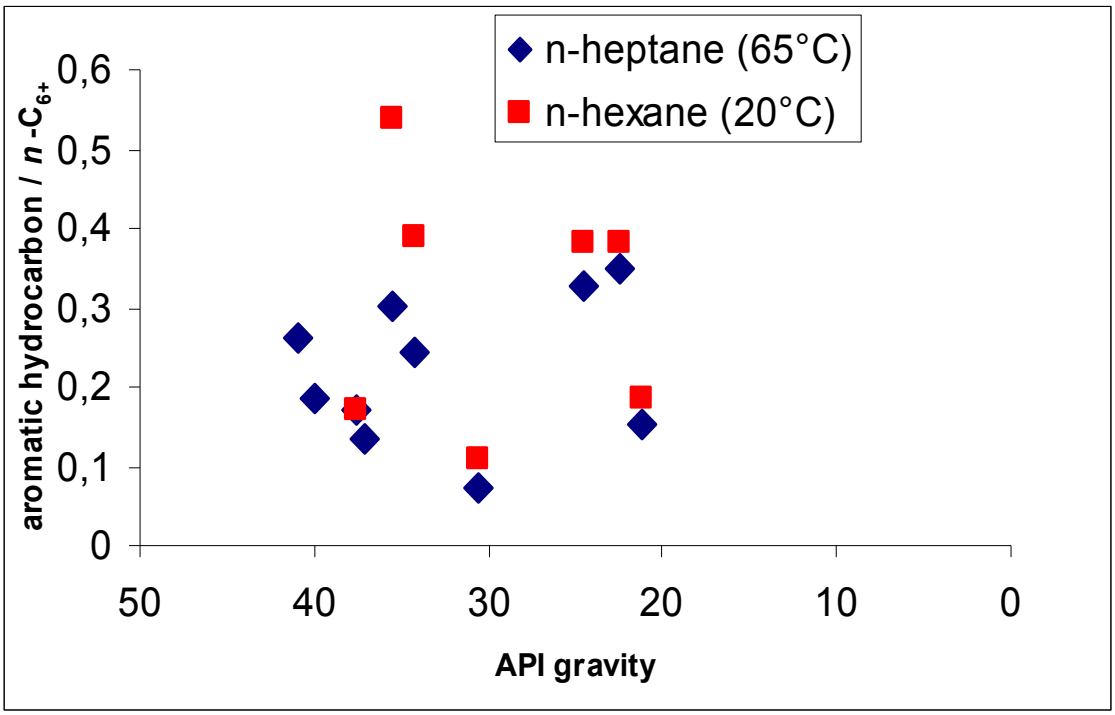

Fig 68 Aromaticity of asphaltene pyrolysates from asphaltenes isolated with *n*-hexane and hot *n*-heptane.

6.7 Conclusions

- Asphaltenes isolated with *n*-pentane, *n*-hexane and *n*-heptane from consecutive precipitation show different amounts of precipitated asphaltenes in that the total amount of asphaltenes decreases with increasing molecular weight of *n*-alkane solvent.
- Asphaltenes isolated with different *n*-alkanes solvents show minor differences in terms of aromaticity, distribution of organic sulphur compounds, and GOR´s, which in turns do not affect the geological prediction of depositional environment obtained from the bulk chemical information of reservoir asphaltenes.

- Related to chemical kinetics and progressive transformation of organic matter, asphaltenes isolated with *n*-pentane show lower reactivity.
- For bulk kinetics and calculated prediction of hydrocarbon generation the asphaltenes precipitated with *n*-pentane differs from the others by higher activation energy and higher geological temperatures values.
- For this sample set, the organic matter which is soluble in *n*-heptane, but insoluble in *n*-pentane and *n*-hexane, is enriched in octadecane/-en and an unknown single compound between *n*-C_8 and *n*-C_9. That same organic matter shows lower amounts of alkylbenzenes and alkylthiophenes in their pyrolysates, indicating differences in the chemical structure of asphaltenes isolated with different *n*-alkane solvents.
- Asphaltenes from Nigerian crude oils isolated with *n*-hexane at room temperature display higher aromaticity than their counterparts separated with hot *n*-heptane.
- This precipitation experiments clearly show, that asphaltene pyrolysates and bulk kinetic parameters of asphaltenes can only be compared to each other, when asphaltenes are precipitated using the same method. Therefore, asphaltenes from Nigerian oils cannot be compared to asphaltenes from Italian and Duvernay samples within this thesis.
- For the further study, we decided to separate asphaltenes from crude oils and source rock bitumen from Southern-Italy, and the Duvernay Formation with *n*-hexane, because the results from this experiment show, that *n*-hexane isolated asphaltenes prove best in terms of bulk kinetics, geological predictions, and structural moieties.
- Further studies on asphaltenes from Nigerian oils were conducted on asphaltenes isolated with hot *n*-heptane to avoid co-precipitation of high waxes.

7. Characterization of asphaltenes from a type II-S sequence

7.1. Bulk kinetic parameters

7.1.1 Introduction

Petroleum formation or hydrocarbon generation is a progressive transformation of organic matter, like kerogen, as a function of time and temperature (Juntgen and Klein, 1975; Tissot and Welte, 1984; Tissot *et al.*, 1987; Schenk *et al.*, 1997). The characterization of hydrocarbon generation of a known organic matter can be described by chemical kinetics in terms of activation energies (Ea) and frequency factor (A). This generating process is accompanied by cracking of numerous covalent bonds (e.g. C-C, C-O, C-S), each having distinct energies. These energies of a given bond type are related to chemical structure of source organic matter and the distribution of covalent bonds in its matrix.

The progress of hydrocarbon generation can be predicted by determining the activation energy distribution and the frequency factor on the basis of pyrolysis experiments. Conventional kinetic models use either a single activation energy and frequency factor set (Welte and Yalcin, 1988) or multiple activation energies with a single frequency factor (Tissot *et al.*, 1978; Delvaux *et al.*, 1990; Reynolds *et al.*, 1995; Dieckmann *et al.*, 1998; Schenk and Horsfield, 1998; Vandenbroucke *et al.*, 1999) to model hydrocarbon generation. Most recently also models containing a distribution of activation energies and a distribution of frequency factors have been applied (Dieckmann, 2005).

Little has been reported about the application of type II-S asphaltenes to kinetic studies. Earlier works mentioned that asphaltenes and related type II kerogens show similar structural features (Béhar *et al.*, 1984; Pelet *et al.*, 1986; Tissot, 1989). Later, several studies focused on kinetics of asphaltenes generated from type II-S kerogens, but without illustrating a clear relationship with genetically related source rock kerogens (Kuo and Michael, 1994; di Primio

and Horsfield, 1996; di Primio *et al.*, 2000; Dieckmann *et al.*, 2002). Di Primio *et al.* (2000) showed that source rock asphaltenes from sulphur-rich settings are less stable than their related kerogens, and explained this discrepancy in that asphaltenes from type II-S settings represent only labile fragments of related kerogens. Di Primio and Horsfield (1996) have shown that the stability of source rock asphaltenes is lower than that of the associated kerogens, and assumed that these results can be directly applied using petroleum asphaltenes. In the present thesis, however, we will later on show that this may be dangerous, since source rock asphaltenes and petroleum asphaltenes have significant structural differences.

The goal of the current study was to compare asphaltenes kinetics from reservoir oils with those of source rock bitumens and related thermally extracted whole rocks, as well as the resulting geological predictions.

7.1.2 Kinetic parameters

Bulk kinetic parameters calculated for four selected thermally-extracted, immature whole rock samples with Tmax ranging from 415-439°C are shown in Fig 69. Three of the four activation energy distributions show generally broad distributions, typical for that of heterogeneous organic matter. The distribution of activation energies generally ranges from 48 – 58 kcal/mole with main activation energies of 53 – 55 kcal/mol and frequency factors of 1.5 – 4.1E+14 s^{-1}. It was already mentioned that sample G000661 differs to the other source rock samples, in that sample G000661 shows an unusual high Rock-Eval Tmax (439°C) within the sample set, and based on biomarkers higher indices for gammacerane, homohopanes, and methylphenanthrenes. Differences for this sample were also observed in terms of kinetic parameters, because kinetic analysis results in one single main activation energy with an Ea of

52 kcal/mol and an A of 3.3E+13 s^{-1}, indicating this type of organic matter to be much more homogenous (type I kerogen) than the sedimentary organic matter preserved in the other samples. With reference to Kenig *et al*. (1990) homogenous organic matter in hypersaline environments point to be originated from lagoonal mats (seagrass), and not to be from microbial mats with different bacterial colonies.

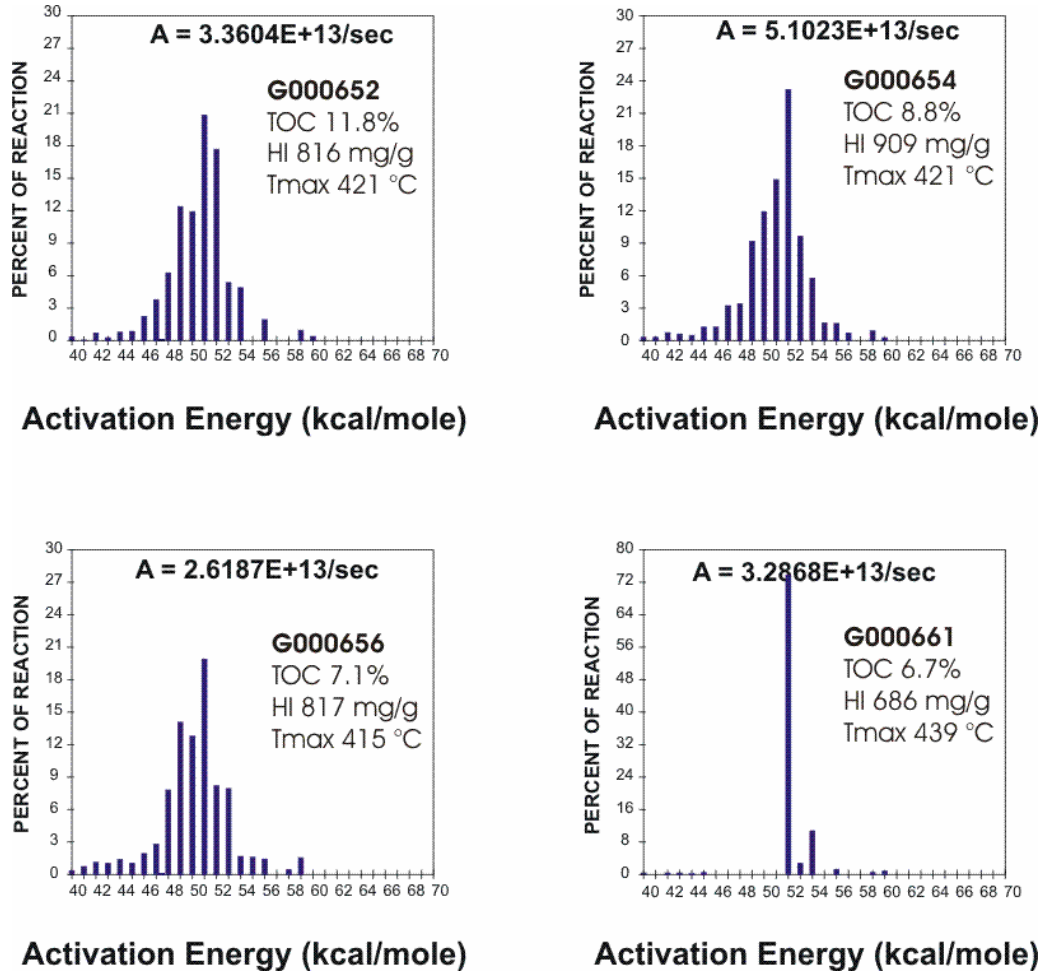

Fig 69 Activation energy distribution (Ea) and the frequency factor (A) calculated for selected source rocks and from South Italy

The activation energy distribution (Ea) and the frequency factor (A) for asphaltenes isolated from the same source rock samples presented before are shown in Fig 70. These asphaltenes show low activation energies with Ea max about 49 kcal/mole and frequency factors ranging

from 9.5E+12 and 4.1E+14 s^{-1}. Only the asphaltene from sample G000652 shows higher Ea max of 55 kcal/mole. Interestingly, the asphaltene isolated from the sample G000661 is different from the related kerogen. The kerogen shows a typical activation energy distribution for homogenous organic matter, whereas the isolated asphaltene is comparable to the more heterogeneous asphaltenes in other samples.

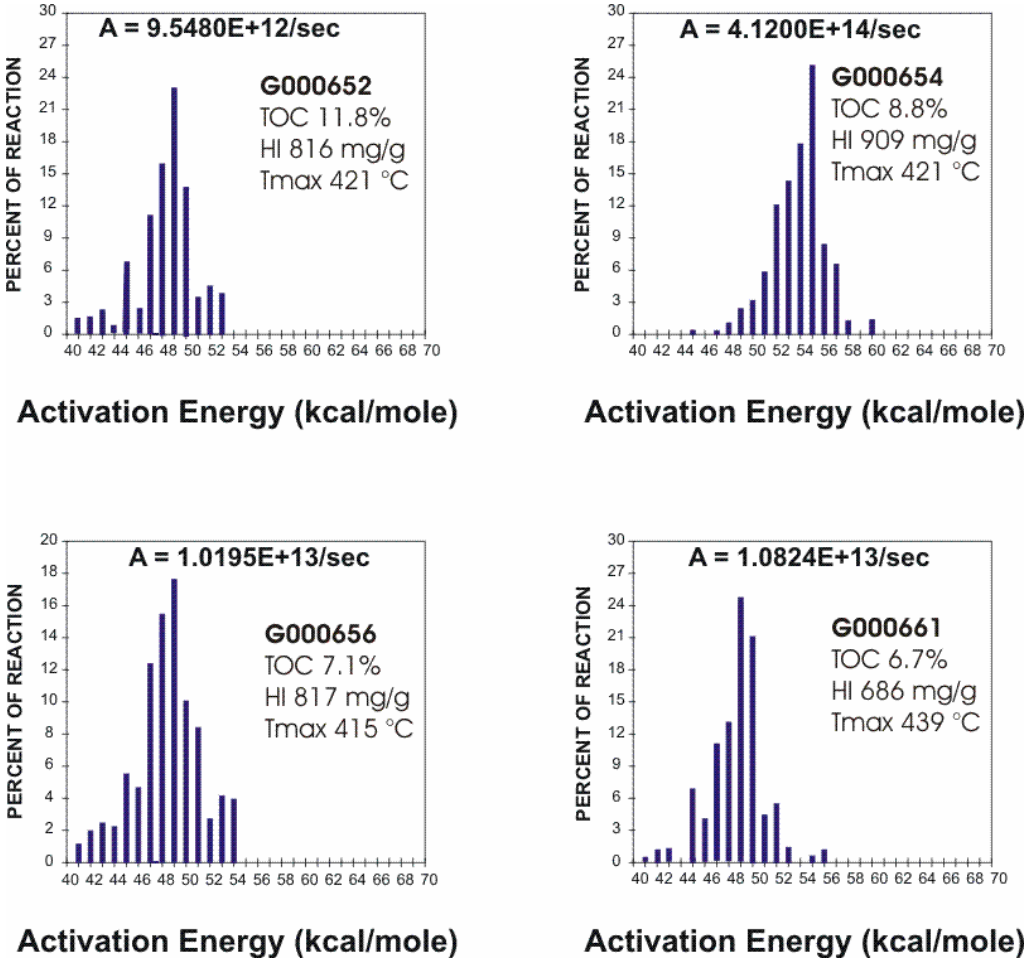

Fig 70 Activation energy distribution (Ea) and the frequency factor (A) calculated for source rock asphaltenes from Italian samples.

Fig 71 shows the activation energy distribution and the frequency factor calculated for the degradation of asphaltenes isolated from crude oils. The investigated reservoir asphaltenes show low activation energies with Ea maxima ranging from 47 to 51 kcal/mole and frequency

factors ranging from 5.5E+11 and 2.6E+13 s^{-1}. The activation energy distributions for the investigated asphaltenes are generally not as broad as those of the source rocks and indicate that the precursor material for the generation of hydrocarbons is significantly more homogeneous than that in the source rock kerogens. The oil asphaltene from sample G000394 shows a wider range of activation energies from 40 to 52 kcal/mol, which might be related to facies variations. This was also observed for the biomarker parameters studied for the related crude oil. Sample G000394 shows the lowest gammacerane index (0.05), indicating a less saline source for this oil.

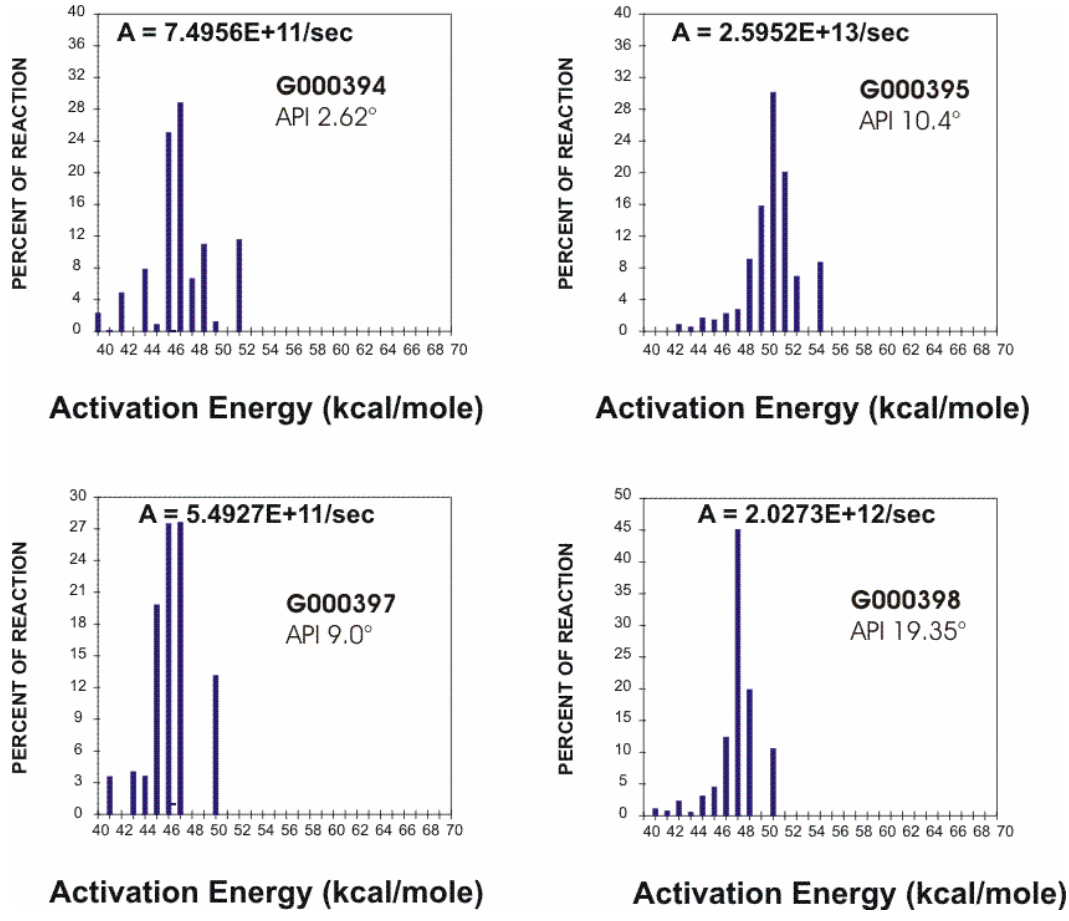

Fig 71 Activation energy distribution (Ea) and the frequency factor (A) calculated for oil asphaltenes from Italian crude oils.

As mentioned, the source rock sample G000661 and the oil sample G000394 differ in terms of biomarkers from the other samples. However, the other samples used for the kinetic analysis show greater similarities to each other based on biomarker parameters. So, the kinetic parameters from those kerogens, source rock asphaltenes and reservoir asphaltenes can compared directly to each other:

Summing up, it can be concluded that reservoir asphaltenes, source rock asphaltenes and related kerogens show distinct differences in terms of kinetic parameters. Both, source rock kerogen and source rock asphaltenes show broader activation energy profiles than the petroleum asphaltenes. In addition, it can be observed that the mean activation energies evaluated on source rock and petroleum asphaltenes are systematically lower than for the source rock kerogens.

7.1.3 Geological prediction of hydrocarbon generation

As a consequence of different kinetic parameters the predictions based on geological heating rates do not result in similar temperatures, as shown in Fig 72 and Fig 73. The onset of the main phase of petroleum formation for the source rock samples was predicted to start at around 80°C under geological conditions, while hydrocarbon generation from both types of asphaltenes starts slightly earlier (Fig 72). Peak petroleum formation ($Tmax_{geol.}$) was found between 118 and 135°C for oil asphaltenes, while source rock asphaltenes cover a range between 124 and 140° and the source rock samples range from 140 to 152°C (Fig 73). At temperatures between 170 to 190° petroleum formation from source rocks as well as from source rock asphaltenes comes to an end, whereas hydrocarbon generation from oil asphaltenes already ends at temperatures between 150 to 165°C. The source rock asphaltenes isolated from sample G000654, however, continue generating hydrocarbons up to 200°C (Fig 72). The calculated geological Tmax is with 140°C also higher than for the other source rock

asphaltenes. This source rock asphaltene do not show major difference based on open-system-pyrolysis, but the related kerogen shows an unusual distribution of alkane / alkene ratios with an entire predominance of alkene for alkyl chain doublets higher than *n*-C_6, so that differences found in bulk kinetic measurements for this sample are probably related to facies variations and different organic input. Additionally, the whole rock sample G000661, which is probably attributed to lagoonal mats differs from other samples in terms of geological predictions. Hydrocarbon generation from the kerogen starts at temperatures about 120°C and peak petroleum formation occurs at 152°C. However, the isolated asphaltene from this sample does not show any difference to other source rock asphaltenes as regards its kinetics of hydrocarbon generation. Fig 73 shows the diagram of calculated geological Tmax versus the Rock-Eval Tmax for source rocks and related asphaltenes. The geological Tmax versus the API gravity for oil asphaltenes is plotted on the right-hand side. The calculated $Tmax_{geol}$ and relevant Rock-Eval data for studied samples are listed in Table 11. As can be seen from Fig 73, predicted geological temperatures for peak hydrocarbon formation is lower for source rock asphaltenes than for related kerogens. Hence, calculated geological Tmax temperatures measured on reservoir asphaltenes are even somewhat lower, suggesting that reservoir asphaltenes are generated during an early stage of hydrocarbon generation. Bearing in mind that the differences in onset temperatures are modest, it cannot be excluded that stable bonds responsible for the generation of late petroleum formation are simply not present in the petroleum asphaltenes. But it is remarkable, that neither calculated temperatures for peak petroleum formation of reservoir asphaltenes nor source rock asphaltenes change systematically with API gravities, or Rock-Eval Tmax. This systematical change of $Tmax_{geol}$ and Rock-Eval Tmax is found for source rock kerogens. Only sample G000652 differs from that, and shows lowest $Tmax_{geol}$ (140°C), whereas the Rock-Eval Tmax is with 421°C intermediate.

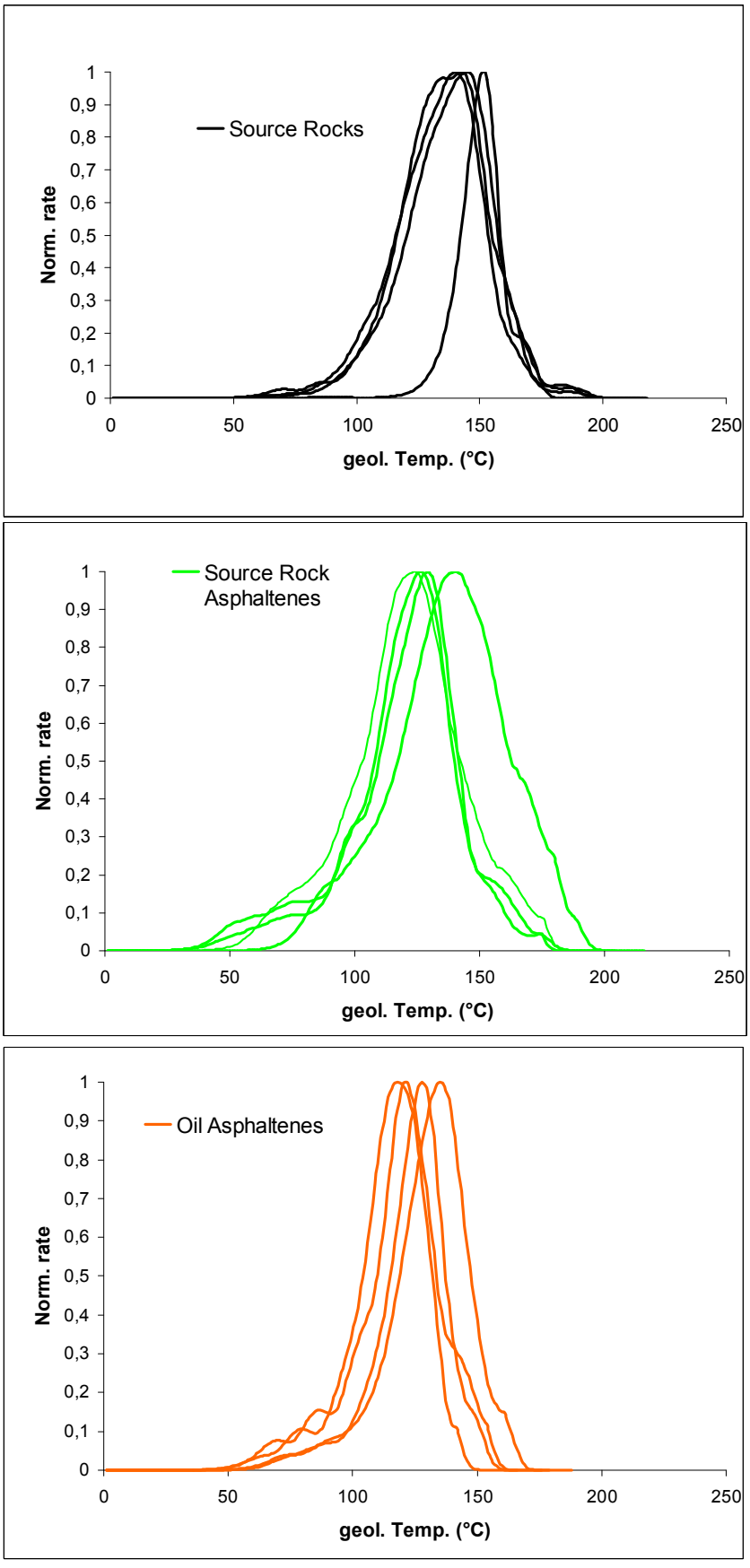

Fig 72 Prediction of bulk petroleum formation from the asphaltenes and source rocks determined for a geological heating rate of 3 K/my using presented samples from Fig 69 -Fig 71.

Schaefer *et al.* (1990) and Dieckmann *et al.* (1998) demonstrated that the activation energies and the frequency factors and consequently the maxima of predicted petroleum formation curves shift to higher temperatures with increasing maturity, which illustrated the structural alteration and effect on petroleum formation during natural maturation within the source rock. This is a well known phenomenon, which is explained by ongoing elimination of labile covalent bonds (Schenk and Horsfield, 1998). But this phenomenon is not observed for the investigated asphaltene samples. On the one hand it has to be considered that the API gravity of the studied oils is unconventionally low and for this reason it is not sure if the studied oils and their asphaltene fractions really represent the original composition of the first formed and trapped oil. Nonetheless, these results correspond to previous work, which showed that oil asphaltenes display higher instability compared to related kerogens (Kuo and Michael, 1994; di Primio and Horsfield, 1996; di Primio *et al.*, 2000). Di Primio *et al.* (2000) illustrated that for the source rock asphaltenes the hydrocarbon formation window predicted always remained in the temperature window predicted for the source rock kerogens. But, it has to be noted that these authors focused on the mean activation energy calculated on the asphaltenes while less stable and more stable potentials were not considered.

sample		HI	Rock-Eval Tmax (°C)	API gravity	$Tmax_{geol}$ (°C)
G000652	kerogen	816	421		140
G000654	kerogen	909	421		145
G000656	kerogen	817	415		142
G000661	kerogen	686	439		152
G000652	s.rock asphaltene	816	421		124
G000654	s.rock asphaltene	909	421		140
G000656	s.rock asphaltene	817	415		126
G000661	s.rock asphaltene	686	439		129
G000394	reservoir asphaltene			2,62	121
G000395	reservoir asphaltene			10,4	135
G000397	reservoir asphaltene			9	118
G000398	reservoir asphaltene			19,35	128

Table 11 The calculated $Tmax_{geol}$ and relevant Rock-Eval data, or API gravity for studied samples.

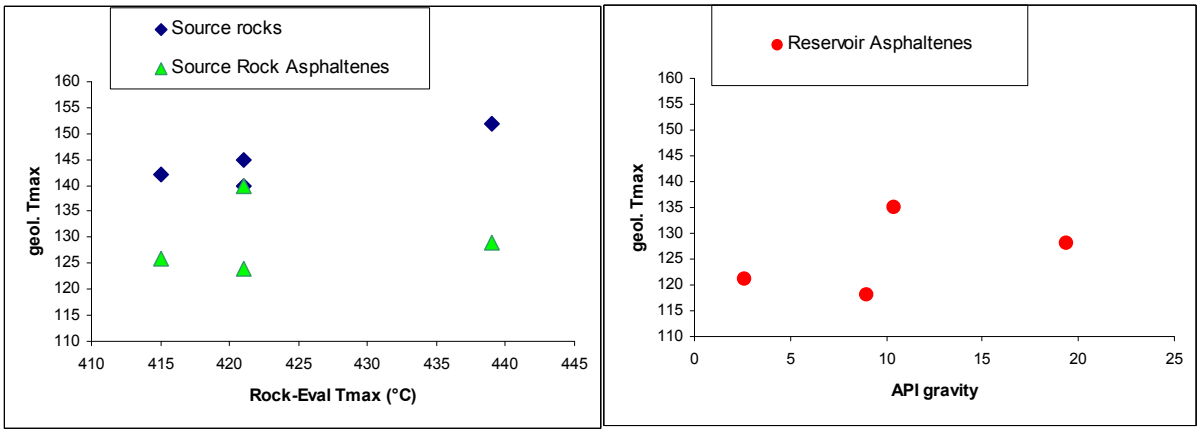

Fig 73 Calculated geological Tmax versus the Rock-Eval Tmax for source rocks and related asphaltenes (left-hand side), and geological Tmax versus the API gravity for oil asphaltenes (right-hand side).

The outcoming results on bulk kinetics for kerogens and asphaltenes from a sulphur-rich sequence confirm previous studies of di Primio *et al.* (1996; 2000) in that source rock asphaltenes are less stable than related kerogens. But the present results show also that structural differences between oil asphaltenes and source rock asphaltenes exist. Oil asphaltenes are slightly less stable but more homogenous than source rock asphaltenes from sulphur-rich sequence.

7.1.4 Organic sulphur content

In order to track structural differences between source rock asphaltenes, reservoir oil asphaltenes and related source rock kerogens, all samples were studied systematically by open system py-GC. A detailed description on pyrolysis is presented in chapter 7.2.

In view of the fact that S-C bond cleavage reactions may be of importance to explain differences in kinetic parameters for asphaltenes and kerogens, it is worth taking a detailed look at different organic sulphur compounds in pyrolysates. Previous studies of Lewan (1985) and Hunt *et al.* (1991) demonstrated that sulphur-rich kerogens are characterised by lower activation energies for petroleum generation than other kerogens, which they attributed to lower bond energies for carbon-sulphur compared to carbon-carbon bonds. Lewan (1998) mentioned sulphur radicals as the rate-controlling factor in petroleum formation in sulphur-rich environments. According to the author, the concentration of initiating sulphur radicals formed during thermal maturation of sedimentary organic matter determines the rate of thermal cracking of the organic matter to petroleum.

Experimentally pyrolysed kerogens have been shown by electron spin resonance spectroscopy to develop free radicals that increase in concentration with increasing thermal stress (Bakr *et al.*, 1991). These free sulphur radicals allow the thermal cracking of C–C bonds to occur at a faster rate and lower thermal stress. The abstraction of a hydrogen atom from an alkyl group initiates thermal cracking of C–C bonds, which then leads to a chain of thermal-cracking reactions (Lewan, 1998). Sulphur radicals are likely derived from cleaved C–S and S–S bonds (Clark and Oriakhi, 1992), and the number of these bonds should be proportional to the rate of thermal cracking (Lewan, 1998).

Oil asphaltenes isolated from heavy sulphur-rich crude oils might be less stable than kerogens and source rock asphaltenes due to sulphur radical reactions because of a) higher organic sulphur content, and therefore more S-C bonds, or b) different, less stable bond types, for

example polysulphide bridges, which are favourable for generating thiyl radicals (Clark and Oriakhi, 1992; Lewan, 1998).

S-rich organic matter is common worldwide and mostly found in sediments from evaporitic and anoxic carbonate platform environments (Sinninghe Damsté *et al.*, 1989; Schaeffer *et al.*, 1995; di Primio and Horsfield, 1996; Mongenot *et al.*, 1997; Baudin *et al.*, 1999). It is well established that kerogen types I-S or II-S originate from incorporation of reduced mineral sulphur (H_2S, S^0 or S_X^{2-}) in functionalised lipids or carbohydrates during early diagenesis (Francois, 1987; Sinninghe Damsté and de Leeuw, 1989; van Kaam-Peters *et al.*, 1998). This incorporation of sulphur into the structure of organic matter, from the H_2S produced by sulphate-reducing bacteria under anoxic conditions, occurs during early diagenesis in the upper layers of the sediment (Hartgers *et al.*, 1997). The proportions of alkylated thiophenes in pyrolysates are representative of the relative enrichment of organic sulphur in the respective source rocks, which in turn gives information about the depositional environment (Sinninghe Damsté *et al.*, 1989; de Leeuw and Sinninghe Damsté, 1990; Eglinton *et al.*, 1990b; di Primio and Horsfield, 1996).

Fig 74 shows the ternary diagram of 2,3-dimethylthiophene, o-xylene, and *n*-$C_{9:1}$ after Eglinton *et al.* (1990b) for source rock kerogens and source rock asphaltenes, as well as reservoir asphaltenes for the samples from Italy. However, it has to be questioned if the ternary diagram after Eglinton *et al.* (1990b) can be used to determine the organic sulphur content for the samples from Southern Italy. The sulphur-rich kerogens and as well their related asphaltenes show unusual low amounts of 2,3-dimethylthiophene. This leads to misinterpretation for characterization of those samples in terms of organic sulphur content. An explanation might be that the precursor resulting in 2,3-dimethylthiophene already destabilize during thermal extraction before the analysis at temperatures lower than 300°C. Therefore, we suggest the use of 2,4-dimethylthiophene instead of 2,3-dimethylthiophene in

this ternary diagram for the samples from Italy, like shown in Fig 75. Here, it can be seen that the source rock pyrolysates are enriched in 2,4-dimethylthiophene as compared to products formed from the reservoir asphaltenes. Following the definition of Eglinton *et al.* (1990b), the source rocks fall into the range of type II-S kerogen. Reservoir asphaltenes are more paraffinic and show lower contents of organic sulphur and aromatic compounds. The source rock asphaltenes are intermediate in terms of organic sulphur content.

Fig 76 compares pairs of kerogens and related asphaltenes in term of organic sulphur content and maturity. Here, the ratio of 2,4-dimethylthiophene / (o-xylene + *n*-$C_{9:1}$) versus Rock-Eval Tmax for kerogens and source rock asphaltenes is plotted (left). Right-hand side of Fig 76 shows that same ratio versus the API gravity for oil asphaltenes. As can be seen from this figure, kerogens show a trend of decreasing ratio of 2,4-dimethylthiophene / (o-xylene + *n*-$C_{9:1}$) with increasing maturity. Source rock asphaltenes show similar trend, but lower organic sulphur content over the entire maturity range. The ratios of 2,4-dimethylthiophene / (o-xylene + *n*-$C_{9:1}$) for oil asphaltene pyrolysates are very similar independent of the API gravity. However, the two asphaltenes isolated from the crude oils G000394 (2.62° API) and G000401 (33.5° API), differ and show lowest content of organic sulphur. Both samples showed already differences in their biomarker distribution with lowest gammacerane indices, so that these oils represent probably another subfamily within the studied oil samples, like mentioned before in the biomarker chapter 5.1.2.2. The two asphaltenes samples are thus marked with A´ in Fig 76. It has also to be noticed, that the sample G000394 (2.62°API) was used for the kinetic analysis. This samples shows definitely lowest organic sulphur content, but the asphaltene was not observed to show a different reactivity than other studied oil asphaltene samples.

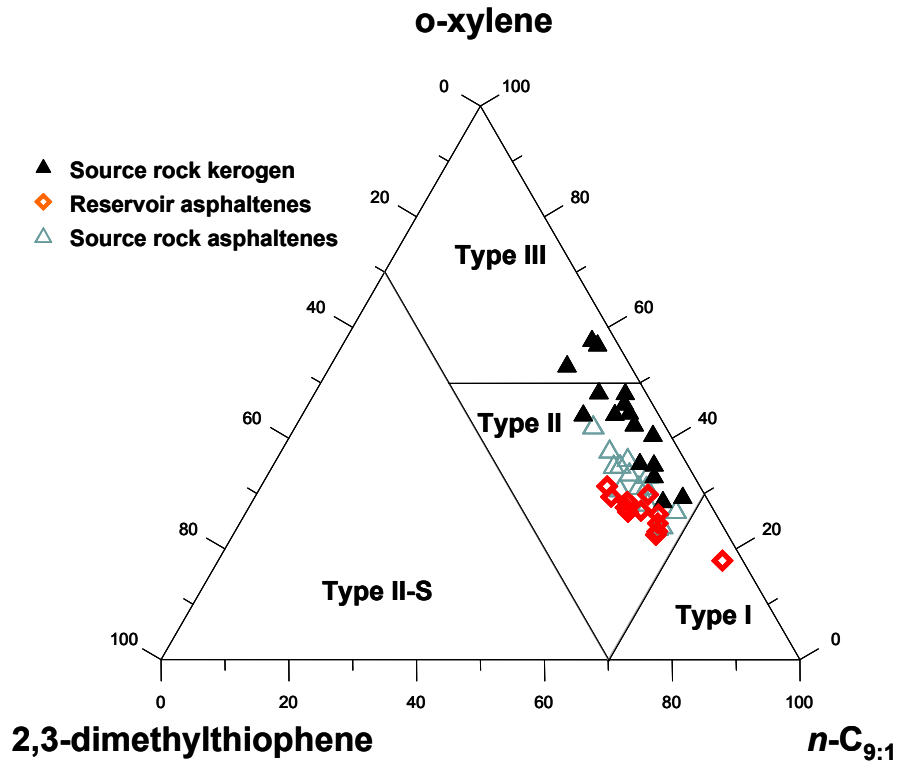

Fig 74 Ternary diagram of 2,3-dimethylthiophene, o-xylene, and *n*-$C_{9:1}$ for source rock kerogen, source rock asphaltenes, and reservoir asphaltenes from Southern Italy (after Eglinton (1990b)).

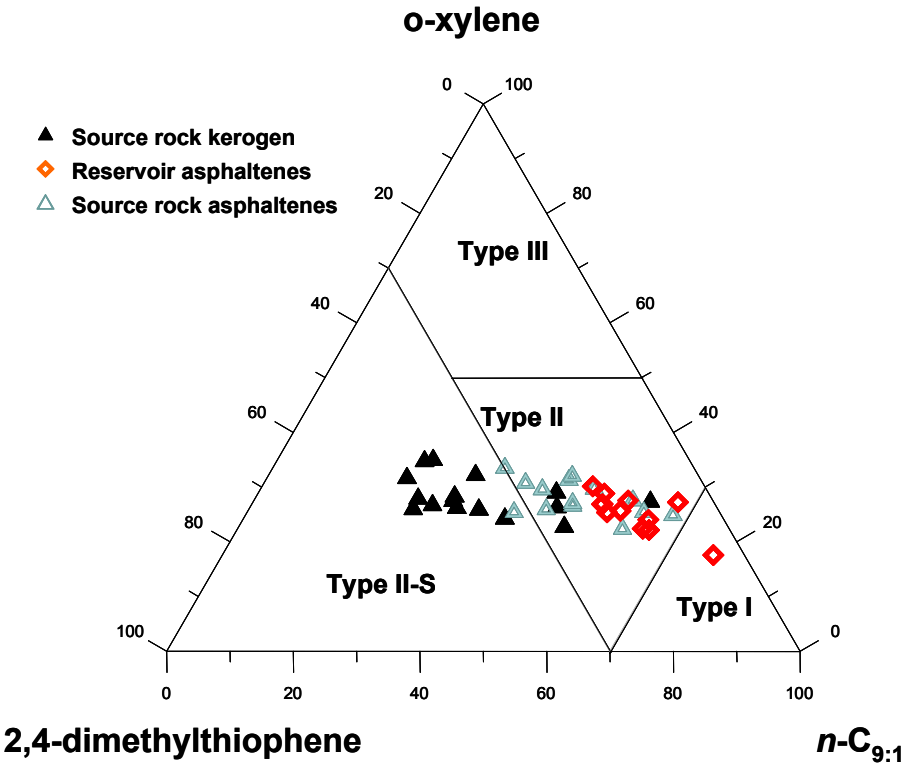

Fig 75 Ternary diagram of 2,4-dimethylthiophene, o-xylene, and *n*-$C_{9:1}$ for source rock kerogen, source rock asphaltenes, and reservoir asphaltenes from Southern Italy (modified after Eglinton (1990b)).

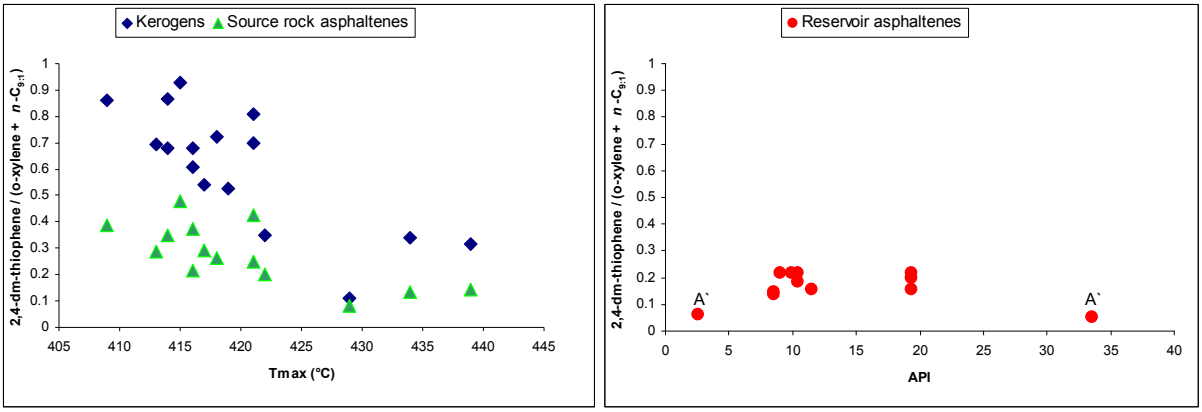

Fig 76 Ratio of 2,4-dimethylthiophene / (o-xylene + *n*-$C_{9:1}$) versus Rock-Eval Tmax for kerogens and source rock asphaltenes (left), and that same ratio versus the API gravity for oil asphaltenes (right).

Di Primio and Horsfield (1996) published the application of a ternary diagram using 2,5-dimethylthiophene, toluene and *n*-$C_{9:1}$ + *n*-$C_{25:1}$. This diagram was established by their study on samples from the same petroleum system like investigated in this study. Fig 77 shows this ternary diagram for the present sample set. Kerogens, as well asphaltenes show higher variations and plot mainly in the field of intermediate sulphur content. The samples here do not predict the same sulphur-rich field like observed from di Primio and Horsfield (1996) for their samples. The reason is explained by a co-elution of 2,5-dimethylthiophene with m,p-xylene in the chromatograms from open-system-pyrolysis. Therefore, the whole peak area of 2,5-dimethylthiophene cannot be quantified, which leads to lower predictions of organic sulphur content like shown in Fig 77.

Fig 78(left) shows the ratio of 2,5-dimethylthiophene / (toluene + *n*-$C_{9:1}$ + *n*-$C_{25:1}$) versus Rock-Eval Tmax for kerogens and source rock asphaltenes. Here, source rock asphaltenes do not demonstrate lower sulphur contents than related kerogens. As well, this plot shows that the amount of organic sulphur for kerogens and source rock asphaltenes decreases with increasing maturity. As well, in Fig 78(right) oil asphaltenes are not so different in terms of

organic sulphur content compared to kerogens and related source rock asphaltenes. The two asphaltenes isolated from the oils supposed to be a different subfamily (A´) demonstrate again lowest sulphur content.

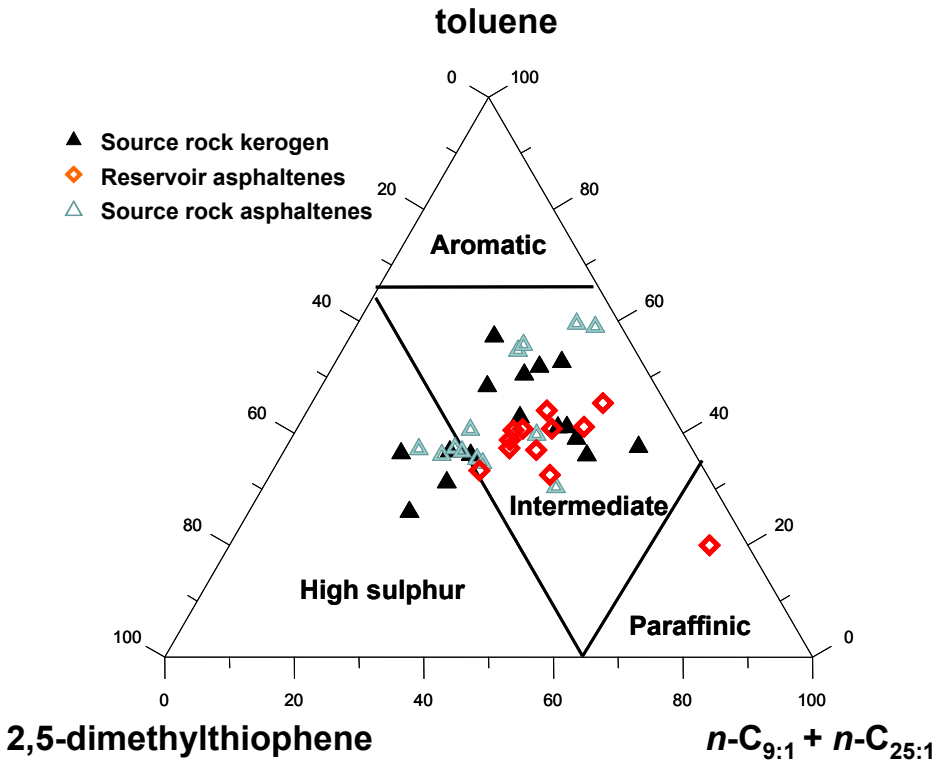

Fig 77 Ternary diagram of 2,5-dimethylthiophene, toluene, and *n*-$C_{9:1}$ + *n*-$C_{25:1}$ for source rock kerogen, source rock asphaltenes, and reservoir asphaltenes from Southern Italy (after di Primio and Horsfield (1996)).

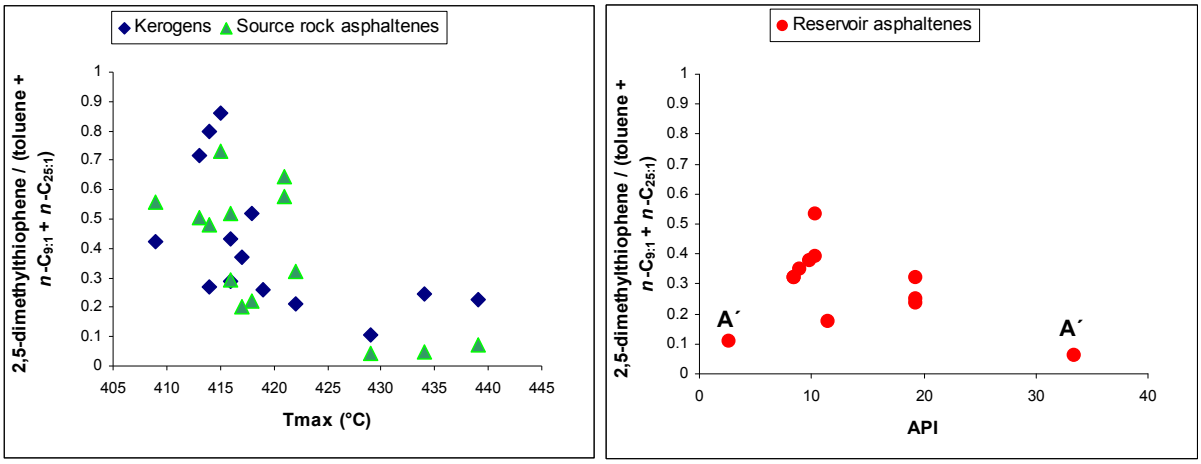

Fig 78 Ratio of 2,5-dimethylthiophene / (toluene + *n*-$C_{9:1}$ + *n*-$C_{25:1}$) versus Rock-Eval Tmax for kerogens and source rock asphaltenes (left), and that same ratio versus the API gravity for oil asphaltenes (right) (after di Primio and Horsfield (1996)).

Since kerogens and both types of asphaltenes show such strong changes in the abundance within different dialkylthiophenes, it is thus the best to calculate a ratio with the sum of alkylthiophenes in order to compare the organic sulphur content in those kerogens and asphaltenes. In order to do so, the following sums were intended to establish a diagram:

Σ alkylthiophenes = 2-methylthiophene + 3- methylthiophene + 2,5-methylthiophene + 2,4-methylthiophene + 2,3-methylthiophene + ethylthiophene + ethylmethylthiophene

Σ C_1-C_2 alkylbenzenes = toluene + ethylbenzene + m,p-xylene + o-xylene

Σ C_7-C_{10} alkenes = *n*-$C_{7:1}$ + *n*-$C_{8:1}$ + *n*-$C_{9:1}$ + *n*-$C_{10:1}$

Fig 79 shows the ternary diagram with these sums of alkylthiophenes, alkylbenzenes and alkenes. Here it is clearly evident that source rock kerogens are richer in organic sulphur than both types of asphaltenes. Source rock asphaltenes demonstrate similar amounts of organic sulphur as oil asphaltenes, but they are different in terms of aromaticity / paraffinicity. Oil asphaltenes are more paraffinic, whereas source rock asphaltenes show higher aromaticity even than source rock kerogens.

Fig 80 shows the ratio of Σ alkylthiophenes / (Σ C_1-C_2 alkylbenzenes + Σ C_7-C_{10} alkenes) for kerogens and related source rock asphaltenes (left) and for oil asphaltenes (right) in terms of maturity. Like observed before, source rock kerogens show highest content of organic sulphur and decreasing amounts of organic sulphur with increasing maturity. Lowering sulphur content with increasing maturity has been explained by Orr and Sinninghe Damsté (1990) by disproportion into H_2S and pyrobitumen.

At least, the amount of organic sulphur in asphaltenes and kerogen cannot explain the lower stability or higher reactivity for asphaltenes obtained from bulk kinetic measurements.

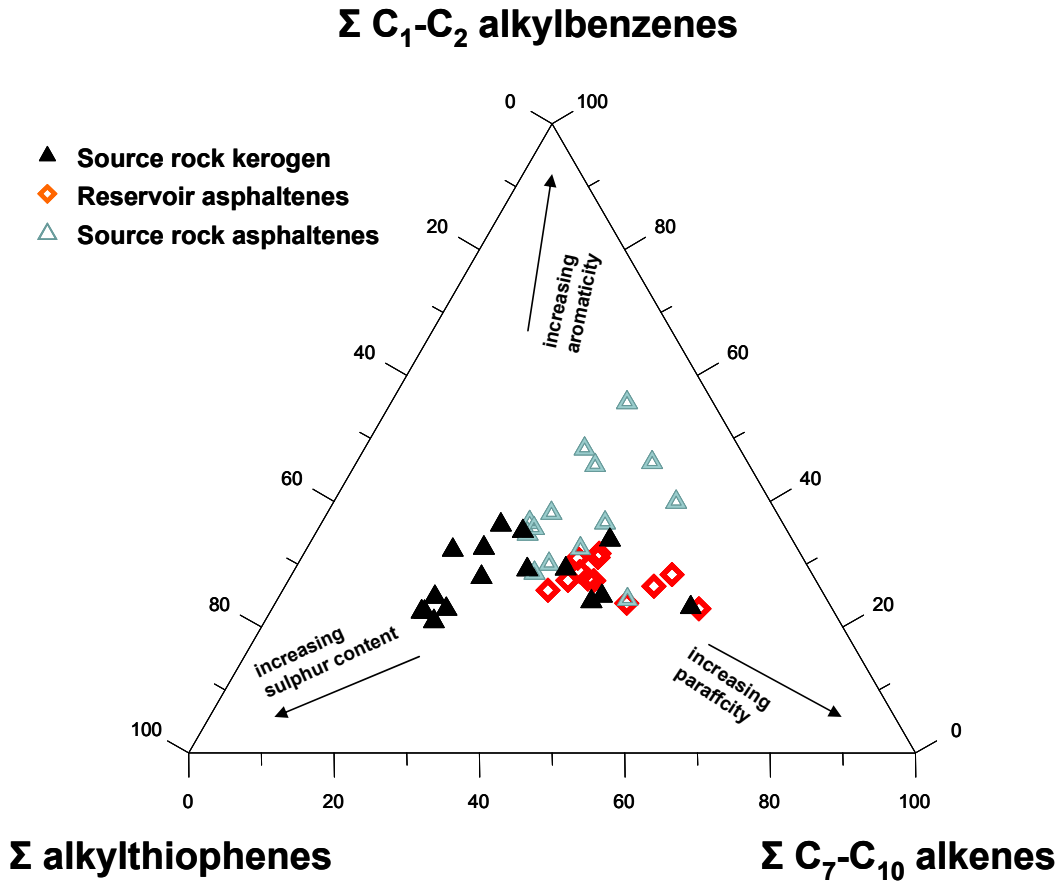

Fig 79 Ternary diagram with Σ alkylthiophenes, Σ C_1-C_2 alkylbenzenes, and Σ C_7-C_{10} alkenes for source rock kerogen, source rock asphaltenes, and reservoir asphaltenes from Southern Italy.

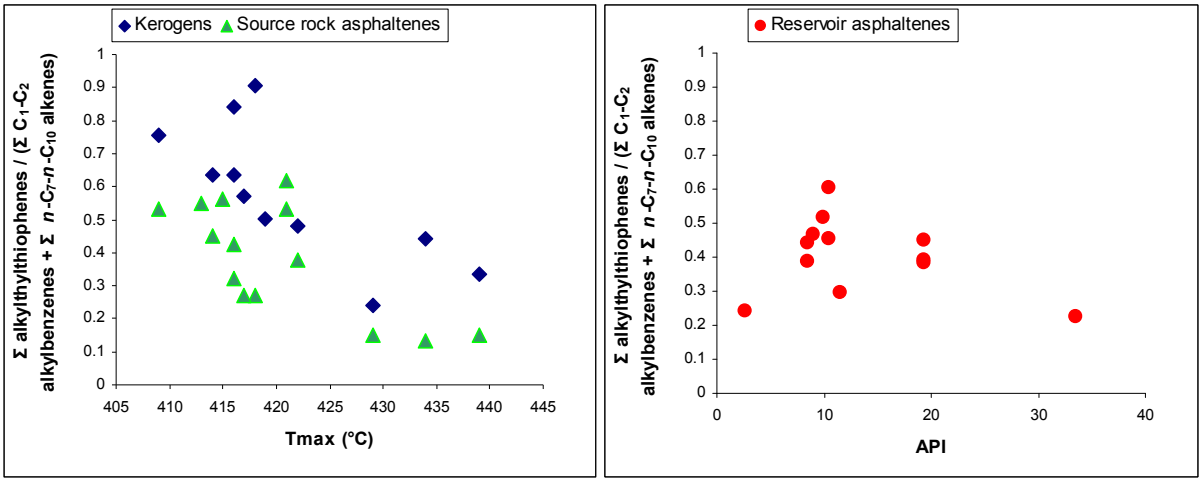

Fig 80 Ratio of Σ alkylthiophenes / (Σ C_1-C_2 alkylbenzenes + Σ C_7-C_{10} alkenes) versus Tmax for kerogens and related source rock asphaltenes (left) and versus API for oil asphaltenes (right).

7.1.5 Discussion on heterolytic versus homolytic cleavages (S-C vs. S-S bonds)

The present observations are in clear contrast to the general assumption, that the enrichment of sulphur and aromatic compounds, which are both known to be formed from macromolecules at lower thermal stress, are responsible for the instability of asphaltenes sourced from type I-S or II-S kerogen. The less stabile oil asphaltenes and source rock asphaltenes contain the lower amounts of organic sulphur compared to the related kerogens. This surely indicates that different precursor molecules are incorporated in asphaltenes and source rock kerogens, and that the higher reactivity of asphaltenes is not only related to the amount of C-S bonds, but probably more to the position and type of sulphur bonds within the macromolecule (Tomic *et al.*, 1995; Mongenot *et al.*, 1997; Riboulleau *et al.*, 2000).

The major sulphur compounds in kerogens are alkylsulphides, di(poly)sulphides and thiophenes, based on data published by various authors, who mainly studied kerogens by XANES spectroscopy (George and Gorbaty, 1989; Waldo *et al.*, 1991; Eglinton *et al.*, 1994; Kasrai *et al.*, 1994; Nelson *et al.*, 1995; Sarret *et al.*, 1999; Riboulleau *et al.*, 2000; Sarret *et al.*, 2002).

The incorporation of sulphur may be intermolecular (polysulphides and sulphides) and/or intramolecular (thiophenes) (Sinninghe Damsté and de Leeuw, 1989; Sinninghe Damsté *et al.*, 1989; Kohnen *et al.*, 1993; Riboulleau *et al.*, 2000).

Riboulleau *et al.* (2000) presented that the major sulphur forms in kerogen from Kashpir oil shales are alkylsulphides and in lesser amount di(poly)sulphides. Similar distributions of sulphur species in the Monterey kerogens were published by Nelson *et al*. (1995) and Eglinton *et al*. (1990b; 1994), based on XANES spectroscopy. In contrast, the kerogen of the carbonate rich lagoon of Orbagnoux in France was shown to contain thiophenes as the major sulphur form and in lesser amount di(poly)sulphides and sulphides (Mongenot *et al.*, 1997; Sarret *et al.*, 2002). Sarret *et al*. (2002) have also shown, that aromatisation of the non-

thiophenic sulphur forms in kerogens from Orbagnoux occurs upon the thermal stress. Sarret *et al*. (1999) have studied asphaltenes isolated from bitumens from different basins in France, Spain, and Middle East by XANES spectroscopy. The authors mentioned that dibenzothiophenes are the dominant forms of sulphur in the most asphaltene macromolecules, but asphaltenes from Cassaber in the Aquitaine Basin contain higher yields of sulfones and sulfates, probably resulted from ester-bonded sulfates with an insertion of an oxygen atom in a C–S bond.

These features imply that sulphur incorporation can vary for different source rocks and asphaltenes. And it is known that S-C bonds in thiophenes are more thermally stable than similar bonding types in polysulphides or thioester (Baskin and Peters, 1992; Tomic *et al.*, 1995). From that point of view it is likely that S-rich precursor molecules in asphaltenes from Southern Italy are more closely associated with preferential cleavage of weak polysulphide and/or thioester bonds, while source rock kerogens are characterised by more stable heteroaromatic precursor molecules. This would also correlate with the concept of sulphur radicals (Lewan, 1998), because it is known that homolytic cleavages (polysulphides and thioester) are favourable for the generation of sulphur radicals (thiyls), which allows the thermal cracking of C–C bonds at lower thermal stress (Clark and Oriakhi, 1992; Lewan, 1998).

7.1.6 Conclusion

- The onset of the main phase of petroleum formation for the source rock samples was predicted to start at around 80°C under geological conditions, while hydrocarbon generation from both types of asphaltenes starts slightly earlier.
- Source rock asphaltenes and oil asphaltenes from a type II-S sequence are thermally less stable than kerogens. Bulk kinetic measurements indicated slightly lower activation energies and frequency factors for the transformation of asphaltenes to petroleum than those for source rock kerogens.
- The predictions from oil asphaltenes resulted in tighter temperature ranges, indicating that the reactive part of the oil asphaltenes is more homogeneous than of source rock kerogens, and source rock asphaltenes.
- No obvious structural links were found that could directly explain the observed reactivity differences from bulk kinetic measurements. But, the amount of organic sulphur is not proportional to the reactivity of petroleum generation from asphaltenes at lower thermal stress. More likely is, that kerogens and asphaltenes posses different positions and types of sulphur bonds resulting in cracking of covalent bonds at different levels of thermal stress.

7.2 Elemental analysis

Differences in the elemental composition between source rock asphaltenes and oil asphaltenes are obvious when looking at their atomic H/C and O/C ratios. Fig 81 illustrates the results of elemental analysis for asphaltenes from Southern-Italy, which support the aliphatic character of all samples. The elemental compositions measured on oil asphaltenes from Southern-Italy show lower atomic O/C ratios compared to source rock asphaltenes. Additionally, source rock asphaltenes are spreading in the Van-Krevelen-diagram more than oil asphaltenes do, indicating higher variability, which was also observed for their pyrolysis products. Oil asphaltenes are defining the zone of type I organic matter, whereas source rock asphaltenes plot in the zone of organic matter type II.

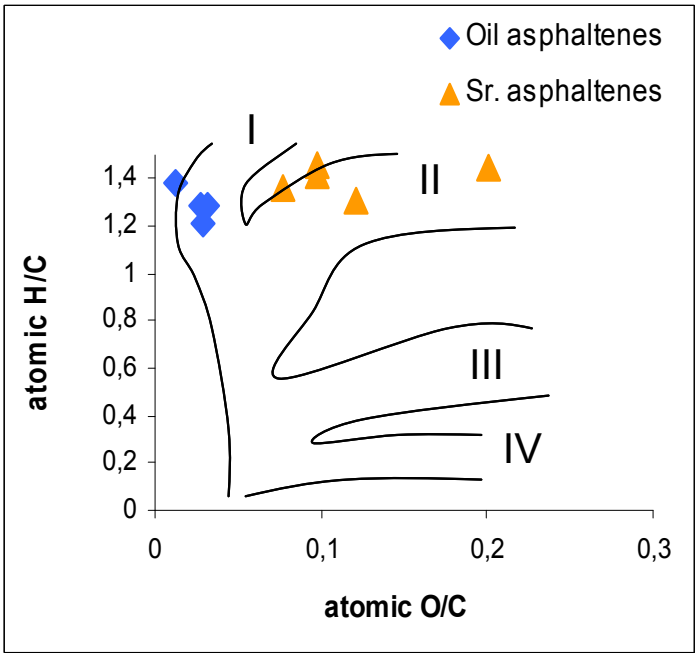

Fig 81 Van-Krevelen diagram showing the results of elemental analysis of the asphaltene samples from Southern-Italy (after Peters (1986), Tissot and Welte (1984).

The same compositional difference for reservoir and source rock asphaltenes was reported from Castex (1985), who studied the elemental composition of oil and bitumen asphaltenes

from various basins worldwide. The author showed that source rock asphaltenes are always characterised by higher O/C ratios compared to oil asphaltenes from the same petroleum basin. The H/C values for the studied asphaltenes from Italy are relative high and range between 1.21 and 1.44 for both types of asphaltenes. Castex (1985) and Tissot and Welte (1984) proposed an average H/C ratio of 1.16 for oil asphaltenes, and of 1.18 for source rock asphaltenes. However, Eglinton *et al*. (1990a) have reported that H/C ratios from oil asphaltenes isolated from sulphur-rich Monterey petroleums show also higher values, which range between 1.22 and 1.32.

Several studies, like Castex (1985) and Pellet *et al*. (1986), proposed that the H/C and O/C ratios of asphaltenes in source rocks decreases with increasing burial and thermal maturation. Fig 82 shows the atomic H/C and O/C ratios versus the API for investigated oil asphaltenes (top), and the same ratios versus HI for source rock asphaltenes (bottom). Since the bitumen asphaltene samples for this analysis are all within a short range of Tmax, the HI is preferred to investigate maturity effect. The elemental compositions and calculated ratios for the Italian asphaltenes, as well as relevant Rock-Eval data are presented in Table 12. As can be seen from Fig 82 oil asphaltenes neither bitumen asphaltenes show a trend of atomic H/C and O/C ratios with API or HI. This explains that the variations of atomic ratios within the asphaltenes are probably related to facies variations and not to maturity.

When comparing the asphaltene isolated from the long-time-stored sample G000404 with the asphaltene isolated from the fresher counterpart G000395, there are major differences observed for the atomic H/C and O/C ratios. The asphaltene from stored oil show lower atomic O/C and higher atomic H/C ratio as the asphaltene from the fresher oil.

Sample		H (%)	C (%)	N (%)	H/C	O/C	HI	Tmax (°C)	API
G000393	oil asphaltene	8.34	77.76	0.65	1.29	0.03			9.9
G000395	oil asphaltene	8.29	77.49	0.64	1.28	0.03			10.4
G000396	oil asphaltene	7.88	78.09	0.67	1.21	0.03			11.5
G000404	oil asphaltene	9.03	78.54	0.72	1.38	0.01			10.4
G000648	s.r. asphaltene	8.71	71.7	0.66	1.46	0.10	691	416	
G000649	s.r. asphaltene	8.5	71.85	0.71	1.42	0.10	763	414	
G000652	s.r. asphaltene	8.33	73.26	1.18	1.36	0.08	816	421	
G000654	s.r. asphaltene	7.88	65.46	0.43	1.44	0.20	909	421	
G000656	s.r. asphaltene	7.71	70.52	0.97	1.31	0.12	817	415	

Table 12 Elemental compositions and calculated ratios for asphaltenes from Southern Italy.

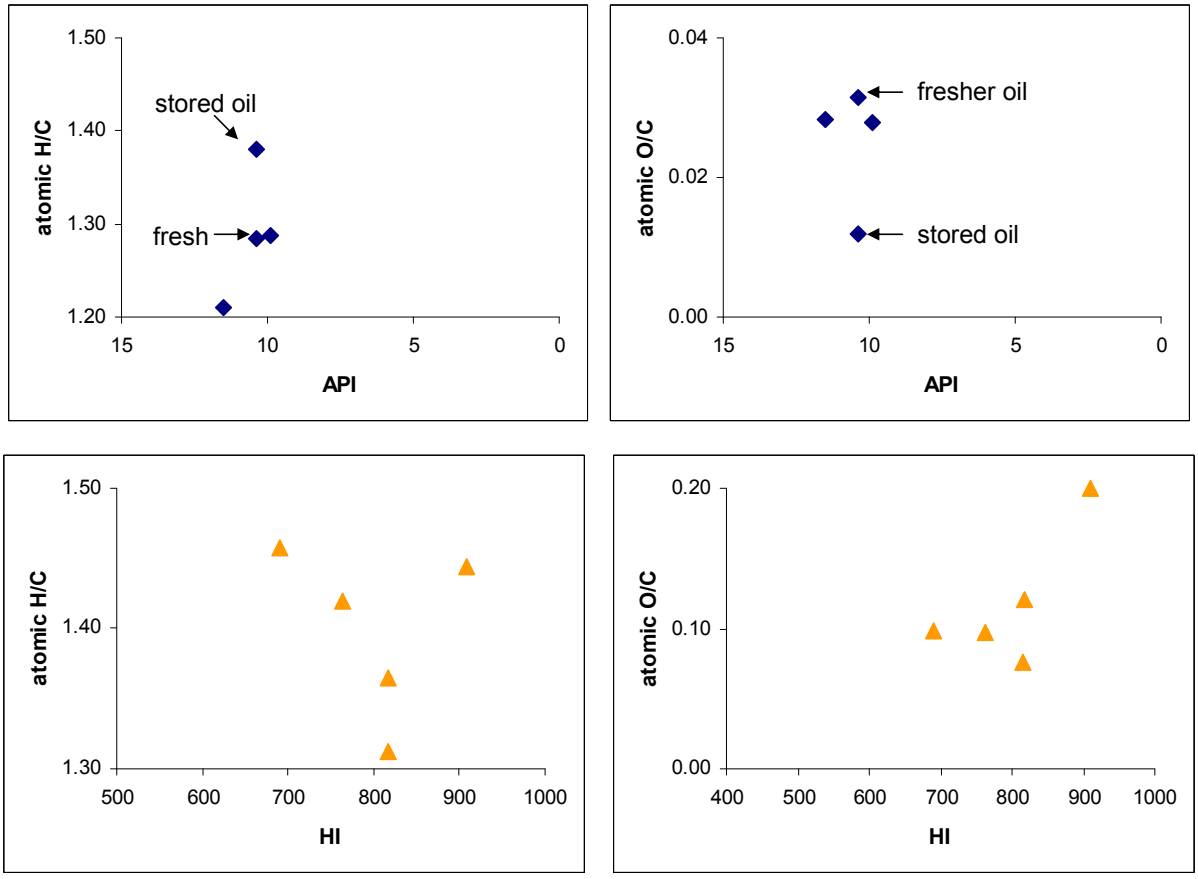

Fig 82 The atomic H/C and O/C ratios versus the API for investigated oil asphaltenes (top), and the same ratios versus HI for source rock asphaltenes (bottom).

7.3 Pyrolysis

7.3.1 Pyrolysis as a structural tool

For further characterisation of kerogens and asphaltenes open-system-pyrolysis-GC and GC-MS were used to study organic matter in terms of their structural moieties, such as aromaticity, alkyl chain distribution and structures related to organic sulphur. The term pyrolysis has been defined as "chemical degradation reaction that is induced by thermal energy alone" (Ericsson and Lattimer, 1988). Open-system-pyrolysis-GC is a method of rapidly cracking organic matter into smaller molecular fragments at the temperature range of 300-600°C for short period of time, i.e. a heating rate of 40°C/min. These products released over this temperature range in a flow of inert carrier gas are analysed by GC for bulk composition. The advantage of pyrolysis, especially when coupled with GC or GC-MS (Giraud, 1970; Horsfield *et al.*, 1983), is that the volatile products are formed according to the same principles as in natural catagenesis, i.e. thermal cleavage reactions (Horsfield, 1997). Kerogens, as well as asphaltenes degrade upon pyrolysis to yield many compound types including hydrocarbons, ketones, alcohols, nitriles and thiols, as represented by cyclic and acyclic, saturated and unsaturated carbon skeletons (Rovere *et al.*, 1983; Wilson *et al.*, 1983). The most commonly components seen by pyrolysis-GC are doublets of alkane/alk-1-enes, alkylbenzenes, alkylnaphthalenes, alkylthiophenes and alkylphenols. The composition of pyrolysates is also predicated on the classical types of organic matter (Larter, 1984; Béhar and Vandenbroucke, 1987; Horsfield, 1989; Horsfield, 1990; Tegelaar and Noble, 1994). The molecular composition and structure of kerogens and also asphaltenes, since those are fragments of parent kerogens (Béhar and Pelet, 1985; Pelet *et al.*, 1986; Jones *et al.*, 1988), is complex and determined by its biological precursors and the modifications brought about during diagenesis and catagenesis (Rullkötter and Michaelis, 1990). Fig 83 illustrates the structural differences between immature kerogens after Béhar and Vandenbroucke (1987),

each showing characteristic structural moieties upon pyrolysis (Larter and Senftle, 1985; Øygard *et al.*, 1988; Horsfield, 1989; Larter and Horsfield, 1993; Tegelaar and Noble, 1994). As well, high proportions of polar compounds are generated during pyrolysis of all kerogen types (Urov, 1980; Castelli *et al.*, 1990; Landais *et al.*, 1991) and tarry residues are deposited in the GC interface. Larter and Horsfield (1993) have demonstrated that pyrolysis predicts bulk compositional features of kerogens. The authors have for example shown in their study that the alkylphenol content of Carboniferous coal pyrolysates in the United States is directly proportional to the hydroxyl oxygen content determined by wet chemical methods (Yarzab *et al.*, 1979; Senftle *et al.*, 1986), pointing to phenolic structures in pyrolysates being proportionally representative of oxygen-substituted benzoid structures in kerogens. In addition, Eglinton *et al.* (1990b) have illustrated that the relative abundance of alkylthiophenes versus aromatic plus aliphatic hydrocarbons were proportional to the atomic S/C ratio, suggesting that pyrolytic sulphur species are proportionally representative of kerogen-bond-sulphur molecules. However, pyrolysis products, such as alkylthiophenes themselves do not occur in natural systems, and they are probably released as long-chain thiophenes due to lower temperatures and longer reaction times under geological conditions (Sinninghe Damsté *et al.*, 1990).

On the premise that kerogen composition directly controls the types and yields of volatile products generated during natural maturation, it can be concluded that the abundance and distribution of resolved pyrolysis products give informations about the bulk compositions of natural petroleums, such as paraffinicity and aromaticity (Horsfield, 1997).

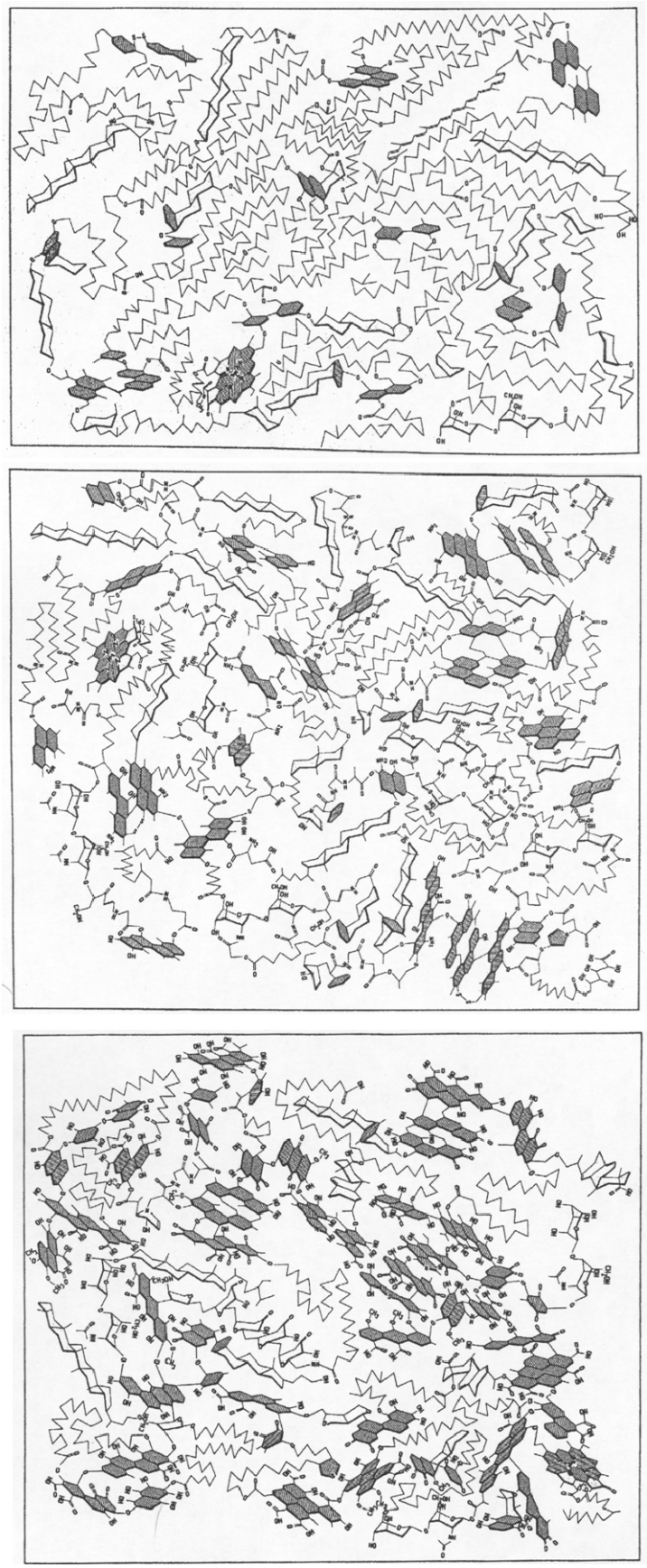

Fig 83 Conceptual models of kerogen structure after Béhar and Vandenbroucke (1987). Figure illustrates the structure of selected type I (top), type II (middle), and type III kerogens (bottom) at the immature stage.

Because asphaltenes are fragments of kerogens, their pyrolysates show a strong compositional resemblance to the parent kerogen (Béhar and Pelet, 1985; Pelet *et al.*, 1986; Jones *et al.*, 1988). Thus pyrolysis-gas chromatography (py-GC) of asphaltenes isolated from crude oils or rock extracts have been the subject of several previous investigations, which provided informations for source rock correlation (Béhar *et al.*, 1984; Béhar and Pelet, 1985; Cassani and Eglinton, 1986; Solli and Leplat, 1986; Jones *et al.*, 1988; Horsfield, 1989; Horsfield *et al.*, 1991; Muscio *et al.*, 1991; Horsfield *et al.*, 1993; Horsfield *et al.*, 1994). Examples for the use of py-GC include analysis of biomarker skeletons in asphaltenes for correlating crude oils and likely sources (Béhar and Pelet, 1985; Cassani and Eglinton, 1986; Jones *et al.*, 1988; Horsfield *et al.*, 1991), as well as for the prediction of petroleum gas-oil ratios (Horsfield *et al.*, 1991; Muscio *et al.*, 1991; Horsfield *et al.*, 1993).

The investigation by open-system-pyrolysis for the present study focus on main topics, described as followed:

- To emphasize structural similarities and dissimilarities between kerogens, source rock asphaltenes, as well as oil asphaltenes
- To correlate structural moieties, such as organic sulphur content to differences found in the analysis of bulk kinetic measurements, which was already discussed in the previous chapter
- To compare facies recognition from pyrolysates of kerogens, source rock and oil asphaltenes
- To study maturity control on asphaltenes

7.3.2 Composition of pyrolysates

Fig 84 - Fig 86 show selected chromatograms of open system pyrolysis GC experiments on thermally extracted whole rock (Fig 84), source rock asphaltenes (Fig 85), and oil asphaltenes (Fig 86).

The asphaltene and whole rock py-GC chromatograms show a similar distribution pattern of alkanes and alkenes. All samples are characterised by a (bi)-modal distribution of *n*-alkyl chains. The most dominant aromatic hydrocarbon is toluene, in some samples additionally m,p-xylene and ethylbenzene, which have been described as products from non-condensed aromatic moieties, such as carotenoids (Béhar and Vandenbroucke, 1987; Hartgers *et al.*, 1994b; Stout and Boon, 1994). Further compound classes formed in the course of open pyrolysis from the kerogen as well as from the both asphaltene types are alkylated thiophenes and alkylated naphthalenes. A study by py-GC-MS showed also the presence of alkylthiolanes, primarily benzothiolane in minor abundance in kerogen pyrolysates of the Italian samples. But these compounds were not detected in all pyrolysates.

Characteristic of pyrolysates is the occurrence of prist-1-ene, and sometimes also prist-2-ene. Several studies suggest different precursors for prist-1-ene. Chappe *et al.* (1982) proposed bound diphytanyl ethers of archaebacteria. Goossens *et al.* (1984) candidate tocopherols, and Höld *et al.* (2001) mentioned tocopherols and an unknown sulphur-bond precursor for prist-1-ene precursors. Other workers for example suggested chlorophyll *a* (Ishiwatari *et al.*, 1991) or phenol–phytol condensation products (Li *et al.*, 1995). Larter and Horsfield (1993) showed in their study that the prist-1-ene precursor in flash pyrolysis is the same as that which produces pristane in the subsurface. Phytane precursors in kerogens are less well understood, and no single phytene isomer dominates open-system pyrolysates.

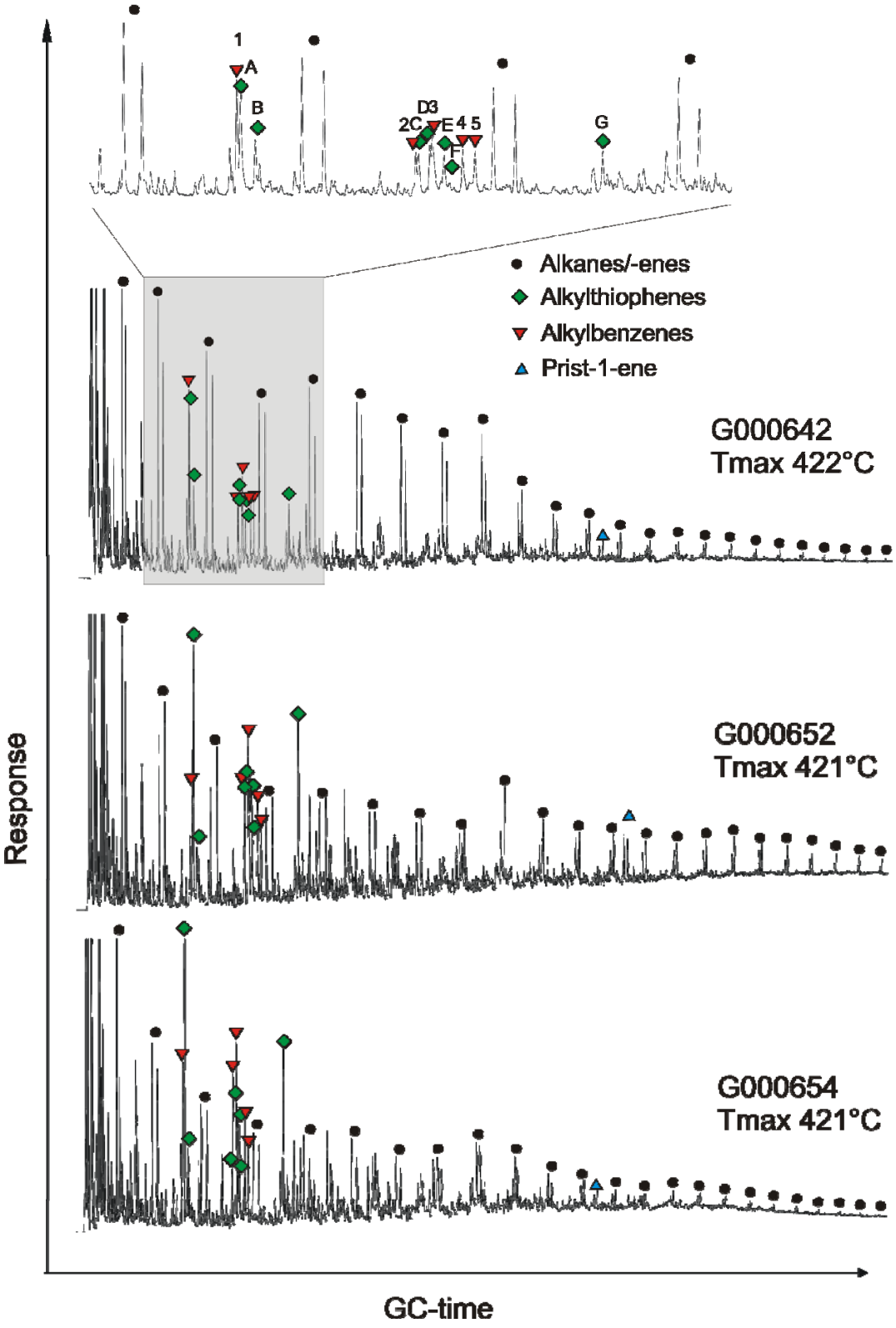

Fig 84 Selected chromatograms from open-system pyrolysis GC for source rock kerogens from Italy. Alkane/-ene doublets, most abundant thiophenes, and alkylbenzenes are marked. Alkylbenzenes are corresponding to retention time from left to the right: toluene (1), ethylbenzene (2), m,p-xylene (3), styrene (4) and o-xylene (5). Alkylthiophenes are from left to right: 2-methylthiophene (A), 3-methylthiophene (B), ethylthiophene (C), 2,5-dimethylthiophene (D), 2,4-dimethylthiophene (E), 2,3-dimethylthiophene (F), and ethylmethylthiophene (G).

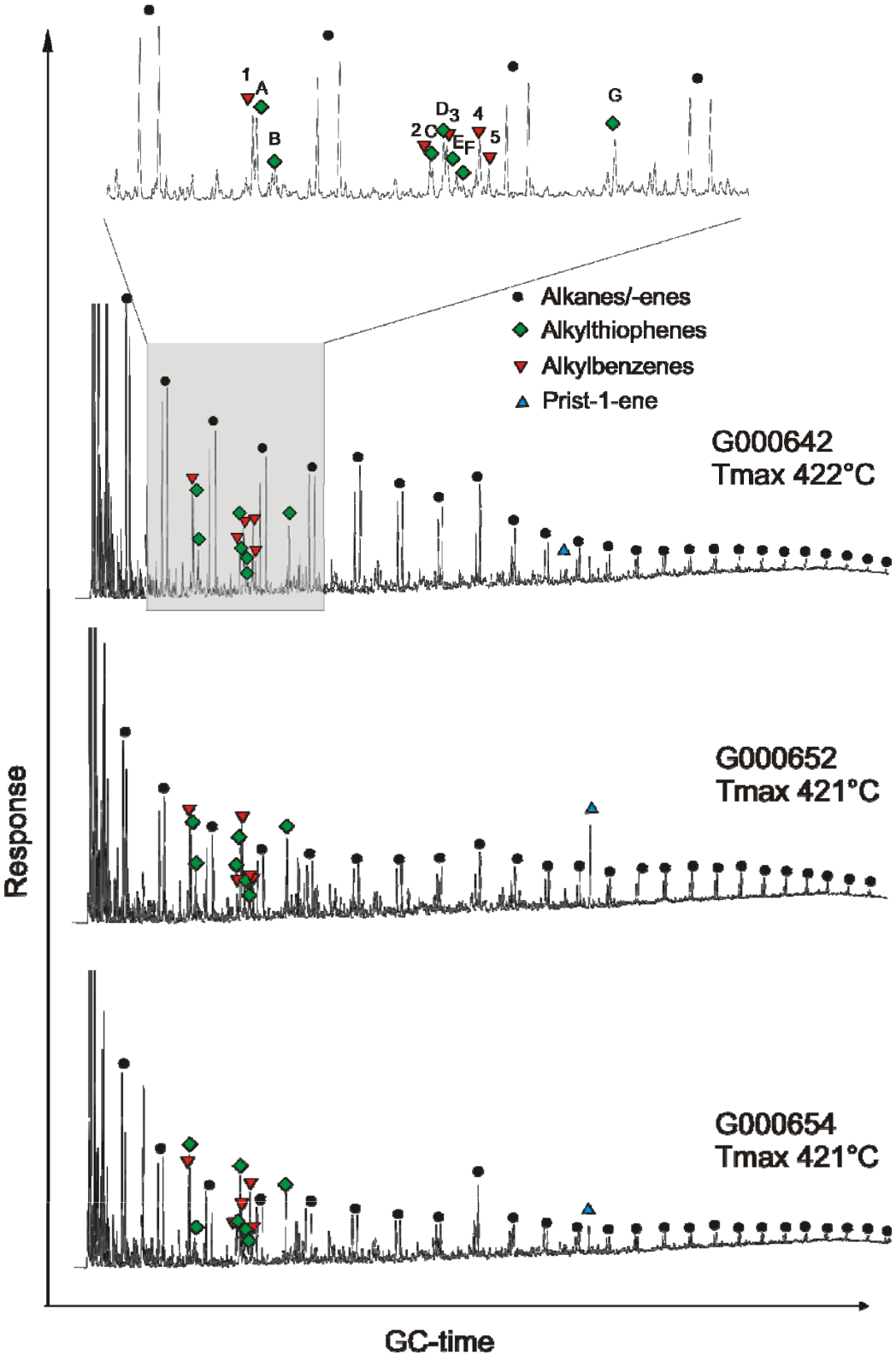

Fig 85 Selected chromatograms from open-system pyrolysis GC for source rock asphaltenes from Italy. Alkane/-ene doublets, most abundant thiophenes, and alkylbenzenes are marked. Alkylbenzenes are corresponding to retention time from left to the right: toluene (1), ethylbenzene (2), m,p-xylene (3), styrene (4) and o-xylene (5). Alkylthiophenes are from left to right: 2-methylthiophene (A), 3-methylthiophene (B), ethylthiophene (C), 2,5-dimethylthiophene (D), 2,4-dimethylthiophene (E), 2,3-dimethylthiophene (F), and ethylmethylthiophene (G).

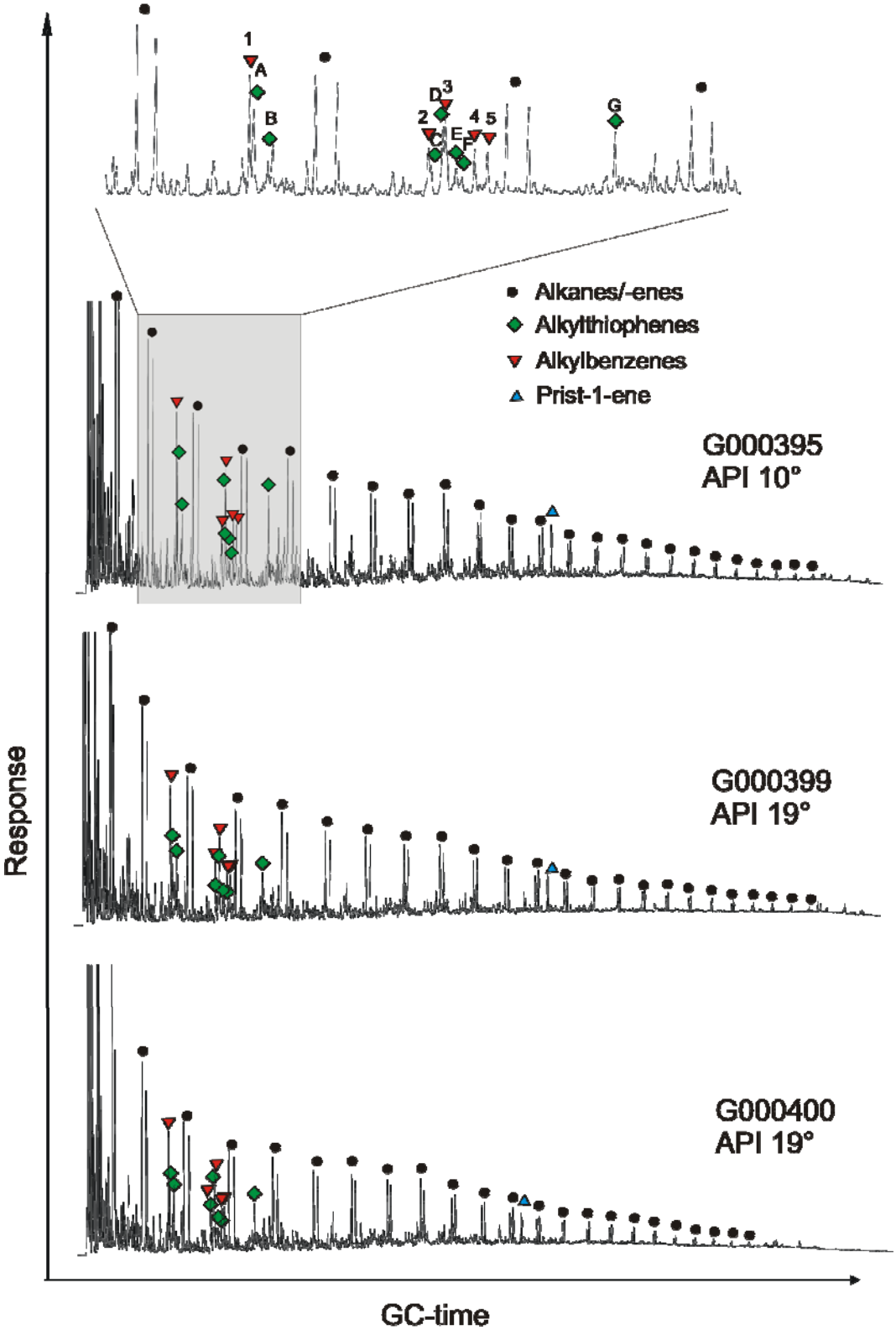

Fig 86 Selected chromatograms from open-system pyrolysis GC for petroleum asphaltenes from Italy. Alkane/-ene doublets, most abundant thiophenes, and alkylbenzenes are marked. Alkylbenzenes are corresponding to retention time from left to the right: toluene (1), ethylbenzene (2), m,p-xylene (3), styrene (4) and o-xylene (5). Alkylthiophenes are from left to right: 2-methylthiophene (A), 3-methylthiophene (B), ethylthiophene (C), 2,5-dimethylthiophene (D), 2,4-dimethylthiophene (E), 2,3-dimethylthiophene (F), and ethylmethylthiophene (G).

7.3.3 Aliphatic hydrocarbons

Linear aliphatic structures in kerogens and asphaltenes crack to give *n*-alkane and *n*-alkene doublets during open-system-pyrolysis, as shown in Fig 84 - Fig 86. The relative abundance of each homologue is controlled to variable degrees by the chain length of the precursor moiety in the macromolecule and the secondary reactions that occur during pyrolytic cleavage (Horsfield, 1997). The probable precursors of these alkane/-ene chains are either fragments of lipids / fatty acids incorporated within the organic matter of kerogens (Douglas and Larter, 1980; Larter *et al.*, 1983) and/or preserved aliphatic-rich biopolymers (Nip *et al.*, 1986; Horsfield, 1989; Horsfield *et al.*, 1994). Alkenes are readily formed on pyrolysis by elimination reactions and even if not strictly lipid in origin they suggest aliphatic chains with relatively few side chains (Bracewell and Robertson, 1987). However, Horsfield (1997) pointed out that not all subtle features in *n*-alkane/-ene distributions can be related to the actual chain length distribution in the macromolecule, since intramolecular radical transfer processes after scission of *n*-alkyl chains may have taken place.

Less biodegraded oils from South-Italy show higher amount of *n*-C_{14} and *n*-C_{15} (Fig 20), normally indicative of bacterial contribution, like sulphate-reducing bacteria (Grimalt *et al.*, 1992; Russel *et al.*, 1997), cyanobacterial mats (Boon *et al.*, 1983), microbial populations (Volkman *et al.*, 1980; Grimalt and Albaigés, 1987; de las Heras *et al.*, 1997), as well as of microalgae (Grice *et al.*, 2003). These higher amounts of *n*-C_{14} and *n*-C_{15} are also found in pyrolysates of kerogens and asphaltenes from the Italian sample set. Whereas crude oils show a dominance of *n*-C_{15}, pyrolysates show a higher peak in *n*-C_{14} alkane/-ene. Various authors found these unusual maximum of *n*-C_{14} or *n*-C_{15} in oils or bitumen from the Lorca Basin (Grimalt and Albaigés, 1987; Grimalt *et al.*, 1992; Russel *et al.*, 1997) or in samples from Ribesalbes (de las Heras *et al.*, 1997), which the authors linked to input of microbial mats. Abdullah (1999) described the occurrence of a maximum in *n*-C_{14} in pyrolysates of Triassic

shallow marine shales of Central Spitsbergen, whereas pyrolysates of Triassic deep marine shales of Spitsbergen do not display this maximum. Therefore, the occurrence of this alkane/-ene in pyrolysates might be referred to a photosynthetic specimen. Grice *et al.* (2003) found as well a maximum in *n*-C_{14} within the alkane distribution of pyrolysates from kerogens from the Sdom Formation of the Dead Sea in Israel. The authors referred the maximum of *n*-C_{14} alkane/-ene to be a pyrolysis product of algaenan biopolymer which occurs in cell walls of microalgaes. Since *n*-C_{14} and *n*-C_{15} are ubiquitous, their occurrence in pyrolysates from the Italian samples cannot refer to a specific biogenic input. As well, their slightly enhanced concentrations point more to an unusual source. Interesting for the present study is that kerogen pyrolysis products show higher maximum in *n*-C_{14} than products from source rock asphaltenes. Fig 87 shows a plot of the ratio of *n*-C_{14} / (*n*-C_{13} + *n*-C_{15}) versus HI for kerogens and source rock asphaltenes (left), and the same ratio versus API gravity for reservoir asphaltenes (right). The kerogens show higher ratios, respectively higher contents of *n*-C_{14} than related asphaltenes. The kerogens with high HI values display highest ratios, indicating that with high biomass input the biological precursor molecule is favourable associated with the kerogens structure than with the macromolecule structure of the related source rock asphaltene. It is also obvious that the difference between kerogens and related asphaltenes increases with increasing HI. Kerogens show a decreasing trend of that ratio with decreasing HI. The opposite trend is observed for source rock asphaltenes. In comparison to them, for the reservoir asphaltenes the ratio slightly decreases with increasing API, or maturity respectively. Here, over the API range the *n*-C_{14} alkane/-ene in pyrolysates of reservoir asphaltenes reveals more similarity to kerogen pyrolysates in their range of HI than to pyrolysates of source rock asphaltenes.

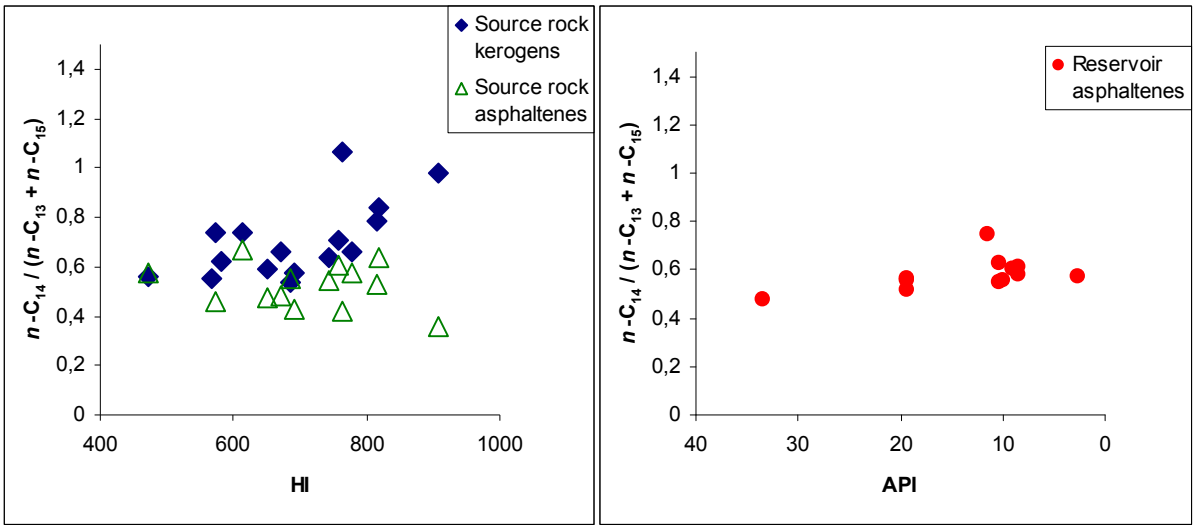

Fig 87 Ratio of *n*-C_{14} / (*n*-C_{13} + *n*-C_{15}) versus HI for kerogens and source rock asphaltenes (left), and the same ratio versus API gravity for reservoir asphaltenes (right).

More interesting findings result also from the comparison of alkanes to alkenes in doublets obtained from py-GC chromatograms of whole rocks and asphaltenes. The distribution of certain *n*-alkanes and *n*-alkenes may also provide information on the organic matter. For example Horsfield (1997) reported a predominance of C_6, C_{10} and C_{14} *n*-alk-1-enes for algal kerogen pyrolysates of torbanites pointing to an algal origin of the original organic matter. Another application for the alkane/alkene ratio obtained from pyrolysates was published by Ishiwatari *et al*. (1995). These authors used this ratio to study the evolution in time for organic matter in sinking particles in oceans, based on their assumption that the alkane/alkene ratio for same organic matter varies over time. There are significant differences observed between kerogen and asphaltene pyrolysates from samples from Southern Italy, when comparing their distribution of *n*-alkane and *n*-alkenes. All reservoir asphaltenes show a predominance of alkane in the range of *n*-C_6-*n*-C_{14}. For alkane/-ene doublets of higher carbon number the distribution changes and reveal a predominance of alkenes in pyrolysates of oil asphaltenes. Pyrolysates of source rock asphaltenes show a different distribution pattern of alkane/alkene

ratios. Here, alkenes are predominant over the whole range, except for *n*-C_6 and *n*-C_{10} doublets, where the *n*-alkanes are dominant. Whole rock pyrolysates show higher variations. Most of their pyrolysates indicate a predominance of alkane in the range of *n*-C_6-*n*-C_{14}. In terms of alkane/alkene ratios pyrolysates of kerogens provide thus higher similarities to oil asphaltenes than to source rock asphaltenes. However, some whole rocks like sample G000652 in Fig 84 demonstrate an entire predominance of alkenes for doublets with higher carbon number than *n*-C_6. These observed differences of kerogens and both types of asphaltenes are not outlined to explain by different thermal reaction processes during pyrolysis for whole rocks and asphaltenes, since major differences are found between oil and bitumen asphaltenes. Therefore, this observation may also be attributed to different concentrations of precursor molecules, like different concentrations of certain fatty acids, associated with oil and source rock asphaltenes.

Fig 88 shows the *n*-alkyl-chain distributions from open-system pyrolysis experiments in a ternary diagram established by Horsfield (1989). The author has illustrated that this diagram allows organic matter typing as well as the typing of petroleum expected to be formed from the studied source rocks. Larter and Horsfield (1993) explained that neither *n*-alkyl pyrolysates distribution nor chain length are controlled by random chain scission during pyrolysis. Later on, Horsfield (1997) as well as Schenk and Horsfield (1998) pointed out that the reactions leading to the formation of *n*-alkanes and -alkenes under laboratory conditions are comparable to the formation of *n*-alkanes under geological conditions. Fig 88 illustrates that the type of petroleum formed from asphaltenes and kerogens is very similar. Pyrolysates of whole rocks plot mainly at the boundary of paraffinic-naphtenic-aromatic low-wax and high-wax oil generating facies. The definitions of petroleum type for each field in the ternary diagram were adapted from Horsfield (1989; 1997). The plot of kerogens in Fig 88a comply with previous observations by di Primio and Horsfield (1996).

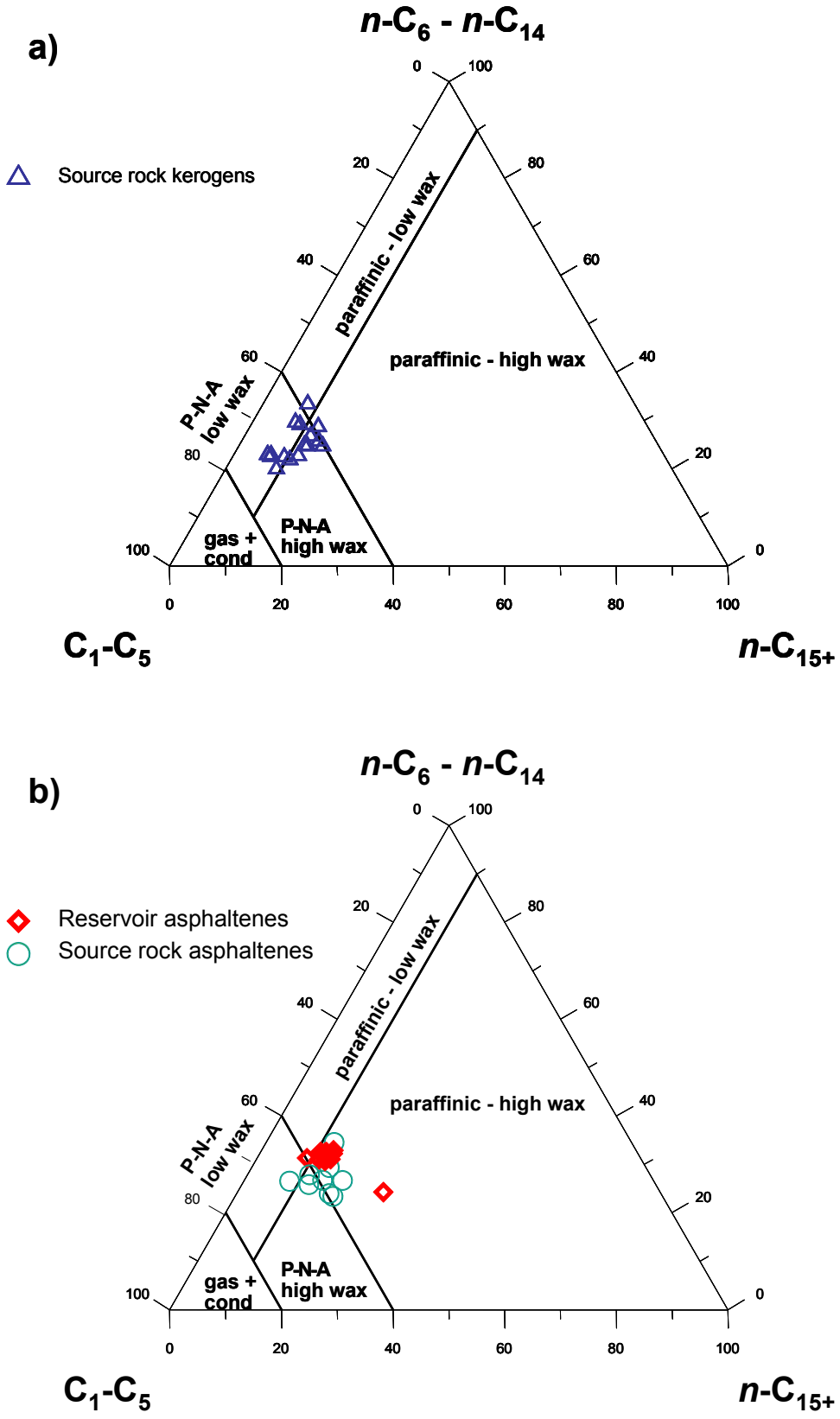

Fig 88 n-alkane/alkene distributions after Horsfield (1989) of investigated pyrolysates for a) source rock kerogens, b) source rock and reservoir asphaltenes from Southern Italy.

The low-wax P-N-A crude oil generating facies is generally associated with shales and carbonates of high petroleum generating potential (Horsfield, 1989). Their organic matter is derived from algal and bacterial inputs containing autochthonous material in abundance. Examples for this facies are the Devonian Woodford Shale, the Jurassic Kimmeridge Clay, Posidonia Shale and Toarcian Shale, as well as the Cretaceous Fischschiefer (Thomas *et al.*, 1985; Horsfield, 1989; Lafargue and Béhar, 1989; Muscio *et al.*, 1991; Horsfield, 1997). The discrepancy between the prediction of low-wax mixed-base crude oil obtained from the kerogen alkyl-chain distribution and the heavy crude oils found in nature, was already discussed in di Primio and Horsfield (1996) as well in Horsfield (1997). The alkane/-ene distributions for asphaltenes pyrolysates are shown in Fig 88b. This figure shows that products formed from both macromolecules are systematically similar, even when oil asphaltene pyrolysates show slightly higher amounts of *n*-C_6-C_{14}. The asphaltenes plot mainly at the triple point of the paraffinic-naphtenic-aromatic (P-N-A) low- and high-wax, as well as high-wax paraffinic oil generating facies. This was also observed by di Primio and Horsfield (1996).

Fig 89 illustrates the ratio of (C_1-C_5) / *n*-C_{6+} obtained from pyrolysates versus a) Tmax, b) HI for kerogens and source rock asphaltenes, and c) versus API for reservoir asphaltenes. All diagrams show for comparison reasons from left to right increasing maturity, or respectively maturity expressed by HI and API. From Fig 89a it can be seen that kerogen pyrolysates are not getting much richer in gas with increasing Tmax. In contrast to Fig 89b were the ratio is plotted versus the HI. Here, kerogen pyrolysates show slightly higher ratios with decreasing HI. Oil and source rock asphaltenes show similar ratios (Fig 89b,c) over their entire range of API and HI respectively.

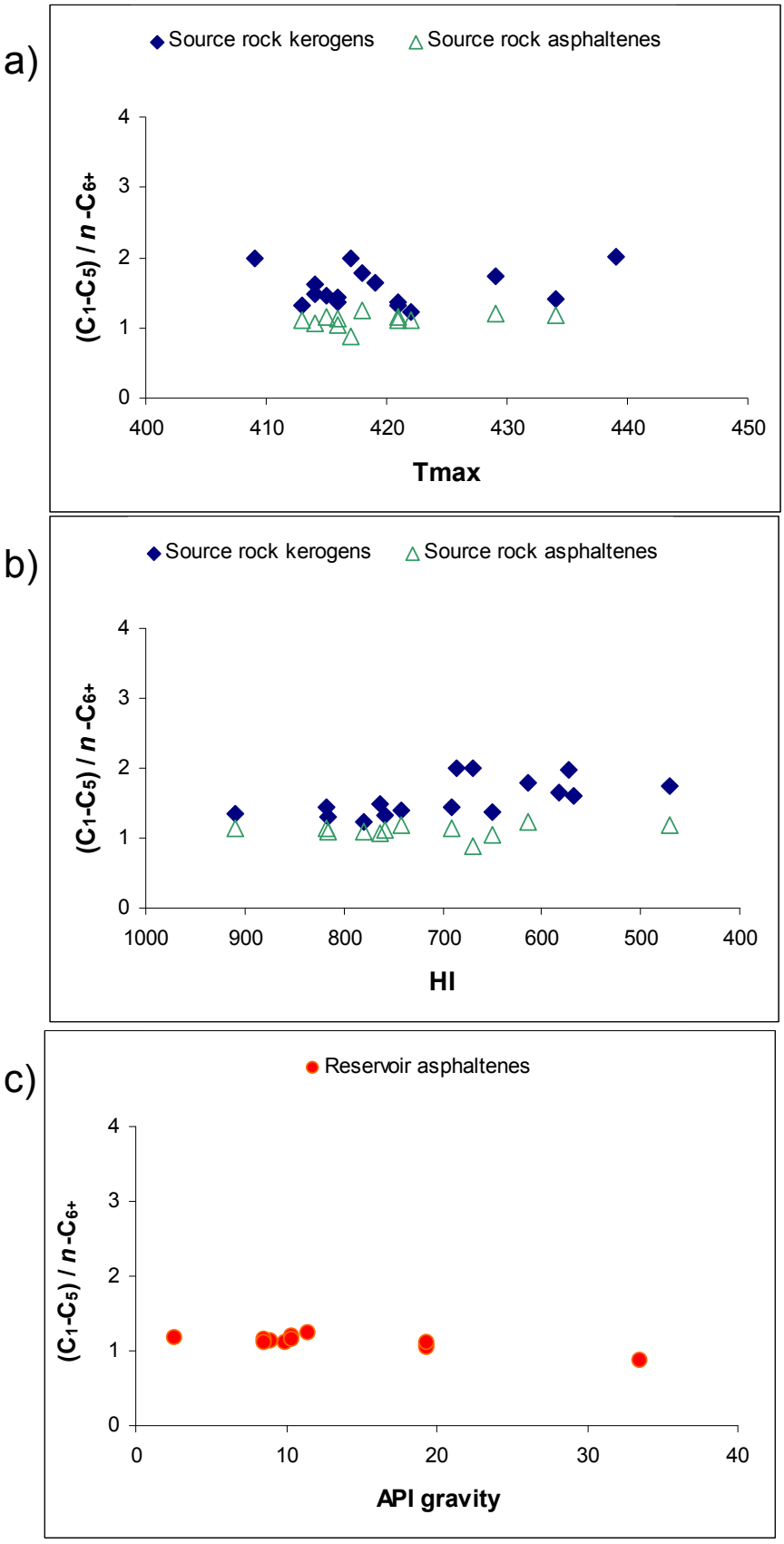

Fig 89 Ratio of (C_1-C_5) / *n*-C_{6+} obtained from pyrolysates versus a) Tmax, b) HI for kerogens and source rock asphaltenes, and c) versus API for reservoir asphaltenes.

7.3.4 Aromatic hydrocarbons

The major resolved aromatic pyrolysis products in all organic matter types are C_1-C_2 alkylbenzenes. Kerogen and asphaltenes from Southern Italy reflect a dominance of toluene. Some kerogens and related source rock asphaltenes show also high yields of ethylbenzene and m,p-xylene, which might even exceed the toluene concentration. However, as it can be seen from Fig 90, the ratio o-xylene / (m,p-xylene + o-xylene) is very similar for kerogens and oil asphaltenes. In contrast, source rock asphaltenes present slightly lower ratios of o-xylenes / Σ xylenes.

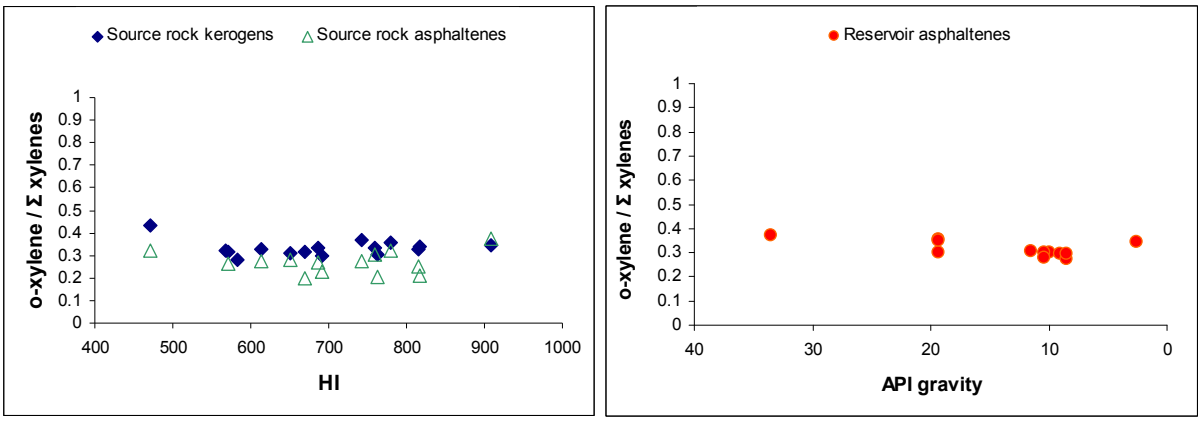

Fig 90 Ratio of o-xylene / (m,p-xylene + o-xylene) versus the hydrogen index for source rock kerogens and related asphaltenes (left side), and that same ratio versus the API gravity for reservoir asphaltenes (right side).

Moreover differences between kerogen and asphaltene pyrolysates are observed when comparing ratios of different aromatic hydrocarbons, like for example toluene / Σ xylenes. This ratio versus HI and API is illustrated in Fig 91 for kerogens and source rock asphaltenes (left) and oil asphaltenes (right). Here it is demonstrated that asphaltenes from Southern Italy show higher amounts of toluene compared to other aromatic hydrocarbons than kerogens. Different concentrations of precursor molecules for the different alkylbenzenes in asphaltenes than in kerogens might be an explanation for this observation.

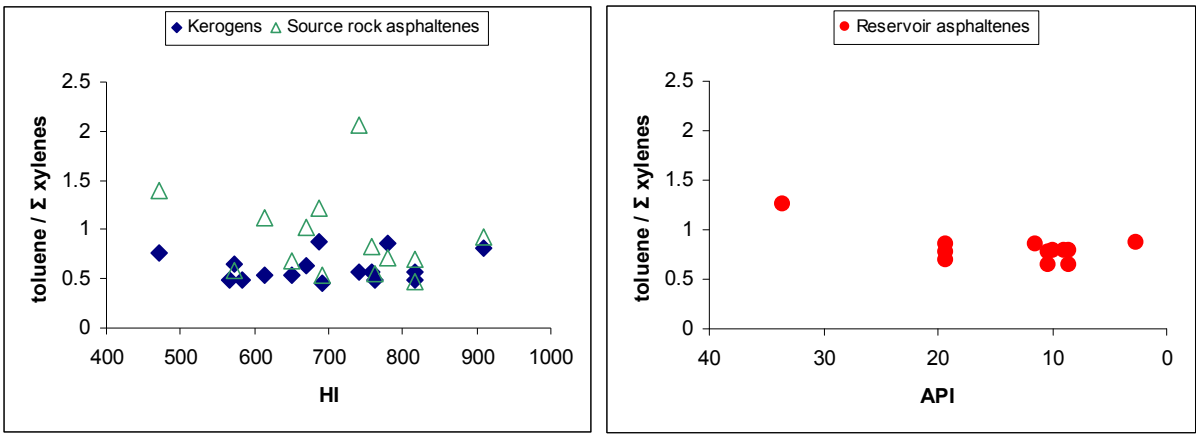

Fig 91 Ratio of toluene / (m,p-xylene + o-xylene) versus the hydrogen index for source rock kerogens and related asphaltenes (left), and that same ratio versus the API gravity for reservoir asphaltenes (right).

Fig 92 compares petroleum asphaltene pyrolysates and crude oils with pyrolysates of kerogens and source rock asphaltenes in terms of their general enrichment of aromatic structures. This aromaticity is here expressed as the ratio of aromatic hydrocarbons / *n*-C_{6+}, using the sum of C_1-C_2 alkylbenzenes. Left side of Fig 92 shows that ratio versus HI for kerogens and related bitumen asphaltenes. The same ratio is shown on the right side versus API for crude oils and related reservoir asphaltenes. For the sample set under study kerogens and source rock asphaltenes are very similar in terms of aromaticity, even when their ratios for aromaticity are spreading much in Fig 92. In marked contrast, oil asphaltenes are more paraffinic and crude oils show even the lowest aromaticity.

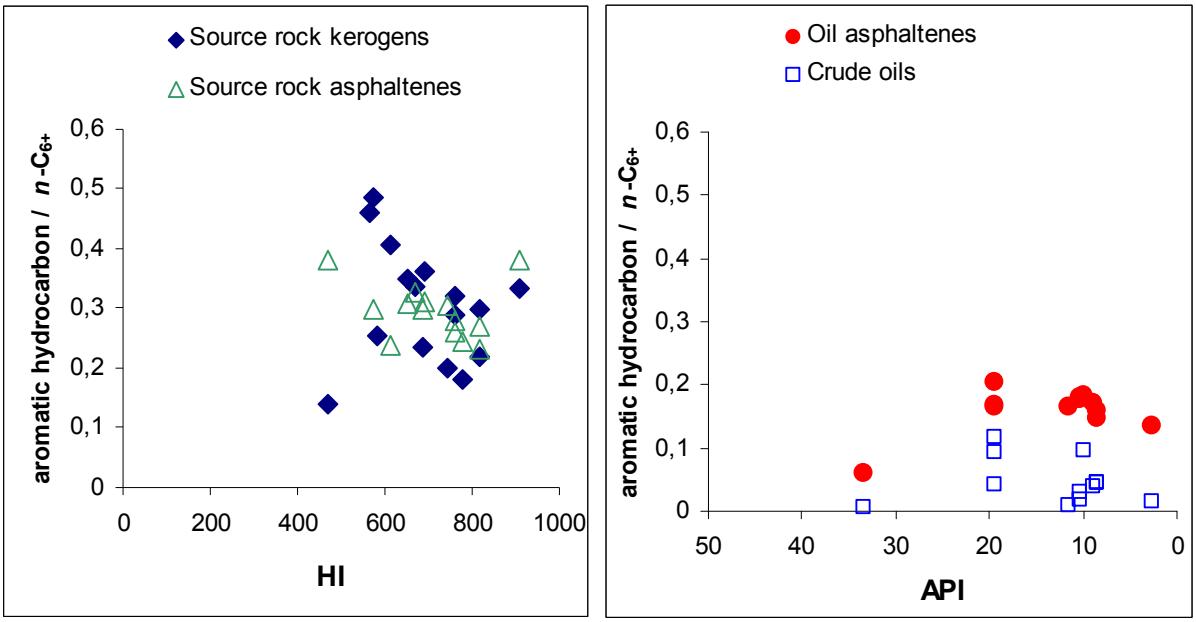

Fig 92 Ratio of aromatic compounds / *n*-C_{6+} versus the hydrogen index for source rock asphaltenes and kerogens (left-hand-side), and versus the API gravity (right-hand-side) respectively for reservoir asphaltenes and natural oils for the samples from S-Italy

However, it is remarkable that source rock asphaltenes and petroleum asphaltenes show dramatic differences when it comes to the characterization of the pyrolysis products. This is of special interest when bearing in mind that several studies in the past such as Pelet *et al.* (1986), Eglinton *et al.* (1990a) among others built on similar characteristics of source rock asphaltenes and petroleum asphaltenes rather than on major differences between these both asphaltene types.

7.3.5 Alkylthiophenes

In evaporitic environments hydrogen sulphide generated by sulphate-reducing bacteria binds to the organic molecules, increasing their potential for preservation (Sinninghe Damsté *et al.*, 1990). The composition of the formed organic-sulphur molecules has been studied in varies previous works in terms of sulphurization process or biogenic inputs originally present at deposition (Sinninghe Damsté *et al.*, 1988; Sinninghe Damsté *et al.*, 1989; de Leeuw and Sinninghe Damsté, 1990; Eglinton *et al.*, 1990b; Kohnen *et al.*, 1991; Kohnen *et al.*, 1993; Sinninghe Damsté *et al.*, 1993; Stankiewicz *et al.*, 1996; de las Heras *et al.*, 1997; Russel *et al.*, 1997; Sinninghe Damsté *et al.*, 1998). The reaction can affect selectively the composition of the free lipid components, so that the analysis of the sulphide-bound biolipids can provide important additional information about palaeoenvironments (Sinninghe Damsté *et al.*, 1990; Kohnen *et al.*, 1991). Also some authors ascribed the sulphurization process of molecules with H_2S to originate from thermochemical sulphate reduction (TSR); a process whereby sulphate minerals and petroleum react together (Heydari, 1997; Putschew *et al.*, 1998; Cai *et al.*, 2003).

Previous (chapter 7.1.4), it was reported that pyrolysates of source rock kerogens and of both types of asphaltenes differ in their concentrations of alkylated thiophenes, which represent the relative enrichment of organic sulphur (Fig 74 - Fig 80). Beside the total organic sulphur content, pyrolysates of both types of asphaltenes and kerogens differ in ratios of specific thiophenes. Sinninghe Damsté *et al.* (1990) explained the generation of alkylthiophenes by pyrolysis depending on the type of bond between the thiophene structure and kerogens, and hence the biological precursor of individual thiophene. Fig 93 after Sinninghe Damsté *et al.* (1990) shows some precursor molecules and their pyrolysis product found in pyrolysates.

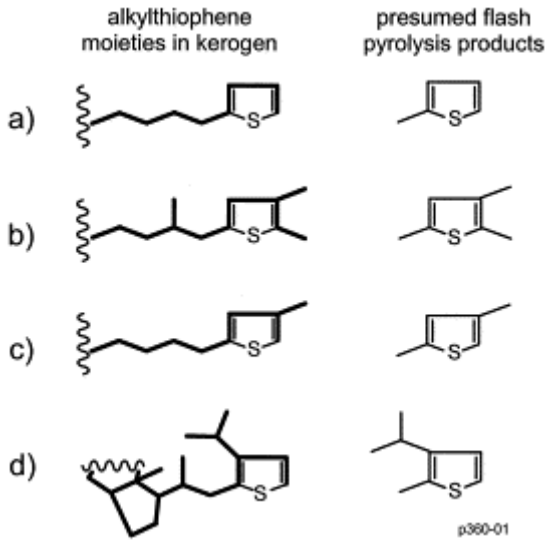

Fig 93 Postulated products of sulphur-containing moieties in kerogens generated upon flash pyrolysis (Sinninghe Damsté *et al.*, 1990).

With reference to these authors, precursor molecules with a linear carbon skeleton (a) derived from normal fatty acids yield upon pyrolysis mainly 2-methylthiophene or 2,5-dimethylthiophene. The isoprenoid thiophenes (b) and thiophenes with branched carbon skeleton (c) originated from isoprenoid alcohols will probably form 3-methylthiophene, 2,3- or 2,4-dimethylthiophene, and trimethylthiophenes upon pyrolysis. Precursor molecules for branched carbon skeletons might be unsaturated olefins, which are common in algae or cyanobacteria (Han and Calvin, 1969). The steroidal carbon skeletons (d) from steroids of higher plants and algae form thiophenes with more complex side chains found in pyrolysates. Based on this assumption, the distribution of thiophenes in pyrolysates reflects the distribution of precursor molecules in the organic matter, and therefore also the biological input found in kerogens and asphaltenes.

As mentioned before, pyrolysates of both types of asphaltenes and kerogens differ in ratios of specific thiophenes. For example 2-methylthiophene is the most prominent within the

asphaltene and kerogen pyrolysates. The ratio of 2-methylthiohene/3-methylthiophene is about 3:1 for pyrolysates of kerogens and lower for reservoir and bitumen asphaltenes. This is interesting, because we know that 2- and 3-methylthiophenes are related to different organic precursor molecules. Fig 94 shows a ternary diagram with the use of 2-methylthiophene, 3-methylthiophene, and 2,5-dimethylthiophene for both types of asphaltenes and source rock kerogens from Southern-Italy. As it can be seen from this plot, source rock kerogens from Southern-Italy are enriched in 2-methylthiophene compared to asphaltenes, whereas both types of asphaltenes show slightly higher concentrations of 2,5-dimethylthiophene compared to parent kerogens. A comparison of bitumen and oil asphaltenes from Southern-Italy shows that most bitumen asphaltenes are somewhat depleted in 3-methylthiophenes. This surly indicates that biogenic precursor molecules of those compounds occur in different concentrations in the macromolecular structure of kerogens, reservoir and source rock asphaltenes.

In addition, the kerogens show a nice trend, which can be related to the hydrogen indices (HI) based on Rock-Eval data (Fig 95). Samples with increasing HI show decreasing amount of 3-methylthiophene. The sample with the highest HI value of 909 mg HC/g TOC (G000654), display with less than 10% lowest content of 3-methylthiophene, whereas the amount of this thiophene increases disproportional with HI. The sample G000646 shows a HI of 471 mg HC/g TOC, and in this diagram a content of 3-methylthiophene about 30%. Beside, the amount of 2,5-dimethylthiophene decreases with decreasing HI values, which results in this observed trend for source rock kerogens.

The observed correlation with HI indicates that isoprenoid precursor molecules, resulting in 3-methylthiophene in pyrolysates proportionally a) decreases with increasing input of hydrogen-rich biomass, and/or b) the amounts of 2-methylthiophene and 2,5-dimethylthiophene decreases with increasing maturity. The latter is also supported by the

methylthiophene ratio found in oil asphaltene pyrolysates, which increases with increasing API for most oil asphaltenes. As well, previous studies of Eglinton *et al.* (1990b) have reported decreasing amounts of 2-methylthiophene with increasing maturity pointing to increasing proportions of branched versus linear isomers during maturation. A comparison of this 3-methylthiophene ratio for kerogens and both types of asphaltenes versus maturity parameters is shown in Fig 96 and Fig 97.

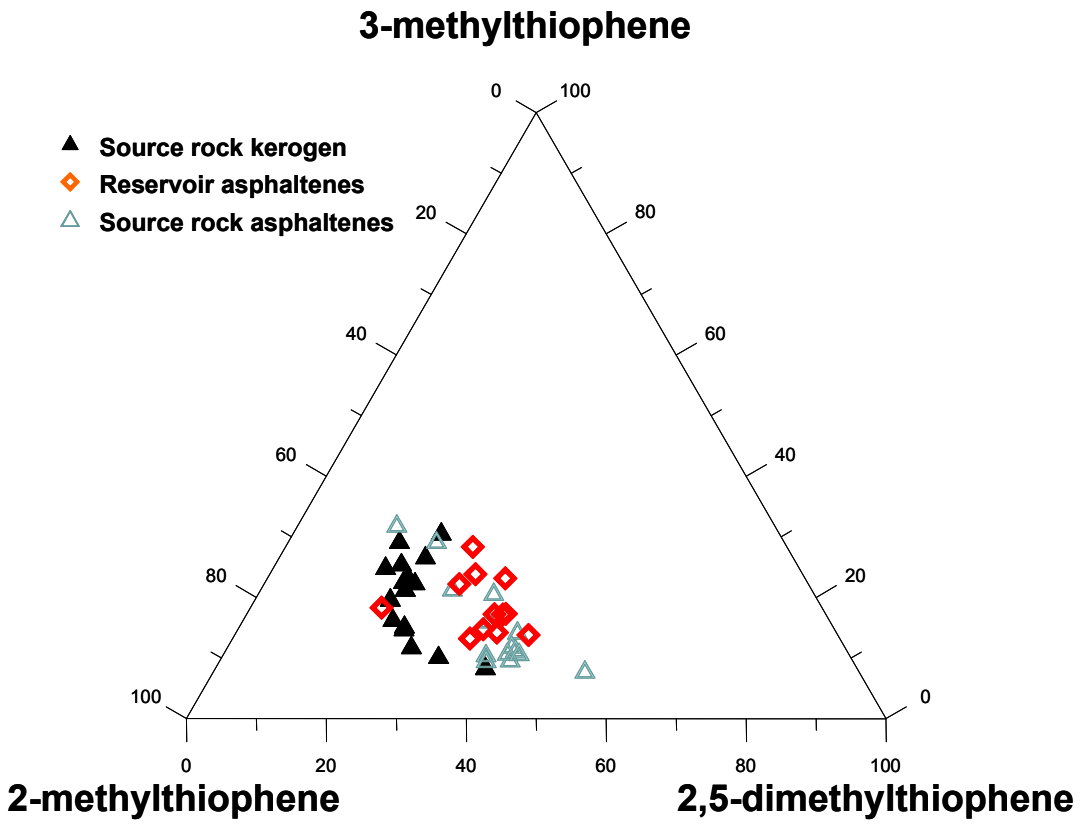

Fig 94 Ternary diagram of 2-methylthiophene, 3-methylthiophene and 2,5-dimethylthiophene for kerogens and both types of asphaltenes from Southern Italy.

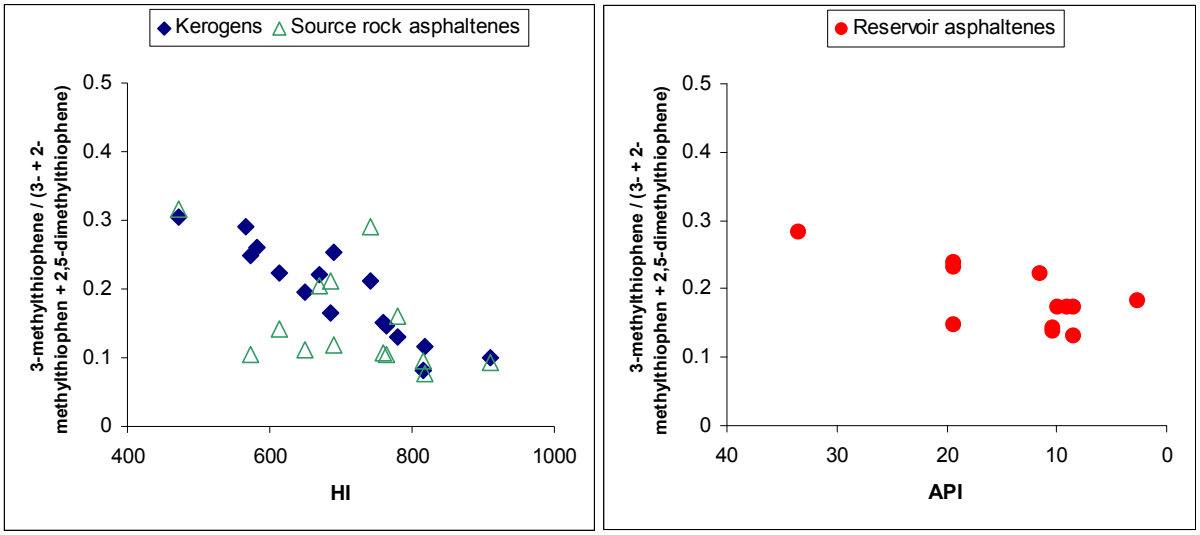

Fig 95 Diagram with the ratio of 3-methylthiopene/ (3- + 2-methylthiophene + 2,5-dimethylthiophene) versus HI for the kerogens and source rock asphaltenes (left) and versus API for reservoir asphaltenes from Southern Italy.

Fig 96 shows the ratio of 3-methylthiopene/ (3- + 2-methylthiophene + 2,5-dimethylthiophene) versus Tmax (left) and versus the maturity parameter C_{29} 20*S*/(20*S*+20*R*) obtained from source rock bitumen (right). Both diagrams do not show a clear trend with maturity parameters, which might be related to an inaccuracy of biomarker parameters and also Tmax for immature source rocks. Perhaps, this ratio within immature source rocks and related bitumen asphaltenes from Southern Italy might also be affected by facies variations, i.e. biogenic input expressed by HI. However, Eglinton *et al.* (1990b) reported that with increasing maturity the ratio of linear (2-methylthiophene) versus branched isomers (3-methylthiophene) decreases, which would lead to higher 3-methylthiophene ratios for pyrolysates of higher thermal stress. And this is found for kerogens from Italy of decreasing HI.

Nevertheless, later on we will see that the 3-methylthiophene ratio obtained from kerogen pyrolysates show also some unusual generation characteristic of methylthiophenes with

higher thermal stress. This will be discussed in the following by the interpretation of data from stepwise-open-system-pyrolysis.

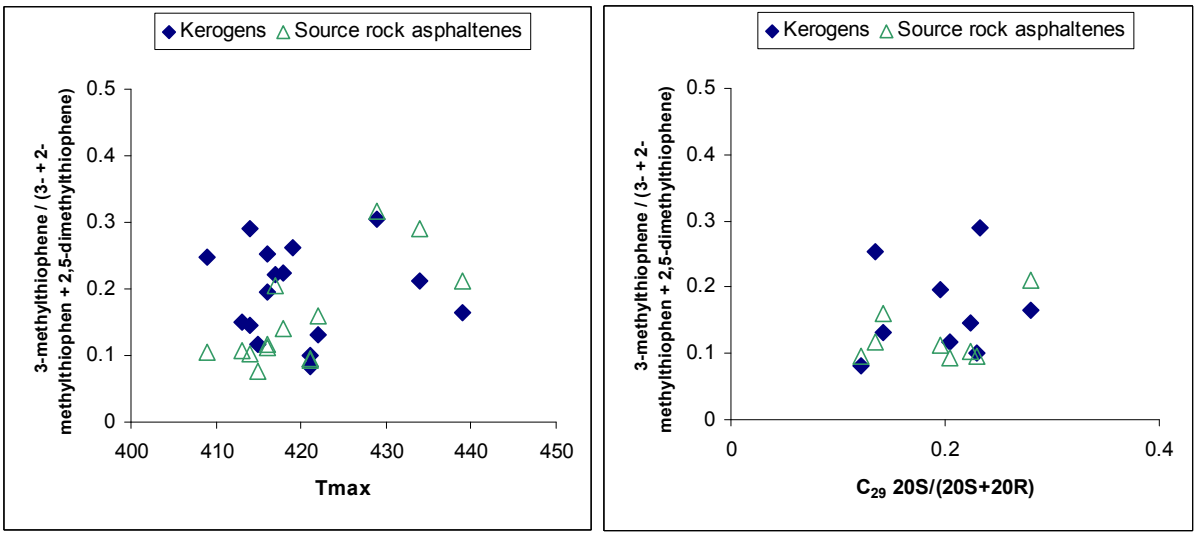

Fig 96 Diagram with the 3-methylthiopene ratio versus Tmax (left) and versus maturity parameter C_{29} 20*S*/(20*S*+20*R*) (right) for the kerogens and source rock asphaltenes from Southern Italy.

The 3-methylthiophene ratio found in pyrolysates from oil asphaltenes shows a relationship to maturity. In Fig 97 the ratio of 3-methylthiophene/ (3- + 2-methylthiophene + 2,5-dimethylthiophene) of oil asphaltene pyrolysates versus the maturity parameters C_{27} $\beta\beta/(\beta\beta+\alpha\alpha)$ (left) and C_{29} 20*S*/(20*S*+20*R*) (right) obtained from related crude oils. The data are spreading somewhat, because the sterane parameters in most crude oils are affected by biodegradation and also by long-time-storing. As well an additional facies control on the 3-methylthiophene ratio cannot be excluded. However, this ratio of pyrolysates from oil asphaltenes increases with increasing biomarker maturity parameter of related oils, pointing to a primarily maturity control of those thiophenes in oil asphaltene pyrolysates. Thus, this ratio obtained from oil asphaltenes pyrolysates has also potential to reconstruct the original maturity for biodegraded oils from Southern Italy.

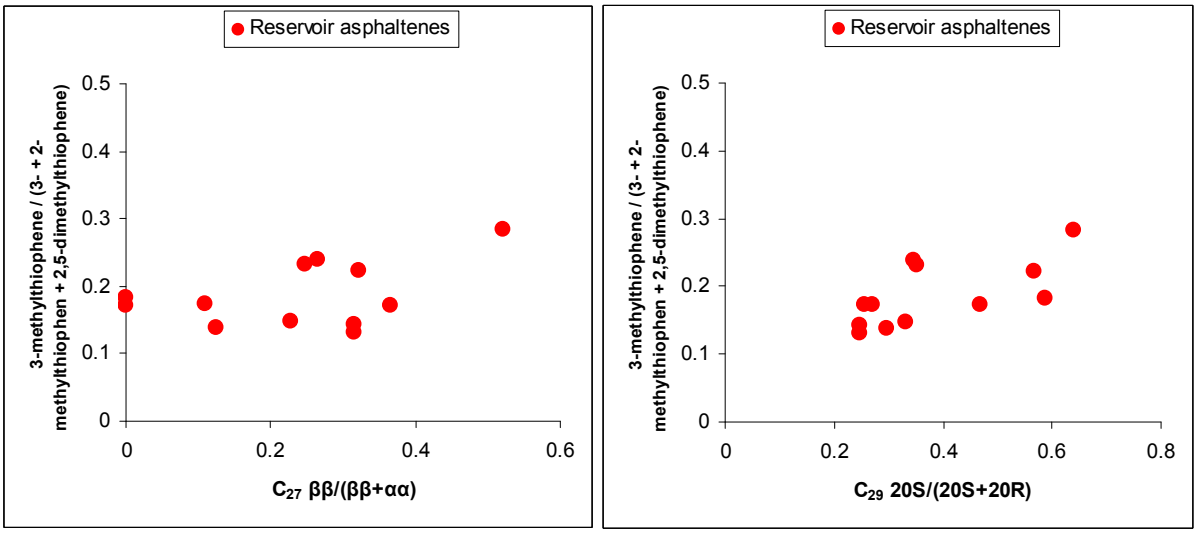

Fig 97 Diagram with the 3-methylthiopene ratio of oil asphaltene pyrolysates versus maturity parameters C_{27} *ββ/(ββ+αα)* (left) and versus C_{29} 20*S*/(20*S*+20*R*) (right) obtained from crude oils from Southern Italy.

Because of the limited maturity range of studied source rocks from Southern Italy, we employed stepwise-open-system-pyrolysis-GC in order to assess generation characteristics of kerogens during thermal maturation. One kerogen sample (G000652), the related source rock asphaltene sample (G000652), and one oil asphaltene sample (G000395) have been heated up by pyrolysis technique with an heating-rate of 5.0 K/min to a specific end-temperature of 350, 380, 400, 420, 450 and 500 °C. The pyrolysis products released up to the decided end-temperature were collected in a liquid nitrogen-cooled trap, and finally released by heating the trap to 300°C and measured online by gas-chromatography. Thus, this technique provides a comparison of specific moieties released from kerogens or asphaltenes within different temperature ranges. Fig 98 shows three selected chromatograms from stepwise-open-system pyrolysis GC of the oil asphaltene sample G000395 with the temperature ranges of 300-380°C (top), 300-420°C (middle), and 300-450°C (bottom). As it can be seen, the oil asphaltene, same for the kerogen, released already high amounts of isoprenoids, for example prist-1-ene, at lower thermal stress. Additionally, the pyrolysates of the oil asphaltene in that range of low temperatures (< 380°C) show higher aromaticity, higher hump, and higher

concentrations of alkylthiophenes relative to aromatic and aliphatic structures compared to pyrolysates with higher pyrolysis end-temperatures. The pyrolysates of the oil asphaltene with a temperature range up to 450°C is more paraffinic and demonstrate lower concentrations of alkylthiophenes relative to aromatic and aliphatic structures.

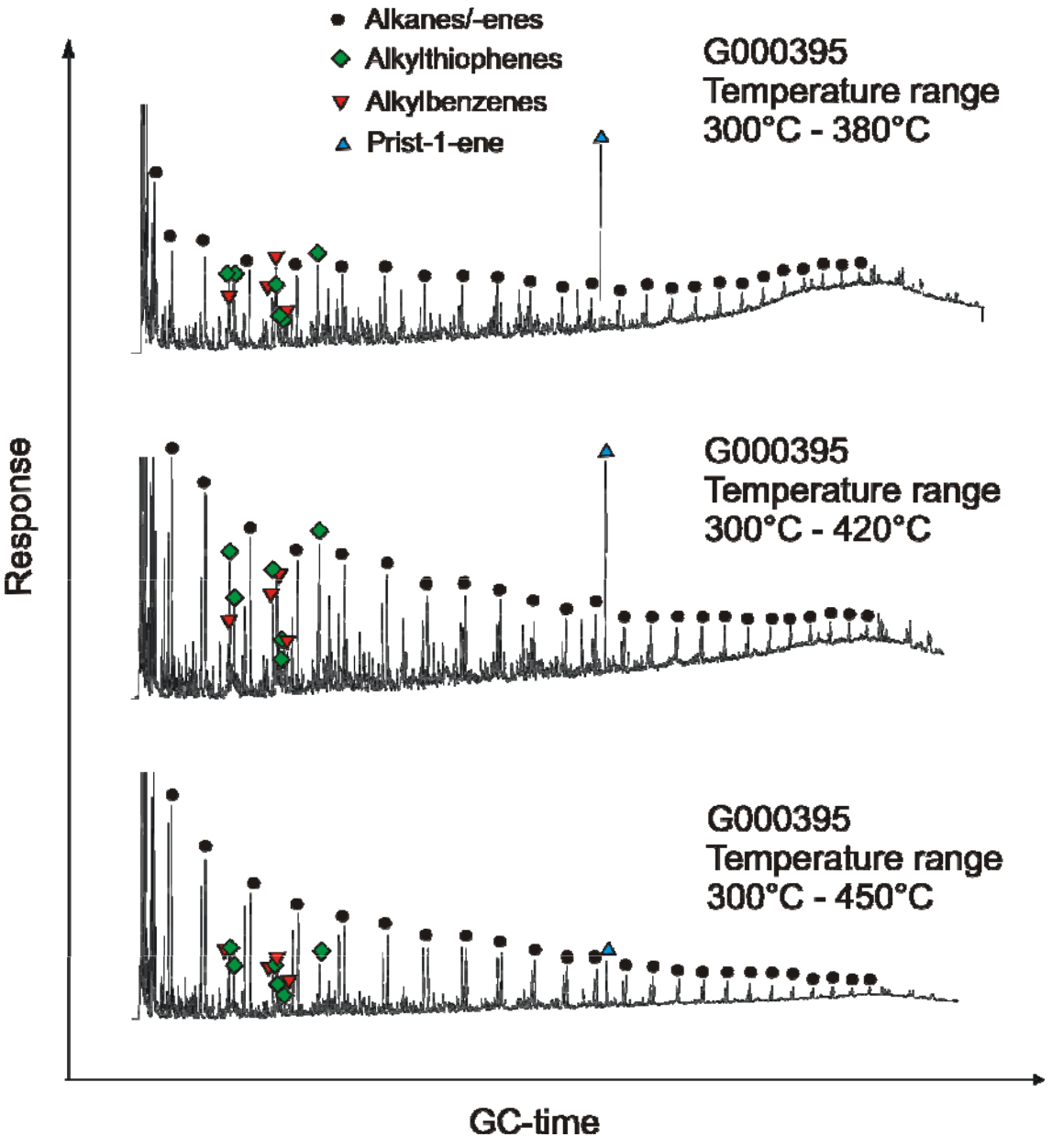

Fig 98 Selected chromatograms from stepwise-open-system pyrolysis GC of oil asphaltene sample G000395 from Southern Italy. Alkane/-ene doublets, most abundant thiophenes, and alkylbenzenes are marked. Alkylbenzenes are corresponding to retention time from left to the right: toluene, ethylbenzene, m,p-xylene, and o-xylene. Alkylthiophenes are from left to right: 2-methylthiophene, 3-methylthiophene, 2,5-dimethylthiophene, 2,4-dimethylthiophene, 2,3-dimethylthiophene, and ethylmethylthiophene.

Fig 99 (left) shows the ratios of (2,3- + 2,4-dimethylthiophene) /(o-xylene + n-$C_{9:1}$) obtained from pyrolysates of the kerogen, source rock asphaltene, and oil asphaltene sample versus stepwise-pyrolysis end-temperatures. At low temperatures < 350°C all pyrolysates show relative low concentrations of dimethylthiophenes compared to aromatic and aliphatic structures. Between pyrolysis end-temperatures of 380–400 °C the pyrolysates of asphaltenes, and even higher marked in the pyrolysates of the kerogen, show highest amounts of dimethylthiophenes. With increasing temperatures this ratio build up on 2,3- and 2,4-dimethylthiophenes decreases, indicating lower organic sulphur content for those samples at higher thermal stress. This was also reported by Orr and Sinninghe Damsté (1990). Right side of Fig 99 shows the ratio using 2,5-dimethylthiophene established by di Primio and Horsfield (1996). Here it is also illustrated that with increasing thermal stress (> 400 °C) the amount of 2,5-dimethylthiophene decreases relative to aromatic and aliphatic structures. The ratio of Σ alkylthiophenes / (Σ C_1-C_2 alkylbenzenes + Σ n-$C_{7:1}$ - $C_{10:1}$ alkenes), which was presented in Fig 79, show the same trend with increasing thermal stress for asphaltenes and the kerogen sample, like demonstrated in Fig 100 (left).

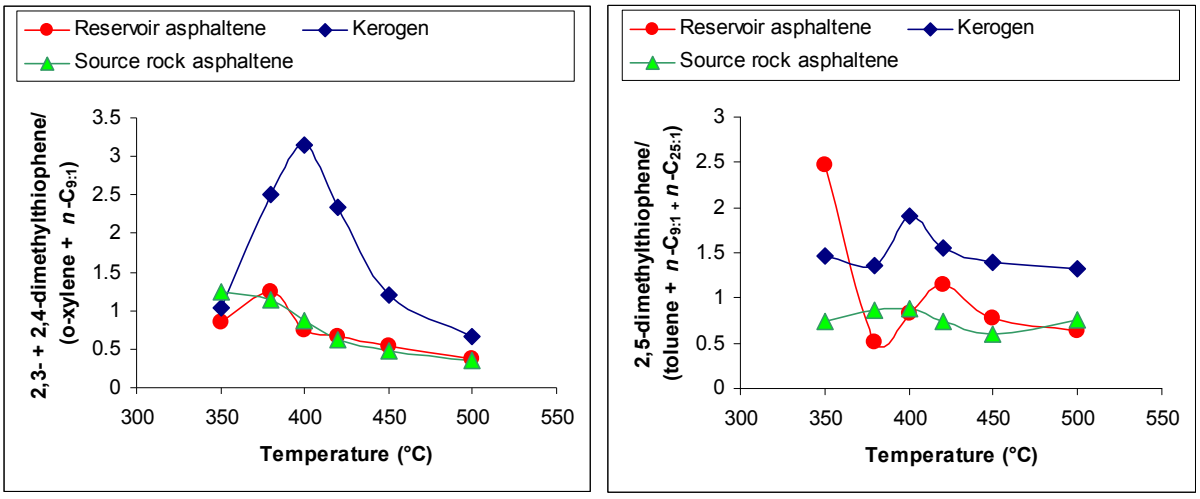

Fig 99 Ratios of (2,3- + 2,4-dimethylthiophene) /(o-xylene + n-$C_{9:1}$) obtained from pyrolysates of the kerogen, source rock asphaltene, and oil asphaltene sample versus stepwise-pyrolysis end-temperatures (left), and the ratio of 2,5-dimethylthiophene) /(toluene + n-$C_{9:1}$+ n-$C_{25:1}$) versus these temperatures (right).

Fig 100 (right) demonstrates the ratio of 3-methylthiophene/ (3- + 2-methylthiophene + 2,5-dimethylthiophene) for asphaltene and kerogen pyrolysates versus the end-temperature of the stepwise-pyrolysis. The oil asphaltene pyrolysates show an increasing 3-methylthiophene ratio with increasing thermal stress up to the pyrolysis temperature of 420°C. For higher temperatures this ratio slightly decreases again. Source rock asphaltene and kerogen pyrolysates show a decreasing trend of the 3-methylthiophene ratio with increasing thermal stress already for temperatures higher than 380°C. Eglinton *et al.* (1990b) reported that with increasing maturity the ratio of linear (2-methylthiophene) versus branched isomers (3-methylthiophene) decreases, which would lead to higher 3-methylthiophene ratios for pyrolysates of higher thermal stress. But that is only observed for the kerogen at low thermal stress (< 380°C). This illustrates that at high thermal stress pyrolysates of kerogens from a carbonate sequence from Southern Italy do not follow the common tendency of decreasing linear isomers with increasing maturity like reported by Eglinton *et al.* (1990b). Moreover, at high temperatures they show an inversely release of linear and branched isomers with increasing thermal stress.

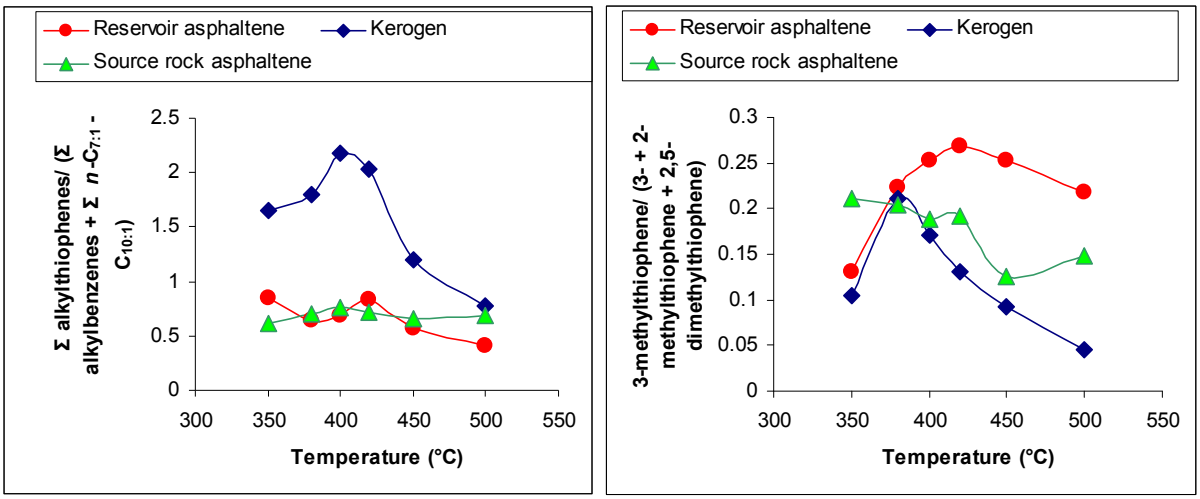

Fig 100 Ratio of Σ alkylthiophenes / (Σ C_1-C_2 alkylbenzenes + Σ *n*-$C_{7:1}$ - $C_{10:1}$ alkenes) obtained from pyrolysates of the kerogen, source rock asphaltene, and oil asphaltene sample versus stepwise-pyrolysis end-temperatures (left), and the ratio of 3-methylthiophene/ (3- + 2-methylthiophene + 2,5-dimethylthiophene) for asphaltene and kerogen pyrolysates versus the end-temperature of the stepwise-pyrolysis (right).

7.3.6 Discussion on structural differences between asphaltenes and kerogens

Such strong observed differences between the different asphaltene types and kerogens in terms of their structural moieties are often ascribed to the thermal degradation (Durand and Monin, 1980; Béhar *et al.*, 1984; Castex, 1985; Pelet *et al.*, 1986; Calemma and Iwanski, 2002). Thermal maturation is associated with the release of alkylated thiophenes and aromatic structures prior to expulsion. However, such an effect would result in the release of low stable bonds within the structure of the low maturity asphaltenes and therefore would stabilize the asphaltenes. Fig 72 shows that asphaltenes form petroleum at even slightly lower temperatures than kerogens, and therefore stabilization due to a retard in asphaltene expulsion may not play a role here. Pellet *et al*. (1986) explained differences in the aromaticity between asphaltenes and kerogens in that asphaltenes are smaller molecules containing fewer cross-linkages than kerogens. With reference to Pellet *et al*. (1986) kerogens have more numerous aromatic nuclei, or if the number of nuclei is the same, they contain more rings. This however, may explain the structural differences between kerogens and reservoir asphaltenes. But, the results from this chapter clearly show that source rock asphaltenes are not so different to related kerogens in terms of aromaticity. As well the presented results illustrate that both types of asphaltenes and kerogens possess different concentrations of structural moieties linked to specific biogenic precursors, and that even at lowest maturity stage of kerogens, related asphaltenes and the oil asphaltenes. The found systematic differences between the parent kerogens and asphaltenes, as well as among both types of asphaltenes are thus unlikely related to thermal evolution.

There might be other reasons for this discrepancy in terms of aromaticity between kerogens and asphaltenes. Fractionation through physical *in-situ* precipitation and/or physico-chemical adsorption of more aromatic asphaltenes in the source rock milieu seems to be a likely possibility.

We know that asphaltenes isolated with solvents of increasing carbon number show increasing aromaticity (Speight *et al.*, 1984). Considering that first formed hydrocarbons are dominated by alkanes of higher carbon number than common solvents (Horsfield, 1997), *in-situ* precipitated asphaltenes should be characterized by much higher aromaticity than asphaltenes isolated with common solvents like *n*-C_5 to *n*-C_7. However, our results from the precipitation experiments on the effect of temperature of solvent showed that precipitation with hot solvent lead to less aromatic asphaltenes. This was shown for the asphaltenes isolated from the Nigerian crude oils. Referring structural differences between both asphaltene types to *in-situ* precipitation would also mean that asphaltenes have already precipitated and deposited in the source rock environment. Oil asphaltenes would thus be only the soluble part of this precipitation.

Processes related to the origin and occurrence of asphaltenes in the subsurface have been proposed by Wilhelms and Larter (1994a; 1994b). They suggest the existences of asphaltene precursors, so called asphaltene-precursor-entities (APE). According to these authors, asphaltene-molecules are kept in solution by steric stabilization and due to changes in solvent properties of the oil these APE´s start to aggregate and probably form lyophilic micelles. High pressure in the source rock kitchen may have an effect on the initial composition of expelled fluids, in that in high pressure regimes the expelled petroleum contains more polar compounds. This, however, implies that the composition and characteristics of asphaltenes are controlled by the composition of oil in which the relevant asphaltenes are dissolved. This mechanism outlined alone will lead to hydrocarbon fluids saturated in asphaltenes, which will lose high asphaltene amounts during migration to shallower depth. Such asphaltenes can also be found along migration pathways in carrier rocks and dominate macromolecules within so called tar mats (Dahl and Speers, 1986; Wilhelms and Larter, 1994a, b; Ehrenberg *et al.*, 1995; Dou *et al.*, 1998; Khavari-Khorasani *et al.*, 1998).

The hypothesis of *in-situ* precipitation might thus have an impact, conceivable when bearing in mind that compositional fractionation is of relevance for controlling expelled and retained petroleum components in source rocks (Pepper, 1992; Sandvik *et al.*, 1992; Pan *et al.*, 2002), which in turn may have an impact on the composition of different asphaltenes or asphaltene-precursor-entities (APE) for expelled and retained fluids.

Another explanation for differences in aromaticity of kerogens and both types of asphaltenes is their physico-chemical adsorption behaviour (Gallant, 1984; Larsen and Li, 1997; Ritter, 2003). Since asphaltenes are induced dipoles, which agglomerate into colloids of different aggregation states, it is clear that more aromatic colloids will easier adsorb onto the mineral surface due to their higher polarity. Additionally, factors like enhanced diffusion (Thomas and Clouse, 1990), solvent swelling thermodynamics (Suuberg *et al.*, 1994), and chemical composition of the source rock (Bantignies *et al.*, 1998; Standal *et al.*, 1999; da Silva Ramos *et al.*, 2001) will also control the adsorption behaviour.

At the very least, a network of different factors seems to influence the fractionation to more aromatic source rock asphaltenes and more paraffinic reservoir asphaltenes.

Summarized and with reference to previous works (Pelet *et al.*, 1986; Larter and Horsfield, 1993; Wilhelms and Larter, 1994a, b) the asphaltene-precursor-entities (APE) are generated together with first-formed bitumen (B_1) from parent kerogen (K) during thermal evolution.

$$\mathbf{K \rightarrow B_1 + APE}$$

These asphaltene-precursor-entities (APE) in steric solution seem to be fractionated due to different processes like compositional fractionation, migration etc into a more aromatic fraction (APE_{arom}) soluted in retained fluids (B_{re}) and a more paraffinic fraction (APE_{paraf}) soluted in the expelled oils (O_{exp}).

$$\mathbf{B_1 + APE \rightarrow (B_{re} + APE_{arom}) + (O_{exp} + APE_{paraf})}$$

7.3.7 Conclusions

- Source rocks asphaltenes, related kerogens, and oil asphaltenes in a petroleum system from Southern Italy show major structural differences and differ in aromaticity and organic sulphur content. Highest aromaticity was found in pyrolysates of source rocks asphaltenes, medium from kerogens, and lowest aromaticity in pyrolysates formed from petroleum asphaltenes.
- The highest organic sulphur content was identified in kerogen pyrolysates, whereas pyrolysates of both types of asphaltenes do not show a major difference in the content of organic sulphur. With increasing maturity the content of organic sulphur relative to aromatic and aliphatic structures decreases for asphaltenes as well as for kerogens.
- The proportionally increasing of 3-methylthiophene in kerogen pyrolysates with decreasing HI provides a maturity parameter for immature source rocks at low levels of thermal stress. For oil asphaltene pyrolysates the thiophenes ratio of branched (3-methylthiophene) versus linear isomers (2-methylthiophene, 2,5-dimethylthiophene) can be used to assess the original maturity of strong biodegraded oils.
- For the facies recognition based on the alkyl chain distribution of pyrolysates kerogens predict the field of the paraffinic-naphtenic-aromatic low-wax oil generating facies. Both asphaltene types plot at a triple point predicting P-N-A low and high wax, as well as paraffinic oil generating facies. These predictions however do not correlate with the asphaltic natural oils found in this petroleum system.
- Pyrolysates from both asphaltene types as well from kerogens show differences which can be attributed to different concentrations of biogenic precursors within the asphaltene and kerogen macromolecules. These differences were identified for example in that:

- Source rock asphaltenes show a predominance of alkenes in their alkane / alkene ratios. Oil asphaltenes however show a predominance of alkanes in the range of *n*-C_6-*n*-C_{14} and predominance of alkenes for alkane/-ene doublets of higher carbon number. Whole rock pyrolysates show higher variations, but are more similar to oil asphaltene pyrolysates than to those of source rock asphaltenes.
- Kerogen pyrolysis products show higher maximum in *n*-C_{14}, which is attributed to certain algae or cyanobacteria, than products from source rock asphaltenes and reservoir asphaltenes.
- Pyrolysates of source rock asphaltenes show slightly lower ratios of o-xylenes / Σ xylenes compared to kerogens and oil asphaltenes, whose pyrolysates show similar ratios of those xylenes. As well, source rock asphaltene pyrolysates illustrate higher amounts of toluene compared to xylenes than kerogens, whereas the toluene/ xylenes ratios for oil asphaltene pyrolysates are intermediate.

7.4 Compositional kinetic predictions from petroleum asphaltenes

7.4.1 Introduction

MSSV pyrolysis is used to simulate the processes of petroleum generation (Horsfield *et al.*, 1989). Like all simulation methods, for example dry confined-system-pyrolysis (Monthioux *et al.*, 1985; Monthioux, 1988; Béhar and Hatcher, 1995; Prinzhofer *et al.*, 2000), multiple cold trap pyrolysis (Tang and Stauffer, 1994; Tang and Béhar, 1995), or hydrous pyrolysis (Eglinton *et al.*, 1988; Barth *et al.*, 1989; Baskin and Peters, 1992; Lewan, 1993), it assumes that reaction pathways are the same under laboratory conditions and nature, and only the reaction rates may differ. This is of course based on the fact that temperature is the main driving force of thermal gas and oil formation, and hence artificial generation of hydrocarbons under laboratory conditions can be extrapolated to natural systems. In the case of MSSV pyrolysis , a comparison with natural maturity series in Mexico (Santamaria and Horsfield, 2003) and the North Sea (di Primio and Skeie, 2004) have verified the utility of the approach. In the last years a lot of works on simulation of gas/oil formation from potential source rocks have been published, including the simulation of in-source petroleum formation and in-source cracking as well as in-reservoir cracking of oil to gas (Juntgen and Klein, 1975; Quigley and Mackenzie, 1988; Béhar *et al.*, 1991; Horsfield and Düppenbecker, 1991; Schenk *et al.*, 1997; Dieckmann *et al.*, 1998; Vandenbroucke *et al.*, 1999; Wavrek and Lara, 1999; Dieckmann *et al.*, 2000b; Michels *et al.*, 2002; Santamaria and Horsfield, 2003; di Primio and Skeie, 2004; Dieckmann *et al.*, 2004; Erdmann and Horsfield, 2006). Where bulk kinetic parameters of asphaltene decomposition are very useful for determining the timing of oil generation (Khavari-Khorasani *et al.*, 1998; Skeie *et al.*, 2004; Keym *et al.*, 2006), compositional kinetic analysis calculated from MSSV experiments provides invaluable data for determining the actual products that will be released from the asphaltene, i.e. kerogen under specific geologic

conditions. These gained data on generation temperatures can be used for basin modelling to quantify source potential. This was for example shown by Dieckmann *et al.* (1998) for their study on Toarcian Shales and by Erdmann and Horsfield (2006) for the Norwegian North Sea. Up to now nobody has illustrated that compositional kinetics from oil asphaltenes provide reliable results on geological predictions of oil and gas formation, or prediction of the molecular composition of the C_{6+} hydrocarbon fraction. Therefore, for the present study micro-scale sealed vessel pyrolysis (MSSV) experiments were applied on the reservoir asphaltene sample G000395 in order to investigate the petroleum and gas generation characteristics. The outcoming results were compared in terms of chemical structural differences, as well as differences in gas formation, isotopic composition of generated gas and compositional kinetics to MSSV pyrolysates formed from an immature source rock kerogen (G000652) of the same sample set from Southern-Italy investigated by Fuhrmann (2005).

7.4.2 Composition of MSSV pyrolysates

Progressive changes in gross petroleum composition which might occur during maturation of a kerogen or asphaltene can be simulated by MSSV pyrolysis experiments (Horsfield *et al.*, 1989). Here, the MSSV pyrolysis technique was performed with the oil asphaltene sample G000395 using three heating-rates of 0.2, 0.7 and 5.0 K/min. The MSSV pyrolysates of the thermally extracted oil asphaltene show the presents of *n*-alkanes, aromatic hydrocarbons, alkylthiophenes, as well as the isoprenoids pristane and phytane. Fig 101 shows GC traces for four experimental temperatures using a heating-rate of 5.0 K/min. The chromatograms point to the variability of hydrocarbons formed in this experiment. Fig 102 shows four

chromatograms of similar temperatures using a heating-rate of 0.2 K/min, in order to demonstrate a gross compositional changeability of generated hydrocarbons with different heating-rates.

MSSV pyrolysates of the oil asphaltene show high amounts of unresolved compounds at low experimental temperatures, like illustrated in Fig 101 for 380°C. Pyrolysates of closed-system pyrolysis show pristane and phytane at lower experimental temperatures (Eglinton *et al.*, 1988). For the studied asphaltene MSSV pyrolysates the generation of pristane and phytane ended at 460°C for the heating-rate of 5.0K/min, and at 420°C for 0.2K/min. As well alkylated thiophenes are present in products from artificial maturation experiments, and do not occur in crude oils. The absence of alkylated thiophenes in natural products is explained by different reaction processes in high-temperature laboratory and low-temperature natural maturation systems. In nature alkylated thiophenes are released as long-chain thiophenes due to lower temperatures and longer reaction times (Sinninghe Damsté *et al.*, 1990). For the present investigation the formation of alkylthiophenes ended at 510°C for the heating-rate of 5.0K/min, and at 455°C for 0.2K/min.

As well, the reservoir asphaltene pyrolysates show the occurrence of alkylnaphthalenes, mainly 2- and 1-methylnaphthalenes, which show increasing amount with increasing temperatures. Only for slower heating-rates the formation of those naphtenoaromatics was finished at 560°C (0.7K/min) and 550°C (0.2K/min). A similar characteristic is observed for alkylbenzenes. These alkylbenzenes show also increasing amounts with increasing artificial temperatures, and the total yields of toluene, ethylbenzene and xylenes are still increasing at 580°C, which was the end-temperature of this experiment. In contrast to that, the trimethylbenzenes which occur in lower abundance in asphaltene pyrolysates showed already decreasing amounts compared to toluene and xylenes at 520°C (0.2K/min) and did not occur anymore at 540°C (0.2K/min).

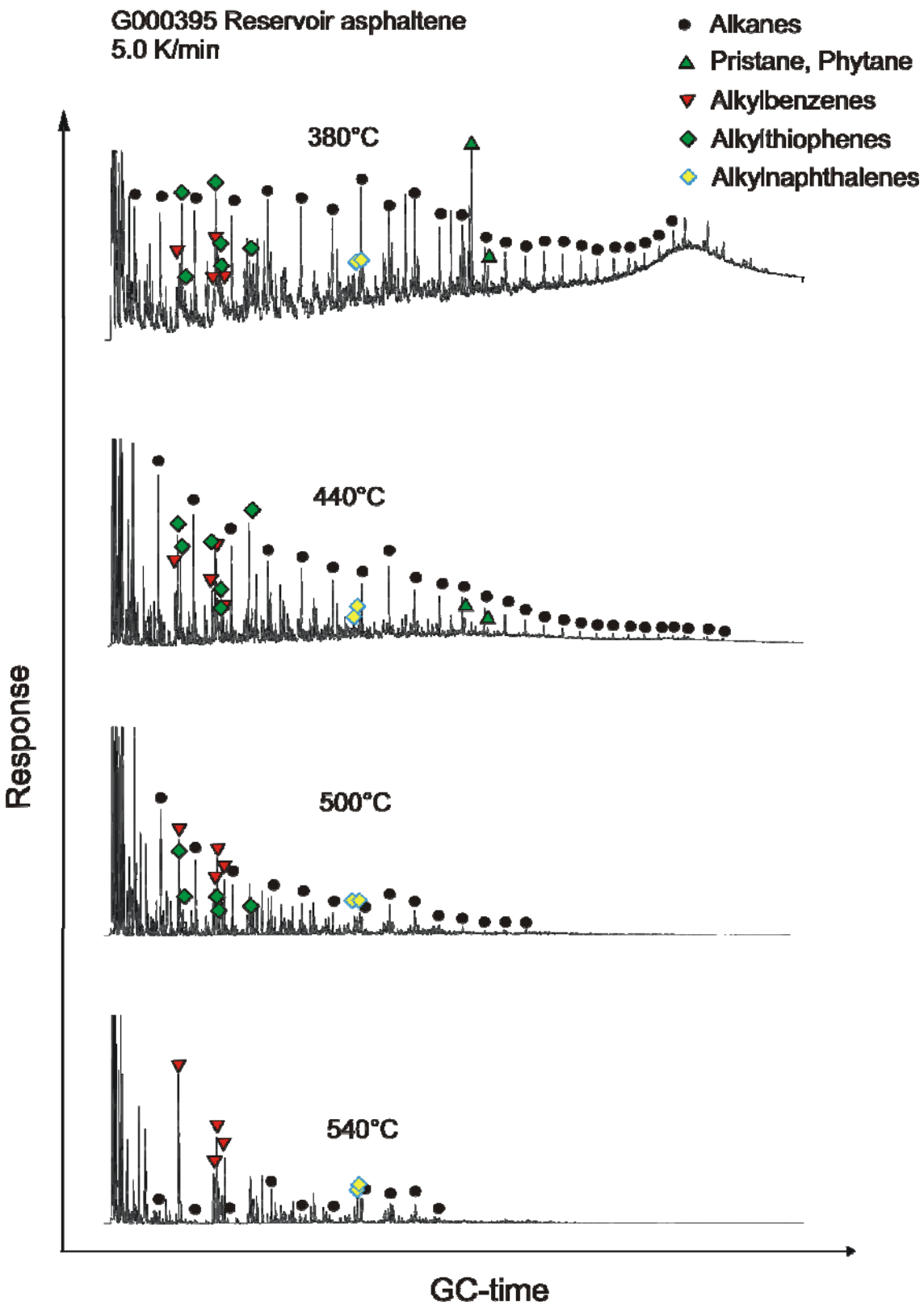

Fig 101 Selected chromatograms from MSSV pyrolysis GC of oil asphaltene sample G000395 using a heating-rate of 5.0 K/min. Alkanes, most abundant thiophenes, alkylnaphthalenes and alkylbenzenes are marked. Alkylbenzenes are corresponding to retention time from left to the right: toluene, ethylbenzene, m,p-xylene, and o-xylene. Alkylnaphthalenes are 2- and 1-methylnaphthalene. Alkylthiophenes are from left to right: 2-methylthiophene, 3-methylthiophene, 2,5-dimethylthiophene, 2,4-dimethylthiophene, 2,3-dimethylthiophene, and ethylmethylthiophene.

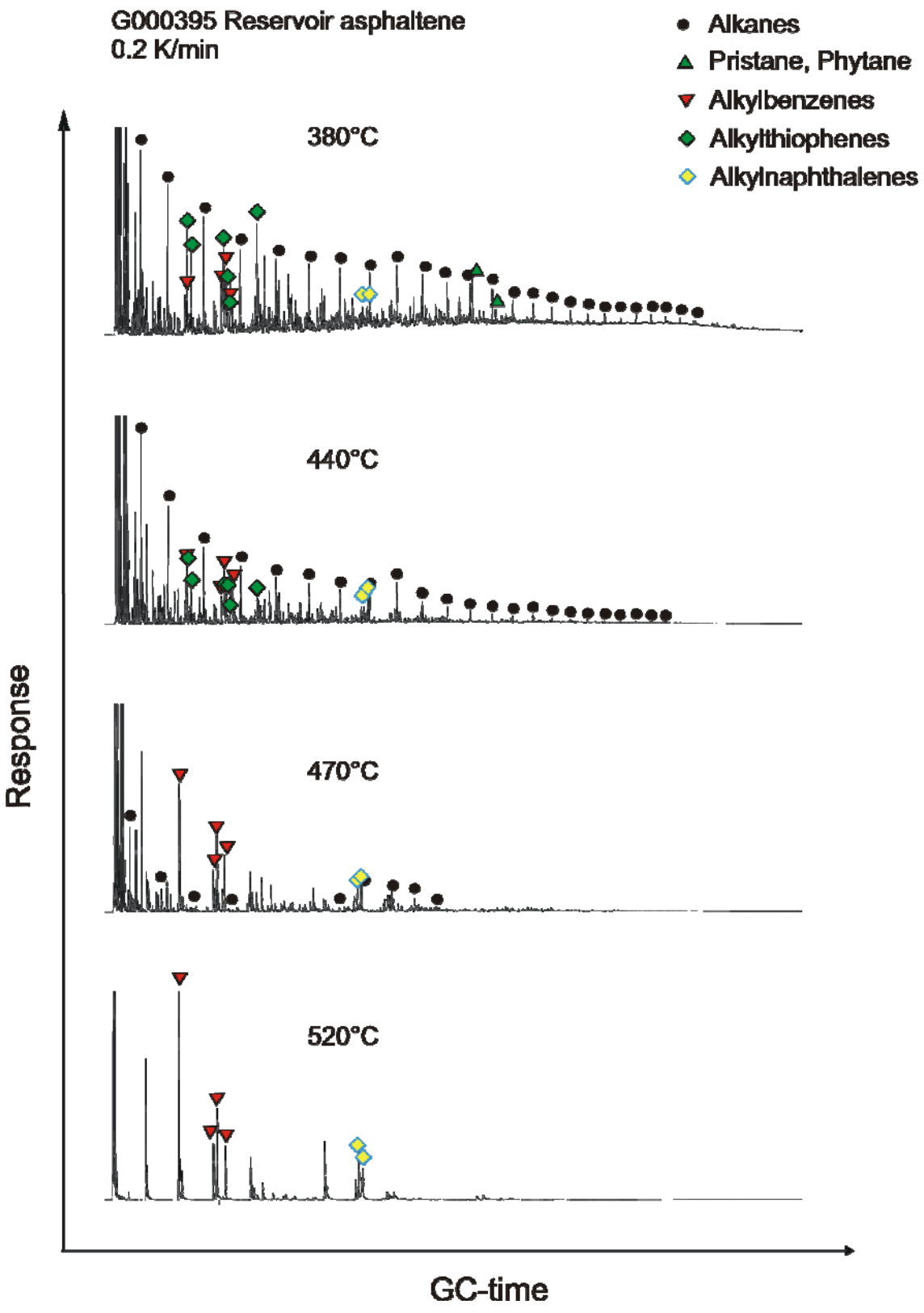

Fig 102 Selected chromatograms from MSSV pyrolysis GC of oil asphaltene sample G000395 using a heating-rate of 5.0 K/min. Alkanes, most abundant thiophenes, alkylnaphthalenes and alkylbenzenes are marked. Alkylbenzenes are corresponding to retention time from left to the right: toluene, ethylbenzene, m,p-xylene, and o-xylene. Alkylnaphthalenes are 2- and 1-methylnaphthalene. Alkylthiophenes are from left to right: 2-methylthiophene, 3-methylthiophene, 2,5-dimethylthiophene, 2,4-dimethylthiophene, 2,3-dimethylthiophene, and ethylmethylthiophene.

Fig 103 presents the diagrams with the concentrations of hydrocarbon fractions (C_{1-5}, C_{6-14}, C_{15+}, C_{total}, and methane) in asphaltene MSSV pyrolysates for the different heating rates. It is obvious that the generation of hydrocarbons starts between 310°C (0.2 K/min) and 370°C (5.0K/min). Peak hydrocarbon formation (max. of C_{total}) is obtained at 475°C for a heating-rate of 5.0K/min, and at 420°C for 0.2K/min. For all heating-rates the hydrocarbon generation starts with the C_{6-14} and C_{15+} fractions. But maximum yields of the C_{15+} fraction are already achieved at relative low temperatures of 410°C (0.2 K/min) and 460°C (5.0K/min). The C_{6-14} fraction show maximum yields at slightly higher temperatures of 430°C (0.2 K/min) and 480°C (5.0K/min).

Dieckmann *et al.* (2000a) have shown that a significant heating rate dependency of maximum yields for different compound classes exists. On a molecular level the heating rate dependency can lead to the enrichment of *n*-alkanes with decreasing heating rate. This was in the present experiment only observed when comparing the hydrocarbon fractions from the fast heating-rate of 5.0K/min with those of the slower heating-rates. But between the heating-rates of 0.7K/min and 0.2K/min this characteristic was not monitored. The maximum yields of the compound classes are rather higher at a heating-rate of 0.7K/min than at 0.2K/min. At present we have no unequivocal explanation for this, but it is possible that the quantification of total yields of pyrolysates for 0.2K/min did not fit anymore to the measured internal butane standard due to a drop of the column quality.

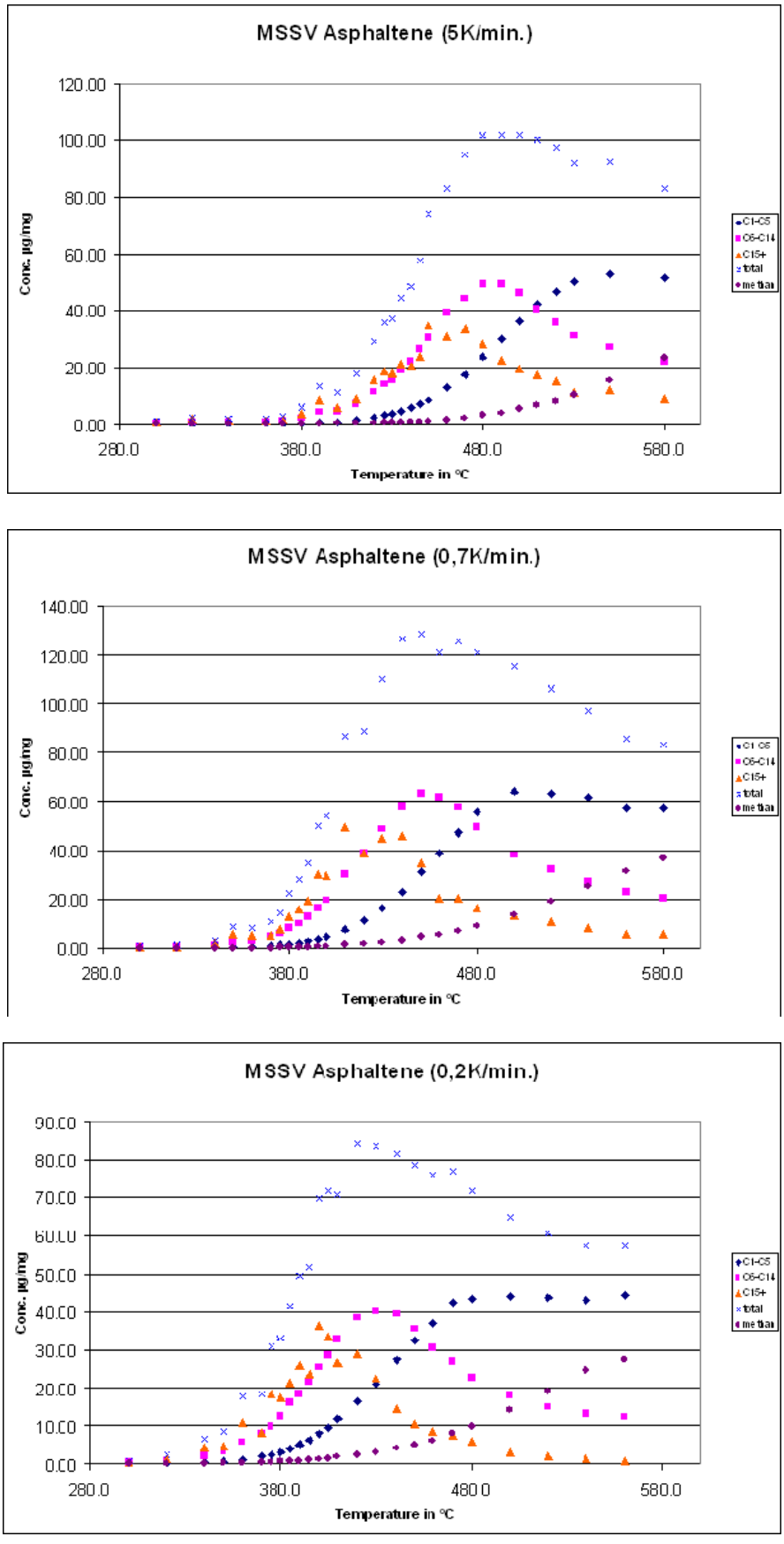

Fig 103 Diagrams showing the total concentrations of hydrocarbon fractions formed from the Italian asphaltene for the heating rates of 5.0K/min (top), 0.7K/min (middle), and 0.2K/min (bottom).

7.4.3 Gas formation

The primary formation of methane is associated with chemical reaction of macromolecular organic matter. The secondary gas formation can be calculated from measured formation rates using the method described by Dieckmann *et al.* (1998). The secondary gas formation originates from the degradation of high molecular weight hydrocarbons and thus can be identified in the generation curves as the point where the apex of the C_{6+} range is exceeded. For that reason secondary gas is predictable by subtraction the amount of generated C_{6+} hydrocarbons from the apex of C_{6+}. Because only 70% of cracked oil can be transformed to gas the calculated sum has to multiplicate with the stoichiometrical factor of 0.7. The formation of primary gas was calculated from the difference between the total gas ($C_{1\text{-}5tot.}$) and the previously evaluated secondary gas.

Gas formation takes place through primary cracking reactions at low temperatures of source rock kerogens or asphaltenes, and through secondary cracking of oil at high temperatures. It is suggested that primary reactions are based on reactions involving the cleavage of thermally unstable bonds, and on reactions based on demethylation of aromatic functional groups (Cramer, 2004). Secondary gas formation are related to defunctionalisation of cross-linked ring structures or cracking of long-chain hydrocarbons, as well as polymerisation and condensation reactions (Quigley and Mackenzie, 1988; Béhar *et al.*, 1991; Pepper and Dodd, 1995; Boreham *et al.*, 1998; Dieckmann *et al.*, 1998; Vandenbroucke *et al.*, 1999; Wendebourg, 2000; Payne and Ortoleva, 2001; Teinturier *et al.*, 2003; Cramer, 2004). The extent of aromatisation, demethylation, ring opening and defunctionalisation is proportional with MSSV temperature, i.e. with a specific maturity stage.

The formation of the C_1-C_5 fraction (whole gas), primary and the secondary gas formation for the different heating rates of the present study on oil asphaltene pyrolysates are presented in

Fig 104. The gas formation from primary cracking reactions shows explicit maximums in our laboratory experiments. The maximum yields of the primary gas fraction are achieved at temperature of 440°C (0.2 K/min) to 515°C (5.0K/min). In contrast, the gas generation curves from secondary cracking shown in Fig 104 are in or close to the plateau area. It may however be possible that methane formation is not finished at those temperatures. Krooss *et al.* (1995) have shown that methane formation for example from coal samples at 2 °C/min laboratory heating rates comes to an end at around 800 °C, while at 600 °C, which marks the temperature limit of routine closed system pyrolysis experiments, only the half of the potential methane is formed. Since we are investigating asphaltenes from a marine carbonate sequence, those high temperature proposed by Krooss *et al.* (1995) however, will not be expected.

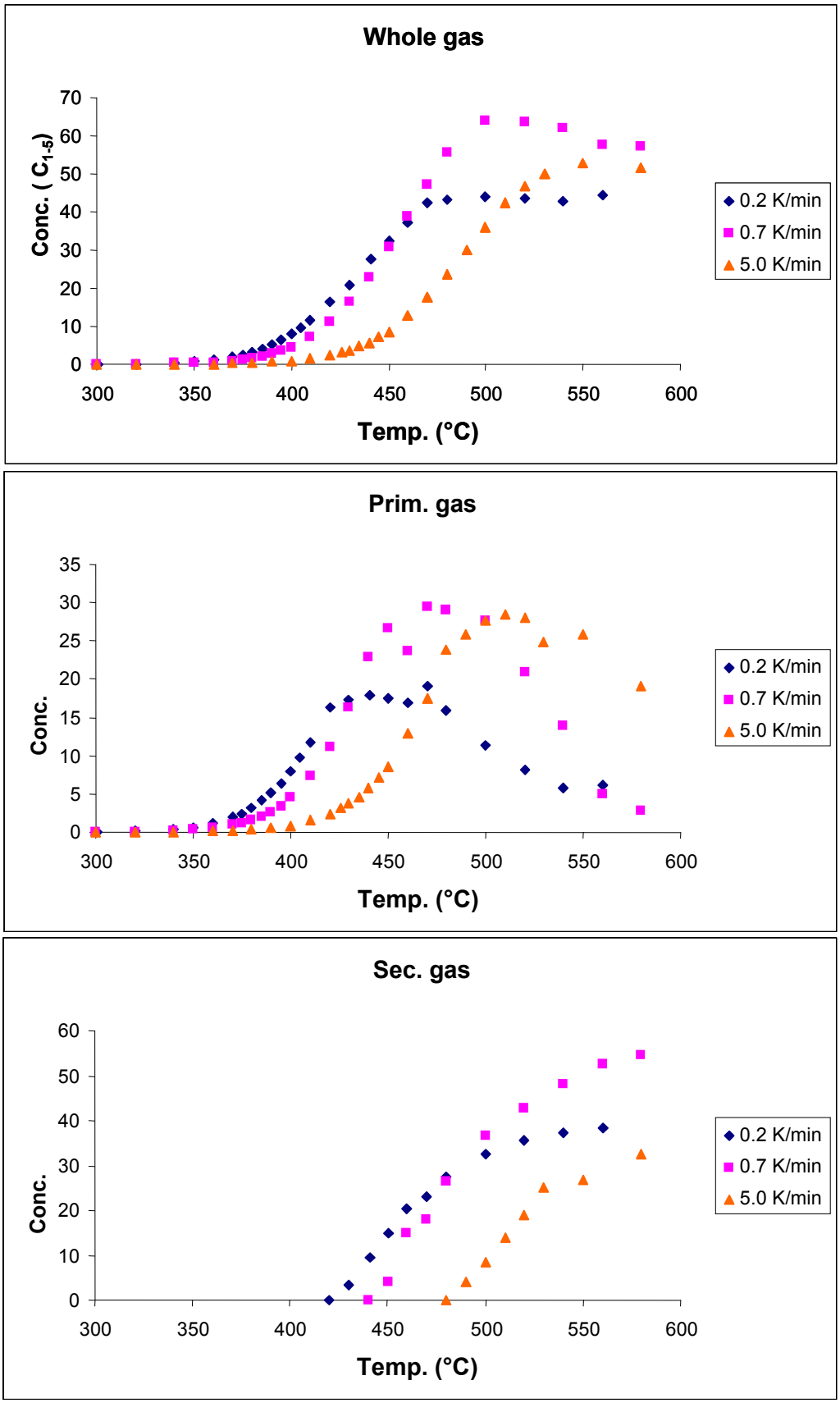

Fig 104 Diagrams showing the formation of the C_1-C_5 fraction (whole gas), primary and the secondary gas formation at specific laboratory temperatures for different heating rates.

7.4.4 Comparison of asphaltene MSSV pyrolysates with natural oils

As mentioned before do pyrolysates of closed-system pyrolysis show pristane and phytane at lower experimental temperatures (Eglinton *et al.*, 1988). Burnham (1989) has shown that the the Pristane Formation Index (PFI), the sum of pristane and pristene, is independent of formation temperature at constant precursor conversion for pyrolysis of several petroleum source rocks over a wide range of pressures and temperatures.

Fig 105 shows the diagram of the ratios of pr/*n*-C_{17} and ph/*n*-C_{18} after Peters *et al.* (1999) for oil asphaltene pyrolysates (0.7 K/min.) and natural oils from Southern Italy. Whereas crude oils predict the field of type II organic matter, the asphaltene pyrolysates plot mainly in the field of mixed organic matter type. As illustrated before in Fig 39 crude oils from Southern Italy do not show a trend of these pristane and phytane ratios with the API gravity. Oil asphaltene pyrolysates instead show a simulated maturity trend of decreasing pr/*n*-C_{17} and ph/*n*-C_{18} ratios with increasing thermal stress. The simulated maturity trend for asphaltene pyrolysates suggest that the ratio of pristane over phytane does not change within the low maturity stage, but in Fig 105 it is also obvious that with continuing maturation the ratio of pristane over phytane slightly increases and pyrolysates of higher temperatures shift to type III organic matter in this diagram. The same characteristic was reported by Tang and Stauffer (1995) for closed-system pyrolysates of Monterey kerogens. The authors mentioned that at higher maturity the decomposition of phytane may be slightly faster than of pristane. This assumption could as well explain the higher pr/*n*-C_{17} ratio for the mature crude oil sample G000401, which differs from the other oils by a higher pristane/phytane ratio. However, later on we will see that asphaltene MSSV pyrolysates from Duvernay and Nigeria do not show the same characteristic. The observed slight pristane over phytane dominance at high thermal stress might therefore be only characteristic for sulphur-rich petroleum systems, like Monterey or Southern Italy.

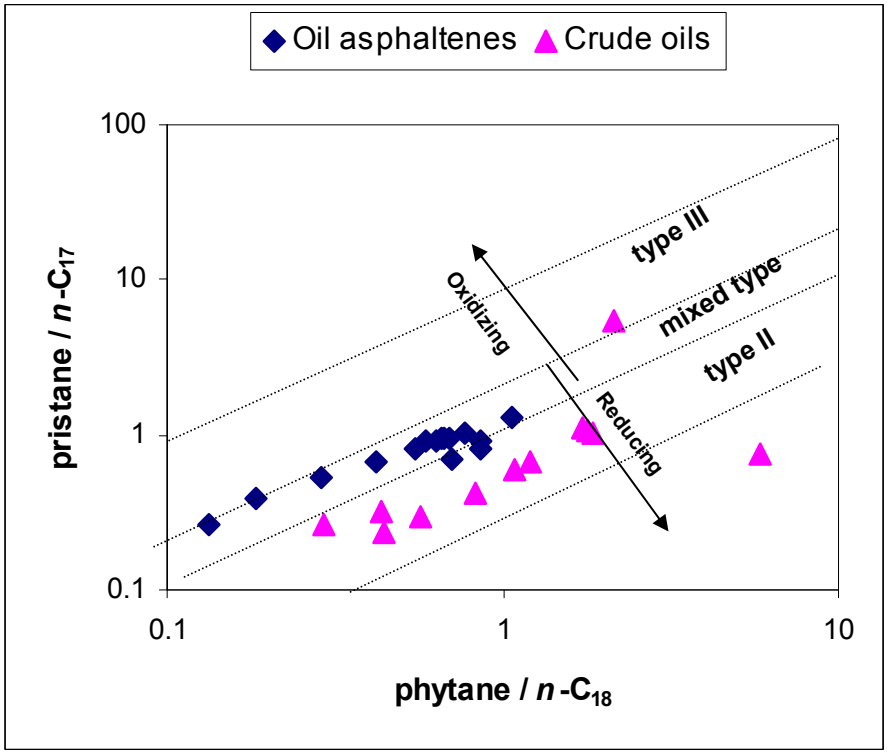

Fig 105 Diagram with the ratios of pristane/*n*-C_{17} versus phytane/*n*-C_{18} for MSSV asphaltene pyrolysates in comparison to natural oils from Southern Italy (after Peters *et al.* , 1999).

7.4.5 Comparison of MSSV pyrolysates of oil asphaltenes and kerogens

By comparing generated hydrocarbons from reservoir asphaltenes and kerogens there were some differences in terms of structural moieties, such as aromaticity, sulphur content and gas generation recognized. The data on MSSV pyrolysates formed from an immature source rock kerogen (G000652) of the same sample set from Southern-Italy are obtained from Fuhrmann (2005).

7.4.5.1 Aromaticity and organic sulphur content

Fig 106 shows the ratio of aromatic compounds and *n*- C_{6+} alkanes versus the MSSV-temperature, representative for a specific maturity stage. The single points in this figure correspond to the composition of artificially generated products at a specific MSSV temperature. It is obvious that the aromaticity of artificial formed products from the kerogen show stronger heating-rate dependency, whereas the aromaticity of asphaltene products does not vary much within the different heating rates.

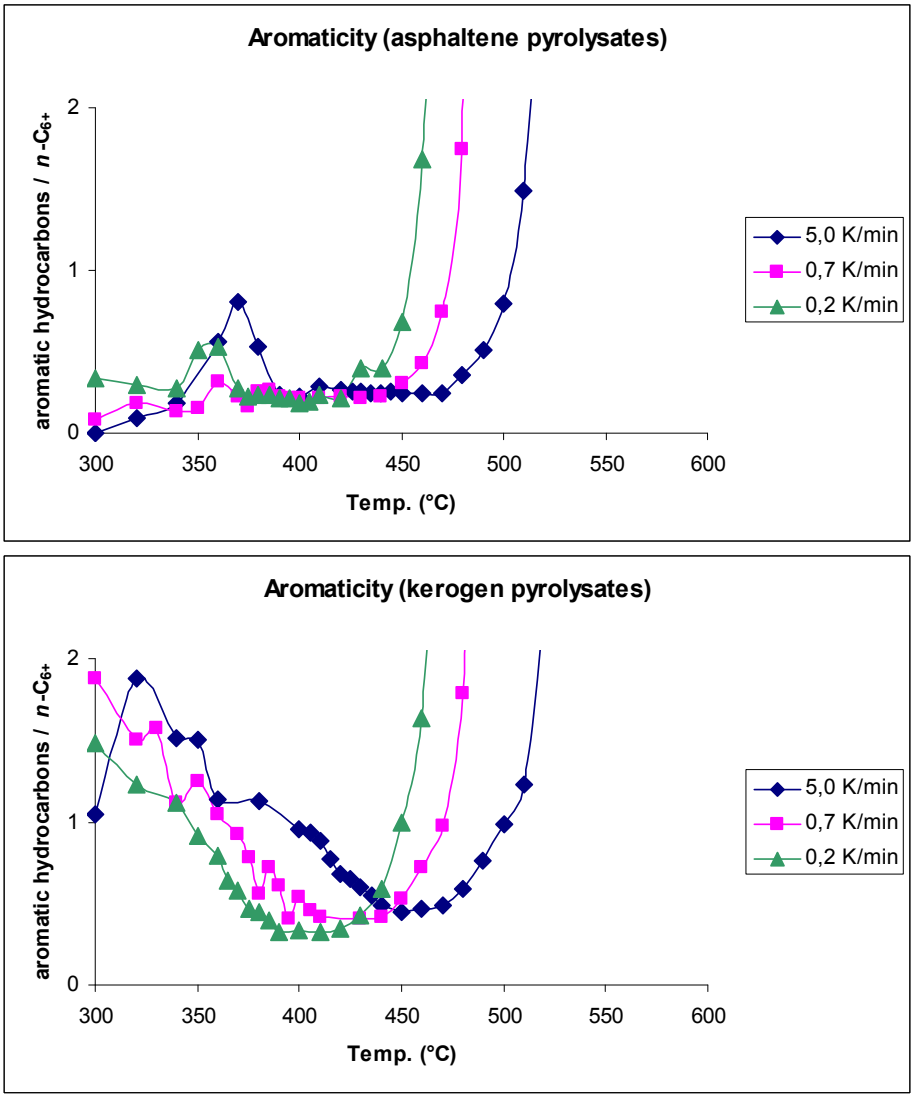

Fig 106 The aromaticity as ratio of aromatic compounds and *n*-C_{6+} alkanes calculated from asphaltene and source rock pyrolysates.

When comparing both diagrams, it is evident that the products generated from the oil asphaltene differ from those generated from the kerogen at a similar temperature stage, with higher aromaticity for kerogen products than for formed products from the petroleum asphaltenes. As well, the aromaticity of kerogen products changes successive within the MSSV-temperature range, and asphaltene products display a more or less constant aromaticity until the temperature where alkane generation decreases. At these temperatures the aromaticity of MSSV products considerably increases, which happens at slightly lower temperatures for asphaltene products than for kerogen products. This is also confirmed when taking a look at specific produced compounds at high MSSV temperatures. At 580 – 600°C kerogen products show still the presence of *n*-hexane and *n*-heptane. In comparison the same compounds are already absent in asphaltene products at 520°C (0.2K/min) and 550°C (5.0K/min.). It is remarkable that products formed at low temperatures from kerogens have 20 times higher aromaticity than those formed from asphaltenes. Products from asphaltenes show a high peak of aromaticity in the low temperature range between 355°C (0.2K/min) and 375°C (5.0K/min), which is not observed for kerogen products, because aromaticity is extremely high anyway in kerogens products at low temperatures. The sudden increase in the aromaticity for asphaltene products between 350 – 380 °C is referred to a strong release of toluene and o-xylene at these temperatures, indicating thermal cracking of specific precursor molecules.

As mentioned before low-molecular-weight alkylthiophenes are present in MSSV products but absent in natural products. Because MSSV products from both organic matter types show major differences in terms of content and distribution of thiophenes it is of interest to take a

more detailed look at it. Fig 107 shows the ternary diagram of 2,3-dimethylthiophene, o-xylene, and *n*-C_9 for asphaltenes (left) and kerogen MSSV products (right) (after Eglinton *et al.* (1990). Single MSSV products of specific temperatures plot along the sketched lines for corresponding heating rate. Kerogen products show a clear heating-rate dependency for the generation of 2,3-dimethylthiophene, with higher amounts of 2,3-dimethylthiophene for faster heating rates. Bearing in mind that crude oils are generated during geological heating-rates, this observation underlines the suggestion of Sinninghe Damsté *et al.* (1990), that low-molecular-weight alkylthiophenes in natural systems are released as long-chain thiophenes due to lower temperatures and longer reaction times. As well, it is obvious in Fig 107 that asphaltene products do not predict the generation of type II-S in this diagram. Moreover, asphaltene products predict the generation of type I or type II organic matter. Kerogen products instead plot in the zone, which defines type II-S (high heating-rate) or type II (low heating-rate) reflecting the sulphur-rich nature of investigated samples from this petroleum system. At temperatures where aromatization is getting more dominant (high temperatures) the products of both types predict increasingly the field of type III.

Additionally, asphaltene products and their kerogen counterparts differ very strong in terms of heating-rate dependency and the generation of *n*-nonane. While the generation of *n*-C_9 and alkylthiophenes from the oil asphaltene ends at the same temperatures, the generation of *n*-nonane from kerogens is ended at temperatures between 460 – 500°C, where the generation of sulphur compound still continues. Furthermore, from Fig 107 it is obvious that the conventional plot after Eglinton *et al*. (1990b) is not reliable for predictions of products formed from asphaltenes.

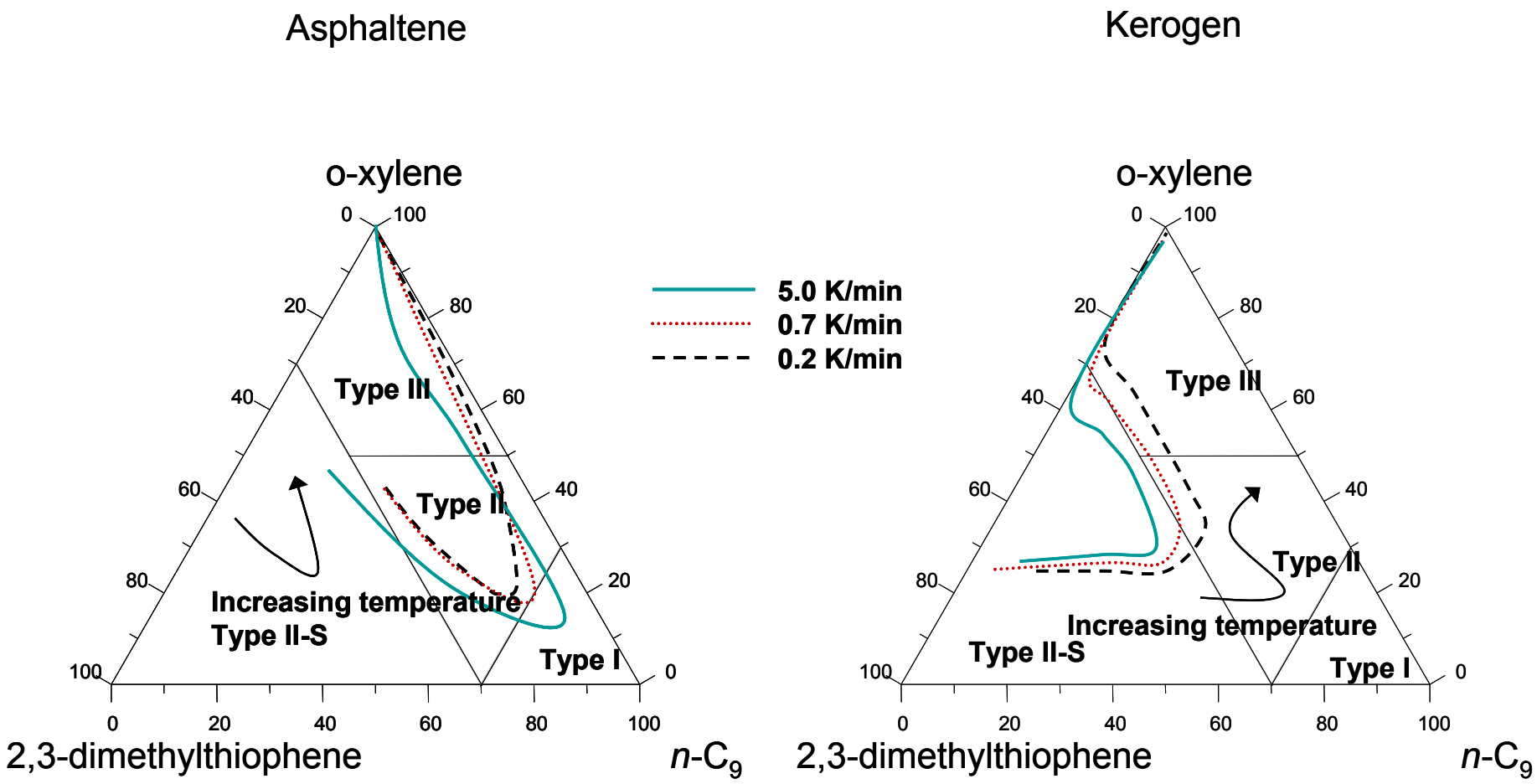

Fig 107 Ternary diagram of 2,3-dimethylthiophene, o-xylene, and *n*-C_9 for asphaltene (left) and kerogen MSSV pyrolysates (right) (after Eglinton *et al.* (1990b)).

7.4.5.2 Alkyl-chain length distribution and gas formation

Fig 108 presents the ternary diagrams for the alky-chain distribution at different heating rates for MSSV pyrolysates of oil asphaltene (top) and kerogen (bottom). It is observed that with increasing heating rate the generated hydrocarbons from the oil asphaltene show higher contents of the C_6-C_{14} and the C_{15+} *n*-alky-chains. With low heating rate of 0.2K/min the maximum yield of C_6-C_{14} fraction is reached at 28%. In comparison with a high heating rate of 5.0K/min the maximum yield plot at 36%. These heating-rate dependencies of yields of alkanes, aromatics and NSO compounds have already described in previous works (Juntgen and Klein, 1975; Stout *et al.*, 1976; Burnham and Happe, 1984; Schaefer *et al.*, 1990; Michels *et al.*, 1995; Horsfield, 1997; Dieckmann *et al.*, 2000a; Michels *et al.*, 2002; Dieckmann *et al.*, 2004). Horsfield (1997) illustrated that *n*-alkanes, aromatics and alkylated thiophenes generated from a Posidonia Shale kerogen show pronounced systematic variations in maximum yields at different rates of heating. The generated hydrocarbons from the sulphur-rich kerogen from Southern Italy do not demonstrate such strong heating-rate dependency like shown for pyrolysates of the oil asphaltene. The alkyl-chain distributions for the kerogen MSSV pyrolysates show only a very slight increasing of the C_6-C_{14} and the C_{15+} *n*-alky-chain contents with faster heating-rate.

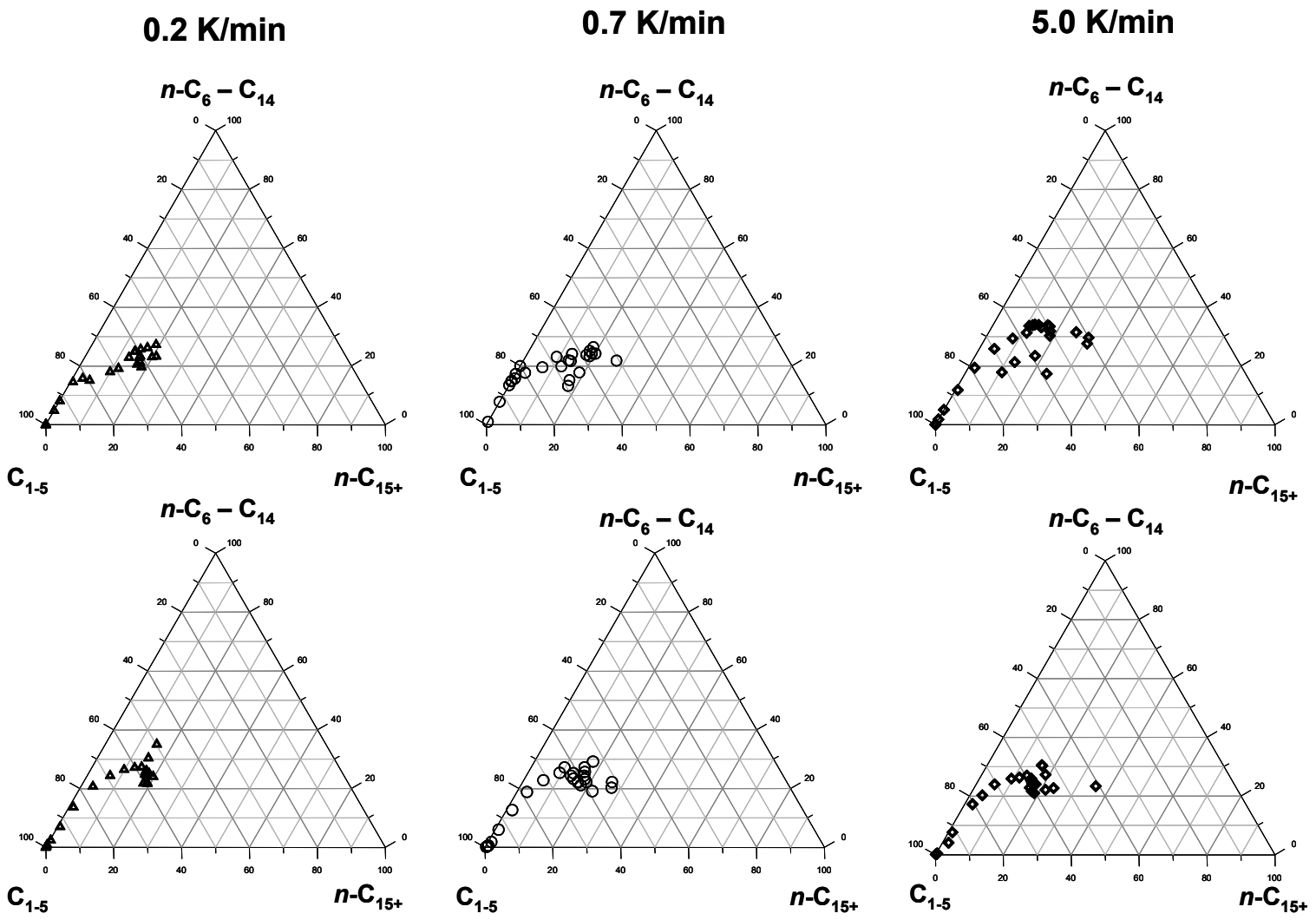

Fig 108 Ternary diagrams of the alky-chain distribution at different heating rates for MSSV pyrolysates of oil asphaltene (top) and kerogen (bottom).

Fig 109 shows that the GOR´s of MSSV pyrolysates of oil asphaltenes and kerogens are different. Pyrolysates of kerogens show higher GOR´s than pyrolysates of asphaltenes. The divergence between the GOR of pyrolysates from both organic matter types increases with increasing maturation temperature and may be an indication of the generally lower gas potential in the asphaltene structures, or even different gas precursor molecules in the asphaltenes relative to the kerogens.

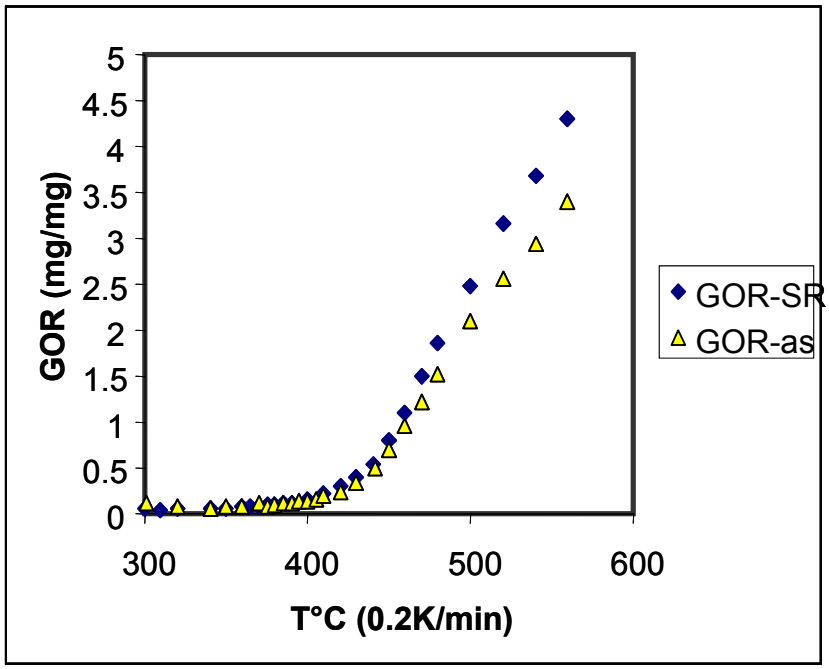

Fig 109 GOR of MSSV pyrolysates of the oil asphaltene and the of the kerogen sample at a heating rate of 0.2K/min

7.4.5.3 Carbon isotopic composition

In order to investigate the difference in gas generation we studied the isotopic composition of methane, ethane and propane formed from the kerogen sample G000652, the related bitumen asphaltene, and from the reservoir asphaltene G000395 by GC-IRMS.

Gas chromatography–isotope ratio mass spectrometry (GC–IRMS) has been widely applied in the various fields of organic geochemistry, e.g. identifying organic source (Freeman *et al.*, 1990; Bjorøy *et al.*, 1991; Rieley *et al.*, 1991; Collister *et al.*, 1994; Odden *et al.*, 2002), correlating oil with possible source rocks (Bjorøy *et al.*, 1994; Chung *et al.*, 1994; Mycke *et al.*, 1994; Rooney *et al.*, 1998; Xiong and Geng, 2000), and reconstructing palaeoenvironment and palaeoclimate (Ruble *et al.*, 1994; Schoell *et al.*, 1994; Kenig *et al.*, 1995). Useful information on $\delta^{13}C$ values of *n*-alkanes has been previously presented by Wilhelms *et al.* (1994), who compared the isotopic composition of *n*-alkanes and isoprenoids alkanes in oils and associated asphaltene pyrolysates derived from different types of source rocks.

Fig 110 displays the carbon isotopic compositions of individual *n*-alkanes from *n*-C_1 to *n*-C_3 for products formed from reservoir and source rock asphaltenes, and related kerogens.

The $\delta^{13}C$ values of methane for products formed from source rock kerogens range from -44 up to -42‰ for temperature between 360 – 440°C. The carbon isotopic composition of methane formed from source rock asphaltene is similar for the same temperature range. In contrast, methane formed from petroleum asphaltenes shows $\delta^{13}C$ values from -47 to -45‰ for temperatures between 360 – 440°C, indicating a lighter isotopic composition of the methane generated. The same systematic is observed for the generation of ethane and propane from the different organic matter types. The isotopic composition of gas formed from petroleum asphaltenes is lighter for the whole gas range, whereas products formed from source rock asphaltenes show heaviest carbon isotope composition.

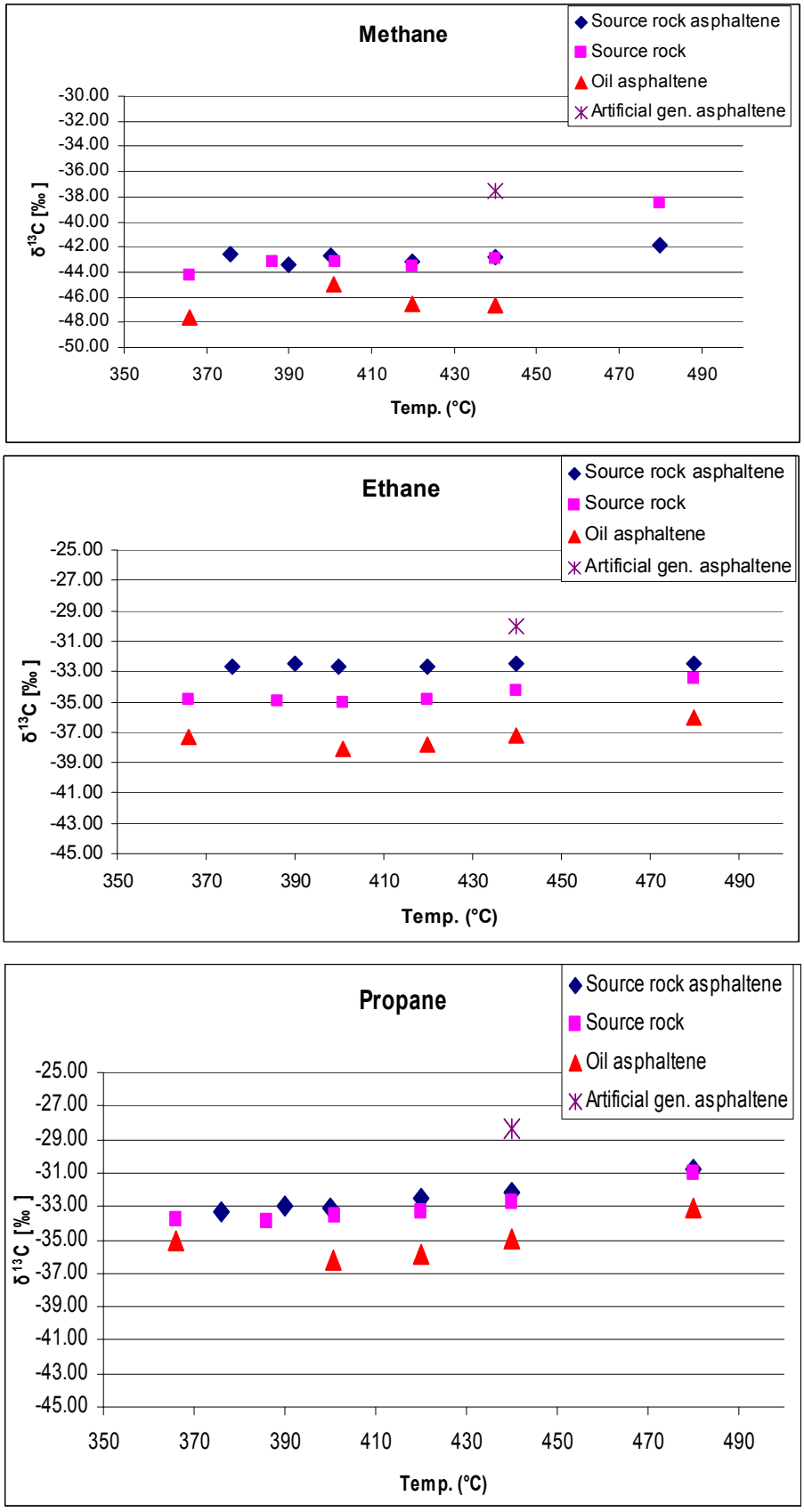

Fig 110 Carbon isotopic composition $\delta^{13}C$ [‰] for the gas fraction of products formed from source rock kerogen, source rock asphaltene, and oil asphaltene, as well as for an artificial generated asphaltene.

The explanation for this discrepancies in $\delta^{13}C$ values for asphaltenes and kerogens may be increasing maturity or phase fractionation, which all may result in isotopically heavier components in organic matter (Galimov, 1974; Bjorøy *et al.*, 1990; Bjorøy *et al.*, 1991; Bjorøy *et al.*, 1994; Mycke *et al.*, 1994; Rooney *et al.*, 1998; Odden *et al.*, 2002). This is of course expected from the models of isotope fractionation, where the lightest products are released first in the maturation process. Although increasing maturity usually leads to isotopically heavy products, the isotopic shift is generally very small (Clayton, 1991; Bjorøy *et al.*, 1992; Chung *et al.*, 1994; Collister *et al.*, 1994; Xiong and Geng, 2000; Odden *et al.*, 2002), and do not excite 2‰ (Chung and Sackett, 1979). Therefore, the different $\delta^{13}C$ values between oil asphaltenes and kerogens in our study cannot be explained by maturity alone. As well the differences in isotope composition between source rock asphaltenes and kerogens are not related to maturity, since both underwent parallel thermal history. Odden *et al.* (2002) investigated isotopic compositions of asphaltenes from different oil fields in the Northern Sea, and showed that the isotope composition varies with terrestrially influenced facies. Previous works suggested that differences in isotopic values can also be referred to organic inhomogenities (Bjorøy *et al.*, 1994; Chung *et al.*, 1994; Rooney *et al.*, 1998). At least the difference in terms of isotopic composition for gas formed from both types of asphaltenes and kerogens can only be explained by different precursor molecules of gas within the different organic matter types. This indicates different gas formation processes and probably different precursor molecules in petroleum and source rock asphaltenes. However, main difference in isotopic composition of formed gas is related between petroleum asphaltenes and source rock kerogens or source rock asphaltenes respectively. This of course hampers the use of isotopic composition of gas formed from petroleum asphaltenes for identifying source rock environment, or oil – source correlation for the present type II-S petroleum system.

In Fig 110 there is also the carbon isotopic composition for an artificial generated asphaltene plotted. A major difficulty in using artificial maturation experiments is that the temperatures and heating-rates usually applied are much higher than those in sedimentary basins. Cracking reaction rates are kinetically controlled (Landais *et al.*, 1994; Horsfield, 1997) consequently, data generated under laboratory conditions cannot be compared directly to natural data. But in our study we wanted to investigate to what extent artificial formed asphaltenes differ to natural formed counterparts. Therefore, we sealed in total ca. 30g of pure extracted source rock sample (G000652) in different small glass tubes, each with max. 5 g of pulverized sample. The sealed glass tubes were heated up to 400°C with a heating rate of 5.0 K/min to simulate peak hydrocarbon generation. After that, generated bitumen was extracted and asphaltenes were isolated and investigated by Py-GC and GC–IRMS in the same way described for source rock and oil asphaltenes.

Methane formed from the artificial generated asphaltene is with a $\delta^{13}C$ value of -37.5‰ for 440°C much heavier than methane formed from natural asphaltenes or kerogen. The same systematic is observed for the generation of ethane and propane from the artificial generated asphaltene, which shows higher $\delta^{13}C$ values than products formed from natural formed asphaltenes and kerogens as well. This of course indicates that oil-source rock correlation using artificial formed asphaltenes from laboratory experiments may lead to misinterpretations.

7.4.6 MSSV compositional kinetics

7.4.6.1 Kinetic parameters

Kinetic parameters were calculated for the generation of primary gas, secondary gas and the oil like C_{6+} compounds formed from petroleum asphaltenes and source rocks at different heating rates. Primary and secondary gas was calculated following the method reported by Dieckmann *et al.* (1998; 2000b). At this the formation of secondary gas results from the decrease of the C_{6+} curve at high temperatures.

Fig 111 compares the resulting kinetic parameters calculated for the petroleum asphaltenes and the source rock sample. The primary formation of gas and the formation of oil from the asphaltene show and Emean of 52kcal/mol with a frequency factor of 6.3E+13 s^{-1} and 1.35E+14 s^{-1}, respectively. The frequency factor for the generation of secondary gas is slightly higher with 7.7E+14 s^{-1}. In addition the Emean is much higher than those calculated for the primary reaction with 62kcal/mol. The kinetic parameters evaluated for the formation of relevant fractions from the source rock show a broader range of variations. The broader variation of kinetic parameters calculated for the different petroleum fraction is in good correspondence to characteristics observed for the bulk kinetic parameters. The formation of primary gas is controlled by an Emean of 50Kcal/mol and a frequency factor of 2.93E+12 s^{-1}. The formation of secondary gas resulted in kinetic parameters which are slightly higher than those evaluated on secondary gas formation from asphaltenes with an Emean of 66kcal/mol and a frequency factor of1E+16 s^{-1}. Last but not least kinetic calculated for the generation of C_{6+} compounds from the source rock are very similar to those calculated for C_{6+} formation from the petroleum asphaltenes with an Emean of 57 kcal/mol and a frequency factor of 4.67E+15 s^{-1}.

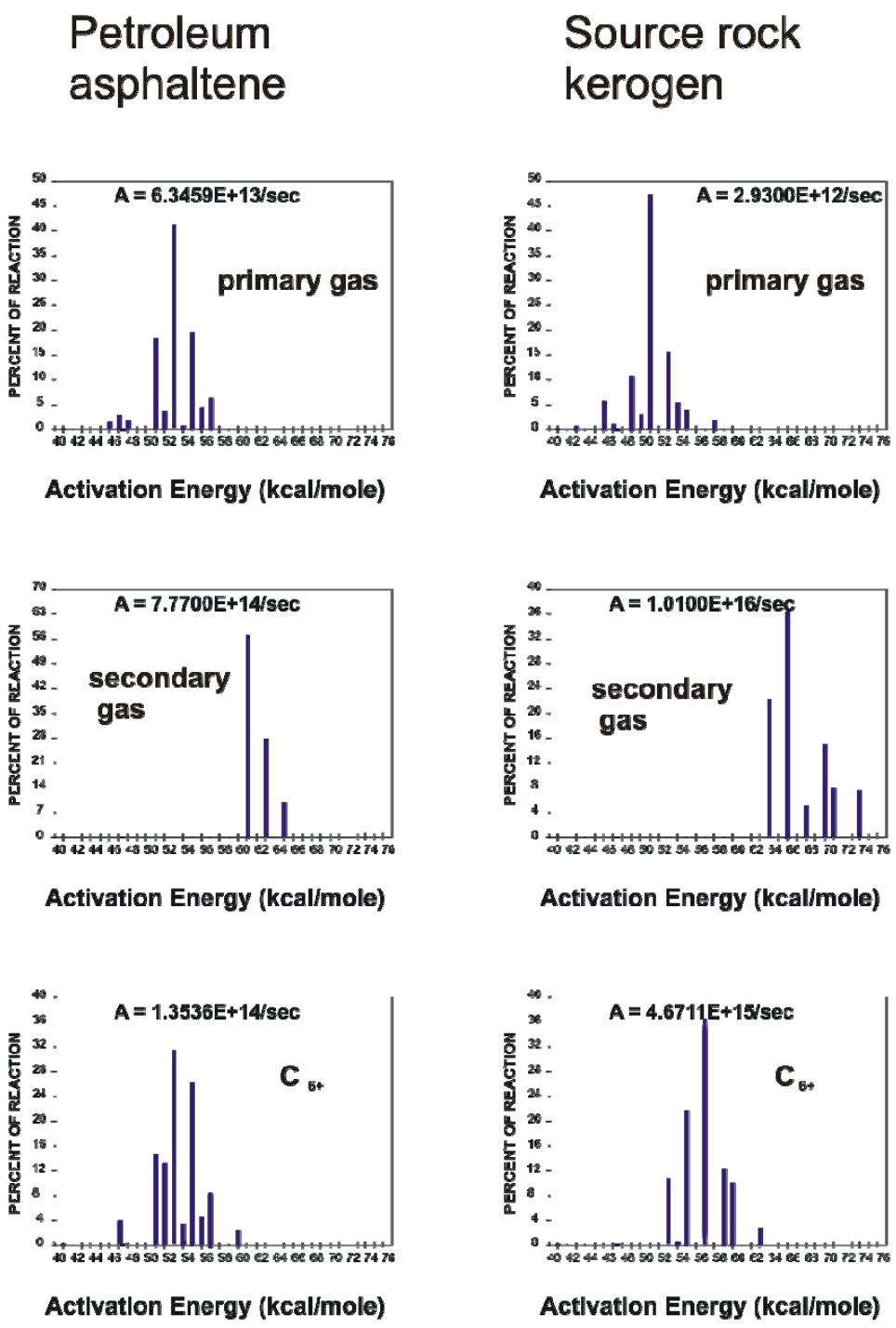

Fig 111 Kinetic parameters calculated for the petroleum asphaltene and the source rock sample from Southern Italy.

7.4.6.2 Geological predictions of oil and gas formation

Fig 112 compares the prediction of primary gas, secondary gas and C_{6+} formation from the Italian asphaltene and the source rock samples under geological heating conditions of 3.3K/my. Although we have observed some differences in the kinetic parameters for the different petroleum fractions, there are strong similarities under geological conditions. The formation of C_{6+} oil like compounds starts at around 100°C for both source type and comes to its end at around 180°C. Slight, but insignificant differences can be seen at Tmax temperatures with $Tmax_{geol}$ 140°C for the asphaltenes and 150°C for the source rock products respectively.

The timing of primary gas formation for the source rock kerogen and the oil asphaltene are nearly identical and cover a temperature range from 100 to 180°C (Tmax 145°C) when predicted to a geological heating rate of 3.3K/my.

The formation of secondary gas from the source rock MSSV pyrolysates and the asphaltene MSSV pyrolysates show some differences. Secondary gas formation from the source rock covers a much broader temperature range under geological conditions (170-280°C) than secondary gas formation from the asphaltene products (170-240°C). However, it is remarkable that both the onsets as well as the Tmaxgeol are very similar.

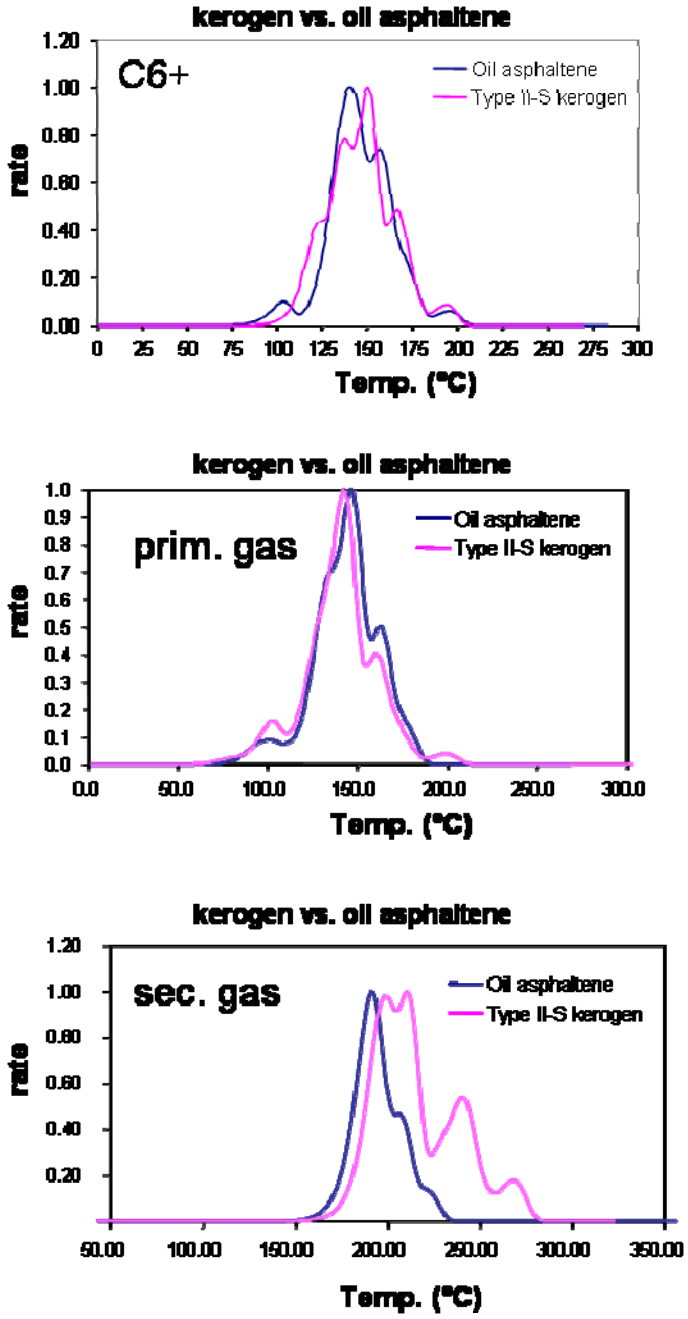

Fig 112 The prediction of primary gas, secondary gas and C_{6+} formation from the asphaltene and the source rock samples under geological heating conditions of 3.3K/my.

7.4.6.3 Molecular compositional C_{6+} kinetics

In the present chapter we have illustrated that products formed from petroleum asphaltenes may bridge the gap between products formed from source rock kerogen and those found in nature, since the aromaticity as well as the amount of sulphur containing compounds formed from asphaltenes were much closer to compositional characteristics found in natural oils than in kerogen MSSV pyrolysates.

For that reason we transformed the compositional information from artificial maturation experiments on petroleum asphaltenes into compositional kinetic model for C_{6+} formation.

In order to do so following procedure was applied

1. The individual laboratory temperature range of the individual activation energy potentials in the activation energy distribution was evaluated.
    a. E.g. 48Kcal/mol and A = 1.535E+14 correspond to reactions which take place between 310 and 340°C under laboratory conditions at 0.2K/min.
    b. This type of reconstruction was performed for all the different potentials individually.
2. MSSV compositions are measured cumulative, but activation energies represent the instantaneous reactions. For that reason MSSV compositional information must be transformed into instantaneous compositional information. For step one, we know the temperature range covered by each individual potential. Picking now the onset as well as the end temperature of each individual temperature range from the MSSV generation curves is used to define the percentage of the potentials responsible for the formation of specific fractions. Here, the quantitative differences of individual petroleum fraction were calculated from composition formed at the onset and the end

temperature of the individual temperature ranges, which finally gives the instantaneous compositional characteristics formed by the individual activation energy potentials.

3. For our compositional characterization we used the *n*-C_{6-14}, *n*- C_{15+}, aromatics and the sum of NSO compounds (e.g. alkylthiophenes, phenols etc.), based on the assumption that resolved compounds characterize natural petroleum composition (Horsfield, 1989, 1997).

The resulting compositional kinetic set is illustrated in Fig 113. The outcoming result predict an oil rich in NSO compounds and aromatic hydrocarbons, which reflects the characteristics of the natural, non-degraded crude oils from Southern Italy.

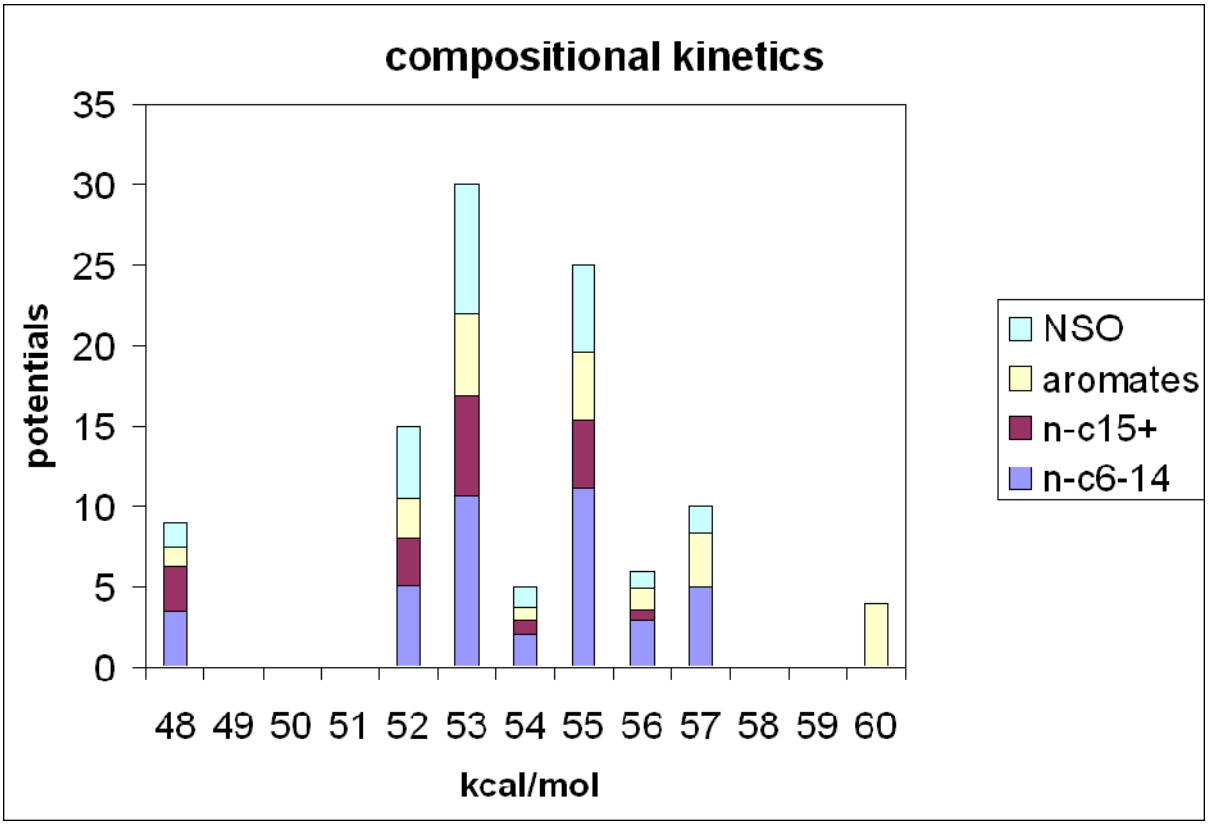

Fig 113 The resulting compositional kinetic set for the MSSV-analysis of the Italian reservoir asphaltene.

7.4.6.4 Discussion on the geological prediction for Southern Italy

Previous studies have shown that the formation of single compounds or hydrocarbon fractions from Italian source rock kerogen show heating rate dependency. It was also mentioned that this heating rate dependence may explain the compositional differences between closed system pyrolysis products and natural oils with petroleum formed using fast heating rates formed high amounts of aromatics, alkylated thiophenes etc. which cannot be found in natural products formed under geological heating conditions. For that reason we concluded that the application of the conventional kinetic models on compound fraction generation from laboratory experiments must result in geological predictions which are not valid.

Heavy oils, found, for example in the Monterey Petroleum System in the United States, Venezuela and Southern Italy (Powell, 1984; Zumberge, 1984; Baskin and Peters, 1992; Mattavelli *et al.*, 1993; Reynolds *et al.*, 1995; di Primio and Horsfield, 1996) are considered to be the products of early petroleum generation of oil-prone, sulphur-rich kerogens (Gransch and Posthuma, 1974; Orr, 1986). The alkyl chain length distribution of kerogen and asphaltene pyrolysates indicate the generation of low-wax mixed-base crude oils in nature. This discrepancy between oil prediction and naturally occurring heavy oils is generally explained in that thermally labile polysulphide bridges rupture very easily to produce low API gravity asphaltene-rich petroleum (Orr, 1986). As well for closed-system pyrolysis the molecular composition of these oils differs from that of pyrolysates, since major proportions of high molecular weight compounds of aromatic/asphaltic oils are thermally involatile and thus cracked to secondary products during MSSV pyrolysis (Horsfield, 1997). Therefore, the compositional kinetic model shows probably an underestimation of NSO contents at lower activation energies.

Another discrepancy between oil prediction using sulphur-rich kerogens or asphaltenes and naturally occurring heavy oils is based on the fact that most natural heavy oils from Southern

Italy are strongly, or at best initially biodegraded, leading to additional differences in the molecular composition of pyrolysates and natural oils. An overprint of biodegradation cannot be predicted by simulated oil generation using pyrolysis methods.

7.4.7 Conclusions

- Detailed compositional information from non-isothermal MSSV pyrolysis clearly showed that hydrocarbons formed from the Italian oil asphaltenes show lower aromaticity than hydrocarbons formed from source rock kerogen do. As well show these hydrocarbons lower content of organic sulphur than those formed from kerogens, which is closer to the composition of natural formed products.
- Compositional kinetics support the oil prone character of the petroleum asphaltenes from Italy: C_{6+} oil like kinetics and geological predictions are nearly identical when comparing oil formed from petroleum asphaltenes with that formed from the kerogen.
- Primary gas and secondary gas kinetics for Southern Italy evaluated on petroleum asphaltene MSSV pyrolysates result in similar geological prediction as gas formation from the source rock kerogen. However, the GOR of product formed from the asphaltenes is much lower than that formed from the kerogen.
- The simulation experiments using MSSV pyrolysis illustrated that compositional features of hydrocarbons formed from asphaltenes are very similar to compositional feature found for natural petroleum. This was especially the case of n-C_{6-14}, *n*-C_{6+}, aromatic compounds and NSO like compounds. For that reason a compositional kinetic model for C_{6+} formation was build up for the asphaltenes

from the Italian Petroleum System. This model reflects the major characteristics of non-degraded oils formed in this area.

- Carbon isotopic composition for gas generation from closed-system experiments show higher $\delta^{13}C$ values for gas formed from source rock asphaltenes and kerogens than for gas formed from petroleum asphaltenes, which hampers the use of isotopic composition of gas formed from petroleum asphaltenes for identifying source rock environment, or oil – source correlation for the present type II-S petroleum system.

8 Characterization of asphaltenes from a type II sequence

8.1 Bulk kinetic parameters

In order to compare asphaltene kinetics from type II-S with bulk kinetics from asphaltenes from a type II, pure marine sequence, we compared asphaltenes from reservoir oils with those of source rock bitumen as well as related source rock kerogens from the Duvernay Formation of the Western Canada Sedimentary Basin (WCSB).

Dieckmann *et al.* (2002) applied bulk kinetic concepts on oils formed from marine carbonate source rocks and illustrated that due to the lean organic content of the source rock, asphaltenes were degraded prior to expulsion. Such stabilisation was supported by previous results from Khavari-Khorasani *et al.* (1998) who studied kinetics on asphaltenes which precipitated along a migration route and which was originally generated in carbonate source rocks as well. Most recently Skeie *et al.* (2004) have applied asphaltene kinetics precipitated from type II marine oil on an exploration area, in order to represent the oil generating facies of the heterogeneous Draupne Formation. Here the kinetics of petroleum asphaltenes were similar to the kerogen of the organic rich and marine Draupne Facies, while the mixed type II/III facies, which still has an oil prone character, was proposed to be unimportant for oil accumulation. The underlying assumption that oil asphaltenes from type II marine oils really fit to the full oil generation window of the relevant source rock was not proven, especially when considering that oil-asphaltenes formed from sulphur rich source rocks do not fit.

8.1.1 Kinetic parameters

In order to show how far kinetic parameters calculated on source rock kerogens and asphaltenes can be compared to each other, one selected immature whole rock sample (G000542 with Tmax 419°C), the related asphaltene isolated from bitumen of the same source rock sample, and one petroleum asphaltene precipitated from a Redwater oil with the lowest API gravity (36° API) were investigated in terms of their bulk kinetic parameters. All these samples were taken within the Redwater area in order to ensure that they can be related to each other without any risk of facies variations or significant migration effects. As well the maturity parameter Ts / (Ts + Tm) of 0.56 (respectively 0.6 %Ro) for this oil and Ts / (Ts + Tm) values of 0.5 for source rock bitumen from the Redwater area (Dieckmann, 1998) prove low maturity and same maturity stage for these samples (Fig 40). Fig 114 illustrates the distribution of activation energies and frequency factors evaluated on these immature samples. Interestingly the kinetic parameters for these three samples are very similar, with Emean values of 54kcal/mol and associated frequency factors of around 5.0E+13 s^{-1}. The range of activation energies for the source rock asphaltenes are slightly tighter than those calculated for the source rock kerogen and for the petroleum asphaltene. This however is quite insignificant because the difference does not significantly influence outcomes when later on these kinetics are used to extrapolate petroleum formation to geological conditions.

In order to study the effect of thermal maturity on bulk kinetic parameters of source rock asphaltenes, additionally two selected asphaltenes isolated from more mature source rock samples (G000631 with Tmax of 431°C, G000600 with Tmax 438°C) were investigated by bulk pyrolysis. The resulted activation energy distribution (Ea) and frequency factors (A) for those source rock asphaltenes are presented in Fig 115. As reference for the immature Redwater samples the kinetic parameters for the whole rock sample shown in Fig 114 are replotted in Fig 115 to ensure a better comparison.

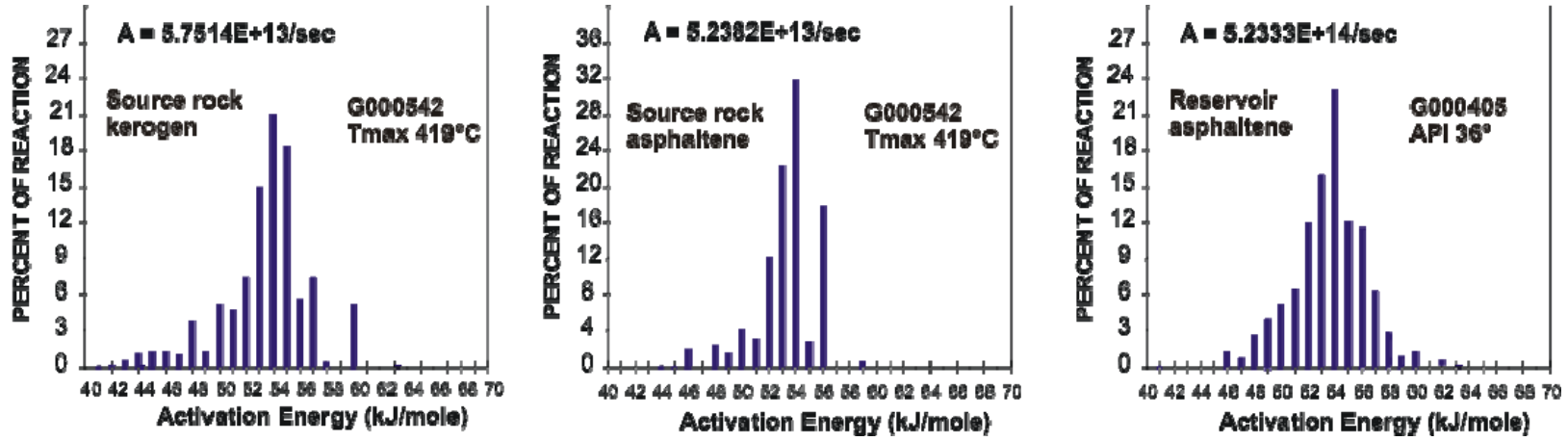

Fig 114 Activation energy distribution and frequency factor for an immature whole rock sample, related source rock asphaltene, and oil asphaltenes isolated from a low mature crude oil.

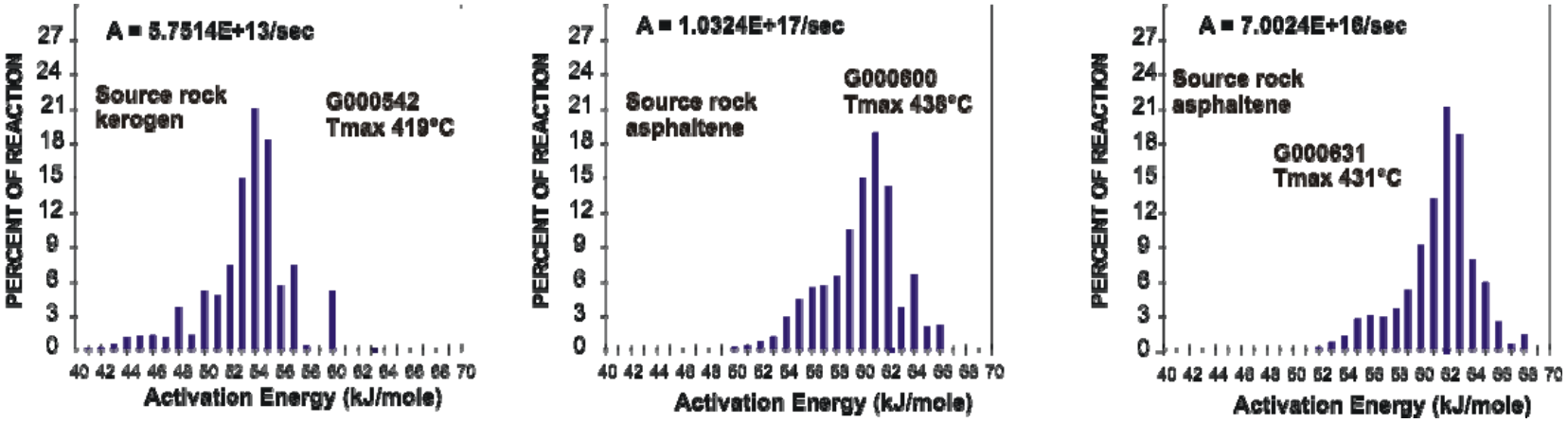

Fig 115 Energy distribution and frequency factor for the immature whole rock sample, and two selected source rock asphaltenes isolated from source rocks of higher maturity.

From Fig 115 it becomes clear that the stability of the asphaltenes precipitated from the source rock samples of increasing maturity is influenced by the increasing level of thermal stress, which asphaltenes have experienced in the geological past. The Emean value for the immature source rock asphaltene sample (G000542) was calculated to be 54 kcal/mol, associated with a frequency factor of 5.24E+13 s^{-1}. The activation energies range from 46 to 56 kcal/mole is very close to that previously reported by Dieckmann *et al.* (2002) for asphaltenes from Italy. When the maturity of the source rock increases it can be observed that mean activation energies increase to 61-62 kcal/mol for sample G000631 and G000600. This increase is associated with higher frequency factors of 7.0E+16 to 1.0E+17 s^{-1} and activation energies covering potentials which range from 54 to 68 kcal/mole. These higher mean activation energies may indicate that thermal stress resulted in a loss of less stable bonds within the source rock asphaltenes. It must however be noted that such a strong shift in kinetic parameters cannot exclusively be a result of the maturation process. One indication may be the presence of a slightly bimodal activation energy profile, with a first maximum at around 56-58 kcal/mol and a second maximum of 61-62 kcal/mol. This bimodal profile may indicate that the first maximum resulted from the same organic matter as that studied for the most immature sample, while the second maximum is a result of a significant contribution from a more stable facies within the Duvernay source rock. Facies variations in the Duvernay Formation were observed before by Li *et al.* (1997) and were shown also to affect the petroleum formation characteristics of the Duvernay Formation in some wells such as Forgotson Burk in the study area (Dieckmann, 1998).

8.1.2 Geological prediction of hydrocarbon generation

Fig 116 shows the prediction for a geological heating rate of 3.3 K/my for the immature samples presented in Fig 114 from the Redwater area. As mentioned before with regard to the kinetic parameter characteristics, the petroleum formation windows predicted for geological heating conditions of 3.3 K/my result in a nearly identical temperatures and time windows of 100°C for the onset, 150°C for the temperature of 50 % conversion and 165°C predicted for the end of petroleum formation. This information indicates that the asphaltenes in the Redwater oil have nearly exactly the sample bulk structural characteristics as the source rock kerogen and therefore could be used if the source rock were not available. Previous studies by di Primio *et al.* (2000) do not support these data, since these authors illustrated that the petroleum formation window using the Snorre oil asphaltenes are much tighter than those predictions using a series of Draupne source rock samples. However, the tighter character of Snorre petroleum asphaltenes relative to the source rock predictions was most probably a result of the extreme variability in kinetic parameters monitored in that Draupne source rocks. In addition the low and high end activation energy potentials were eliminated from the kinetics presented by di Primio *et al.* (2000), because the major focus of the study was on the Emean rather than on the full distribution of activation energies. This elimination was performed in order to avoid any potential risk of contamination at that time. In our sample set however contamination is absent or insignificant, because of the extensive precipitation procedure and tests with Rock-Eval analysis in order to check for the possible presence of a residual S1 (free hydrocarbons). In addition, the good fit of source rock asphaltenes and the source rock kerogen in the immature sample as well as the higher stabilities of source rock asphaltenes (Fig 115) precipitated from the more mature samples prove that co-precipitation of non-asphaltic macromolecules does not play any significant role here.

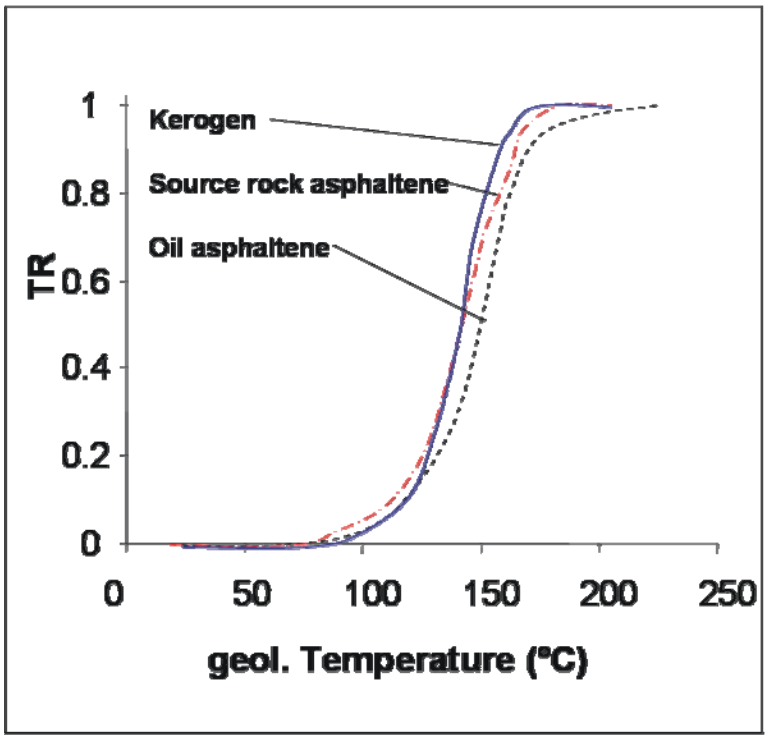

Fig 116 Extrapolation to geological conditions for transformation behaviour of asphaltenes and source rock kerogens of the samples from the Duvernay Formation using presented samples from Fig 114.

Fig 117 illustrates the prediction of bulk petroleum formation from the three source rock asphaltenes extracted from samples of different maturities and compares those with prediction based on kinetics evaluated on the immature source rock sample G000542 reported before. Fig 118 shows the diagram with a plot of resulted geological temperatures ($Tmax_{geol}$) versus the Tmax obtained from Rock-Eval for the three source rock asphaltenes and the immature source rock sample G000542. First of all, in Fig 117 it can be seen that the petroleum formation curves predicted for the asphaltenes isolated from more mature sample shift to higher temperatures. This however becomes only obvious for the geological Tmax which shift from 151°C for the immature sample (G000542) to 169°C for the more mature sample G000631 with a Rock-Eval Tmax of 431°C. Nevertheless the shift of these curves is not systematic since the asphaltene sample precipitated from the most mature sample G000600

(Tmax 438°C) plots with a $Tmax_{geol}$ of 156°C between the immature and the intermediate mature sample. For that reason it must be assumed the kinetics from source rock asphaltenes do not strictly follow the effects of thermal stress which the associated source rock may have seen in the geological past. It can however be seen that the petroleum formation from the most immature sample from which the asphaltenes were precipitated show a perfect fit to the parent kerogen.

A slight shift can also be observed for the onset temperatures of petroleum formed from source rock asphaltenes with an onset temperature of 80°C for the immature and most mature asphaltene samples, and an onset at about 90°C for the intermediate mature sample. The onset temperature for hydrocarbon generation from the whole rock reference sample is also slightly higher than for the related asphaltene.

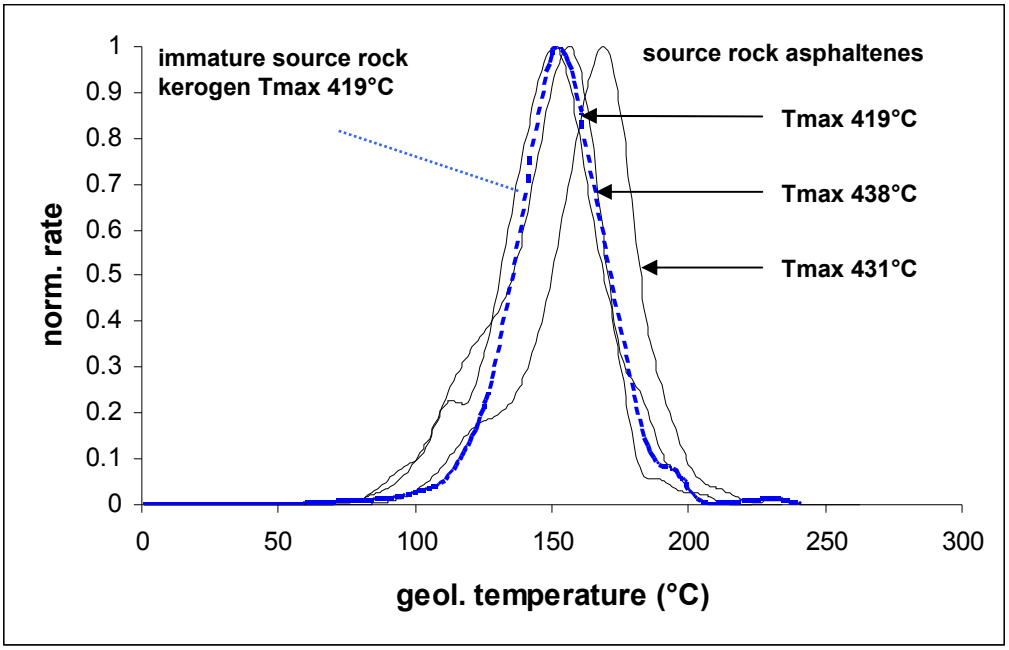

Fig 117 Extrapolation of bulk petroleum formation rates for a geological heating rate of 3°C/my for asphaltenes extracted from mature source rock samples compared to an immature source rock sample presented in Fig 115.

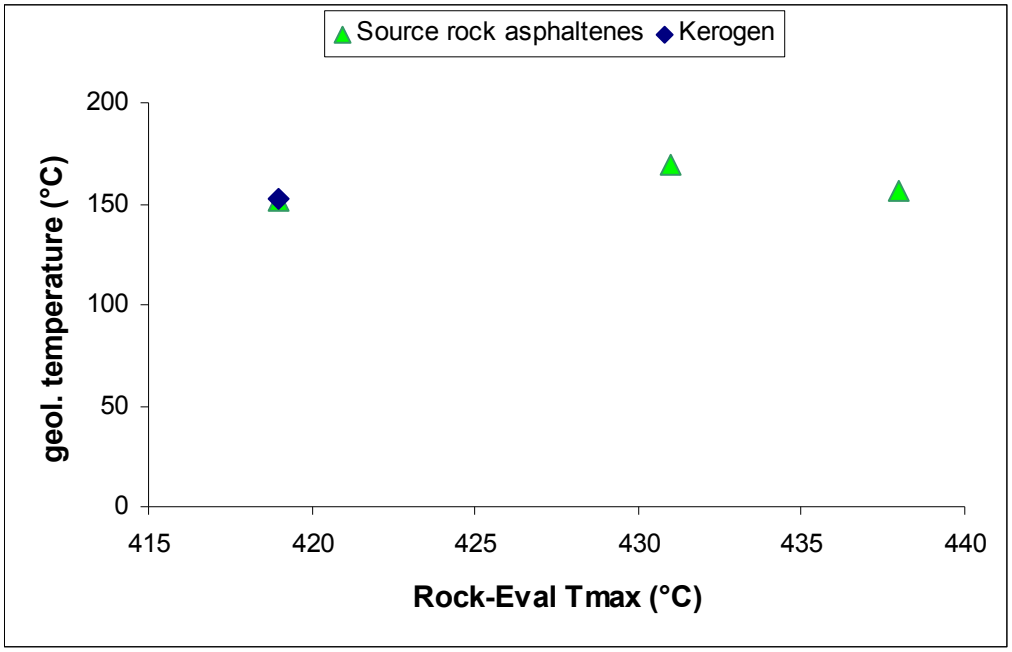

Fig 118 Calculated geological Tmax versus the Rock-Eval Tmax for source rock asphaltenes and the kerogen reference sample

8.1.3 Conclusions

- Oil asphaltenes from a type II sequence differ from oil asphaltenes from sulphur-rich sequences in that petroleum asphaltenes precipitated from the low mature Duvernay oils can be used to reconstruct the timing of source rock transformation as well as the compositional characteristics of natural oil in the petroleum system. These results are especially important for petroleum systems where the source rock is not drilled. This is because:
  - Bulk Petroleum generation kinetics evaluated for the transformation of petroleum asphaltenes and source rock asphaltenes from type II sequence are similar to those calculated for the transformation of related immature source rocks. Consequently the extrapolations of petroleum formation to geological heating conditions are very similar.

8.2 Elemental analysis

The elemental compositions measured on one oil asphaltene isolated from the immature crude oil G000405 (API 36°) and on four source rock asphaltenes with maturities between 414 – 421 °C Tmax is presented in Fig 119. Both types of asphaltenes show similar characteristics like observed for asphaltenes from Southern Italy. As shown for Southern Italy, the oil asphaltene from Duvernay show a lower atomic O/C ratio compared to source rock asphaltenes. An H/C ratio of 1.03 for the oil asphaltenes, and ratios between 1.07 and 1.20 for source rock asphaltenes were measured, which is closed to the average ratios for asphaltenes from marine organic matter published by Castex (1985) and Béhar *et al.* (1984). Both types of asphaltenes from the Duvernay Formation plot in the zone defined as type II in Fig 119. The elemental compositions and calculated ratios for the Duvernay asphaltenes, as well as relevant Rock-Eval data are presented in Table 13.

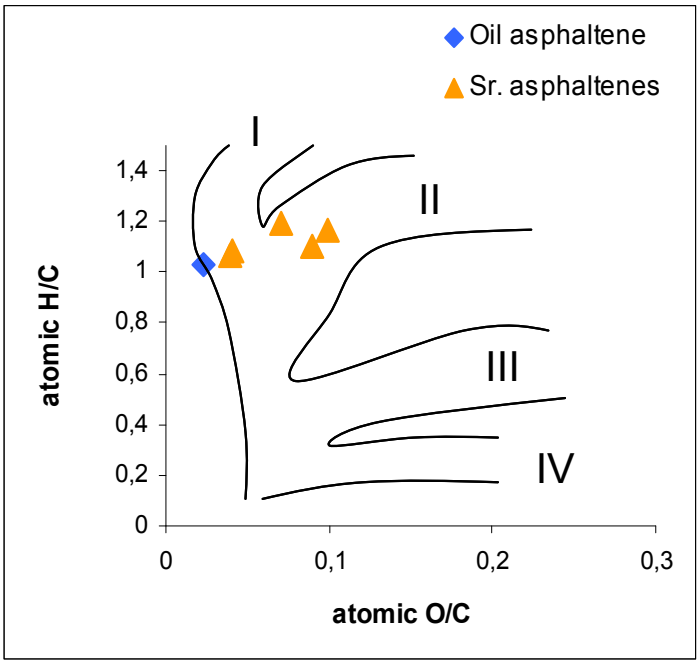

Fig 119 Van-Krevelen diagram showing the results of elemental analysis of the asphaltene samples from Duvernay (after Peters (1986), Tissot and Welte (1984).

Sample		H (%)	C (%)	O (%)	N (%)	H/C	O/C	HI	Tmax (°C)	API
G000549	s.r. asphaltene	7,28	80,28	4,31	2,78	1,09	0,04	577	416	
G000570	s.r. asphaltene	7,12	77,23	9,21	1,29	1,11	0,09	412	414	
G000583	s.r. asphaltene	7,11	79,86	4,15	3,48	1,07	0,04	631	421	
G000592	s.r. asphaltene	7,22	74,6	9,9	3,3	1,16	0,10	473	421	
G000615	s.r. asphaltene	7,63	76,51	7,24	3,51	1,20	0,07	591	415	
G000405	oil asphaltene	7,16	83,74	2,51	1	1,03	0,02			36

Table 13 Elemental compositions and calculated ratios for asphaltenes from the Duvernay Formation.

Interestingly, Duvernay source rock asphaltenes yield relative high concentrations of nitrogen, which can be attributed to nitrogen-containing bases. Li *et al*. (1997) conducted a quantitative study of pyrrolic nitrogen compounds on a series of source rock extracts taken from the Duvernay Formation. The authors stated that with increasing thermal maturity, concentrations of various pyrrolic nitrogen compounds in the rock extracts increase drastically. The atomic N/C ratios of selected source rock asphaltenes within the present study do not correlate to that observation. Fig 120 (left) shows a plot of atomic N/C of bitumen asphaltenes versus the HI of related source rocks. The selected bitumen asphaltenes are all extracted from immature source rock samples and they do not cover a full maturity trend, but their atomic N/C ratios vary highly with the HI. This makes clear that the elemental nitrogen concentration in these source rock asphaltenes might be more associated to facies variations than to thermal maturation.

Castex (1985) proposed that the H/C and O/C ratios of asphaltenes in source rocks decreases with increasing burial and thermal maturation. This was neither observed for the H/C nor for the O/C ratio of the asphaltenes from Southern Italy. Moreover, the source rock asphaltenes from Duvernay show a more or less inversed trend of atomic O/C with HI, like shown in Fig 120 (right). This illustrates that variation in atomic ratios of studied asphaltenes are more likely related to facies variations than to thermal maturation.

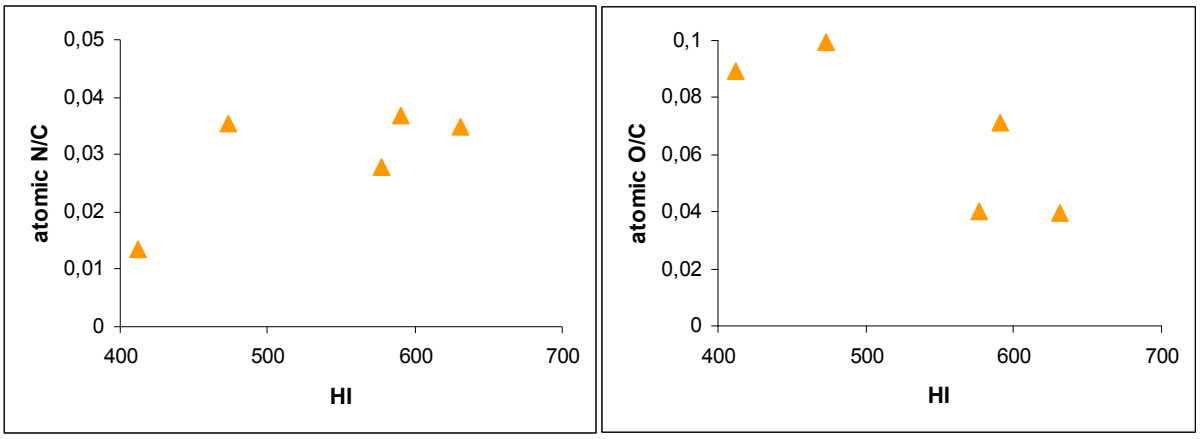

Fig 120 Diagrams with atomic N/C ratio of bitumen asphaltenes versus the HI of related source rocks (left), and atomic O/C ratio of those asphaltenes versus the HI of related source rocks from the Duvernay Formation (right).

8.3 Pyrolysis

8.3.1 Composition of pyrolysates

Fig 121 to Fig 123 show selected chromatograms of open system pyrolysis GC experiments on source rock kerogens (Fig 121), source rock asphaltenes (Fig 122), and from oil asphaltenes (Fig 123). All the illustrated samples increase in thermal maturity from the top to the bottom of the relevant figure.

The chromatograms from asphaltenes and kerogens performed by open-system pyrolysis show a similar distribution pattern of alkanes and alkenes. All samples are characterised by a (bi)-modal distribution of *n*-alkyl chains. Most dominant aromatic hydrocarbons are toluene and xylenes, which have been described as products from non-condensed aromatic moieties, like carotenoids (Béhar and Vandenbroucke, 1987; Hartgers *et al.*, 1994b; Stout and Boon, 1994). A prominent structural moiety for the Duvernay Formation is the occurrence of 1,2,3,4-tetramethylbenzene (TMB) in natural and pyrolysis products, which can be traced to the *β*-cleavage of diaromatic carotenoid moieties (Requejo *et al.*, 1992; Hartgers *et al.*, 1994a; Hartgers *et al.*, 1994b; Clegg *et al.*, 1997). For immature source rocks and for most source rock asphaltenes the concentration of tetramethylbenzene even exceed concentrations of other aromatic hydrocarbons.

Alkylthiophenes are as well present in pyrolysates from kerogens and asphaltenes, but they show lower concentrations than thiophenes in pyrolysates from the Italian samples.

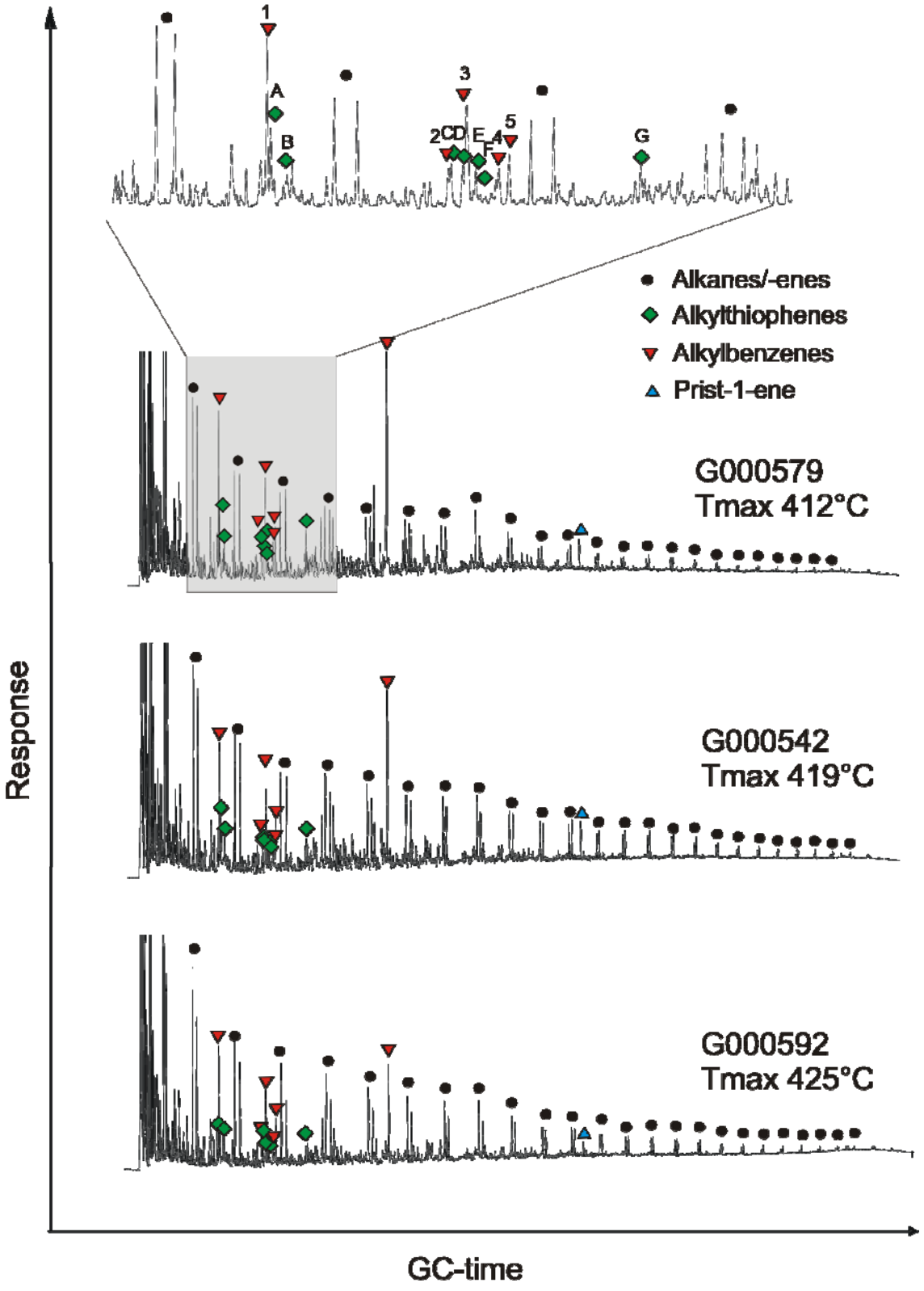

Fig 121 Selected chromatograms from open-system pyrolysis GC for source rock kerogens from the Duvernay Formation. Alkane/-ene doublets, most abundant thiophenes, and alkylbenzenes are marked. Alkylbenzenes are corresponding to retention time from left to the right: toluene (1), ethylbenzene (2), m,p-xylene (3), styrene (4), o-xylene (5), and 1,2,3,4-tetramethylbenzene. Alkylthiophenes are from left to right: 2-methylthiophene (A), 3-methylthiophene (B), ethylthiophene (C), 2,5-dimethylthiophene (D), 2,4-dimethylthiophene (E), 2,3-dimethylthiophene (F), and ethylmethylthiophene (G).

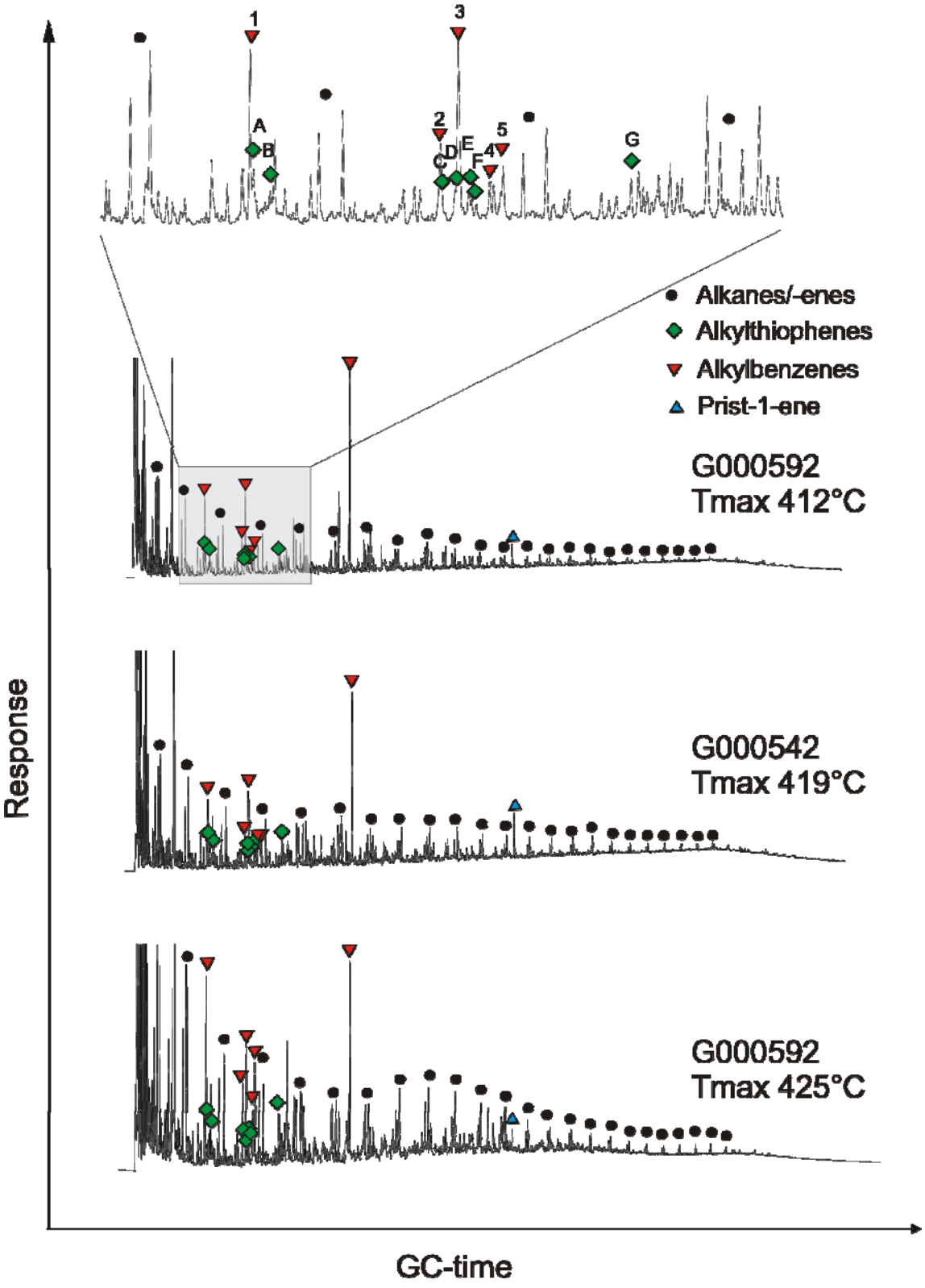

Fig 122 Selected chromatograms from open-system pyrolysis GC for source rock asphaltenes from the Duvernay Formation. Alkane/-ene doublets, most abundant thiophenes, and alkylbenzenes are marked. Alkylbenzenes are corresponding to retention time from left to the right: toluene (1), ethylbenzene (2), m,p-xylene (3), styrene (4), o-xylene (5), and 1,2,3,4-tetramethylbenzene. Alkylthiophenes are from left to right: 2-methylthiophene (A), 3-methylthiophene (B), ethylthiophene (C), 2,5-dimethylthiophene (D), 2,4-dimethylthiophene (E), 2,3-dimethylthiophene (F), and ethylmethylthiophene (G).

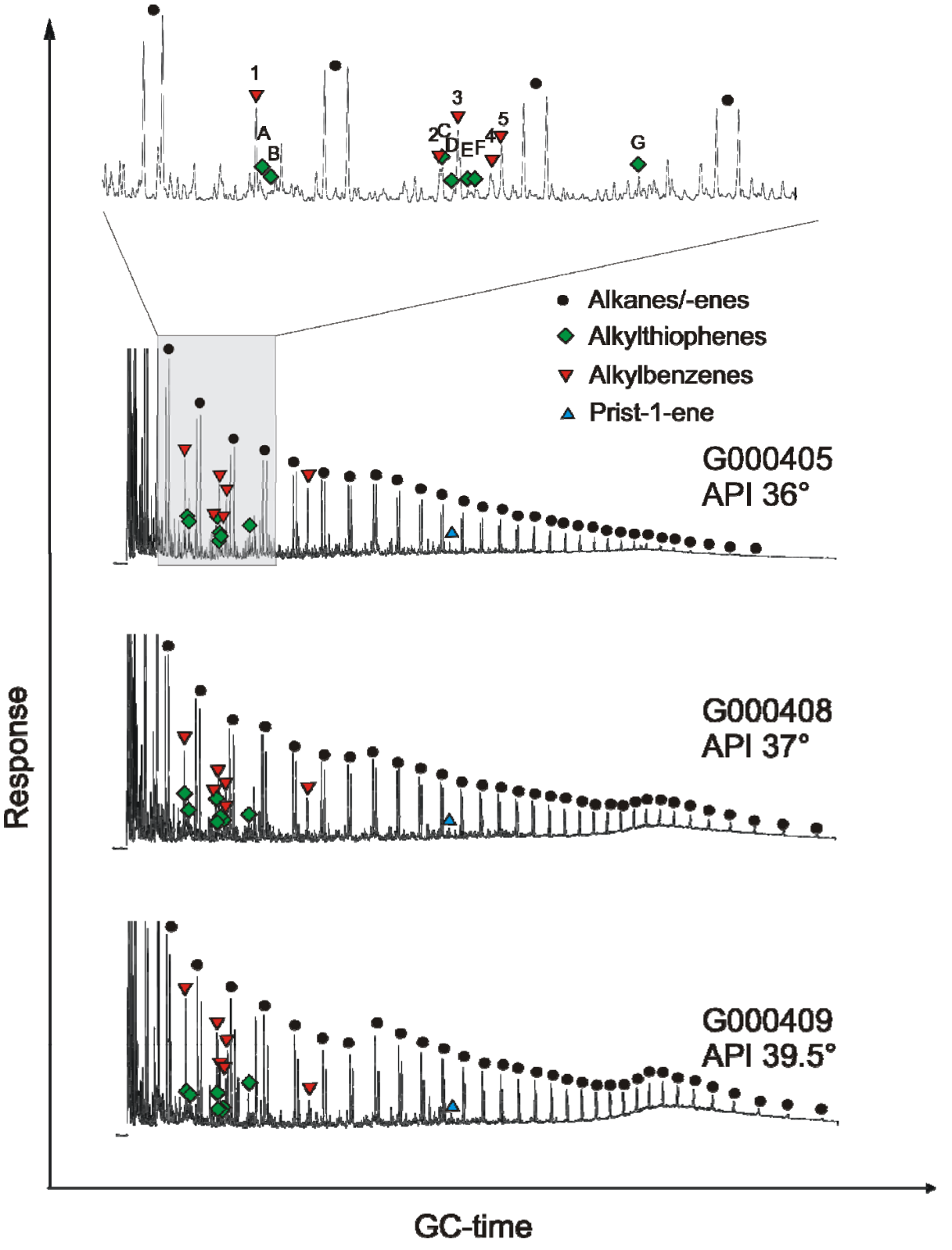

Fig 123 Selected chromatograms from open-system pyrolysis GC for petroleum asphaltenes from the Duvernay Formation. Alkane/-ene doublets, most abundant thiophenes, and alkylbenzenes are marked. Alkylbenzenes are corresponding to retention time from left to the right: toluene (1), ethylbenzene (2), m,p-xylene (3), styrene (4), o-xylene (5), and 1,2,3,4-tetramethylbenzene. Alkylthiophenes are from left to right: 2-methylthiophene (A), 3-methylthiophene (B), ethylthiophene (C), 2,5-dimethylthiophene (D), 2,4-dimethylthiophene (E), 2,3-dimethylthiophene (F), and ethylmethylthiophene (G).

8.3.2 Aliphatic hydrocarbons

The (bi)-modal distribution of *n*-alkyl chains for kerogens and asphaltenes shows a minor peak in *n*-C_{14}, which is generally more sticking out in pyrolysates of oil asphaltenes.

The alkane / alkene ratios of *n*-alkyl chain doublets show systematic differences for pyrolysates of Duvernay kerogens and asphaltenes, like reported before for the Italian samples. Petroleum asphaltenes isolated from low-mature crude oils show a predominance of alkanes up to *n*-C_{14} or *n*-C_{15}, which then changes and alkenes are getting more dominant. The asphaltenes isolated from more mature oils show a predominance of alkanes up to *n*-C_{28} doublets. Similar to bitumen asphaltenes from Southern Italy, the pyrolysates of asphaltenes isolated from Duvernay source rock bitumen are predominated by alkenes in their *n*-alkyl chain doublets. However, most source rock asphaltenes present a single predominance of alkanes in *n*-C_6, *n*-C_{10}, and *n*-C_{12}. Most pyrolysates of Duvernay kerogens show a similar alkane / alkene ratio distribution as pyrolysates of oil asphaltenes. For kerogens, alkane is predominant up to *n*-C_{16} or *n*-C_{17}, but all kerogens demonstrate a high single dominance of alkene either in *n*-C_{10} or *n*-C_{11}.

Fig 124 shows the ternary diagram of alkyl chain distribution for pyrolysates of kerogens and asphaltenes from the Duvernay Formation. This diagram has been introduced to predict the characteristics of oil generated from a certain source by its pyrolysates (Horsfield, 1989). Kerogens and source rock asphaltenes predict both the field of the paraffinic-naphtenic-aromatic low-wax oil generating facies. This supports the original assumption, that general structural features of a source rock can be found in the relevant asphaltene fractions (Muscio *et al.*, 1991; Horsfield *et al.*, 1993). However, a slight difference between kerogens and related source rock asphaltenes is observed in that the asphaltene pyrolysates show slightly higher amounts of C_1-C_5.

When comparing the products from source rocks with those from oil asphaltenes, it becomes clear that source rock products contain lower amounts of *n*- C_{15+}, while the ratio of C_{1-5}/*n*-C_6-C_{14} is similar. Thus pyrolysates of oil asphaltenes even predict the field of paraffinic high wax oil generating facies. Since the Duvernay Formation is a well defined marine petroleum system, the possibility of explaining higher yields in *n*-alkyl-chain precursor material by a lacustrine input, can be excluded. With regard to the presented chromatograms in Fig 121 - Fig 123 it can be seen that asphaltenes isolated from Duvernay crude oils are enriched in long-chain C_{15+} *n*-alkyl chains, and in contrast to kerogens they show *n*-alkyl doublets up to *n*-C_{37}. In this characteristic feature the oil asphaltenes reflect very well the crude oil characteristics, which also show *n*-alkanes up to *n*-C_{37} in their whole-oil chromatograms (Fig 38).

A positive fit between asphaltenes and kerogens through oil window maturities and a misfit between these different organic matter types at higher maturity has previously also been observed by Muscio *et al.* (1991) for a maturity sequence from the Toarcian shale. At present we have no unequivocal explanation for this observation. However, it cannot be excluded that due to the low quantities of asphaltenes in such samples and the low precipitation efficiency these differences reflect the limits of the pyrolysis-GC technique in handling very low amounts of sample material. But it must be assumed that the potential of the Duvernay oil asphaltenes to form gas may be lower than that for the kerogen. This is supported for the oil asphaltenes, since that fraction contains very low amounts of 1,2,3,4-TMB, a compound which has been proposed as marking specific gas precursor material in source rocks (Muscio *et al.*, 1994). In addition, source rock asphaltenes are enriched in 1,2,3,4-TMB and they show also a higher potential to form gas, which support the observations of Muscio *et al*. (1994). From that point of view the differences of the *n*-alkyl chain distribution for Duvernay

pyrolysates are linked to the structural characteristics of Duvernay kerogens and both types of asphaltenes.

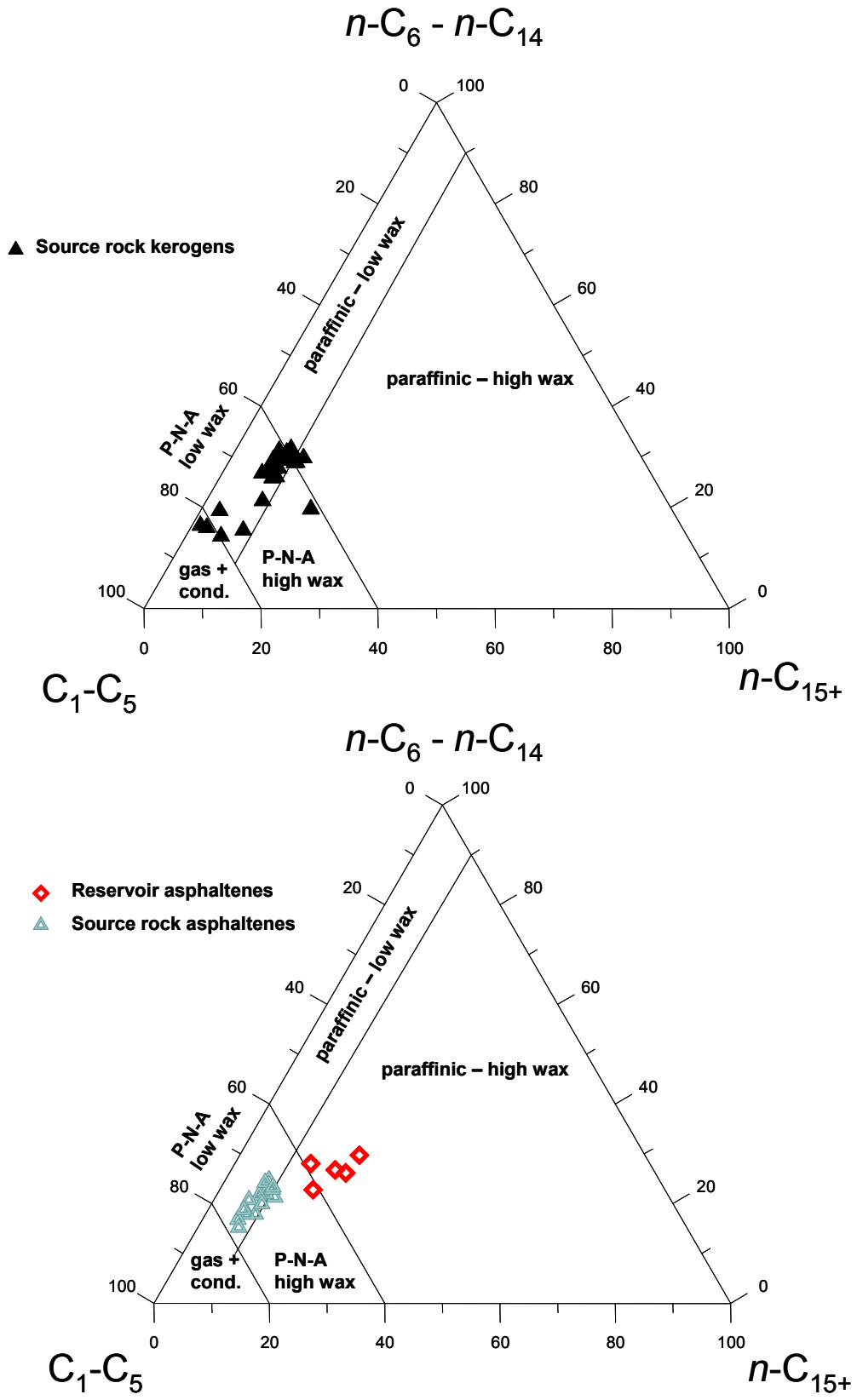

Fig 124 Ternary diagram of alkyl chain distribution for pyrolysates of kerogens and asphaltenes from the Duvernay Formation.

Fig 125 illustrates the gas generation characteristics of kerogens, source rock asphaltenes and oil asphaltenes with ongoing maturity. The diagram shows the ratio of (C_1-C_5) / *n*-C_{6+} versus Tmax for kerogens and related asphaltenes (left), and versus API for oil asphaltenes (right). As it can be seen the kerogens show a sudden increasing of gas generation at Tmax higher than 440°C. Interesting is that kerogens of lowest maturity also show higher gas generation characteristics than kerogens of intermediate maturity. This is also observed for the source rock asphaltenes, which demonstrate highest potential of gas formation at lower levels of maturity. Later on, we will see that immature kerogens and source rock asphaltenes show higher amounts of 1,2,3,4-TMB. The relationship of gas generation and 1,2,3,4-TMB is thus in agreement with previous study of Muscio *et al.* (1994). The same gas generation characteristic is as well found for the oil asphaltenes. Asphaltenes from low mature Duvernay oils show higher potential to form gas than asphaltenes isolated from intermediate mature oils, whereas the potential again increases for asphaltenes extracted from the oil of highest maturity. This trend for oil asphaltenes correlates also with the amount of 1,2,3,4-TMB in these samples, which is illustrated in the next chapter.

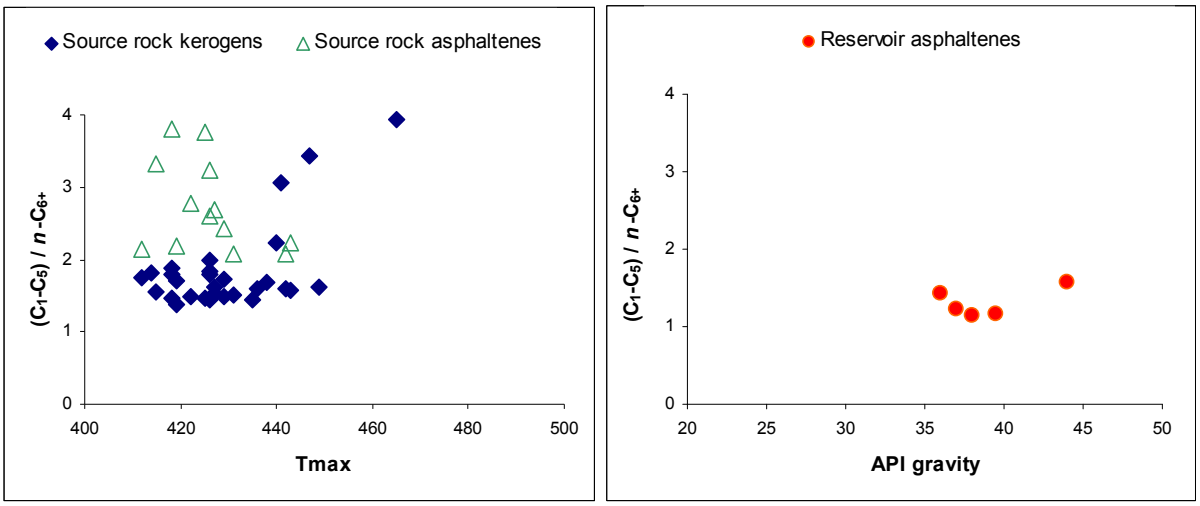

Fig 125 The ratio of (C_1-C_5) / *n*-C_{6+} versus Tmax for kerogens and related asphaltenes (left), and versus API for oil asphaltenes (right).

8.3.3 1,2,3,4-tetramethylbenzene as specific geomarker

A prominent structural moiety for the Duvernay Formation is the occurrence of 1,2,3,4-tetramethylbenzene (TMB) in natural and pyrolysis products, which can be traced to the *β*-cleavage of diaromatic carotenoid moieties (Requejo *et al.*, 1992; Hartgers *et al.*, 1994a; Hartgers *et al.*, 1994b; Clegg *et al.*, 1997). The biological precursor is related to a specific green sulphur bacteria (*Chlorobiacea*), known to reproduce only in sulphate and hydrogen sulphide-rich water bodies (Abella *et al.*, 1980). Since this biogenic related alkylbenzene is abundant in pyrolysis products, as well as in natural products, it has use as geomarker. Fig 126 on the left side shows the ratio 1,2,3,4-tetramethylbenzene / (*n*-C_{11} + *n*-C_{12}) versus the hydrogen index for source rock asphaltenes and kerogens. The plot contains only those source rocks from which asphaltenes have been extracted. Right side of Fig 126 shows the same ratio versus API gravity respectively for natural oils and reservoir asphaltenes.

Interestingly, the source rock asphaltenes are most enriched in 1,2,3,4-TMB compared to the source rock kerogen. In contrast reservoir asphaltene pyrolysates show significantly lower amounts of 1,2,3,4 TMB relative to *n*-C_{11} and *n*-C_{12} alkyl-chain, when compared to than the source rock kerogen and especially to source rock asphaltene pyrolysates. This difference supports also the previous discussed structural differences in terms of gas generation and 1,2,3,4-TMB for Duvernay asphaltenes and kerogens.

A very interesting finding result from the comparison of the 1,2,3,4-TMB ratio in the products formed from the oil asphaltenes and those measured in the natural oil. Here it is obvious that the ratio from oil asphaltene pyrolysates fits exactly to those measured the naturally formed crude oils as shown in Fig 126.

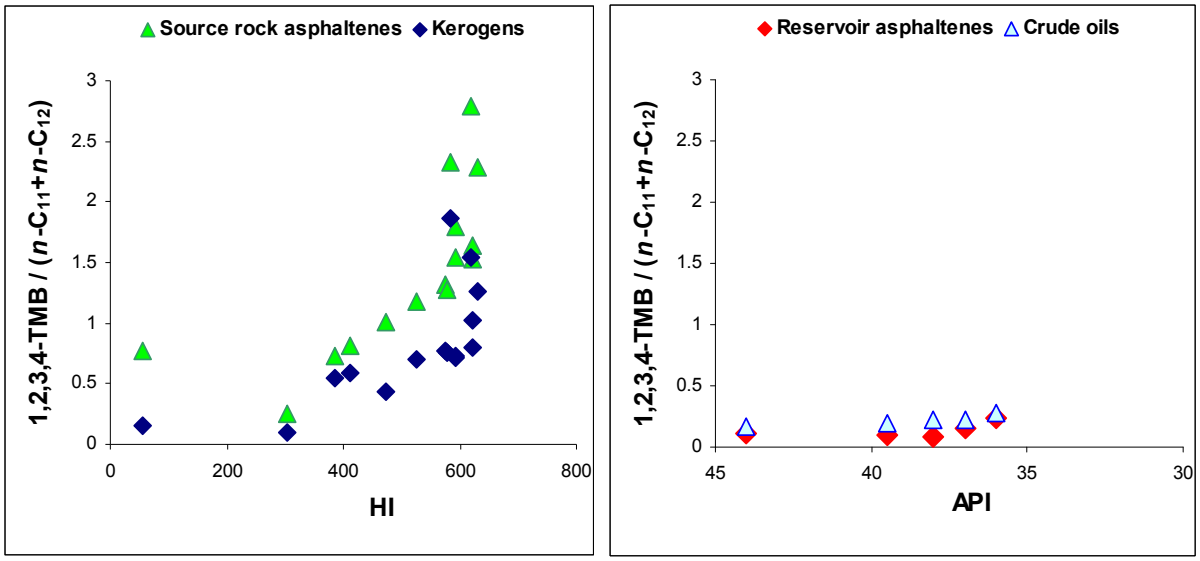

Fig 126 Ratio of 1,2,3,4-tetramethylbenzene / (n-C_{11} + n-C_{12}) versus the hydrogen index for source rock asphaltenes and kerogens (left), and versus the API gravity for natural oils and reservoir asphaltenes (right) for the samples from the Duvernay Formation.

8.3.4 Aromatic hydrocarbons

For the Duvernay Formation we found a similar characteristic of pyrolysates in terms of aromaticity as for the Italian samples. Fig 127 illustrates the ratio of aromatic hydrocarbons versus n-C_{6+} alkyl-chains as a function of the transformation ratio calculated after Espitalié *et al.* (1987) for source rock asphaltenes and related kerogens from the Duvernay sample set. Due the homogeneous character of the Duvernay Formation, it can be assumed that a decrease in TR, based on HI, is directly related to an increase of thermal maturity. On the right hand side of Fig 127 the same ratio is plotted as a function of Tmax. For both diagrams within Fig 127 it is obvious that low mature samples contain significantly higher amounts of aromatic compounds than products formed from more mature equivalents. However, when focusing on

samples of low maturity, the highest aromaticity can be observed in the products formed from the source rock asphaltenes, as well supported by the ratio of 1,2,3,4-TMB found in pyrolysates of kerogens and source rock asphaltenes shown in Fig 126.

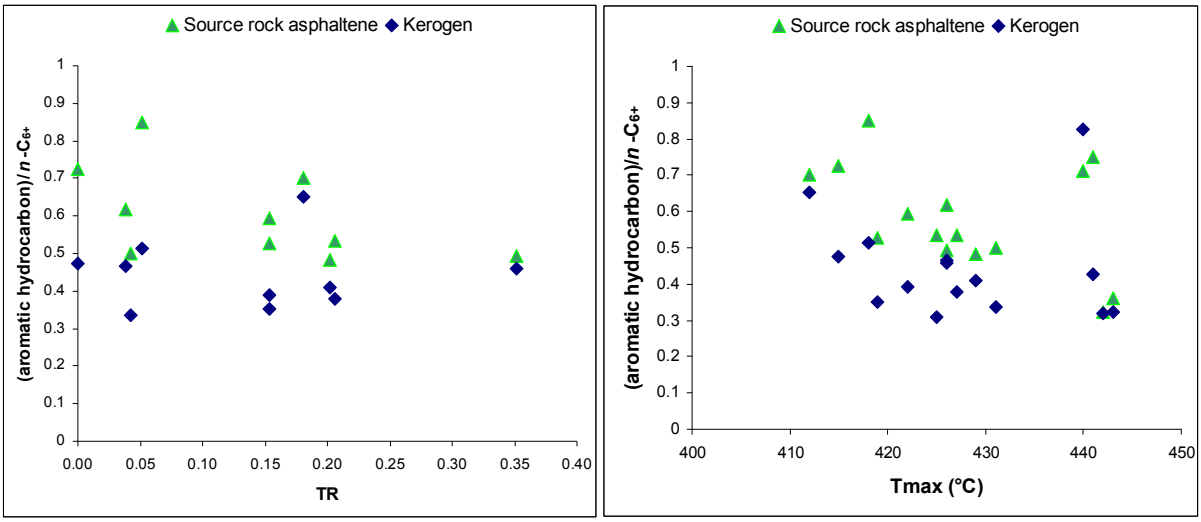

Fig 127 Ratio of aromatic compounds / *n*-C_{6+} versus the transformation ratio (left) and versus Tmax (right) for source rock asphaltenes and kerogens from the Duvernay Formation

Fig 128 compares the aromaticity of pyrolysates from kerogens and source rock asphaltenes as a function of HI (left) with those of oil asphaltenes as a function of the API gravity (right). This diagram shows all investigated kerogens over the maturity range, while the previous two diagrams showed kerogen-asphaltene-pairs. In this figure it is obvious that oil asphaltene products demonstrate the lowest aromaticity, while source rock kerogens seem to represent an intermediate between both types of asphaltenes at low levels of maturity. Here, it is also obvious that the aromaticity of oil asphaltene pyrolysates decreases with increasing API. Source rock asphaltenes and parent kerogens show the same trend of decreasing aromaticity with increasing maturity for their immature stage of maturity. Through lack of *n*-C_{6+} aliphatic

hydrocarbons samples of high maturity (Tmax > 440°C, or HI < 200 mg HC/g TOC) show again increasing aromaticity

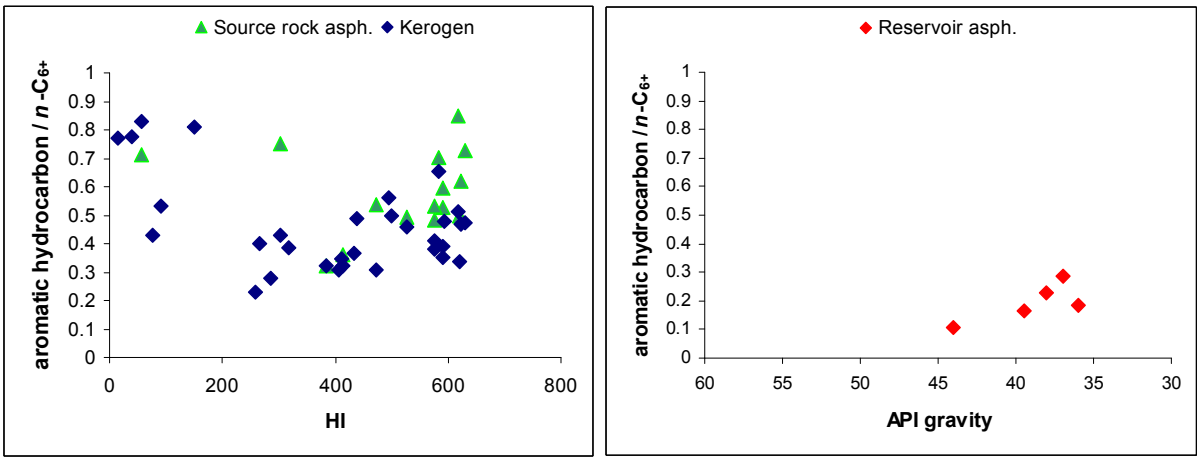

Fig 128 Ratio of aromatic compounds / *n*-C_{6+} versus the HI for source rock asphaltenes and kerogens (left), and versus the API for oil asphaltenes (right) from the Duvernay Formation.

For the samples from Southern Italy we found as well differences within the ratios of aromatic hydrocarbons, like shown for the ratio of toluene / Σ xylenes (Fig 91). The asphaltenes and parent kerogens from the Duvernay Formation display as well differences within the same ratio of toluene / (m,p-xylene + o-xylene), like illustrated in Fig 129. As opposed to highest toluene / Σ xylenes ratios in pyrolysates of the source rock asphaltenes from Italy, source rock asphaltenes from Duvernay show lowest ratios for toluene compared to their related kerogens, as well to oil asphaltenes. Here, for the Duvernay Formation it can also be seen that that ratio for kerogens and oil asphaltenes increases with increasing maturity, which points to higher amounts of toluene in pyrolysates of more mature samples. In contrast, this ratio obtained from source rock asphaltene pyrolysates does not apply to ongoing thermal maturation for the studied samples.

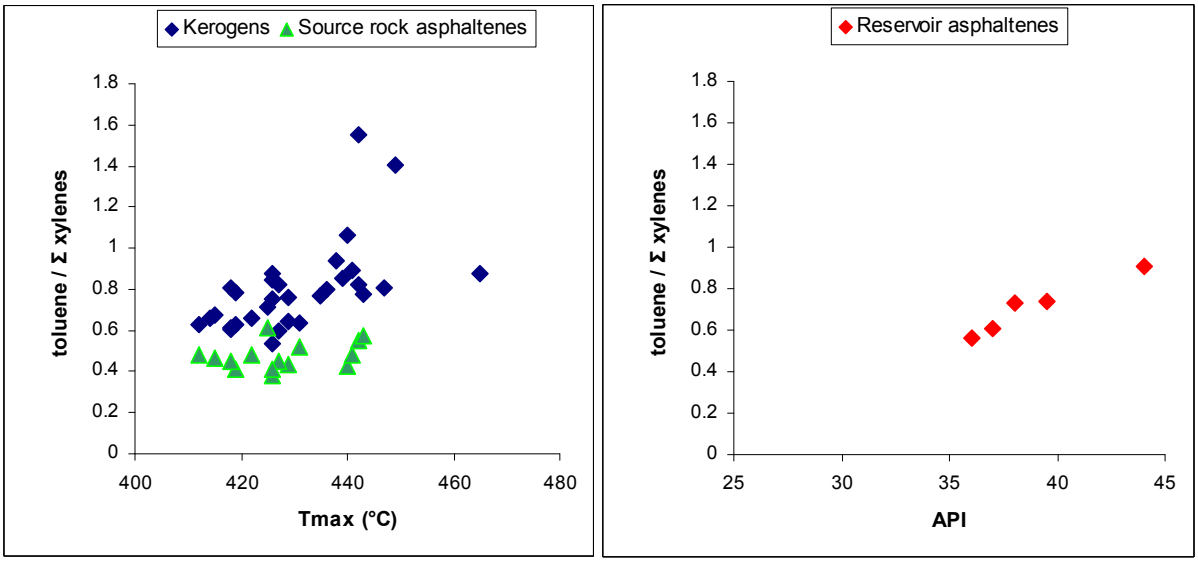

Fig 129 Ratio of toluene / (m,p-xylene + o-xylene) versus Tmax for source rock kerogens and related asphaltenes (left), and the same ratio versus the API gravity for reservoir asphaltenes (right) from the Duvernay Formation.

8.3.5 Alkylthiophenes

Fig 130 illustrates the ternary diagram of 2,3-dimethylthiophene, o-xylene, and *n*-$C_{9:1}$ after Eglinton *et al.* (1990b) for source rock kerogen (top), as well as source rock asphaltenes and reservoir asphaltenes (bottom) for the samples from the Duvernay Formation.

Based on these three compounds it can be seen that for the majority of the samples predict the field of type II organic matter. A major systematic difference between asphaltenes and kerogens is a slightly higher proportion of 2,3-dimethylthiophene in products formed from the source rock kerogens. Oil asphaltenes reflect in contrast to source rock asphaltenes a higher paraffinicity, a structural feature, which was also reported for the alkyl chain distribution, and also found for pyrolysates from Italian samples. High mature kerogen and source rock asphaltene samples (>Tmax 440°C) are depleted in thiophenes and alkanes and therefore they shift to the type III field in this diagram.

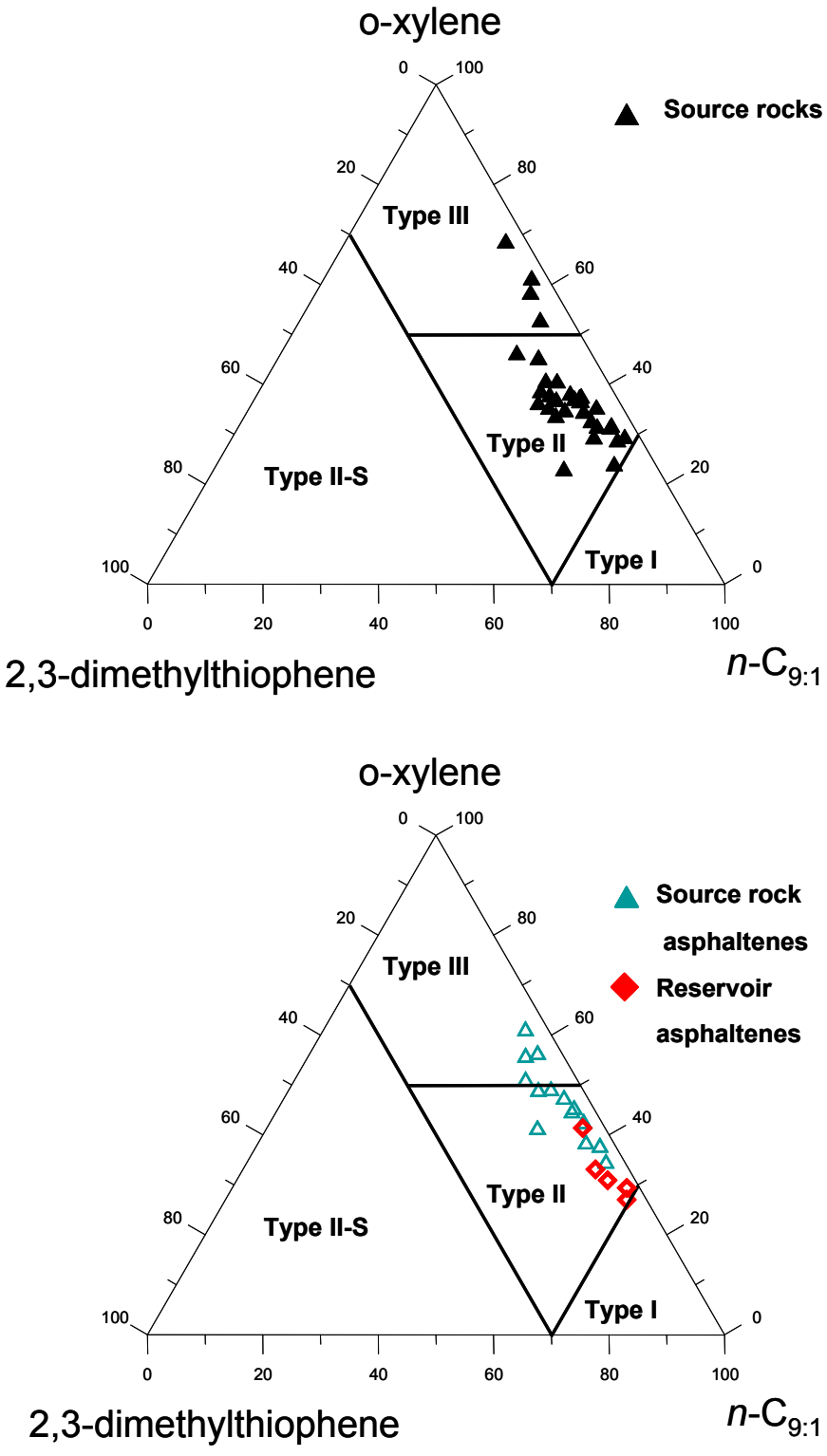

Fig 130 Ternary diagram of 2,3-dimethylthiophene, o-xylene, and *n*-$C_{9:1}$ after Eglinton *et al.* (1990b) for source rock kerogen (top), as well as source rock asphaltenes and reservoir asphaltenes (bottom) for the samples from the Duvernay Formation

Fig 131 illustrates the ratio of 2,3-dimethylthiophene / (o-xylene + *n*-$C_{9:1}$) versus Rock-Eval Tmax for kerogens and source rock asphaltenes (left), and versus the API gravity for oil asphaltenes (right) over a broad maturity range. The content of 2,3-dimethylthiophene in pyrolysates of kerogens and related source rock asphaltenes decreases with increasing maturity, which correlates to studies of Orr and Sinninghe Damsté (1990). Pyrolysates of oil asphaltenes show as well highest ratios of 2,3-dimethylthiophene / (o-xylene + *n*-$C_{9:1}$) for samples of lower API gravity. But, similar to the Italian samples, both types of asphaltenes from the Duvernay Formation show lower amounts of 2,3-dimethylthiophenes, i.e. lower organic sulphur content (Eglinton *et al.*, 1990b), as their parent kerogens.

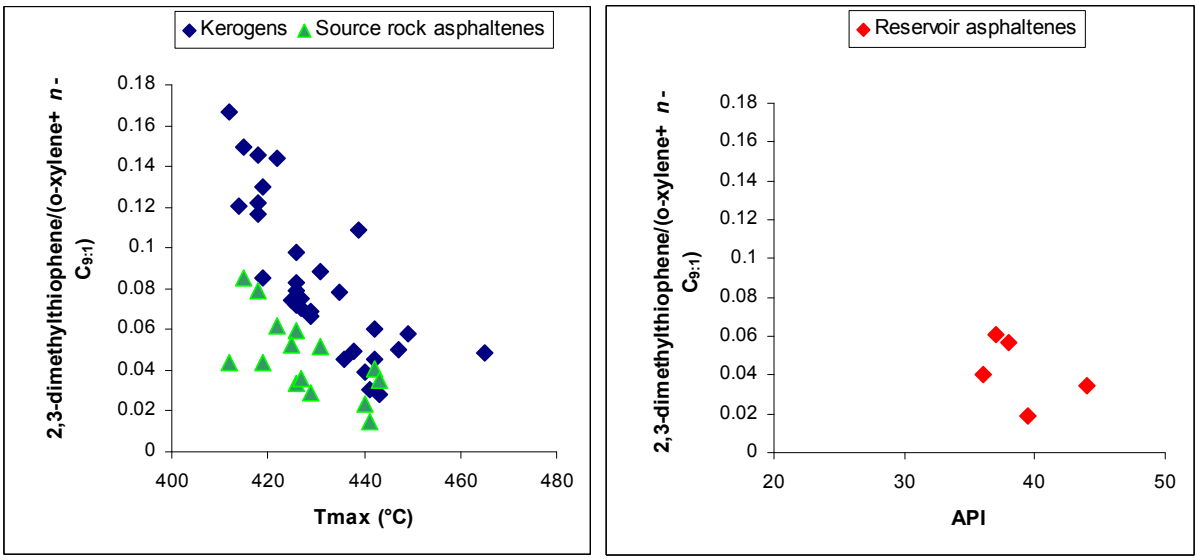

Fig 131 Ratio of 2,3-dimethylthiophene / (o-xylene + *n*-$C_{9:1}$) versus Rock-Eval Tmax for kerogens and source rock asphaltenes (left), and that same ratio versus the API gravity for oil asphaltenes (right).

Fig 132 illustrates the ratio of 3-methylthiopene/ (3- + 2-methylthiophene + 2,5-dimethylthiophene) versus Tmax (left) for kerogens and source rock asphaltenes, and versus the API gravity for oil asphaltenes from the Duvernay Formation. As opposed to the Italian

kerogens, the kerogens and source rock asphaltenes from the Duvernay Formation show a clear trend of that ratio versus thermal maturation. As published by Eglinton *et al* (1990b) the amount of 3-methylthiophene relative to thiophenes of linear precursor isomers increases with increasing maturity. This is for pyrolysates of Duvernay oil asphaltenes only observed for the lower API range. However, differences are also found, in that pyrolysates of source rock asphaltenes display lowest ratios for 3-methylthiopene/ (3- + 2-methylthiophene + 2,5-dimethylthiophene) compared to oil asphaltenes and parent kerogens.

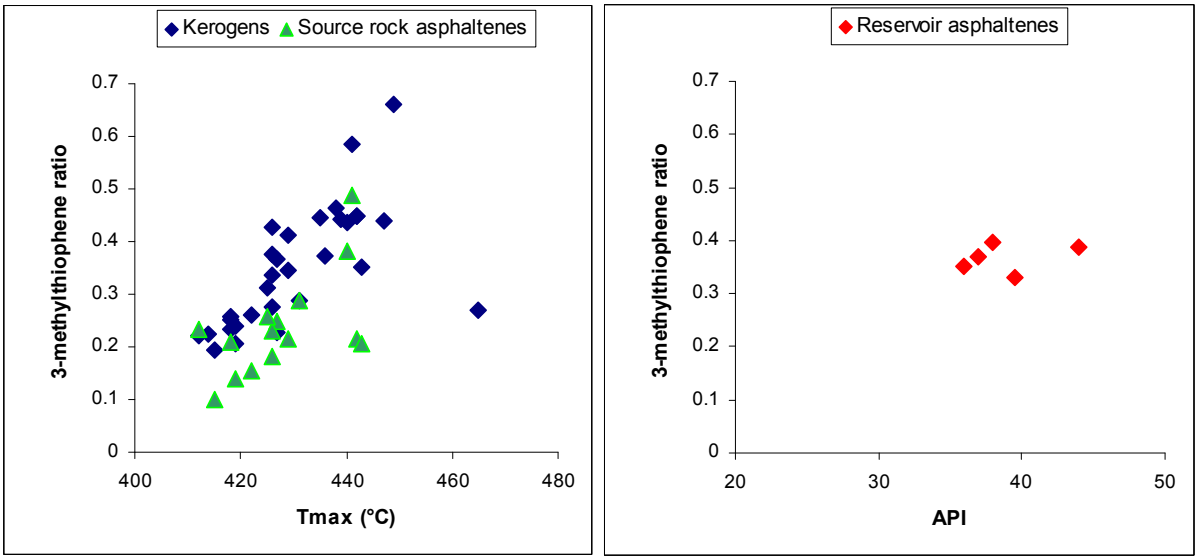

Fig 132 Ratio of 3-methylthiopene/ (3- + 2-methylthiophene + 2,5-dimethylthiophene) versus Tmax (left) for kerogens and source rock asphaltenes, and versus the API gravity for oil asphaltenes from the Duvernay Formation.

8.3.6 Conclusions

- The molecular composition of pyrolysates formed from petroleum asphaltenes and source rock asphaltenes from the Duvernay Formation are extremely different. The aromaticity of source rock asphaltene pyrolysates is much higher than the aromaticity of pyrolysates from petroleum asphaltenes. Interestingly, pyrolysates formed from immature kerogens represent intermediate aromaticity.
- The aromaticity of natural oils from Duvernay is much lower than those of pyrolysates from source rock kerogens and source rock asphaltenes. However, petroleum asphaltenes pyrolysates fit exactly to the aromaticity of the natural oils. This feature indicates that petroleum asphaltene pyrolysates can be used for petroleum compositional predictions, while the application of kerogen and source rock asphaltene pyrolysates is very limited.
- Source rock asphaltenes as well parent kerogens show decreasing aromaticity of their pyrolysates with ongoing maturity, up to a maturity stage, where the aromaticity increases through lack of aliphatic hydrocarbons in their pyrolysates
- Geochemical facies markers such as the 1,2,3,4-TMB/(n-C_{11}+n-C_{12}) ratio as well as the distribution of alkyl chains in products formed from petroleum asphaltenes cannot not be used for source rock organofacies characterization. Kerogens and source rock asphaltenes predict both the field of the paraffinic-naphtenic-aromatic low-wax oil generating facies based on the alkyl chain distribution, whereas oil asphaltenes predict the field of paraffinic high wax oil generating facies. Pyrolysates of oil asphaltenes do however copy molecular characteristics of natural oils.
- Pyrolysates of source rock and oil asphaltenes show lower organic sulphur content than related parent kerogens, and show decreasing amounts of organic sulphur with increasing thermal maturation, just as pyrolysates of kerogens do.

8.4 Compositional kinetic predictions from petroleum asphaltenes

8.4.1 Composition of MSSV pyrolysates

In order to compare products from artificial maturation experiments from asphaltenes from different depositional environments, we applied additionally MSSV analysis for an asphaltene precipitated from a low mature crude oil (API 36°) from the Duvernay Petroleum System. Because of low amounts of asphaltenes we conducted this study with the use of one heating rate of 0.7 K/min.

Fig 133 shows GC traces for four experimental temperatures using a heating-rate of 0.7 K/min. The MSSV pyrolysates of the Duvernay reservoir asphaltene show a bimodal distribution pattern of homologues *n*-alkanes. These pyrolysates from the Duvernay asphaltene show lower amounts of unresolved compounds at low temperatures than those previously presented for MSSV pyrolysates of the Italian oil asphaltene (Fig 101 Fig 102). As well pristane/phytane and alkylthiophenes formed from the Duvernay asphaltene still occur at higher experimental temperatures than monitored for the oil asphaltene from Southern Italy.

For the studied Duvernay asphaltene MSSV pyrolysates the generation of pristane and phytane ended at 460°C for the heating-rate of 0.7K/min, and at 430°C for Italian asphaltene MSSV pyrolysates using the same heating rate. The formation of alkylthiophenes from the Duvernay asphaltene ended at 470°C (0.7K/min), and already at 460°C (0.7K/min) for the Italian MSSV asphaltene pyrolysates. The Duvernay reservoir asphaltene pyrolysates show increasing amounts of 2- and 1-methylnaphthalenes up to the end-temperature of 580°C, whereas the generation of those naphtenoaromatics was finished at 560°C (0.7K/min) for the Italian asphaltene. Interestingly, the Duvernay pyrolysates show very high yields of ethylbenzene at lower thermal stress, which decreases with increasing simulated maturation.

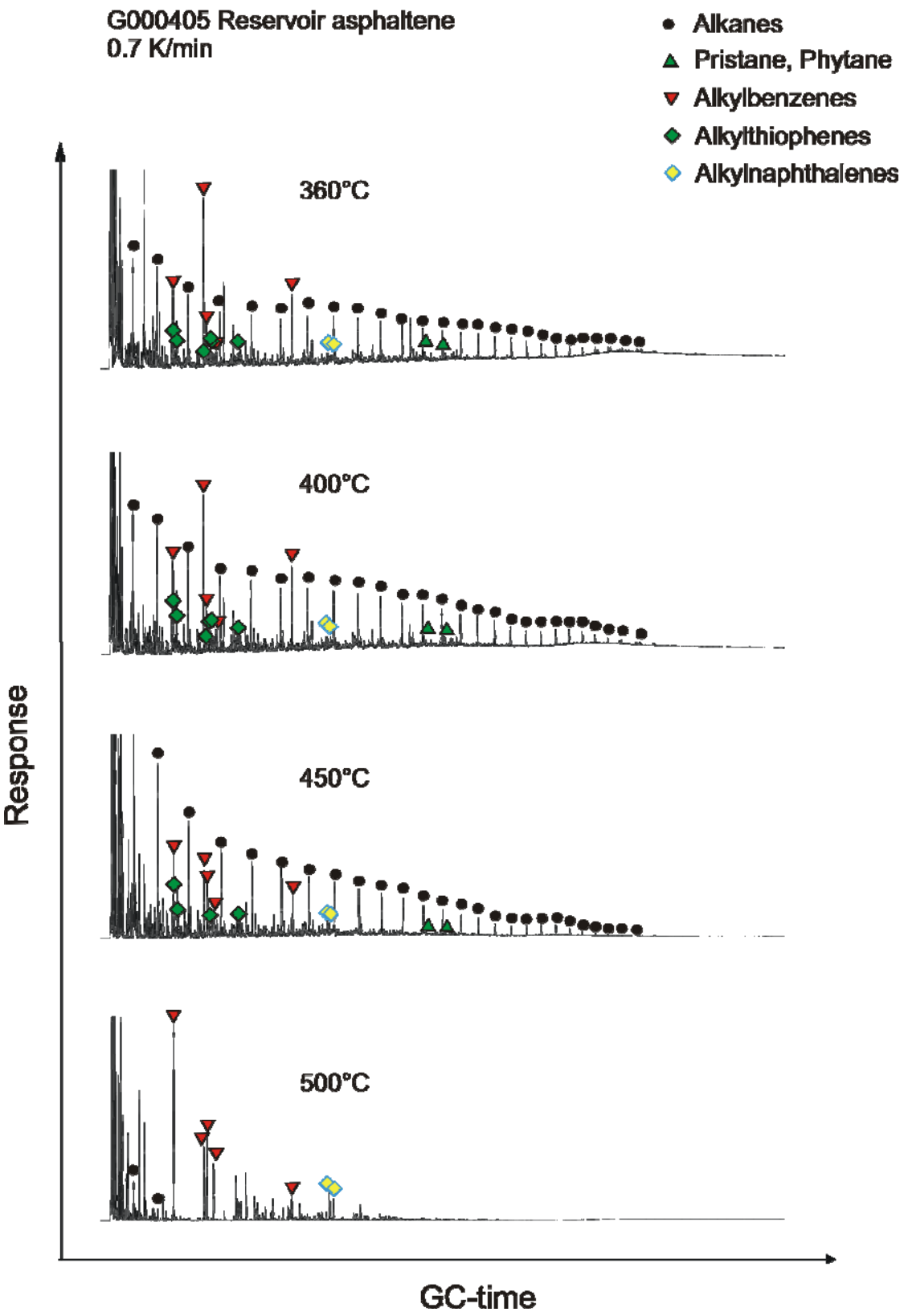

Fig 133 Selected chromatograms from MSSV pyrolysis GC of oil asphaltene sample G000405 using a heating-rate of 0.7 K/min. Alkanes, most abundant thiophenes, alkylnaphthalenes and alkylbenzenes are marked. Alkylbenzenes are corresponding to retention time from left to the right: toluene, ethylbenzene, m,p-xylene, and o-xylene. Alkylnaphthalenes are 2- and 1-methylnaphthalene. Alkylthiophenes are from left to right: 2-methylthiophene, 3-methylthiophene, 2,5-dimethylthiophene, 2,4-dimethylthiophene, 2,3-dimethylthiophene, and ethylmethylthiophene.

8.4.2 Gas and oil formation

The hydrocarbon generation curves of the total concentrations of different hydrocarbon fractions (methane, C_{1-5}, C_{6-14} and C_{15+}) are shown in Fig 134.

It is obvious that the generation of artificial formed hydrocarbons starts at 330°C (0.7 K/min). First formed compound classes are the C_{6-14} and C_{15+} fraction. The secondary cracking of these fractions starts at 445°C (0.7 K/min). The formation of the C_1-C_5 fraction (whole gas), primary and the secondary gas formation are presented in Fig 135. The secondary gas formation was calculated from measured formation rates using the method described by Dieckmann *et al.* (1998).

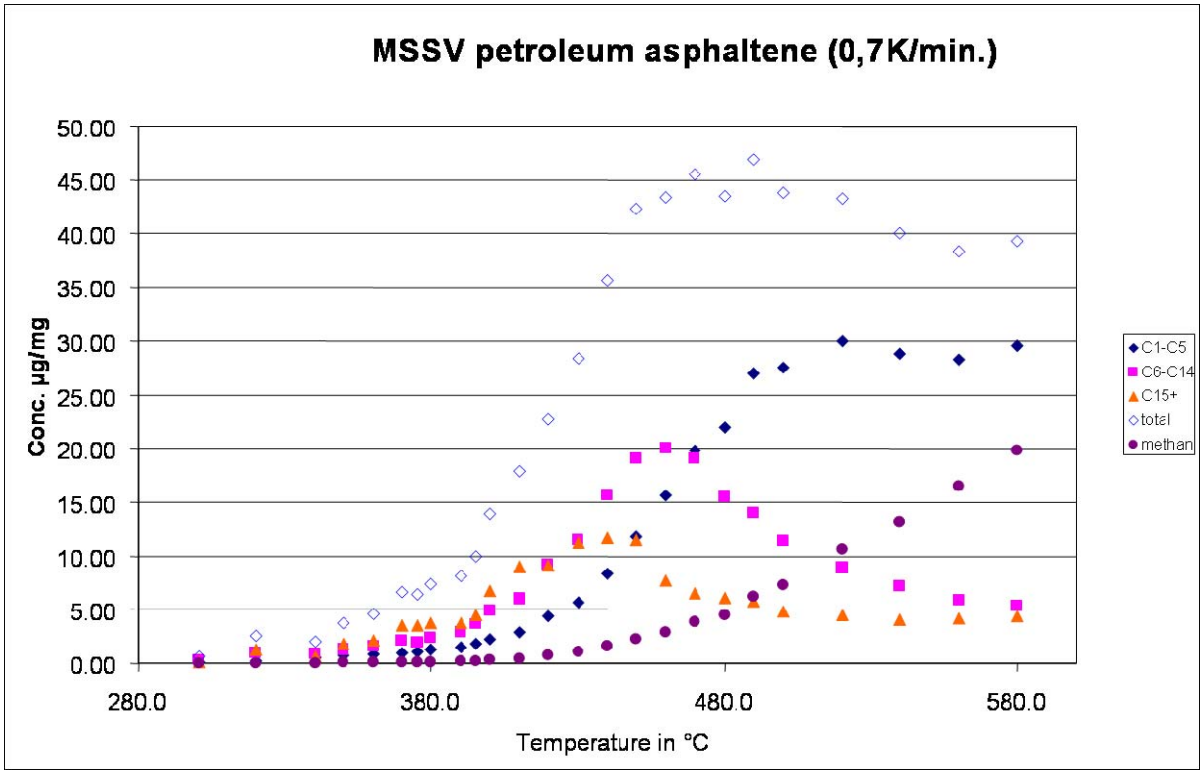

Fig 134 Total concentrations of hydrocarbon fractions for a heating rate of 0.7 K/min of MSSV-analysis of an oil asphaltene from the Duvernay Formation.

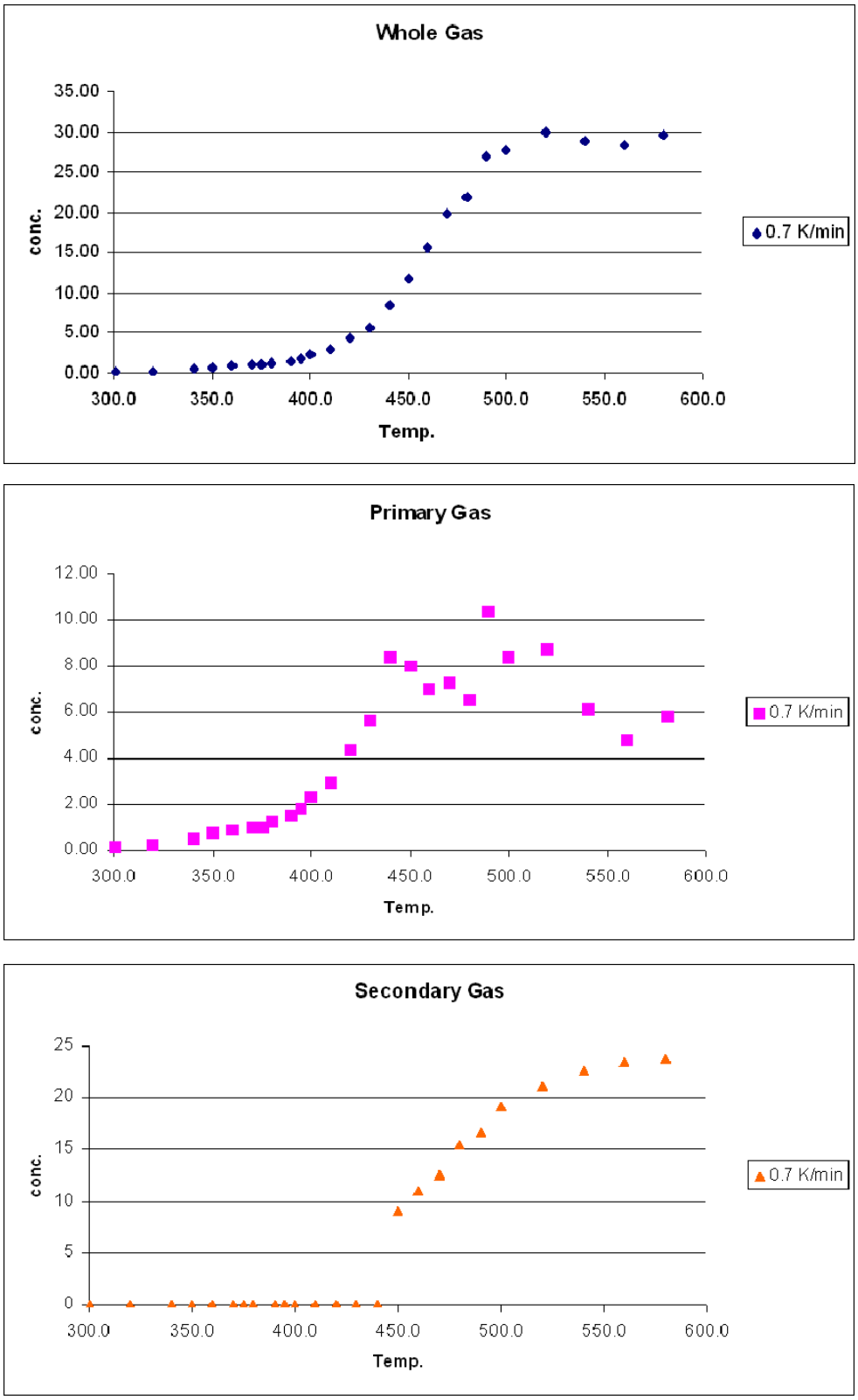

Fig 135 The formation of the C_1-C_5 fraction (whole gas), primary and the secondary gas formation for one heating rate.

8.4.3 Comparison of asphaltene MSSV pyrolysates with natural oils

Fig 136 shows the diagram of the ratios of pri/*n*-C_{17} and phy/*n*-C_{18} after Peters *et al.* (1999) for oil asphaltene and kerogen pyrolysates (0.7 K/min.) and natural oils from Duvernay. The MSSV data on the Duvernay kerogen are taken from Dieckmann (1998). The crude oils show a clear trend of decreasing pri/*n*-C_{17} and phy/*n*-C_{18} with increasing API gravity. The asphaltene as well kerogen pyrolysates show a simulated maturity trend of decreasing ratios with increasing thermal stress. Remarkable is that products from MSSV-analysis of Duvernay source rocks show different ratios of pri/*n*–C_{17} vs. phy/*n*–C_{18} than natural oils do. At low thermal stress kerogen pyrolysates demonstrate lower pri/*n*–C_{17} ratios than crude oils, whereas at high thermal stress this ratio increases, leading to a wrong facies prediction. This observation correlates to the characteristic of faster phytane decomposition for closed-system kerogen pyrolysates at high temperatures reported by Tang and Stauffer (1995). But, this is not observed for the Duvernay oil asphaltene pyrolysates. These show very similar pri/*n*–C_{17} and phy/*n*–C_{18} ratios as found for the natural oils. They plot along the same straight line, which allows the use for correlation as facie indicator. Nevertheless, it is remarkable that crude oils have higher amounts of pristane and phytane relative to asphaltene pyrolysates from MSSV, which might be related to the differences of natural and artificial heating rates.

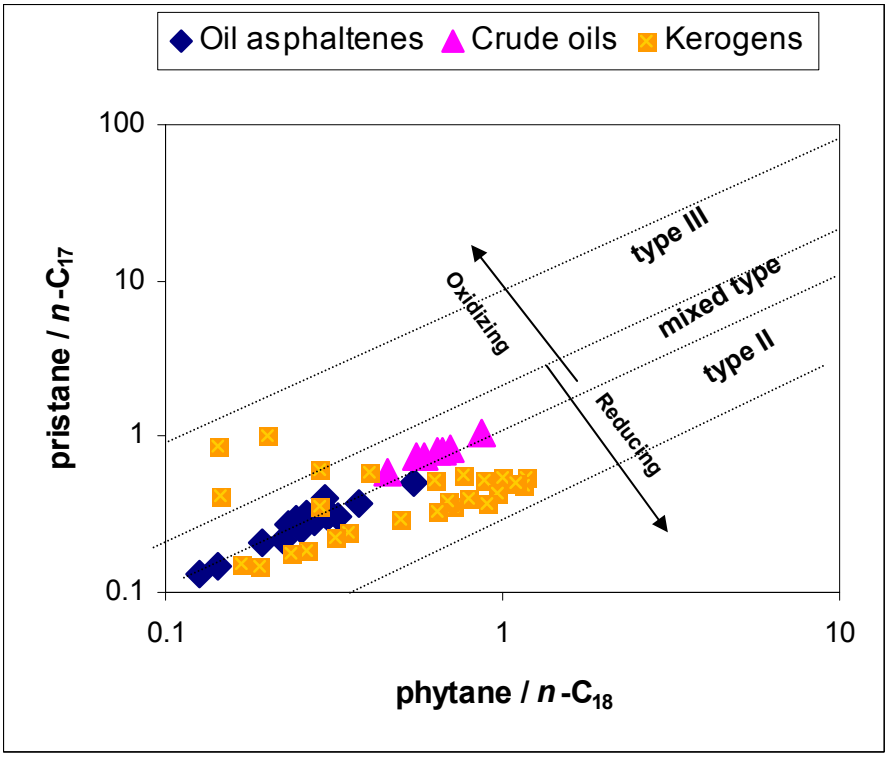

Fig 136 Diagram with the ratios of pristane/*n*-C_{17} versus phytane/*n*-C_{18} for MSSV asphaltene and kerogen pyrolysates (both at 0.7K/min) in comparison to natural oils from the Duvernay Petroleum System (after Peters *et al.* , 1999).

8.4.4 Comparison of MSSV pyrolysates of oil asphaltenes and kerogens

A comparison of artificial formed hydrocarbons from the Duvernay oil asphaltene and source rock kerogen in terms of aromaticity and gas generation show the same characteristics described before for MSSV pyrolysates from Southern Italy. In the following this is shown for the structural moieties, like *n*-alkyl chain length distribution, the generation of primary and secondary gas, and aromaticity of formed hydrocarbons.

Fig 137 shows the ternary diagrams of *n*-alkyl-chain distribution for MSSV pyrolysates from the Duvernay oil asphaltene compared to MSSV pyrolysates from the kerogen for a heating rate of 0.7 K/min. For both the hydrocarbon generation starts with the enrichment of *n*-C_6-C_{14} and *n*-C_{15+} compounds. But products from asphaltenes reaches total maximum amounts of *n*-C_6-C_{14} of 30% and total maximum amounts of *n*- C_{15+} of 20%, whereas products from kerogen show lower maximum yields of these compound classes. With increasing temperatures the samples plot along the axis in direction to the *n*-C_1-C_5 fraction. With the ratio of (C_1-C_5)/(C_6-C_{14}) versus temperature it is confirmed that kerogen MSSV pyrolysates are more gas prone than the asphaltene pyrolysates from an immature crude oil (Fig 138). Below, the Fig 138b shows the ratio of C_1/(C_2-C_5) versus temperature for products from asphaltene and kerogen. The gas formation of kerogens is dryer than pyrolysates from oil asphaltenes at lower thermal stress of 320-430°C (0.7K/min). With increasing MSSV temperature the pyrolysates of kerogen and asphaltene are similar in terms of gas wetness, up to 540°C (0.7K/min), where kerogen pyrolysates show again the formation of dryer gas.

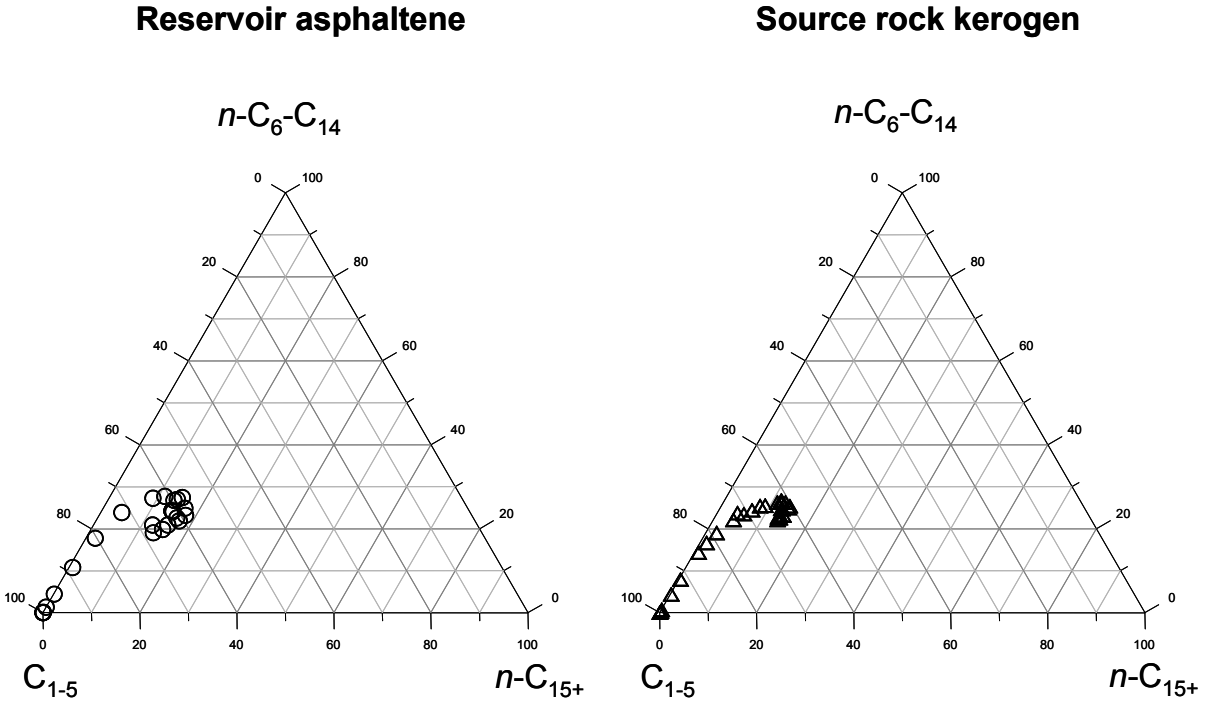

Fig 137 Ternary diagrams of *n*-alkyl-chains for MSSV pyrolysates of the oil asphaltene compared to MSSV pyrolysates from the kerogen for a heating rate of 0.7 K/min.

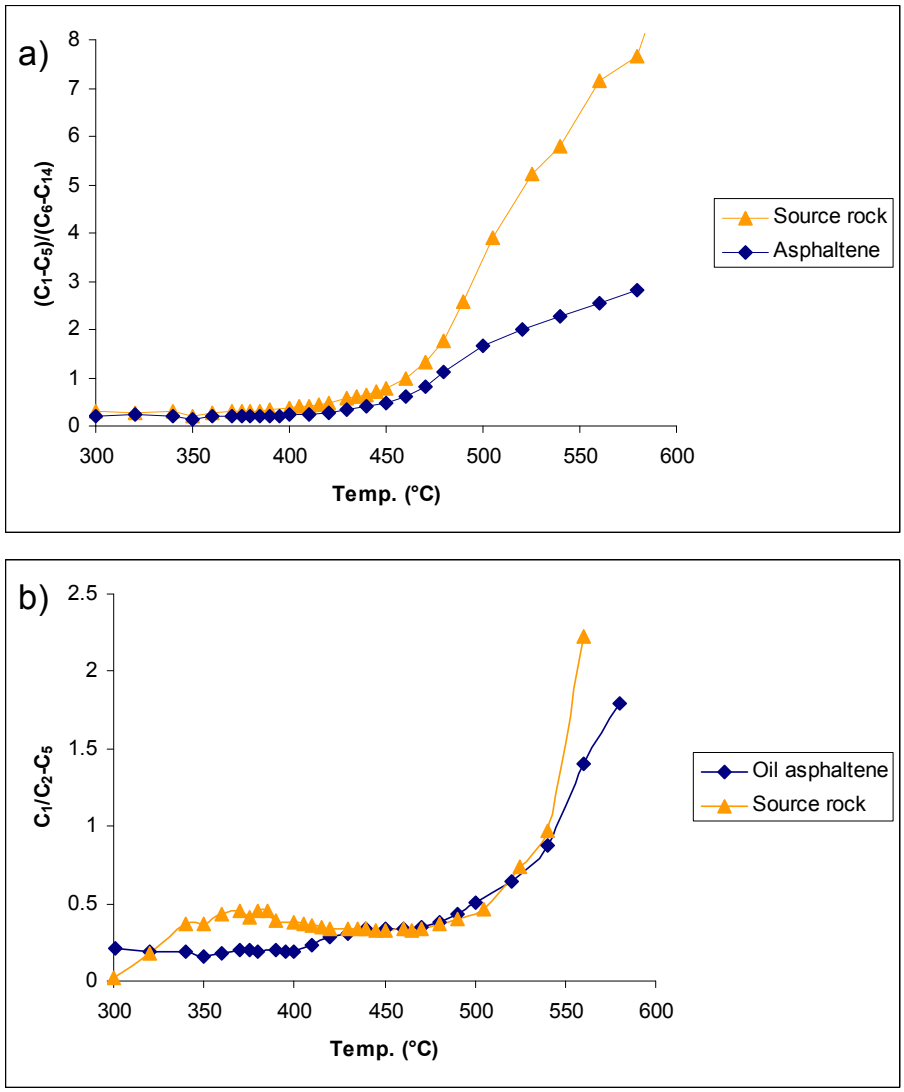

Fig 138 a) The ratio of $(C_1\text{-}C_5)/(C_6\text{-}C_{14})$ versus temperature for hydrocarbons formed from kerogen and from the Duvernay oil asphaltene, and b) the ratio of $C_1/(C_2\text{-}C_5)$ versus temperature for asphaltene and kerogen MSSV pyrolysates.

A comparison of MSSV pyrolysates from the oil asphaltene and the kerogen from Duvernay in terms of primary and secondary gas formation is shown in Fig 139. It can be seen that primary gas formation from Duvernay asphaltenes starts slightly earlier than from the source rock sample, while timing of secondary gas formation from asphaltenes and source rock kerogens seems to be identical under laboratory conditions.

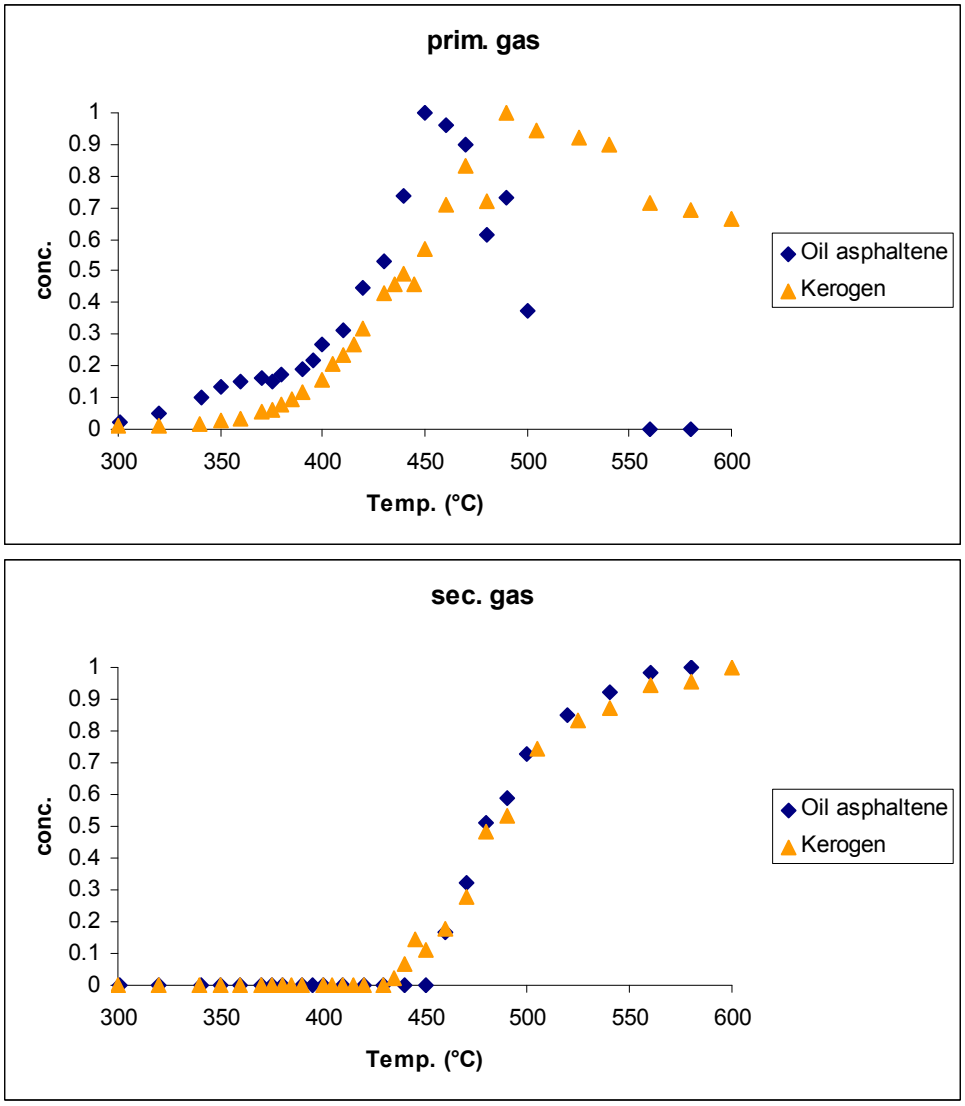

Fig 139 Primary and secondary gas formation obtained from oil asphaltene and kerogen MSSV pyrolysates at a heating rate of 0.7K/min.

Fig 140a illustrates the ratio o-xylene/*n*-C_9 calculated from asphaltene and source rock MSSV pyrolysates. Hydrocarbons formed from source rock kerogens are more aromatic relative to hydrocarbons formed from the oil asphaltene. This is supported by the ratio of 1,2,3,4-

tetramethylbenzene / (n-C_{11} + n-C_{12}) shown in Fig 140b. These observations are in consistency with results achieved by open-system-pyrolysis.

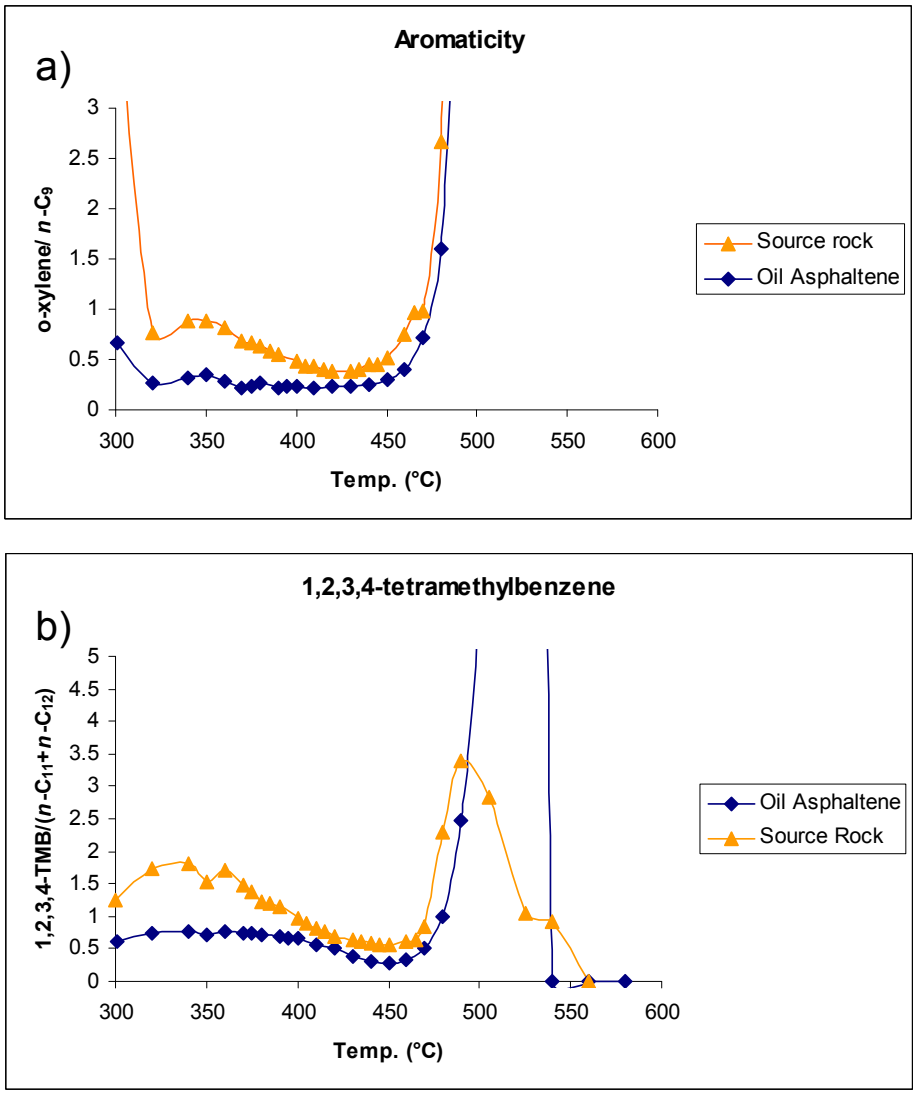

Fig 140 The ratio of o-xylene/n-C_9 calculated from asphaltene and source rock MSSV pyrolysates, and b) the ratio of 1,2,3,4-tetramethylbenzene / (n-C_{11} + n-C_{12}) for hydrocarbons formed from the asphaltene and the source rock kerogen.

8.4.5 Conclusions

- The pyrolysates from artificial maturity experiments on Duvernay petroleum asphaltenes show lower aromaticity than products from source rock kerogens, which confirm the results from Southern-Italy.

- Hydrocarbons formed from asphaltenes are enriched in *n*-C_6-C_{14} and total maximum of *n*- C_{15+}, whereas hydrocarbons formed from kerogens show lower maximum yields of these compound classes. In contrast kerogen products are more gas prone than the asphaltene from an immature crude oil.

- The GOR of hydrocarbons formed from the asphaltene is much lower than that formed from the kerogen. As well, MSSV pyrolysates of asphaltenes and kerogens differ in terms of the gas wetness in that gas formed from kerogens is generally dryer at low and at high thermal stress. Primary gas formation from Duvernay asphaltenes starts slightly earlier than from the source rock sample, while timing of secondary gas formation from asphaltenes and source rock kerogens seems to be identical under laboratory conditions.

- The products from artificial maturity experiments on petroleum asphaltenes show higher similarity to natural oils in terms of pristane and phytane ratios, which allows facies correlation.

9 Characterization of asphaltenes from a deltaic sequence

9.1 Bulk kinetic parameters

9.1.1 Kinetic parameters

We applied asphaltene kinetics from one Nigerian sample (G000506 API 21.1°) to predict geological peak hydrocarbon generation and compared resulted $Tmax_{geol}$ with data from literature. Due to high contents of high wax compounds, it was not possible to evaluate kinetic parameters for all asphaltenes isolated with *n*-hexane at room temperatures from the Nigerian oils. Only the most biodegraded oil sample (G000506 API 21.1°) contained enough asphaltenes isolated with hot *n*-heptane for reasonable asphaltene kinetics and resulting geological predictions. The bulk kinetic parameters calculated for this selected oil asphaltene sample G000506 (API 21.1°) is shown in Fig 141. The Emean calculated for that asphaltene sample was calculated to be 54 kcal/mole associated with a frequency factor of 9.79E+13 s^{-1}. The activation energies lower than 53 kcal/mole and higher than 56 kcal/mole were eliminated to avoid contamination risk due to occluded maltenes or waxy compounds following the approach proposed by di Primio *et al.* (2000). Organic matter from type II/III or type III displays normally a much broader activation energy distribution. Occluded material will probably have an impact on the activation energy distribution. One indication may be the presence of a bi- or polymodal activation energy profile, with energy highs beside the maximum of Emean, which in turns exert influence the calculated geological predictions, resulting in improbable low prediction for peak hydrocarbon generation and onset temperatures. Samples with a polymodal activation energy distribution were thus not used for kinetic investigations. Because the major focus of this study was on the Emean and peak hydrocarbon generation rather than on the full distribution of activation energies, the elimination of the low and high end activation energy potentials from the kinetics is therefore

favorable to calculate geological peak hydrocarbon generation without the risk of impact due to contamination. The risk of contamination and the consequences for kinetic parameters are illustrated by Geng and Liao (2002). These authors reported very unusual activation energy distributions and frequency factors for asphaltenes precipitated from different petroleum types. Some of the kinetics result in laboratory hydrocarbon generation curves which cannot be correct, because they describe temperatures which are more common for bitumen evaporation rather than from cracking reactions in macromolecular organic matter.

The computed peak hydrocarbon generation rate curve for geological predictions show a $Tmax_{geol}$ of 145°C for the oil asphaltene sample G000506 (Fig 141).

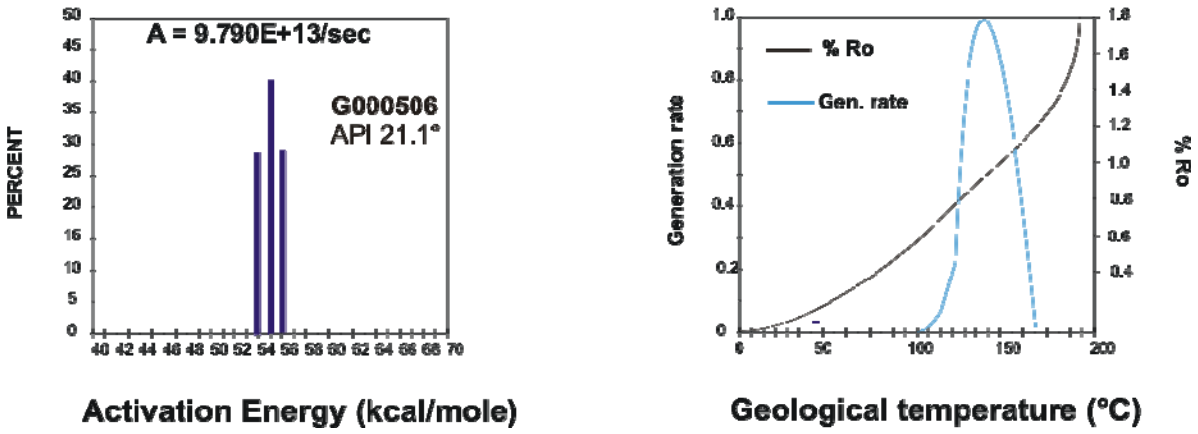

Fig 141 Activation energy distribution (Ea) and the frequency factor (A) calculated for selected petroleum asphaltene from Nigeria (left), and calculated peak hydrocarbon generation rate curve for geological prediction (right).

9.1.2 Discussion on predicted geological temperatures for Nigeria onshore

Since the exact location of studied samples is not known, it is difficult to correlate the measured peak hydrocarbon generation obtained from the oil asphaltene with data for hydrocarbon formation in Nigeria from literature. The oil generation in the Niger delta system

is very complex with local variations of temperature, burial history, and deformations related to tectonic effects (Beka and Oti, 1995). Additionally, in the northern part of the Benue trough potential source rocks have experienced thermal pulses due to cretaceous and tertiary volcanism (Ehinola *et al.*, 2005). Evamy *et al.* (1978) set the top of the present-day oil window in the Niger Delta at the 115° C isotherm. In the north-western portion of the delta, the oil window lies in the upper Akata Formation and the lower Agbada Formation (Tuttle *et al.*, 1999). To the southeast, the top of the oil window is stratigraphically lower (up to 4000' below the upper Akata/lower Agbada sequence) (Evamy *et al.*, 1978). Some researchers (Nwachukwu and Chukwura, 1986; Stacher, 1995) attribute the distribution of the top of the oil window to the thickness and sand/shale ratios of the overburden Benin Formation and variable proportions of the Agbada Formation. As an illustration the average cross-section through the Nigeria delta is presented in Fig 142.

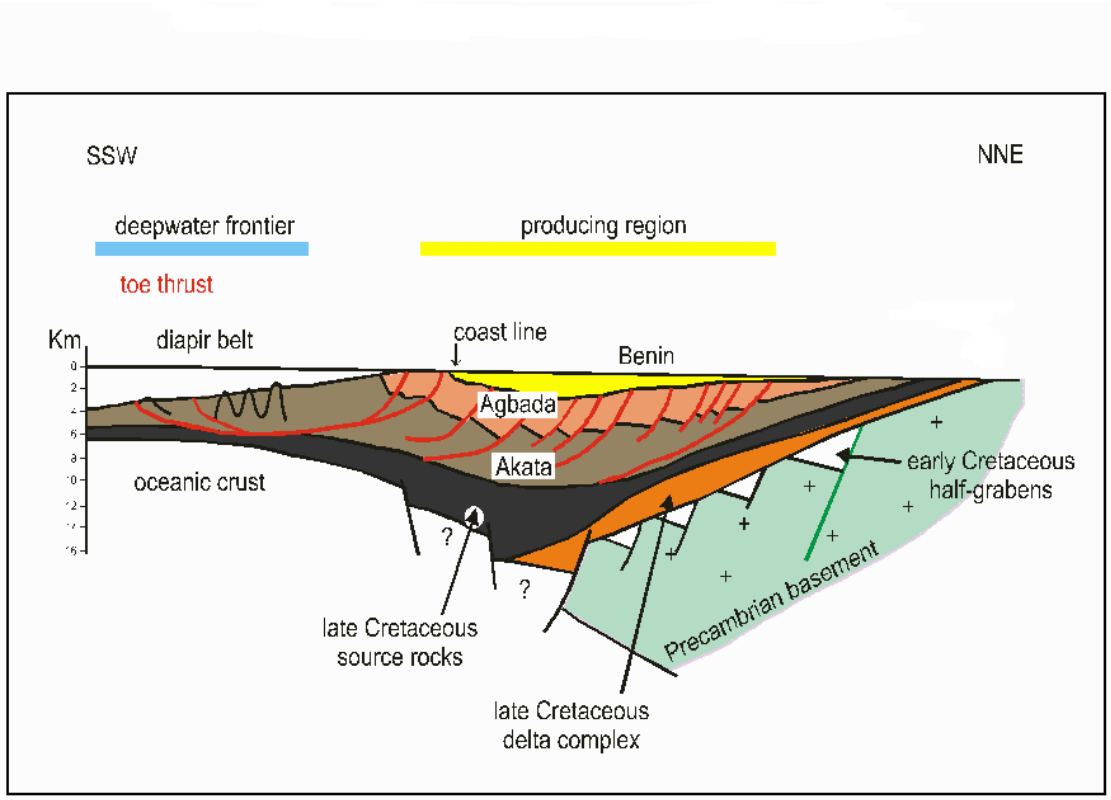

Fig 142 Averaged cross-section through the Niger delta (after Thomas (1995)).

The sandy continental sediment of the Benin Formation has the lowest thermal gradient (1.3 to 1/8°C/100 m); the paralic Agbada Formation has an intermediate gradient (2.7°C/100 m); and the marine, over-pressured Akata Formation has the highest (5.5°C/100 m) (Ejedawe *et al.*, 1984)

Fig 143 shows a burial history chart after Tuttle *et al*. (1999), modified from Ekweozor and Daukoru (1994) for the Oben-1 well, located 80 km northeast the town Port Harcourt in the northern portion of the delta. In the late Eocene, the Akata/Agbada formational boundary in the vicinity of this well entered the oil window at approximately 0.6 R_o (Stacher, 1995) and temperatures of 115°C (Evamy *et al.*, 1978). The Akata/Agbada formational boundary in this region is currently at a depth of about 4,300 m, with the upper Akata Formation in the wet gas/condensation generating zone (vitrinite reflectance value >1.2; (Tissot and Welte, 1984)). The lowermost part of the Agbada Formation here entered the oil window in the Late Oligocene.

The measured peak hydrocarbon generation at $Tmax_{geol}$ 145°C obtained from asphaltene kinetics would - with regard to the presented area of Oben-1-well - refer to the lower part of the Agbada Formation as potential source rock. This correlates with the high abundance of oleanane derived from angiosperms in studied crude oils, which type to a source younger than mid-cretaceous (Tuttle *et al.*, 1999). Peak hydrocarbon generation for those oils would have occurred at the boundary of Oligocene/Miocene and in depths of 3500 m, based on the projected burial curve in Fig 143. Additionally, Mosto Onuoha and Ekine (1999) published the subsurface temperatures and heat flow of various wells in the Anambra Basin of Nigeria onshore. They showed that subsurface temperatures in Nigeria onshore vary to a great deal, depending on well site, burial and the hydraulic flow systems in the basin. Several wells in the Anambra Basin provide temperatures of less than 120 °C in depths of 3500 – 4000 m,

indicating that source rocks are very immature. But, some wells in the western part of the basin showed temperatures of 140-155 °C in depths of 3500-4000 m at the Akata/Agbada boundary. A calculated peak hydrocarbon generation for geological temperatures at 145°C in Nigeria onshore seems therefore be realistic.

In addition, biomarker maturity parameters of crude oils showed an early to near peak hydrocarbon generation corresponding to vitrinite reflectance values of about 0.75 percent for studied oils, which correlates also to the lower Agbada Formation in the western part of the Anambra Basin.

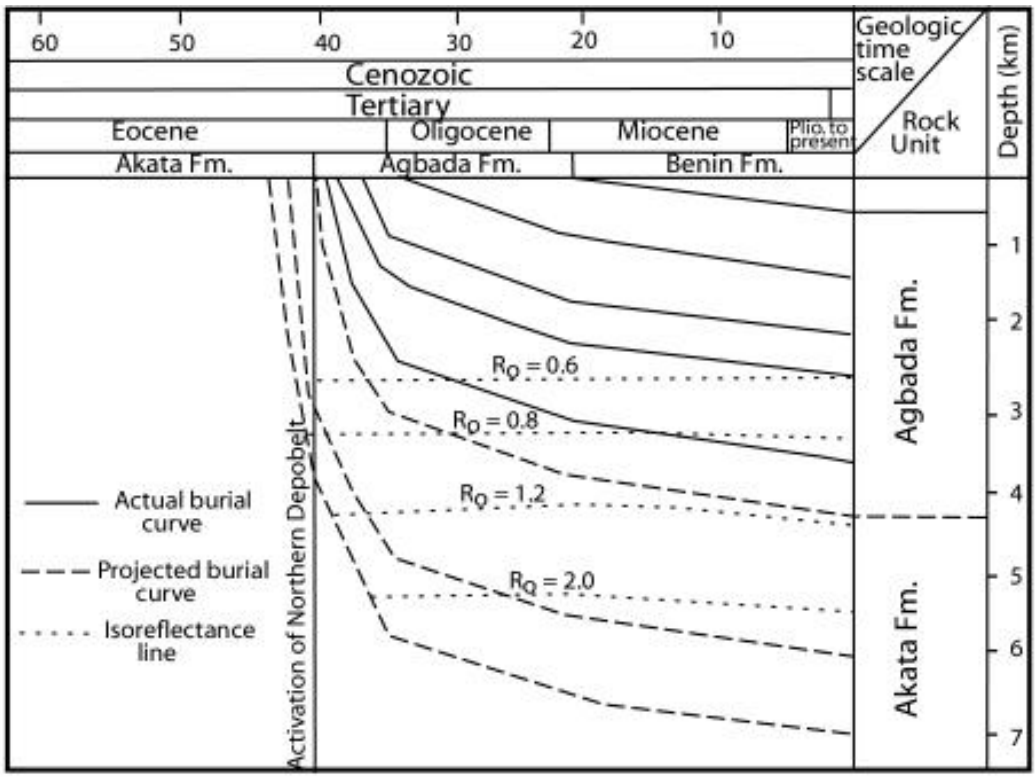

Fig 143 Burial history chart for the northern portion of the Niger Delta. Data for the Oben-1 well (Tuttle *et al.*, 1999).

9.2 Pyrolysis

9.2.1 Composition of pyrolysates

Fig 144 shows selected chromatograms of open-system-pyrolysis GC experiments on oil asphaltenes. All the illustrated samples increase in API gravity of related oils from the top to the bottom of the relevant figure. The great similarity of asphaltene pyrolysates from this sample set cite to the same origin of investigated oils. The reservoir asphaltenes are extraordinary in that they contain alkane/-ene duplets even higher than *n*-C_{40} derived from land plant input (Peters *et al.*, 2005).

Most important aromatic hydrocarbons in asphaltene pyrolysates are C_1-C_2 alkylbenzenes, with a dominance of styrene and toluene. As well, those pyrolysates contain alkylphenols in low quantities, which are indicative for vitrinitic terrestrial organic matter (Larter and Senftle, 1985). Alkylthiophenes are absent in these pyrolysates, which cite to very low organic sulphur content in petroleum asphaltenes isolated from the Nigerian crude oils.

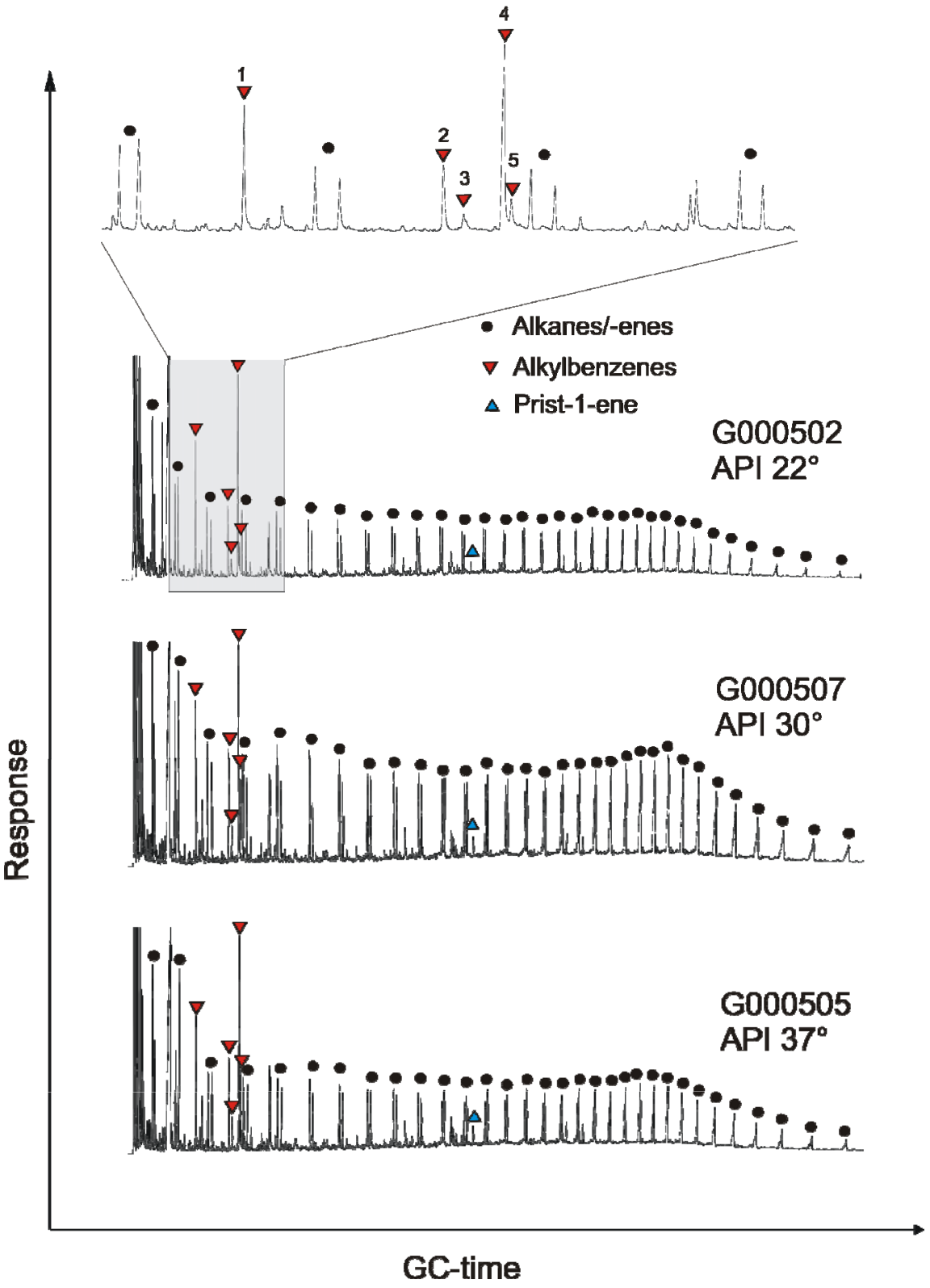

Fig 144 Selected chromatograms from open-system pyrolysis GC for petroleum asphaltenes from Nigeria. Alkane/-ene doublets and alkylbenzenes are marked. Alkylbenzenes are corresponding to retention time from left to the right: toluene (1), ethylbenzene (2), m,p-xylene (3), styrene (4), and o-xylene (5).

9.2.2 Aliphatic hydrocarbons

The asphaltenes show distinct even over odd carbon numbered preference of alkane/-ene duplets in the range of *n*-C_{12} to *n*-C_{22}, which normally suggest high thermal maturity. This observed even-predominance related to thermal maturity is also proved by high API gravities (API up to 41°). But it is also known that odd or even carbon numbered preference of alkanes in this range can be affected by organic matter input (Hatch *et al.*, 1987; Peters *et al.*, 2005). A further characteristic feature of studied oil asphaltenes is that they show increasing amount of *n*-alkane duplets higher than *n*-C_{22} as a result of terrestrial input (Tissot and Welte, 1984). This increasing content of *n*-alkanes higher than *n*-C_{22} was already observed in the crude oils, but is stronger marked in asphaltene pyrolysates. In comparison to whole oil characteristics, the isolated asphaltenes do not exhibit a peak in *n*-C_{22}, as well as a slight predominance of odd over even carbon number alkanes is only observed in the range between *n*-C_{25} and *n*-C_{29}. A similar predominance of *n*-alkanes in that range has been documented in pyrolysates of terrigenous organic matter from other fluviodeltaic environments (van de Meent *et al.*, 1980; Thomas, 1982; Kelley *et al.*, 1985; Dong *et al.*, 1986), but has also be found in pyrolysates of algal kerogens (Goth *et al.*, 1988; Horsfield *et al.*, 1994) and in biopolymers from lower and higher plants as well as bacteria (Chalansonnet *et al.*, 1988; Fukushima *et al.*, 1989; van Bergen *et al.*, 1994).

The alkane / alkene ratio of doublets in asphaltene pyrolysates from Nigeria shows a predominance of alkane up to *n*-C_{15}. For doublets of higher carbon number all asphaltene pyrolysates illustrate a predominance of alkenes.

Fig 145 shows the *n*-alkyl-chain distribution after Horsfield (1989) of investigated pyrolysates from Nigerian oil asphaltenes. The plot of the oil asphaltenes predict to source depositional environment which generate high-wax P-N-A-oils or paraffinic oils. The high-wax, paraffinic-naphtenic-aromatic (P-N-A) crude oil generating facies usually occurs in lower

delta plain and inner shelf environments and commonly intercalates with the high-wax paraffinic oil generating facies (Horsfield, 1997), The P-N-A oil facies is as well characteristic for many tertiary coals from Southeast Asia and Australia (Kelley *et al.*, 1985; Horsfield, 1989, 1997). Most asphaltenes from Nigeria plot in the field of the high-wax, paraffinic crude oil generating facies, which was originally defined using pyrolysates of lacustrine environments (Horsfield, 1989). This changes between high-wax P-N-A-oils or paraffinic oils obtained from alkane /-ene distribution of oil asphaltenes is probably resulted from facies inhomogenities (Fig 146). The amount of the *n*-C_6-C_{14} fraction for all oil asphaltenes is nearly similar, whereas the main difference is related to the amount of the *n*-C_{15+}, or respectively the C_1-C_5 fraction.

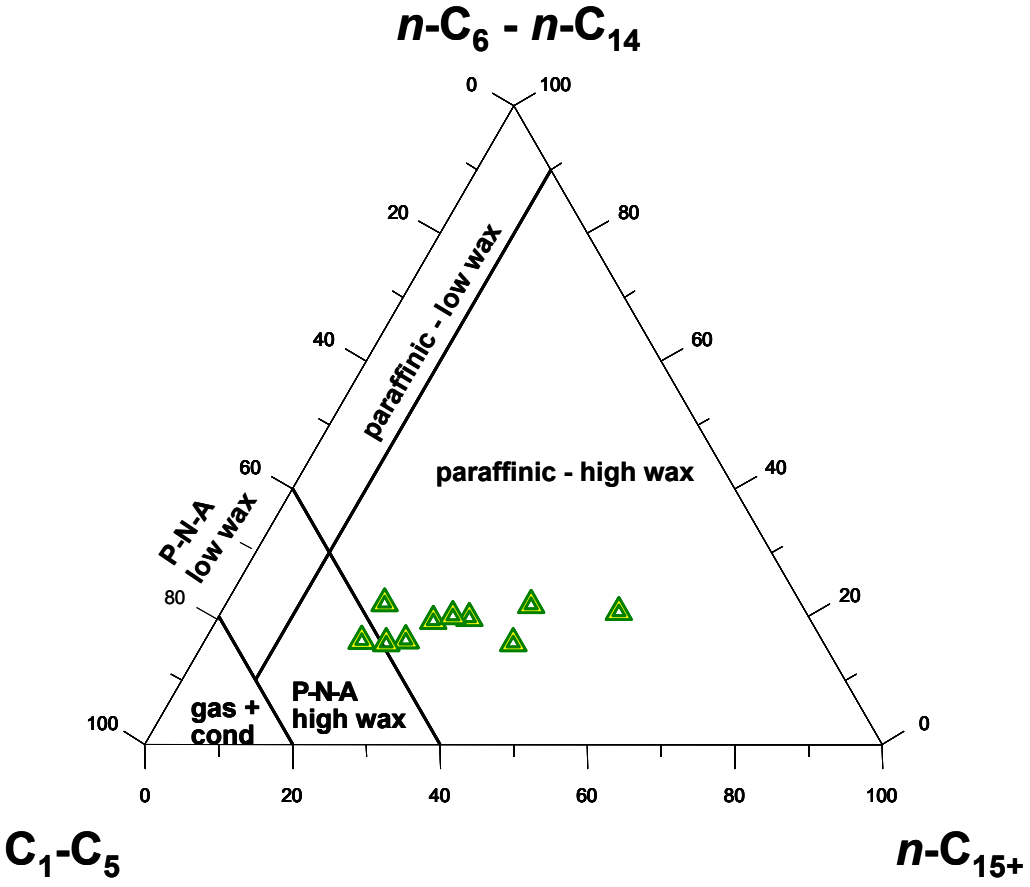

Fig 145 Alkane/alkene distributions after Horsfield (1989) of investigated pyrolysates for the Nigerian asphaltene samples.

Fig 146 shows the three different plots with the ratio C_1-C_5 / *n*-C_{6+} attained from the alkane/alkene distribution of oil asphaltenes pyrolysates versus a) the API gravity of related oils, b) the ratio pristane / *n*-C_{17} of related oils, and c) the sterane ratio of αααC_{29} / ααα(C_{27} + C_{28} + C_{29}) measured in related oils.

As it can be seen from Fig 146, there is no observed trend for the alkane / alkene distribution of asphaltene pyrolysates with increasing or decreasing API-gravity. As well, this distribution shows no trend with the ratio of pristane / *n*-C_{17} of related oils. That ratio was chosen to investigate if the redox potential of the environmental deposition has an impact on the alkane/-ene distribution of asphaltene pyrolysates. More oxic conditions are better indicated by this pristane ratio than by the ratio using phytane as shown for Nigerian oils in Fig 49. The pristine / *n*-C_{17} ratio for less degraded oils is very similar, pointing to identical redox conditions of environmental deposition for the studied samples. Such a trend of alkane distribution of pyrolysates and oxicity was for example published by Sachsenhofer *et al*. (1996), who studied kerogen pyrolysates of late cretaceous lacustrine shales of the Eastern Alps. In contrast, alkalinity for example is proposed to have no effect on the alkane/-ene distribution of pyrolysates, like published by Horsfield *et al*. (1994), who investigated freshwater and alkaline lacustrine sediments of the Green River Formation. Fig 146c shows a good correlation of alkane/-ene distribution from asphaltene pyrolysates with the biomarker parameter αααC_{29} / ααα(C_{27} + C_{28} + C_{29}) of related petroleums. That correlation is at least very good for less degraded oils, since asphaltenes from stronger biodegraded oils have probably been more affected by a contamination, which will be discussed in the follow. From Fig 146c it is obvious that the ratio C_1-C_5 / *n*-C_{6+} of asphaltene pyrolysates decreases with decreasing ratio of αααC_{29} / ααα(C_{27} + C_{28} + C_{29}) of related less degraded oils. This illustrates facies variations, which control the alkane/-ene distribution of oil asphaltenes, and supports as well facies differences of source rocks in the deltaic environment.

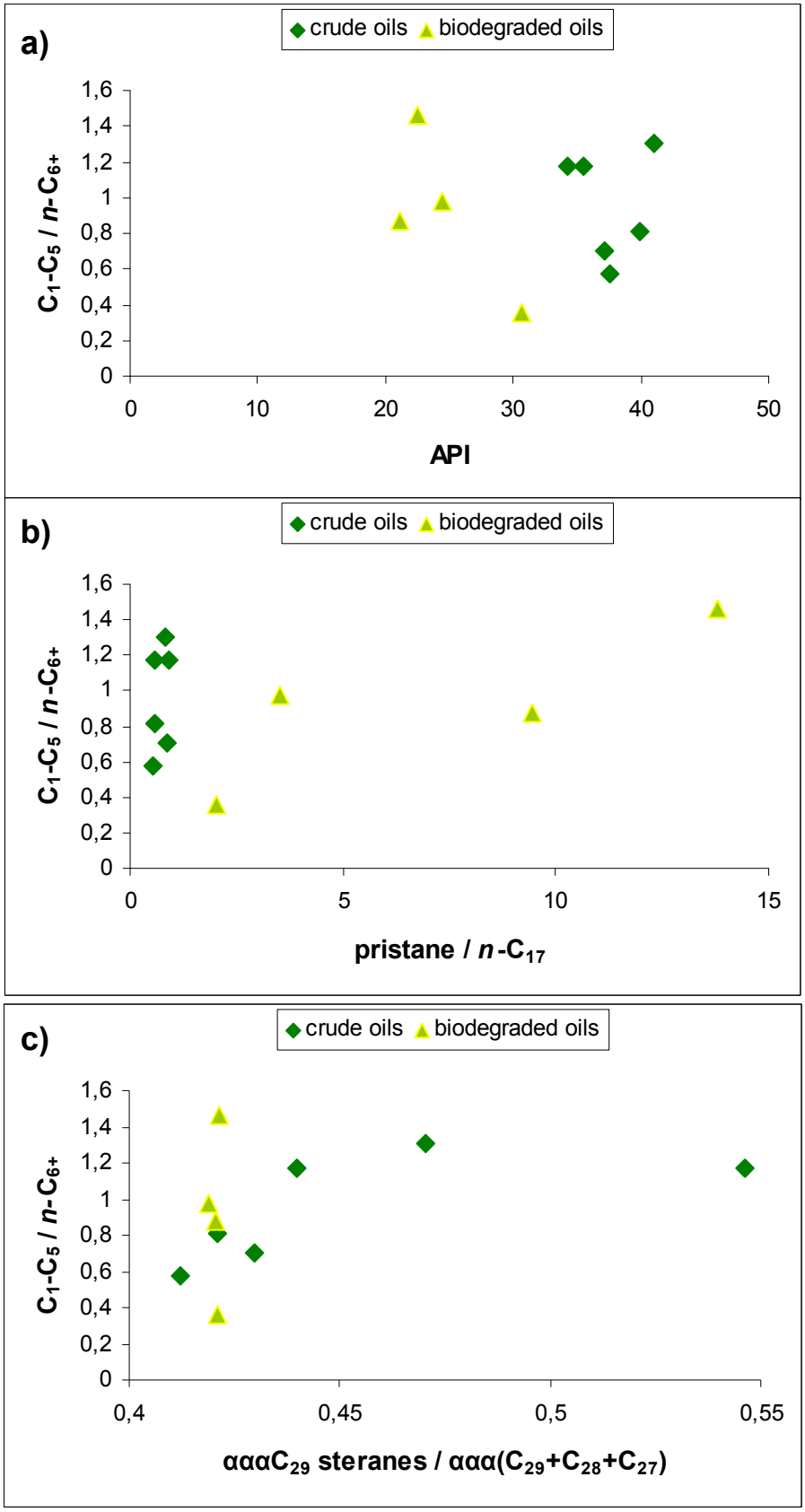

Fig 146 The ratio C_1-C_5 / *n*-C_{6+} of oil asphaltenes pyrolysates versus a) the API gravity of related oils, b) the ratio pristane / *n*-C_{17} of related oils, and c) the ratio of $\alpha\alpha\alpha C_{29}$ steranes / $\alpha\alpha\alpha(C_{27} + C_{28} + C_{29})$ measured in related oils.

In addition, from Fig 146c it is also evident that asphaltenes isolated from crude oils sourced from organic matter with higher terrestrial input show higher gas potential. This illustrates that structural moieties, like alkane distribution obtained from oil asphaltene pyrolysates, can typify basic gas generation potential of parent deltaic source rocks.

9.2.3 Aromatic hydrocarbons

Fig 147 shows the ratio of aromatic compounds / *n*-C_{6+} versus the API gravity for reservoir asphaltenes and natural oils from Nigeria. The natural oils show higher aromaticity than related reservoir asphaltenes. This is in contrast to the observations on samples from Italy, and can be in part cited to the precipitation method used for the isolation of asphaltenes from the Nigerian crude oils (see also Fig 68, p. 144). Additionally, it was shown in Fig 56, p. 120, that some oils from Nigeria have experienced evaporitic fractionation, which increases the aromaticity of those oils.

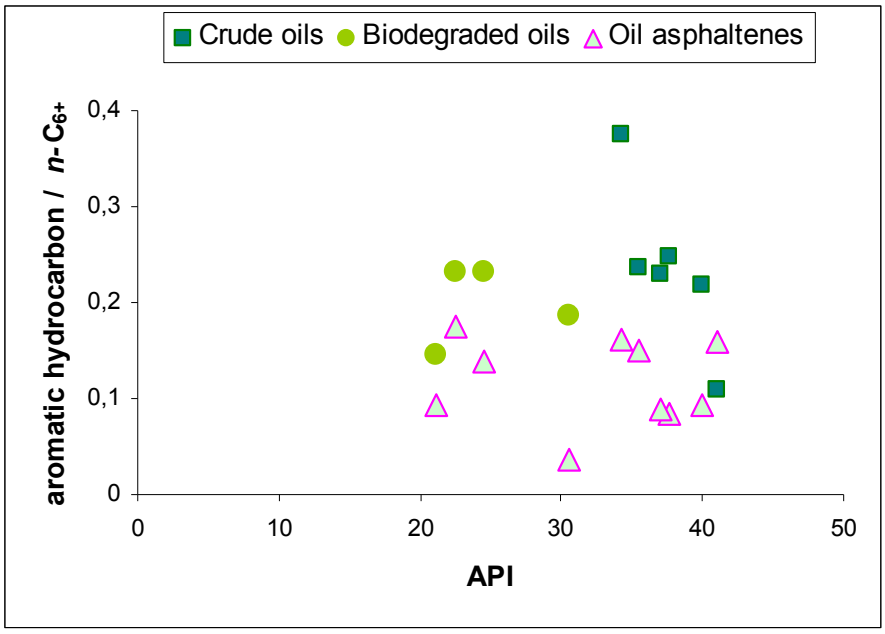

Fig 147 Ratio of aromatic compounds / *n*-C_{6+} versus the API gravity for reservoir asphaltenes and natural oils for the samples from Nigeria.

All pyrolysates of investigated asphaltenes from Nigeria show high yields of styrene (Fig 144). The origin of styrene in pyrolyzed organic matter is often attributed to land plant precursors, such as lignin (Li *et al.*, 2003; Dignac *et al.*, 2005) or monoterpenes derived from spores and pollen (Fabbri *et al.*, 2002). But, styrene is ubiquitous in pyrolysates, for that linking styrene to a specific precursor should be undertaken with caution. As well, high concentrations of styrene can arise by a contamination with synthetic polymers (Dignac *et al.*, 2005), which occur for example in sampling and storing repositories or in some drilling fluids (Darley and Gray, 1988). The high yields of styrene in asphaltene pyrolysates might therefore only be in part, if ever, indicative for terrestrial organic matter. As well, monoterpenes derived from spores and pollen are trace compounds in crude oils (Bauer *et al.*, 1983), and thus unlikely the source of such high yields of styrene in asphaltene pyrolysates.

9.2.4 Discussion on evidence of contamination

The unusual high yields of styrene within all oil asphaltene pyrolysates point to a probable contamination of asphaltenes. This was supported by a study of non-isothermal-closed-system-pyrolysis-GC (MSSV) of thermally extracted oil asphaltenes. Chromatograms of this study showed unusual high yields of various alkylbenzenes, such as methylstyrene, propylbenzene, and ethylmethylbenzenes, especially at lower thermal stress. Horsfield (1984) reported that for example methylstyrene can occur in pyrolysates of coal macerals, but normally with lower abundance than found in Nigerian oil asphaltene pyrolysates, which show at low temperatures total yield of methylstyrene even higher than those of xylenes or

toluene. Larter and Senftle (1985) described a similar high abundance of styrene and methylstyrene in pyrolysates of polystyrene, which they used as internal polymeric standard for their quantitative pyrolysis-GC studies. A comparison of the distribution of those alkylbenzenes in hydrocarbons formed from Nigerian oil asphaltenes with the alkylbenzene distribution from pyrolysates of synthetics (McNeill *et al.*, 1998; Yoshioka *et al.*, 2000; Kim, 2001; Liou, 2003; Dignac *et al.*, 2005) show indeed high similarities. Polystyrene and also polyvinyl-containing synthetics show up on pyrolysis high amounts of styrene, methylstyrene and ethylmethylbenzenes, as well as the occurrence of propylbenzene, butylbenzene, and ethylxylenes, just as found in pyrolysates of Nigerian oil asphaltenes. This alkylbenzene distribution of oil asphaltene pyrolysates point thus to a contamination of those asphaltenes with a synthetic material. Since all asphaltenes demonstrate this alkylbenzene distribution, it is unlikely that the contamination has occurred during the precipitation procedure of these asphaltenes from Nigerian oils. It is more likely that crude oils are already "contaminated" for example with synthetic drilling fluids (Darley and Gray, 1988), synthetic antifoulants to control microbial growth in crude oils (Demirbas, 2002), or dispersants to avoid asphaltene precipitation in the well bore (Mansoori, 1995). Especially dispersants have a strong association with the asphaltene fraction in crude oils, because they work by surrounding the asphaltene molecules similar to natural resins (Mansoori, 1995). During the precipitation of asphaltenes from these oils with generally low asphaltene contents, the synthetic material is concentrated in the isolated asphaltenes.

For the previous discussed bulk kinetic analysis this contamination might not have greater impact, since the hydrocarbon prediction focussed on Emean calculated for that asphaltene sample, which is certainly referred to the organic matter. The activation energies lower than 53 kcal/mole and higher than 56 kcal/mole were eliminated to avoid contamination risk.

As well the alkane/alkene distribution in asphaltene pyrolysates seems not to be affected by contamination. Polysynthetics generate only low amounts of aliphatic structures during thermal decomposition (Dignac *et al.*, 2005). Additionally, their pyrolysates show a very high predominance of alkenes (Kim, 2001), but the alkane/alkene doublets of asphaltene pyrolysates do not reflect this characteristic. This is also explained by the decomposition characteristics of synthetics. Polystyrene- and polyvinyl-containing materials decompose at lower temperatures than 300°C, which is the temperature of thermal extraction of the asphaltenes. Aliphatic hydrocarbons formed from the synthetic material have probably been volatized during asphaltenes thermal cleaning, whereas aromatic structures built a tar-like residue after decomposition of synthetics (McNeill *et al.*, 1998). Probably this tar-like residue generates alkylbenzenes in high abundance during the pyrolysis of the asphaltenes.

For the further study on the compositional kinetic predictions from oil asphaltenes this contamination has to be taken into account. Especially, when considering that synthetics also generate high amounts of alkylphenols and alkylnaphthalenes, which are also found in MSSV-products of Nigerian oil asphaltenes

9.2.5 Conclusions

- Bulk kinetic measurements on one oil asphaltene sample predict peak hydrocarbon generation for geological temperatures of 145°C. This predicted temperature correlates with hydrocarbon generation for example in the western part of the Anambra Basin in Nigeria onshore.
- The *n*-alkyl-chain distribution after Horsfield (1989) of investigated pyrolysates from Nigerian oil asphaltenes predict the facies generating high-wax P-N-A-oils or paraffinic oils. The high-wax, paraffinic-naphtenic-aromatic (P-N-A) crude oil generating facies usually occurs in lower delta plain and inner shelf environments.
- The changes for facies recognition based on the *n*-alkyl chain length distribution of asphaltene pyrolysates correlates with facies changes due to variations of terrestrial input obtained from biomarker parameters of related crude oils.
- Oil asphaltene pyrolysates show lower aromaticity than related Nigerian crude oils.
- However, oil asphaltenes isolated from Nigerian crude oils show a clear evidence of being contaminated with synthetic material.

9.3 Compositional kinetic predictions from petroleum asphaltenes

For further studies we analysed asphaltenes from a strong biodegraded crude oil G000506 (API 21.1°) of the Nigerian sample set by MSSV. Due to the low amount of asphaltenes precipitated from the oils it was not possible to perform MSSV experiments on three full heating rates. For this reason two full heating rates of 0.2 and 5.0 K/min was measured while 8 tubes were artificially heated at 0.7K/min in order to verify the kinetic model.

9.3.1 Composition of MSSV pyrolysates

The MSSV pyrolysates of the thermally extracted Nigerian oil asphaltene show the presents of *n*-alkanes, aromatic hydrocarbons, alkylphenols, alkylnaphthalenes, as well as the isoprenoids pristane and phytane. Alkylthiophenes are also absent in oil asphaltene pyrolysates of MSSV pyrolysis.

Fig 148 - Fig 149 show GC traces for four experimental temperatures using a heating-rate of 5.0 K/min and 0.2 K/min. The oil asphaltene MSSV pyrolysates show relative low amounts of unresolved compounds compared to MSSV pyrolysates of asphaltenes from Duvernay and especially from Southern Italy. The generation of hydrocarbons formed from the Nigerian oil asphaltene starts at low thermal stress with the formation of *n*-C_{15+} alkanes, and with increasing temperatures the amount of *n*- C_{15+} decreases relative to alkanes of lower carbon number. Pristane and phytane formed from the Nigerian asphaltene are still generated at slightly higher temperatures than reported for the oil asphaltene from Southern Italy. For the

Nigerian asphaltene MSSV pyrolysates the generation of those compounds ended at 470°C for the heating-rate of 5.0K/min, and at 450°C for 0.2K/min. As well, the reservoir asphaltene pyrolysates show the occurrence of alkylnaphthalenes, which show increasing amount with increasing temperatures. Beside methylnaphthalenes, the pyrolysates show also dimethyl- and trimethylnaphthalenes in relative high abundance. The formation of these naphtenoaromatics was finished at 580°C (5.0K/min) and 550°C (0.2K/min), whereat it was monitored that dimethyl- and even more trimethylnaphthalenes decompose faster at higher temperatures than the methylnaphthalenes.

The presence of abundant alkylphenols, like cresols, is characteristic of pyrolysates from type III organic matter having terrestrial organic input (Larter and Senftle, 1985; Nip *et al.*, 1988; Mukhopadhyay *et al.*, 1995). During MSSV pyrolysis the alkylphenols are already generated at low thermal stress and they show increasing amounts with increasing thermal stress. At the highest MSSV temperature of 580°C most of the alkylphenols, like the cresols, are still present at a heating rate of 5.0 K/min, whereas at a heating rate of 0.2 K/min these alkylphenols are virtually absent at a temperature of 530°C. Dimethyl- and ethylphenol start to decompose faster at high experimental temperatures and are virtually absent in the pyrolysates of already 500°C (0.2 K/min).

The amount of alkylbenzenes relative to paraffinic hydrocarbons increases with increasing thermal stress. Remarkable is that the abundance of C_1-C_2 alkylbenzenes display a strong correlation with simulated maturity. At low thermal stress ethylbenzene show very high yields compared to other alkylbenzenes, which was also observed for asphaltene MSSV pyrolysates from the Duvernay oil asphaltene. With increasing MSSV temperatures the amount of ethylbenzene decreases continuously relative to other alkylbenzenes. The amount of toluene in the Nigerian MSSV pyrolysates increases continuously relative to other compounds with

increasing temperature. As well the ratio of m,p-xylene / o-xylene decreases with increasing simulated maturation.

However, it has to be considered that the contamination of the oil asphaltene might have influenced the total yields of aromatic hydrocarbons, like alkylbenzenes, alkylphenols etc. found in the pyrolysates of closed-system analysis.

Fig 150 presents the diagrams with the concentrations of hydrocarbon fractions (C_{1-5}, C_{6-14}, C_{15+}, C_{total}, and methane) in asphaltene MSSV pyrolysates for the heating rates of 5.0 K/min (top) and 0.2 K/min (bottom). It can be seen that the generation of hydrocarbons starts between 310°C (0.2 K/min) and 350°C (5.0K/min). Peak hydrocarbon formation (max. of C_{total}) is obtained at 500°C for a heating-rate of 5.0K/min, and at 445°C for 0.2K/min. In comparison to the asphaltene MSSV pyrolysates from Southern Italy show the Nigerian pyrolysates an onset of hydrocarbon generation at slightly lower temperatures, but a peak hydrocarbon generation at slightly higher simulated maturity. The maximum yields of the C_{15+} fraction are already achieved at relative low temperatures of 420°C (0.2 K/min) and 460°C (5.0K/min), which is very similar to the observation for asphaltene pyrolysates from Southern Italy. The C_{6-14} fraction formed from the Nigerian oil asphaltene show maximum yields at temperatures of 445°C (0.2 K/min) and 495°C (5.0K/min).

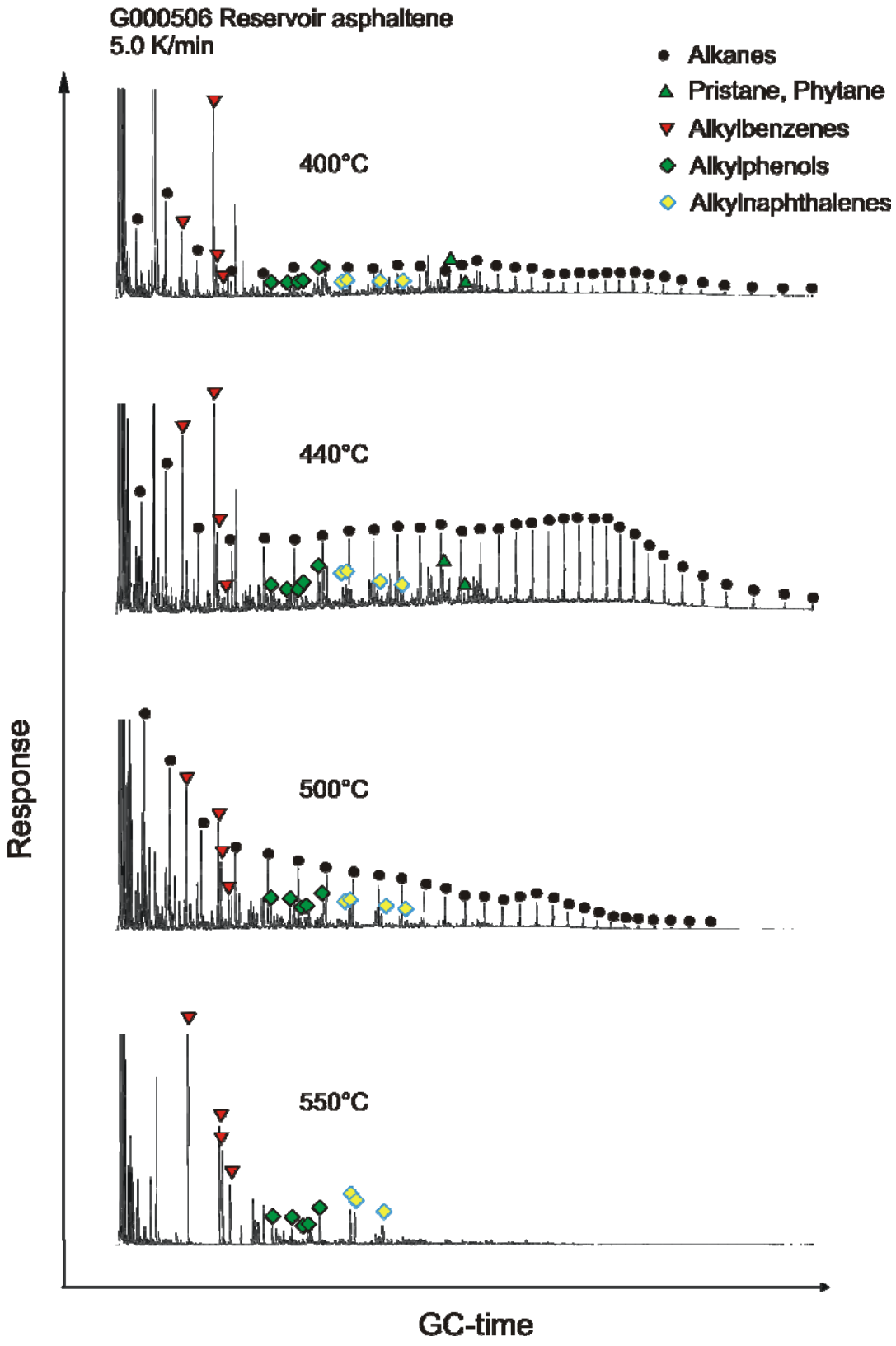

Fig 148 Selected chromatograms from MSSV pyrolysis GC of oil asphaltene sample G000506 using a heating-rate of 5.0 K/min. Alkanes, most abundant alkylphenols, alkylnaphthalenes and alkylbenzenes are marked. Alkylbenzenes are corresponding to retention time from left to the right: toluene, ethylbenzene, m,p-xylene, and o-xylene. Alkylnaphthalenes are from left to right: 2- and 1-methylnaphthalene, dimethylnaphthalene, and trimethylnaphthalene. Alkylphenols are from left to right: o-cresol, m,p-cresol, ethylphenol, dimethylphenol, and trimethylphenol.

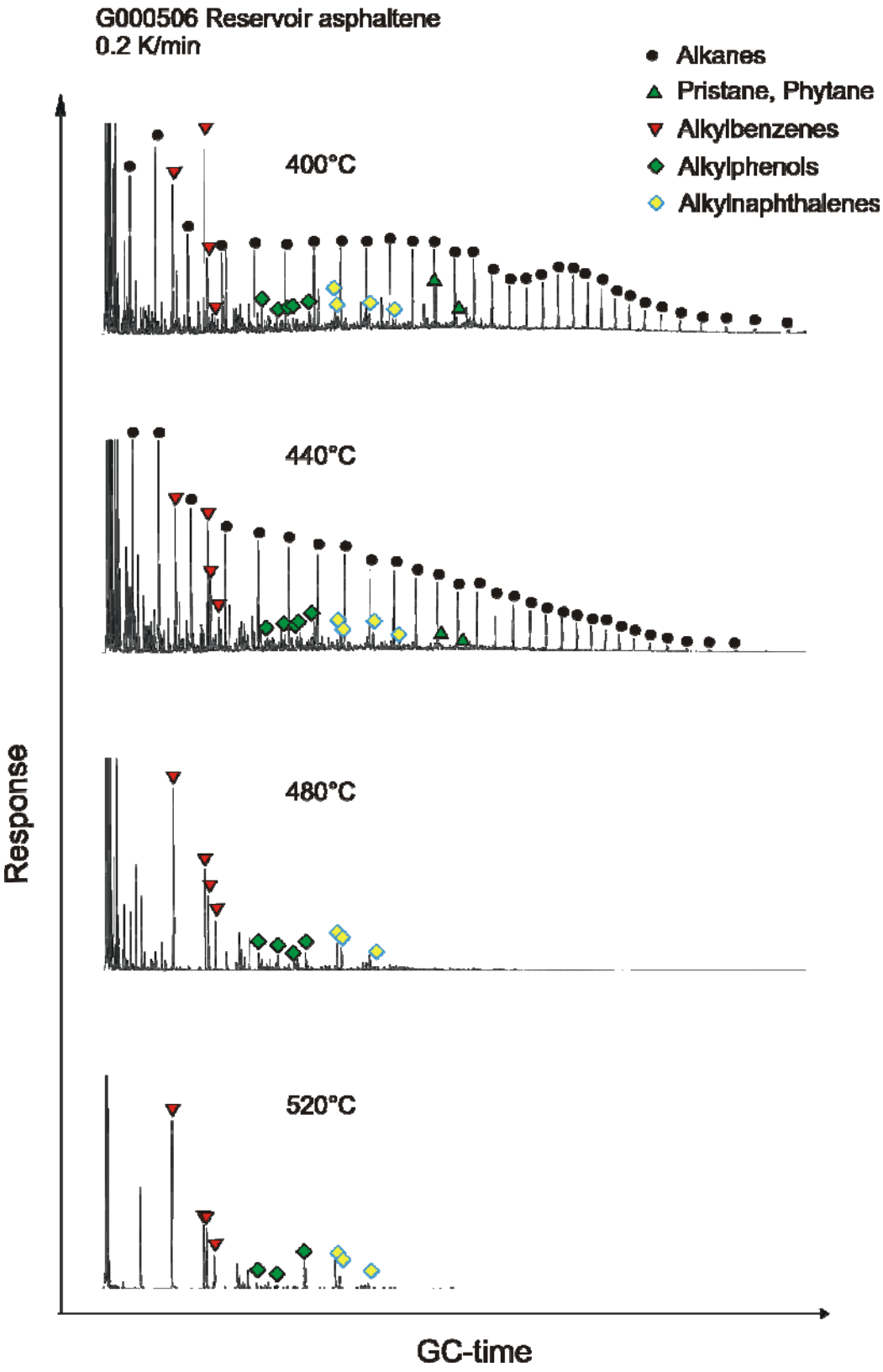

Fig 149 Selected chromatograms from MSSV pyrolysis GC of oil asphaltene sample G000506 using a heating-rate of 0.2 K/min. Alkanes, most abundant alkylphenols, alkylnaphthalenes and alkylbenzenes are marked. Alkylbenzenes are corresponding to retention time from left to the right: toluene, ethylbenzene, m,p-xylene, and o-xylene. Alkylnaphthalenes are from left to right: 2- and 1-methylnaphthalene, dimethylnaphthalene, and trimethylnaphthalene. Alkylphenols are from left to right: o-cresol, m,p-cresol, ethylphenol, dimethylphenol, and trimethylphenol.

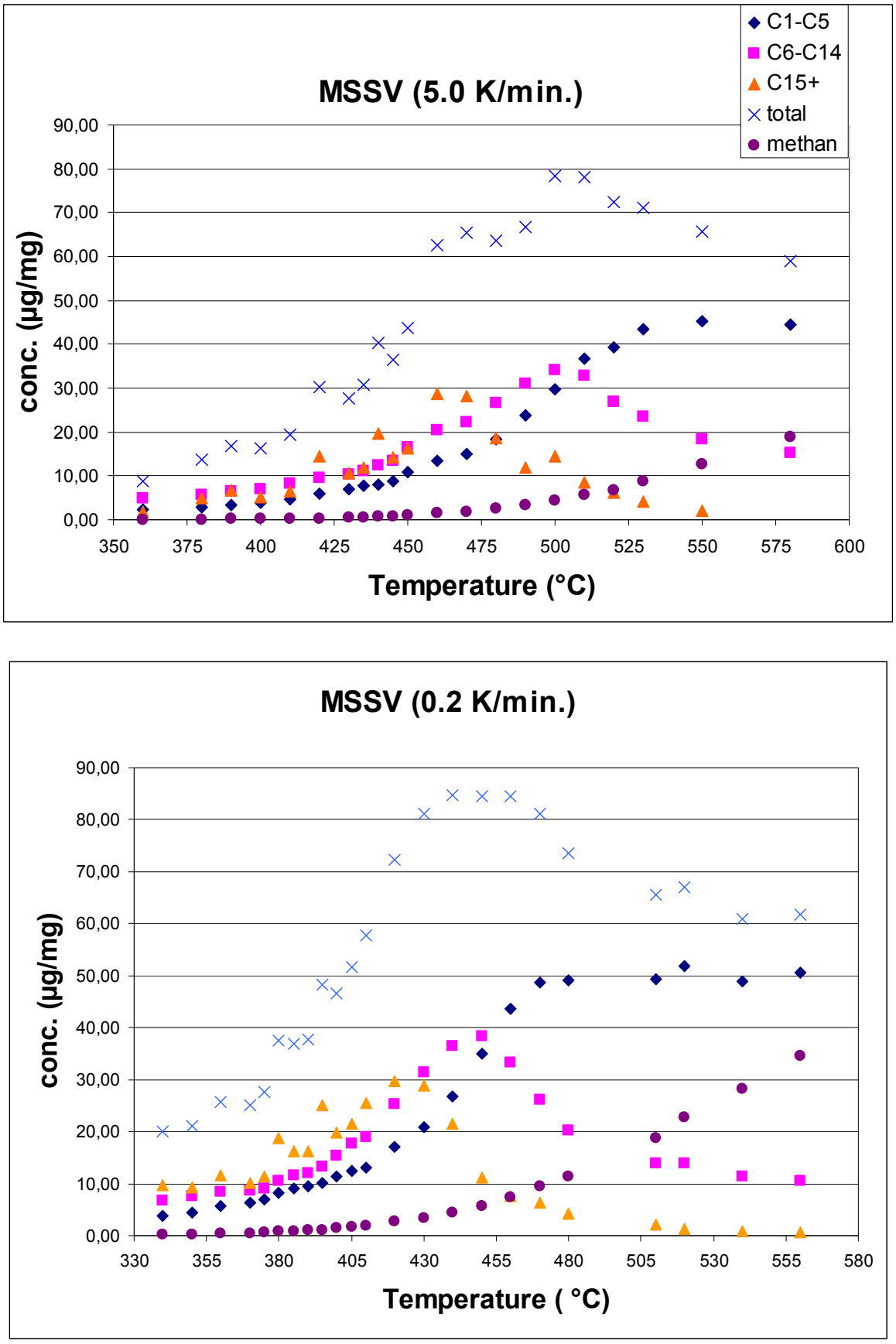

Fig 150 MSSV pyrolysis cumulative concentrations for total products, methane, total gas (C_1-C_5), and oil fractions C_6-C_{14}, and C_{15+} at heating rates of 5.0 K/min (top) and 0.2 K/min (bottom).

9.3.2 Gas formation and *n*-alkyl chain length distribution

Fig 151 shows the primary gas formation C_1-C_5 and the secondary gas formation for products from the Nigerian asphaltene for two different heating rates. The gas formation was calculated from measured formation rates using the method described by Dieckmann *et al.* (1998). Primary gas formation for the Nigerian asphaltene reaches maximum yields at 455°C (0.2K/min) and 490°C (5K/min) respectively. The secondary cracking starts with low heating rate at 430°C and for a heating rate of 5.0K/min the secondary gas formation starts at 470°C. Both features prove that gas formation from the oil asphaltenes follow the law of chemical reaction kinetics.

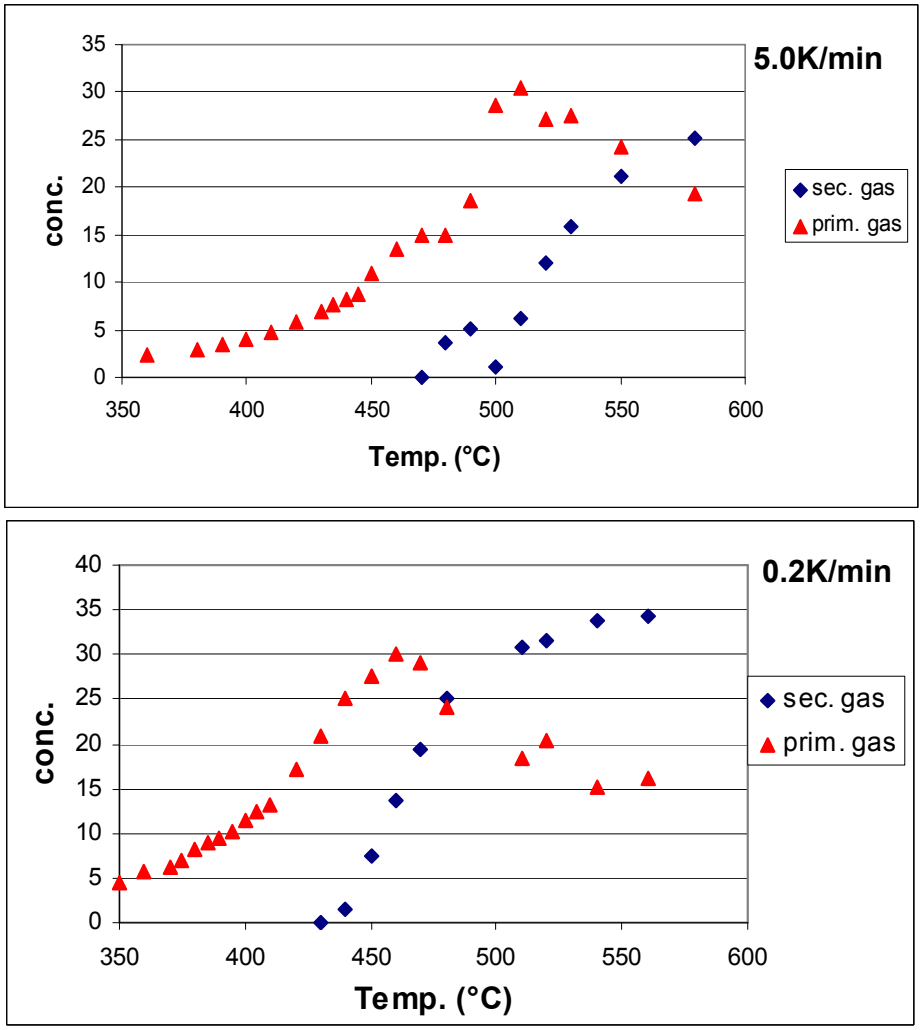

Fig 151 The formation of the primary and the secondary gas obtained from Nigerian oil asphaltene pyrolysates for the two heating rates of 5.0 K/min (top) and 0.2 K/min (bottom).

Fig 152 presents the ternary diagrams for the *n*-alky-chain length distribution of hydrocarbons formed from the Nigerian oil asphaltene for two different heating rates. As for the Italian sample set artificial formed products from Nigerian asphaltenes show higher contents of the C_6-C_{14} and the C_{15+} *n*-alky chains at faster heating rates. With low heating rate of 0.2K/min, while a maximum of 25% was reached at 5K/min. This heating rate dependency is more obvious for the C_{15+} *n*-alky chain fraction. Here, the maximum yield is reached at 32% for the low heating rate of 0.2K/min, and at 41% for 5.0K/min.

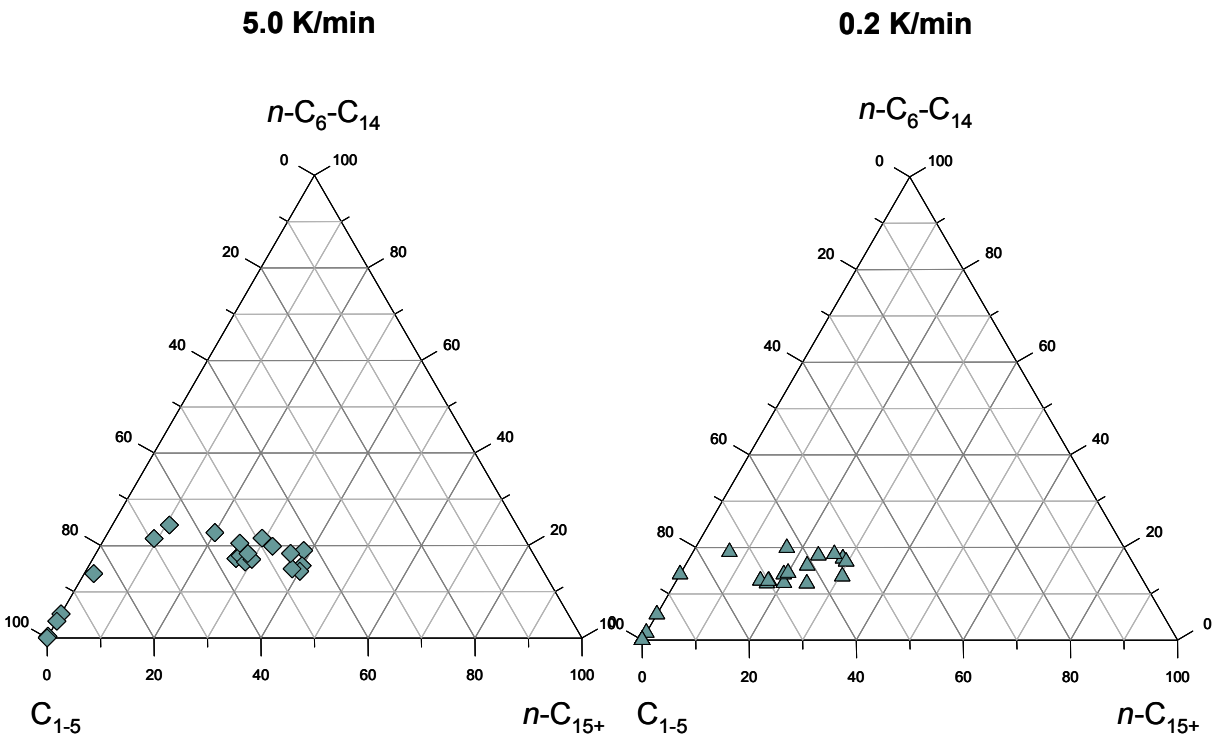

Fig 152 The ternary diagrams for the *n*-alky-chain length distribution of hydrocarbons formed from the oil asphaltene for two heating rates.

9.3.3 Aromatic hydrocarbons

9.3.3.1 Aromaticity

A strong heating rate dependency is as well observed for the aromaticity of hydrocarbons formed from the Nigerian oil asphaltene. Fig 153 illustrates the ratio o-xylene/*n*-C_9 as the degree of aromaticity calculated from the asphaltene MSSV pyrolysates. Hydrocarbons formed at a heating rate of 0.2 K/min show lower aromaticity than at faster heating rate. Such strong heating rate dependency for the aromaticity of hydrocarbons formed from oil asphaltenes was not observed for the Italian asphaltene MSSV pyrolysates (see Fig 106 with the sum of aromatics vs. n-C_{6+} for Italian pyrolysates).

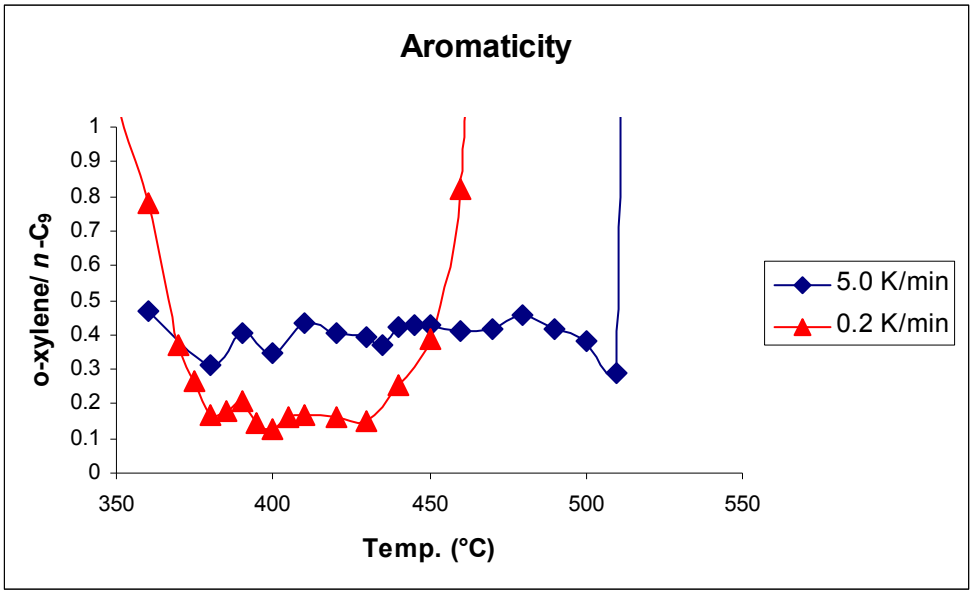

Fig 153 Aromaticity as ratio of o-xylene/*n*-C_9 calculated from Nigerian oil asphaltene MSSV pyrolysates at two different heating rates.

9.3.3.2 Generation of alkylbenzenes and alkylphenols

As noted before do alkylbenzenes in asphaltene pyrolysates show a relationship of simulated maturation temperatures and continuously distribution changes within those alkylbenzenes. Fig 154a illustrates the ratio of ethylbenzene / Σ C_1-C_2 alkylbenzenes calculated from asphaltene pyrolysates at the heating rates of 5.0 and 0.2 K/min. This ratio decreases with increasing MSSV temperature, and is higher for hydrocarbons formed at faster heating rate. In contrast to that increases the ratio of toluene / Σ C_1-C_2 alkylbenzenes obtained from those asphaltene pyrolysates with the simulated maturation temperatures (Fig 154b). As well the toluene ratio show a heating rate dependency in that hydrocarbons at lower heating rate are enriched in toluene relative to other alkylbenzenes. Fig 154c shows the ratio of o-xylene / Σ xylenes of pyrolysates versus the MSSV temperatures for the two heating rates. Here, the xylene ratios are very similar for pyrolysates of both heating rates. Only the temperature range where this ratio increases continuously shows a heating rate dependency. For MSSV pyrolysates of lower heating rate the xylene ratio increases continuously between 370 and 455°C, and then the ratio slightly decreases again with ongoing thermal stress. Pyrolysates of faster heating rate demonstrate a continuously increasing xylene ratio between 360 and 480°C. Interestingly the maxima of the xylene ratios at 455°C (0.2 K/min) and 480°C (5.0 K/min) are very close to the maxima of primary gas formation with 455°C (0.2K/min) and 490°C (5K/min), as well to the peak hydrocarbon formation with 445°C for 0.2 K/min and 500°C for a heating rate of 5.0 K/min.

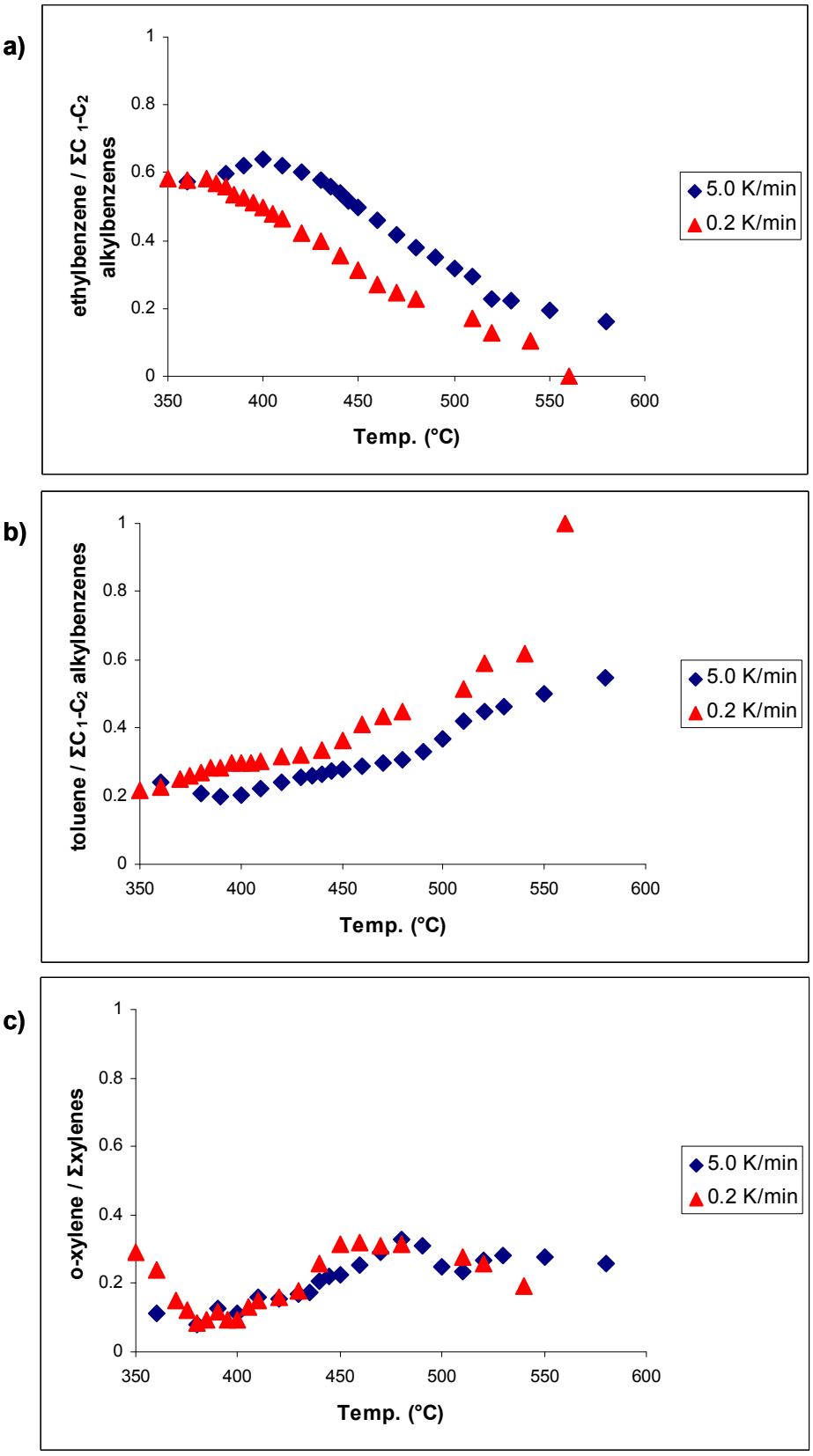

Fig 154 Distribution of alkylbenzenes obtained from oil asphaltene pyrolysates, a) ratio of ethylbenzene / Σ C_1-C_2 alkylbenzenes, b) ratio of toluene / Σ C_1-C_2 alkylbenzenes, c) ratio of o-xylene / Σ xylenes of pyrolysates versus the MSSV temperatures.

Phenolic compounds are common in living organisms and sedimentary organic matter, as well they are trace compounds in petroleums (Ioppolo *et al.*, 1992; Ioppolo-Armanios *et al.*, 1995; Taylor *et al.*, 1997; Lucach *et al.*, 2002). In plants they occur as combinations of esters or glycosides or as complex polymeric structures such as lignins and tannins (Ribéreau-Gayon, 1972). Phenolic compounds occur in many families of angiosperms and gymnosperms as constituents of heartwoods, seeds, fruits, leaves, pigments of flowers and essential oils, and have also been identified in fungi (Ribéreau-Gayon, 1972).

Ioppolo-Armanios *et al.* (1995) proposed that the occurrence of alkylphenols in petroleum is controlled initially by alkylation and isomerization of precursors in source rocks during diagenesis and catagenesis. Several workers have shown that these alkylphenols also interact with the mineral matrix in the source rocks (Issacson and Frink, 1984; Laquer and Manahan, 1987; Sandvik *et al.*, 1992). After expulsion from the source rocks, the concentrations and relative abundance is determined mainly by a 3-phase partitioning between petroleum, water and solids like rocks and organics during migration and within the reservoir (Lucach *et al.*, 2002). This partitioning process leads to a reduction of phenol concentrations with increasing migration distance, which is used as indicator of relative petroleum migration distance (Larter *et al.*, 1996; Galimberti *et al.*, 2000; Larter *et al.*, 2000; Lucach *et al.*, 2002). As well the different solubility of alkylphenol isomers in water was used to determine the effects of biodegradation or water-washing of petroleums (Bennet and Larter, 1997; Taylor *et al.*, 1997; Taylor *et al.*, 2001).

For the present study we focussed on the relative concentrations as well as on the distribution of different alkylphenols formed from the oil asphaltene with increasing simulated maturity. Since the total yields of alkylphenols are probably affected by the contaminant the results of this investigation are rather of qualitative than of quantitative nature.

Fig 155 illustrates the ratio of different alkylphenols and *n*-alkane with increasing MSSV temperature. In Fig 155a the ratio of Σ cresols / *n*-C_{11} versus experimental maturation temperature for two heating rates is shown. With increasing temperature the amount of cresols decreases relative to alkanes until the temperature where the alkane generation decreases. The same is observed for the ratios of Σ dimethylphenols / *n*-C_{12} (Fig 155b) and trimethylphenol / *n*-C_{12} (Fig 155c). Remarkable is that the generation of all alkylphenols show a very strong heating rate dependency, with higher amounts for a faster heating rate of 5.0 K/min. This at least explains the relative low concentrations of alkylphenols in petroleums when calculated the generation of these compounds to a geological heating rate. As well from Fig 155 it gets clear that the concentration of alkylphenols relative to alkanes is not only controlled by partitioning processes, but also by thermal maturity.

Fig 156 shows the distribution of alkylphenols, like the ratios of Σ cresols / Σ dimethylphenols (a), Σ cresols / trimethylphenol (b), and Σ dimethylphenols / trimethylphenol (c) calculated from the Nigerian oil asphaltene pyrolysates. The ratio of Σ cresols / Σ dimethylphenols is remarkable constant with increasing MSSV temperature. A slight heating rate dependency is observed in that the ratio is slightly higher at lower heating rate. In contrast to that both other ratios with the use of trimethylphenol show a rapid increasing with increasing MSSV temperature, illustrating a strong thermal control for the distribution of these alkylphenols.

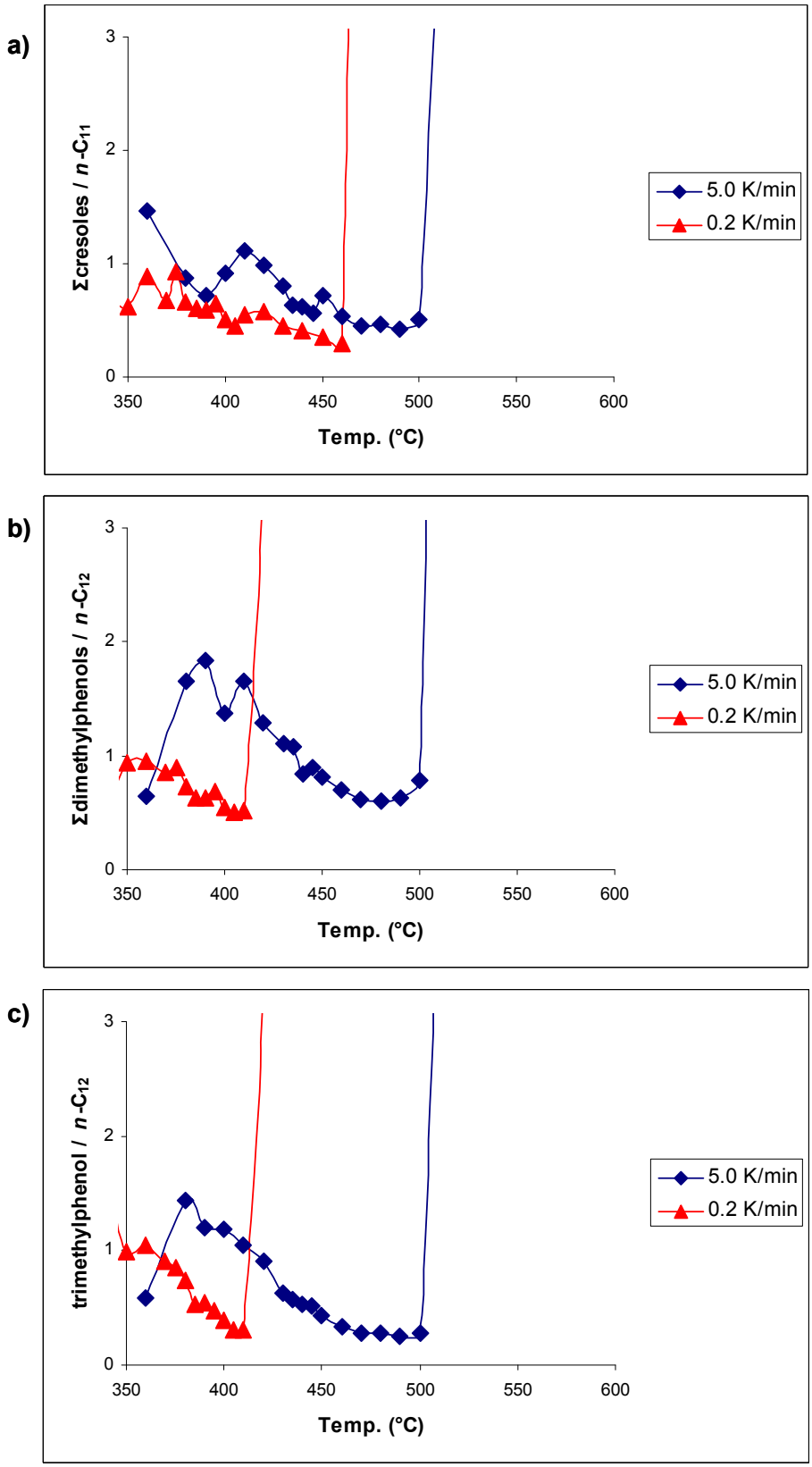

Fig 155 Ratio of different alkylphenols and *n*-alkane with increasing MSSV temperature, a) Σ cresols / *n*-C_{11}, b) Σ dimethylphenols / *n*-C_{12} , c) trimethylphenol / *n*-C_{12}.

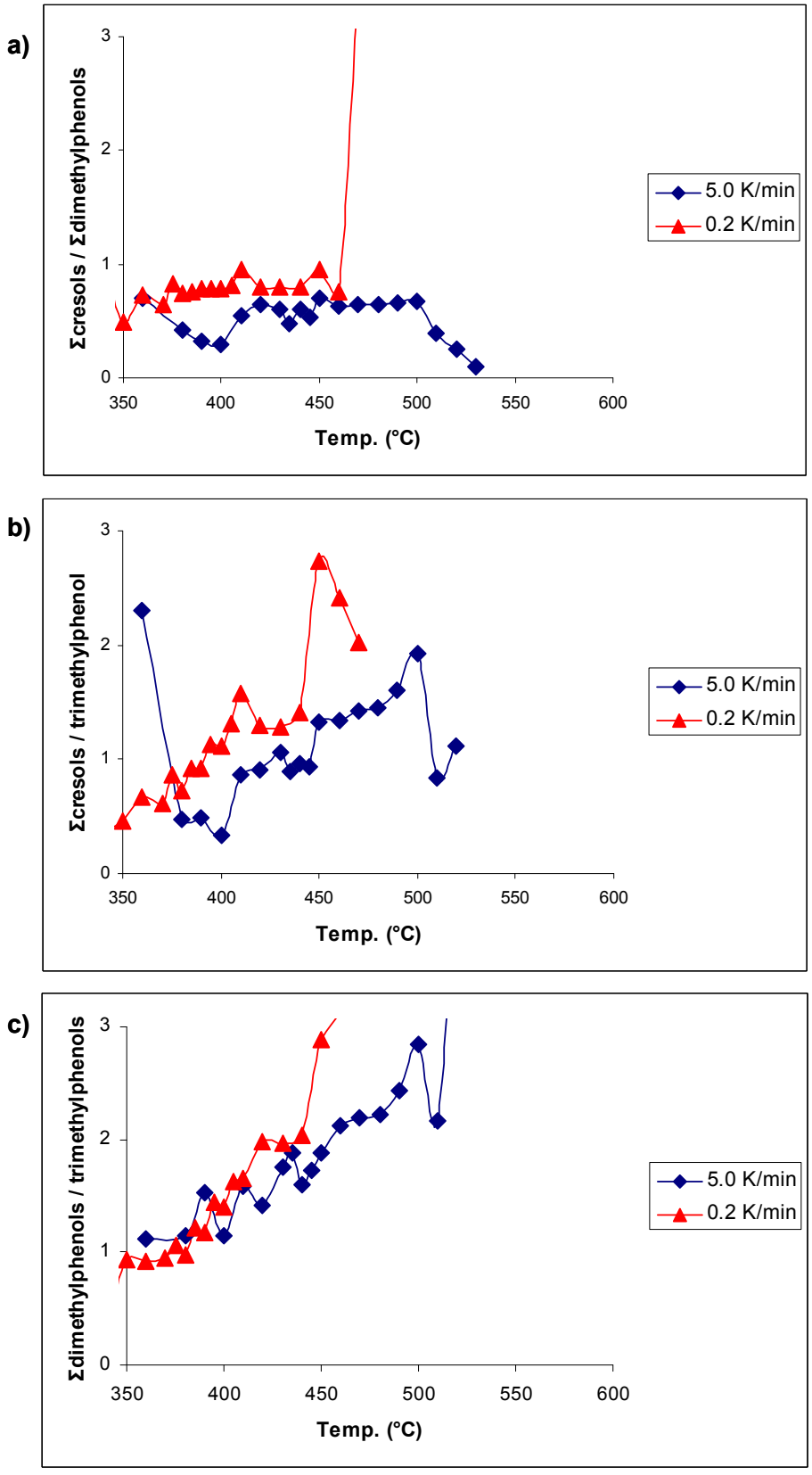

Fig 156 Distribution of different alkylphenols with increasing MSSV temperature, a) Σ cresols / Σ dimethylphenols, b) Σ cresols / trimethylphenol, c) Σ dimethylphenols / trimethylphenol.

9.3.4 Comparison of MSSV pyrolysates with natural oils

Fig 157 shows the diagram of the ratios of pri/*n*-C_{17} and phy/*n*-C_{18} after Peters *et al.* (1999) for oil asphaltene pyrolysates (0.2 K/min.) and natural oils from Nigeria onshore. As shown before in Fig 49 do the crude oils not show a clear trend of pri/*n*-C_{17} and phy/*n*-C_{18} with the API gravity. Only the biodegraded oils show a decreasing trend of pristane/*n*-C_{17} versus phytane/*n*-C_{18} with increasing API, explained by ongoing depletion of *n*-alkanes due to microbial alteration. The asphaltene pyrolysates however show a simulated maturity trend of decreasing ratios with increasing thermal stress. The asphaltene pyrolysates demonstrate a slightly higher ratio of pri/*n*-C_{17} as the related crude oils and plot in the field of type III organic matter, illustrating their nature to be sourced of predominantly terrestrial organic matter.

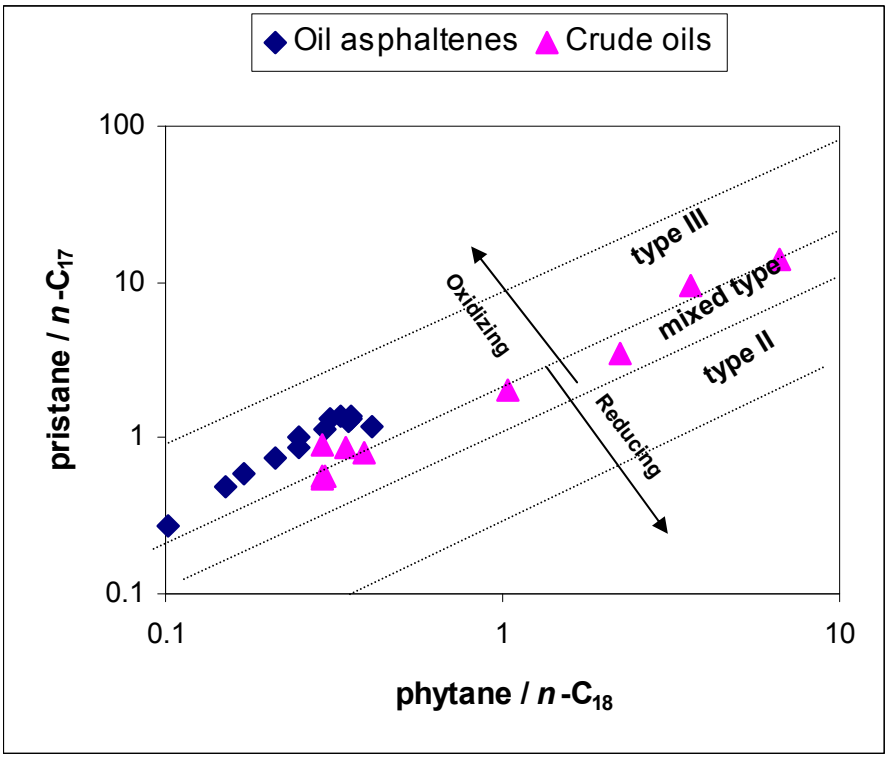

Fig 157 Diagram with the ratios of pristane/*n*-C_{17} versus phytane/*n*-C_{18} for MSSV asphaltene pyrolysates (0.2K/min) in comparison to natural oils from Nigeria onshore (after Peters *et al.* , 1999).

9.3.5 Compositional kinetic parameter

9.3.5.1 Kinetic parameters

Kinetic parameters for the generation of the C_{6+} oil like fraction and the formation of primary as well as secondary gas were also evaluated on asphaltenes precipitated from Nigerian oil. Primary and secondary gas was calculated following the method reported by Dieckmann *et al.* (1998; 2000b). At this the formation of secondary gas results from the decrease of the C_{6+} curve at high temperatures. Since secondary gas formation originates from the degradation of high molecular weight hydrocarbons and thus can be identified in the generation curves as the point where the apex of the C_{6+} range is exceeded. For that reason secondary gas is predictable by subtraction the amount of generated C_{6+} hydrocarbons from the apex of C_{6+}. Because only 70% of cracked oil can be transformed to gas the calculated sum has to be multiplicated with the stoichiometrical factor of 0.7. The formation of primary gas was calculated from the difference between the total gas (C_1-$_{5tot.}$) and the previously evaluated secondary gas. Since no source rock sample from the petroleum system was provided to this project, it is not possible to compare the result archived in the asphaltene with those archived on relevant source rock samples in this area. However, based on the results evaluated on the other sample types within this study, it can be expected that the resulting geological prediction are very similar to those from the source rocks and that compositional characteristics may even better simulated.

Kinetic parameters for the different petroleum fraction are shown in Fig 158. The formation of primary gas is characterized by a broad activation energy distribution with an Emean of 56-58 kcal/mol and a Frequency Factor of 7.91 E+13 s^{-1}. This is much lower as the set of kinetic parameters calculated for the generation secondary gas which is defined by an Emean of 68kcal/mol and a frequency factor of 3.48E+16 s^{-1}. The formation of C_{6+} compounds is also

characterized by high activation energies and a high frequency factor with Emean 64kcal/mol and 2.6E+17 s^{-1}. These high values together with the early potential for the generation of gas may support that the original source rock of these oils correspond to a type II/III organic matter. This type of assumption is also supported by the occurrence of significant amounts of alkylphenols and alkylated benzenes in the MSSV pyrolysates.

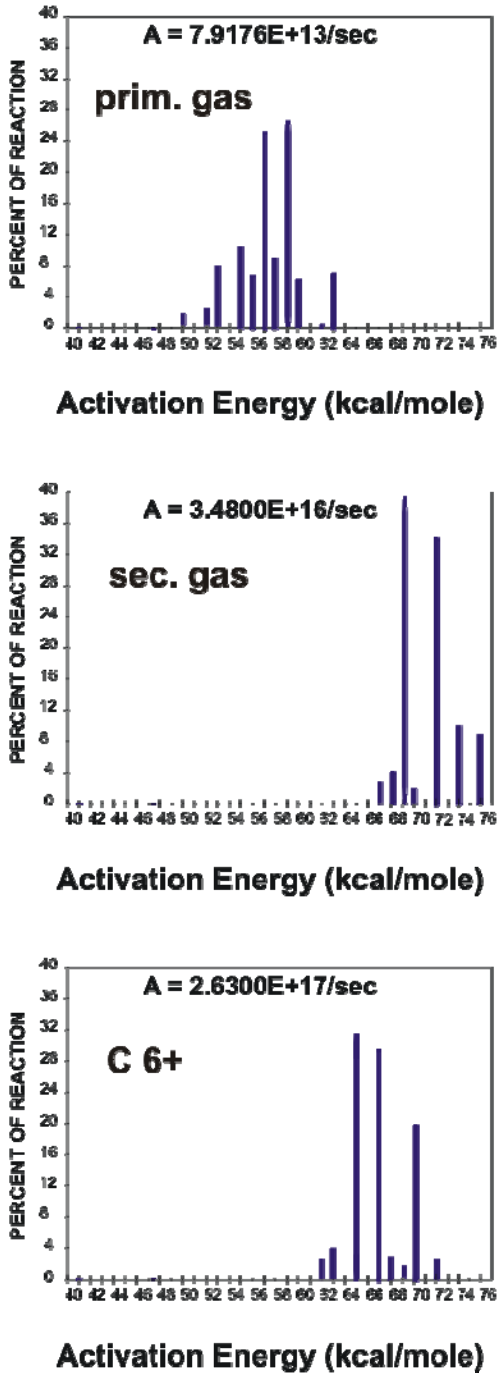

Fig 158 Kinetic parameters for the different petroleum fraction formed from the Nigerian petroleum asphaltene.

9.3.5.2 Geological predictions of oil and gas formation

Fig 159 shows the calculated predictions for primary and secondary gas formation from the Nigerian asphaltene pyrolysates for heating conditions of 3.3K/my**.** Predicted to these geological heating conditions, it can be seen that the initial phase of hydrocarbon formation from the Nigerian asphaltenes is dominated by primary gas formation. The formation of this gas type was predicted to start at around 100°C ($Tmax_{geol}$. 170°). At 200°C the formation of primary gas comes to its end.

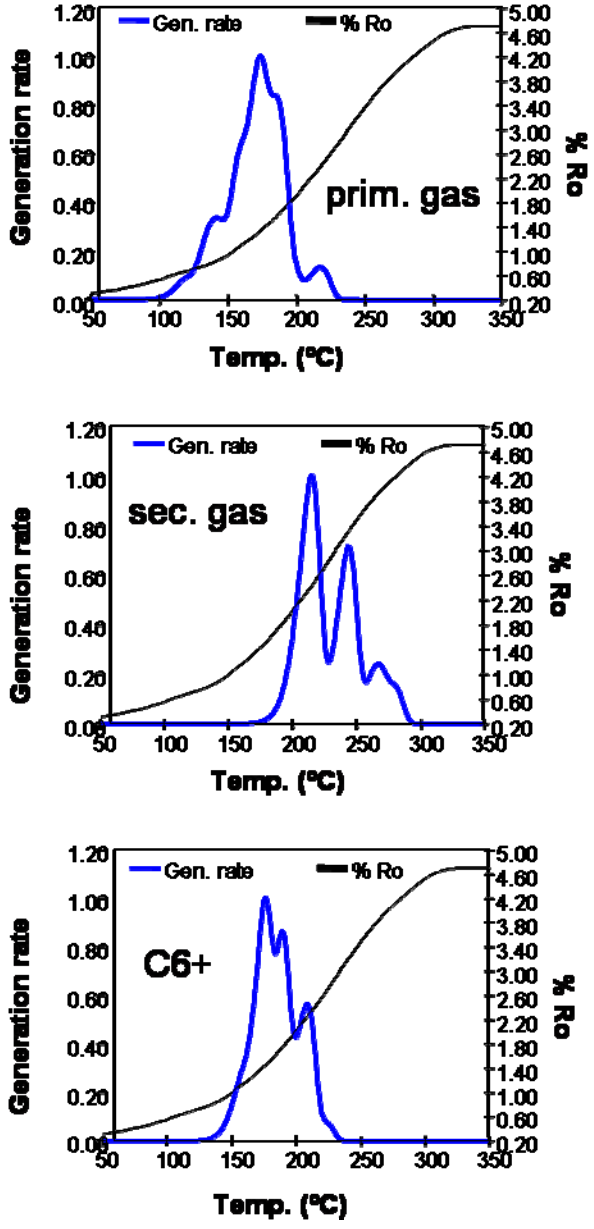

Fig 159 Calculated predictions for primary and secondary gas formation for heating conditions of 3.3K/my.

9.3.5.3 Molecular compositional C_{6+} kinetics

Fig 160 illustrates the resulting detailed compositional kinetic model for the generation of oil like C_{6+} compounds from the Nigerian petroleum asphaltene. The compositional kinetic prediction was calculated using the same method described before for the Italian sample set. In correspondence to the type of organic matter and the oil type found in the Nigerian area, the kinetics describes the formation of relative NSO lean, but saturate-rich oil. However, the contamination of the Nigerian oil asphaltenes has probably influenced the compositional kinetic prediction to a smaller degree, especially for the fractions of aromatic hydrocarbons and NSO. Nevertheless, beside the characteristic leanness of NSO fraction do the resulting prediction show other typical characteristics of Nigerian oils, such as the formation of relative high amounts of *n*-C_{15+} at lower activation energies.

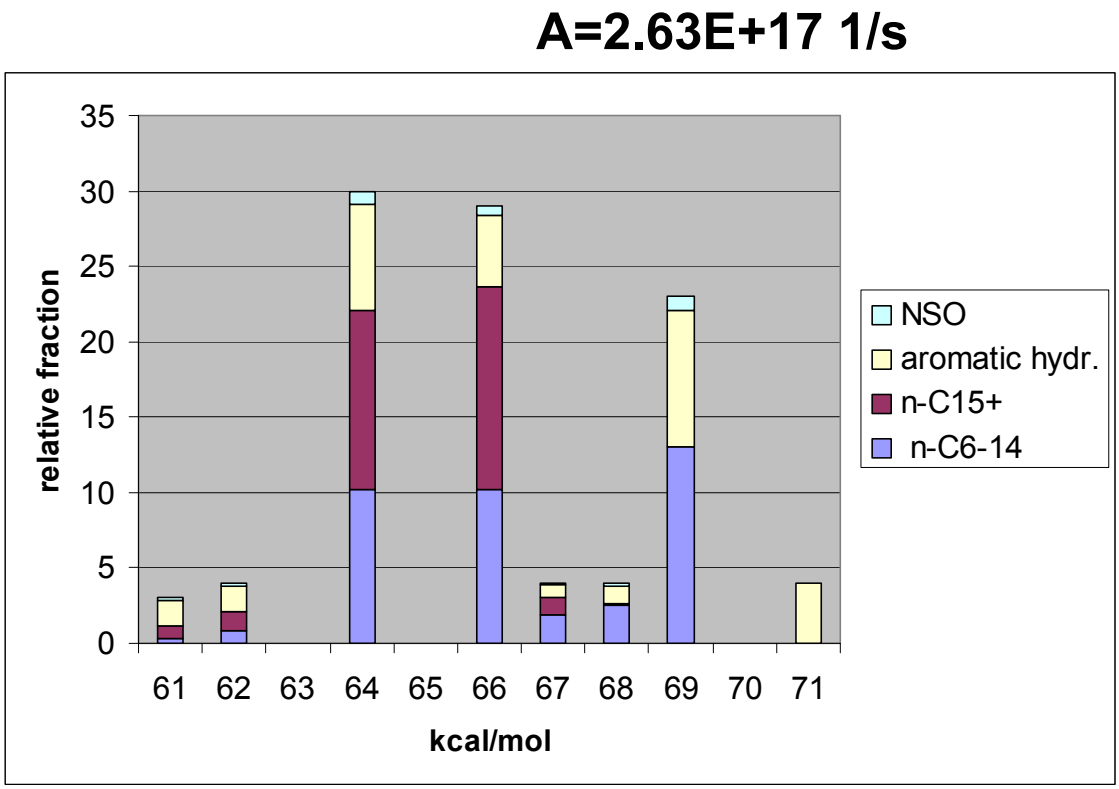

Fig 160 Detailed compositional kinetic model for the generation of oil like C_{6+} compounds from the Nigerian petroleum asphaltenes.

9.3.6 Conclusions

- Hydrocarbons formed from the Nigerian reservoir asphaltene show a strong heating rate dependency for the *n*-alky-chain length distribution with higher contents of the C_6-C_{14} and the C_{15+} *n*-alky chains at faster heating rate. This heating rate dependency is also observed for the generation of aromatic hydrocarbons. These formed at a heating rate of 0.2 K/min show lower aromaticity than at faster heating rate.
- Alkylbenzenes in asphaltene pyrolysates show a relationship of simulated maturation temperatures and continuously distribution changes. The ratio of ethylbenzene / Σ C_1-C_2 alkylbenzenes calculated from asphaltene pyrolysates decreases with increasing MSSV temperature, and is higher for hydrocarbons formed at faster heating rate. The ratio of toluene / Σ C_1-C_2 alkylbenzenes increases continuously with increasing temperature and demonstrate a heating rate dependency in that hydrocarbons at lower heating rate are enriched in toluene relative to other alkylbenzenes. The ratios of o-xylene / Σ xylenes of pyrolysates are very similar for pyrolysates of both heating rates. Only the temperature range where this ratio increases continuously shows a heating rate dependency. For MSSV pyrolysates of lower heating rate the xylene ratio increases continuously between 370 and 455°C, and then the ratio slightly decreases again with ongoing thermal stress. Pyrolysates of faster heating rate demonstrate a continuously increasing xylene ratio between 360 and 480°C. Interestingly the maxima of the xylene ratios at 455°C (0.2 K/min) and 480°C (5.0 K/min) are very close to the maxima of primary gas formation with 455°C (0.2K/min) and 490°C (5K/min), as well to the peak hydrocarbon formation with 445°C for 0.2 K/min and 500°C for a heating rate of 5.0 K/min.

- As well alkylphenols show a very strong heating rate dependency, with higher amounts relative to alkanes for a faster heating rate. Additionally the abundance of alkylphenols generated from the reservoir asphaltene, relative to alkanes, as well as the distribution of these alkylphenols is primary controlled by thermal maturity.
- Compositional kinetic parameters of oil and gas formation obtained from oil asphaltene pyrolysates show high values together with the early potential for the generation of gas, which may support that the original source rock of these oils correspond to a type II/III organic matter.
- For the formation of C_{6+} compound fraction the predicted onset temperatures are quite high for Nigeria onshore. This may be explained with the higher stability of the original organic matter preserved in the source rock. The simulation experiments using MSSV-pyrolysis illustrated that compositional features of hydrocarbons formed from Nigerian asphaltenes are very similar to compositional feature found for natural petroleum. For that reason a compositional kinetic model for C_{6+} formation was build up for the asphaltenes from Nigeria onshore. This model reflects the major characteristics of NSO lean oils formed in this delta system.

10 Synopsis

Heavy crude oils and source rock bitumens from Southern Italy show different levels of thermal maturity based on biomarker maturity parameters. Less degraded and non stored oils demonstrate an early stage of thermal maturity using the parameters C_{27} $\beta\beta/(\beta\beta+\alpha\alpha)$ and C_{29} 20*S*/(20*S*+20*R*), whose values correspond to an vitrinite reflectance value of 0.7 – 0.8 %Ro. Bitumen show an immature stage of maturity, corresponding to a vitrinite reflectance of 0.4 – 0.5 %Ro. Biomarker parameters for oil-source correlation do not show a clear relationship between crude oils and source rocks. But, the unusual high concentrations of gammacerane and dinosteranes in oils and bitumens point to be of same origin. Based on the biomarker parameters of gammacerane and % C_{29} sterane the heavy crude oils from Southern Italy can be divided into two subfamilies. Pyrolysates of asphaltenes isolated from those oils of different subfamilies show as well differences in structural moieties, such as different organic sulphur content and xylene distributions, which highlights the use of asphaltenes to characterise variations in facies. Light hydrocarbon parameters for the crude oils from Southern Italy do not reflect low mature characteristics of studied oils. The low mature, heavy oils show an overestimation of oil maturity based on Thompson´s light hydrocarbon parameters, due to high concentrations of *n*-C_7 in the first phase of oil generation. Long-time storing affected strongly the characteristics of light hydrocarbons with stored oils being enriched in 2- and 3-methylhexane relative to their fresher equivalents. The storage effect on studied oils has also influenced biomarker maturity parameters and the *n*-alkane distribution. But asphaltenes isolated from stored oils and isolated from related fresher oils are very similar in terms of structural moieties investigated by open-system-pyrolysis. Thus the pyrolysates of asphaltenes isolated from long-time-stored oils can be used for oil-source correlations. Low API crude oils from Southern Italy are affected by biodegradation, indicated by an unusual high % of GC-unresolved compounds (hump), depletion of certain alkanes and even of light

hydrocarbons. For the studied Italian oils the biomarker parameters Ts/(Ts+Tm) and C_{29}Ts index are grossly affected by microbial metabolism. As well, an anaerobic biodegradation is indicated by the ongoing depletion of o-xylene with decreasing API gravity for these oils.

Bulk kinetic measurements proved that the kinetics of petroleum asphaltenes from type II-S source rocks do not represent the full hydrocarbon generation window of the related source rock kerogens. Source rock asphaltenes and oil asphaltenes are less thermally stable than kerogens. Bulk kinetic measurements indicated slightly lower activation energies and frequency factors for the transformation of asphaltenes to petroleum than those for source rock kerogens. However, the predictions from asphaltene resulted in tighter temperature ranges, indicating that the reactive part of the asphaltenes is more homogeneous than the source rock kerogens. Reservoir asphaltenes from type II sequences differ in terms of kinetic parameters and their application for oil – source correlation from type II-S asphaltenes. However, no obvious structural links were found that could directly explain the observed reactivity differences from bulk kinetic measurements. But, the amount of organic sulphur is not proportional to the reactivity of petroleum generation from asphaltenes at lower thermal stress. More likely is, that kerogens and asphaltenes posses different positions and types of sulphur bonds resulting in cracking of covalent bonds at different levels of thermal stress.

Source rocks asphaltenes, related kerogens, and oil asphaltenes in a petroleum system from Southern Italy show major structural differences and differ in aromaticity and organic sulphur content. Highest aromaticity was found in pyrolysates of source rocks asphaltenes, medium from kerogens, and lowest aromaticity in pyrolysates formed from petroleum asphaltenes. The highest organic sulphur content was identified in kerogen pyrolysates, whereas pyrolysates of both types of asphaltenes do not show a major difference in the content of organic sulphur. With increasing maturity the content of organic sulphur relative to aromatic and aliphatic structures decreases for asphaltenes as well as for kerogens. The proportionally

increasing of 3-methylthiophene in kerogen pyrolysates with decreasing HI provides a maturity parameter for immature source rocks at low levels of thermal stress. For oil asphaltene pyrolysates the thiophenes ratio of branched (3-methylthiophene) versus linear isomers (2-methylthiophene, 2,5-dimethylthiophene) can be used to assess the original maturity of strong biodegraded oils. For the facies recognition based on the alkyl chain distribution of pyrolysates kerogens predict the field of the paraffinic-naphtenic-aromatic low-wax oil generating facies. Both asphaltene types plot at a triple point predicting P-N-A low EndNote>□(1996; 2000)□ in that source rock asphaltenes are less stable than related . But the presethe asphaltic natural oils found in this petroleum system. Pyrolysates from both asphaltene types as well from kerogens show differences which can be attributed to different concentrations of biogenic precursors within the asphaltene and kerogen macromolecules, indicated for example in different alkane / alkene ratios, xylene distributions, and toluene/ xylenes ratios obtained from pyrolysates of kerogens and both asphaltene types.

Detailed compositional information from non-isothermal MSSV pyrolysis clearly showed that hydrocarbons formed from the Italian oil asphaltenes show lower aromaticity than hydrocarbons formed from source rock kerogen do. As well show these hydrocarbons lower content of organic sulphur than those formed from kerogens, which is closer to the composition of natural formed products. The compositional kinetics supports the oil prone character of the petroleum asphaltenes from Italy. The C_{6+} oil like kinetics and geological predictions are nearly identical when comparing oil formed from petroleum asphaltenes with that formed from the kerogen. Primary gas and secondary gas kinetics for Southern Italy evaluated on petroleum asphaltene MSSV pyrolysates result in similar geological prediction as gas formation from the source rock kerogen. However, the GOR of product formed from the asphaltenes is much lower than that formed from the kerogen. Carbon isotopic composition for gas generation from closed-system experiments show higher $\delta^{13}C$ values for

gas formed from source rock asphaltenes and kerogens than for gas formed from petroleum asphaltenes, which hampers the use of isotopic composition of gas formed from petroleum asphaltenes for identifying source rock environment, or oil – source correlation for the present type II-S petroleum system.

The simulation experiments using MSSV pyrolysis illustrated that compositional features of hydrocarbons formed from asphaltenes are very similar to compositional feature found for natural petroleum. This was especially the case of n-C_{6-14}, *n*-C_{6+}, aromatic compounds and NSO like compounds. For that reason a compositional kinetic model for C_{6+} formation was build up for the asphaltenes from the Italian petroleum system. This model reflects the major characteristics of non-degraded oils formed in this area. Nevertheless, the compositional kinetic model shows probably an underestimation of NSO contents at lower activation energies, since major proportions of naturally occurring high molecular weight compounds of aromatic/asphaltic oils are thermally involatile and thus cracked to secondary products during MSSV pyrolysis.

Low mature oils from Duvernay show Ts/(Ts+Tm) values, which correspond to a vitrinite reflectance of 0.65 %Ro, and those values from more mature oils correspond to a vitrinite reflectance up to 1.1 Ro%. Values obtained from C_{29} 20*S*/(20*S*+20*R*) measured on bitumen yield a vitrinite reflectance of 0.6 %Ro for immature source rocks. Bitumen of mature source rocks yield a correlated vitrinite reflectance of 0.8 Ro% based on the Ts/(Ts+Tm) parameter. The distribution of αααC_{27}, C_{28} and C_{29} steranes in crude oils and source rock bitumen from the Duvernay Formation points to same facies for oils and source rocks. Based on light hydrocarbon parameters the studied oils do not show any indications of a secondary overprint such as biodegradation or water washing. Therefore, their compositional characteristics such

as aromaticity and paraffinicity can later be compared directly to the products formed from the kerogens and asphaltenes.

Bulk Petroleum generation kinetics evaluated for the transformation of petroleum asphaltenes and source rock asphaltenes from type II sequence are similar to those calculated for the transformation of related immature source rocks. Consequently the extrapolations of petroleum formation to geological heating conditions are very similar. Oil asphaltenes from a type II sequence differ in that to oil asphaltenes from sulphur-rich sequences in that petroleum asphaltenes precipitated from the low mature Duvernay oils can be used to reconstruct the timing of source rock transformation as well as the compositional characteristics of natural oil in the petroleum system. These results are especially important for petroleum systems where the source rock is not drilled. However, the molecular composition of pyrolysates formed from petroleum asphaltenes and source rock asphaltenes from the Duvernay Formation are very different. The aromaticity of pyrolysates formed from source rock asphaltenes is much higher than the aromaticity of pyrolysates formed from petroleum asphaltenes. Interestingly, products formed from immature kerogens represent intermediate aromaticity. The aromaticity of natural oils from Duvernay is much lower than those of pyrolysates formed from source rock kerogens and source rock asphaltenes. However, petroleum asphaltenes pyrolysates fit exactly to the aromaticity of the natural oils. This feature indicates that petroleum asphaltene products can be used for petroleum compositional predictions, while the application of kerogen and source rock asphaltene products is very limited. Source rock asphaltenes as well parent kerogens show a decreasing aromaticity of their pyrolysates with ongoing maturity, up to a maturity stage, where the aromaticity increases through lack of aliphatic hydrocarbons in their pyrolysates. Geochemical facies markers such as the 1,2,3,4-TMB/(n-C_{11}+n-C_{12}) ratio as well as the distribution of alkyl chains in petroleum asphaltene pyrolysates cannot not be used for source rock organofacies characterization. Kerogens and source rock asphaltenes predict

both the field of the paraffinic-naphtenic-aromatic low-wax oil generating facies based on the alkyl chain distribution, whereas oil asphaltenes predict the field of paraffinic high wax oil generating facies. Pyrolysates of oil asphaltenes do however copy molecular characteristics of natural oils. Pyrolysates of source rock and oil asphaltenes show lower organic sulphur content than related parent kerogens, and show decreasing amounts of organic sulphur with increasing thermal maturation, just as pyrolysates of kerogens do.

The pyrolysates from artificial maturity experiments on Duvernay petroleum asphaltenes show lower aromaticity than products from source rock kerogens, which confirm the results from Southern-Italy. Hydrocarbons formed from asphaltenes are enriched in *n*-C_6-C_{14} and total maximum of *n*- C_{15+}, whereas hydrocarbons formed from kerogens show lower maximum yields of these compound classes. In contrast kerogen products are more gas prone than the asphaltene from an immature crude oil. The GOR of hydrocarbons formed from the oil asphaltene is much lower than that formed from the kerogen. As well, MSSV pyrolysates of asphaltenes and kerogens differ in terms of the gas wetness in that gas formed from kerogens is generally dryer at low and at high thermal stress. Primary gas formation from Duvernay asphaltenes starts slightly earlier than from the source rock sample, while timing of secondary gas formation from asphaltenes and source rock kerogens seems to be identical under laboratory conditions. As well, the hydrocarbons from artificial maturity experiments on petroleum asphaltenes show higher similarity to natural oils in terms of pristane and phytane ratios, which allows facies correlation.

The studied Nigerian oils are all of same stage of maturity, corresponding to a vitrinite reflectance of about 0.8 %Ro. These oils show minor facies variations probably due to different terrestrial organic matter input indicated by their biomarker distributions. Biodegraded oil samples are all of very similar facies pointing to the same oil with different

ranks of biodegradation. The extent of biodegradation following the common scales for the most degraded oils is about 4/5, and there is no indication of asphaltene biodegradation. The light hydrocarbon parameters from Nigerian oils distinguish unaltered from biodegraded oils. However, most oils have experienced secondary overprint due to evaporitic fractionation. Thus, only their compositional characteristics in terms of paraffinicity should be compared directly to the pyrolysates formed from oil asphaltenes.

Bulk kinetic measurements on one oil asphaltene sample predict peak hydrocarbon generation for geological temperatures of 145°C. This predicted temperature correlates with hydrocarbon generation for example in the western part of the Anambra Basin in Nigeria onshore. The *n*-alkyl-chain distribution of investigated pyrolysates from Nigerian oil asphaltenes predicts the facies generating high-wax P-N-A-oils or paraffinic oils. The high-wax, paraffinic-naphtenic-aromatic (P-N-A) crude oil generating facies usually occurs in lower delta plain and inner shelf environments. The changes for facies recognition based on the *n*-alkyl chain length distribution of asphaltene pyrolysates correlates with facies changes due to variations of terrestrial input obtained from biomarker parameters of related crude oils.

Hydrocarbons formed from the Nigerian reservoir asphaltene show a strong heating rate dependency for the *n*-alky-chain length distribution with higher contents of the C_6-C_{14} and the C_{15+} *n*-alky chains at faster heating rate. This heating rate dependency is also observed for the generation of aromatic hydrocarbons, like alkylbenzenes and alkylphenols. These formed at lower heating rate show lower aromaticity than at faster heating rate. Alkylbenzenes in asphaltene pyrolysates show a relationship of simulated maturation temperatures and continuously distribution changes. The ratio of ethylbenzene / Σ C_1-C_2 alkylbenzenes calculated from asphaltene pyrolysates decreases with increasing MSSV temperature, and is higher for hydrocarbons formed at faster heating rate. The ratio of toluene / Σ C_1-C_2 alkylbenzenes increases continuously with increasing temperature and demonstrate a heating

rate dependency in that hydrocarbons at lower heating rate are enriched in toluene relative to other alkylbenzenes. The ratios of o-xylene / Σ xylenes of pyrolysates are very similar for pyrolysates of both heating rates. Only the temperature range where this ratio increases continuously shows a heating rate dependency. Interestingly, the temperatures for the maxima of the xylene ratios are very close to temperatures of the maxima of primary gas formation, as well to the peak hydrocarbon formation.

Compositional kinetic parameters of oil and gas formation obtained from oil asphaltene pyrolysates show high values together with the early potential for the generation of gas, which may support that the original source rock of these oils correspond to a type II/III organic matter. For the formation of C_{6+} compound fraction the predicted onset temperatures are quite high for Nigeria onshore. This may be explained with the higher stability of the original organic matter preserved in the source rock. The simulation experiments using MSSV-pyrolysis illustrated that compositional features of hydrocarbons formed from Nigerian asphaltenes are very similar to compositional feature found for natural petroleum. For that reason a compositional kinetic model for C_{6+} formation was build up for the asphaltenes from Nigeria onshore. This model reflects the major characteristics of NSO lean oils formed in this delta system.

11 References

Abdullah, W.H., (1999). Organic facies variations in the Triassic shallow marine and deep marine shales of central Spitsbergen, Svalbard. Marine and Petroleum Geology 16 (5), 467-481.

Abella, C., Moutesinos, E., Guerrero, R.M., (1980). Field studies on the competition between the purple and green sulfur bacteria for available light. Dev. Hydrobiol. 3, 173-181.

Acevedo, S., Gutierrez, L.B., Negrin, G., Pereira, J.C., (2005). Molecular Weight of Petroleum Asphaltenes: A Comparison between Mass Spectrometry and Vapor Pressure Osmometry. Energie and Fuels 19 (4), 1548 -1560.

Aeckersberg, F., Bak, F., Widdel, F., (1991). Anaerobic oxidation of saturated hydrocarbons to CO2 by a new type of sulfate-reducing bacterium. Archives of Microbiology 156, 5-14.

Afanasev, A.N., Matishev, V.A., Syunyaev, Z.I., Farafonov, V.V., (1993). Melting and crystallization of paraffins. Chemistry and Technology of Fuels and Oils 29, 549-554.

Agrawala, M., Yarranton, H.W., (2001). Asphaltene association model analogous to linear polymerization. Ind. Eng. Chem. Res. 40, 4664-4672.

Albaigés, J., Algaba, J., Clavell, E., Grimalt, J.O., (1986). Petroleum geochemistry of the Tarragona Basin (Spanish Mediterranean off-shore). Organic Geochemistry 8, 293-297.

Alboudwarej, H., Akbarzadeh, K., Beck, J., Svrcek, W.Y., Yarranton, H.W., (2003). Regular Solution Model for Asphaltene Precipitation from Bitumens and Solvents. AIChE Journal 49 (11), 2948-2956.

Alboudwarej, H., Beck, J., Svrcek, W.Y., Yarranton, H.W., (2002). Sensitivity of asphaltene properties to seperation techniques. Energy & Fuels 16, 462-469.

Albrecht, P., Ourission, G., (1969). Diagenesis des hydrocarbures satures dans une serie sedimentaire epaisse (Douala, Cameroum). Geochim. Cosmochim. Acta 33, 138-142.

Almehaideb, R.A., (2004). Asphaltene precipitation and deposition in the near wellbore region: a modeling approach. Journal of Petroleum Science and Engineering 42 (2-4), 157-170.

Ancheyta, J., Centeno, G., Trejo, F., Marroquin, G., Garcia, J.A., Tenorio, E., Torres, A., (2002). Extraction and characterization of asphaltenes from different crude oils and solvents. Energie and Fuels 16, 1121-1127.

Andersen, S., Speight, J., (2001). Petroleum resins separation, character, and role in petroleum. Petroleum Science and Technology 19, 1-34.

Andersen, S.I., Speight, J.G., (1999). Thermodynamic models for asphaltene solubility and precipitation. Journal of Petroleum Science and Engineering 22 (1-3), 53-66.

Audino, M., Grice, K., Alexander, R., Kagi, R.I., (2002). Origin of macrocyclic alkanes in crude oils from the algaenan of Botryococcus braunii. Organic Geochemistry 33, 979-984.

Baker, E.W., Louda, J.W., (1986). Porphyrins in the geological record. In: R.B. Johns (Ed.), Biological Markers in the Sedimentary Record. Elsevier, pp. 121-223.

Bakr, M., Akiyama, M., Sanadia, Y., (1991). In situ high temperature ESR measurements for kerogen maturation. Organic Geochemistry 17 (3), 321-328.

Bakr, M.M.Y., Wilkes, H., (2002). The influence of facies and depositional environment on the occurrence and distribution of carbazoles and benzocarbazoles in crude oils: a case study from the Gulf of Suez, Egypt. Organic Geochemistry 33, 561-580.

Balba, M.T., Al-Awadhi, N., Al-Daher, R., (2003). Bioremediation of oil-contaminated soil: microbiological methods for feasibility assessment and field evaluation. Water, Air and Soil Pollution 144 (1-4), 419-440.

Bantignies, J.-L., Cartier, D., Moulin, C., Dexpert, H., (1998). Asphaltene adsorption on kaolinite characterized by infrared and X-ray absorption spectroscopies. Journal of Petroleum Science and Engineering 20 (3-4), 233-237.

Bao, J., Li, M., (2001). Unprecedented occurrence of novel C26-C28 21-norcholestanes and related triaromatic series in evaporitic lacustrine sediments. Organic Geochemistry 32 (8), 1031-1036.

Barbe, A., Grimalt, J.O., Pueyo, J.J., Albaigés, J., (1990). Characterization of model evaporitic environments through the study of lipid components. Organic Geochemistry 16 (4-6), 815-828.

Barth, T., Borgund, A.E., Hopland, A.E., (1989). Generation of organic compounds by hydrous pyrolysis of a Kimmeridge Oil shale-bulk results and activation energy calculations. Organic Geochemistry 14 (1), 69-76.

Baskin, D.K., Peters, K.E., (1992). Early generation characteristics of a sulfur-rich Monterey kerogen. American Association of Petroleum Geologists Bulletin 76 (1), 1-13.

Bastow, T.P., van Aarssen, B.G.K., Herman, R., Alexander, R., Kagi, R.I., (2003). The effect of oxidation on the distribution of alkylphenols in crude oils. Organic Geochemistry 34 (8), 1103-1111.

Baudin, F., Tribovillard, N., Laggoun-Defarge, F., Lichtfouse, E., Monod, O., Gardin, S., (1999). Depositional environment of a Kimmeridgian carbonate 'black band' (Akkuyu Formation, south-western Turkey). Sedimentology 46 (4), 589-602.

Bauer, P.E., Dunlap, N.K., Arseniyadis, S., Watt, D.S., Seifert, W.K., Moldowan, J.M., (1983). Synthesis of biological markers in fossil fuels. J. of Organic Chemistry 48, 4493-4497.

Bäuml, E., Mayr, H., (1985). Cycloadditionen des Triphenylallenyl-Kations mit Cyclopentadien - Studium des Reaktionsmechanismus unter stabilen Ionen-Bedingungen. Chemische Berichte 118 (2), 694-703.

Beeder, J., Nilsen, R.K., Thorstensen, T., Torsvik, T., (1996). Penetration of sulfate reducers through a porous North Sea oil reservoir. Applied and Environmental Microbiology 62, 3551-3553.

Béhar, F., Beaumont, V., Penteado, B.H.L., (2001). Rock-Eval 6 technology: Performances and developments. Oil and Gas Science and Technology 56, 111-134.

Béhar, F., Hatcher, P.G., (1995). Artificial coalification of a fossil wood from Brown coal by confined system pyrolysis. Energie and Fuels 9 (6), 984-994.

Béhar, F., Pelet, R., (1985). Pyrolysis-gas chromatography applied to organic geochemistry - structural similarities between kerogens and asphaltenes from related rock extracts and oils. Journal of Analytical and Applied Pyrolysis 8, 173-187.

Béhar, F., Ungerer, P., Kressmann, S., Rudkiewicz, J.L., (1991). Thermal evolution of crude oils in sedimentary basins: experimental simulation in a confined system and kinetic modeling. Revue de l'Institut Francais du Petrole 46 (2), 151-181.

Béhar, F., Vandenbroucke, M., (1987). Chemical modelling of kerogens. Organic Geochemistry 11 (1), 15-24.

Béhar, F.H., Pelet, R., Roucache, J., (1984). Geochemistry of asphaltenes, Advances in Organic Geochemistry 1983. Pergamon, Oxford-New York International, pp. 587-595.

Beka, F.T., Oti, M.N., (1995). The distal offshore Niger Delta: frontier prospects of a mature petroleum province. In: M.N. Oti, G. Postma (Eds.), Geology of Deltas. A.A. Balkema, Rotterdam, pp. 237-241.

Beneo, E., (1952). The search for oil in Sicily. Petroleum Times 56 (1424), 180-181.

Beneo, E., (1955). Les resultats des etudes pour la recherche petrolifere en Sicile. Proceedings - World Petroleum Congress = Actes et Documents - Congres Mondial du Petrole 59 (1506), 109-124.

Beneo, E., (1956). Risultati degli studi volti alla ricerca petrolifera in Sicilia; the results of the studies on petroleum exploration in Sicily. Bollettino del Servizio Geologico d'Italia.

Benkhelil, J., (1989). The evolution of the Cretaceous Benue Trough, Nigeria. Journal of African Earth Sciences 8, 251-282.

Bennet, B., Larter, S.R., (1997). Partition behaviour of alkylphenols in crude oil/brine systems under subsurface conditions. Geochim. Cosmochim. Acta 61 (20), 4393-4402.

Berridge, S.A., Thew, M.T., Loriston-Clarke, A.G., (1968). The formation and stability of emulsions of water in crude petroleum and similar stocks. Journal of the Institute of Petroleum 54, 333-357.

Bertrand, P., Behar, F., Durand, B., (1986). Composition of potential oil from humic coals in relation to their petrographic nature. Organic Geochemistry 10 (1-3), 601-608.

Bird, C.W., Lynch, J.M., (1974). Formation of hydrocarbons by microorganisms. Chem. Soc. Rev. 3, 309-328.

Bissada, K.K., Elrod, L.W., Robinson, C.R., Darnell, L.M., Szymczyk, H.M., Trostle, J.L., (1993). Geochemical inversion. A modern approach to inferring source-rock identity from characteristics of accumulated oil and gas. Energy Exploration and Exploitation 11, 295–328.

Bjorøy, M., Hall, K., Gillyon, P., Jumeau, J., (1991). Carbon isotope variations in n-alkanes and isoprenoids of whole oils. Chemical Geology 93 (1-2), 13-20.

Bjorøy, M., Hall, K., Jumeau, J., (1990). Stable carbon isotope ratio analysis on single components in crude oils by direct gas chromatography--isotope analysis. Trends in Analytical Chemistry 9 (10), 331-337.

Bjorøy, M., Hall, P.B., Hustad, E., Williams, J.A., (1992). Variation in stable carbon isotope ratios of individual hydrocarbons as a function of artificial maturity. Organic Geochemistry 19 (1-3), 89-105.

Bjorøy, M., Hall, P.B., Moe, R.P., (1994). Stable carbon isotope variation of n-alkanes in Central Graben oils. Organic Geochemistry 22 (3-5), 355-381.

Blumer, M., Robertson, J.C., Gordon, J.E., Sass, J., (1969). Phytol-derived C19 di- and triolefinic hydrocarbons in marine zooplankton and fishes. Biochemistry 8, 4067-4074.

Bodrossy, L., Murrell, J.C., Dalton, H., Kalman, M., Puskas, L.G., Kovacs, K.L., (1995). Heat-tolerant methanotrophic bacteria from the hot water effluent of a natural gas field. Applied and Environmental Microbiology 61, 3549-3555.

Boon, J.J., de Leeuw, J.W., Hoeck, V.G., Vosjan, J.H., (1977). The significance of taxonomical value of iso- and anteiso-monoenoic fatty acids and branched-hydroxy acids in Desulfovibrio desulfuricans. J. Bacteriol. 129, 1183-1191.

Boon, J.J., Hines, H., Burlingame, A.L., (1983). Organic geochemical studies of Solar Lake laminated cyanobacterial mats. Advances in Organic Geochemistry 1981, 207-227.

Bordenave, M.L., (1993). The sedimentation of organic matter. In: M.L. Bordenave (Ed.), Applied Petroleum Geochemistry. Editions Technip, Paris, pp. 217-278.

Bordenave, M.L., Espitalié, J., Leplat, P., Oudin, J.L., Vandenbroucke, M., (1993). Screening tecniques for source rock evaluation. In: M.L. Bordenave (Ed.), Applied Petroleum Geochemistry. Editions Technip, Paris, pp. 219–224.

Boreham, C.J., Golding, S.D., Glikson, M., (1998). Factors controlling the origin of gas in Australian Bowen Basin coals. Organic Geochemistry 29 (1-3), 347-362.

Boreham, C.J., Hope, J.M., Hartung-Kagi, B., (2001). Understanding source, distribution and preservation of Australian natural gas: A geochemical perspective. Aus. Petrol. Explor. Assoc. J. 41, 523-547.

Boreham, C.J., Horsfield, B., Schenk, H.J., (1999). Predicting the quantities of oil and gas generated from Australian Permian coals, Bowen Basin using pyrolytic methods. Marine and Petroleum Geology 16 (2), 165-188.

Boreham, C.J., Powell, T.G., (1991). Variation in pyrolysate composition of sediments from the Jurassic Walloon Coal Measures, eastern Australia as a function of thermal maturation. Organic Geochemistry 17 (6), 723-733.

Boussingault, M., (1837). Memoire sur la composition des bitumens. Annals de Chimie Physyque 64, 141.

Bracewell, J.M., Robertson, G.W., (1987). Characteristics of soil organic matter in temperate soils by Curie-point pyrolysis-mass spectrometry. II. The effect of drainage and illuviation in B horizons. European Journal of Soil Science 38 (2), 191-198.

Brosse, E., Loreau, J.P., Frixa, A., (1989). La Distribution de la matiere organique dans la formation de Noto, roche-mere du bassin de Ragusa (Sicile), Applications de la petrologie organique en geologie, 5; 5. Societe Geologique de France, Paris, France, pp. 951-955.

Brosse, E., Riva, A., Santucci, S., Bernon, M., Loreau, J.P., Frixa, A., Laggoun, D.F., (1990). Some sedimentological and geochemical characters of the Late Triassic Noto Formation, source rock in the Ragusa Basin (Sicily), Advances in organic geochemistry, 1989; Part II, Molecular geochemistry; proceedings of the 14th international meeting on Organic geochemistry, 16; 4-6. Pergamon, Oxford-New York, International, pp. 715-734.

Burnham, A.K., (1989). On the validity of the Pristane Formation Index. Geochim. Cosmochim. Acta 53 (7), 1693-1697.

Burnham, A.K., Braun, R.L., Gregg, H.R., Samoun, A.M., (1987). Comparison of methods for measuring kerogen pyrolysis rates and fitting kinetic parameters. Energy and Fuels 1, 452-458.

Burnham, A.K., Braun, R.L., Samoun, A.M., (1988). Further comparison of methods for measuring kerogen pyrolysis rates and fitting kinetic parameters. In: L. Mattavelli, L. Novelli (Eds.), Advances in Organic Geochemistry 1987. Pergamon, Oxford-New York International, pp. 839-845.

Burnham, A.K., Happe, J.A., (1984). On the mechanism of kerogen pyrolysis. Fuel 63 (10), 1353-1356.

Butler, R.W.H., Grasso, M., Gardiner, W., Sedgeley, D., (1997). Depositional patterns and their tectonic controls within the Plio-Quaternary carbonate sands and muds of onshore and offshore SE Sicily (Italy). Marine and Petroleum Geology 14 (7-8), 879-892.

Cabrera, L., Cabrera, M., Gorchs, R., de las Heras, F.X.C., (2002). Lacustrine basin dynamics and organosulphur compound origin in a carbonate-rich lacustrine system (Late Oligocene Mequinenza Formation, SE Ebro Basin, NE Spain). Sedimentary Geology 148 (1-2), 289-317.

Cai, C., Worden, R.H., Bottrell, S.H., Wang, L., Yang, C., (2003). Thermochemical sulphate reduction and the generation of hydrogen sulphide and thiols (mercaptans) in Triassic carbonate reservoirs from the Sichuan Basin, China. Chemical Geology 202 (1-2), 39-57.

Caldwell, M.E., Garrett, R.M., Prince, R.C., Suflita, R.M., (1998). Anaerobic biodegradation of long-chain n-alkanes under sulfate-reducing condition. Environmental Science and Technology 32, 2191-2195.

Calemma, V., Iwanski, P., (2002). Structural characterisation of asphaltenes of different origins. Energie and Fuels 9, 225-230.

Campos, P.G., Grimalt, J.O., Berdie, L., Lopez-Quintero, J.O., Navarrete-Reyes, L.E., (1996). Organic geochemistry of Cuban oils--I. The northern geological province. Organic Geochemistry 25 (8), 475-488.

Cañipa-Morales, N.K., Galan-Vidal, C.A., Guzman-Vega, M.A., Jarvie, D.M., (2003). Effect of evaporation on C7 light hydrocarbon parameters. Organic Geochemistry 34 (6), 813-826.

Carauta, A.N.M., Seidl, P.R., Chrisman, E.C.A.N., Correia, J.C.G., de Menechini, P.O., Silva, D.M., Leal, K.Z., de Menezes, S.M.C., de Souza, W.F., Teixeira, M.A.G., (2005). Modeling solvent effects on asphaltene dimers. Energy & Fuels 19 (4), 1245 - 1251.

Carbognani, L., (1992). Molecular structure of asphaltene of venezuelan crude. In: Techn. Rept. INTEVEP S.A. Centro de Investigación y Apoyo Tecnológico, Filial de Petróleos de Venezuela.

Carpentier, B., Huc, A.Y., Gely, J.P., Blanc-Valleron, M.M., (1993). Geological and geochemical modeling, an approach for understanding organic cyclic sedimentation in evaporitic sequences. Application to the Mulhouse Basin (France). Organic Geochemistry 20 (8), 1153-1163.

Cassani, F., Eglinton, G., (1986). Organic geochemistry of Venezuelan extra-heavy crude oils. 1. Pyrolysis of asphaltenes: a technique for the correlation and maturity evaluation of crude oils. Chem. Geol. 56, 167-183.

Castelli, A., Chiaramonte, M.A., Beltrame, P.L., Carniti, P., del Bianco, A., Stroppa, F., (1990). Thermal degradation of kerogen by hydrous pyrolysis. A kinetic study. Organic Geochemistry 16 (1-3), 75-82.

Castex, H., (1985). Resins and asphaltenes: Evolution as a function of organic-matter type and burial. Revue de l´Institut Francais du Petrole 40 (2), 169-189.

Catalano, R., Di, S.E., Infuso, S., Sulli, A., Vail, P.R., Vitale, F.P., (1994). Sequence stratigraphy in active tectonic setting; Plio-Pleistocene of Tyrrhenian Sea and Sicily; comparison with the Gulf of Mexico, AAPG annual convention, 1994;. American Association of Petroleum Geologists and Society of Economic Paleontologists and Mineralogists, Tulsa, OK, United States, pp. 118-119.

Catalano, R., Di Stefano, P., Sulli, A., Vitale, F.P., (1996). Paleogeography and structure of the central Mediterranean: Sicily and its offshore area. Tectonophysics 260 (4), 291-323.

Catalano, R., Merlini, S., Sulli, A., (2002). The structure of western Sicily, central Mediterranean. Petroleum Geoscience 8 (1), 7-18.

Chaillan, F., Le Fleche, A., Bury, E., Phantavong, Y.-h., Grimont, P., Saliot, A., Oudot, J., (2004). Identification and biodegradation potential of tropical aerobic hydrocarbon-degrading microorganisms. Research in Microbiology 155 (7), 587-595.

Chalansonnet, S., Largeau, C., Casadevall, E., Berkaloff, C., Peniguel, G., Couderc, R., (1988). Cyanobacterial resistant biopolymers. Geochemical implications of the properties of Schizothrix sp. resistant material. Organic Geochemistry 13 (4-6), 1003-1010.

Chappe, B., Albrecht, P., Michaelis, W., (1982). Polar lipids of archaebacteria in sediments and petroleums. Science 217 (4554), 65-66.

Chen, J., Summons, R.E., (2001). Complex patterns of steroidal biomarkers in Tertiary lacustrine sediments of the Biyang Basin, China. Organic Geochemistry 32 (1), 115-126.

Chow, N., Wendte, J., Stasiuk, L.D., (1995). Productivity versus preservation controls on two organic-rich carbonate facies in the Devonian of Alberta; sedimentological and organic petrological evidence. Bulletin of Canadian Petroleum Geology 43 (4), 433-460.

Chung, H.M., Claypool, G.E., Rooney, M.A., Squires, R.M., (1994). Source characteristics of marine oils as indicated by carbon isotopic ratios of volatile hydrocarbons. Bulletin of the American Association of Petroleum Geologists 78, 396-408.

Chung, H.M., Sackett, W.M., (1979). Use of stable carbon isotope compositions of pyrolytically derived methane as maturity indices for carbonaceous materials. Geochimica et Cosmochimica Acta 43 (12), 1979-1988.

Cimino, R., Correra, S., del Bianco, A., Lockhart, T.P., (1995). Asphaltenes: Fundamentals and applications. In: E.Y. Sheu, O.C. Mullins (Eds.). Plenum Press, New York, pp. 97-130.

Clark, P.D., Oriakhi, C.O., (1992). Studies on the stability of organic disulfide–polysulfide sulfur solvents used in sour gas production. Energie and Fuels 6, 474-477.

Clayton, C.J., (1991). Effect of maturity on carbon isotope ratios of oils and condensates. Organic Geochemistry 17 (6), 887-899.

Clayton, J.L., (1998). Geochemistry of coalbed gas - A review. International Journal of Coal Geology 35 (1-4), 159-173.

Clayton, J.L., Rice, D.D., Michael, G.E., (1991). Oil-generating coals of the San Juan Basin, New Mexico and Colorado, U.S.A. Organic Geochemistry 17 (6), 735-742.

Clegg, H., Horsfield, B., Stasiuk, L., Fowler, M.G., Vliex, M., (1997). Geochemical characterisation of organic matter in Keg River Formation (Elk Point Group, Middle Devonian), La Crete Basin, Western Canada. Organic Geochemistry 26 (11-12), 627-643.

Coates, J.D., Woodward, J.C., Allen, J., Philip, P., Lovley, D.R., (1997). Anaerobic degradation of polycyclic aromatic hydrocarbons and alkanes in petroleum-contaminated harbor-sediments. Applied and Environmental Microbiology 63, 3589-3593.

Coleman, J.M., (1988). Dynamic changes and processes in the Mississippi River delta. Geological Society of America Bulletin 100, 999-1015.

Collister, J.W., Lichtfouse, E., Hieshima, G., Hayes, J.M., (1994). Partial resolution of sources of n-alkanes in the saline portion of the Parachute Creek Member, Green River Formation (Piceance Creek Basin, Colorado). Organic Geochemistry 21 (6-7), 645-659.

Colombo, U., Sironi, G., (1959). Geochemical analysis of Italian oils and asphalts. Proceedings - World Petroleum Congress = Actes et Documents - Congres Mondial du Petrole.

Connan, J., Dessort, D., (1987). Novel family of hexacyclic hopanoid alkanes (C32---C35) occurring in sediments and oils from anoxic paleoenvironments. Organic Geochemistry 11 (2), 103-113.

Connan, J., Lacrampe-Couloume, G., Magot, M., (1997). Anaerobic biodegradation of petroleum in reservoirs: a widespread phenomenon in nature. In: Abstracts Part I, 18th IMOG, Maastricht, Netherlands.

Connan, J., Nissenbaum, A., (2004). The organic geochemistry of the Hasbeya asphalt (Lebanon): comparison with asphalts from the Dead Sea area and Iraq. Organic Geochemistry 35 (6), 775-789.

Corbett, L.W., Petrossi, U., (1978). Differences distillation and solvent separated asphalt residua. Ind. Eng. Chem. Prod. Res. Dev. 17, 342-346.

Cramer, B., (2004). Methane generation from coal during open system pyrolysis investigated by isotope specific, Gaussian distributed reaction kinetics. Organic Geochemistry 35 (4), 379-392.

Creaney, S., Allan, J., (1990). Hydrocarbon generation and migration in the Western Canada sedimentary basin, Classic petroleum provinces, 50;. Geological Society of London, London, United Kingdom, pp. 189-202.

Creaney, S., Allan, J., Cole, K.S., Fowler, M.G., Osadetz, K.G., Macqueen, R.W., Snowdon, L.R., Riediger, C.L., (1994). Petroleum generation and migration in the Western Canada sedimentary basin, Geological atlas of the Western Canada sedimentary basin. Canadian Society of Petroleum Geologists, Calgary, AB, Canada | Alberta Research CouncilEdmonton, AB.

Creek, J.L., (2005). Freedom of action in the state of asphaltenes: Escape from conventional wisdom. Energie and Fuels 19, 1212-1224.

Curiale, J.A., (1987). Steroidal hydrocarbons of the Kishenehn Formation, northwest Montana. Organic Geochemistry 11, 233-244.

da Rocha Filho, G.N., Brodzki, D., Djega-Mariadassou, G., (1993). Formation of alkanes, alkylcycloalkanes and alkylbenzenes during the catalytic hydrocracking of vegetable oils. Fuel 72 (4), 543-549.

da Silva Ramos, A.C., Haraguchi, L., Notrispe, F.R., Loh, W., Mohamed, R.S., (2001). Interfacial and colloidal behavior of asphaltenes obtained from Brazilian crude oils. Journal of Petroleum Science and Engineering 32 (2-4), 201-216.

Dahl, B., Speers, G.C., (1986). Geochemical characterization of a tar mat in the Oseberg field Norwegian sector, north sea. Organic Geochemistry 10 (1-3), 547-558.

Damuth, J.E., (1994). Neogene gravity tectonics and depositional processes on the deep Niger Delta continental margin. Marine and Petroleum Geology 11, 320-346.

Darley, H.C.H., Gray, G.R., (1988). Composition and Properties of Drilling and Completion Fluids. Gulf Professional Publishing.

de Boer, R.B., Leerlooyer, K., Eigner, M., van Bergen, A., (1995). Screening of Crude Oils for Asphalt Precipitation: Theory, Practice and the Selection of Inhibitors. SPE Production and Facilities, 55-61.

de las Heras, F.X., Grimalt, J.O., Lopez, J.F., Albaigés, J., Sinninghe Damsté, J.S., Schouten, S., de Leeuw, J.W., (1997). Free and sulphurized hopanoids and highly branched isoprenoids in immature lacustrine oil shales. Organic Geochemistry 27, 41-63.

de Leeuw, J.W., Sinninghe Damsté, J.S., (1990). Organic sulfur compounds and other biomarkers as indicators of palaeosalinity, In: Geochemistry of sulfur in fossil fuels, 429. American Chemical Society, Washington, DC, United States, pp. 417-443.

del Carmen Garcia, M., Carbognani, L., Orea, M., Urbina, A., (2000). The influence of alkane class-types on crude oil wax crystallization and inhibitors efficiency. Journal of Petroleum Science and Engineering 25 (3-4), 99-105.

Delvaux, D., Martin, H., Leplat, P., Paulet, J., (1990). Geochemical characterization of sedimentary organic matter by means of pyrolysis kinetic parameters, Advances in organic geochemistry 1989; Part I, Organic geochemistry in petroleum exploration, 16; 1-3. Pergamon, Oxford-New York, International, pp. 175-187.

Demirbas, A., (2002). Asphaltene yields from five types of fuels via different methods. Energy Conversion and Management 43 (8), 1091-1097.

Derenne, S., Largeau, C., Berkaloff, C., (1996). First example of an algaenan yielding an aromatic-rich pyrolysate. Possible geochemical implications on marine kerogen formation. Organic Geochemistry 24 (6-7), 617-627.

Deroo, G., Powell, T.G., Tissot, B., McCrossen, R.G., (1977). The origin and migration of petroleum in the Western Canada Sedimentary Basin, Alberta: A geochemical and thermal maturation study. Bulletin of the Geological Society of Canada 262.

Devai, I., Delaune, R.D., Patrick Jr., W.H., Gambrell, R.P., (2001). Changes in methylmercury concentration during storage: effect of temperature. Organic Geochemistry 32 (5), 755-758.

di Primio, R., (1995). The generation and migration of sulphur-rich petroleums in a low-maturity carbonate source rock sequence from Italy. In: Forschungszentrum Jülich, PhD-thesis, pp. 197.

di Primio, R., Dieckmann, V., Mills, N., (1998). PVT and phase behaviour analysis in petroleum exploration. Organic Geochemistry 29, 207-222.

di Primio, R., Horsfield, B., (1996). Predicting the generation of heavy oils in carbonate/evaporitic environments using pyrolysis methods. Organic Geochemistry 24 (10-11), 999-1016.

di Primio, R., Horsfield, B., Guzman, V.M.A., (2000). Determining the temperature of petroleum formation from the kinetic properties of petroleum asphaltenes. Nature (London) 406 (6792), 173-176.

di Primio, R., Skeie, J.E., (2004). Development of a compositional kinetic model for hydrocarbon generation and phase equilibria modelling: A case study from Snorre Field, Norwegian North Sea. In: J.M. Cubitt, W.A. England, S.R. Larter (Eds.), Understanding Petroleum Reservoirs: Towards an Integrated Reservoir Engineering and Geochemical Approach, 237, Geological Society Special Publication. Geological Society Publishing House, London, pp. 157-174.

di Stefano, P., (1990). The Triassic of Sicily and the Southern Apennines. Bolettino della Società Geoligica Italiana 109 (3), 21-37.

Didyk, B.M., Simoneit, B.R.T., Brassell, S.C., Eglinton, G., (1978). Organic geochemical indicators of palaeoenvironmental conditions of sedimentation. Nature 272 (5650), 216-222.

Dieckmann, V., (1998). Zur Vorhersage der Erdöl- und Erdgaszusammensetzungen durch die Integration von Labor- und Fallstudien. Forschungszentrum Jülich, PhD-thesis, 285.

Dieckmann, V., (2005). Modelling petroleum formation from heterogeneous source rocks: the influence of frequency factors on activation energy distribution and geological prediction. Marine and Petroleum Geology 22 (3), 375-390.

Dieckmann, V., Caccialanza, P.G., Galimberti, R., (2002). Evaluating the timing of oil expulsion: about the inverse behaviour of light hydrocarbons and oil asphaltene kinetics. Organic Geochemistry 33 (12), 1501-1513.

Dieckmann, V., Fowler, M., Horsfield, B., (2004). Predicting the composition of natural gas generated by the Duvernay Formation (Western Canada Sedimentary Basin) using a compositional kinetic approach. Organic Geochemistry 35 (7), 845-862.

Dieckmann, V., Horsfield, B., Schenk, H.J., (2000a). Heating rate dependency of petroleum-forming reactions: implications for compositional kinetic predictions. Organic Geochemistry 31 (12), 1333-1348.

Dieckmann, V., Schenk, H.J., Horsfield, B., (2000b). Assessing the overlap of primary and secondary reactions by closed- versus open-system pyrolysis of marine kerogens. Journal of Analytical and Applied Pyrolysis 56 (1), 33-46.

Dieckmann, V., Schenk, H.J., Horsfield, B., Welte, D.H., (1998). Kinetics of petroleum generation and cracking by programmed-temperature closed-system pyrolysis of Toarcian Shales. Fuel 77 (1-2), 23-31.

Dignac, M.-F., Houot, S., Francou, C., Derenne, S., (2005). Pyrolytic study of compost and waste organic matter. Organic Geochemistry 36 (7), 1054-1071.

Dong, J.Z., Katoh, T., Itoh, H., Ouchi, K., (1986). n-paraffins obtained by extraction and mild stepwise hydrogenation of Wandoan coal. Fuel 65 (8), 1073-1078.

Dou, L., Zhu, Y., Yang, T., Xu, S., Ping, X., (1998). Origins of heavy oils in the Erlian Basin, NE China. Marine and Petroleum Geology 15 (8), 769-781.

Douglas, A.G., Larter, S.R., (1980). The origin of algal kerogens. In: International Geological Congress, Abstracts, 2, pp. 770.

Durand, B., Monin, J.C., (1980). Elemental analysis of kerogens. In: B. Durand (Ed.), Kerogen. Editions Technip., Paris, pp. 113-141.

Durand, B., Paratte, M., (1983). Oil potential of coals: a geochemical approach. Petroleum geochemistry and exploration of Europe, Published by Blackwell Scientific; Geological Society Special Publication 12, Editors Brooks J., 255-265.

Eglinton, G., Douglas, A.G., Rowland, S.J., (1988). Release of aliphatic, aromatic and sulphur compounds from Kimmeridge kerogen by hydrous pyrolysis: a quantitative study. Organic Geochemistry 13 (4-6), 655-663.

Eglinton, T.I., Irvine, J.E., Vairavamurthy, A., Zhou, W., Manowitz, B., (1994). Formation and diagenesis of macromolecular organic sulfur in Peru margin sediments. Organic Geochemistry 22 (3-5), 781-799.

Eglinton, T.I., Sinninghe Damsté, J.S., Kohnen, M.E.L., de Leeuw, J.W., (1990a). Rapid estimation of the organic sulphur content of kerogens, coals and asphaltenes by pyrolysis-gas chromatography. Fuel 69, 1394-1404.

Eglinton, T.I., Sinninghe Damsté, J.S., Kohnen, M.E.L., de Leeuw, J.W., Larter, S.R., Patience, R.L., (1990b). Analysis of maturity-related changes in the organic sulfur composition of kerogens by flash pyrolysis-gas chromatography, In: Geochemistry of sulfur in fossil fuels, 429. American Chemical Society, Washington DC, United States, pp. 529-565.

Ehinola, O.A., Joshua, E.O., Opeloye, S.A., Ademola, J.A., (2005). Radiogenic heat production in the Cretaceous sediments of Yola Arm of Nigeria Benue Trough: Implications for thermal history and hydrocarbon generation. Journal of Applied Sciences 5 (4), 696-701.

Ehrenberg, S.N., Skjevrak, I., Gilje, A.E., (1995). Asphaltene-rich residues in sandstone reservoirs of Haltenbanken province, mid-Norwegian continental shelf. Marine and Petroleum Geology 12 (1), 53-69.

Ejedawe, J.E., Coker, S.J.L., Lambert-Aikhionbare, D.O., Alofe, K.B., Adoh, F.O., (1984). Evolution of oil-generative window and oil and gas occurrence in Tertiary Niger Delta Basin. AAPG Bulletin 68, 1744-1751.

Ekweozor, C.M., Daukoru, E.M., (1994). Northern delta depobelt portion of the Akata-Agbada(!) petroleum system, Niger Delta, Nigeria, The petroleum system; from source to trap, 60;. American Association of Petroleum Geologists, Tulsa, OK, United States, pp. 599-613.

Ekweozor, C.M., Okogun, J.I., Ekong, D.E.U., Maxwell, J.R., (1979). Preliminary organic geochemical studies of samples from the Niger delta (Nigeria) I. Analyses of crude oils for triterpanes. Chemical Geology 27 (1-2), 11-28.

Ekweozor, C.M., Okogun, J.I., Ekong, D.E.U., Maxwell, J.R., (1981). C24-C27 Degraded triterpanes in Nigerian petroleum: novel molecular markers of source/input or organic maturation? Journal of Geochemical Exploration 15 (1-3), 653-662.

Ekweozor, C.M., Telnaes, N., (1990). Oleanane parameter: Verification by quantitative study of the biomarker occurrence in sediments of the Niger delta. Organic Geochemistry 16 (1-3), 401-413.

Ekweozor, C.M., Udo, O.T., (1988). The oleananes: Origin, maturation and limits of occurence in Southern Nigeria sedimentary basins. Organic Geochemistry 13 (1-3), 131-140.

Eneogwe, C., Ekundayo, O., (2003). Geochemical correlation of crude oils in the NW Niger Delta, Nigeria. Journal of Petroleum Geology 26 (1), 95-103.

Eneogwe, C.I., (2004). The invariance ratio in isoheptanes: a powerful tool for oil-oil correlation in the Tertiary Niger Delta, Nigeria. Organic Geochemistry 35 (8), 989-992.

Erdmann, M., Horsfield, B., (2006). Enhanced late gas generation potential of petroleum source rocks via condensation reactions: Evidence from the Norwegian North Sea. Geochim. Cosmochim. Acta 70, 3943-3956.

Ericsson, I., Lattimer, R.P., (1988). Pyrolysis nomenclature. Journal of Analytical and Applied Pyrolysis 14, 219-221.

Escobedo, J., Mansoori, G.A., (1997). Viscometric principles of the onsets of colloidal asphaltene flocculation in paraffinic oils and asphaltene micellization in aromatics. SPE Production and Facilities, 116.

Escobedo, J., Mansoori, G.A., Balderas-Joers, C., Carranza-Becerra, L.J., Mendez-Garcia, M.A., (1997). Heavy organic deposition during oil production from a hot deep reservoir: a field experience. In: 5th Latin American and Caribbean Petroleum Engineering Conference and Exhibition. Society of Petroleum Engineers.

Espinat, D., Ravey, J.C., (1993). Colloidal structure of asphaltene solutions and heavy-oil fractions studied by small-angle neutron and X-ray scattering. In: SPE International Symposium, New Orleans.

Espitalié, J., Deroo, G., Marquis, F., (1985). La pyrolyse Rock-Eval et ses applications - première/deuxième partie. Revue de l´Institut Francais du Petrole 40 (5-6), 563-579.

Espitalié, J., Marquis, F., Sage, L., (1987). Organic geochemistry of the Paris Basin. In: J.M. Brooks, K. Glennie (Eds.), Petroleum Geology of North West Europe. Graham and Trotman, London, pp. 71-86.

Evamy, B.D., Haremboure, J., Kamerling, P., Knaap, W.A., Molloy, F.A., Rowlands, P.H., (1978). Hydrocarbon habitat of Tertiary Niger Delta. AAPG Bulletin 62, 1-39.

Fabbri, D., Prati, S., Vassura, I., (2002). Molecular characterisation of organic material in air fine particles (PM10) using conventional and reactive pyrolysis-gas chromatography-mass spectrometry. J. Environ. Monitoring 4, 210-215.

Facca, G.C., Roberti, G., Sommariva, E., (1951). Italian crude oil analyses. Proceedings - World Petroleum Congress = Actes et Documents - Congres Mondial du Petrole.

Flory, P.J., (1953). Principles of polymer chemistry. Cornell University Press, Ithaca, NY, pp. 495-518.

Fowler, M., Brooks, P.W., (1990). Organic geochemistry as an aid in the interpretation of the history of oil migration into different reservoirs at the Hibernia K-18 and Ben Nevis I-45 wells, Jeanne d´Arc Basin, offshore eastern Canada. Organic Geochemistry 16, 461-475.

Fowler, M.G., Douglas, A.G., (1987). Saturated hydrocarbon biomarkers in oils of Late Precambrian age from Eastern Siberia. Organic Geochemistry 11, 201-213.

Francois, R., (1987). A study of sulphur enrichment in the humic fraction of marine sediments during early diagenesis. Geochimica et Cosmochimica Acta 51 (1), 17-27.

Freeman, K.H., Hayes, J.M., Trendel, J.-M., Albrecht, P., (1990). Evidence from carbon isotope measurements for diverse origins of sedimentary hydrocarbons. Nature 343 (6255), 254-256.

Fuhrmann, A., (2005). Predicting petroleum phase and composition. In: Internal Report. GFZ-Potsdam, Potsdam.

Fukushima, K., Morinaga, S., Uzaki, M., Ochiai, M., (1989). Hydrocarbons generated by pyrolysis of insoluble kerogen-like materials isolated from microbially degraded plant residues. Chem. Geol. 76, 131-141.

Galimberti, R., Dolci, D., Caccialanza, P.G., Caldiero, L., Dieckmann, V., (2003). Anomalous behaviour of C7 paraffinicity parameters in carbonate sourced Italian oils. In: IMOG 2003, Book of abstracts, part I., Krakow, pp. 146-147.

Galimberti, R., Ghiselli, C., Chiaramonte, M.A., (2000). Acidic polar compounds in petroleum: a new analytical methodology and applications as molecular migration indicies. Organic Geochemistry 31, 1375-1386.

Galimov, E.M., (1974). Organic geochemistry of carbon isotopes. In: B.P. Tissot, F. Bienner (Eds.), Advances in Organic Geochemistry 1973. Editions Technip, Paris, pp. 439-452.

Gallant, R.W., (1984). Physical properties of hydrocarbons. Gulf Publishing Vol. 2.
Gallego, J.R., González-Rojas, E., Peláez, A.I., Sánchez, J., García-Martínez, M.J., Llamas, J.F., (2006). Effectiveness of bioremediation for the prestige fuel spill: a summary of case studies. In: Advanced Technology in the Environmental Field.
Galloway, W.E., Hobday, D.K., (1996). Terrigenous Clastic Depositional Systems. Springer, Berlin.
Galtsev, V.E., Ametov I.M., Grinberg, O.Y., (1995). Asphaltene association in crude oil as studied by ENDOR. Fuel 74, 670.
Gelin, F., Sinninghe Damsté, J.S., Harrison, W.N., Maxwell, J.R., de Leeuw, J.W., (1995). Molecular indicators for palaeoenvironmental change in a Messinian evaporitic sequence (Vena del Gesso, Italy): III. Stratigraphic changes in the molecular structure of kerogen in a single marl bed as revealed by flash pyrolysis. Organic Geochemistry 23 (6), 555-566.
Geng, A., Liao, Z., (2002). Kinetic studies of asphaltene pyrolyses and their geochemical applications. Applied Geochemistry 17 (12), 1529-1541.
George, G.N., Gorbaty, M.L., (1989). Sulfur K-edge X-ray absorption spectroscopy of petroleum asphaltenes and model compounds. Journal of the American Chemical Society 111, 3186–3192.
Giraud, A., (1970). Application of pyrolysis and pyrolysis gas chromatography to the geochemical characterisation of kerogen in sedimentary rocks. AAPG Bulletin 54, 439-455.
Giunta, G., (1993). Elementi per un modello cinematico delle Maghrebidi siciliane. Mem. Soc. Geol. Ital. 47, 297-311.
Goossens, H., de Leeuw, J.W., Schenck, P.A., Brassell, S.C., (1984). Tocopherols as likely precursors of pristane in ancient sediments and crude oils. Nature 312, 440-442.
Goth, K., de Leeuw, J.W., Püttmann, W., Tegelaar, E.W., (1988). Origin of messel oil shale. Nature 336, 759-761.
Gransch, J.A., Posthuma, J., (1974). On the origin of sulphur in crudes. In: B. Tissot, F. Bienner (Eds.), Advances in Organic Geochemistry 1973, Paris, pp. 727-739.
Grice, K., Schouten, S., Blokker, P., Derenne, S., Largeau, C., Nissenbaum, A., Sinninghe Damsté, J.S., (2003). Structural and isotopic analysis of kerogens in sediments rich in free sulfurised Botryococcus braunii biomarkers. Organic Geochemistry 34, 471-482.
Grice, K., Schouten, S., Nissenbaum, A., Charrach, J., Sinninghe Damsté, J.S., (1998a). A remarkable paradox: Sulfurised freshwater algal (Botryococcus braunii) lipids in an ancient hypersaline euxinic ecosystem. Organic Geochemistry 28 (3), 195-216.
Grice, K., Schouten, S., Peters, K.E., Sinninghe Damsté, J.S., (1998b). Molecular isotopic characterisation of hydrocarbon biomarkers in Palaeocene-Eocene evaporitic, lacustrine source rocks from the Jianghan Basin, China. Organic Geochemistry 29 (5-7), 1745-1764.
Grimalt, J.O., Albaigés, J., (1987). Sources and occurrence of C12-C22 n-alkane distributions with even carbon-number preference in sedimentary environments. Geochimica et Cosmochimica Acta 51, 1379-1384.
Grimalt, J.O., de Wit, R., Teixidor, P., Albaigés, J., (1992). Lipid biogeochemistry of Phormidium and Microcoleus mats. Organic Geochemistry 26, 509-530.
Grimalt, J.O., Torras, E., Albaigés, J., (1988). Bacterial reworking of sedimentary lipids during sample storage. Organic Geochemistry 13 (4-6), 741-746.
Grimalt, J.O., Yruela, I., Saiz-Jimenez, C., Toja, J., de Leeuw, J.W., Albaigés, J., (1991). Sedimentary lipid biogeochemistry of an hypereutrophic alkaline lagoon. Geochimica et Cosmochimica Acta 55, 2555-2577.
Groenzin, H., Mullins, O.C., (2001). Molecular size and structure of asphaltenes. Petroleum Science and Technology 19 (1&2), 219-230.

Gürgey, K., (1998). Geochemical effects of asphaltene separation procedures; changes in sterane, terpane, and methylalkane distributions in maltenes and asphaltene co-precipitates, Advances in organic geochemistry 1997; proceedings of the 18th international meeting on Organic geochemistry; Part II, Biogeochemistry, 29; 5-7. Pergamon, Oxford-New York, International, pp. 1139-1147.

Gussow, W.C., (1968). Migration of reservoir fluids. Journal of Petroleum Technology, 353-363.

Haack, R.C., Sundararaman, P., Diedjomahor, J.O., Xiao, H., Gant, N.J., May, E.D., Kelsch, K., (2000). Niger Delta petroleum systems, Nigeria, Petroleum systems of South Atlantic margins, 73;. American Association of Petroleum Geologists, Tulsa, OK, United States, pp. 213-231.

Haas, J., (2002). Origin and evolution of late Triassic backplatform and intraplatform basins in the Transdanubian range, Hungary. Geologica Carpathica 53 (3), 159-178.

Halpern, H.I., (1995). Development and applications of light-hydrocarbon-based star diagrams. AAPG Bulletin 79 (6), 801-815.

Han, J., Calvin, M., (1969). Hydrocarbon distribution of algae and bacteria and microbiological activity in sediments. Proc. Natl. Acad. Sci. USA 64, 436-445.

Han, J., McCarthy, E.D., Van Hoeven, W., Calvin, M., Bradley, W.H., (1968). Organic geochemical studies, II. A preliminary report on the distribution of aliphatic hydrocarbons in algae, in bacteria, and in a recent lake sediment. In: Proceedings of the National Academy of Sciences, 59, (USA), pp. 29-33.

Hanson, A.D., Zhang, S.C., Moldowan, J.M., Liang, D.G., Zhang, B.M., (2000). Molecular organic geochemistry of the Tarim basin, Northwest China. American Association of Petroleum Geologists Bulletin 84 (8), 1109-1128.

Harms, G., Zengler, K., Rabus, R., Aeckersberg, F., Minz, D., Rossello-Mora, R., (1999). Anaerobic oxidation of o-xylene, m.xylene, and homologous alkylbenzenes by new types of sulfate-reducing bacteria. Applied and Environmental Microbiology 65, 999-1004.

Hartgers, W.A., Lopez, J.F., Sinninghe Damsté, J.S., Reiss, C., Maxwell, J.R., Grimalt, J.O., (1997). Sulfur-binding in recent environments: II. Speciation of sulfur and iron and implications for the occurrence of organo-sulfur compounds. Geochimica et Cosmochimica Acta 61 (22), 4769-4788.

Hartgers, W.A., Sinninghe Damsté, J.S., de Leeuw, J.W., (1994a). Geochemical significance of alkylbenzene distributions in flash pyrolysates of kerogens, coals, and asphaltenes. Geochimica et Cosmochimica Acta 58 (7), 1759-1775.

Hartgers, W.A., Sinninghe Damsté, J.S., Requejo, A.G., Allan, J., Hayes, J.M., Ling, Y., Xie, T.-M., Primack, J., de Leeuw, J.W., (1994b). A molecular and carbon isotopic study towards the origin and diagenetic fate of diaromatic carotenoids*1. Organic Geochemistry 22 (3-5), 703-725.

Hatch, J.R., Jacobson, S.R., Witzke, B.J., Risatti, J.B., Anders, D.E., Watney, W.L., Newell, K.D., Vuletich, A.K., (1987). Possible Middle Ordovician organic carbon isotope eccursion: Evidence from Ordovician oils and hydrocarbon source rocks, Mid-Continent, and East-Central United States. Amer. Assoc. of Petrol. Geol. Bull. 71, 1342-1354.

Head, I.M., Jones, M., Larter, S.R., (2003). Biological activity in the deep subsurface and the origin of heavy oil. Nature 426, 344-352.

Heath, D.J., Lewis, C.A., Rowland, S.J., (1997). The use of high temperature gas chromatography to study the biodegradation of high molecular weight hydrocarbons. Organic Geochemistry 26 (11-12), 769-785.

Hetenyi, M., Brukner-Wein, A., Sajgo, C., Haas, J., Hamor-Vido, M., Szanto, Z., Toth, M., (2002). Variations in organic geochemistry and lithology of a carbonate sequence

deposited in a backplatform basin (Triassic, Hungary). Organic Geochemistry 33 (12), 1571-1591.

Hetenyi, M., Sajgo, C., Veto, I., Brukner-Wein, A., Szanto, Z., (2004). Organic matter in a low productivity anoxic intraplatform basin in the Triassic Tethys. Organic Geochemistry 35 (11-12), 1201-1219.

Heydari, E., (1997). The role of burial diagenesis in hydrocarbon destruction and H2S accumulation, Upper Jurassic Smackover Formation, Black Creek Field, Mississippi. AAPG Bulletin 81, 26-45.

Higby Schweitzer, M., (2004). Molecular paleontology: some current advances and problems. Annales de Paleontologie 90 (2), 81-102.

Hirschberg, A., de Jong, L.N.J., Schipper, B.A., Meijer, J.G., (1984). Influence of temperature and pressure on asphaltene flocculation. Society of Petroleum Engineers Journal, 283-293.

Hofmann, P.M., Huc, A.Y., Carpentier, B., Schaeffer, P., Albrecht, P., Keely, B.J., Maxwell, J.R., Sinninghe Damsté, J.S., de Leeuw, J.W., Leythaeuser, D., (1993). Organic matter of Mulhouse basin, France: a synthesis. Organic Geochemistry 8, 1105-1123.

Holba, A.G., Dzou, L.I., Wood, G.D., Ellis, L., Adam, P., Schaeffer, P., Albrecht, P., Greene, T., Hughes, W.B., (2003). Application of tetracyclic polyprenoids as indicators of input from fresh-brackish water environments. Organic Geochemistry 34 (3), 441-469.

Höld, I.M., Schouten, S., van der Gaast, S.J., Sinninghe Damsté, J.S., (2001). Origin of prist-1-ene and prist-2-ene in kerogen pyrolysates. Chemical Geology 172 (3-4), 201-212.

Holton, J., (1999). Southern Italy; 2, Four geologic settings dominate oil, gas fields of Italy, Sicily. Oil and Gas Journal 97 (49), 81-84.

Hong, E., Watkinson, P., (2004). A study of asphaltene solubility and precipitation. Fuel 83 (14-15), 1881-1887.

Hoover, W.F., (1953). Italy has four favorable areas for oil and gas search. Oil and Gas Journal 51 (38), 381-383.

Horsfield, B., (1984). Pyrolysis studies and petroleum exploration. In: J. Brooks, D.H. Welte (Eds.), Advances in Petroleum Geochemistry. Academic Press, London, pp. 247-298.

Horsfield, B., (1989). Practical criteria for classifying kerogens: Some observations from pyrolysis-gas chromatography. Geochimica et Cosmochimica Acta 53 (4), 891-901.

Horsfield, B., (1990). The rapid characterization of kerogens according to source quality, compositional heterogeneity and thermal lability. Rev. Palaeobot. Palynol. 65, 357-365.

Horsfield, B., (1997). The bulk composition of first-formed petroleum in source rocks. In: D.H. Welte, B. Horsfield, D.R. Baker (Eds.), Petroleum and Basin Evolution. Springer, Heidelberg, pp. 337–402.

Horsfield, B., Curry, D.J., Bohacs, K., Littke, R., Rullkötter, J., Schenck, H.J., Radke, M., Schaefer, R.G., Carroll, A.R., Isaksen, G., Witte, E.G., (1994). Organic geochemistry of freshwater and alkaline lacustrine environments, Green River Shale, Wyoming. In: N. Telnaes, G.W. van Graas, K. Øygard (Eds.), Advances in Geochemistry 1993, 22. Organic Geochemistry, pp. 415-440.

Horsfield, B., Dembicki, H., Ho, T.T.Y., (1983). Some potential applications of pyrolysis to basin studies. J. Geol. Soc. 140, 431-443.

Horsfield, B., Disko, U., Leistner, F., (1989). The micro-scale simulation of maturation; outline of a new technique and its potential applications, Geologic modeling; aspects of integrated basin analysis and numerical simulation, 78; 1. Springer International, Berlin, Federal Republic of Germany, pp. 361-374.

Horsfield, B., Düppenbecker, S.J., (1991). The decomposition of Posidonia Shale and Green River Shale kerogens using Microscale Sealed Vessel (MSSV) pyrolysis. Journal of Analytical and Applied Pyrolysis 20, 107-123.

Horsfield, B., Düppenbecker, S.J., Schenck, H.J., Schaefer, R.G., (1993). Kerogen typing concepts designed fpr the quantitative geochemical evaluation of petroleum potential. In: A.G. Doré, J.H. Augustson, C. Hermanrud, D.J. Stewart, O. Sylta (Eds.), Basin modelling: advances and applications, Vol. 3. NPF Spec. Publ. Elsevier, Amsterdam, pp. 243-249.

Horsfield, B., Heckers, J., Leythaeuser, D., Littke, R., Mann, U., (1991). A study of Holzener Asphaltkalk, Northern Germany: observations regarding the distribution, composition and origin of organic matter in an exhumed petroleum reservoir. Marine and Petroleum Geology 8, 198-211.

Horstad, I., Larter, S.R., (1997). Petroleum migration, alteration, and remigration within Troll Field, Norwegian North Sea. Bull. Am. Assoc. Petrol. Geol. 81, 222-248.

Hotier, G., Robin, M., (1983). Action de divers diluants sur les produits pétroliers lourds : mesure, interprétation et prévision de la floculation des asphaltènes. Revue de l'Institut Français du Pétrole 38 (1), 101-120.

Hsieh, M., (1999). Characterization of waxes in high pour-point crude oils. University of Oklahoma, Norman, OK, United States, pp. 113.

Hsieh, M., Philip, P., (2001). Ubiquitous occurence of high molecular weight hydrocarbons in crude oils. Organic Geochemistry 32, 955-966.

Hsieh, M., Philip, P., del Rio, J.C., (2000). Characterization of high molecular weight biomarkers in crude oils. Organic Geochemistry 31, 11581-1588.

Hu, Y.-F., Guo, T.-M., (2001). Effect of temperature and molecular weight of n-alkane precipitants on asphaltene precipitation. Fluid Phase Equilibria 192 (1-2), 13-25.

Hu, Y.-F., Li, S., Liu, N., Chu, Y.-P., Park, S.J., Mansoori, G.A., Guo, T.-M., (2004). Measurement and corresponding states modeling of asphaltene precipitation in Jilin reservoir oils. Journal of Petroleum Science and Engineering 41 (1-3), 169-182.

Huang, D., Li, J., Zhang, D., (1990). Maturation sequence of continental crude oils in hydrocarbon basins in China and its significance. Organic Geochemistry 16, 521-529.

Hubbard, R.L., Stanfield, K.E., (1948). Determination of asphaltenes, oils, and resins in asphalt. Analytical Chemistry, 460-461.

Hunt, J.M., Lewan, M.D., Hennet, R.J.-C., (1991). Modelling oil generation with time-temperature index graphs based on the Arrhenius equation. AAPG Bulletin 75, 795-807.

Ibrahim, H.H., Idem, R.O., (2005). A method for evaluating the kinetics of n-heptane-induced asphaltene precipitation from various Saskatchewan crude oils during light hydrocarbon flooding. Fuel 84 (2-3), 311-314.

Ignasiak, T., Kemp-Jones, A.V., Strausz, O.P., (1977). The molecular structure of Athabasca asphaltene. Cleavage of the carbon-sulfur bonds by radical ion electron transfer reactions. Organic geochemistry 42, 312-320.

Ioppolo, M., Alexander, R., Kagi, R.I., (1992). Identification and analysis of C0-C3 phenols in some Australian crude oils. Organic Geochemistry 18, 603-609.

Ioppolo-Armanios, M., Alexander, R., Kagi, R.I., (1995). Geosynthesis of organic compounds: I. Alkylphenols. Geochim. Cosmochim. Acta 59, 3017-3027.

Isaksen, G., Bohacs, K., (1995). Geological controls of source rock geochemistry through relative sea level; Triassic, Barents Sea. In: B.J. Katz (Ed.), Petroleum Source Rocks. Springer, Berlin, pp. 25–50.

Ishiwatari, M., Ishiwatari, R., Sakashita, H., Tatsumi, T., Tominaga, H.-o., (1991). Pyrolysis of chlorophyll a after preliminary heating at a moderate temperature: Implications for the origin of prist-1-ene on kerogen pyrolysis. Journal of Analytical and Applied Pyrolysis 18 (3-4), 207-218.

Ishiwatari, R., Yamamoto, S., Handa, N., (1995). Characterization of sinking particles in the ocean by pyrolysis--gas chromatography/mass spectrometry. Journal of Analytical and Applied Pyrolysis 22, 75-89.

Issacson, J.P., Frink, C.R., (1984). Nonreversible sorption of phenolic compounds by sediment fractions: the role of sedimentary organic matter. Environmental Science and Technology 18, 43-48.

James, A.T., Burns, B.J., (1984). Microbial alteration of subsurface natural gas accumulations. Assoc. Petrol. Geol. 68, 957-960.

Jarvie, D.M., Walker, P.R., Price, L.C., (1997). Geochemical comparison of Paleozoic oils, Williston Basin, U.S.A, AAPG Rocky Mountain Section meeting; abstracts, 81; 7. American Association of Petroleum Geologists, Tulsa, OK, United States, pp. 1226.

Jeng, W.-L., Huh, C.-A., (2004). Lipids in suspended matter and sediments from the East China Sea Shelf. Organic Geochemistry 35 (5), 647-660.

Jiamo, F., Guoying, S., Jiayou, X., Eglington, G., Gowar, A.P., Rongfen, J., Shanfa, F., Pingang, P., (1990). Application of biological markers in the assessment of paleoenvironments of Chinese non-marine sediments. Organic Geochemistry 16, 769-779.

Jobson, A.M., Cook, F.D., Westlake, D.W.S., (1979). Interaction of aerobic and anerobic bacteria in petroleum biodegradation. Chemical Geology 24, 355-366.

Johns, R.B., Gillan, F.T., Volkman, J.K., (1980). Early diagenesis of phytyl esters in a contemporary temperate intertidal sediment. Geochimica et Cosmochimica Acta 44, 183-188.

Jones, D.M., Douglas, A.G., (1987). Hydrocarbon Distributions in Crude Oil Asphaltene Pyrolyzates. 1. Aliphatic Compounds. Energie and Fuels 1, 468-476.

Jones, D.M., Douglas, A.G., Connan, J., (1988). Hydrous pyrolysis of asphaltenes and polar fractions of biodegraded oils, Advances in organic geochemistry 1987; Part II, Analytical geochemistry; proceedings of the 13th international meeting on Organic geochemistry, 13; 4-6. Pergamon, Oxford-New York, International, pp. 981-993.

Jones, P.J., Philp, R.P., (1990). Oils and source rocks from Pauls Valley, Anadarko Basin, Oklahoma, U.S.A. Applied Geochemistry 5, 429–448.

Juntgen, H., Klein, J., (1975). Entstehung von Erdgas aus kohligen Sedimenten. Erdoel und Kohle, Erdgas, Petrochemie 28 (2), 65-73.

Justwan, H., Dahl, B., Isaksen, G.H., (2006). Geochemical characterisation and genetic origin of oils and condensates in the South Viking Graben, Norway. Marine and Petroleum Geology 23, 213–239.

Juyal, P., Merino-Garcia, D., Andersen, S.I., (2005). Effect on molecular interactions of chemical alteration of petroleum asphaltenes. I. Energy & Fuels 19 (4), 1272 - 1281.

Kafka, F.T., Kirkbride, R.K., (1959). The Ragusa oil field, Sicily. Proceedings - World Petroleum Congress = Actes et Documents - Congres Mondial du Petrole.

Kampfer, P., Steiof, M., Becker, P.M., Dott, W., (1993). Characterization of chemoheterotrophic bacteria associated with the in situ bioremediation of a waste-oil contaminated site. Microb. Ecol. 26, 161-188.

Kanaly, A.R., Harayama, S., (2000). Biodegradation of high-molecular weight polycyclic aromatic hydrocarbons. J. Bacteriol. 182, 2059-2067.

Kaneda, T., (1967). Fatty acids in the genus Bacillus. I. Iso- and anteiso acids as characteristic constituents of lipids in 10 species. J. Bacteriol. 93, 894-903.

Kasrai, M., Bancroft, G.M., Brunner, R.W., Jonasson, R.G., Brown, J.R., Tan, K.H., Feng, X., (1994). Sulphur speciation in bitumens and asphaltenes by X-ray absorption fine structure spectroscopy. Geochimica et Cosmochimica Acta 58 (13), 2865-2872.

Kawanaka, S., Leontaritis, K.J., Park, S.J., Mansoori, G.A., (1989). Thermodynamic and colloidal models of asphaltene flocculation. In: ACS Symposium. American Chemical Society, Washington, DC.

Keely, B.J., Sinninghe Damsté, J.S., Betts, S.E., Yue, L., de Leeuw, J.W., Maxwell, J.R., (1993). A molecular stratigraphic approach to palaeoenvironmental assessment and the recognition of changes in source inputs in marls of the Mulhouse Basin (Alsace, France). Organic Geochemistry 20 (8), 1165-1186.

Kelley, P.A., Bissada, K.K., Burda, B.H., Elrod, L.W., Pfeiffer, R.N., (1985). Pretoleum generation potential of coals and organic-rich deposits: significance in tertiary coal-rich basins. Proc. Ind. Petrol. Assoc. 14, 3-21.

Kenig, F., Huc, A.Y., (1989). Incorporation of sulfur in organic matter during early diagenesis as thiophene, Abstracts of papers; 197th ACS national meeting, 197. American Chemical Society, Washington, DC, United States, pp. GEOC 12.

Kenig, F., Huc, A.Y., Purser, B.H., Oudin, J.L., (1990). Sedimentation, distribution and diagenesis of organic matter in a recent carbonate environment, Abh Dhabi, U.A.E. In: F. Béhar, B. Durand (Eds.), Advances in Organic Geochemistry 1989, 16, pp. 735-747.

Kenig, F., Sinninghe Damsté, J.S., Frewin, N.L., Hayes, J.M., de Leeuw, J.W., (1995). Molecular indicators for palaeoenvironmental change in a Messinian evaporitic sequence (Vena del Gesso, Italy). II: High-resolution variations in abundances and 13C contents of free and sulphur-bound carbon skeletons in a single marl bed. Organic Geochemistry 23 (6), 485-526.

Keym, M., Dieckmann, V., (2006). Predicting the timing and characteristics of petroleum formation using tar mats and petroleum asphaltenes: A case study from the Northern North Sea. Journal of Petroleum Geology 29 (1), 273-296.

Keym, M., Dieckmann, V., Horsfield, B., Erdmann, M., Galimberti, R., Kua, L.-C., Leith, L., Podlaha, O., (2006). Source rock heterogeneity of the Upper Jurassic Draupne Formation, North Viking Graben, and its relevance to petroleum generation studies. Organic Geochemistry 37 (2), 220-243.

Khavari-Khorasani, G., Dolson, J.C., Michelsen, J.K., (1998). The factors controlling the abundance and migration of heavy versus light oils, as constrained by data from the Gulf of Suez. Part I. The effect of expelled petroleum composition, PVT properties and petroleum system geometry. Organic Geochemistry 29 (1-3), 255-282.

Kim, S., (2001). Pyrolysis kinetics of waste PVC pipe. Waste Management 21 (7), 609-616.

Kleemann, G., Poralla, K., Englert, G., Kjosen, H., Liaaen-Jensen, S., Neunlist, S., Rohmer, M., (1990). Tetrahymanol from the phototrophic bacterium Rhodopseudomonas palustris: first report of a gammacerane triterpene from a prokaryote. J. Gen. Microbiol. 136, 2551-2553.

Kocabas, I., Islam, M.R., (1998). A wellbore model for predicting asphaltene plugging. In: SPE annual technical conference, New Orleans, pp. 671-679.

Kohnen, M.E.L., Sinninghe Damsté, J.S., Baas, M., van Dalen, A.C.K., de Leeuw, J.W., (1993). Sulphur-bound steroid and phytane carbon skeletons in geomacromolecules: Implications for the mechanism of incorporation of sulphur into organic matter. Geochimica et Cosmochimica Acta 57 (11), 2515-2528.

Kohnen, M.E.L., Sinninghe Damsté, J.S., de Leeuw, J.W., (1991). Biases from natural sulphurization in palaeoenvironmental reconstruction based on hydrocarbon biomarker distributions. Nature 349, 775-778.

Koopmans, M.P., Rijpstra, W.I.C., Klapwijk, M.M., de Leeuw, J.W., Lewan, M.D., Sinninghe Damsté, J.S., (1999). A thermal and chemical degradation approach to decipher pristane and phytane precursors in sedimentary organic matter. Organic Geochemistry 30, 1089-1104.

Koots, J.A., Speight, J.G., (1975). Relation of petroleum resins to asphaltenes. Fuel 54, 179.

Kotarba, M.J., Clayton, J.L., Rice, D.D., Wagner, M., (2002). Assessment of hydrocarbon source rock potential of Polish bituminous coals and carbonaceous shales. Chemical Geology 184 (1-2), 11-35.

Krooss, B.M., Littke, R., Mueller, B., Frielingsdorf, J., Schwochau, K., Idiz, E.F., (1995). Generation of nitrogen and methane from sedimentary organic matter: implications on the dynamics of natural gas accumulations. In: Processes of Natural Gas Formation, Amsterdam, Netherlands, pp. 291-318.

Kruge, M.A., Mastalerz, M., Solecki, A., Stankiewicz, B.A., (1996). Organic geochemistry and petrology of oil source rocks, Carpathian Overthrust region, southeastern Poland--implications for petroleum generation. Organic Geochemistry 24 (8-9), 897-912.

Kuo, L.C., Michael, E.G., (1994). A multicomponent oil-cracking kinetics model for modeling preservation and composition of reservoired oils. Organic Geochemistry 21 (8-9), 911-925.

Kvenvolden, K.A., (1962). Normal paraffin hydrocarbons in sediments from San Francisco Bay, California. Amer. Assoc. of Petrol. Geol. Bull. 46, 1643-1652.

La Londe, R.T., Ferrara, L.M., Hayes, M.P., (1987). Low-temperature, polysulfide reactions of conjugated ene carbonyls: A reaction model for the geologic origin of S-heterocycles. Organic Geochemistry 11 (6), 563-571.

Lafargue, E., Béhar, F., (1989). Application of a new preparative pyrolysis technique for the determination of source rock types and oil / source rock correlations. Geochim. Cosmochim. Acta 53, 2973-2983.

Lafargue, E., Marquis, F., Pillot, D., (1998). Rock-Eval 6 applications in hydrocarbon exploration, production and soil contamination studies. Revue de l'Institut Français du Petrolé 53 (4), 421-437.

Lafargue, E., Marquis, F., Pillot, D., Bernard, M., Beauducel, G., Antonas, R., Burwood, R., (1997). Rock Eval 6; a new generation of Rock-Eval pyrolyser for a wider use in petroleum Exploration/production and in soil contamination studies, 1997 AAPG International Conference and Exhibition. American Association of Petroleum Geologists, Tulsa, OK, United States, pp. 1393.

Landais, P., Michels, R., Elie, M., (1994). Are time and temperature the only constraints to the simulation of organic matter maturation? Organic Geochemistry 22 (3-5), 617-630.

Landais, P., Zaugg, P., Monin, J.C., Kister, J., Muller, J.F., (1991). Experimental simulation of the natural coalification of coal maceral concentrations. Bull. Soc. Geol. Fr. 2, 211-217.

Laquer, F.C., Manahan, S.E., (1987). Solution factors affecting the adsorption of phenol onto a siltstone. Chemosphere 16, 1431-1445.

Larsen, J.W., Li, S., (1997). An initial comparison of the interactions of Type I and III kerogens with organic liquids. Organic Geochemistry 26 (5-6), 305-309.

Larter, S.R., (1984). Application of analytical pyrolysis techniques to kerogen characterization and fossil fuel exploration/exploitation. In: K. Voorhees (Ed.), Analytical pyrolysis, methods and application. Butterworth, London, pp. 212-275.

Larter, S.R., Aplin, A.C., (1995). Reservoir geochemistry: methods, applications and opportunities. In: J.M. Cubitt, W.A. England (Eds.). Geological Society Special Puiblication, London, pp. 5-32.

Larter, S.R., Bowler, B.F.J., Clarke, E., Wilson, C., Moffatt, B., Bennet, B., Yardley, G., Carruthers, D., (2000). An experimental investigation of geochromatography during secondary migration of petroleum performed under subsurface conditions with a real rock. Geochemical Transactions 9.

Larter, S.R., Bowler, B.F.J., Li, M., Chen, M., Brincat, D., Bennet, B., Noke, K., Donohoe, P., Simmons, D., Kohnen, M.E.L., Allan, J., Telnaes, N., Horstad, I., (1996). Molecular indicators of secondary oil migration distances. Nature 383, 593-597.

Larter, S.R., Horsfield, B., (1993). Determination of structural components of kerogens using analytical pyrolysis methods. In: M.H. Engel, S.A. Macko (Eds.), Organic Geochemistry. Plenum Press, pp. 271-287.

Larter, S.R., Senftle, J.T., (1985). Improved kerogen typing for petroleum source rock analysis. Nature 318, 277-280.

Larter, S.R., Solli, H., Douglas, A.G., (1983). Phytol containing melanoidins and their bearing on the fate of isoprenoid structures in sediments. Wiley, Chichester.

Larter, S.R., Wilhelms, A., Head, I.M., Koopmans, M.P., Aplin, R., di Primio, R., Zwach, C., Erdmann, M., Telnaes, N., (2003). The controls on the composition of biodegraded oils in the deep subsurface - part 1: biodegradation rates in petroleum reservoirs. Organic Geochemistry 34, 601-613.

Lentini, F., Catalano, S., Carbone, S., (1996). The external thrust system in southern Italy; a target for petroleum exploration. Petroleum Geoscience 2 (4), 333-342.

Leon, O., Contreras, E., Rogel, E., (2001). Amphiphile adsorption on asphaltene particles: adsorption isotherms and asphaltene stabilization. Colloids and Surfaces A: Physicochemical and Engineering Aspects 189 (1-3), 123-130.

Leontaritis, K.J., Mansoori, G.A., (1988). Asphaltene deposition: a survey of field experiences and research approaches. Journal of Petroleum Science and Engineering 3 (1), 229-239.

Lewan, M.D., (1985). Evaluation of petroleum generation by hydrous pyrolysis experiments. Phil. Trans. R. Soc. Lond. A 315, 123-134.

Lewan, M.D., (1993). Laboratory simulation of petroleum formation: hydrous pyrolysis. In: M.H. Engel, S.A. Macko (Eds.), Organic Geochemistry. Plenum, New York, pp. 419–442.

Lewan, M.D., (1998). Sulphur-radical control on petroleum formation rates. Nature 391, 164-166.

Li, M., Larter, S.R., Taylor, P., Jones, D.M., Bowler, B., Bjorøy, M., (1995). Biomarkers or not biomarkers? A new hypothesis for the origin of pristane involving derivation from methyltrimethyltridecylchromans (MTTCs) formed during diagenesis from chlorophyll and alkylphenols. Organic Geochemistry 23 (2), 159-167.

Li, M., Yao, H., Fowler, M.G., Stasiuk, L.D., (1998). Geochemical constraints on models for secondary petroleum migration along the Upper Devonian Rimbey-Meadowbrook reef trend in central Alberta, Canada, Advances in organic geochemistry 1997; proceedings of the 18th international meeting on Organic geochemistry; Part 1, Petroleum geochemistry, 29; 1-3. Pergamon, Oxford-New York, International, pp. 163-182.

Li, M., Yao, H., Stasiuk, L.D., Fowler, M.G., Larter, S.R., (1997). Effect of maturity and petroleum expulsion on pyrrolic nitrogen compound yields and distributions in Duvernay Formation petroleum source rocks in central Alberta, Canada. Organic Geochemistry 26 (11-12), 731-744.

Li, X., Matuschek, G., Herrera, M., Wang, H., Kettrup, A., (2003). Investigation of pyrolysis of Chinese coals using thermal analysis/mass spectrometry. J. of Thermal Analysis and Calorimetry 71, 601-612.

Liou, T.H., (2003). Pyrolysis kinetics of electronic packaging material in a nitrogen atmosphere. J. of Hazard Materials 103 (1-2), 107-123.

Littke, R., Leythaeuser, D., Radke, M., Schaefer, R.G., (1990). Petroleum generation and migration in coal seams of the Carboniferous Ruhr Basin, northwest Germany. Organic Geochemistry 16 (1-3), 247-258.

Louis, M., (1964). Etudes geochimiques sur les "Schisters cartons" du Toarcian du Basin de Paris. In: G.B. Hosbson, M.C. Louis (Eds.), Advances in Organic Geochemistry. Pergamon Press, New York, pp. 84-95.

Lovley, D.R., Coates, J.D., Woodward, J.C., Phillips, E.J.P., (1995). Benzene oxidation coupled to sulfate reduction. Applied and Environmental Microbiology 61, 953-958.

Lucach, S.O., Bowler, B.F.J., Frewin, N.L., Larter, S.R., (2002). Variation in alkylphenol distribution in a homogenous oil suite from the Dhahaban petroleum system of Oman. Organic Geochemistry 33, 581-594.

Mackenzie, A.S., (1984). Application of biological markers in petroleum geochemistry. In: J. Brooks, D.H. Welte (Eds.), Advances in Petroleum Geochemistry, 1. Academic Press, London, pp. 115-214.

Mackenzie, A.S., McKenzie, D., (1983). Isomerization and aromatization of hydrocarbons in sedimentary basins formed by extension. Geology Magazin 120, 417-470.

Magnier, C., Huc, A.Y., (1995). Pyrolysis of asphaltenes as a tool for reservoir geochemistry. Organic Geochemistry 23 (10), 963-967.

Magnier, C., Trindade, L.A.F., (1999). Light hydrocarbon analyses in reservoir geochemistry. Revista Latino Americana de Geoquímica Orgánica 5, 25-37.

Mana Capelli, S., Busalmen, J.P., de Sanchez, S.R., (2001). Hydrocarbon bioremediation of a mineral-base contaminated waste from crude oil extraction by indigenous bacteria. International Biodeterioration and Biodegradation 47 (4), 233-238.

Mango, F.D., (1990). The origin of light hydrocarbons in petroleum; a kinetic test of the steady-state catalytic hypothesis. Geochimica et Cosmochimica Acta 54 (5), 1315-1323.

Mango, F.D., (1994). The origin of light hydrocarbons in petroleum; ring preference in the closure of carbocyclic rings. Geochimica et Cosmochimica Acta 58 (2), 895-901.

Mansoori, G.A., (1995). Arterial blockage in the petroleum and natural gas industries - heavy organics (asphaltene / bitumen, resin, organometallics, paraffin / wax, diamondoids, etc.) deposition from petroleum fluids. In: online-report. uic.edu.

Mansoori, G.A., (1996). Arterial blockage in the petroleum and natural gas industries (causes & effects, economic implications, & preventive measures. In: Asphaltene and wax conference, London, pp. 2.

Mansoori, G.A., (1999). Modeling of asphaltene and other heavy organics depositions. Journal of Petroleum Science and Engineering 17, 101.

Marcusson, J., Burchart, H., Wilke, P., (1931). Die natürlichen und künstlichen Asphalte. Wilhelm Engelmann, Leipzig.

Margesin, R., Schinner, F., (2000). Biodegradation and bioremediation of hydrocarbons in extreme environments. Appl. Microbiol. Biotechnol. 56, 650-663.

Marquez, N., Ysambertt, F., de la Cruz, C., (1999). Three analytical methods to isolate and characterize vanadium and nickel porphyrins from heavy crude oil. Analytica Chimica Acta 395 (3), 343-349.

Marzi, R., Rullkötter, J., (1992). Qualitative and quantitative evolution and kinetics of biological marker transformations - laboratory experiments and application to the Michigan Basin. In: J.M. Moldowan, P. Albrecht, R.P. Philp (Eds.), Biological markers in Sediments and Petroleum. Pretence Hall, Englewood Cliffs, pp. 18-41.

Matsumo, G., Torii, T., Hanya, T., (1982). High abundance of algal 24-ethylcholesterol in Antartic lake sediment. Nature 299, 52-54.

Mattavelli, L., Novelli, L., (1990a). Burial history influence on the generation of some Italian oils, AAPG annual convention with DPA/ EMD divisions and SEPM, an associated society; technical program with abstracts, 74; 5. American Association of Petroleum Geologists, Tulsa, OK, United States, pp. 714.

Mattavelli, L., Novelli, L., (1990b). Geochemistry and habitat of oils in Italy. AAPG Bulletin 74, 1623–1639.

Mattavelli, L., Pieri, M., Groppi, G., (1993). Petroleum exploration in Italy: a review. Marine and Petroleum Geology 10 (5), 410-425.

McKirdy, D.M., Alridge, A.K., Ypma, P.J., (1983). A geochemical comparison of some crude oils from pre-Ordovician carbonate rocks. In: M. Bjorøy (Ed.), Advances in Organic Geochemistry 1981, pp. 99–107.

McLean, J.D., Kilpatrick, P.K., (1997). Effects of asphaltene solvency on stability of water-in-crude oil emulsions. Journal of Colloid and Interface Science 189, 242-253.

McNeill, I.C., Memetea, L., Mohammed, M.H., Fernandes, A.R., Ambidge, P., (1998). Polychlorinated dibenzodioxins and dibenzofurans in PVC pyrolysis. Polymer Degradation and Stability 62 (1), 145-155.

Mello, M.R., Gaglianone, P.C., Brassell, S.C., Maxwell, J.R., (1988). Geochemical and biological marker assessment of depositional environments using Brazilian offshore oils. Marine and Petroleum Geology 5 (3), 205-223.

Meredith, W., Kelland, S.J., Jones, D.M., (2000). Influence of biodegradation on crude oil acidity and carboxylic acid composition. Organic Geochemistry 31, 1059-1073.

Metzger, P., Templier, J., Largeau, C., Casadevall, E., (1986). A n-alkatriene and some n-alkadienes from the A race of the green alga Botryococcus braunii. Phytochemistry 25, 1869.

Meyers, P.A., Ishiwatari, R., (1993). The early diagenesis of organic matter in lacustrine sediments. In: M.H. Engel, S.A. Macko (Eds.), Advances in Organic Geochemistry 1993. Pergamon, Oxford-New York International, pp. 185-209.

Michels, R., Enjelvin-Raoult, N., Elie, M., Mansuy, L., Faure, P., Oudin, J.-L., (2002). Understanding of reservoir gas compositions in a natural case using stepwise semi-open artificial maturation. Marine and Petroleum Geology 19 (5), 589-599.

Michels, R., Landais, P., Torkelson, B.E., Philp, R.P., (1995). Effects of effluents and water pressure on oil generation during confined pyrolysis and high-pressure hydrous pyrolysis. Geochimica et Cosmochimica Acta 59 (8), 1589-1604.

Mitchell, D.L., Speight, J.G., (1973). The solubility of asphaltenes in hydrocarbon solvents. Fuel 53, 149-152.

Moldowan, J.M., Seifert, W.K., Gallegos, E.J., (1985). Relationship between petroleum composition and depositional environment of petroleum source rocks. AAPG Bulletin (American Association of Petroleum Geologists) 69 (8), 1255-1268.

Monaco, C., Tortorici, L., Catalano, S., (2000). Tectonic escape in the Sicanian mountains (Western Sicily). Mem. Soc. Geol. Ital. 55.

Mongenot, T., Boussafir, M., Derenne, S., Lallier-Verges, E., Largeau, C., Tribovillard, N.-P., (1997). Sulphur-rich organic matter from bituminous laminites of Orbagnoux (France, Upper Kimmeridgian). The role of early vulcanization. Bulletin - Societe Geologique de France 168 (3), 331-341.

Monteagudo, J.E.P., Lage, P.L.C., Rajagopal, K., (2001). Towards a polydisperse molecular thermodynamic model for asphaltene precipitation in live-oil. Fluid Phase Equilibria 187-188, 443-471.

Monthioux, M., (1988). Expected mechanisms in nature and in confined-system pyrolysis. Fuel 67 (6), 843-847.

Monthioux, M., Landais, P., Monin, J.C., (1985). Comparison between natural and artificial maturation series of humic coals from the Mahakam delts, Indonesia. Organic Geochemistry 8 (4), 275-292.

Moretti, I., Brosse, E., Delahaye, S., Roure, F., Mattavelli, L., (1990). Analysis of subsidence and modeling of oil formation in the Ragusa Basin (Iblean Plateau, Southeast Sicily), AAPG annual convention with DPA/ EMD divisions and SEPM, an associated

society; technical program with abstracts, 74; 5. American Association of Petroleum Geologists, Tulsa, OK, United States, pp. 725.

Moschopedis, S.E., Parkash, S., Speight, J., (1979). Thermal decomposition of asphaltenes. Fuel 57, 431-434.

Mosto Onuoha, K., Ekine, A.S., (1999). Subsurface temperature variations and heat flow in the Anambra Basin, Nigeria. Journal of African Earth Sciences 28 (3), 641-652.

Mousavi-Dehghani, S.A., Riazi, M.R., Vafaie-Sefti, M., Mansoori, G.A., (2004). An analysis of methods for determination of onsets of asphaltene phase separations. Journal of Petroleum Science and Engineering 42 (2-4), 145-156.

Mukhopadhyay, P.K., Gormly, J.R., Zumberge, J.E., (1989). Generation of hydrocarbons from the Tertiary coals of Texas--Coal as potential source rock for liquid hydrocarbons in a deltaic basin? Organic Geochemistry 14 (3), 351-352.

Mukhopadhyay, P.K., Wade, J.A., Kruge, M.A., (1995). Organic facies and maturation of Jurassic/Cretaceous, and possible oil-source rock correlation based on pyrolysis of asphaltenes, Scotian Basin, Canada. Organic Geochemistry 22, 85-104.

Mulaski, H., Coulon, C., Popoff, M., Baudin, P., (1995). 40Ar/39Ar chronology, petrology and geodynamic setting of Mesozoic to early Cenozoic magmatism from the Benue Trough, Nigeria. Journal of the Geological Society 152, 311-326.

Muscio, G.P.A., Horsfield, B., Welte, D.H., (1991). Compositional changes in the macromolecular organic matter (kerogens, asphaltenes, and resins) of a naturally matured source rock sequence from northern Germany as revealed by pyrolysis methods. In: D. Manning (Ed.), Organic geochemistry advances and applications in energy and the natural environment. Manchester University Press, Manchester, pp. 447-449.

Muscio, G.P.A., Horsfield, B., Welte, D.H., (1994). Occurrence of thermogenic gas in the immature zone; implications from the Bakken in-source reservoir system. In: M.H. Engel, S.A. Macko (Eds.), Advances in Organic Geochemistry 1993. Pergamon, Oxford-New York International, pp. 461-476.

Musser, B.J., Kilpatrick, P.K., (1998). Molecular characterization of wax isolated from a variety of crude oils. Energie and Fuels 12, 715-725.

Mycke, B., Hall, K., Leplat, P., (1994). Carbon isotopic composition of individual hydrocarbons and associated gases evolved from micro-scale sealed vessel (MSSV) pyrolysis of high molecular weight organic material. Organic Geochemistry 21 (6-7), 787-800.

Myhr, M.B., Schou, L., Skjetne, T., Krane, J., (1990). Characterization of asphaltenes and co-precipitated material from a Californian crude oil, Advances in organic geochemistry, 1989; Part II, Molecular geochemistry; proceedings of the 14th international meeting on Organic geochemistry, 16; 4-6. Pergamon, Oxford-New York, International, pp. 931-941.

Nali, M., Caccialanza, G., Ghiselli, C., Chiaramonte, M.A., (2000). Tmax of asphaltenes: a parameter for oil maturity assessment. Organic Geochemistry 31 (12), 1325-1332.

Navale, V., (1994). Comparative study of low and high temperature hydrous pyrolysis products of monoglyceryl diether lipid from archaebacteria. Journal of Analytical and Applied Pyrolysis 29, 33-43.

Nellensteyn, F.J., (1924). The constitution of asphalt. Journal of the Institute of Petroleum Technology 10, 311.

Nelson, B.C., Eglinton, T.I., Seewald, J.S., Vairavamurthy, M.A., Miknis, F.P., (1995). Transformations in organic sulfur speciation during maturation of Monterey shale: constraints from laboratory experiments. In: M.A. Vairavamurthy, M.A.A. Schoonen (Eds.), Geochemical Transformations in Sedimentary Sulfur, 612. ACS Symposium Series, Washington, pp. 138–166.

Nilsen, R.K., Beeder, J., Thorstensen, T., Torsvik, T., (1996). Distribution of thermophilic marine sulfate reducers in North Sea oil field waters and reservoir oils. Applied and Environmental Microbiology 62, 1793-1798.

Nilsen, R.K., Torsvik, T., (1996). Methanococcus thermolithotrophicus isolated from North sea oil field reservoir waters. Applied and Environmental Microbiology 62, 728-731.

Nip, M., de Leeuw, J.W., Schenck, P.A., (1988). The characterization of eight maceral concentrates by means of Curie point pyrolysis-gas chromatography-mass spectrometry. Geochim. Cosmochim. Acta 52, 637-648.

Nip, M., Tegelaar, E.W., Brinkhuis, H., de Leeuw, J.W., Schenck, P.A., Holloway, P.J., (1986). Analysis of modern and fossil plant cuticles by Curie point Py-GC and Curie point Py-GC-MS; recognition of a new, highly aliphatic and resistant biopolymer, Advances in Organic Geochemistry 1985. Pergamon International, Oxford-New York, pp. 769-778.

Nissenbaum, A., Baedecker, M.J., Kaplan, I.R., (1972). Organic geochemistry of Dead Sea sediments. Geochimica et Cosmochimica Acta 36 (7), 709-727.

Novelli, L., Mattavelli, L., (1988). Geochemistry and habitat of oils in Italy, 1988 AAPG annual convention with DPA/ EMD divisions and SEPM, an associated society; abstracts, 72; 2. American Association of Petroleum Geologists, Tulsa, OK, United States, pp. 229.

Novelli, L., Welte, D.H., Mattavelli, L., Yalcin, M.N., Cinelli, D., Schmitt, K.J., (1988). Hydrocarbon generation in southern Sicily. A three dimensional computer aided basin modeling study. Organic Geochemistry 13 (1-3), 153-164.

Nwachukwu, J.I., Chukwura, P.I., (1986). Organic matter of Agbada Formation, Niger Delta, Nigeria. AAPG Bulletin 70, 48-55.

Nwachukwu, J.I., Oluwole, A.F., Asubiojo, O.I., Filby, R.H., Grimm, C.A., Fitzgerald, S., (1995). A geochemical evaluation of Niger Delta crude oils, Geology of deltas. A.A Balkema, Rotterdam, Netherlands.

Obaje, N.G., Wehner, H., Abubakar, M.B., Isah, M.T., (2004). Nasara-I Well, Gongola Basin (upper Benue Trough, Nigeria); source-rock evaluation. Journal of Petroleum Geology 27 (2), 191-206.

Odden, W., Barth, T., Talbot, M.R., (2002). Compound-specific carbon isotope analysis of natural and artificially generated hydrocarbons in source rocks and petroleum fluids from offshore Mid-Norway. Organic Geochemistry 33 (1), 47-65.

Odden, W., Patience, R.L., van Graas, G.W., (1998). Application of light hydrocarbons (C (sub 4) -C (sub 13)) to oil/ source rock correlations; a study of the light hydrocarbon compositions of source rocks and test fluids from offshore Mid-Norway. Organic Geochemistry 28 (12), 823-847.

Oh, K., Ring, T.A., Deo, M.D., (2004). Asphaltene aggregation in organic solvents. Journal of Colloid and Interface Science 271 (1), 212-219.

Orr, W.L., (1986). Kerogen/ asphaltene/ sulfur relationships in sulfur-rich Monterey oils, Advances in organic geochemistry, 1985; Part I, Petroleum geochemistry, 10; 1-3. Pergamon, Oxford-New York, International, pp. 499-516.

Orr, W.L., Sinninghe Damsté, J.S., (1990). Geochemistry of sulfur in petroleum systems. In: W.L. Orr, C.M. White (Eds.), Geochemistry of sulfur in fossil fuels. Am. Chem. Soc., Washington DC, pp. 2-29.

Ostlund, J.-A., Lofroth, J.-E., Holmberg, K., Nyden, M., (2002). Flocculation Behavior of Asphaltenes in Solvent/Nonsolvent Systems. Journal of Colloid and Interface Science 253 (1), 150-158.

Øygard, K., Larter, S.R., Senftle, J.T., (1988). The control of maturity and kerogen type on quantitative analytical pyrolysis data. In: L. Mattavelli, L. Novelli (Eds.), Advances in Organic Geochemistry 1987. Pergamon Press, Oxford, pp. 1153-1162.

Palmer, S.E., (1993). Effects of biodegradation and water washing on crude oil composition. In: M.H. Engel, S.A. Macko (Eds.), Organic Geochemistry. Plenum Press, New York, pp. 511-533.

Pan, C., Geng, A., Liao, Z., Xiong, Y., Fu, J., Sheng, G., (2002). Geochemical characterization of free versus asphaltene-sorbed hydrocarbons in crude oils: implications for migration-related compositional fractionations. Marine and Petroleum Geology 19 (5), 619-632.

Park, S.J., Mansoori, G.A., (1988). Aggregation and deposition of heavy organics in petroleum crude. Energy Sources 10, 109.

Parra-Barraza, H., Hernandez-Montiel, D., Lizardi, J., Hernandez, J., Herrera Urbina, R., Valdez, M.A., (2003). The zeta potential and surface properties of asphaltenes obtained with different crude oil/n-heptane proportions*. Fuel 82 (8), 869-874.

Payne, D.F., Ortoleva, P.J., (2001). A model for lignin alteration--part I: a kinetic reaction-network model. Organic Geochemistry 32 (9), 1073-1085.

Pelet, R., Béhar, F., Monin, J.C., (1986). Resins and asphaltenes in the generation and migration of petroleum. Organic Geochemistry 10 (1-3), 481-498.

Pepper, A.S., (1992). Estimating the petroleum expulsion behavior of source rocks: A novel quantitative approach. Geological Society Special Publication, London No. 59, 149-163.

Pepper, A.S., Dodd, T.A., (1995). Simple kinetic models of petroleum formation. Part II: oil-gas cracking. Marine and Petroleum Geology 12 (3), 321-340.

Peramanu, S., Clarke, P.F., Pruden, B.B., (1999). Flow loop apparatus to study the effect of solvent, temperature and additives on asphaltene precipitation. Journal of Petroleum Science and Engineering 23 (2), 133-143.

Perez, A., Luzon, A., Roc, A.C., Soria, A.R., Mayayo, M.J., Sanchez, J.A., (2002). Sedimentary facies distribution and genesis of a recent carbonate-rich saline lake: Gallocanta Lake, Iberian Chain, NE Spain. Sedimentary Geology 148 (1-2), 185-202.

Peters, K.E., (1986). Guidelines for evaluating petroleum source rock using programmed pyrolysis. AAPG Bulletin 70 (3), 318-329.

Peters, K.E., Fraser, T.H., Amris, W., Rustanto, B., Hermanto, E., (1999). Geochemistry of crude oils from Eastern Indonesia. AAPG Bulletin 83 (12), 1927-1942.

Peters, K.E., Moldowan, J.M., Sundararaman, P., (1990). Effects of hydrous pyrolysis on biomarker thermal maturity parameters: Monterey phosphatic and siliceous members. Organic Geochemistry 15 (3), 249-265.

Peters, K.E., Walters, C.C., Moldowan, J.M., (2005). The Biomarker Guide. Cambridge University Press, U.K.

Peterson, J.A., (1994). Regional geology and hydrocarbon resource potential, the Mediterranean Sea region. U. S. Geological Survey, Reston, VA, United States, pp. 118.

Pfeiffer, J.P., (1950). The Properties of Asphaltic Bitumen. Elsevier, Amsterdam.

Pfeiffer, J.P., Saal, R.N.J., (1940). Asphaltic bitumen as colloid system. Journal of Physical Chemistry 44, 139-149.

Philppi, G.T., (1965). On the depth, time and mechanism of petroleum generation. Geochim. Cosmochim. Acta 29, 1021-1049.

Pina, A., Mougin, P., Béhar, F., (2006). Characterisation of asphaltenes and modelling of flocculation – state of the art. Oil and Gas Science and Technology – Rev. IFP 61 (3), 319-343.

Pineda-Flores, G., Boll-Argüello, G., Lira-Galeana, C., Mesta-Howard, A.M., (2004). A mircobial consortium isolated from a crude oil sample that uses asphaltenes as a carbon and energy source. J. Biodegradation 15, 145-151.

Powell, T.G., (1984). Some aspects of the hydrocarbon geochemistry of a middle Devonian barrier reef complex, western Canada. In: J.G. Palacas (Ed.), Petroleum geochemistry and source rock potential of carbonate rocks, 18. American Association of Petroleum Geologists Bulletin Studies in Geology, pp. 45-62.

Powell, T.G., Boreham, C.J., (1994). Terrestrially sourced oils: where do they exist and what are our limits of knowledge? - a geochemical perspective. Coal and coal-bearing strata as oil-prone source rocks?, Published by Geological Society of London, Special Publication, 77, Editors Scott A.C. and Fleet A.J., 11-29.

Powell, T.G., Boreham, C.J., Smyth, M., Russell, N., Cook, A.C., (1991). Petroleum source rock assessment in non-marine sequences: pyrolysis and petrographic analysis of Australian coals and carbonaceous shales. Organic Geochemistry 17 (3), 375-394.

Premovic, P.I., Dordevic, D.M., Pavlovic, M.S., (2002). Vanadium of petroleum asphaltenes and source kerogens (La Luna Formation, Venezuela): isotopic study and origin. Fuel 81 (15), 2009-2016.

Premovic, P.I., Jovanovic, L.S., (1997). Are vanadyl porphyrins products of asphaltene/kerogen thermal breakdown? Fuel 76 (3), 267-272.

Premovic, P.I., Jovanovic, L.S., Nikolic, G.S., (1996). Thermal stability of the asphaltene/kerogen vanadyl porphyrins. Organic Geochemistry 24 (8-9), 801-814.

Premuzic, E., Lin, M.S., (1999). Induced biochemical conversions of heavy crude oils. J. Pet. Sci. Eng. 22, 171-180.

Prinzhofer, A., Mello, M.R., Takaki, T., (2000). Geochemical characterization of natural gas: A physical multivariable approach and its applications in maturity and migration estimates. AAPG Bulletin 84 (8), 1152-1172.

Priyanto, S., Mansoori, G.A., Aryadi, S., (2001). Measurement of property relationships of nano-structure micelles and coacervates of asphaltene in a pure solvent. Chemical Engineering Science 56, 6933–6939.

Putschew, A., Schaeffer, P., Schaeffer-Reiss, C., Maxwell, J.R., (1998). Carbon isotope characteristics of the diaromatic carotenoid, isorenieratene (intact and sulfide-bound) and a novel isomer in sediments. Organic Geochemistry 29 (8), 1849-1856.

Quesada, S., Dorronsoro, C., Robles, S., Chaler, R., Grimalt, J.O., (1997). Geochemical correlation of oil from the Ayoluengo field to Liassic black shale units in the southwestern Basque - Cantabrian Basin (Northern Spain). Organic Geochemistry 27, 25-40.

Quigley, T.M., Mackenzie, A.S., (1988). The temperatures of oil and gas formation in the sub-surface. Nature 333 (6173), 549-552.

Rabus, R., Heider, J., (1998). Initial reactions of anaerobic metabolism of alkylbenzenes in denitrifying and sulfate-reducing bacteria. Archives of Microbiology 170, 377-384.

Rabus, R., Widdel, F., (1995). Conversion studies with substrate analogues of toluene in a sulfate-reducing bacterium, strain Tol2. Archives of Microbiology 164, 448-451.

Radke, M., Willsch, H., Welte, D.H., (1980). Preperative hydrocarbon group type determination by automated medium pressure liquid chromatography. Analytical Chemistry 52, 406-424.

Reeves, F., (1953). Italian oil and gas resources. Bulletin of the American Association of Petroleum Geologists 37 (4), 601-653.

Reinhard, M., Shang, S., Kitanidis, P.K., Orwin, E., Hopkins, G.D., Lebron, C.A., (1997). In situ BTEX biotransformation under enhanced nitrate- and sulfate-reducing conditions. Environmental Science and Technology 31, 28-36.

Requejo, A.G., Allan, J., Creaney, S., Gray, N.R., Cole, K.S., (1992). Aryl isoprenoids and diaromatic carotenoids in Paleozoic source rocks and oils from the Western Canada and Williston basins, Advances in organic geochemistry 1991; Part 1, Advances and

applications in energy and the natural environment, 19; 1-3. Pergamon, Oxford-New York, International, pp. 245-264.

Requejo, A.G., Wielchowsky, C.C., Klosterman, M.J., Sassen, R., (1994). Geochemical characterization of lithofacies and organic facies in Cretaceous organic-rich rocks from Trinidad, East Venezuela Basin, Advances in organic geochemistry 1993; proceedings of the 16th international meeting on Organic geochemistry, 22; 3-5. Pergamon, Oxford-New York, International, pp. 441-459.

Reynolds, J.G., Burnham, A.K., Mitchell, T.O., (1995). Kinetic analysis of California petroleum source rocks by programmed temperature micropyrolysis. Organic Geochemistry 23 (2), 109-120.

Ribéreau-Gayon, P., (1972). Plant Phenolics. Olivier and Boyd, Great Britain.

Riboulleau, A., Derenne, S., Sarret, G., Largeau, C., Baudin, F., Connan, J., (2000). Pyrolytic and spectroscopic study of a sulphur-rich kerogen from the "Kashpir oil shales" (Upper Jurassic, Russian platform). Organic Geochemistry 31 (12), 1641-1661.

Riediger, C.L., Fowler, M., Brooks, P.W., Snowdon, L.R., (1990). Triassic oils and potential Mesozoic source rocks, Peace River Arch area, Western Canada Basin. Organic Geochemistry 16, 295-305.

Riediger, C.L., Fowler, M., Snowdon, L.R., MacDonald, R., Sherwin, M.D., (1999). Origin and alteration of Lower Cretaceous Mannville Group oils from the Provost oil field, east central Alberta, Canada. Bulletin of Canadian Petroleum Geology 47 (1), 43-62.

Rieley, G., Collier, R.J., Jones, D.M., Eglinton, G., Eakin, P.A., Fallick, A.E., (1991). Sources of sedimentary lipids deduced from stable carbon-isotope analyses of individual compounds. Nature 352 (6334), 425-427.

Risatti, J.B., Rowland, S.J., Yon, D.A., Maxwell, J.R., (1984). Stereochemical studies of acyclic isoprenoids. XII. Lipids of methanogenic bacteria and possible contributions to sediments. In: P.A. Schenck, J.W. de Leeuw, G.W.M. Lijmbach (Eds.), Advances in Organic Geochemistry 1983, pp. 93-104.

Ritter, U., (2003). Solubility of petroleum compounds in kerogen: implications for petroleum expulsion. Organic Geochemistry 34 (3), 319-326.

Riva, A., Caccialanza, P.G., Quagliaroli, F., (1988). Recognition of 18beta (H)oleanane in several crudes and Tertiary-Upper Cretaceous sediments; definition of a new maturity parameter, Advances in organic geochemistry 1987; Part II, Analytical geochemistry; proceedings of the 13th international meeting on Organic geochemistry, 13; 4-6. Pergamon, Oxford-New York, International, pp. 671-675.

Riva, A., Riolo, B., Mycke, B., Ocampo, R., Callot, H.J., Albrecht, P., Nali, M., (1989). Molecular parameters in Italian carbonate oils: reconstruction of past depositional environments. In: IMOG 1989, Book of abstracts, Paris, pp. 335.

Robinson, N., Eglinton, G., Brassel, S.C., Cranwell, P.A., (1984). Dinoflagellate origin for sedimentary 4-a-methylsteroids and 5a(H)-stanols. Nature 308, 439-442.

Rodrigues, D.C., Koike, L., Reis, F.d.A.M., Alves, H.P., Chang, H.K., Trindade, L.A., Marsaioli, A.J., (2000). Carboxylic acids of marine evaporitic oils from Sergipe-Alagoas Basin, Brazil. Organic Geochemistry 31 (11), 1209-1222.

Rontani, J.F., Bosser-Joulak, F., Rambeloarisou, E., Bertrand, J.C., Giusti, G., (1985). Analytical study of Asthart crude oil asphaltenes biodegradation. Chemosphere 14 (9), 1413-1422.

Rooney, M.A., Vuletich, A.K., Griffith, C.E., (1998). Compound-specific isotope analysis as a tool for characterizing mixed oils: an example from the West of Shetlands area. Organic Geochemistry 29 (1-3), 241-254.

Rovere, C.E., Crisp, P.T., Ellis, J., Bolton, P.D., (1983). Chemical characterization of shale oil from Condor, Australia. Fuel 62, 1274-1282.

Rowland, S.J., (1990). Production of acyclic isoprenoid hydrocarbons by laboratory maturation of methanogenic bacteria. Organic Geochemistry 15, 9-16.

Rowland, S.J., Alexander, R., Kagi, R.I., Jones, D.M., Douglas, A.G., (1986). Microbial degradation of aromatic components of crude oils: A comparison of laboratory and field observations. Organic Geochemistry 9, 153-161.

Roy, K., (1999). Kinetische Untersuchungen zur Hochtemperaturpyrolyse und -oxidation von Cyclopentadien und Cyclopentadienyl mit Hilfe der Stoßwellentechnik. In: PhD-thesis, Fakultät für Chemie. Universität Stuttgart, pp. 155.

Rubinstein, I., Spyckerelle, C., Strausz, O.P., (1979). Pyrolysis of asphaltenes; a source of geochemical information. Geochimica et Cosmochimica Acta 43 (1), 1-6.

Ruble, T.E., Bakel, A.J., Paul Philp, R., (1994). Compound specific isotopic variability in Uinta Basin native bitumens: paleoenvironmental implications. Organic Geochemistry 21 (6-7), 661-671.

Rueter, P., Rabus, R., Wilkes, H., Aeckersberg, F., Rainey, F.A., Jannasch, H.W., (1994). Anaerobic oxidation of hydrocarbons in crude oil by new types of sulphate-reducing bacteria. Nature 372, 455-458.

Rullkötter, J., Aizenshtat, Z., Spiro, B., (1984). Biological markers in bitumens and pyrolyzates of Upper Cretaceous bituminous chalks from the Ghareb Formation (Israel). Geochim. Cosmochim. Acta 48, 151–157.

Rullkötter, J., Michaelis, W., (1990). The structure of kerogens and related materials. A review of recent progress and future trends. In: B. Durand, F. Behar (Eds.), Advances in Organic Geochemistry 1989. Pergamon Press, Oxford, pp. 829-852.

Rullkötter, J., Spiro, B., Nissenbaum, A., (1985). Biological marker characteristics of oils and asphalts from carbonate source rocks in a rapidly subsiding graben, Dead Sea, Israel. Geochim. Cosmochim. Acta 49, 1357–1370.

Russel, M., Grimalt, J.O., Hartgers, W.A., Taberner, C., Rouchy, J.M., (1997). Bacterial and algal markers in sedimentary organic matter deposited under natural sulphuruzation conditions (Lorca Basin, Murcia, Spain). Organic Geochemistry 26, 605-625.

Ruvo, L., Aldegheri, A., Galimberti, R., Nembrini, E., Rossi, L., Ruspi, R., (2003). Multi-disciplinary study of the heavy-oil reservoirs in the Armatella Field, Sicily. Petroleum Geoscience 9 (3), 265-276.

Sachsenhofer, R.F., Curry, D.J., Horsfield, B., Rantitsch, G., Wilkes, H., (1996). Characterisation of organic matter in late Cretaceous black shales of the Eastern Alps (Kainach Gosau-Group, Austria). Organic Geochemistry 23, 915-929.

Saiz-Jimenez, C., (1995). The origin of alkylbenzenes and thiophenes in pyrolysates of geochemical samples. Organic Geochemistry 23 (1), 81-85.

Sandvik, E.I., Young, W.A., Curry, D.J., (1992). Expulsion from hydrocarbon sources: The role of organic absorption. Organic Geochemistry 19, 77-87.

Santamaria, O.D., Horsfield, B., (2003). Gas generation potential of Upper Jurassic (Tithonian) source rocks in the Sonda de Campeche, Mexico, The circum-Gulf of Mexico and the Caribbean; hydrocarbon habitats, basin formation, and plate tectonics, 79;. American Association of Petroleum Geologists, Tulsa, OK, United States, pp. 349-363.

Sarret, G., Connan, J., Kasrai, M., Bancroft, G.M., Charrie-Duhaut, A., Lemoine, S., Adam, P., Albrecht, P., Eybert-Berard, L., (1999). Chemical forms of sulfur in geological and archeological asphaltenes from Middle East, France, and Spain determined by sulfur K- and L-edge X-ray absorption near-edge structure spectroscopy. Geochimica et Cosmochimica Acta 63 (22), 3767-3779.

Sarret, G., Mongenot, T., Connan, J., Derenne, S., Kasrai, M., Michael Bancroft, G., Largeau, C., (2002). Sulfur speciation in kerogens of the Orbagnoux deposit (Upper

Kimmeridgian, Jura) by XANES spectroscopy and pyrolysis. Organic Geochemistry 33 (8), 877-895.

Schaefer, G., Hattwig, S., Unterste, W.M., Hupe, K., Heerenklage, J., Lueth, J.C., Kaestner, M., Eschenbach, A., Stegmann, R., Mahro, B., (1995). PAH-degradation in soil; microbial activation or inoculation? A comparative evaluation with different supplements and soil materials, Contaminated soil '95; proceedings of the Fifth international FZK/ TNO conference, 5;. Kluwer Academic Publishers, Dordrecht - Boston - London, Netherlands, pp. 415-416.

Schaefer, R.G., Schenk, H.J., Hardelauf, H., Harms, R., (1990). Determination of gross kinetic parameters for petroleum formation from Jurassic source rocks of different maturity levels by means of laboratory experiments, Advances in organic geochemistry 1989; Part I, Organic geochemistry in petroleum exploration, 16; 1-3. Pergamon, Oxford-New York, International, pp. 115-120.

Schaeffer, P., Reiss, C., Albrecht, P., (1995). Geochemical study of macromolecular organic matter from sulfur-rich sediments of evaporitic origin (Messinian of Sicily) by chemical degradations. Organic Geochemistry 23 (6), 567-581.

Schaeffer-Reiss, C., Schaeffer, P., Putschew, A., Maxwell, J.R., (1998). Stepwise chemical degradation of immature S-rich kerogens from Vena del Gesso (Italy). Organic Geochemistry 29 (8), 1857-1873.

Schantz, S.S., Elliot, P.L., (1994). Economic implications of solids in crude and their ultimate fate in the refining process. In: NPRA Annual Meeting, San Antonio, USA.

Schenk, H.J., Dieckmann, V., (2004). Prediction of petroleum formation: the influence of laboratory heating rates on kinetic parameters and geological extrapolations. Marine and Petroleum Geology 21 (1), 79-95.

Schenk, H.J., Horsfield, B., (1998). Using natural maturation series to evaluate the utility of parallel reaction kinetics models: an investigation of Toarcian shales and Carboniferous coals, Germany. Organic Geochemistry 29 (1-3), 137-154.

Schenk, H.J., Horsfield, B., Krooss, B., Schaefer, R.G., Schwochau, K., (1997). Kinetics of petroleum formation and cracking, Petroleum and basin evolution; insights from petroleum geochemistry, geology and basin modeling. Springer, Berlin, Federal Republic of Germany.

Schmid, H., Kubassa, F., Herdy, R., (1948). Kinetische Untersuchungen der Dimerisierung von Cyclopentadien. Monatsheft für Chemie 79 (5), 430-438.

Schoell, M., Schouten, S., Sinninghe Damsté, J.S., de Leeuw, J.W., Summons, R.E., (1994). A molecular organic carbon isotope record of Miocene climate changes. Science 263 (5150), 1122-1125.

Seifert, W.K., Moldowan, J.M., (1978). Applications of steranes, terpanes and monoaromatics to the maturation, migration and source of crude oils. Geochim. Cosmochim. Acta 42, 77–95.

Seifert, W.K., Moldowan, J.M., (1986). Use of biological markers in petroleum exploration. In: R.B. Johns (Ed.), Methods in Geochemistry and Geophysics, 24, pp. 261-290.

Senftle, J.T., Larter, S.R., Bromley, B.W., Brown, J.H., (1986). Quantitative chemical characterization of vitrinite concentrates using pyrolysis-gas chromatography. Rank variation of pyrolysis products. Organic Geochemistry 9 (6), 345-350.

Sheu, E.Y., Mullins, O.C., (1995). Asphaltenes fundamentals and applications. Plenum Press., New York.

Sheu, E.Y., Shields, M.B., (1995). Asphaltene surface activity at oil-water interfaces. Society of Petroleum Engineers Journal, 523-532.

Sheu, E.Y., Tar, M.M.D., Storm, D.A., (1991). Solution properties of colloids formed by petroleum vacuum residues. Macromolecular Reports A28, 159-175.

Sinninghe Damsté, J.S., de las Heras, F.X.C., van Bergen, P.F., de Leeuw, J.W., (1993). Characterization of Tertiary Catalan lacustrine oil shales; discovery of extremely organic sulphur-rich Type I kerogens. Geochimica et Cosmochimica Acta 57 (2), 389-415.

Sinninghe Damsté, J.S., de Leeuw, J.W., (1989). Analysis, structure and geochemical significance of organically-bound sulphur in the geosphere: state of the art and future research. Organic Geochemistry 16, 1077–1101.

Sinninghe Damsté, J.S., Eglinton, T.I., de Leeuw, J.W., Schenck, P.A., (1989). Organic sulphur in macromolecular sedimentary organic matter; I, Structure and origin of sulphur-containing moieties in kerogen, asphaltenes and coal as revealed by flash pyrolysis. Geochimica et Cosmochimica Acta 53 (4), 873-889.

Sinninghe Damsté, J.S., Eglinton, T.I., Rijpstra, W.I.C., de Leeuw, J.W., (1990). Characterisation of organically-bound sulfur in high-molecular-weight sedimentary organic matter using flash pyrolysis and Raney Ni desulfurisation. In: W.L. Orr, C.M. White (Eds.), Geochemistry of Sulfur in Fossil Fuels, 429. ACS Symposium Series, Washington DC, pp. 486-528.

Sinninghe Damsté, J.S., Frewin, N.L., Kenig, F., de Leeuw, J.W., (1995). Molecular indicators for palaeoenvironmental change in a Messinian evaporitic sequence (Vena del Gesso, Italy). I: Variations in extractable organic matter of ten cyclically deposited marl beds. Organic Geochemistry 23 (6), 471-483.

Sinninghe Damsté, J.S., Kock-van Dalen, A.C., de Leeuw, J.W., Schenck, P.A., (1988). Identification of homologous series of alkylated thiophenes, thiolanes, thianes and benzothiophenes present in pyrolysates of sulphur-rich kerogens. Journal of Chromatography A 435, 435-452.

Sinninghe Damsté, J.S., Kohnen, M.E.L., Horsfield, B., (1998). Origin of low-molecular-weight alkylthiophenes in pyrolysates of sulphur-rich kerogens as revealed by micro-scale sealed vessel pyrolysis. Organic Geochemistry 29 (8), 1891-1903.

Skeie, J.E., di Primio, R., Karlsen, D.A., (2004). An integrated basin modelling study applying asphaltene kinetics from reservoired petroleum in the Snorre Area, northern North Sea. In: J.M. Cubitt, W.A. England, S.R. Larter (Eds.), Understanding Petroleum Reservoirs: Towards an Integrated Reservoir Engineering and Geochemical Approach, Geological Society Special Publication 237. Geological Society Publishing House, London, pp. 138-156.

Solli, H., Leplat, P., (1986). Pyrolysis-gas chromatography of asphaltenes and kerogens from source rocks and coal - a comparative structural study, Advances in Organic Geochemistry 1985. Pergamon, Oxford-New York International, pp. 313-329.

Speight, J.G., (1999). The chemistry and technology of petroleum. Marcel Dekker, Inc., New York.

Speight, J.G., Long, R.B., Trowbridge, T.D., (1984). Factors influencing the separation of asphaltenes from heavy petroleum feedstocks. Fuel 63 (5), 616-620.

Speight, J.G., Wernick, D.L., Gould, K.A., Overfield, R.E., Rao, B.M.L., (1985). Molecular Weight and Association of Asphaltenes: a Critical Review. Oil and Gas Science and Technology 40 (1), 51-61.

Spiecker, P.M., Gawrys, K.L., Trail, C.B., Kilpatrick, P.K., (2003). Effects of petroleum resins on asphaltene aggregation and water-in-oil emulsion formation. Colloids and Surfaces A: Physicochemical and Engineering Aspects 220 (1-3), 9-27.

Spielmann, R., Cramers, C.A., (1972). Cyclopentadienic compounds as intermediates in the thermal degradation of phenols. Kinetics of the thermal decomposition of cyclopentadiene. J. Chromatographia 5 (12), 295-300.

Stacher, P., (1995). Present understanding of the Niger Delta hydrocarbon habitat. In: M.N. Oti, G. Postma (Eds.), Geology of Deltas. A.A. Balkema, Rotterdam, pp. 257-267.

Standal, S., Haavik, J., Blokhus, A.M., Skauge, A., (1999). Effect of polar organic components on wettability as studied by adsorption and contact angles. Journal of Petroleum Science and Engineering 24 (2-4), 131-144.

Stankiewicz, B.A., Kruge, M.A., Mastalerz, M., Salmon, G.L., (1996). Geochemistry of the alginite and amorphous organic matter from Type II-S kerogens. Organic Geochemistry 24 (5), 495-509.

Stark, J.L., Asomaning, S., (2005). Synergies between asphaltene stabilizers and demulsifying agents giving improved demulsification of asphaltene-stabilized emulsions. Energy & Fuels 19 (4), 1342 - 1345.

Stefani, M.M., Burchell, M.T., (1993). A review of the Upper Triassic source rocks of Italy, Generation, accumulation, and production of Europe's hydrocarbons; III, 3;, pp. 169-178.

Stetter, K.O., Huber, R., Blöchl, E., Knurr, M., Eden, R.D., Fielder, M., Cash, H., Vance, I., (1993). Hyperthermophilic archea are thriving in deep North Sea and Alaskan oil reservoirs. Nature 365, 743-745.

Stoakes, F.A., Creaney, S., (1984). Sedimentology of a carbonate source rock: the Duvernay Formation of Alberta Canada. In: Proceedings of the 1984 Canadian Society of Petroleum Geologists Core Conference, Carbonates in Subsurface and Outcrop (Ed. by E. L.), pp. 132-147.

Stoakes, F.A., Creaney, S., (1985). Controls on the accumulation and subsequent maturation and migration history of a carbonate source rock. In: SEPM Core Workshop Proceedings, Golden, Colorado.

Storm, D.A., de Canio, S.J., Sheu, E.Y., (1994). Sludge formation during heavy oil conversion, in asphaltene particles in fossil fuel exploration, recovery, refining, and production processes. In: M.K. Sharma, T.F. Yen (Eds.). Plenum Press, New York, pp. 81-90.

Stout, N.D., Koskinas, G.J., Raley, J.H., Santor, S.D., Opila, R.L., Rothman, A.J., (1976). Pyrolysis of oil shale: effects of thermal history on oil yield. Q. Colo. Sch. Mines 71 (4), 153-172.

Stout, S.A., Boon, J.J., (1994). Structural characterization of the organic polymers comprising a lignite's matrix and megafossils. Organic Geochemistry 21 (8-9), 953-970.

Summons, R.E., Thomas, J., Maxwell, J.R., Boreham, C.J., (1992). Secular and environmental constraints on the occurrence of dinosterane in sediments. Geochimica et Cosmochimica Acta 56 (6), 2437-2444.

Summons, R.E., Volkman, J.K., Boreham, C.J., (1987). Dinosterane and other steroidal hydrocarbons of dinoflagellate origin in sediments and petroleum. Geochimica et Cosmochimica Acta 51 (11), 3075-3082.

Sun, Y., Xu, S., Lu, H., Cuai, P., (2003). Source facies of the Paleozoic petroleum systems in the Tabei uplift, Tarim Basin, NW China: implications from aryl isoprenoids in crude oils. Organic Geochemistry 34 (4), 629-634.

Suuberg, E.M., Otake, Y., Langer, M.J., Leung, K.T., Milosavljevie, I., (1994). Coal macromolecular structure analyses: solvent swelling thermodynamics and its implications. Energy and Fuels 8, 1247–1262.

Suzuki, T., Ito, Y., Takegami, Y., Watanabe, Y., (1982). Chemical structure of tar-sand bitumens by 13C and 1H NMR spectroscopy method. Fuel 61, 402-410.

Talling, J.F., Wood, A.B., Prosser, M.V., Baxter, R.M., (1973). The upper limit of photosynthetic productivity by phytoplankton: Evidence from Ethiopian soda lakes. Freshwater Biol. 3, 53-76.

Talukdar, S.C., Dow, W.G., (1990). Geochemistry of oils provides optimism for deeper exploration in atlantic off Trinidad. Oil and Gas Journal 12, 118-122.

Tang, Y., Béhar, F., (1995). Rate constants and activation energies of n-alkanes generation from type II kerogen in open and closed pyrolysis systems. Energie and Fuels 9, 507-512.

Tang, Y., Stauffer, M., (1994). Development of multiple cold trap pyrolysis. Journal of Analytical and Applied Pyrolysis 28 (2), 167-174.

Tang, Y., Stauffer, M., (1995). Formation of pristene, pristane and phytane: kinetic study by laboratory pyrolysis of Monterey source rock. Organic Geochemistry 23 (5), 451-460.

Tannenbaum, E., Aizenshtat, Z., (1985). Formation of immature asphalt from organic-rich carbonate rocks; I, Geochemical correlation. Organic Geochemistry 8 (2), 181-192.

Taylor, P.N., Bennet, B., Jones, D.M., Larter, S.R., (2001). The effect of biodegradation and water washing on the occurrence of alkylphenols in crude oils. Organic Geochemistry 32, 341-358.

Taylor, P.N., Larter, S.R., Jones, D.M., Dale, J.D., Horstad, I., (1997). The effect of oil water rock partitioning on the occurrence of alkylphenols in petroleum systems. Geochim. Cosmochim. Acta 61, 3295-3339.

Tegelaar, E.W., Noble, R.A., (1994). Kinetics of hydrocarbon generation as a function of the molecular structure of kerogen as revealed by pyrolysis-gas chromatography. In: N. Telnaes, G.W. van Graas, K. Øygard (Eds.), Advances in Organic Geochemistry 1993. Pergamon Press, Oxford, pp. 543-574.

Teinturier, S., Elie, M., Pironon, J., (2003). Oil-cracking processes evidence from synthetic petroleum inclusions. Journal of Geochemical Exploration 78-79, 421-425.

Teixidor, P., Grimait, J.O., Pueyo, J.J., Rodriguez-Valera, F., (1993). Isopranylglycerol diethers in non-alkaline evaporitic environments. Geochimica et Cosmochimica Acta 57 (18), 4479-4489.

ten Haven, H.L., (1996). Applications and limitations of Mango's light hydrocarbon parameters in petroleum correlation studies, Proceedings of the 17th international meeting on Organic chemistry; Part III, Origin of natural gases; petroleum geochemistry, impact of organic geochemistry on exploration; migration and expulsion of oil and gas, 24; 10-11. Pergamon, Oxford-New York, International, pp. 957-976.

ten Haven, H.L., de Leeuw, J.W., Peakman, T.M., Maxwell, J.R., (1986). Anomalies in steroid and hopanoid maturity indices. Geochimica et Cosmochimica Acta 50 (5), 853-855.

ten Haven, H.L., de Leeuw, J.W., Rullkötter, J., Sinninghe Damsté, J.S., (1987). Restricted utility of the pristane/phytane ratio as environmental indicator. Nature 330, 641.

ten Haven, H.L., Rohmer, M., Rullkotter, J., Bisseret, P., (1989). Tetrahymanol, the most likely precursor of gammacerane, occurs ubiquitously in marine sediments. Geochimica et Cosmochimica Acta 53 (11), 3073-3079.

Thanh, N.X., Hsieh, M., Philp, R.P., (1999). Waxes and asphaltenes in crude oils. Organic Geochemistry 30 (2-3), 119-132.

Thomas, B.M., (1982). Land-plant source rocks for oil and their significance in Australian basins. APEA J. 22, 164-178.

Thomas, B.M., Moller-Pederson, P., Whitaker, M.F., Shaw, N.D., (1985). Organic facies and hydrocarbon distributions in the Norwegian North Sea. In: B.M. Thomas (Ed.), Petroleum Geochemistry in Exploration of the Norwegian shelf. Graham and Trotman, London, pp. 3-26.

Thomas, D., (1995). Nigeria; 1, Exploration gaps exist in Nigeria's prolific delta. Oil and Gas Journal 93 (44), 66-71.

Thomas, M.M., Clouse, J.A., (1990). Primary migration by diffusion through kerogen: II. Hydrocarbon diffusivities in kerogen. Geochimica et Cosmochimica Acta 54 (10), 2781-2792.

Thompson, K.F.M., (1983). Classification and thermal history of petroleum based on light hydrocarbons. Geochimica et Cosmochimica Acta 47 (2), 303-316.

Thompson, K.F.M., (1988). Gas-condensate migration and oil fractionation in deltaic systems. Marine and Petroleum Geology 5 (3), 237-246.

Thompson, K.F.M., Kennicutt, M.C.I., (1990). Classification of offshore Gulf of Mexico oils and gas-condensates, Gulf Coast oils and gases; their characteristics, origin, distribution, and exploration and production significance, 9;. Society of Economic Paleontologists and Mineralogists, Austin, TX, United States, pp. 183.

Thompson, S., Cooper, B.S., Barnard, P.C., (1994). Some examples and possible explanations for oil generation from coals and coaly sequences. Coal and coal-bearing strata as oil-prone source rocks?, Published by Geological Society of London; Special Publication, 77, Editors Scott A.C. and Fleet A.J., 119-137.

Thouand, G., Bauda, P., Oudot, J., Kirsch, G., Sutton, C., Vidalie, J.F., (1999). Laboratory evaluation of crude oil biodegradation with commercial or natural microbial inocula. Can. J. Microbiol. 45, 106-115.

Tissot, B., (1989). The geochemistry of resins and asphaltenes, Characterization of heavy crude oils and petroleum residues. Petroleum Industry Press, Beijing, pp. 2-10.

Tissot, B., Deroo, G., Hood, A., (1978). Geochemical study of the Uinta Basin; formation of petroleum from the Green River Formation. Geochimica et Cosmochimica Acta 42 (10), 1469-1486.

Tissot, B.P., Pelet, R., Ungerer, P., (1987). Thermal history of sedimentary basins, maturation indices, and kinetics of oil and gas generation. AAPG Bulletin 71 (12), 1445-1466.

Tissot, B.P., Welte, D.H., (1984). Petroleum Formation and Occurrence. Springer-Verlag.

Tomic, J., Béhar, F., Vandenbroucke, M., Tang, Y., (1995). Artificial maturation of Monterey kerogen (Type II-S) in a closed system and comparison with Type II kerogen: implications on the fate of sulfur. Organic Geochemistry 23 (7), 647-660.

Tortorici, L., Monaco, C., Mazzoli, S., Bianca, M., (2001). Timing and modes of deformation in the western Sicilian thrust system, southern Italy. Journal of Petroleum Geology 24 (2), 191-211.

Trejo, F., Centeno, G., Ancheyta, J., (2004). Precipitation, fractionation and characterization of asphaltenes from heavy and light crude oils. Fuel 83 (16), 2169-2175.

Trindade, L.A.F., Philp, R.P., Mizusaki, A.M.P., dos Santos, R.L.A., Tchouparova, E., Siamak Djafarian, M., (1996). Geochemical characterization of waxy oils from the Dom Joao oil field, Reconcavo Basin, Brazil. In: Proceedings of the 5th Latin American Organic Geochemistry Congress, Cancun, Mexico, pp. 281-283.

Tuttle, M.L.W., Charpentier, R.R., Brownfield, M.E., (1999). The Niger Delta Petroleum System: Niger Delta Province, Nigeria, Cameroon, and Equatorial Guinea, Africa. In: Open File Report 99-50H. U.S. Geological Survey.

Udo, O.T., Ekweozor, C.M., (1990). Significance of oleanane occurrence in shales of Opuama Channel Complex, Niger Delta. Energie and Fuels 4, 248-254.

Ukpabio, E.J., Comet, P.A., Sassen, R., Brooks, J.M., (1994). Triterpenes in a Nigerian oil. Organic Geochemistry 22 (2), 323-329.

Urov, K.E., (1980). Thermal decomposition of kerogens - mechanism and analytical application. Journal of Analytical and Applied Pyrolysis 1, 323-338.

van Bergen, P.F., Collinson, M.E., Sinninghe Damsté, J.S., de Leeuw, J.W., (1994). Chemical and microscopical characterization of inner seed coats of fossil watter plants. Geochim. Cosmochim. Acta 58, 231-239.

van de Meent, D., Brown, S.C., Philp, R.P., Simoneit, B.R.T., (1980). Pyrolysis-high resolution gas chromatography and pyrolysis gas chromatography-mass spectrometry of kerogens and kerogen precursors. Geochim. Cosmochim. Acta 44, 999-1013.

van Kaam-Peters, H.M.E., Schouten, S., Köster, J., Sinninghe Damsté, J.S., (1998). Control on the molecular and carbon isotopic composition of organic matter depositted in a Kimmeridgian euxinic shelf sea: evidence for preservation of carbohydrates through sulfurisation. Geochimica et Cosmochimica Acta 62, 3259–3284.

Vandenbroucke, M., Béhar, F., Rudkiewicz, J.L., (1999). Kinetic modelling of petroleum formation and cracking; implications from the high pressure/ high temperature Elgin Field (UK, North Sea). Organic Geochemistry 30 (9), 1105-1125.

Vaz dos Santos Neto, E., Hayes, J.M., Takaki, T., (1998). Isotopic biogeochemistry of the Neocomian lacustrine and Upper Aptian marine-evaporitic sediments of the Potiguar Basin, Northeastern Brazil. Organic Geochemistry 28 (6), 361-381.

Venkatesan, M.I., (1989). Tetrahymanol: its widespread occurence and geochemical significance. Geochimica et Cosmochimica Acta 53, 3095-3101.

Venkateswaran, K., Hoaki, T., Kato, M., Maruyama, T., (1995). Microbial degradation of resins fractioned from arabian light crude oil. Can. J. Microbiol. 41, 418-424.

Versteegh, G.J.M., Blokker, P., Wood, G.D., Collinson, M.E., Sinninghe Damsté, J.S., de Leeuw, J.W., (2004). An example of oxidative polymerization of unsaturated fatty acids as a preservation pathway for dinoflagellate organic matter. Organic Geochemistry 35, 1129–1139.

Volkman, J.K., (1986). A review of sterol markers for marine and terrigenous organic matter. Organic Geochemistry 9, 83-99.

Volkman, J.K., Alexander, R., Kagi, R.I., Rowland, S.J., Sheppard, P.N., (1984). Biodegradation of aromatic hydrocarbons in crude oils from the Barrow Sub-basin in Western Australia. Organic Geochemistry 6, 619-632.

Volkman, J.K., Johns, R.B., Gillan, F.T., Perry, G.J., Bavor, H.J., (1980). Microbial sediments of an intertidal sediment - 1. Fatty acids and hydrocarbons. Geochimica et Cosmochimica Acta 44, 1133-1143.

Volova, T.G., Kalacheva, G.S., Zhila, N.O., (2003). Specificity of lipid composition in two Botryococcus strains, the producers of liquid hydrocarbons. Russian Journal of Plant Physiology 50 (5), 627-633.

von Soxhlet, F., (1879). Die gewichtsanalytische Bestimmung des Milchfettes. Polytechnisches J. 232, 461.

Waldo, G.S., Carlson, R.M.K., Moldowan, J.M., Peters, K.E., Penner-Hahn, J.E., (1991). Sulfur speciation in heavy petroleums: Information from X-ray absorption near-edge structure. Geochimica et Cosmochimica Acta 55, 801-814.

Waples, D.W., Machihara, T., (1990). Application of sterane and triterpane biomarkers in petroleum exploration. Bulletin of Canadian Petroleum Geology 38 (3), 357–380.

Waples, D.W., Machihara, T., (1991). Biomarkers for Geologists. A Practical Guide to the Application of Steranes and Triterpanes in Petroleum Geology. The American Association of Petroleum Geologists, Tulsa, Oklahoma.

Wavrek, D.A., Lara, M.E., (1999). Risk reduction in gas exploration; application of compositional kinetic analysis to the deep Neuquen Basin, Argentina, American Association of Petroleum Geologists 1999 annual meeting, 1999;. American Association of Petroleum Geologists and Society of Economic Paleontologists and Mineralogists, Tulsa, OK, United States, pp. A146.

Wehner, H., (2005). Zur Genese von Kohlenwasserstoffen im Oberen Benue Trog, Nigeria. BGR-report, Hannover.

Welte, D.H., Yalcin, M.N., (1988). Basin modelling; a new comprehensive method in petroleum geology, Advances in organic geochemistry 1987; Part I, Organic geochemistry in petroleum exploration; proceedings of the 13th international meeting on organic geochemistry, 13; 1-3. Pergamon, Oxford-New York, International, pp. 141-151.

Wendebourg, J., (2000). Modeling multi-component petroleum fluid migration in sedimentary basins. Journal of Geochemical Exploration 69-70, 651-656.

Werner, A., Béhar, F., de Hemptinne, J.C., Béhar, E., (1996). Thermodynamic properties of petroleum fluids during expulsion and migration from source rocks. Organic Geochemistry 24 (10-11), 1079-1095.

Wever, H.E., (2000). Petroleum and source rock characterization based on C (sub 7) star plot results; examples from Egypt. AAPG Bulletin 84 (7), 1041-1054.

Wiehe, I.A., Yarranton, H.W., Akbarzadeh, K., Rahimi, P.M., Teclemariam, A., (2005). The paradox of asphaltene precipitation with normal paraffins. Energy & Fuels 19 (4), 1261 - 1267.

Wikimedia Foundation, (2006). Soxhlet extractor. In: Wikipedia online encyclopedia.

Wilhelms, A., Larter, S.R., (1994a). Origin of tar mats in petroleum reservoirs. Part I: introduction and case studies. Marine and Petroleum Geology 11 (4), 418-441.

Wilhelms, A., Larter, S.R., (1994b). Origin of tar mats in petroleum reservoirs. Part II: formation mechanisms for tar mats. Marine and Petroleum Geology 11 (4), 442-456.

Wilhelms, A., Larter, S.R., Hall, K., (1994). A comparative study of the stable carbon isotopic composition of crude oil alkanes and associated crude oil asphaltene pyrolysate alkanes. Organic Geochemistry 21 (6-7), 751-759.

Wilkes, H., Boreham, C.J., Harms, G., Zengler, K., Rabus, R., (2000). Anaerobic degradation and carbon isotopic fractionation of alkylbenzenes in crude oil by sulphate-reducing bacteria. Organic Geochemistry 31, 101-115.

Wilson, M.A., Philp, R.P., Gillam, A.H., Gilbert, T.D., Tate, K.R., (1983). Comparison of the structures of humic substances from aquatic and terrestrial sources by pyrolysis gas chromatography-mass spectrometry. Geochim. Cosmochim. Acta 47, 497-502.

Withers, N., (1983). Dinoflagellate sterols. In: P.J. Scheuer (Ed.), Marine Natural Products 5. Academic Press, pp. 87-130.

Wu, J., Prausnitz, J.M., Firoozabadi, A., (2000). Molecular Thermodynamics of Asphaltene Precipitation in Reservoir Fluids. AIChE Journal 46 (1), 197-209.

Xiao, X., Wilkins, R.W.T., Zufa, L., Jiamo, F., (1998). A preliminary investigation of the optical properties of asphaltene and their application to source rock evaluation. Organic Geochemistry 28 (11), 669-676.

Xiong, Y., Geng, A., (2000). Carbon isotopic composition of individual n-alkanes in asphaltene pyrolysates of biodegraded crude oils from the Liaohe Basin, China. Organic Geochemistry 31 (12), 1441-1449.

Yang, X., Kilpatrick, P., (2005). Asphaltenes and waxes do not interact synergistically and coprecipitate in solid organic deposits. Energy & Fuels 19 (4), 1360 - 1375.

Yarzab, R.F., Abdel-Basset, Z., Given, P.H., (1979). Hydroxyl content of coals. Geochim. Cosmochim. Acta 43, 281-287.

Yen, T.F., Chilingarian, G.V., (1994). Asphaltenes and asphalt, 1. Developments in Petroleum Science. Elsevier, Amsterdam.

Yoshioka, T., Akama, T., Uchida, M., Okuwaki, A., (2000). Analysis of two stages dehydrochlorination of poly(vinyl chloride) using TG-MS. Chemistry Letters 29 (4), 322.

Younes, M.A., (2005). Petroleum geochemistry and potential source rock correlation in the Shushan Basin, North Western Desert, Egypt. Pet. Sci. Technol. 23 (5-6), 507-536.

Youngblood, W.W., Blumer, M., Guillard, R.L., Fiore, F., (1971). Saturated and unsaturated hydrocarbons in marine benthic algae. Marine Biology 8, 190-201.

Zekri, A.Y., Chaalal, O., (2005). Effect of temperature on biodegradation of crude oil. Energie Sources 27 (1-2), 233-244.

Zengler, K., Richnow, H.H., Rossello-Mora, R., Michaelis, W., Widdel, F., (1999). Methane formation from long-chain alkanes by anaerobic microorganisms. Nature 401, 266-269.

Zhang, S., Liang, D., Gong, Z., Wu, K., Li, M., Song, F., Song, Z., Zhang, D., Wang, P., (2003). Geochemistry of petroleum systems in the eastern Pearl River Mouth Basin: evidence for mixed oils. Organic Geochemistry 34 (7), 971-991.

Zhang, X., Young, L.Y., (1997). Carboxylation as an initial reaction in the anaerobic metabolism of naphthalene and phenanthrene by sulfidogenic consortia. Applied and Environmental Microbiology 63, 4759-4764.

Zumberge, J.E., (1984). Source rocks of the La Luna Formation (Upper Cretaceous, in the Middle Magdalena Valley, Colombia). In: J.G. Palacas (Ed.), Petroleum geochemistry and source rock potential of carbonate rocks. American Association of Petroleum Geologists Bulletin in Geology Sciences, pp. 127-134.

Appendix

Sample info	TOC (%)	S1 (mg/g)	S2 (mg/g)	S3 (mg/g)	Tmax (°C)	PP (mg/g)	PI (wt ratio)	HI (mg HC/g TOC)	OI (mg CO2/g TOC)
G000642	4,39	0,51	34,18	0,67	422	34,69	0,01	779	15
G000645	3,46	1,18	25,67	0,45	434	26,85	0,04	742	13
G000646	0,41	1,34	1,93	0,16	429	3,27	0,41	471	39
G000647	2,93	0,23	17,97	0,51	418	18,20	0,01	613	17
G000648	1,37	0,32	9,46	0,62	416	9,78	0,03	691	45
G000649	6,76	1,59	51,56	0,58	414	53,15	0,03	763	9
G000650	1,29	0,30	7,32	0,57	414	7,62	0,04	567	44
G000651	2,34	0,35	15,21	0,66	416	15,57	0,02	650	28
G000652	11,80	1,43	96,23	0,85	421	97,66	0,01	816	7
G000653	2,89	0,52	19,35	0,67	417	19,87	0,03	670	23
G000654	8,76	1,66	79,64	0,84	421	81,30	0,02	909	10
G000655	4,03	0,53	30,60	0,79	413	31,13	0,02	759	20
G000656	7,05	1,69	57,61	0,59	415	59,30	0,03	817	8
G000657	0,75	0,16	4,37	0,55	419	4,53	0,04	583	73
G000660	0,67	0,09	3,83	0,38	409	3,92	0,02	572	57
G000661	6,65	0,71	45,65	0,68	439	46,36	0,02	686	10

PP = S1 + S2
PI = S1 / (S1 + S2)
HI = (S2 / TOC) x 100
OI = (S3 / TOC) x 100

Rock-Eval pyrolysis data for source rocks from South Italy

Sample	Formation	Depth (m)	TOC (%)	S1	S2	S3	HI	OI	PI	Tmax
G000541	Redwater	1144.3	3.05	0.43	13.34	1.53	437.38	50.16	0.03	419
G000542	Redwater	1147.3	5.36	0.79	31.7	1.51	591.42	28.17	0.02	419
G000545	Redwater	1153.9	9.33	1.89	55.38	2.36	593.57	25.29	0.03	418
G000546	Redwater	1157.2	4.69	0.92	23.17	1.69	494.03	36.03	0.04	414
G000548	Tomahawk	2335.3	5.72	3.67	30.09	0.63	526.05	11.01	0.11	426
G000549	Tomahawk	2335.8	6.53	4.54	37.69	0.4	577.18	6.13	0.11	429
G000550	Tomahawk	2336.2	8.26	4.03	47.59	0.88	576.00	11.00	0.08	427
G000553	Tomahawk	2338.8	9.57	6.21	59.52	0.46	621.94	4.81	0.09	426
G000559	Leduc	1783.5	0.61	0.21	1.57	0	257.38	0	0.12	435
G000560	Norbuck	2640.6	0.74	0.34	0.11	0	14.86	0	0.76	442
G000562	Norbuck	2648.3	4.36	1.91	1.75	0.28	40.14	6.42	0.52	465
G000564	Forgotsen Burk	1934.2	9.71	5.46	37.39	0.22	385.07	2.27	0.13	442
G000570	Forgotsen Burk	1944.8	10.30	5.75	42.52	0.47	412.82	4.56	0.12	443
G000575	Imperial Armena 3	1575.4	1.94	0.7	7.87	0.46	405.67	23.71	0.08	429
G000579	Can Gulf Dom Red.	1146.7	14.80	6.16	86.37	3.91	583.58	26.42	0.07	412
G000581	Can Gulf Dom Red.	1153.2	3.25	0.68	16.23	1.52	499.38	46.77	0.04	418
G000583	Can Gulf Dom Red.	1155.8	7.60	2.6	47.96	2.43	631.05	31.97	0.05	415
G000586	Imperial Kingman	1404.2	2.37	0.74	9.77	0.78	412.24	32.91	0.07	427
G000587	Imperial Kingman	1404.5	3.21	0.99	13.88	1	432.4	31.15	0.07	426
G000592	Imperial Kingman	1406.7	3.37	0.79	15.96	0.96	473.59	28.49	0.05	425
G000593	Imperial Kingman	1416.9	1.78	0.38	5.64	0.72	316.85	40.45	0.06	426
G000596	Ferrybank	2243.3	5.03	4.58	14.39	0.35	286.08	6.96	0.24	436
G000598	Ferrybank	2245.3	0.73	0.46	1.10	0.16	150.68	21.92	0.29	439
G000600	Ferrybank	2248.6	4.04	3.86	10.70	0.5	264.85	12.38	0.27	438
G000601	Imperial Cynthia	2971.5	1.48	0.71	0.82	0.44	55.41	29.73	0.46	440
G000602	Imperial Cynthia	2971.9	1.28	0.73	0.97	0.24	75.78	18.75	0.43	449
G000603	Imperial Cynthia	2973.7	4.19	3.65	12.70	0.23	303.1	5.49	0.22	441
G000607	Imperial Cynthia	2976.1	1.90	1.72	1.75	0.22	92.11	11.58	0.5	447
G000610	Sarcee et al Pibroc	1395.7	9.37	3.29	57.97	1.35	618.68	14.41	0.05	418
G000615	Sarcee et al Pibroc	1402.9	8.47	2.2	50.10	1.41	591.5	16.65	0.04	422
G000617	Banff Aguit Ram River	4610.7	1.33	0.11	0.02	0.18	1.5	13.53	0.85	
G000622	Banff Aguit Ram River	4623.3	5.35	0.37	0.27	0.58	5.05	10.84	0.58	548
G000624	Banff Aguit Ram River	4623.9	2.01	0.1	0.08	0.34	3.98	16.92	0.56	542
G000631	Banff Imperial	1677.6	5.54	3.46	34.40	0.31	620.94	5.6	0.09	431

Rock-Eval pyrolysis data for source rocks from the Duvernay Formation.

sample	Well	Ali %	Arom %	NSO %	API - gravity
G000393	A	21.33	21.71	56.96	9.9
G000394	A	10.25	21.41	68.34	2.62
G000395	A	16.05	19.52	64.43	10.4
G000396	A	17.98	22.98	59.04	11.5
G000397	A	16.06	19.06	64.88	9
G000398	B	36.57	27.17	36.26	19.35
G000399	B	35.64	27.55	36.81	19.35
G000400	B	36.83	26.07	37.10	19.35
G000401	C	78.23	13.25	8.52	33.5
G000402	A	14.29	20.04	65.67	8.5
G000403	A	13.79	20.52	65.69	8.5
G000404	A	17.22	16.38	66.40	10.4

Data of MPLC analysis for Italian crude oils.

Sample	Formation	Depth (m)	API	Ali%	Aro%	NSO%
G000405	Redwater	943 - 999	36	48.3	28.3	23.4
G000406	Leduc Woodbend	1623 - 1631	38	66.1	23.2	10.7
G000407	Homeglen Rimbey	2410 - 2411	44	70.8	21	8.3
G000408	Leduc Woodbend	1522 - 1548	37	61.6	24.2	14.3
G000409	Judy Creek	2575 - 2577	39.5	69.2	21.8	9.1
G000410	West Pembina	3069	39.37	85.6	11.7	2.7
G000411	West Pembina	3753 - 3761	52.36	64.1	32.1	3.8
G000412	West Pembina	3364 - 3380	47.1	87.3	11	1.8

Data of MPLC analysis for Duvernay crude oils.

Sample		Gammacerane Index	Homohop. Index	C_{31} Homohop. Izom.-Index	C_{32} Homohop. Izom.-Index	Ts/(Ts+Tm)	Hop-Mor-Ratio H/(H+M)	C_{29}Ts Index	20S/(20S+20R) αααC_{29}	ββ/(ββ+αα) C_{27}	Pr/Ph
G000393	crude oil	0.35	0.04	0.53	0.57	0.44	0.80	0.23	0.57	0.67	0.62
G000394	crude oil	0.05	0.06	0.57	0.59	0.05	0.92	0.04	0.58	0.53	0.50
G000395	crude oil	0.36	0.05	0.50	0.50	0.29	0.86	0.16	0.57	0.71	0.40
G000396	crude oil	0.30	0.03	0,57	0.57	0.29	0.88	0.11	0.60	0.65	0.56
G000397	crude oil	0.33	0.02	0.51	0.54	0.32	0.86	0.12	0.53	0.70	0.40
G000398	crude oil	0.35	0.07	0.59	0.60	0.41	0.87	0.18	0.67	0.63	0.55
G000399	crude oil	0.36	0.07	0.59	0.60	0.43	0.88	0.15	0.62	0.65	0.66
G000400	crude oil	0.36	0.07	0.57	0.61	0.44	0.88	0.24	0.59	0.65	0.65
G000401	crude oil	0.12	n.d.	0.58	0.69	0.69	0.94	0.40	n.d.	0.53	n.d.
G000402	crude oil	0.32	0.05	0.53	0.54	0.27	0.87	0.11	0.56	0.69	0.45
G000403	crude oil	0.30	0.03	0.55	0.57	0.28	0.88	0.11	0.64	0.69	0.37
G000404	crude oil	0.31	0.04	0.50	0.54	0.33	0.85	0.15	0.53	0.70	0.41
G000642	bitumen	0.33	0.11	0.19	0.18	0.11	0.80	0.11	0.17	0.71	n.d.
G000648	bitumen	0.45	0.02	0.21	0.29	0.12	0.84	0.19	0.20	0.83	n.d.
G000649	bitumen	0.33	0.07	0.23	0.20	0.06	0.83	0.07	0.18	0.76	n.d.
G000650	bitumen	0.37	0.08	0.18	0.07	0.16	0.90	0.14	0.19	0.87	n.d.
G000651	bitumen	0.19	0.11	0.23	0.18	0.08	0.85	0.22	0.25	0.77	n.d.
G000652	bitumen	0.14	0.03	0.19	0.17	0.04	0.80	0.09	0.17	0.77	n.d.
G000654	bitumen	0.27	0.08	0.21	0.11	0.05	0.79	0.09	0.08	0.71	n.d.
G000656	bitumen	0.22	0.06	0.25	0.24	0.06	0.80	0.15	0.32	0.72	n.d.
G000661	bitumen	0.46	0.13	0.56	0.53	0.36	0.89	0.19	0.44	0.68	n.d.

Gammacerane Index = gammacerane / (gammacerane + C_{29} 17α(H), 21β(H)-homohopane)

Homohopane Index = C_{35}-homohopane / (C_{31}- + C_{32}- + C_{33}- + C_{34}- + C_{35}-homohopane)

C_{31} Homohopane Izom.-Index = 22S C_{31}-homohopane / (22S + 22R C_{31}-homohopane)

C_{32} Homohopane Izom.-Index = 22S C_{32}-homohopane / (22S + 22R C_{32}-homohopane)

Ts/(Ts+Tm) = C_{27} 18α(H)-trisnorhopane II / (C_{27} 18α(H)-trisnorhopane II + C_{27} 17α(H)-trisnorhopane)

Hopane-Moretane-Ratio = C_{29} 17α(H), 21β(H)-homohopane / (C_{29} 17α(H), 21β(H)-homohopane + βα-moretane)

C_{29}Ts Index = C_{29} 18α-(H)-30-norneohopane / (C_{29} 18α-(H)-30-norneohopane + C_{29} 17α(H)-hopane)

Sterane-Isom. 20S/(20S+20R) αααC_{29} = C_{29} 5α(H), 14α(H), 17α(H) 20S / (ααα20S + ααα20R)

Sterane-Isom. ββ/(ββ+αα) C_{27} = C_{27} 14β(H), 17β(H) / (ββ + αα)

Biomarker distribution for crude oils and selected source rock bitumens.

Sample		% αααC_{27}	% αααC_{28}	% αααC_{29}	Sterane-Isom. C_{29} ββ/(ββ+αα)	Sterane-Isom. 20S/(20S+20R)	Ts/(Ts+Tm)	Homohop. Index	Pr/Ph
G000405	crude oil	36.00	17.00	46.00	0.73	0.62	0.52	0.08	1.32
G000406	crude oil	38.00	16.00	46.00	0.72	0.64	0.68	0.14	1.42
G000407	crude oil	41.00	0.00	59.00	0.66	0.66	0.8	0.00	1.61
G000409	crude oil	41.00	19.00	40.00	0.71	0.61	0.74	0.00	1.86
G000410	crude oil				0.4	-	-	-	1.94
G000411	crude oil	-	-	-	-	0.74	0.36	0.11	1.92
G000412	crude oil	-	-	-	-	-	-	-	1.94
42714*	bitumen	26.00	18.00	55.00	0.43	-	-		
42725*	bitumen	33.00	19.00	47.00	0.5	0.58	0.56	0.07	
42728*	bitumen	34.00	18.00	48.00	0.58	0.61	0.52	0.07	
42746*	bitumen	35.00	19.00	46.00	0.4	0.6	0.47	0.06	
42765*	bitumen	30.00	17.00	53.00	0.36	0.58	0.3	0.06	
G000596	bitumen	35.00	19.00	45.00	0.65	0.64	0.73	0.12	
42779*	bitumen	-	-	-	-	0.52	0.56	0.12	
42790*	bitumen	28.00	18.00	54.00	0.41	0.46	0.31	0.05	
42795*	bitumen	25.00	22.00	53.00	0.39	0.5	0.34	0.11	
42802*	bitumen	33.00	20.00	47.00	0.49	0.61	0.41	0.06	
42811*	bitumen	36.00	19.00	45.00	0.45	0.61	0.42	0.07	

Sterane-Isom. ββ/(ββ+αα) C_{29} = C_{29} 14β(H), 17β(H) / (ββ + αα)

Sterane-Isom. 20S/(20S+20R) αααC$_{29}$ = C_{29} 5α(H), 14α(H), 17α(H) 20S / (ααα20S + ααα20R)

Ts/(Ts+Tm) = C_{27} 18α(H)-trisnorhopane II / (C_{27} 18α(H)-trisnorhopane II + C_{27} 17α(H)-trisnorhopane)

Homohopane Index = C_{35}-homohopane / (C_{31}- + C_{32}- + C_{33}- + C_{34}- + C_{35}-homohopane)

Pr/Ph = pristane /phytane

Biomarker parameter for Duvernay crude oils and source rock bitumen after Dieckmann (1998). The marked (*) source rock bitumen are not part of the sample set for the present study.

Sample	Ts/(Ts+Tm)	C_{29}Ts Index	Moretane Ratio M/(H+M)	Oleanane Index O/H	Oleanane-Hop. O/(O+H) Ratio	Homohop. Index	C_{31} Homohop. Izom.-Index	C_{32} Homohop. Izom.-Index	C_{35} Homohop. Izom.-Index
G000502	0.52	0.20	0.10	1.01	0.50	0.03	0.58	0.56	0.58
G000503	0.51	0.23	0.10	1.01	0.50	0.03	0.59	0.56	0.59
G000504	0.59	0.20	0.08	0.98	0.49	0.03	0.58	0.58	0.54
G000505	0.53	0.16	0.09	0.99	0.50	0.03	0.58	0.57	0.56
G000506	0.51	0.20	0.10	1.02	0.50	0.03	0.59	0.57	0.58
G000507	0.54	0.18	0.09	0.98	0.49	0.03	0.58	0.56	0.58
G000508	0.61	0.19	0.07	0.98	0.49	0.03	0.58	0.58	0.55
G000509	0.58	0.19	0.12	1.05	0.51	0.02	0.57	0.58	0.55
G000510	0.44	0.14	0.12	1.03	0.51	0.02	0.56	0.56	0.55
G000511	0.53	0.15	0.10	0.99	0.50	0.02	0.57	0.57	0.54

Sample	Sterane-Isom. 20S/(20S+20R) αααC_{27}	Sterane-Isom. 20S/(20S+20R) αααC_{28}	Sterane-Isom. 20S/(20S+20R) αααC_{29}	Sterane-Isom. 20S/(20S+20R) αααC_{30}	Sterane-Isom. ββ/(ββ+αα) C_{29}	% αααC_{27}	% αααC_{28}	% αααC_{29}	Pr/Ph
G000502	0.43	0.20	0.36	0.43	0.48	31.54	26.58	41.88	2.51
G000503	0.44	0.21	0.35	0.40	0.49	31.48	26.37	42.15	1.94
G000504	0.47	0.22	0.40	0.46	0.51	31.65	26.24	42.11	2.00
G000505	0.44	0.20	0.37	0.41	0.48	31.88	26.92	41.20	2.20
G000506	0.45	0.20	0.36	0.43	0.51	31.27	26.66	42.06	1.82
G000507	0.44	0.21	0.36	0.41	0.48	31.12	26.77	42.11	2.96
G000508	0.48	0.27	0.41	0.49	0.55	29.29	26.73	43.98	2.18
G000509	0.47	0.25	0.38	0.48	0.50	23.01	22.35	54.64	3.70
G000510	0.43	0.19	0.33	0.44	0.46	29.97	27.04	42.99	3.39
G000511	0.44	0.21	0.36	0.44	0.50	28.12	24.82	47.06	2.47

Ts/(Ts+Tm) = C_{27} 18α(H)-trisnorhopane II / (C_{27} 18α(H)-trisnorhopane II + C_{27} 17α(H)-trisnorhopane)

C_{29}Ts Index = C_{29} 18α-(H)-30-norneohopane / (C_{29} 18α-(H)-30-norneohopane + C_{29} 17α(H)-hopane)

Moretane-Ratio = C_{30} βα-moretane/ (C_{30} βα-moretane +C_{30} 17α(H), 21β(H)-homohopane)

Oleanane Index = 18α(H)-oleanane / C_{30} 17α(H), 21β(H)-homohopane

Homohopane Index = C_{35}-homohopane / (C_{31}- + C_{32}- + C_{33}- + C_{34}- + C_{35}-homohopane)

C_{31} Homohopane Izom.-Index = 22S C_{31}-homohopane / (22S + 22R C_{31}-homohopane)

Sterane-Isom. 20S/(20S+20R) αααC_{27} = C_{27} 5α(H), 14α(H), 17α(H) 20S / (ααα20S + ααα20R)

Sterane-Isom. ββ/(ββ+αα) C_{29} = C_{29} 14β(H), 17β(H) / (ββ + αα)

% αααC_{27} = αααC_{27} sterane / ααα(C_{27} + C_{28} + C_{29})

Pr/Ph = pristane /phytane

Biomarker parameter for Nigerian crude oils.

Italy asphaltene	n-c6-14	n-c15+	aromates	NSO
48.0	3.4	2.9	1.1	1.5
49.0	0.0	0.0	0.0	0.0
50.0	0.0	0.0	0.0	0.0
51.0	0.0	0.0	0.0	0.0
52.0	5.1	3.0	2.5	4.5
53.0	10.7	6.2	5.1	8.0
54.0	2.0	0.8	0.9	1.3
55.0	11.2	4.2	4.2	5.4
56.0	2.9	0.6	1.4	1.1
57.0	5.0	0.0	3.4	1.6
58.0	0.0	0.0	0.0	0.0
59.0	0.0	0.0	0.0	0.0
60.0	0.0	0.0	4.0	0.0
Frequency Factor	1.45E+14 1/s	1.45E+14 1/s	1.45E+14 1/s	1.45E+14 1/s

Compositional kinetic predictions for hydrocarbons formed from oil asphaltene from Southern Italy.

activation energies (kcal/mol)	n-C6-14	n-C15+	aromatic hydr.	NSO
61.0	0.3	0.9	1.6	0.2
62.0	0.8	1.3	1.8	0.2
63.0	0.0	0.0	0.0	0.0
64.0	10.2	11.8	7.1	0.9
65.0	0.0	0.0	0.0	0.0
66.0	10.2	13.5	4.7	0.6
67.0	1.9	1.1	0.8	0.1
68.0	2.5	0.1	1.2	0.2
69.0	13.1	0.0	9.0	1.0
70.0	0.0	0.0	0.0	0.0
71.0	0.0	0.0	4.0	0.0
Frequency Factor	2.63E+17	2.63E+17	2.63E+17	2.63E+17

Compositional kinetic predictions for hydrocarbons formed from oil asphaltene from Nigeria onshore.